frontiers | Research Topics

Plant-soil-microbial interactions in arid areas

Edited by
Lu Gong, Xiao-Dong Yang and Yanju Liu

Published in
Frontiers in Plant Science

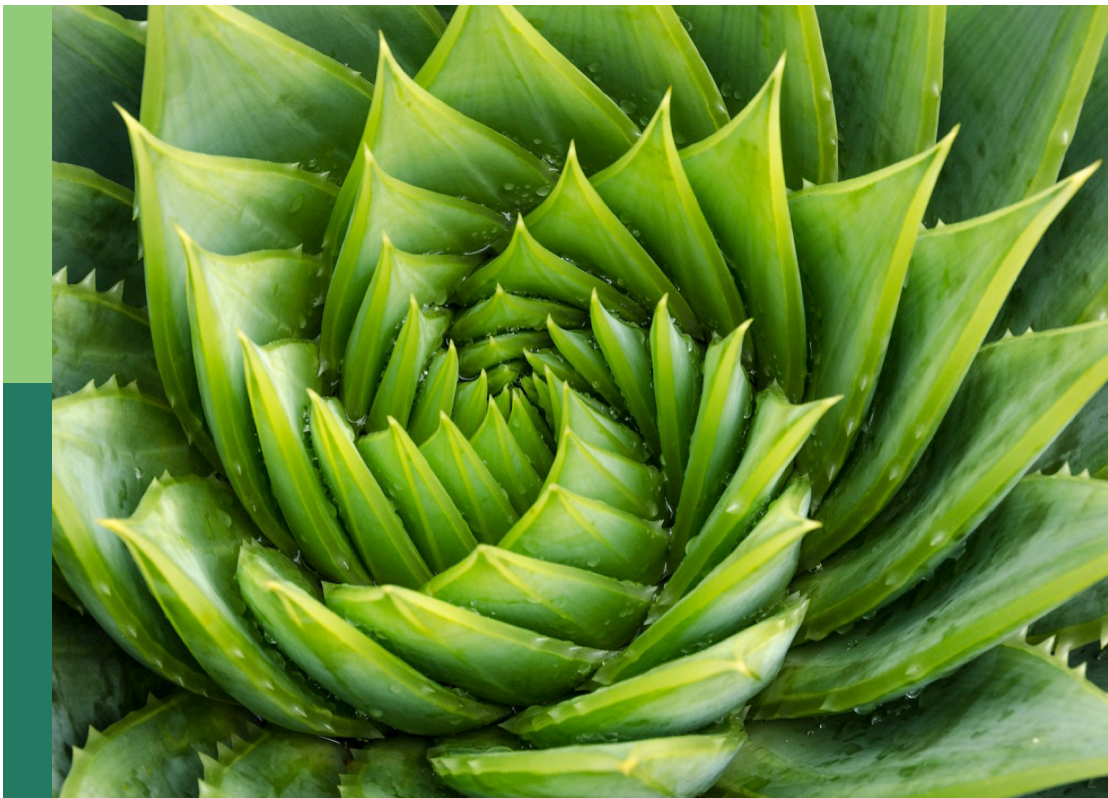

ISSN 1664-8714
ISBN 978-2-8325-7102-6
DOI 10.3389/978-2-8325-7102-6

Generative AI statement
Any alternative text (Alt text) provided alongside figures in the articles in this ebook has been generated by Frontiers with the support of artificial intelligence and reasonable efforts have been made to ensure accuracy, including review by the authors wherever possible. If you identify any issues, please contact us.

About Frontiers

Frontiers is more than just an open access publisher of scholarly articles: it is a pioneering approach to the world of academia, radically improving the way scholarly research is managed. The grand vision of Frontiers is a world where all people have an equal opportunity to seek, share and generate knowledge. Frontiers provides immediate and permanent online open access to all its publications, but this alone is not enough to realize our grand goals.

Frontiers journal series

The Frontiers journal series is a multi-tier and interdisciplinary set of open-access, online journals, promising a paradigm shift from the current review, selection and dissemination processes in academic publishing. All Frontiers journals are driven by researchers for researchers; therefore, they constitute a service to the scholarly community. At the same time, the *Frontiers journal series* operates on a revolutionary invention, the tiered publishing system, initially addressing specific communities of scholars, and gradually climbing up to broader public understanding, thus serving the interests of the lay society, too.

Dedication to quality

Each Frontiers article is a landmark of the highest quality, thanks to genuinely collaborative interactions between authors and review editors, who include some of the world's best academicians. Research must be certified by peers before entering a stream of knowledge that may eventually reach the public - and shape society; therefore, Frontiers only applies the most rigorous and unbiased reviews. Frontiers revolutionizes research publishing by freely delivering the most outstanding research, evaluated with no bias from both the academic and social point of view. By applying the most advanced information technologies, Frontiers is catapulting scholarly publishing into a new generation.

What are Frontiers Research Topics?

Frontiers Research Topics are very popular trademarks of the *Frontiers journals series*: they are collections of at least ten articles, all centered on a particular subject. With their unique mix of varied contributions from Original Research to Review Articles, Frontiers Research Topics unify the most influential researchers, the latest key findings and historical advances in a hot research area.

Find out more on how to host your own Frontiers Research Topic or contribute to one as an author by contacting the Frontiers editorial office: frontiersin.org/about/contact

Plant-soil-microbial interactions in arid areas

Topic editors
Lu Gong — Xinjiang University, China
Xiao-Dong Yang — Ningbo University, China
Yanju Liu — The University of Newcastle, Australia

Citation
Gong, L., Yang, X.-D., Liu, Y., eds. (2025). *Plant-soil-microbial interactions in arid areas*. Lausanne: Frontiers Media SA. doi: 10.3389/978-2-8325-7102-6

Table of contents

05 Editorial: Plant-soil-microbial interactions in arid areas
Huimin Wang, Lu Gong, Xue Wu, Yanju Liu and Xiaodong Yang

08 Root exudates facilitate the regulation of soil microbial community function in the genus *Haloxylon*
Deyan Wu, Xuemin He, Lamei Jiang, Wenjing Li, Hengfang Wang and Guanghui Lv

21 Soil bacterial community characteristics and influencing factors in different types of farmland shelterbelts in the Alaer reclamation area
Cuiping Tian, Xue Wu, Bota Bahethan, Xianyao Yang, Qianqian Yang and Xiantao Wang

33 Arbuscular mycorrhizal fungi alleviate Mn phytotoxicity by altering Mn subcellular distribution and chemical forms in *Lespedeza davidii*
Gao Pan, Jiayao Hu, Zhen Zi, Wenying Wang, Xinhang Li, Xiaoli Xu and Wensheng Liu

47 Enhancing sugarcane's drought resilience: the influence of Streptomycetales and Rhizobiales
Mianhe Chen, Yuanjun Xing, Chunyi Chen and Ziting Wang

59 Spatial heterogeneity of soil factors enhances intraspecific variation in plant functional traits in a desert ecosystem
Yong-chang Wang, Xue-ni Zhang, Ji-fen Yang, Jing-ye Tian, Dan-hong Song, Xiao-hui Li and Shuang-fu Zhou

71 Impacts of plant root traits and microbial functional attributes on soil respiration components in the desert-oasis ecotone
Jinlong Wang, Guanghui Lv, Jianjun Yang, Xuemin He, Hengfang Wang and Wenjing Li

87 Silicon enhanced phosphorus uptake in rice under dry cultivation through root organic acid secretion and energy distribution in low phosphorus conditions
Hao Jiang, Wanchun Li, Zixian Jiang, Yunzhe Li, Xinru Shen, Min Nuo, Hongcheng Zhang, Bei Xue, Guangxin Zhao, Ping Tian, Meiying Yang and Zhihai Wu

103 Exogenous carbon inputs alleviated salt-induced oxidative stress to cotton in salinized field by improving soil aggregate structure and microbial community
Weidi Li, Mingtao Zhong, Haijiang Wang, Xiaoyan Shi, Jianghui Song, Jingang Wang and Wenxu Zhang

121 Specific soil factors drive the differed stochastic assembly of rhizosphere and root endosphere fungal communities in pear trees across different habitats
Yunfeng Liu, Zhenzhou Wang, Xiang Sun, Xueli He and Yuxing Zhang

135 Soil and climate factors affect the nutrient resorption characteristics of desert shrub roots in Xinjiang, China
Yan Luo, Wenya Wei, Yaxuan Wang, Tianai Xue and Kaijuan Du

151 Impact of seasonal changes on root-associated microbial communities among phreatophytes of three basins in desert ecosystem
Yulin Zhang, Yi Du, Zhaobin Mu, Waqar Islam, Fanjiang Zeng, Norela C. T. Gonzalez and Zhihao Zhang

171 Effects of vegetation restoration on soil fungi community structure and assembly process in a semiarid alpine mining region
Yuanyuan Xue, Wei Liu, Qi Feng, Meng Zhu, Jutao Zhang, Lingge Wang, Zexia Chen and Xuejiao Li

frontiers | Frontiers in Plant Science

TYPE Editorial
PUBLISHED 21 October 2025
DOI 10.3389/fpls.2025.1704520

OPEN ACCESS

EDITED AND REVIEWED BY
Yongjiang Zhang,
University of Maine, United States

*CORRESPONDENCE
Xiaodong Yang
xjyangxd@sina.com

RECEIVED 13 September 2025
ACCEPTED 10 October 2025
PUBLISHED 21 October 2025

CITATION
Wang H, Gong L, Wu X, Liu Y and Yang X (2025) Editorial: Plant-soil-microbial interactions in arid areas. *Front. Plant Sci.* 16:1704520. doi: 10.3389/fpls.2025.1704520

Editorial: Plant-soil-microbial interactions in arid areas

Huimin Wang[1,2], Lu Gong[2], Xue Wu[2], Yanju Liu[3] and Xiaodong Yang[1,2]*

[1]Department of Geography & Spatial Information, Ningbo University, Ningbo, China, [2]Institute of Ecology and Environment, Xinjiang University, Urumqi, China, [3]Global Centre for Environmental Remediation (GCER), The University of Newcastle (UON), Newcastle, NSW, Australia

KEYWORDS

drought stress, environmental filtering, microbial community assembly, plant stress resistance, stochastic processes

Editorial on the Research Topic
Plant-soil-microbial interactions in arid areas

Arid and semi-arid regions account for approximately 40-42% of the Earth's terrestrial surface and represent a critical component of global ecosystems (Lewin et al., 2024). Under long-term water and nutrient limitations, these regions have shaped a large number of species adapted to drought, salinity, and nutrient-poor conditions, which maintain ecosystem stability through deep root systems, leaf morphological traits, and osmotic regulation mechanisms (Schenk and Jackson, 2002). Meanwhile, soils in arid regions serve as important reservoirs of carbon and nutrients, and their physicochemical properties and microbial activities exert profound effects on plant survival and ecosystem processes (Schimel et al., 2007). With the increasing frequency of drought events and the intensification of environmental stresses (IPCC, 2021), elucidating the mechanisms of plant-soil-microbe interactions has become a central scientific issue in arid ecology. In this Research Topic, we have collected 12 articles focusing on plant-soil-microbial interactions in arid regions. These studies include four major aspects: the physiological and chemical mechanisms underlying plant-soil-microbial interactions, microbial community assembly, the regulation of nutrient and carbon cycling mediated by plant-soil-microbial interactions, and the application of these interactions in agriculture and ecosystem restoration. By integrating these findings, this Research Topic delineates a clear scientific trajectory: from elucidating the fundamental mechanisms of plant-soil-microbe interactions, to revealing the patterns of microbial community assembly, and finally to their applications in agriculture and ecological restoration. These studies not only advance our understanding of ecosystem functioning in arid regions but also provide a scientific foundation and practical guidance for the sustainable use and management of these vulnerable ecosystems in the future.

In addition to water scarcity, plants in arid regions are also subjected to multiple other limiting stresses, such as salinity and phosphorus deficiency (Tian et al.; Wang et al.). Under these adverse conditions, soil microorganisms play a critical role in supporting plant survival and growth through various mechanisms. For example, under drought stress, Streptomycetales alleviate nutrient limitations caused by reduced enzymatic activity in plants through the 1-aminocyclopropane-1-carboxylate (ACC) deaminase and the production of secondary metabolites such as indole-3-acetic acid (IAA), thereby

enhancing nutrient absorption by sugarcane roots. Rhizobiales counteract drought stress by supporting nitrogen acquisition in sugarcane and producing siderophores to facilitate iron uptake. The synergistic effect of these microorganisms collectively enhances the drought tolerance of sugarcane (Chen et al.). Furthermore, Pan et al. found that inoculation with arbuscular mycorrhizal fungi (AMF) could alleviate manganese stress on *Lespedeza davidii*. Specifically, AMF enhance plant stress resistance by increasing the content of osmotic adjustment substances (e.g., soluble sugars, soluble proteins, free proline), enhancing antioxidant enzyme activities, and reducing membrane lipid peroxidation products, thereby strengthening plant stress tolerance. These studies provide important theoretical support for a deeper understanding of plant-soil-microbe interactions in arid ecosystems.

Microbial community assembly represents a central regulatory element in plant-soil-microbe interactions, providing a foundation for understanding these complex relationships. To clarify microbial community assembly, researchers have conducted extensive experimental studies across different contexts, including artificial vegetation restoration sequences, drought stress gradients, and comparisons between rhizosphere and bulk soils. The results show that stochastic processes (such as dispersal limitation and ecological drift) play an important role in microbial community assembly. By analyzing the microbial communities in the root endosphere, rhizosphere, and bulk soil across three seasons, Zhang et al. found that microbial community assembly was dominated by stochastic processes, with dispersal limitation being the core stochastic process; only bacteria and fungi in bulk soil were regulated by deterministic processes (homogeneous selection) in some seasons. Similarly, in studies on *Pyrus betulifolia*, Liu et al. (2025) further confirmed that both the rhizosphere and endosphere fungal communities were dominated by stochastic processes, and the proportion of these processes in the endosphere was significantly higher than in the rhizosphere. This difference can be attributed to the more enclosed environment of the endosphere and the smaller size of its microbial species pool, which amplifies the influence of ecological drift on community assembly. However, in addition to stochastic processes, environmental filtering (such as the selective effects of factors like soil pH, salinity, nutrients, and moisture) also plays a crucial role in the community assembly. For example,Xue et al. found that dispersal limitation and homogeneous selection dominated the assembly process, with their relative contributions changing dynamically with the duration of artificial vegetation restoration. Among these factors, soil texture and phosphorus were identified as key drivers. These findings provide strong evidence for the crucial role of stochastic processes in microbial community assembly in arid regions.

Plant-soil-microbial interactions play a significant role in nutrient and carbon cycling in terrestrial ecosystems. Root exudates, the functional regulation of microbial communities, and their interactions with soil collectively determine ecosystem productivity, nutrient cycling, and energy flow. Wu et al. , using *Haloxylon ammodendron* and *Haloxylon persicum* as study species, demonstrated that these plants actively shape the structure and function of their rhizosphere microbial communities through root exudates, including triterpenes and fatty acids, which act as key signaling molecules. The enriched beneficial microbes, such as Actinomycetales and Proteobacteria, participate in and drive soil carbon and nutrient cycling. The study by Wang et al. elucidated the regulatory role of plant-soil-microbial interactions in carbon cycling. In the desert-oasis ecotone, microbial community structures differ significantly between rhizosphere and bulk soils. In rhizosphere soil, Proteobacteria and Actinobacteria are relatively abundant; these microorganisms promote heterotrophic respiration by accelerating the degradation of root exudates and the turnover of organic carbon. In contrast, bulk soils are mainly dominated by Actinobacteria, which maintain basal respiration by decomposing recalcitrant soil organic carbon. Luo et al. found that desert shrubs adapt to nutrient-poor environments by differentially regulating root nutrient resorption efficiencies for nitrogen (N), phosphorus (P), and potassium (K). Overall, these plants exhibit a "prioritized K resorption" pattern. Moreover, C_4 plants show higher K resorption efficiency, whereas C_3 plants display higher N and P resorption efficiencies. Additionally, plants dynamically adjust their nutrient resorption efficiencies in response to changes in soil properties and climatic factors to better adapt to arid and nutrient-poor environments.

Furthermore, elucidating the mechanisms underlying plant-soil-microbe interactions and applying this knowledge to improve soil quality and optimize nutrient management are central goals for achieving sustainable agriculture and effective ecosystem restoration. Li et al. (2025) found that exogenous carbon application can regulate the structure of soil microbial communities and further enhance plant antioxidant systems, thereby alleviating the effects of salt stress on cotton. Under low-phosphorus conditions, silicon addition can promote the secretion of malic and succinic acids from plant roots, enhance acid phosphatase activity, and enrich phosphorus-solubilizing microbes, including *Bradyrhizobium*, *Paenibacillus*, *Bacillus*, and *Fusarium*, thereby forming an effective "organic acid-microbe" phosphorus system and improving plant phosphorus uptake (Jiang et al.). These studies provide important theoretical and practical support for sustainable agricultural development and ecological restoration.

The aforementioned studies have systematically elucidated the important role of plant-soil-microbial interactions in arid-land ecosystems, providing a solid theoretical foundation for improving plant stress resistance and resource use efficiency through microbial strategies. Despite significant progress made in terms of mechanisms and application potential, future research should further explore the interactive effects of multiple stress factors (such as drought, salinization, and heavy metals) in arid regions, as well as the long-term dynamic patterns of plant-soil-microbial interactions. This will contribute to the development of innovative solutions for the sustainable development of arid regions under global climate change.

Author contributions

HW: Writing – original draft. LG: Writing – review & editing. XW: Writing – review & editing. YL: Writing – review & editing. XY: Writing – review & editing.

Funding

The author(s) declare financial support was received for the research and/or publication of this article. This work was supported by the National Natural Science Foundation of China (Grant Nos. 42261065).

Acknowledgments

We thank all the authors and reviewers that have contributed to this Research Topic.

Conflict of interest

The authors declare that the research was conducted in the absence of any commercial or financial relationships that could be construed as a potential conflict of interest.

Generative AI statement

The author(s) declare that no Generative AI was used in the creation of this manuscript.

Any alternative text (alt text) provided alongside figures in this article has been generated by Frontiers with the support of artificial intelligence and reasonable efforts have been made to ensure accuracy, including review by the authors wherever possible. If you identify any issues, please contact us.

Publisher's note

References

IPCC (2021). *Climate Change 2021: The Physical Science Basis. Contribution of Working Group I to the Sixth Assessment Report of the Intergovernmental Panel on Climate Change* (Cambridge, United Kingdom and New York, NY, USA: Cambridge University Press). doi: 10.1017/9781009157896

Lewin, A., Murali, G., Rachmilevitch, S., and Roll, U. (2024). Global evaluation of current and future threats to drylands and their vertebrate biodiversity. *Nat. Ecol. Evol.* 8, 1448–1458. doi: 10.1038/s41559-024-02450-4

Li, W., Zhong, M., Wang, H., Shi, X., Song, J., Wang, J., et al. (2025). Exogenous carbon inputs alleviated salt-induced oxidative stress to cotton in salinized field by improving soil aggregate structure and microbial community. *Front. Plant Sci.* 16. doi: 10.3389/fpls.2025.1522534

Liu, Y., Wang, Z., Sun, X., He, X., and Zhang, Y. (2025). Specific soil factors drive the differed stochastic assembly of rhizosphere and root endosphere fungal communities in pear trees across different habitats. *Front. Plant Sci.* 16. doi: 10.3389/fpls.2025.1549173

Schenk, H. J., and Jackson, R. B. (2002). Rooting depths, lateral root spreads and below-ground/above-ground allometries of plants in water-limited ecosystems. *J. Ecol.* 90, 480–494. doi: 10.1046/j.1365-2745.2002.00682.x

Schimel, J., Balser, T. C., and Wallenstein, M. (2007). Microbial stress-response physiology and its implications for ecosystem function. *Ecology* 88, 1386–1394. doi: 10.1890/06-0219

frontiers | Frontiers in Plant Science

TYPE Original Research
PUBLISHED 19 September 2024
DOI 10.3389/fpls.2024.1461893

OPEN ACCESS

EDITED BY
Yanju Liu,
The University of Newcastle, Australia

REVIEWED BY
Geeta Chhetri,
Korea Institute of Industrial Technology, Republic of Korea
Wen Zhang,
Ecology Institute of Shandong Academy of Sciences, China

*CORRESPONDENCE
Guanghui Lv
guanghui_xju@sina.com

RECEIVED 09 July 2024
ACCEPTED 02 September 2024
PUBLISHED 19 September 2024

CITATION
Wu D, He X, Jiang L, Li W, Wang H and Lv G (2024) Root exudates facilitate the regulation of soil microbial community function in the genus *Haloxylon*. *Front. Plant Sci.* 15:1461893. doi: 10.3389/fpls.2024.1461893

Root exudates facilitate the regulation of soil microbial community function in the genus *Haloxylon*

Deyan Wu[1,2], Xuemin He[1,2], Lamei Jiang[3,4], Wenjing Li[1,2], Hengfang Wang[1,2] and Guanghui Lv[1,2]*

[1]College of Ecology and Environment, Xinjiang University, Urumqi, Xinjiang, China, [2]Key Laboratory of Oasis Ecology of Ministry of Education, Xinjiang University, Urumqi, Xinjiang, China, [3]College of Life Science, Xinjiang Agricultural University, Urumqi, Xinjiang, China, [4]Key Laboratory for Ecological Adaptation and Evolution of Extreme Environment Biology, Xinjiang Agricultural University, Urumqi, Xinjiang, China

Introduction: Root exudates act as the "language" of plant-soil communication, facilitating crucial interactions, information exchange, and energy transfer between plants and soil. The interactions facilitated by root exudates between plants and microorganisms in the rhizosphere are crucial for nutrient uptake and stress resilience in plants. However, the mechanism underlying the interaction between root exudates and rhizosphere microorganisms in desert plants under drought conditions remains unclear, especially among closely related species.

Methods: To reveal the ecological strategies employed by the genus Haloxylon in different habitats. Using DNA extraction and sequencing and UPLC-Q-Tof/MS methods, we studied root exudates and soil microorganisms from two closely related species, *Haloxylon ammodendron (HA)* and *Haloxylon persicum (HP)*, to assess differences in their root exudates, soil microbial composition, and interactions.

Results: Significant differences were found in soil properties and root traits between the two species, among which soil water content (SWC) and soil organic carbon (SOC) in rhizosphere and bulk soils ($P < 0.05$). While the metabolite classification of root exudates was similar, their components varied, with terpenoids being the main differential metabolites. Soil microbial structure and diversity also exhibited significant differences, with distinct key species in the network and differential functional processes mainly related to nitrogen and carbon cycles. Strong correlations were observed between root exudate-mediated root traits, soil microorganisms, and soil properties, although the complex interactions differed between the two closely relative species. The primary metabolites found in the network of *HA* include sugars and fatty acids, while *HP* relies on secondary metabolites, steroids and terpenoids.

Discussion: These findings suggest that root exudates are key in shaping rhizosphere microbial communities, increasing microbial functionality, fostering symbiotic relationships with hosts, and bolstering the resilience of plants to environmental stress.

KEYWORDS

root exudates, genus *Haloxylon*, soil microorganisms, root traits, rhizosphere

1 Introduction

Rhizosphere refers to the narrow region of soil that surrounds and is influenced by plant roots, where various interactions between roots and microorganisms that inhabit their root vicinity, and high concentrations of plant-derived organic exudates and mucilage (Korenblum et al., 2020; Vieira et al., 2020). Root exudates, serving as the "language" of rhizosphere communication, are pivotal in facilitating interactions, information exchange, and energy transfer between plants and soil (Venturi and Keel, 2016; Zhao et al., 2021). Root exudates comprise various compounds, such as amino acids, organic acids and other secondary metabolites, which are vital for plant functional metabolic pathways, with their composition affecting the physicochemical properties and nutrient availability of rhizosphere soil (Bais et al., 2006; Zhalnina et al., 2018).

Soil microorganisms are crucial components of the soil ecosystem, playing a vital role in maintaining ecological balance and nutrient cycling (Cui et al., 2018; Sahu et al., 2019). Root exudates as a medium for the co-evolution of plants and microorganisms (Morgan et al., 2005), they extend the functional traits of plants by participating in a series of processes, including nutrient acquisition, growth promotion, and enhancing the ability to resist environmental stress (Bai et al., 2022). Root exudates stimulate microbial colonization at the root-rhizosphere soil interface, affecting the relative abundance and activity of soil microorganisms (Yin et al., 2013; Ribbons et al., 2016). This process enhances resource acquisition and adaptation to adverse environments (Haichar et al., 2014), such as drought and salinization, representing the evolutionary response of plants to external environment changes (Yin et al., 2013). The preference of soil microorganisms for root exudates drives the assembly of rhizosphere microbial communities (Zhalnina et al., 2018), allowing plants to selectively promote beneficial microorganisms (Bulgarelli et al., 2015), while deterring pathogenic or detrimental ones (Venturi and Keel, 2016). A previous study found that *Arabidopsis* and *Ageratina adenophora* could recruit beneficial bacteria by releasing specific compounds from root exudates to promote growth (Harbort et al., 2020; Sun et al., 2021). Root exudates facilitate plant-microbial community interactions that affect plant growth and adaptation, fostering mutualistic relationships or antagonizing soil microorganisms to affect plant growth (Eppinga et al., 2006; Kardol et al., 2007).

Root exudates play an important role in interspecies chemical communication, acting as chemical signals between plant roots and other soil organisms (including the roots of neighboring plants), and inducing changes in root behavior (Bais et al., 2006; Semchenko et al., 2014; Xia et al., 2019). Plants can modify soil pH through changes in root exudate composition, which affects pathogen and beneficial microbial colonization (Lareen et al., 2016). Manipulating plant traits to enhance plant-microbial interactions that increase plant resilience to adversity and optimize soil nutrient cycling (De Vries et al., 2020). These interactions are crucial for maintaining and stabilizing ecosystem functions. For example, plant root traits and the composition of rhizosphere microbial communities promote plant yields (Lareen et al., 2016). These traits and exudates adjust in response to resource competition among species (Meier et al., 2020; Wen et al., 2019) and they are intricately linked to resource acquisition and utilization functions, such as the contents of roots N and P in roots (Cui et al., 2018; Sun et al., 2021). Hence, further observation is needed to assess the relationship between these rhizosphere microbes and plant community dynamics mediated by plant traits (Chai et al., 2019). Moreover, rhizosphere microbes play a crucial role in fostering host phenotypic plasticity, aiding host plant adaptation to environmental conditions (De La Fuente Cantó et al., 2020). However, studies on the role and regulation of root exudates in the rhizosphere environment of desert soils remain relatively few, which are affected by various factors and conditions, especially congenerics plants. Therefore, the mechanism underlying the interaction between exudates and their rhizosphere microorganisms in closely related species under drought conditions remains unclear.

Root exudation mediated plant-soil microbial interactions are crucial in facilitating active plant adaptation to microenvironment and stress resistance (De Vries et al., 2020). These exudates modify the soil properties to help plants withstand the stress of adversity (Baetz and Martinoia, 2014; Zhu et al., 2009). In the Gurbantunggut Desert, two closely related species, *Haloxylon ammodendron* (C. A. Mey.) Bunge, primarily inhabiting on the plain saline-alkali land, and *Haloxylon persicum* Bge. ex Boiss. et Buhse, grows on the sand soil of the dunes with a distinct species distribution mode (Song et al., 2006). Studies have explored environmental factors as potential causes for this pattern but have not reached a

consensus. This study focuses on root exudates and investigates root characteristics, exudates, soil environmental factors, rhizosphere microorganisms, and their interactions. It analyzed root exudates composition, soil microbial community structure variations, and the interplay among environmental factors, plant traits, and rhizosphere microorganisms. Therefore, this study aims to elucidate the ecological adaptation strategies employed by the genus *Haloxylon* in different habitats. The findings may help elucidate the underlying mechanism and distribution pattern of desert plants adapting to harsh environments. It also seeks to provide valuable insights that can greatly contribute to desertification control and ecological restoration efforts.

2 Materials and methods

2.1 Study site

The research site was situated in the Ebinur Lake Wetland National Nature Reserve, Xinjiang (83°32′–83°35′E, 44°35′–44°42′N). In this region, the average annual precipitation was approximately 100 mm, with annual evaporation rates >1600 mm, an average annual temperature range of 6–8°C and approximately 2800 h of sunshine annually (Wang et al., 2022). The long-term scarcity of precipitation resulted in severe drought stress in the local ecosystem (Li et al., 2022a). The soil is predominantly gray desert soil, aeolian sandy, meadow soil, and swamp soils (Wang et al., 2022). The local zonal vegetation consisted of sparse, extreme xeromorphic shrubbery, and dominant shrubs in this ecosystem included *H. ammodendron* (*HA*), *H. persicum* (*HP*), *Tamarix ramosissima, Nitraria schoberi, Reaumuria soongorica*, and *Halimodendron halodendron.*

2.2 Sample collection

Based on previous investigation and research in the study area, *HA* is primarily distributed on the saline-alkali land near the river bank of the Akikesu River, and *HP* grows on the semi-fixed dune far away from the river bank. In July 22 to 25, 2021, we chose four sample sites of *HA* approximately 0.5 km from the riverbank towards the Akikesu River, and four sample sites of *HP* approximately 3.5 km from the riverbank, matching in height and size, to collect plant root exudates, and rhizosphere and bulk soil samples (Supplementary Figure S1).

Rhizosphere and bulk soil samples were collected from four *HA* and *HP*, respectively. The plants selected from each site of *HA* or *HP* were collected from depth of 0 ~ 40 cm,1 ~ 2 m away from the trunk. All roots at each site are placed in sterile bags to prepare rhizosphere soil samples. In addition, four bare soil samples were collected on unvegetated ground about 10 m away from the plants, at a depth of about 0-40 cm, and these samples were uniformly mixed to form bulk soil samples.

Each root of the plant, measuring approximately 20 cm in length, was selected from the four cardinal directions, ensuring the roots remained undamaged. The soil clinging to the root surface was carefully rinsed off with distilled water. Following a modified version of the *in situ* sample collection method (Phillips et al., 2018), the primary steps were as follows: the cleaned root was placed in a sterile bag filled with sterile glass sand (1 mm particle size) as the culture medium. Simultaneously, a carbon-free nutrient solution (Jakoby et al., 2020) was injected to provide essential nutrients for healthy root development. The opening of the bag was sealed to prevent impurities, and then the aseptic bag, which was wrapped in tin foil, was covered with soil. After 24 h of root recovery, the growth medium was washed with the nutrient solution to collect the exudates, combining all samples from each tree.

After extraction, 16 roots were randomly selected from the roots of both *HA* and *HP*. Their surface moisture was adsorbed using filter paper. The roots were then scanned. Following that, they were analyzed using WinRHIZO software. Subsequently, the scanned roots underwent drying at 65°C for 48 h and then weighed. Follow the methods used in previous studies (Li et al., 2022a), Rhizosphere soil samples were collected by adding a Phosphate Buffered Saline (PBS) solution into the sterile, aseptic bag containing roots. The solution underwent a rinsing process, during which turbidity was collected and subsequently centrifuged. After removing the supernatant, the precipitated material was used as the rhizosphere soil and stored at −20°C until measurement. Supplementary Table S1 depicts the soil properties of the samples, which were evaluated using soil measurement methods.

2.3 DNA extraction, high-throughput sequencing and processing

Total soil genomic DNA was extracted from soil using the MoBio Power Soil DNA Isolation Kit (MoBio Laboratories, Carlsbad, CA, USA).The bacterial PCR amplification employed primers 515F (5' - GTGCCAGCMGCCGCGG - 3') and 907R (5' - CCGTCAATTCM TTTRAGTTT -3') (Christner et al., 2001), while the fungal PCR amplification used primers ITS_1F (5' - CTTGGTCATTTA GAGGAAGTAA - 3') and ITS2R (5' - GCTGCGTTCTTCATC GATGC - 3') (Gardes and Bruns, 1993). PCR amplification was conducted in a 20 μL reaction system using TransGen AP221-02. The PCR products were detected on 2% agarose gel electrophoresis and QuantiFluor was used for quantitative detection ^{TM}-ST blue fluorescence quantification system. A cDNA library was constructed on the Illumina MiSeq platform (Illumina San Diego, USA) and high-throughput sequencing (MiSeq PE300) of the PCR amplified fragments was performed.

Utilizing the UPARSE platform version 7.1, gene sequence clustering and elimination of chimeras were executed to achieve 97% ASV convergence towards taxa. The annotation and Bayesian algorithms, and RDP classifier were used for the species classification

analysis. After flattening, 2,201 bacterial ASVs (23,444 sequence reads) and 634 fungal ASVs (2,783 sequence reads) were obtained.

2.4 Determination of root exudates via UPLC-Q-Tof/MS

The *HA* and *HP* exudates were concentrated to approximately 5 mL using a Rotary evaporator at 45°C and 120 r/min. They were then transferred to a low-temperature freeze dryer until they became solid powder. Subsequently, 1.5 mL of 70% methanol aqueous solution was added for re-dissolution, followed by a 30-min ultrasound treatment. After centrifugation at 10000 rpm/min for 5 min, 200 µL of the solution was taken and placed into a 2 mL volumetric bottle, then passed through a 0.22-µm filter membrane for use. The samples were separated using a Waters Acuity H-Class ultra-high performance liquid chromatograph (FTN automatic sampler, four-element liquid chromatography pump) and ACQUITY UPLC® BEH C18 column (1.7 µm, 2.1 mm×100 mm) at a temperature of 45°C. The flow rate was maintained at 0.4 mL/min with an injection volume of 2.0 µL.

The MS^E mode was employed for data collection, capturing mass spectrum data in positive ion and sensitivity modes. Data storage utilized the centroid mode, and a real-time mass number correction was achieved using a leucine enkephalin (LE) standard solution, with a 5 µL/min flow rate. Mass Lynx v4.1 software was employed to facilitate MS data collection, which was then imported into UNIFI for peak identification and chemical composition retrieved through the Natural Products database. The obtained products were compared with the KEGG database, followed by metabolite classification and enrichment analyses of the root exudates.

2.5 Statistical analysis

Root traits and soil properties were expressed as mean ± standard error (SD). Before statistical analysis of the data, the "shapiro.test" and "Bartlet.test" functions were used to test the normality and variance homogeneity of the data, respectively. If the data do not conform to the normal distribution, or the variance between the groups was not uniform, the "kruskal.test" function was used for non-parametric tests. Metabolites from root exudates were classified using the KEGG database, with classification statistics conducted using the *reshape2* package. Pathway enrichment analysis was conducted using Metabo Analyst 6.0. Orthogonal partial least squares discriminant analysis (OPLS-DA) was used to differentiate intergroup variations in the root exudates of both species, and the variable importance in projection (VIP) of OPLS-DA was calculated. Root exudates that satisfy both criteria of $|\log2FC| > 1.5$ and a t-test with a P-value < 0.05 were selected for statistical analysis as metabolites exhibiting significant differences.

The bacterial and fungal network at the family level was constructed based on the Pearman correlation matrix. ASV units with abundance < 20 were excluded, and only correlations satisfying the conditions ($r > 0.8$ and $P < 0.05$) were considered, and the degree of a node in the network determines its criticality. The network was visualized, and its topological properties were obtained using Gephi (v 0.9.2). Differential bacteria and fungi communities' analysis were conducted using *ggpubr* package.

The *devtools* and *linkET* packages were utilized for correlation and Mantel analyses involving root traits, environmental factors, root exudates, rhizosphere soil bacteria, and fungi. Node and edge data were obtained using the *igraph* package. Cytoscape (v 3.9.1) facilitated the prediction of root exudates and microbial functional pathways, along with network visualization of soil properties and root traits ($r > 0.8$ and $P < 0.05$).

All statistical analyses were conducted using R 4.1.3 (http://www.r-project.org/), with the *ggplot2* package used for mapping in statistical analyses (http://www.r-project.org/).

3 Results

3.1 Difference analysis of root traits and soil properties of genus *Haloxylon*

Significant differences were observed in soil pH, soil water content (SWC), soil salt content (SA), soil organic carbon (SOC), soil total phosphorus (TP), soil available phosphorus (AP), and soil total nitrogen (TN) between *HA* and *HP* treatments ($P < 0.05$). However, no significant differences were observed in soil nitrate nitrogen (NN) ($P > 0.05$). SWC and SOC exhibited significant differences between the rhizosphere and bulk soil of the two species, whereas TN and soil ammonium nitrogen (AN) showed significant differences in the soil of the two species ($P < 0.05$) (Table 1).

Significant differences were observed in root characteristics between *HA* and *HP* treatments (Figure 1). The root surface area (RS), mean root diameter (RD), root volume (RV), and nitrogen (N) content of *HA* were significantly higher than those of *HP* ($P < 0.01$). In contrast, carbon (C) and phosphorus (P) contents, specific root length (SRL), specific surface area (SRA), and root tissue density (RLD) of *HP* were significantly higher than those of *HA* ($P < 0.05$).

3.2 Composition and difference analysis of root exudates of genus *Haloxylon*

By chemical composition analysis, 263 and 261 positive and negative ion compounds were identified in the root secretions of *HA* and *HP* (Figure 2A), and the common compounds accounted for 68.8% and 77.4%, respectively. These compounds were compared using the KEGG database, and 85 positive and 83 negative ion metabolites were identified. The OPLS-DA analysis of metabolites accounted for 65.45% and 73.13% of the variance, respectively (Figure 2B). The predictive power of the positive and negative models was high at 0.982 and 0.98($Q^2Y>0.9$, $R^2Y>Q^2Y$), respectively. This indicated a significant difference in metabolites between the root exudates of *HA* and *HP*.

According to the Phytochemical compounds in the KEGG compounds, the metabolites identified in the root exudates of the

10.3389/fpls.2024.1461893

TABLE 1 Soil property comparison of soil from genus *Haloxylon*.

Soil properties	Unit	HAR	HAB	HPR	HPB
pH	–	8.24 ± 0.20Aa	8.01 ± 0.30Aa	7.29 ± 0.14Ab	7.24 ± 0.18Ab
SWC	%	13.53 ± 1.56Aa	5.31 ± 0.17Ba	1.03 ± 0.11Ab	0.19 ± 0.00Bb
SA	$g.kg^{-1}$	7.59 ± 2.17Aa	4.80 ± 0.90Aa	1.12 ± 0.07Ab	1.00 ± 0.13Ab
SOC	$g.kg^{-1}$	10.84 ± 4.59Aa	4.67 ± 1.37Ba	1.12 ± 0.16Bb	1.38 ± 0.08Ab
TN	$g.kg^{-1}$	1.89 ± 0.72Aa	1.56 ± 0.68Aa	0.76 ± 0.10Ab	0.55 ± 0.13Bb
AN	$mg.kg^{-1}$	3.77 ± 1.73Aa	1.86 ± 0.61Aa	1.28 ± 0.17Aa	0.67 ± 0.17Bb
NN	$mg.kg^{-1}$	11.43 ± 5.72Aa	6.27 ± 2.75Aa	2.70 ± 0.25Aa	3.05 ± 0.33Aa
TP	$g.kg^{-1}$	1.32 ± 0.22Aa	1.37 ± 0.34Aa	0.65 ± 0.04Ab	0.69 ± 0.02Ab
AP	$mg.kg^{-1}$	43.61 ± 19.17Aa	33.98 ± 14.58Aa	9.63 ± 0.77Ab	8.09 ± 1.80Ab

Different capital letters indicate significant differences between the rhizosphere and bulk soil, while the same capital letters denote insignificant differences. Different lowercase letters indicate significant differences between the rhizosphere soils of the genus Haloxylon, or between their bulk soil, whereas the same lowercase letters denote no significant differences between them. HAR and HPR represent the rhizosphere soil of *HA* and *HP*, HAB and HPB represent the bulk soil of *HA* and *HP*. SOC, Soil organic carbon; SA, soil salt content; TN, soil total nitrogen; TP, soil total phosphorus; AN, Soil ammonium nitrogen; NN, soil nitrate nitrogen; AP, Soil available phosphorus.

two species were categorized mainly into alkaloids, fatty acid-related compounds, flavonoids, phenylpropanoids, terpenoids, and shikimate/acetate malonate pathway-derived compounds. Among these, triterpenoids were the most abundant, followed by steroids and fatty acids. The classification of KEGG metabolite compounds, metabolite pathways, and enrichment were comparable to the root exudates of both species (Figures 2C, D; Supplementary Figure S2).

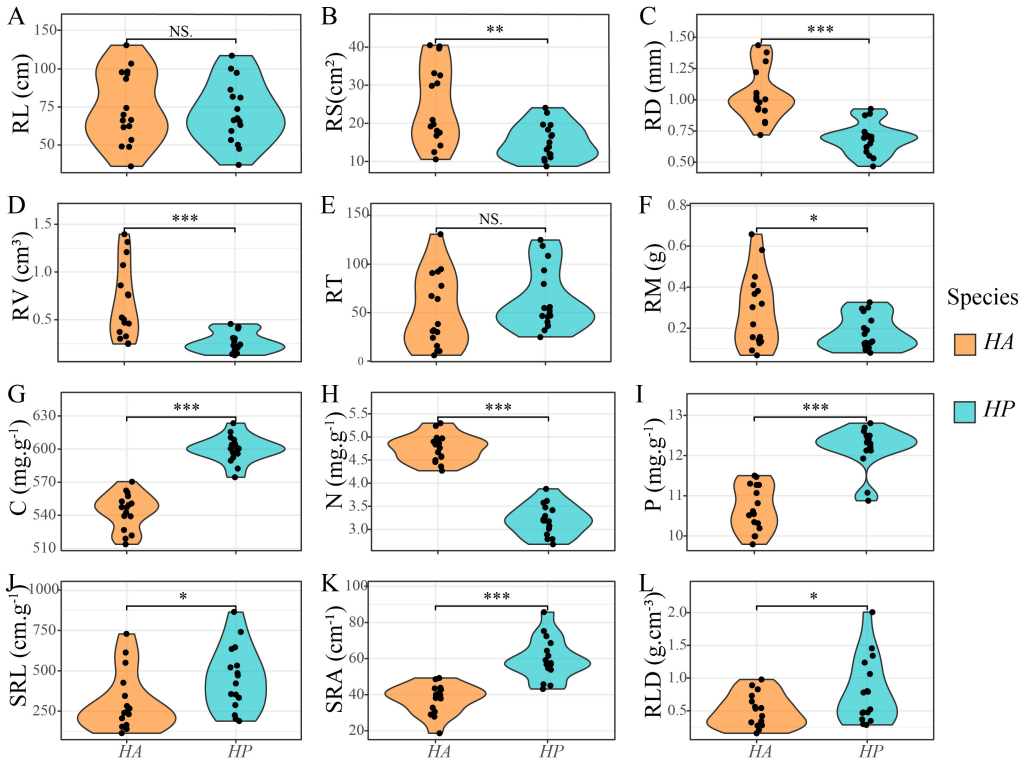

FIGURE 1
Differences in root traits between *Haloxylon* species. **HA** represent **H. ammodendron**, and *HP* represent *H. persicum*. **(A)** RL, root length; **(B)** RS, root surface area; **(C)** RD, average root diameter; **(D)** RV, root volume; **(E)** RT, number of root tips; **(F)** RM, dry weight of root biomass; **(G)** C, root carbon content; **(H)** N, root nitrogen content; **(I)** P, root phosphorus content; **(J)** SRL, specific root length; **(K)** SRA, specific surface area; **(L)** RLD, root tissue density. *, **, *** indicated significant levels of $P < 0.05$, $P < 0.01$, and $P < 0.001$ respectively, while NS indicated no significant level.

10.3389/fpls.2024.1461893

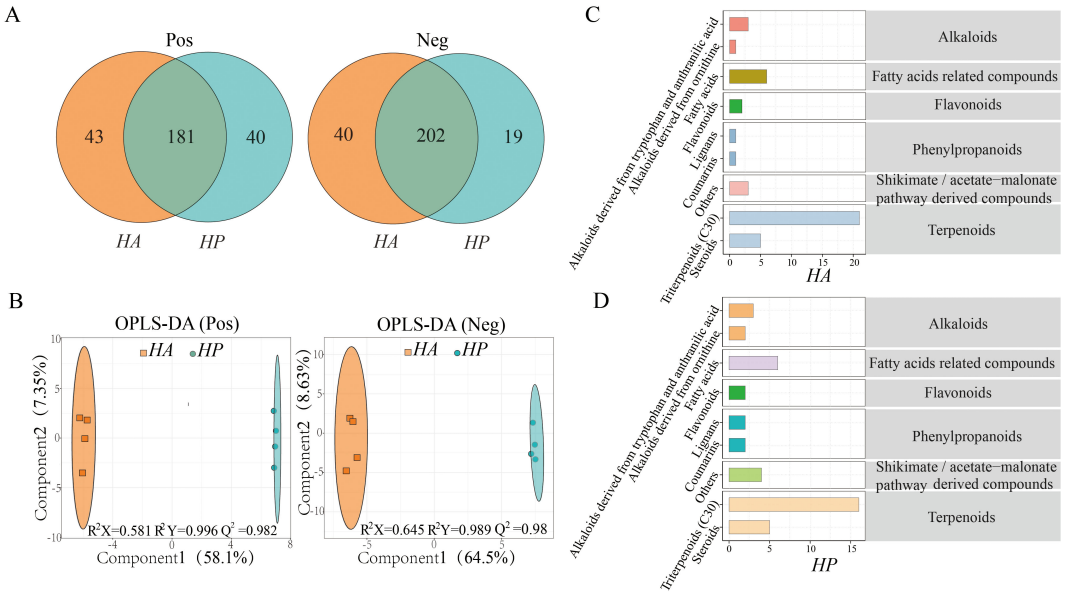

FIGURE 2
Comparison of root exudate composition in the genus *Haloxylom*. **(A)**, the root exudate composition. **(B)**, the OPLS-DA of the root exudates. **(C, D)** illustrate the root exudate compositions of the two species in the KEGG database.

Based on the OPLS-DA analysis (|log2FC|>1.5, P<0.05), 622 metabolites were identified between *HA* and *HP*, comprising 30 positive and 32 negative ions. Among these, 23 metabolites in *HP* exhibited higher content (7 positive and 16 negative ions), while 39 metabolites (23 cations and 16 anions) showed higher content in *HA* (Figures 3A, B). The significantly different metabolites in the root exudates of the two species were further analyzed using clustering heat maps and VIP bar graphs (FC > 2 or FC < 0.5,

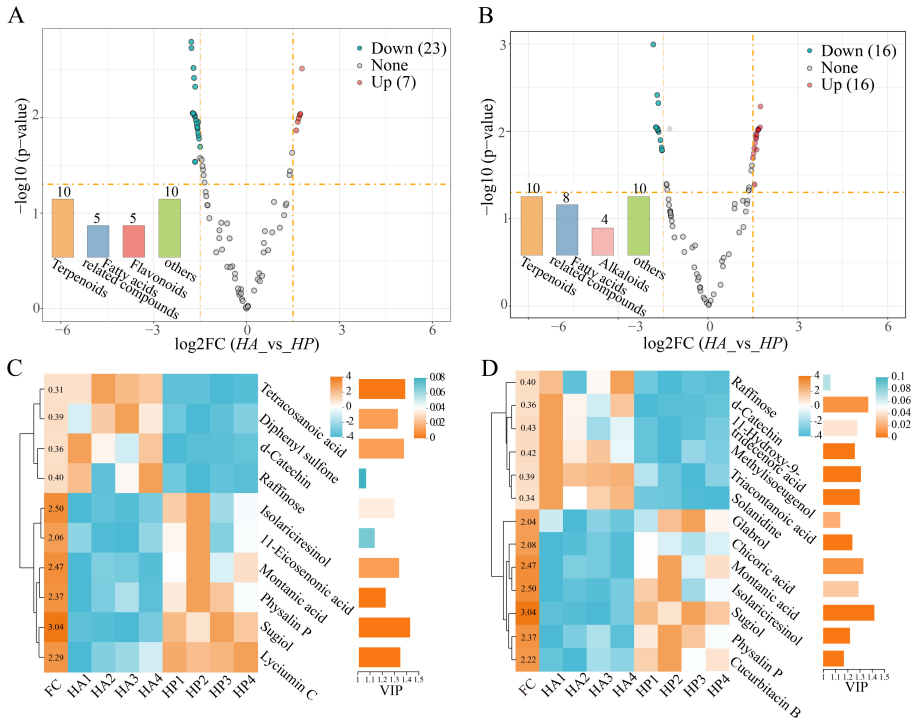

FIGURE 3
Difference in root exudates within the genus *Haloxylon*. **(A, B)** represent the volcano plot, with exudates that increased and decreased twofold, as shown in orange and blue, respectively, while other metabolites are depicted in gray. **(C, D)** displayed the Heatmap cluster and VIP analysis of the differential exudates between the two species. **(A, C)** are the positive ion metabolites. **(B, D)** are the negative ion metabolites of exudates.

10.3389/fpls.2024.1461893

VIP > 1) (Figures 3C, D). Terpenoid compounds emerged as the primary differential metabolites in the root exudates of the two species, with fatty acid-related compounds showing higher levels in *HP* than those of *HA*.

3.3 Analysis of soil microbial community of genus *Haloxylon*

At the phylum level, 11 phyla with relative abundances exceeding 1% were identified, with Actinobacteria (31.53%) and Proteobacteria (29.36%) emerging as dominant bacteria. Among the dominant fungi, Ascomycota (54.15%) and Basidiomycota (25.34%) were the dominant groups (Figures 4A, B), and the community structure displayed significant differences (Supplementary Figure S3). Regarding soil bacteria diversity, significant differences were observed in the Chao and Shannon indices for *HA* ($P < 0.05$), along with a significant difference in the Chao index for *HP* ($P < 0.05$). Significant differences were observed in the Chao and Shannon indices of soil bacteria between bulk *HA* and *HP* samples ($P < 0.01$). However, no significant difference ($P > 0.05$) was observed in the rhizosphere soil bacterial diversity index between the two plants. Regarding the soil fungi diversity, the Chao index showed a significant difference ($P < 0.01$), while the Shannon diversity index did not exhibit a significant difference ($P > 0.05$) (Figure 4C). Furthermore, the rhizosphere fungal diversity surpassed that of the bulk soil. Additionally, differences were observed in the species of soil bacteria and fungi within the *Haloxylon* genus (Supplementary Figure S4).

The network association between soil bacteria and fungi was analyzed using Spearman's correlation ($|r|>0.8$, $P<0.05$) (Figures 4D, E; Supplementary Table S3). The numbers and edge interaction ratios within the bacterial and fungal interaction networks of both species were similar. However, the co-occurrence network of *HA* exhibited a higher gram density, average degree, and average clustering coefficient than that of *HP* while showing lower modularity and average path length. Key species in the co-occurrence network of *HA* included Woeseiaceae, Halomonadaceae, and unclassified_Rhizobiales among bacteria, and Phaeococcomycetaceae and Pleosporaceae among fungi. In contrast, Thermoanaerobaculaceae, Cyclobacteriaceae, and Glycomycetaceae bacteria, along with Didymosphaeriaceae, Cordycipitaceae, and Microascaceae fungi, were identified as keystone species in the network of *HP*.

The Tax4Fun analysis of KEGG pathways in soil bacteria of the genus *Haloxylon* revealed that carbohydrate and amino acid metabolism and membrane transport were the primary metabolic pathways (Figure 5A). Differential functional pathways were identified using the Wilcoxon test ($P<0.05$) (Figure 5B), highlighting significant differences in the following pathways: carbohydrate metabolism, signal transduction, metabolism of cofactors and vitamins, and energy metabolism in the soil bacteria of *HP*, with metabolism of other amino acids, infectious disease, and cellular community-prokaryotes of *HA*. Furthermore,

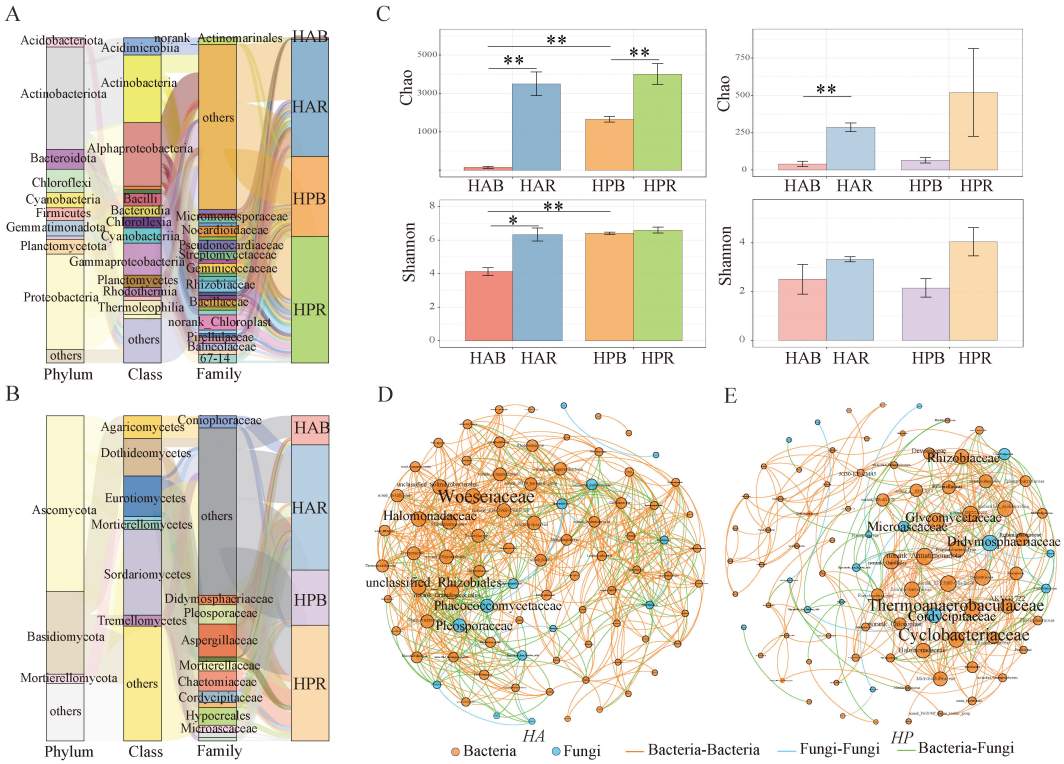

FIGURE 4
Soil bacterial and fungal communities of genus *Haloxylon*. **(A, B)** show the composition of soil bacterial and fungal communities at the phylum level. **(C)** displays the soil microbial diversity comparison between *HA* and *HP*, indicated by *$P < 0.05$, **$P < 0.01$. **(D)** depicts the networks of soil microbial communities at the family level for *HA*, and **(E)** is the networks for *HP*, with the circle size representing the number of degrees. HAR and HAB refer to the rhizosphere and bulk soil of *HA*, respectively, while HPR and HPB denote the rhizosphere and bulk soil of *HP*, respectively.

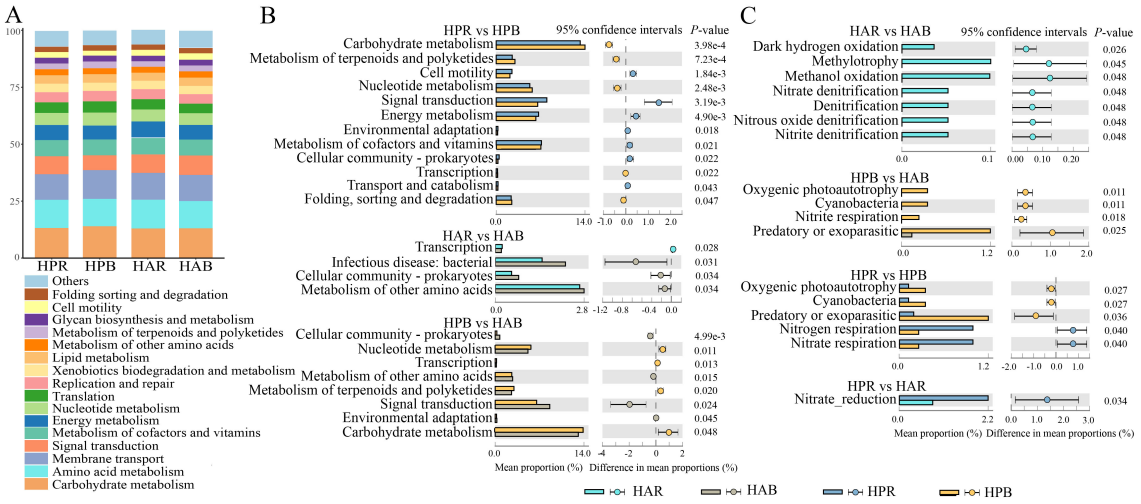

FIGURE 5
Function prediction and differential analysis of soil bacteria in the genus *Haloxylon*. **(A)** shows the composition of bacterial functional pathways at the KEGG class level, **(B)** presents the comparison of predicted functional pathways between groups, and **(C)** illustrates the difference in FAPROTAX functional prediction among groups.

carbohydrate metabolism, signal transduction, and nucleotide metabolism differed between the bulk soils of both species. The FAPROTAX database was utilized to predict differential functional processes in soil bacteria ($P<0.05$), with a focus on nitrogen and carbon cycle-related processes (Figure 5C).

We used FUNGuild function prediction and Wilcoxon test ($P<0.05$) to examine differences in soil fungal function within the genus *Haloxylon*. The primary functions identified for soil fungi in *Haloxylon* were Saprotroph and Sybiotrophs (Figure 6A). Significant differences were observed in the functional prediction of Undefined Saprotroph, Endophyte-Lichen Parasite-Plant Pathogen, and Arbuscular Mycorrhizal and Animal in soil fungi of *HP*, with Dung Saprotroph-Saprotroph in soil fungi of *HA*. Arbuscular Mycorrhiza function exhibited significant differences in rhizosphere soil fungi between the two species but not in bulk soil (Figure 6B).

3.4 Correlation analysis of root traits, exudates, and microorganisms of genus *Haloxylon*

At the family level, we conducted an analysis of the correlation between bacteria, fungi, root exudates, and root traits in the genus *Haloxylon* using the Mantel test. The RL, RS, RD, RV, and RT of the root trait of *HA* showed strong correlations with soil bacteria and root exudates but weak correlations with fungi (Figure 7A). Additionally,

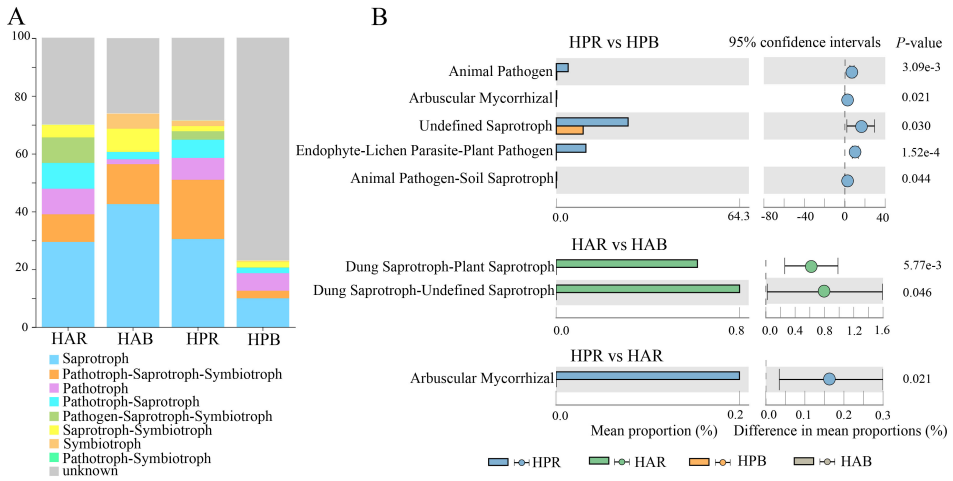

FIGURE 6
Prediction and differential analysis of fungal functional groups in the genus *Haloxylon*. **(A)** displays the relative abundance proportion of fungal functional prediction by FUNGuild. **(B)** presents the comparison of predicted functional pathways among groups.

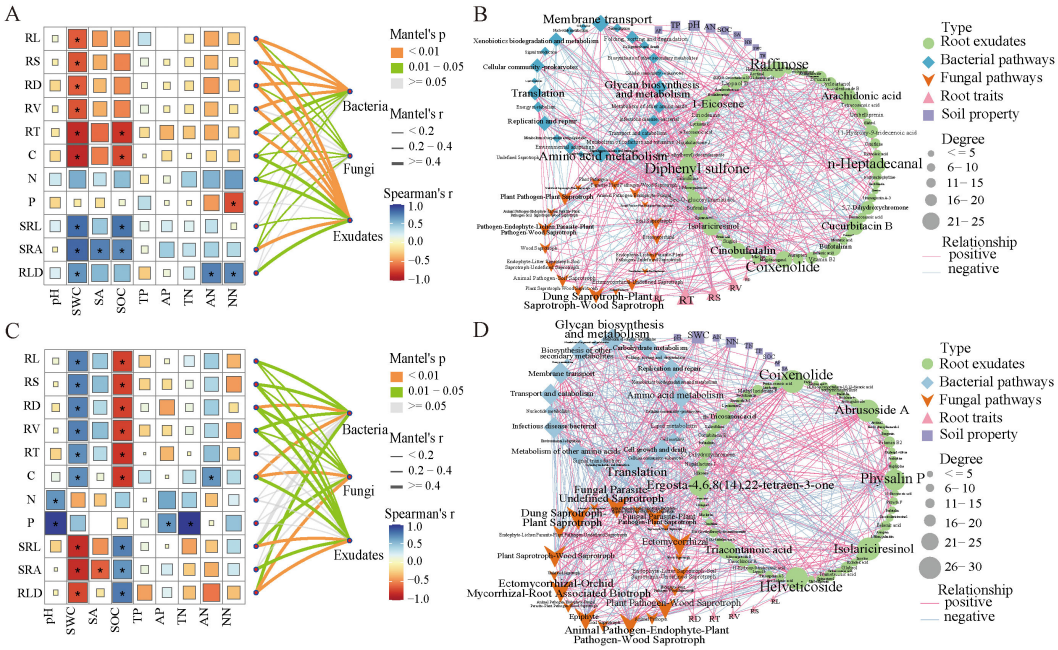

FIGURE 7
Correlation analysis between plant traits, soil environmental factors, and Mantel test of bacteria, fungi, and root exudates in the genus *Haloxylon*. **(A, C)** depict the Mantel test. **(B, D)** show the correlation network of bacteria, fungi, root exudates, soil properties, and root traits in the two *Haloxylon* species. **(A, B)** are for *HA*, while **(C, D)** represent *HP*. * indicated significant levels of $P < 0.05$.

root traits were significantly correlated with SWC. In contrast, the RD, C, and RLD of the root traits of *HP* exhibited strong correlations with soil bacteria, fungi, and root exudates, and the root traits were significantly correlated with both SWC and SOC (Figure 7C).

Functional pathways prediction and Pearson's correlation ($|r| > 0.8$, $P < 0.05$) revealed strong correlations between bacterial and fungal functions, root exudates, root traits, and soil properties (Figures 7B, D). Key hubs in the correlation network included root exudates such as Raffinose, n-heptadecanal, Coixenolide, and Diphenyl sulfone, with predicted microbial functions such as amino acid metabolism, membrane transport, glycan biosynthesis, and metabolism, dung saprotroph-plant saprotroph-wood saprotrophs, root traits T and S, and soil pH. The root exudates of *HP*, including isolariciresinol, abbrusoside A, helveticoside, physalin P, and coixenolide, along with predicted functional pathways, such as glycan biosynthesis and metabolism, biosynthesis of other secondary metabolites, membrane transport, dung saprotroph-plant saprotrophs, ectomycorrhizal function, root traits D and T, and soil SWC and NN, emerged as key hubs in the correlation network.

4 Discussion

4.1 Composition of root exudates within the genus *Haloxylon*

The quantity and quality of root exudates vary depending on factors such as plant genotype, soil environment, nutrient conditions, plant growth stage, and physiological state (Mommer et al., 2016). Root exudates from *HA* and *HP* plants exhibit significant differences in metabolite composition (Figures 2A, B), indicating variations in the components of the root exudates among different plant genotypes, consistent with previous studies (Ziegler et al., 2016). Plant-derived secondary metabolites affect the complexity of interactions with biological and abiotic environmental factors (Enebe and Babalola, 2018). Terpenoids—a major chemical defense in plants—play an essential role in species competition and co-evolution (Fujii et al., 2012). The root exudates of *Haloxylon* exhibit significantly higher levels of triterpernoids than those of other compounds, with fatty acids and steroids following (Figures 2C, D). These may be adaptive strategies closely related species employ to thrive in desert and drought-stressed environments. Triterpenoids and fatty acids serve as signaling molecules, actively contributing to plant stress responses that support overall plant growth (Li et al., 2022b).

Stress affects protein synthesis and nucleic acid metabolism in plants, leading to increased secretion of organic acids and amino metabolites, such as oxalic acid and proline, during periods of stress (Canarini et al., 2016; Xiang et al., 2019). The metabolic pathways observed in the *Haloxylon* genus primarily include metabolic and organic system pathways, with significantly enriched pathways such as galactose metabolism, riboflavin metabolism, and arginine biosynthesis pathway. These pathways are closely linked to adaptation strategies for harsh desert environments, particularly in enhancing drought resistance through improved arginine and proline metabolism (Shi et al., 2013). The physiological and ecological response mechanisms of *Haloxylon* to environmental stress may slightly involve terpenoids and fatty acids as the primary differential metabolites in root exudates between the two species (Figure 3). The composition of root exudates is affected and

constrained by factors such as plant species, genotype, stress conditions, and other environmental factors (Calvo et al., 2019; Vives-Peris et al., 2017).

4.2 Soil microbial communities and functional differences of the genus *Haloxylon*

Many Proteobacteria exhibit eutrophic characteristics, evidenced by rapid growth rates and the ability to utilize diverse substrates (Spain et al., 2009; Zhang et al., 2016). Microbial populations in various plant rhizosphere soils are generally affected by rhizosphere effects (Jing et al., 2023). At the phylum level, the bacterial genus of *Haloxylon* predominantly belonged to Proteobacteria and Actinobacteria, while fungi mainly belonged to Ascomycota and Basidiomycota (Figures 4A, B). Rhizosphere effect plays a vital role in shaping differences in microbial composition and diversity between rhizosphere soil and bulk soil (Qiu et al., 2022; Vieira et al., 2020). Rhizosphere available resources, specifically nutrients, are more abundant, while environmental stress is reduced (Lundberg et al., 2012; Qiu et al., 2022). The rhizosphere of *Haloxylon* shows higher microbial diversity than that of bulk soil, with a distinct composition that is significantly different (Figures 4C; Supplementary Figure S3). This indicates a strong selection of rhizosphere microbial community by two species, highlighting the effect of host plants on rhizosphere microbial community (Gao et al., 2020). The intricate relationships among plant hosts, microorganisms, and the environment strongly correlate with network complexity (Mougi and Kondoh, 2012; Tian et al., 2022). In the soil of the *Haloxylon* genus, the networks of bacteria and fungi exhibit similar levels of complexity (Figures 4D, E; Supplementary Table S2), while the key microbial species in these networks differ. Specifically, the rhizosphere of *HP* shows significant enrichment in Proteobacteria and Bacteroidota, while *HA* is primarily enriched in Bacteroidetes, Cyanobacteria, and Proteobacteria (Supplementary Figure S4). These differences likely stem from interactions between host plant genotypes and soil conditions, enabling adaption to diverse habitat conditions.

Metabolites produced by rhizosphere microbial communities play an important role in providing nutrients to plants or microorganisms, triggering and participating in plant responses to the environment, and enhancing plant stress tolerance (Bai et al., 2022; Sukweenadhi et al., 2015). Plants and microorganisms absorb ammonium salts, nitrates, and other inorganic forms of nitrogen from their environments to synthesize proteins and nitrogen compounds. In the rhizosphere of the *Haloxylon* genus, functional predictions of bacteria primarily revolve around nitrogen metabolism, showing significantly heightened activity than that of the bulk soil. These functions are mainly associated with nitrogen and carbon cycle processes (Figure 5C), indicating the close interaction between rhizosphere plants and soil microorganisms despite variations in the functional groups of rhizosphere microbial communities across different species. Environmental information processing pathways play a vital role in regulating various signaling pathways in bacteria, including responses to toxicity, changes in osmotic pressure, nutrient absorption, and secondary metabolite production (Ma et al., 2022). Similar patterns are observed in the genus *Haloxylon*, particularly focusing on metabolic and environmental information processing pathways, albeit with distinctions between the two species (Figure 5B). These differences likely stem from the physiological and ecological adaptations of plants to environmental stress, developed over long-term evolution, fostering symbiotic relationships with fungi that aid in regulating plant growth and enhancing resistance to harsh environments (Gill et al., 2016). The rhizosphere fungi of both species primarily exhibit saprophytic and saprophytic combinations traits, with higher functional diversity than that of bulk soil (Figure 6). This indicates that greater functional diversity in fungal species contributes to maintaining rhizosphere stability and overall plant health (Wagg et al., 2019).

4.3 Root exudates mediate synergistic interaction between soil properties, microorganisms and the root traits of the genus *Haloxylon*

During the growth phase of plants, roots secrete organic compounds into the surrounding soil environment. These compounds create and sustain a symbiotic relationship between plants and their soil environment, facilitating various biological and abiotic processes (Bais et al., 2006). Root traits are pivotal factors that affect nutrient and water absorption and are crucial for sustaining plant growth (Samejima et al., 2005; Zhang et al., 2009). Here, we found significant correlations between SWC and the root traits of *HA* and SWC, and SOC with the root traits of *HP* (Figures 7A, C). These correlations suggest that desert plants invest heavily in underground structures for water absorption to support their growth during drought periods. Moreover, the microbial communities in the root and rhizosphere also play a critical role. They contribute by supplying essential nutrients and water for plant growth while also participating in producing growth-regulating compounds, such as hormones, organic acids, and amino acids (Bai et al., 2022; Samejima et al., 2005). Strong correlations were observed between the root traits of *HA* and its exudates, soil bacteria, and between the root traits of *HP* and its exudates, soil bacteria, and fungi, indicating a close relationship between root traits and exudates (Meier et al., 2020; Sun et al., 2021; Weemstra et al., 2016). These correlations affect the composition and function of rhizosphere microorganisms (Bulgarelli et al., 2015; Zhalnina et al., 2018). The interactions between plants, soil, and rhizosphere bacteria and fungi mediated by root exudates differ between the two species and are affected by various factors such as soil properties, host plant phenotypes and traits, and abiotic environmental conditions (Berendsen et al., 2012; Vieira et al., 2020).

Roots secrete a range of primary metabolites and secondary metabolites, such as, carbohydrates, alkaloids, terpenes, and phenols (Enebe and Babalola, 2018). These compounds are crucial in shaping and affecting rhizosphere microbial communities and are closely linked to key rhizosphere processes such as carbon and nitrogen cycles (Bulgarelli et al., 2015; Sasse et al., 2018; Vives-Peris et al., 2020). Specifically, our findings reveal that root exudates from *Haloxylon* plants exhibit robust interactions with root traits, soil microbial

functions, and soil properties (Figures 7B, D). The primary metabolites found in root exudates of *HA* include sugars and fatty acids (such as raffinose, n-heptadecanal, and coixenolide), with root traits T and S. Amino acid metabolism, membrane transport, and the soil microorganism pH are closely interconnected. *HP* relies on secondary metabolites, Steroids, and Terpenoids (such as helveticoside, ambrusoside A, and physalin P), with root traits T, and soil microorganisms, for glycan metabolism. The biosynthesis of other secondary metabolites, SWC and NN, exhibit strong mutual interactions, indicating distinct species-specific interactions with their soil environment and microorganisms to enhance adaptability in stressed desert environments (De Vries et al., 2020; Quiza et al., 2015).

We conclude that the interaction between the genus *Haloxylon* growth, soil conditions and microorganisms are a crucial determinant for the exudation profiles observed. This study fills a gap in knowledge about the interactions between plant closely relative species and their subsurface rhizosphere ecological processes in desert ecosystems. However, exudates are dynamic, varying growth stages and season, and also differences in plant species. In this study, specific root exudate components and core microbial flora were not specifically screened, and the interaction between them was not comprehensive enough. This limitation may lead to a lack of depth and clarity in our understanding of how root exudations regulate plant-soil-microbial systems in response to adverse environmental changes. Therefore, in future studies, it is necessary to clarify the function of specific root exudates and coordinate the main beneficial microbial groups to resist stressed environments, so as to better reveal ecological adaptation strategies of plants under harsh environmental conditions and provide scientific basis for the conservation of *Haloxylon* in desert ecosystems and desertification control.

5 Conclusion

The profiles of root exudates in the genus Haloxylon are different, which mediates complex interactions between rhizosphere microorganisms and their hosts. However, these complex interactions manifest differently in the performance of the two species within the soil ecosystem. The findings highlight the significant role of root exudates in responding to soil environmental changes and shaping the structure of the rhizosphere microbial community, synergizing with the host plant, and ecological adaptation mechanisms of *Haloxylon* plants to environmental stressors and contribute to symbiotic relationships with soil microbes. Future studies can deepen our understanding of the complex interactions between desert plants, soil microbial communities, and the environment, ultimately contributing to strategies for enhancing plant resilience and ecosystem sustainability in arid regions.

Data availability statement

The original contributions presented in the study are included in the article/Supplementary Material. Further inquiries can be directed to the corresponding author.

Author contributions

DW: Data curation, Formal analysis, Investigation, Methodology, Software, Visualization, Writing – original draft, Writing – review & editing. XH: Funding acquisition, Project administration, Resources, Supervision, Writing – review & editing. LJ: Data curation, Methodology, Software, Visualization, Writing – review & editing. WL: Investigation, Visualization, Writing – review & editing. HW: Funding acquisition, Project administration, Supervision, Writing – review & editing. GL: Conceptualization, Funding acquisition, Project administration, Supervision, Writing – review & editing.

Funding

The author(s) declare financial support was received for the research, authorship, and/or publication of this article. This research was financially supported by the National Natural Science Foundation of China (32260266), the National Natural Science Foundation of China (3236028) and the National Natural Science Foundation of China (32101360).

Acknowledgments

We thank Zhoukang Li in the Key Laboratory of Oasis Ecology of Xinjiang University for their indispensable help in fieldwork, and Editage (www.editage.cn) for English language editing.

Conflict of interest

The authors declare that the research was conducted in the absence of any commercial or financial relationships that could be construed as a potential conflict of interest.

Publisher's note

Supplementary material

The Supplementary Material for this article can be found online at: https://www.frontiersin.org/articles/10.3389/fpls.2024.1461893/full#supplementary-material

References

Baetz, U., and Martinoia, E. (2014). Root exudates: the hidden part of plant defense. *Trends Plant Sci.* 19, 90–98. doi: 10.1016/j.tplants.2013.11.006

Bai, B., Liu, W., Qiu, X., Zhang, J., Zhang, J., and Bai, Y. (2022). The root microbiome: Community assembly and its contributions to plant fitness. *J. Integr. Plant Biol.* 64, 230–243. doi: 10.1111/jipb.13226

Bais, H. P., Weir, T. L., Perry, L. G., Gilroy, S., and Vivanco, J. M. (2006). The role of root exudates in rhizosphere interactions with plants and other organisms. *Annu. Rev. Plant Biol.* 57, 233–266. doi: 10.1146/annurev.arplant.57.032905.105159

Berendsen, R. L., Pieterse, C. M. J., and Bakker, P. A. H. M. (2012). The rhizosphere microbiome and plant health. *Trends Plant Sci.* 17, 478–486. doi: 10.1016/j.tplants.2012.04.001

Bulgarelli, D., Garrido-Oter, R., Münch, P. C., Weiman, A., Dröge, J., Pan, Y., et al. (2015). Structure and function of the bacterial root microbiota in wild and domesticated barley. *Cell Host Microbe* 17, 392–403. doi: 10.1016/j.chom.2015.01.011

Calvo, O. C., Franzaring, J., Schmid, I., and Fangmeier, A. (2019). Root exudation of carbohydrates and cations from barley in response to drought and elevated CO2. *Plant Soil* 438, 127–142. doi: 10.1007/s11104-019-03998-y

Canarini, A., Merchant, A., and Dijkstra, F. A. (2016). Drought effects on Helianthus annuus and Glycine max metabolites: from phloem to root exudates. *Rhizosphere* 2, 85–97. doi: 10.1016/j.rhisph.2016.06.003

Chai, Y., Cao, Y., Yue, M., Tian, T., Yin, Q., Dang, H., et al. (2019). Soil abiotic properties and plant functional traits mediate associations between soil microbial and plant communities during a secondary forest succession on the loess plateau. *Front. Microbiol.* 10. doi: 10.3389/fmicb.2019.00895

Christner, B. C., Mosley-Thompson, E., Thompson, L. G., and Reeve, J. N. (2001). Isolation of bacteria and 16S rDNAs from Lake Vostok accretion ice. *Environ. Microbiol.* 3, 570–577. doi: 10.1046/j.1462-2920.2001.00226.x

Cui, Y., Fang, L., Guo, X., Wang, X., Wang, Y., Li, P., et al. (2018). Responses of soil microbial communities to nutrient limitation in the desert-grassland ecological transition zone. *Sci. Total Environ.* 642, 45–55. doi: 10.1016/j.scitotenv.2018.06.033

De La Fuente Cantó, C., Simonin, M., King, E., Moulin, L., Bennett, M. J., Castrillo, G., et al. (2020). An extended root phenotype: the rhizosphere, its formation and impacts on plant fitness. *Plant J.* 103, 951–964. doi: 10.1111/tpj.14781

De Vries, F. T., Griffiths, R. I., Knight, C. G., Nicolitch, O., and Williams, A. (2020). Harnessing rhizosphere microbiomes for drought-resilient crop production. *Science* 368, 270–274. doi: 10.1126/science.aaz5192

Enebe, M. C., and Babalola, O. O. (2018). The influence of plant growth-promoting rhizobacteria in plant tolerance to abiotic stress: a survival strategy. *Appl. Microbiol. Biotechnol.* 102, 7821–7835. doi: 10.1007/s00253-018-9214-z

Eppinga, M. B., Rietkerk, M., Dekker, S. C., De Ruiter, P. C., and van der Putten, W. H. (2006). Accumulation of local pathogens a new hypothesis to explain exotic plant invasions. *Oikos* 1, 168–176. doi: 10.1111/j.2006.0030-1299.14625.x

Fujii, K., Aoki, M., and Kitayama, K. (2012). Biodegradation of low molecular weight organic acids in rhizosphere soils from a tropical montane rain forest. *Soil Biol. Biochem.* 47, 142–148. doi: 10.1016/j.soilbio.2011.12.018

Gao, C., Montoya, L., Xu, L., Madera, M., Hollingsworth, J., Purdom, E., et al. (2020). Fungal community assembly in drought-stressed sorghum shows stochasticity, selection, and universal ecological dynamics. *Nat. Commun.* 11, 34. doi: 10.1038/s41467-019-13913-9

Gardes, M., and Bruns, T. D. (1993). ITS primers with enhanced specificity for basidiomycetes - application to the identification of mycorrhizae and rusts. *Mol. Ecol.* 2, 113–118. doi: 10.1111/j.1365-294X.1993.tb00005.x

Gill, S. S., Gill, R., Trivedi, D. K., Anjum, N. A., Sharma, K. K., Ansari, M. W., et al. (2016). Piriformospora indica: potential and significance in plant stress tolerance. *Front. Microbiol.* 7. doi: 10.3389/fmicb.2016.00332

Haichar, F. E. Z., Santaella, C., Heulin, T., and Achouak, W. (2014). Root exudates mediated interactions belowground. *Soil Biol. Biochem.* 77, 69–80. doi: 10.1016/j.soilbio.2014.06.017

Harbort, C. J., Hashimoto, M., Inoue, H., Niu, Y., Guan, R., Rombolà, A. D., et al (2020). Root-secreted coumarins and the microbiota interact to improve iron nutrition in arabidopsis. *Cell Host Microbe* 28, 825–837.e6. doi: 10.1016/j.chom.2020.09.006

Jakoby, G., Rog, I., Megidish, S., and Klein, T. (2020). Enhanced root exudation of mature broadleaf and conifer trees in a Mediterranean forest during the dry season. *Tree Physiol.* 40, 1595–1605. doi: 10.1093/treephys/tpaa092

Jing, H., Wang, H., Wang, G., Liu, G., and Cheng, Y. (2023). The mechanism effects of root exudate on microbial community of rhizosphere soil of tree, shrub, and grass in forest ecosystem under N deposition. *ISME Commun.* 3, 120. doi: 10.1038/s43705-023-00322-9

Kardol, P., Cornips, N. J., van Kempen, M. M. L., Bakx-Schotman, J. M. T., and van der Putten, W. H. (2007). Microbe-mediated plant-soil feedback causes historical contingency effects in plant community assembly. *Ecol. Monogr.* 77, 147–162. doi: 10.1890/06-0502

Korenblum, E., Dong, Y., Szymanski, J., Panda, S., Jozwiak, A., Massalha, H., et al. (2020). Rhizosphere microbiome mediates systemic root metabolite exudation by root-to-root signaling. *Proc. Natl. Acad. Sci.* 117, 3874–3883. doi: 10.1073/pnas.1912130117

Lareen, A., Burton, F., and Schäfer, P. (2016). Plant root-microbe communication in shaping root microbiomes. *Plant Mol. Biol.* 90, 575–587. doi: 10.1007/s11103-015-0417-8

Li, W., Li, Y., Lv, J., He, X., Wang, J., Teng, D., et al. (2022a). Rhizosphere effect alters the soil microbiome composition and C, N transformation in an arid ecosystem. *Appl. Soil Ecol.* 170, 104296. doi: 10.1016/j.apsoil.2021.104296

Li, Y., Zou, J., Zhu, H., He, J., Setter, T. L., Wang, Y., et al. (2022b). Drought deteriorated the nutritional quality of cottonseed by altering fatty acids and amino acids compositions in cultivars with contrasting drought sensitivity. *Environ. Exp. Bot.* 194, 104747. doi: 10.1016/j.envexpbot.2021.104747

Lundberg, D. S., Lebeis, S. L., Paredes, S. H., Yourstone, S., Gehring, J., Malfatti, S., et al. (2012). Defining the core Arabidopsis thaliana root microbiome. *Nature* 488, 86–90. doi: 10.1038/nature11237

Ma, S., Qiao, L., Liu, X., Zhang, S., Zhang, L., Qiu, Z., et al. (2022). Microbial community succession in soils under long-term heavy metal stress from community diversity-structure to KEGG function pathways. *Environ. Res.* 214, 113822. doi: 10.1016/j.envres.2022.113822

Meier, I. C., Tückmantel, T., Heitkötter, J., Müller, K., Preusser, S., Wrobel, T. J., et al. (2020). Root exudation of mature beech forests across a nutrient availability gradient: the role of root morphology and fungal activity. *New Phytol.* 226, 583–594. doi: 10.1111/nph.16389

Mommer, L., Kirkegaard, J., and Van Ruijven, J. (2016). Root–root interactions: towards A rhizosphere framework. *Trends Plant Sci.* 21, 209–217. doi: 10.1016/j.tplants.2016.01.009

Morgan, J. A. W., Bending, G. D., and White, P. J. (2005). Biological costs and benefits to plant–microbe interactions in the rhizosphere. *J. Exp. Bot.* 56, 1729–1739. doi: 10.1093/jxb/eri205

Mougi, A., and Kondoh, M. (2012). Diversity of interaction types and ecological community stability. *Science* 337, 349–351. doi: 10.1126/science.1220529

Phillips, R. P., Erlitz, Y., Bier, R., and Bernhardt, E. S. (2008). New approach for capturing soluble root exudates in forest soils. *Funct. Ecol.* 22, 990–999. doi: 10.1111/j.1365-2435.2008.01495.x

Qiu, L., Kong, W., Zhu, H., Zhang, Q., Banerjee, S., Ishii, S., et al. (2022). Halophytes increase rhizosphere microbial diversity, network complexity and function in inland saline ecosystem. *Sci. Total Environ.* 831, 154944. doi: 10.1016/j.scitotenv.2022.154944

Quiza, L., St-Arnaud, M., and Yergeau, E. (2015). Harnessing phytomicrobiome signaling for rhizosphere microbiome engineering. *Front. Plant Sci.* 6. doi: 10.3389/fpls.2015.00507

Ribbons, R. R., Levy-Booth, D. J., Masse, J., Grayston, S. J., McDonald, M. A., Vesterdal, L., et al. (2016). Linking microbial communities, functional genes and nitrogen-cycling processes in forest floors under four tree species. *Soil Biol. Biochem.* 103, 181–191. doi: 10.1016/j.soilbio.2016.07.024

Sahu, P. K., Singh, D. P., Prabha, R., Meena, K. K., and Abhilash, P. C. (2019). Connecting microbial capabilities with the soil and plant health: Options for agricultural sustainability. *Ecol. Indic.* 105, 601–612. doi: 10.1016/j.ecolind.2018.05.084

Samejima, H., Kondo, M., Ito, O., Nozoe, T., Shinano, T., and Osaki, M. (2005). Characterization of root systems with respect to morphological traits and nitrogen-absorbing ability in the new plant type of tropical rice lines. *J. Plant Nutr.* 28, 835–850. doi: 10.1081/PLN-200055550

Sasse, J., Martinoia, E., and Northen, T. (2018). Feed your friends: do plant exudates shape the root microbiome? *Trends Plant Sci.* 23, 25–41. doi: 10.1016/j.tplants.2017.09.003

Semchenko, M., Saar, S., and Lepik, A. (2014). Plant root exudates mediate neighbour recognition and trigger complex behavioural changes. *New Phytol.* 204, 631–637. doi: 10.1111/nph.12930

Shi, H., Ye, T., Chen, F., Cheng, Z., Wang, Y., Yang, P., et al. (2013). Manipulation of arginase expression modulates abiotic stress tolerance in Arabidopsis: effect on arginine metabolism and ROS accumulation. *J. Exp. Bot.* 64, 1367–1379. doi: 10.1093/jxb/ers400

Song, J., Feng, G., Tian, C.-Y., and Zhang, F.-S. (2006). Osmotic adjustment traits of Suaeda physophora, Haloxylon ammodendron and Haloxylon persicum in field or controlled conditions. *Plant Sci.* 170, 113–119. doi: 10.1016/j.plantsci.2005.08.004

Spain, A. M., Krumholz, L. R., and Elshahed, M. S. (2009). Abundance, composition, diversity and novelty of soil *Proteobacteria*. *ISME J.* 3, 992–1000. doi: 10.1038/ismej.2009.43

Sukweenadhi, J., Kim, Y.-J., Choi, E.-S., Koh, S.-C., Lee, S.-W., Kim, Y.-J., et al. (2015). Paenibacillus yonginensis DCY84T induces changes in Arabidopsis thaliana gene expression against aluminum, drought, and salt stress. *Microbiol. Res.* 172, 7–15. doi: 10.1016/j.micres.2015.01.007

Sun, L., Ataka, M., Han, M., Han, Y., Gan, D., Xu, T., et al. (2021). Root exudation as a major competitive fine-root functional trait of 18 coexisting species in a subtropical forest. *New Phytol.* 229, 259–271. doi: 10.1111/nph.16865

Tian, G., Qiu, H., Li, D., Wang, Y., Zhen, B., Li, H., et al. (2022). Little environmental adaptation and high stability of bacterial communities in rhizosphere rather than bulk soils in rice fields. *Appl. Soil Ecol.* 169, 104183. doi: 10.1016/j.apsoil.2021.104183

Venturi, V., and Keel, C. (2016). Signaling in the rhizosphere. *Trends Plant Sci.* 21, 187–198. doi: 10.1016/j.tplants.2016.01.005

Vieira, S., Sikorski, J., Dietz, S., Herz, K., Schrumpf, M., Bruelheide, H., et al. (2020). Drivers of the composition of active rhizosphere bacterial communities in temperate grasslands. *ISME J.* 14, 463–475. doi: 10.1038/s41396-019-0543-4

Vives-Peris, V., De Ollas, C., Gómez-Cadenas, A., and Pérez-Clemente, R. M. (2020). Root exudates: from plant to rhizosphere and beyond. *Plant Cell Rep.* 39, 3–17. doi: 10.1007/s00299-019-02447-5

Vives-Peris, V., Gómez-Cadenas, A., and Pérez-Clemente, R. M. (2017). Citrus plants exude proline and phytohormones under abiotic stress conditions. *Plant Cell Rep.* 36, 1971–1984. doi: 10.1007/s00299-017-2214-0

Wagg, C., Schlaeppi, K., Banerjee, S., Kuramae, E. E., and van der Heijden, M. G. A. (2019). Fungal-bacterial diversity and microbiome complexity predict ecosystem functioning. *Nat. Commun.* 10, 4841. doi: 10.1038/s41467-019-12798-y

Wang, H., Zhang, R., Cai, Y., Yang, Q., and Lv, G. (2022). Ecological uniqueness and the determinants in arid desert ecosystems of Northwest China. *Glob. Ecol. Conserv.* 34, e02005. doi: 10.1016/j.gecco.2022.e02005

Weemstra, M., Mommer, L., Visser, E. J. W., Van Ruijven, J., Kuyper, T. W., Mohren, G. M. J., et al. (2016). Towards a multidimensional root trait framework: a tree root review. *New Phytol.* 211, 1159–1169. doi: 10.1111/nph.14003

Wen, Z., Li, H., Shen, Q., Tang, X., Xiong, C., Li, H., et al. (2019). Tradeoffs among root morphology, exudation and mycorrhizal symbioses for phosphorus-acquisition strategies of 16 crop species. *New Phytol.* 223, 882–895. doi: 10.1111/nph.15833

Xia, Z., Yu, L., He, Y., Korpelainen, H., and Li, C. (2019). Broadleaf trees mediate chemically the growth of Chinese fir through root exudates. *Biol. Fertil Soils* 55, 737–749. doi: 10.1007/s00374-019-01389-0

Xiang, G., Ma, W., Gao, S., Jin, Z., Yue, Q., and Yao, Y. (2019). Transcriptomic and phosphoproteomic profiling and metabolite analyses reveal the mechanism of NaHCO3-induced organic acid secretion in grapevine roots. *BMC Plant Biol.* 19, 383. doi: 10.1186/s12870-019-1990-9

Yin, H., Li, Y., Xiao, J., Xu, Z., Cheng, X., and Liu, Q. (2013). Enhanced root exudation stimulates soil nitrogen transformations in a subalpine coniferous forest under experimental warming. *Glob. Change Biol.* 19, 2158–2167. doi: 10.1111/gcb.12161

Zhalnina, K., Louie, K. B., Hao, Z., Mansoori, N., Da Rocha, U. N., Shi, S., et al. (2018). Dynamic root exudate chemistry and microbial substrate preferences drive patterns in rhizosphere microbial community assembly. *Nat. Microbiol.* 3, 470–480. doi: 10.1038/s41564-018-0129-3

Zhang, C., Liu, G., Xue, S., and Wang, G. (2016). Soil bacterial community dynamics reflect changes in plant community and soil properties during the secondary succession of abandoned farmland in the Loess Plateau. *Soil Biol. Biochem.* 97, 40–49. doi: 10.1016/j.soilbio.2016.02.013

Zhang, H., Xue, Y., Wang, Z., Yang, J., and Zhang, J. (2009). An alternate wetting and moderate soil drying regime improves root and shoot growth in rice. *Crop Sci.* 49, 2246–2260. doi: 10.2135/cropsci2009.02.0099

Zhao, M., Zhao, J., Yuan, J., Hale, L., Wen, T., Huang, Q., et al. (2021). Root exudates drive soil-microbe-nutrient feedbacks in response to plant growth. *Plant Cell Environ.* 44, 613–628. doi: 10.1111/pce.13928

Zhu, Y., Zhang, S., Huang, H., and Wen, B. (2009). Effects of maize root exudates and organic acids on the desorption of phenanthrene from soils. *J. Environ. Sci.* 21, 920–926. doi: 10.1016/S1001-0742(08)62362-1

Ziegler, J., Schmidt, S., Chutia, R., Müller, J., Böttcher, C., Strehmel, N., et al. (2016). Non-targeted profiling of semi-polar metabolites in Arabidopsis root exudates uncovers a role for coumarin secretion and lignification during the local response to phosphate limitation. *J. Exp. Bot.* 67, 1421–1432. doi: 10.1093/jxb/erv539

frontiers | Frontiers in Plant Science

TYPE Original Research
PUBLISHED 28 October 2024
DOI 10.3389/fpls.2024.1488089

OPEN ACCESS

EDITED BY
Xiao-Dong Yang,
Ningbo University, China

REVIEWED BY
Benfeng Yin,
Chinese Academy of Sciences (CAS), China
Lingjuan Li,
Chengdu University of Technology, China

*CORRESPONDENCE
Xue Wu
wuxue@xju.edu.cn

RECEIVED 29 August 2024
ACCEPTED 09 October 2024
PUBLISHED 28 October 2024

CITATION
Tian C, Wu X, Bahethan B, Yang X, Yang Q and Wang X (2024) Soil bacterial community characteristics and influencing factors in different types of farmland shelterbelts in the Alaer reclamation area.
Front. Plant Sci. 15:1488089.
doi: 10.3389/fpls.2024.1488089

Soil bacterial community characteristics and influencing factors in different types of farmland shelterbelts in the Alaer reclamation area

Cuiping Tian[1,2,3], Xue Wu[1,2,3,4]*, Bota Bahethan[1,2,3], Xianyao Yang[1,2,3], Qianqian Yang[1,2,3] and Xiantao Wang[1,2,3]

[1]College of Ecology and Environment, Xinjiang University, Urumqi, China, [2]Key Laboratory of Oasis Ecology, Ministry of Education, Xinjiang University, Urumqi, China, [3]Xinjiang Jinghe Observation and Research Station of Temperate Desert Ecosystem, Ministry of Education, Jinghe, China, [4]Technology Innovation Center for Ecological Monitoring and Restoration of Desert-Oasis, Ministry of Natural Resources (MNR), Urumqi, China

To investigate the effects of various types of farmland shelterbelts on soil quality and soil bacterial community diversity, this study focused on soil samples from four different shelterbelt types in the Alaer reclamation area, including *Populus euphratica* Oliv.- *Populus tomentosa* Carrière (PP), *Elaeagnus angustifolia* L.- *Populus euphratica* Oliv. (EP), *Populus alba* var. *pyramidalis* Bunge (P), and *Salix babylonica* L. (S). We analyzed their physical, chemical, biological properties as well as the differences in bacterial community structure, and explored the influencing factors on soil microbial community characteristics through microbial correlation network analysis. The results showed that: (1) There were significant differences in soil properties among the four types of farmland shelterbelts ($p < 0.05$), with P soils exhibiting the highest levels of organic matter, total nitrogen, and total phosphorus contents. (2) The Alpha diversity indices of soil bacteria showed significant differences among the four types of farmland shelterbelts ($p < 0.05$), with the P soils displayed the highest Chao1 and Shannon indices. (3) There were differences in the composition and abundance of dominant soil bacterial communities among different farmland shelterbelts, notably, the abundances of Verrucomicrobia, Acidobacteria, and Planctomycetes were significantly higher in P soils compared to the other three types. (4) The complexity of the correlation network between microbial species and environmental factors was highest in EP soils, soil microbial biomass nitrogen and available phosphorus were the main influencing factors. These findings indicated that different types of farmland shelterbelts had significant impacts on soil properties and soil bacterial communities. Soil bacterial communities were regulated by soil properties, their changes reflected a combined effect of soil characteristics and tree species.

KEYWORDS

Alaer reclamation area, farmland shelterbelts, soil properties, soil microorganisms, correlation network analysis

1 Introduction

The farmland shelterbelt system (FSS) is an essential component of agroforestry systems and a key ecological barrier against adverse environmental conditions (Krichen et al., 2017; Wang et al., 2020). This system is widely applied in ecologically fragile areas facing challenges of wind erosion and soil desertification, such as the northern regions of China, including Northwest and Northeast China (Bao et al., 2012; Cerdà et al., 2022). By designing and constructing different types of shelterbelt networks around farmland, FSS aims to resist sand and wind disasters, improve soil properties and quality, increase soil microbial diversity, and promote ecosystem health (Chen et al., 2017; Luca et al., 2018; Cao et al., 2021). In the context of increasingly severe global environmental issues such as climate change, land degradation, and biodiversity loss, the importance of FSS is gradually being recognized worldwide (Haddaway et al., 2018; Fang, 2021). Especially in enhancing agricultural sustainability and ecological restoration, FSS is regarded as an effective ecological engineering measure (Kong et al., 2022).

The surface soil of forest land is an important habitat for microorganisms, many of which are beneficial. The diversity and activity of forest soil microorganisms play a crucial role in the decomposition of organic matter, the release of nutrients, the promotion of matter and energy cycling, and the balance and maintenance of the health and stability of forest soil ecosystems (Breulmann et al., 2012; Edwards et al., 2015; Hacquard and Schadt, 2015; Fang et al., 2016). Previous studies have shown that the abundance of Actinobacteria varies the most among different types of farmland shelterbelts (Zhang J. et al., 2019), while the Proteobacteria and Acidobacteria are most affected by afforestation (Li et al., 2019; Deng et al., 2019a). Actinobacteria can produce extracellular polysaccharides and other substances, improving soil aeration and water retention capacity. Proteobacteria promote nitrogen cycling in the soil, and Acidobacteria are involved in the decomposition of organic matter, all of which have significant effects on soil improvement and nutrient cycling. Studying the characteristics of these microorganisms and their interactions with environmental factors will help improve our understanding of the dynamics of forest soil ecosystems and provide a scientific basis for ecological restoration and management.

Soil microorganisms are extremely sensitive to environmental changes and are influenced by various factors, including soil properties, climate, vegetation, and root activity. Farmland shelterbelts increase the biomass of surface litter and root activity, enhancing the decomposition rate of organic matter and nutrient content in the soil, thereby positively regulating soil microorganisms. Studies have shown that the establishment of farmland shelterbelts significantly increases soil microbial biomass, metabolism, and diversity (Jan et al., 2014; Qiu et al., 2017; Liu et al., 2019). Therefore, it is crucial to explore the impact of soil properties on the structure and diversity of microbial communities. High soil organic matter content promotes processes such as microbial organic matter degradation, nitrogen fixation, and mineral transformation, leading to changes in soil microbial community structure. Soil pH and nitrogen are also key factors determining soil microbial diversity and composition. Previous research results have shown a significant positive correlation between pH and microbial diversity and richness (Bao et al., 2012; Liu et al., 2014). Total nitrogen and alkali-hydrolyzable nitrogen can also directly affect the relative abundance of dominant bacterial phyla (Deng et al., 2019b). The environment regulates the distribution of soil microorganisms, while the characteristics of soil microbial community respond to soil ecological processes and vegetation changes (Rodrigues et al., 2015). However, few studies have comprehensively analyzed and evaluated the combined effects of different types of FSS vegetation changes and understory soil properties on soil microbial community characteristics. Additionally, reports using 16S rDNA high-throughput sequencing technology to study FSS soil microorganisms are relatively scarce.

The Alaer reclamation area is adjacent to the Taklamakan Desert, where frequent wind and sand activities occur. The study indicates that the soil organic matter content in the Aral reclamation area is relatively low, classifying it as lightly salinized soil (Cai et al., 2013). The spatial variation of soil water and salt is significantly influenced by soil texture and topography (Xu and Sun, 2023). Through reclamation and cultivation management, it is possible to effectively improve the degree of soil salinization and significantly increase the microbial biomass in the soil (Wang et al., 2021; Guo et al., 2023). The establishment of Farmland shelterbelts could effectively prevent wind and sand disasters, maintaining high-quality and stable agricultural development and benefiting the construction of high-standard farmland. On this background, it is necessary to study the influence of different types of FSS on soil bacterial community characteristics, which could reveal the ecological protection function of shelterbelts from multiple dimensions. *Populus euphratica* Oliv., *Populus tomentosa* Carrière, *Populus alba* var. *pyramidalis* Bunge, *Elaeagnus angustifolia* L., Salix babylonica L. are commonly used tree species for constructing farmland shelterbelts in the Alaer reclamation area. This study measured and analyzed the soil properties and microbial community structure under different types of farmland shelterbelts during the growing season. In this context, the following questions are proposed: (1) How do soil properties vary among different types of farmland shelterbelts? (2) How do soil bacterial community compositions respond to different types of farmland shelterbelts? (3) What are the influencing factors of soil bacterial community characteristics in different types of farmland shelterbelts? The results of this study will provide a theoretical basis and technical support for the sustainable development of farmland shelterbelt soil in this region, ensuring the long-term stable effectiveness of protective benefits.

2 Materials and methods

2.1 Overview of the study area

The Alaer reclamation area is located in the heart of the Eurasian continent, in the northern part of the Tarim Basin, at

the confluence of the Aksu River, Yarkand River, and Hotan River, in the upper reaches of the Tarim River. Its geographical coordinates are between 40°22′ - 40°57′ N and 80°30′ - 81°58′ E, stretching 281 km from east to west and 180 km from north to south. The region experiences a warm temperate extreme continental arid desert climate. It receives 2800-3000 hours of sunshine annually, has a frost-free period of 200-220 days, an average annual precipitation of about 75 mm, an annual evaporation rate of 1200-1500 mm, and an average annual temperature of approximately 10°C. Natural disasters in the area include wind and sand, droughts, cold waves, and floods, with wind and sand being the most prevalent natural disaster. The primary soil types identified in the area include brown desert soil and saline-alkaline soil.

Following a field survey, four types of farmland shelterbelts were selected as research subjects: *Populus euphratica* Oliv.- *Populus tomentosa* Carrière farmland shelterbelt (PP), *Elaeagnus angustifolia* L.- *Populus euphratica* Oliv. farmland shelterbelt (EP), *Populus alba* var. *pyramidalis* Bunge farmland shelterbelt (P), and *Salix babylonica* L. farmland shelterbelt (S) (Figure 1).

2.2 Soil sample collection

In June 2021, field surveys were conducted in around the city of Alaer. In each type of farmland shelterbelt, three sample plots of 2m × 5m were established in areas with similar site conditions, 12 sample plots in total. The trees in each plot were measured for height and diameter at breast height to determine the average tree height and diameter (Table 1). Based on measurements, one healthy tree without disease or pest damage was selected as the standard tree for each plot.

Under the canopy of standard trees, near the base of roots, surface litter and debris were removed. Using a sterile shovel, soil samples were collected at depth of 0-20 cm, with three repetitions. After mixing the three repetitions thoroughly, the soil was sieved through a 2 mm sieve and divided into three portions. One portion was placed in an aluminum box for soil moisture content determination, one portion was placed in a sterile cryotube, taken back to the laboratory, and stored at -80°C for soil bacterial and microbial biomass determination. The remaining portion was air-dried for pH, electrical conductivity, soil organic carbon, available phosphorus, alkali-hydrolyzable nitrogen, total nitrogen, and total phosphorus determination.

2.3 Soil property analysis

Soil properties were determined according to *Soil Agricultural Chemistry Analysis* (Bao, 2000), pH was measured using the potentiometric method (soil to water ratio 1:5); electrical conductivity (EC) was measured using the conductivity method (soil to water ratio 1:5); soil water content (SWC) was determined using the drying method; soil organic carbon (SOC) was determined

FIGURE 1
Field photos of different types of farmland shelterbelts.

TABLE 1 The structure of different types of farmland shelterbelts.

	Configuration	Average height of trees/m	Diameter at breast height/cm
PP	*Populus euphratica* Oliv. /*Populus tomentosa* Carrière	10.5/16	12.5/21
EP	*Elaeagnus angustifolia* L. /*Populus euphratica* Oliv.	6.5/10.5	15/12.5
P	*Populus alba* var. *pyramidalis* Bunge	22.5	26
S	*Salix babylonica* L.	14.5	13.5

using the potassium dichromate volumetric method; available phosphorus (AP) was determined using the sodium bicarbonate extraction method; alkali-hydrolyzable nitrogen (AN) was determined using the alkaline diffusion method; total nitrogen (TN) was determined using the Nessler's reagent spectrophotometric method; and total phosphorus (TP) was determined using the molybdenum antimony anti-colorimetric method.

Soil microbial biomass was determined according to *Soil Microbial Biomass Determination Methods and Applications* (Wu et al., 2006). Microbial biomass carbon (MBC), microbial biomass nitrogen (MBN), and microbial biomass phosphorus (MBP) were all determined using the chloroform fumigation extraction method.

2.4 Soil DNA extraction and high-throughput sequencing

The TGuide S96 magnetic bead method soil genomic DNA extraction kit (Model: DP812, Tiangen Biotech (Beijing) Co., Ltd.) was used to extract total DNA from soil microorganisms in different types of farmland shelterbelts according to the kit's manual. The nucleic acid concentration was measured using a microplate reader (Manufacturer: Gene Company Limited, Model: Synergy HTX), and amplification was performed based on the measurement results. For bacterial communities, universal bacterial primers 27F (5'-AGRGTTTGATYNTGGCTCAG-3') and 1492R (5'-TASGGHTACCTTGTTASGACTT-3') were used to amplify the full-length region of the bacterial 16S rDNA gene sequence. The PCR products were electrophoresed on 1.8% agarose gel (Manufacturer: Beijing Biotech-Xin Technology Co., Ltd.) to check for integrity. The PCR reaction conditions were as follows: 95°C for 2 min; 25 cycles of denaturation at 98°C for 10 s, annealing at 55°C for 30 s, and extension at 72°C for 1 min 30 s; and a final extension at 72°C for 2 min.

For the constructed libraries, the PacBio SMRTbell Template Prep Kit was used for damage repair, end repair, and adapter ligation of the mixed products. The reaction process was conducted on a PCR instrument, and the final library was recovered using AMpure PB magnetic beads. The PacBio Binding kit was used to bind the library with primers and polymerase before sequencing on the Sequel II sequencer, sequencing and sequence alignment work were undertaken by Beijing Biomarker Technologies Co., Ltd.

2.5 Bioinformatics analysis and data processing

The raw subreads obtained from sequencing were corrected to obtain Circular Consensus Sequencing (CCS) sequences using SMRT Link, version 8.0. The lima software (v1.7.0) was then used to identify CCS sequences of different samples through barcode sequences and to remove chimeras, resulting in Effective CCS sequences. The Effective CCS sequences were clustered into Operational Taxonomic Units (OTUs) at a similarity level of 97% using Usearch v10.0. Using the SILVA reference database, taxonomic annotation of the feature sequences was conducted with a Naïve Bayes classifier in combination with alignment methods. This approach allows for the statistical analysis of community composition at various levels (phylum, class, order, family, genus, species) for each sample.

Data organization and analysis were performed using Excel 2019 and IBM SPSS Statistics 26 software. One-way analysis of variance (One-way ANOVA) using the Waller-Duncan test was employed, and results were presented as mean ± standard error. Origin 2023 software was used for plotting. QIIME 2 software was used to calculate Alpha diversity indices (ACE, Chao1, Simpson, and Shannon). Principal component analysis (PCA) was conducted using R software. The Biomarker Microbial Diversity Analysis Platform (www.biocloud.net) was used for correlation analysis between soil microbial species and environmental factors.

3 Results

3.1 Differences in soil properties among different types of farmland shelterbelts

One-way analysis of variance showed significant differences in soil TP, AP, AN, pH, EC, SWC, MBC, MBP, and MBN among the four types of farmland shelterbelts (Table 2). Among them, P had the highest SOC, TP, TN, AP, AN, SWC, MBC, MBP, and MBN among the four types of farmland shelterbelts, with TP, AP, AN, SWC, MBC, MBP, and MBN significantly higher than the other three types of farmland shelterbelts ($p < 0.05$). The EC of P was the lowest, showing significant differences compared to the other types of farmland shelterbelts ($p < 0.05$). The soils of all four types of farmland shelterbelts were alkaline (pH > 8.3), with S having the highest pH, significantly higher than the other three types of farmland shelterbelts ($p < 0.05$).

3.2 Soil bacterial community characteristics and differences among different types of farmland shelterbelts

A total of 1271 OTUs were detected in the soil bacterial communities of the four types of farmland shelterbelts, with 378 OTU shared among all samples, accounting for 29.74%. The number of unique OTU was highest in S (86), followed by PP (83), P (62), and EP (34). S had the highest total OTU count as well

10.3389/fpls.2024.1488089

TABLE 2 Soil properties of different types of farmland shelterbelts.

	PP	EP	P	S
SOC	4.55 ± 0.26	4.92 ± 0.59	6.03 ± 1.56	3.82 ± 0.40
TP	0.61 ± 0.02**AB**	0.53 ± 0.02**B**	0.65 ± 0.01**A**	0.60 ± 0.04**AB**
TN	0.28 ± 0.01	0.37 ± 0.04	0.46 ± 0.11	0.25 ± 0.02
AP	4.61 ± 1.02**C**	2.62 ± 0.42**C**	32.74 ± 0.54**A**	7.10 ± 0.67**B**
AN	25.45 ± 1.46**B**	33.03 ± 2.41**AB**	46.58 ± 9.36**A**	23.56 ± 0.86**B**
pH	8.73 ± 0.05**AB**	8.49 ± 0.07**BC**	8.30 ± 0.10**C**	8.92 ± 0.13**A**
EC	1538.33 ± 150.58**C**	3926.67 ± 135.44**A**	883.00 ± 83.19**D**	2592.67 ± 197.99**B**
SWC	5.84 ± 0.61**B**	2.42 ± 0.20**C**	12.05 ± 1.02**A**	3.76 ± 0.08**BC**
MBC	45.52 ± 4.55**C**	38.47 ± 2.13**C**	115.41 ± 0.46**A**	73.78 ± 0.81**B**
MBP	4.23 ± 0.38**BC**	6.60 ± 0.89**AB**	7.59 ± 0.89**A**	3.60 ± 0.41**C**
MBN	3.36 ± 0.33**B**	4.25 ± 0.88**B**	11.47 ± 0.36**A**	4.35 ± 1.01**B**

Data in the table are means ± standard error; different capital letters in the same row indicate significant differences at the $p = 0.05$ level.

as the highest number of unique OTUs, while EP had the second-highest total OTU count but the lowest number of unique OTU. P had a higher total OTU count than PP but a lower number of unique OUT (Figure 2).

The coverage indices of all samples were above 0.97. The Chao1 and Shannon indices of EP were significantly lower than those of P ($p < 0.05$), but showed no significant differences compared to PP and S. However, the ACE index of EP was significantly lower than the other three types of farmland shelterbelts. There were no significant differences in the Simpson index among the four types of farmland shelterbelts ($p > 0.05$) (Table 3).

Based on the taxonomic analysis of soil genomic DNA sequences, a total of 23 bacterial phyla and 433 bacterial genera were detected in all soil samples. Specifically, 15 phyla and 204 genera were detected in PP, 16 phyla and 185 genera in EP, 17 phyla and 259 genera in P, and 15 phyla and 201 genera in S.

The top 10 phyla in relative abundance were selected for each type of shelterbelt soil, and a relative abundance bar stack chart was generated (Figure 3A). Proteobacteria was the dominant phylum in all samples, accounting for 30.80% to 58.72% of the total sequences, followed by Bacteroidetes (11.96% - 44.09%), Firmicutes (0.88% - 29.93%), Gemmatimonadetes (0.11% - 5.90%), Actinobacteria (0.58% - 6.45%), Verrucomicrobia (0.13% - 3.82%), Acidobacteria (0.02% to 3.63%), Patescibacteria (0.08% - 4.11%), Planctomycetes (0.12% - 2.18%), and Chloroflexi (0.01% - 0.61%). Proteobacteria, Bacteroidetes, and Firmicutes were the common dominant phyla in the four types of farmland shelterbelts. Bacterial phyla with a relative abundance of more than 1% in P were more abundant than the other three types of farmland shelterbelt.

At the genus level, the proportion of dominant genera was relatively low (Figure 3B), with *Salinimicrobium* (0.09% - 35.96%) and *Halomonas* (0.23% - 31.55%) being the dominant in all four types of farmland shelterbelts. Then it was followed by *Palleronia* (0.08% - 9.05%), *Marinobacter* (0.04% - 11.79%), *Salegentibacter* (0.07% - 5.49%), *Uncultured_bacterium_f_Cyclobacteriaceae* (0.38% - 7.04%), *Pontibacter* (0.03% - 6.39%), *Planococcus* (0.27% - 4.00%), *Pseudomonas* (0.10% - 3.36%), and *Altererythrobacter* (0.05% - 2.92%).

The soil bacteria in the four types of farmland shelterbelts showed differences in the composition and abundance of some

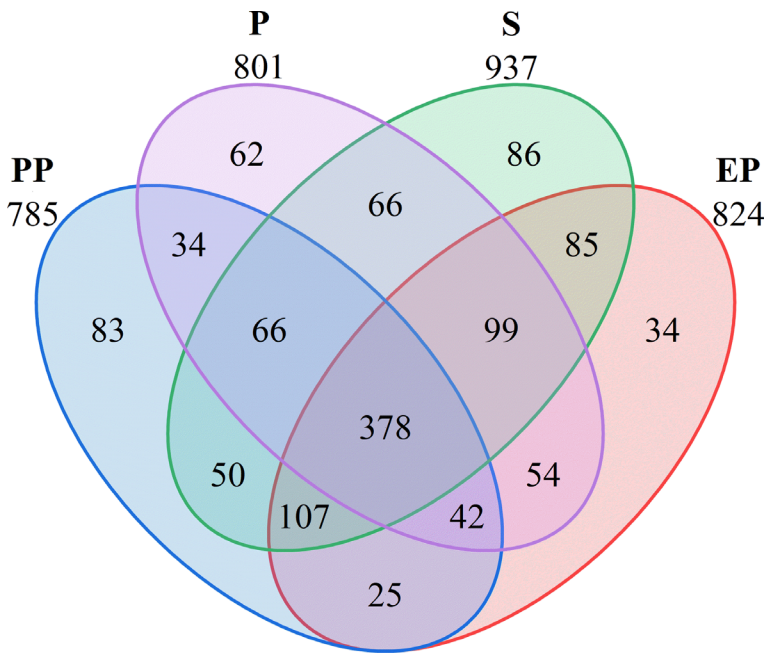

FIGURE 2
Venn diagram of different types of farmland shelterbelts based on OTUs.

10.3389/fpls.2024.1488089

TABLE 3 Alpha diversity analysis of different types of farmland shelterbelts soils.

	PP	EP	P	S
ACE	589.88 ± 48.84**A**	370.76 ± 6.05**B**	660.57 ± 49.86**A**	611.92 ± 83.39**A**
Chao1	555.38 ± 85.32**AB**	372.20 ± 1.18**B**	655.75 ± 43.64**A**	580.90 ± 89.79**AB**
Simpson	0.96 ± 0.02	0.96 ± 0.00	0.99 ± 0.00	0.97 ± 0.01
Shannon	6.47 ± 0.57**AB**	5.96 ± 0.01**B**	7.91 ± 0.02**A**	6.72 ± 0.82**AB**
Coverage	0.97 ± 0.00**B**	0.99 ± 0.00**A**	0.97 ± 0.01**AB**	0.98 ± 0.00**AB**

Data in the table are means ± standard error; different capital letters in the same row indicate significant differences at the 0.05 level.

dominant groups. The abundance of the Verrucomicrobia, Acidobacteria, and Planctomycetes in P was significantly higher than in the other three types of farmland shelterbelts, while the abundance of *Palleronia* in EP was significantly higher. There were no significant differences in the other dominant community at the phylum and genus levels ($p > 0.05$) (Table 4).

3.3 Factors affecting soil bacterial community characteristics

In the PCA plot (Figure 4), the angle between the arrows and the distance projected onto the PC axis indicate that MBN, AP, AN, SWC, TN, MBC, SOC, TP, and MBP are positively correlated with PC1, while EC and pH are negatively correlated with PC1. The lengths of arrow of pH, EC, TN were longer, suggesting that they had greater contributions to PC1 and PC2.

According to the principle of eigenvalues > 1, a total of 3 principal components were extracted (Table 5), with contribution rates of 60.57%, 19.54%, and 10.89% respectively, cumulatively contributing to 91.00%. Soil indicators with factor loadings absolute value ≥ 0.75 were grouped into one component. TN, AP, AN, SWC, MBC, and MBN had high loadings on the first principal component, with values of 0.768, 0.954, 0.858, 0.919, 0.837, and 0.934 respectively.

Based on the correlation analysis between environmental factors (loadings absolute value ≥ 0.75) and microbial taxa (default parameters, genus level, Pearson correlation, correlation threshold 0.3, correlation p-value threshold 0.05, node number 80, edge number 100), a correlation network diagram was constructed, as shown in Figure 5. The complexity of the correlation network in EP was the highest among the four types of farmland shelterbelts, with most bacterial genera showing a positive correlation with environmental factors, and MBN and AP having a significant positive promoting effect on various bacterial genera. The bacterial genera in PP were mostly negatively correlated with environmental factors, with SWC and MBN being the main influencing factors. The relationship differences between bacterial genera and environmental factors in P were not significant, only MBC and SWC had a significant effect on various bacterial genera. The bacterial genera in S were only correlated with AP, MBN, and MBC, and most of them were negatively correlated, with AP having a more significant impact on various bacterial genera. In all four types of farmland shelterbelts, Proteobacteria were significantly influenced by environmental factors, followed by Bacteroidetes and Firmicutes.

4 Discussion

4.1 Different types of farmland shelterbelts on soil environment

Constructing farmland shelterbelts can effectively improve environmental factors within the shelterbelt system, optimize

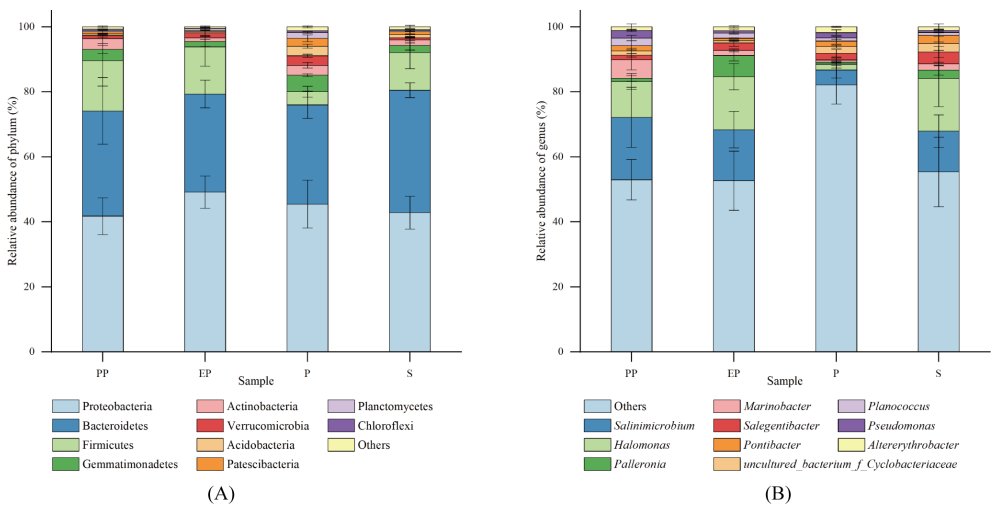

FIGURE 3
Relative abundance of soil bacterial communities at phylum **(A)** and genus **(B)** levels in different types of farmland shelterbelts.

10.3389/fpls.2024.1488089

TABLE 4 Differences in soil bacterial community composition at phylum and genus levels in different types of farmland shelterbelts.

		PP	EP	P	S
	Proteobacteria	41.77 ± 5.67	49.15 ± 4.97	45.48 ± 7.34	42.84 ± 5.06
	Bacteroidetes	32.35 ± 10.24	30.20 ± 4.27	30.51 ± 4.19	37.65 ± 2.28
	Firmicutes	15.47 ± 7.79	14.5 ± 5.95	4.05 ± 1.66	11.61 ± 4.98
	Gemmatimonadetes	3.50 ± 1.21	1.64 ± 1.53	5.12 ± 0.41	2.19 ± 1.43
	Actinobacteria	3.32 ± 1.60	1.16 ± 0.51	3.01 ± 0.82	1.69 ± 0.94
Phylum	**Verrucomicrobia**	**0.92 ± 0.46B**	**1.48 ± 0.71AB**	**2.93 ± 0.48A**	**0.65 ± 0.17B**
	Acidobacteria	**0.51 ± 0.24B**	**0.51 ± 0.50B**	**2.98 ± 0.62A**	**0.94 ± 0.90AB**
	Patescibacteria	0.62 ± 0.35	0.15 ± 0.11	2.40 ± 1.03	0.91 ± 0.69
	Planctomycetes	**0.46 ± 0.08B**	**0.66 ± 0.42B**	**1.75 ± 0.28A**	**0.44 ± 0.30B**
	Chloroflexi	0.37 ± 0.13	0.10 ± 0.09	0.53 ± 0.05	0.23 ± 0.17
	Others	0.72 ± 0.31	0.45 ± 0.23	1.24 ± 0.28	0.85 ± 0.45
	Others	52.96 ± 6.20	52.65 ± 9.09	82.17 ± 5.95	55.38 ± 10.74
	Salinimicrobium	19.21 ± 9.24	15.73 ± 5.60	4.57 ± 2.46	12.53 ± 5.01
	Halomonas	11.05 ± 2.42	16.27 ± 4.06	1.77 ± 1.17	16.2 ± 8.66
	Palleronia	**0.94 ± 0.85B**	**6.55 ± 1.67A**	**0.63 ± 0.23B**	**2.57 ± 1.49AB**
	Marinobacter	5.71 ± 3.11	1.60 ± 0.44	0.65 ± 0.63	1.90 ± 0.56
Genus	*Salegentibacter*	1.44 ± 0.55	2.27 ± 0.97	2.10 ± 1.20	3.64 ± 1.70
	uncultured_bacterium_f_Cyclobacteriaceae	1.31 ± 0.79	0.64 ± 0.18	2.04 ± 0.47	2.70 ± 2.17
	Pontibacter	1.57 ± 1.51	0.82 ± 0.11	1.72 ± 1.00	2.42 ± 1.99
	Planococcus	2.35 ± 0.83	1.59 ± 0.32	0.95 ± 0.43	0.96 ± 0.17
	Pseudomonas	2.39 ± 0.36	0.71 ± 0.45	1.62 ± 0.87	0.56 ± 0.36
	Altererythrobacter	1.07 ± 0.92	1.18 ± 0.31	1.79 ± 0.17	1.13 ± 0.93

Data in the table are means ± standard error; different capital letters in the same row indicate significant differences at the 0.05 level.
Bolded numbers highlight results that are significantly different between groups.

farmland soil conditions, protect vegetation cover, finally enhance the ecological benefits of farmland (Shi et al., 2016). In this study, significant differences were found in soil properties among different types of farmland shelterbelts. The pH value of S was significantly higher than the other three types farmland shelterbelts. The differences in soil pH among different tree species of farmland shelterbelts are consistent with the results of Iovieno et al. (2010), who emphasized the influence of dominant tree species on soil pH in forest stands on the same substrate. The soil SOC, TP, TN, AP, AN, SWC, MBC, MBN, and MBP contents in the P were the highest (Table 1), indicating excellent nutrient condition in the P soil. Then was S, with the AP, AN, MBC, and MBN contents ranking behind, suggesting that the soil nutrient element contents were also at a higher level. The soil nutrient element contents in the PP and EP two composite types of shelterbelt soil was relatively low, indicating pure forest farmland shelterbelts had better nutrient status. Given the similar growth substrates of the studied farmland shelterbelts, the differences in soil nutrient contents are likely caused by different tree species and their litter. Vegetation can adjust the microclimate through shading, frost prevention, and soil moisture regulation. Additionally, the accumulation and decomposition of plant litter, as well as the components of root exudates, including carbohydrates, amino acids, low molecular weight aliphatics and aromatics, fatty acids, enzymes, and hormones, directly or indirectly affect microbial communities, thus affecting soil nutrient contents (Prescott and Grayston, 2013). Liu and Wang (2021) compared the soil nutrients of artificial forests of *Picea crassifolia* Kom., *Larix gmelinii* var. *principis-rupprechtii* (Mayr) Pilg., *Populus cathayana* Rehder, *Betula platyphylla* Sukaczev, the results also showed significant differences in soil nutrients among different artificial forests, with the soil nutrient content of *Populus cathayana* Rehder forests being the highest. This may be because both *Populus alba* var. *pyramidalis* Bunge and *Populus cathayana* Rehder belong to broad-leaved forests, and their abundant litter results in a high input of organic matter to the soil, which is consistent with the results of previous studies (Wang et al., 2008; Shi and Cui, 2010; Lou et al., 2021). Soil humus is a substance formed by organic matter, such as plant residues, microorganisms, and other biological residues. Its content and quality have important effects on soil nutrient cycling and stability. In this study, the P soil has the lowest electrical conductivity, indicating the lowest salt content. As salinity increases, the diversity of bacterial and archaeal communities in desert soils gradually decreases (Zhang K. P. et al., 2019). The MBC, MBN, and MBP contents in the soil of P and S were significantly

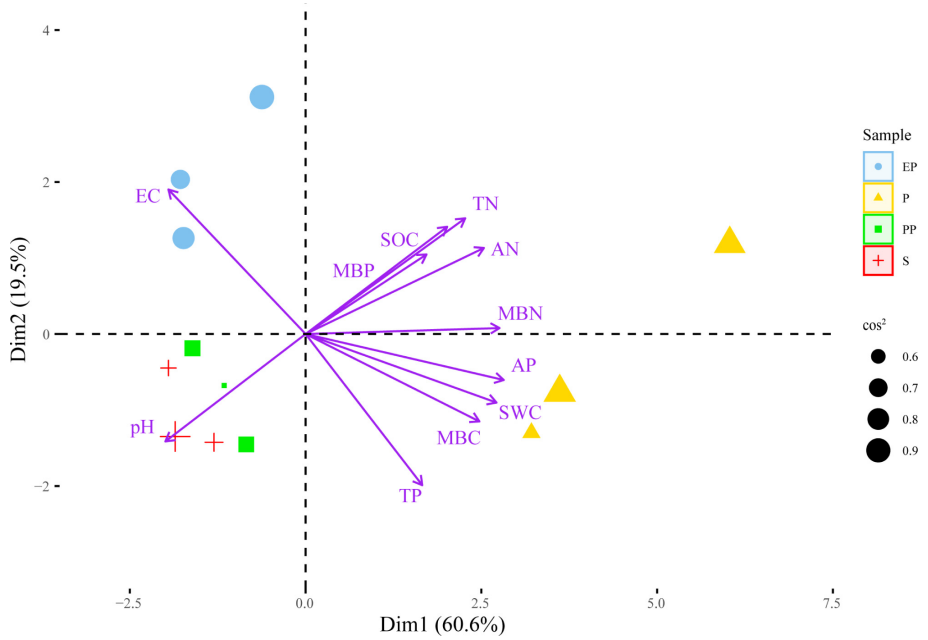

FIGURE 4
Principal component analysis of soil environment and bacterial community structure in different types of farmland shelterbelts.

higher than those in PP and EP. The activity and quantity of soil microorganisms can indirectly promote an increase soil nutrient content (Wang et al., 2015), which may lead to the differences in soil nutrient contents among different tree species. The spatial distribution of the biomass of the main roots of *Populus alba* var. *pyramidalis* Bunge tends to concentrate near soil surface (Zhao et al., 2018), where a thick layer of litter covers the ground, both of which contribute to an increase in soil nutrient content. Consequently, P soil exhibits the highest nutrient content, consistent with the results of Ren et al. (2016) and Yang et al. (2018).

TABLE 5 Load matrix of principal components.

	Dim.1	Dim.2	Dim.3
SOC	0.681	0.478	0.525
TP	0.561	-0.673	0.253
TN	0.768	0.515	0.376
AP	0.954	-0.205	-0.161
AN	0.858	0.383	0.281
pH	-0.675	-0.478	0.408
EC	-0.660	0.644	-0.079
SWC	0.919	-0.305	-0.085
MBC	0.837	-0.389	-0.090
MBP	0.582	0.354	-0.636
MBN	0.934	0.027	-0.138
Eigenvalue	6.663	2.150	1.198
Contribution rate/%	60.572	19.543	10.890
Cumulative contribution rate/%	60.572	80.115	91.004

4.2 The impact of different types of farmland shelterbelts on soil microbial communities

Studying the structure and function of soil microbial communities is of great significance for deepening our understanding in the mechanisms that farmland shelterbelt ecosystems respond to environmental changes (Grosso et al., 2018). The diversity of soil microbial communities in forest land reflects their direct connection with vegetation cover, soil characteristics, and land use types (Gunina et al., 2017). In this study, the number of OTU in composite farmland shelterbelts (PP, EP) was 785 and 824, respectively, while in single-species farmland shelterbelts (P, S), it was 801 and 937, respectively. Composite farmland shelterbelts did not show a significant advantage in microbial diversity (Song et al., 2020). This may be because soil bacterial diversity is not directly related to plant diversity (Johnson et al., 2003), but rather depends more on plant specificity (Porazinska et al., 2003; Eisenhauer et al., 2010; Gunina et al., 2017). The study found significant differences in the Shannon index among the four types of farmland shelterbelts, while the Simpson index showed no significant difference. Additionally, the ACE and Chao1 indices of P were higher than those of the other three types of farmland shelterbelts. This indicates that the richness of soil microbial communities and the relative proportions of species

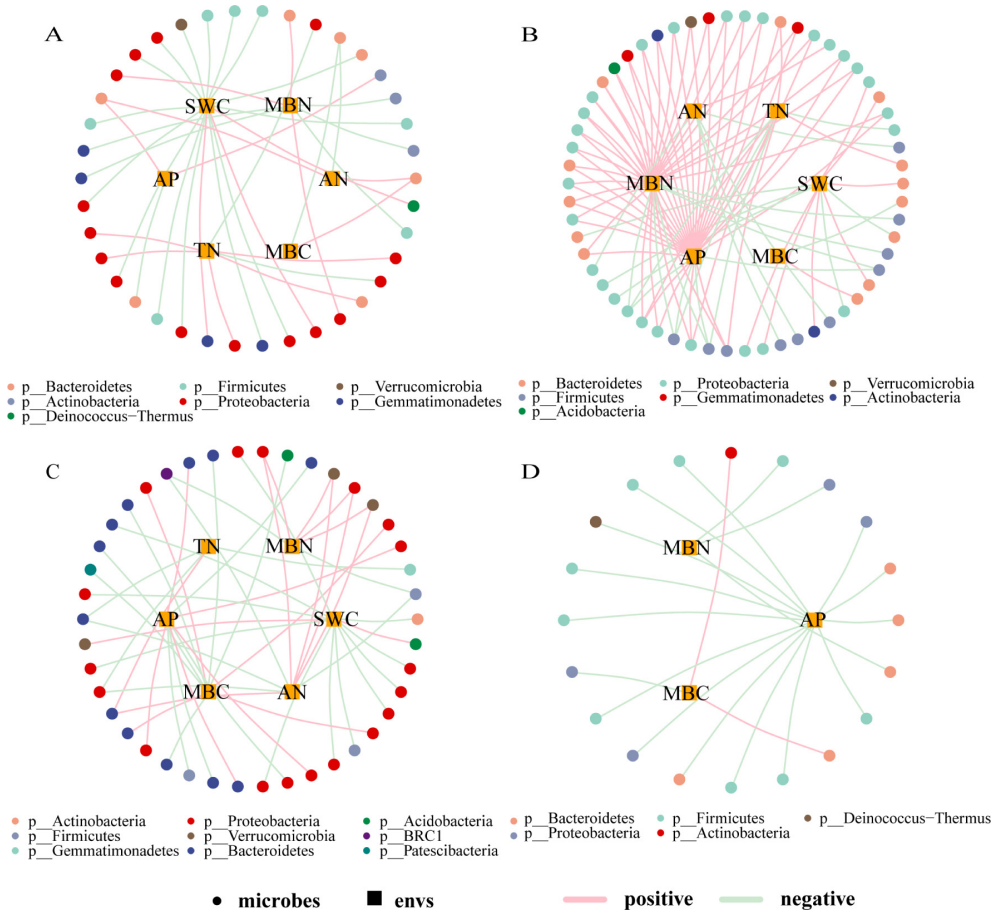

FIGURE 5
Correlation network between soil microbial species and environmental factors in different types of shelterbelts forests **(A)**: PP; **(B)**: EP; **(C)**: P; **(D)**: S. As shown in the legend, the circular nodes are species (outer circle), the square nodes are environmental factors (inner circle), the circular nodes of different colors represent genera at different gate levels, and the line colors represent correlations, with pink being positive and light green being negative.

have undergone significant changes in different types of farmland shelterbelt ecosystems, but the dominant species are similar.

In this study, the Proteobacteria was the dominant phylum in all four types of farmland shelterbelts, which is consistent with the results of a study on artificial farmland shelterbelts in the wind and sand area of northwest Liaoning Province (Zhang, 2020). Proteobacteria have the characteristics of rapid growth and tolerance to environmental changes, including changes in pH, temperature, and strong organic degradation ability. They also form mutualistic symbiotic relationships with other microorganisms, giving them a competitive advantage in soil, hence becoming the dominant phylum. At the phylum level, only the Verrucomicrobia, Acidobacteria, and Planctomycetes in P were significantly higher than the other three types of farmland shelterbelts. Verrucomicrobia has the ability to degrade cellulose and other complex carbohydrates (Nixon et al., 2019). Acidobacteria are often involved in the decomposition of plant exudates, insect remains, and dead branches and leaves in the soil (Liu et al., 2014; Wu et al., 2024), both of which contribute to the degradation of *Populus alba* var. *pyramidalis* Bunge litter. Planctomycetes promote nitrogen biogeochemical cycling (Wei et al., 2020), which positively affects nitrogen cycling and nutrient accumulation in P soils. All three benefits to the effective decomposition of litter, nutrients release and the maintenance of soil nutrient balance, providing a more favorable environment for microbial growth and forming a beneficial cycle. At the genus level, only the genus *Palleronia* in EP was significantly higher than in the other three types of farmland shelterbelts. It belongs to the Proteobacteria and exhibits good tolerance to a wide range of salinities, showing excellent adaptability (Martínez-Checa et al., 2005). The lower SWC and higher EC in EP soils may be the reasons for this result.

4.3 Influence factors of soil bacterial community characteristics in different types of farmland shelterbelts

Resource availability and habitat quality have significant impacts on bacterial community diversity (Yergeau et al., 2015; Wang et al., 2016). In this study, the relationship between soil microbial species and environmental factors showed significant differences among four types of farmland shelterbelts. P soils had higher levels of TN, AP, AN, SWC, MBC, and MBN, S soils had higher levels of AP, MBC,

and MBN, and PP soils had higher levels of TN, AP, AN, SWC, and MBC (Table 2). Better soil conditions will weaken the environmental filtration (Zhou et al., 2014), reducing the dependence of species on the environment. Therefore, the correlations between microbial species and environmental factors in P, S, and PP soils were relatively simple. In contrast, more correlations were observed in the microbial species-environmental factor network in EP soil, which mainly involved SWC, MBN, and AP. Compared to other types, EP soil had lower levels of SWC, MBN, and AP, which could reduce microbial growth, maintenance, and survival rates (Marschner et al., 2001). Therefore, the microbial species in EP soil became more dependent on environmental factors, exhibiting a more complex correlation. This suggests that changes in soil bacterial communities are constrained by forest environment conditions (Gunina et al., 2017), and resource and habitat quality factors play important driving roles in regulating bacterial community diversity.

5 Conclusion

In this study, we comprehensively investigated the impact of different types of farmland shelterbelts on soil, and found that different tree species not only caused changes in soil properties but also influenced soil bacterial communities. In the four different types of farmland shelterbelts, the P soil nutrient content and bacterial diversity were the highest. At the same time, we observed that soil bacterial communities were regulated by soil properties. Soil TN, AP, AN, SWC, MBC, and MBN had a notable impact on bacterial community structure. Significant differences in Verrucomicrobia, Acidobacteria, Planctomycetes, and *Palleronia* were observed among different types of farmland shelterbelts. Due to the complicated effects of tree species and soil properties on soil bacterial community changes, it is difficult to distinguish the pure effects of each factor. Therefore, we conclude that the changes in soil bacterial communities are a comprehensive reflection of soil properties and tree species effects.

Data availability statement

The datasets presented in this study can be found in online repositories. The names of the repository/repositories and accession number(s) can be found below: https://www.ncbi.nlm.nih.gov/, PRJNA1123072.

Author contributions

CT: Writing – original draft, Writing – review & editing, Data curation, Formal analysis, Methodology. XW: Writing – review & editing, Data curation, Methodology, Project administration, Resources. BB: Methodology, Writing – review & editing. XY: Writing – review & editing, Data curation. QY: Writing – review & editing, Formal analysis. XTW: Writing – review & editing, Investigation.

Funding

The author(s) declare financial support was received for the research, authorship, and/or publication of this article. This work was financially supported by the Xinjiang Uygur Autonomous Region Education Department Basic Scientific Project (No. XJEDU2023P005), Sciences Foundation of Xinjiang Uygur Autonomous Region (No. 2024D01C32), National Natural Science Foundation of China (No. 32001145), 2024 Xinjiang Uygur Autonomous Region Postdoctoral Funding Project.

Acknowledgments

The authors would like to express sincere gratitude to Xueying Wang, Pengqi Wang, and Yuanting Gu for their valuable assistance with the experiments.

Conflict of interest

The authors declare that the research was conducted in the absence of any commercial or financial relationships that could be construed as a potential conflict of interest.

Publisher's note

References

Bao, S. D. (2000). *Agricultural chemical analysis of soil. 3ed* (Beijing: China Agricultural Press).

Bao, Y. H., Li, H. Y., and Zhao, H. F. (2012). Effect of shelterbelts on winter wheat yields in sanded farmland of north-western Shandong province, China. *J. Food Agric. Environment.* 10, 1399–1403.

Breulmann, M., Schulz, E., Weißhuhn, K., and Buscot, F. (2012). Impact of the plant community composition on labile soil organic carbon, soil microbial activity and community structure in semi-natural grassland ecosystems of different productivity. *Plant Soil.* 352, 253–265. doi: 10.1007/s11104-011-0993-6

Cai, L. H., Hou, Z. A., Bao, J. P., Feng, W. G., Chen, L., and Gong, W. H. (2013). Analysis of the current status and trends of soil nutrients in the Aral reclamation area. *J. Agric. Reclamation Sci. Xinjiang.* 36, 60–62.

Cao, Q. Q., Li, J. R., Wang, G., Wang, D., Xin, Z. M., Xiao, H. J., et al. (2021). On the spatial variability and influencing factors of soil organic carbon and total nitrogen stocks in a desert oasis ecotone of northwestern China. *Catena.* 206, 105533. doi: 10.1016/j.catena.2021.105533

Cerdà, A., Franch-Pardo, I., Novara, A., Sannigrahi, S., and Rodrigo-Comino, J. (2022). Examining the effectiveness of catch crops as a nature-based solution to

mitigate surface soil and water losses as an environmental regional concern. *Earth Syst. Environment.* 6, 29–44. doi: 10.1007/s41748-021-00284-9

Chen, D., Wei, W., and Chen, L. D. (2017). Effects of terracing practices on water erosion control in China: A meta-analysis. *Earth-Science Rev.* 173, 109–121. doi: 10.1016/j.earscirev.2017.08.007

Deng, J. J., Zhang, Y., Yin, Y., Zhu, X., Zhu, W. X., and Zhou, Y. B. (2019a). Comparison of soil bacterial community and functional characteristics following afforestation in the semi-arid areas. *PeerJ.* 7, E7141. doi: 10.7717/peerj.7141

Deng, J. J., Zhou, Y. B., Yin, Y., Wei, Y. W., Qin, S. J., and Zhu, W. X. (2019b). Soil bacterial community structure characteristics in coniferous forests of montane regions of eastern Liaoning province, China. *Acta ECOLOGICA SINICA.* 39, 997–1008. doi: 10.5846/stxb201803090471

Edwards, J., Johnson, C., Santos-Medellín, C., Lurie, E., Podishetty, N. K., Bhatnagar, S., et al. (2015). Structure, variation, and assembly of the root-associated microbiomes of rice. *Proc. Natl. Acad. Sci.* 112, E911–E920. doi: 10.1073/pnas.1414592112

Eisenhauer, N., Beßler, H., Engels, C., Gleixner, G., Habekost, M., Milcu, A., et al. (2010). Plant diversity effects on soil microorganisms support the singular hypothesis. *Ecology.* 91, 485–496. doi: 10.1890/08-2338.1

Fang, H. Y. (2021). Quantifying farmland shelterbelt impacts on catchment soil erosion and sediment yield for the black soil region, Northeastern China. *Soil Use Management.* 37, 181–195. doi: 10.1111/sum.12591

Fang, X. M., Yu, D. P., Zhou, W. M., Zhou, L., and Dai, L. M. (2016). The effects of forest type on soil microbial activity in Changbai Mountain, Northeast China. *Ann. For. Science.* 73, 473–482. doi: 10.1007/s13595-016-0540-y

Grosso, F., Iovieno, P., Alfani, A., and De Nicola, F. (2018). Structure and activity of soil microbial communities in three mediterranean forests. *Appl. Soil Ecology.* 130, 280–287. doi: 10.1016/j.apsoil.2018.07.007

Gunina, A., Smith, A. R., Godbold, D. L., Jones, D. L., and Kuzyakov, Y. (2017). Response of soil microbial community to afforestation with pure and mixed species. *Plant Soil.* 412, 357–368. doi: 10.1007/s11104-016-3073-0

Guo, K. Y., Feng, L., Li, Y., and Xu, W. L. (2023). Analysis of improvement saline-alkali land of Alar reclamation area in the upper reaches of Tarim river by *Lycium ruthenicum*. *Soil AND FERTILIZER Sci. IN CHINA.* 12, 70–77.

Hacquard, S., and SChadt, C. W. (2015). Towards a holistic understanding of the beneficial interactions across the *populus* microbiome. *New Phytologist.* 205, 1424–1430. doi: 10.1111/nph.13133

Haddaway, N. R., Brown, C., Eales, J., Eggers, S., Josefsson, J., Kronvang, B., et al. (2018). The multifunctional roles of vegetated strips around and within agricultural fields. *Environ. Evidence.* 7, 14. doi: 10.1186/s13750-018-0126-2

Iovieno, P., Alfani, A., and Bååth, E. (2010). Soil microbial community structure and biomass as affected by *pinus pinea* plantation in two mediterranean areas. *Appl. Soil Ecology.* 45, 56–63. doi: 10.1016/j.apsoil.2010.02.001

Jan, L., Lena, A., Gunnar, B., Knut, E., Glòria Palarès, V., and Ingvar, S. (2014). Land-use intensification and agroforestry in the Kenyan highland: Impacts on soil microbial community composition and functional capacity. *Appl. Soil Ecology.* 82, 93–99. doi: 10.1016/j.apsoil.2014.05.015

Johnson, D., Booth, R. E., Whiteley, A. S., Bailey, M. J., Read, D. J., Grime, J. P., et al. (2003). Plant community composition affects the biomass, activity and diversity of microorganisms in limestone grassland soil. *Eur. J. Soil Science.* 54, 671–678. doi: 10.1046/j.1351-0754.2003.0562.x

Kong, T. W., Wang, S., and Liu, B. H. (2022). Effects of farmland shelterbelt transformation on soil aggregate characteristics and soil erodibility. *J. Cent. South Univ. Forestry Technology.* 11, 128–140. doi: 10.14067/j.cnki.1673-923x.2022.11.014

Krichen, K., Vilagrosa, A., and Chaieb, M. (2017). Environmental factors that limit stipa tenacissima l. Germination and establishment in mediterranean arid ecosystems in a climate variability context. *Acta Physiologiae Plantarum.* 39, 175. doi: 10.1007/s11738-017-2475-9

Li, P., Shi, R. J., Zhao, F., Yu, J. H., Cui, X. Y., Hu, J. G., et al. (2019). Soil bacterial community structure and predicted functions in the larch forest during succession at the Greater Khingan Mountains of Northeast China. *Chin. J. Appl. Ecology.* 30, 95–107. doi: 10.13287/j.1001-9332.201901.010

Liu, J. J., Sui, Y. Y., Yu, Z. H., Shi, Y., Chu, H. Y., Jin, J., et al. (2014). High throughput sequencing analysis of biogeographical distribution of bacterial communities in the black soils of Northeast China. *Soil Biol. Biochem.* 70, 113–122. doi: 10.1016/j.soilbio.2013.12.014

Liu, P., Qiu, Y., Wang, Y. T., Wei, Z. P., Fan, J. G., and Cao, B. H. (2019). Seasonal dynamics of soil microbial biomass in typical shelterbelts on the Bohai muddy coast. *Acta ECOLOGICA SINICA.* 39, 363–370.

Liu, R. S., and Wang, D. M. (2021). Soil nutrients and ecostoichiometric characteristics of different plantations in the alpine region of the loess plateau. *J. OF Beijing FORESTRY UNIVERSITY.* 43, 88–95.

Lou, B. Y., Wang, Y. D., Yan, J. S., and Askar, A. (2021). Characteristics of soil ecological stoichiometry of different tree species in sub-frigid desert steppe. *ARID ZONE Res.* 38, 1385–1392. doi: 10.13866/j.azr.2021.05.20

Luca, E. F., Chaplot, V., Mutema, M., Feller, C., Ferreira, M. L., Cerri, C. C., et al. (2018). Effect of conversion from sugarcane preharvest burning to residues green-trashing on SOC stocks and soil fertility status: Results from different soil conditions in Brazil. *Geoderma.* 310, 238–248. doi: 10.1016/j.geoderma.2017.09.020

Marschner, P., Yang, C. H., Lieberei, R., and Crowley, D. E. (2001). Soil and plant specific effects on bacterial community composition in the rhizosphere. *Soil Biol. Biochem.* 33, 1437–1445. doi: 10.1016/s0038-0717(01)00052-9

Martínez-Checa, F., Quesada, E., Martínez-Cánovas, M. J., Llamas, I., and Béjar, V. (2005). *Palleronia marisminoris* gen. Nov., sp. Nov., a moderately halophilic, exopolysaccharide-producing bacterium belonging to the 'alphaproteobacteria', isolated from a saline soil. *Int. J. Systematic Evolutionary Microbiol.* 55, 2525–2530. doi: 10.1099/ijs.0.63906-0

Nixon, S. L., Daly, R. A., Borton, M. A., Solden, L. M., Welch, S. A., Cole, D. R., et al. (2019). Genome-resolved metagenomics extends the environmental distribution of the Verrucomicrobia phylum to the deep terrestrial subsurface. *mSphere.* 4, E00613–E00619. doi: 10.1128/msphere.00613-19

Porazinska, D. L., Bardgett, R. D., Blaauw, M. B., Hunt, H. W., Parsons, A. N., Seastedt, T. R., et al. (2003). Relationships at the aboveground-belowground interface: Plants, soil biota, and soil processes. *Ecol. Monographs.* 73, 377–395. doi: 10.1890/0012-9615(2003)073[0377:rataip]2.0.co;2

Prescott, C. E., and Grayston, S. J. (2013). Tree species influence on microbial communities in litter and soil: Current knowledge and research needs. *For. Ecol. Management.* 309, 19–27. doi: 10.1016/j.foreco.2013.02.034

Qiu, Y., Liu, P., Wei, Z. P., Fan, J. G., Xing, X. Y., Li, R. P., et al. (2017). Effects of four typical shelterbelts on soil microbial biomass, enzyme activities and soil nutrient in the Bohai muddy coast. *Chin. J. Soil Science.* 48, 1119–1125. doi: 10.19336/j.cnki.trtb.2017.05.14

Ren, C. J., Zhao, F. Z., Kang, D., Yang, G. H., Han, X. H., Tong, X. G., et al. (2016). Linkages of C: N: P stoichiometry and bacterial community in soil following afforestation of former farmland. *For. Ecol. Management.* 376, 59–66. doi: 10.1016/j.foreco.2016.06.004

Rodrigues, R., Araújo, R., Costa, C. D., Lima, A., Oliveira, M., Santos, F., et al. (2015). Soil microbial biomass in an agroforestry system of Northeast Brazil. *Trop. Grasslands - Forrajes Tropicales.* 3, 41. doi: 10.17138/tgft(3)41-48

Shi, J., and Cui, L. L. (2010). Soil carbon change and its affecting factors following afforestation in China. *Landscape Urban Planning.* 98, 75–85. doi: 10.1016/j.landurbplan.2010.07.011

Shi, X. L., Li, Y., and Deng, R. X. (2016). Evaluation method for effect of farmland shelterbelts on crop yield based on RS and GIS. *Trans. Chin. Soc. Agric. Eng. (Transactions CSAE).* 32, 175–181.

Song, Z. C., Wang, H., Liu, S. R., Hu, J. J., Ming, A. G., Chen, H., et al. (2020). Relationship between tree species richness and soil microbial diversity and community composition in a mixed planted south subtropical forest. *Acta ECOLOGICA SINICA.* 40, 8265–8273.

Wang, D., Xiao, H. J., Xin, Z. M., Jia, H. T., and Cao, Q. Q. (2020). Effects of different configurations of farmland shelterbelt system on spatital variation of soil moisture content. *J. Soil Water Conserv.* 34, 223–230. doi: 10.13870/j.cnki.stbcxb.2020.05.031

Wang, Q. K., Wang, S. L., and Huang, Y. (2008). Comparisons of litterfall, litter decomposition and nutrient return in a monoculture *Cunninghamia lanceolata* and a mixed stand in southern China. *For. Ecol. Management.* 255, 1210–1218. doi: 10.1016/j.foreco.2007.10.026

Wang, X. G., Li, H., Bezemer, T. M., and Hao, Z. Q. (2016). Drivers of bacterial beta diversity in two temperate forests. *Ecol. Res.* 31, 57–64. doi: 10.1007/s11284-015-1313-z

Wang, X. Q., Wang, C. K., and Han, Y. (2015). Effects of tree species on soil organic carbon density: A common garden experiment of five temperate tree species. *Chin. J. Plant Ecology.* 39, 1033–1043. doi: 10.17521/cjpe.2015.0100

Wang, Y. N., Hu, Y. G., Wang, Z. R., and Li, C. S. (2021). Impacts of reclamation on salinization desert soil microbial community: a case study of Alar oasis. *J. OF DESERT Res.* 41, 126–137.

Wei, Y. R., Wang, Y. J., Ma, Q. L., Li, Q. X., Li, C. H., Li, X., et al. (2020). Effects of silt particles, ammonia nitrogen and water content on structural and functional differentiation of Plantomycetes communities. *Microbiol. China.* 47, 2732–2745. doi: 10.13344/j.microbiol.China.200338

Wu, H. W., Cui, H. L., Fu, C. X., Li, R., Qi, F. Y., Liu, Z. L., et al. (2024). Unveiling the crucial role of soil microorganisms in carbon cycling: A review. *Sci. Total Environment.* 909, 168627. doi: 10.1016/j.scitotenv.2023.168627

Wu, J. S., Lin, Q. M., Huang, Q. Y., and Xiao, H. A. (2006). *Method and application of soil microbial biomass measurement* (Beijing: China Meteorological Press).

Xu, L., and Sun, H. Y. (2023). Research on spatial variation and influencing factors of water and salt in Aksu River Basin in Alar region. *J. Shandong Agric. Univ. (Natural Sci. Edition).* 54, 577–581.

Yang, N., Ji, L., Salahuddin,, Yang, Y. C., and Yang, L. X. (2018). The influence of tree species on soil properties and microbial communities following afforestation of abandoned land in Northeast China. *Eur. J. Soil Biol.* 85, 73–78. doi: 10.1016/j.ejsobi.2018.01.003

Yergeau, E., Bell, T. H., Champagne, J., Maynard, C., Tardif, S., Tremblay, J., et al. (2015). Transplanting soil microbiomes leads to lasting effects on willow growth, but not on the rhizosphere microbiome. *Front. Microbiol.* 6. doi: 10.3389/fmicb.2015.01436

Zhang, J., Xin, Y., and Zhao, Y. S. (2019). Diversity and functional potential of soil bacterial communities in different types of farmland shelterbelts in mid-western Heilongjiang, China. *Forests.* 10, 1115. doi: 10.3390/f10121115

Zhang, K. P., Shi, Y., Cui, X. Q., Yue, P., Li, K. H., Liu, X. J., et al. (2019). Salinity is a key determinant for soil microbial communities in a desert ecosystem. *mSystems*. 4, 1–11. doi: 10.1128/msystems.00225-18

Zhang, Y. (2020). *Study on soil microbial structure and functional characteristics of three plantation forests in the semi-arid areas of northwest Liaoning* (Master: Shenyang Agricultural University) doi: 10.27327/d.cnki.gshnu.2020.000466

Zhao, Y. M., Lei, Y. C., Yang, W. B., Hao, Y. G., Huang, Y. R., Dong, X., et al. (2018). Spatial distribution of main root biomass of farmland shelterbelt. *J. Agric. Sci. Technology.* 9, 86–94. doi: 10.13304/j.nykjdb.2017.0694

Zhou, J. Z., Deng, Y., Zhang, P., Xue, K., Liang, Y. T., Van Nostrand, J. D., et al. (2014). Stochasticity, succession, and environmental perturbations in a fluidic ecosystem. *Proc. Natl. Acad. Sci.* 111, E836–E845. doi: 10.1073/pnas.1324044111

frontiers | Frontiers in Plant Science

TYPE Original Research
PUBLISHED 27 November 2024
DOI 10.3389/fpls.2024.1470063

OPEN ACCESS

EDITED BY
Xiao-Dong Yang,
Ningbo University, China

REVIEWED BY
Xue Wu,
Xinjiang University, China
Lixian Yao,
South China Agricultural University, China

*CORRESPONDENCE
Wensheng Liu
Liuwsairr@163.com

†These authors have contributed equally to this work

RECEIVED 25 July 2024
ACCEPTED 28 October 2024
PUBLISHED 27 November 2024

CITATION
Pan G, Hu J, Zi Z, Wang W, Li X, Xu X and Liu W (2024) Arbuscular mycorrhizal fungi alleviate Mn phytotoxicity by altering Mn subcellular distribution and chemical forms in *Lespedeza davidii*.
Front. Plant Sci. 15:1470063.
doi: 10.3389/fpls.2024.1470063

Arbuscular mycorrhizal fungi alleviate Mn phytotoxicity by altering Mn subcellular distribution and chemical forms in *Lespedeza davidii*

Gao Pan[1,2†], Jiayao Hu[1,2†], Zhen Zi[1], Wenying Wang[1,2], Xinhang Li[1,2], Xiaoli Xu[1,2] and Wensheng Liu[1,2*]

[1]College of Life and Environmental Sciences, Central South University of Forestry and Technology, Changsha, China, [2]Hunan Research Center of Engineering Technology for Utilization of Environmental and Resources Plant, Central South University of Forestry and Technology, Changsha, China

Introduction: Arbuscular mycorrhizal fungi (AMF) can relieve manganese (Mn) phytotoxicity and promote plant growth under Mn stress, but their roles remain unclear.

Methods: In this study, *Lespedeza davidii* inoculated with or without AMF (*Glomus mosseae*) under different Mn concentrations (0 mmol/L, 1 mmol/L, 5 mmol/L, 10 mmol/L, and 20 mmol/L) was cultivated via a pot experiment, and plant biomass, physiological and biochemical characteristics, manganese absorption, subcellular distribution, and chemical forms of Mn were examined.

Results: The results showed that root biomass, stem biomass, leaf biomass, and total individual biomass decreased under high Mn concentrations (above 10 mmol/L), and the inoculated plants had higher biomass than the uninoculated plants. With the increasing Mn concentration, the contents of soluble sugar, soluble protein, free proline, superoxide dismutase (SOD), peroxidase (POD), and catalase (CAT) increased first and then decreased, while the malondialdehyde (MDA) content increased. The contents of soluble sugar, soluble protein, free proline, SOD, POD, and CAT in the inoculated group were higher than those in the uninoculated group at the Mn concentration of 20 mmol/L. The content of MDA in the inoculated plants was lower than that in the uninoculated plants. AMF inoculation enriched most of the manganese in the root system when compared with the non-mycorrhizal treatment. Subcellular distribution of Mn indicated that most of the Mn ions were stored in the cell wall and the vacuoles (the soluble fractions), and the proportion of Mn content in the cell wall components and the vacuole components in leaves in the inoculated group was higher than that in the uninoculated group. Furthermore, the proportions of Mn extracted using ethanol and deionized water in the uninoculated group in stems and roots were higher than those in the inoculated group, which suggested that AMF could convert Mn into inactive forms.

10.3389/fpls.2024.1470063

Discussion: The present study demonstrated that AMF could improve the resistance of *L. davidii* to Mn toxicity by increasing the activity of antioxidant enzymes and altering the subcellular distribution and chemical forms of Mn.

KEYWORDS

arbuscular mycorrhizal fungi, manganese stress, *Lespedeza davidii*, physiological characteristics, subcellular distribution, chemical forms

1 Introduction

Manganese (Mn) is an important essential trace element for plants, as it is involved in plant photosynthesis, enzymatic reactions, and redox activities. However, high concentrations of Mn would lead to destructed chloroplast structure, reduced plant photosynthesis, and inhibited growth for plants (Bai et al., 2021; Lin et al., 2021). They would even harm human health through the food chain (Santos et al., 2017; Luo et al., 2020). However, Mn is also one of the most widely used heavy metals in industry, manganese ore has been exploited for a long time, and large areas of manganese mine wasteland bring heavy Mn pollution. This seriously influences the normal production and living of people in these areas. Therefore, it is urgent to control Mn pollution in these areas as soon as possible.

Of the heavy metal (HM) treatment methods, arbuscular mycorrhizal fungi (AMF)-favored phytoremediation is the most economical and persistent technology with less secondary pollutant effects, which has received much attention in recent years (Riaz et al., 2021). AMF are a kind of widespread soil microorganism, which can coexist with more than 80% of terrestrial plants. These microorganisms have a good symbiotic relationship with plants. They could contribute to increasing plant metal tolerance and improving plant growth performance (Amir et al., 2019; Marro et al., 2022). In addition, AMF can enhance the uptake of mineral nutrition and directly affect the absorption and accumulation of heavy metals in plants under heavy metal stress (Garcia et al., 2018; Boorboori and Zhang, 2022; Riaz et al., 2021). Moreover, AMF (such as *Glomus mosseae*) can widely exist in real-scale wasteland habitats around the world (e.g., USA, China, Mexico, Portugal, and Algeria) (Pan et al., 2023b). Therefore, AMF have a wide prospect for phytoremediation of contaminated soils (Wang et al., 2022).

Plant growth under stress reflects the adaptability of plants to the environment and their bioremediation capability. Appropriate amounts of Mn would contribute to plant growth and development, while excessive amounts of Mn would markedly impair plant growth and reduce plant biomass (Xiao et al., 2020). In addition, Mn accumulation within plants plays a key role in plant survival under stress. Higher concentrations of Mn would easily accumulate in plants from soils and cause damage. AMF could promote the growth of host plants by reducing heavy metal concentrations in shoots and roots (Zhang et al., 2019; Pan et al., 2023a). Understanding the enrichment characteristics of Mn is key to revealing the adaptive mechanism.

In response to high amounts of Mn, plants produce an excessive quantity of reactive oxygen species (ROS), which may result in the malfunctioning of plant cells (Han et al., 2021; Kaya et al., 2022). To prevent the cells from oxidative damage, the defense proteins [e.g., superoxide dismutase (SOD), peroxidase (POD), and catalase (CAT)] would enhance the capacity of plants to combat excessive ROS. AMF could demonstrate high activities of antioxidant enzymes to alleviate oxidative stress and decrease the contents of malondialdehyde (MDA) (Wang et al., 2021a). In addition to the enzymatic defense mechanisms, osmoregulation substances, such as soluble sugar, soluble protein, and free proline, would also be produced to maintain the water balance and energy supply in cells and to perform the protective function.

Subcellular distribution and chemical forms of heavy metal in plants are two internal mechanisms for plants that impart protection against heavy metal toxicity (Wang et al., 2021b). Chelation and compartmentalization play essential roles in alleviating Mn toxicity in plants. Deposition in the cell wall and vacuolar (the soluble fraction) sequestration could prevent HM from entering more vulnerable sites in cells. In addition, Mn would distribute in different chemical forms once taken up by plants. Plants could reduce Mn migration and toxicity by converting highly toxic chemical forms of Mn into less toxic chemical forms in plants. Therefore, investigating the subcellular distribution and chemical forms of Mn in plants was a key step to revealing the role of AMF in plants under stress.

Lespedeza davidii is a shrub of *Lespedeza* in Fabaceae, which is widely distributed in southern China (Zheng et al., 2011b). This plant has a strong ability for biological nitrogen fixation and soil and water conservation (Wang et al., 2021b; Rai et al., 2021). It was reported that the species of Fabaceae could decrease the injury of heavy metals in soybean rhizobia (Doty, 2008). As a Fabaceae plant, *L. davidii* has strong heavy metal resistance. It can grow normally in a variety of habitats. The investigation on the abandoned manganese tailings of Xiangtan, Hunan Province, showed that *L. davidii* grows well and can normally blossom and bear fruits in this area, whose soil Mn concentration reached 52,319 mg/kg. It indicated that this plant has a strong tolerance to Mn pollution (Hu et al., 2022). Therefore, the plant is an important restoration candidate for the manganese mine area. At present, relevant

research on *L. davidii* mainly focuses on its medicinal value (Li and Wang, 1989; Liang and Yan, 2018) and tolerance to Pb stress (Zheng et al., 2011a). The adaptive mechanism of this plant inoculated with AMF under Mn stress has not been systematically studied, which limited the further application of the plant.

In the present study, seedlings of *L. davidii* were cultivated under different Mn concentrations; whether or not to inoculate with AMF, plant growth, physiological and biochemical characteristics, enrichment characteristics, subcellular components, and chemical morphology of Mn were measured. The aim of this study is 1) to determine whether AMF can affect the plant growth of *L. davidii* under Mn stress, 2) to reveal the physiological mechanism of *L. davidii* to Mn stress under the condition of AMF inoculation, and 3) to illustrate whether AMF can regulate the migration and distribution of Mn and its chemical state transformation, and if so, what the regulatory mechanism is.

2 Materials and methods

2.1 Material provision

Seeds of *L. davidii* were collected in Xiangtan manganese tailings, Hunan Province, in November 2019 (28°03′E, 112°55′N). The field investigation revealed that the height of *L. davidii* was approximately 1.4 m. It also showed that the plant had set many flowers and bear fruits. In the present study, over 80 well-growing individuals of *L. davidii* were selected, and their mature and plump fruits were sampled and brought back to the laboratory in cloth bags. The seeds (picked from fruits) were stored at room temperature until seed germination. The average 1000 seed weight of this plant was 9.39 g.

The AMF species [*G. mosseae* (GM)], which was highly resistant to Mn, was obtained from the Institute of Plant Nutrition, Resources and Environment, Beijing Academy of Agriculture and Forestry Sciences, China (Pan et al., 2023a). The fungi were propagated using maize as a host plant, and the mycelium, spores, colonized root fragments, and dried sand–soil were mixed to use as AMF inoculant according to Yang et al. (2014). Average spore densities were 590 per 10 g of air-dried soil.

2.2 Pot experiment

The seed germination and seedling cultivation of *L. davidii* were carried out in the greenhouse of Central Southern University of Forestry and Technology in August 2021. After the seedlings were cultivated for 0.5 years, the uniform 18-cm-tall seedlings of *L. davidii* were chosen and transferred to the pot with a height of 11 cm and a diameter of 18 cm, which was sterilized with 75% ethanol solution. Each pot was filled with 2 kg of sterilized sand mix (pure sand:perlite = 2:1), which was sterilized with high-pressure steam at 121°C for 2 h.

The pot experiment was performed in a completely randomized design with a two factorial scheme with the following variables: five Mn-added levels (0, 1, 5, 10, and 20 mg Mn kg^{-1} soil) (Pan et al., 2023a), two treatments (inoculation with or without GM), and 10 replicates in each treatment, for a total of 100 pots.

The GM inocula were applied at a rate of 5% (w/w) of the weight. The same amounts of the autoclaved inocula were added to uninoculated controls and supplemented with a filtrate obtained from the unsterilized soil solution sieved using an 11-μm sieve to provide the microbial populations accompanying the mycorrhizal fungi (Zhong et al., 2012). The Mn concentration was determined by $MnCl_2{\cdot}4H_2O$, and the same amount of distilled water was set as the control group (CK). The transplanted plants were cultured in the greenhouse (25°C–28°C) for 30 days.

During the growing period, Hoagland nutrient solution was added every 3 days. After 60 days of Mn stress, the plant growth traits, physiological and biochemical indices, Mn content, Mn subcellular components, and chemical forms of *L. davidii* were determined after harvesting.

2.3 Morphological measurements

Plant biomass was measured following plant harvest, and the individual plants were divided into three parts (root, stem, and leaf). All parts were dried for 2 h at 105°C followed by 48 h at 70°C to achieve a constant weight. The biomass of the roots, stems, and leaves of individual plants was determined using an electronic balance.

2.4 Mycorrhizal colonization measurements

To ensure that our inoculation protocol was successful, 60-day-old roots were checked using a combination of bright-field and confocal microscopy (Leica Microsystems GmbH, Wetzlar, Germany). The fresh roots were cut into fragments approximately 1 cm and then stained with 0.05% Trypan Blue according to the method of Phillips and Hayman (1970). Bright-field microscopy was used to assess mycorrhizal infection rate after the Trypan Blue staining (Phillips and Hayman, 1970). The infection rate was determined based on the microstructure of the infected *L. davidii* roots by identifying the internal hyphae, external hyphae, arbuscules, and spores. The AMF infection rate (ratio of infected roots) was quantified on 1-cm-long root segments using the grid-line intersect method under a compound microscope (40 × 10) (Giovannetti and Mosse, 1980). The results showed that the root colonization rates of plants inoculated with GM were 73% ± 2.9%.

2.5 Determination of osmoregulation substances and antioxidant systems

A leaf sample of approximately 0.2 g was ground using a mortar with liquid nitrogen, which was used to determine the physiological and biochemical indices. The activity of SOD was determined using the nitro blue tetrazolium (NBT) method. The amounts of soluble sugar content, free proline content, POD, CAT, and MDA were determined according to the methods of Gao (2000). Soluble

protein content was determined using the method of Bradford (1976) with bovine serum albumin (BSA) as a standard. All the measurements were carried out in five replicates.

2.6 Mn concentration analysis

Mn concentration was determined according to the methods of Xiao et al. (2020). The dried roots, stems, and leaves were ground using a grinder, and the fine powder was weighed and placed in a muffle furnace at 300°C for 2 h followed by 500°C for 5 h. Then, the powders were soaked in concentrated HNO_3:$HClO_4$ (7:3, v/v) using the Kjeldahl method until the samples became a clear liquid (Rao et al., 2011). The samples were diluted to a constant volume (25 mL), and the Mn concentrations were determined using inductively coupled plasma–optical emission spectroscopy (ICP-OES) (iCAP6500, Thermo Scientific, Oxford, UK). Measurements of the plant's Mn concentrations were performed in three replicates (Xiao et al., 2020). The bioconcentration factors (BCFs) were defined as the ratio of metal concentration in plant roots to that in the soil. The transport coefficient (TF) was indicated as the ratio of metal concentration in plant shoots to that in the roots.

2.7 Subcellular fraction extraction

To reveal the effects of various treatments on the distribution of Mn across different subcellular fractions, the concentrations of Mn with different subcellular compartments were determined using the gradient centrifugation technique, and cells were separated into four fractions [cell wall fraction, chloroplast and cell nuclear fraction, mitochondrial fraction, and ribosomal fraction (soluble components)] (Wang et al., 2015). Frozen plant materials were homogenized in cooled extraction buffer [50 mM Tris–HCl, 250 mM sucrose, and 1.0 mM dithioerythritol ($C_4H_{10}O_2S_2$), pH 7.5] using a chilled mortar and pestle. The homogenate was sieved through nylon cloth (80 µm), and the liquid was squeezed from the residue. The residue was washed twice with homogenization buffer; as it contained mainly cell walls and cell wall debris, it was designated as the "cell wall fraction". Then, the supernatant was moved to a new centrifuge tube and centrifuged at 2,000 ×*g* for 15 min, creating a pellet consisting of chloroplasts and cell nuclei. The supernatant was once again removed and centrifuged at 10,000 ×*g* for 20 min, creating a pellet that was considered the mitochondrial fraction. In the end, the final supernatant was considered the ribosomal fraction (including vacuoles). All steps were performed at 4°C, and the subcellular fractions were dried at 70°C to a constant weight (Wang et al., 2015).

2.8 Chemical form extraction

Chemical forms of Mn were extracted in the following order: 1) 80% ethanol, extracting inorganic Mn giving priority to nitrate/nitrite, chloride, and aminophenol manganese; 2) deionized water (d-H_2O), extracting water soluble Mn–organic acid complexes; 3) 1 M NaCl, extracting pectates and protein integrated Mn; 4) 2% acetic acid (HAc), extracting undissolved manganese phosphate; 5) 0.6 M HCl, extracting manganese oxalate; and 6) the residues (Fu et al., 2011).

Frozen tissues were homogenized in an extraction solution using a mortar and pestle, diluted at a ratio of 1:100 (w/v), and shaken for 22 h at 25°C. The homogenate was then centrifuged at 5,000 ×*g* for 10 min, obtaining the first supernatant solution in a conical beaker. The sedimentation was re-suspended twice in an extraction solution, shaken for 2 h at 25°C, and centrifuged at 5,000 ×*g* for 10 min. The supernatants of the three suspensions were then pooled. The residue was extracted with the next extraction solution in the sequence using the same procedure described above. Each pooled solution was evaporated on an electric plate at 70°C to a constant weight.

2.9 Statistical analysis

All results were presented as means ± standard deviation (SD) for the 10 replicates. Two-way ANOVA was used to test the data of *L. davidii* between different Mn concentration treatment groups and inoculation conditions, and Duncan's multiple comparison method (the significance level was set as 0.05) was used to conduct significant difference analysis between different concentrations. Statistical analyses were conducted using the SPSS 22.0 software package (SPSS, Inc., Chicago, IL, USA), and figures were created using SigmaPlot 14.0.

3 Results

3.1 Plant biomass

The two-way ANOVA showed significant and interactive effects of Mn stress and AMF inoculation on plant biomass; all the root biomass, stem biomass, leaf biomass, and total individual biomass of *L. davidii* were significantly affected by Mn concentrations and AMF inoculation ($p < 0.001$). All the root biomass, stem biomass, leaf biomass, and total individual biomass of plants in the AMF-inoculated and uninoculated plants increased first and then decreased (Figures 1A–D). Compared with the uninoculated plants, the root biomass (Figure 1A), stem biomass (Figure 1B), leaf biomass (Figure 1C), and total individual biomass (Figure 1D) of the AMF-inoculated plants were higher. The results showed that the positive effects of AMF on plant biomass compensated for the negative effect of Mn application.

3.2 Physiological characteristics

The two-way ANOVA showed that Mn stress and whether or not to inoculate with AMF had significant effects on the contents of soluble sugar, soluble protein, and free proline in the leaves of *L. davidii* (Figure 2; $p < 0.001$). With the increasing Mn concentration, the contents of soluble sugar (Figure 2A), soluble protein (Figure 2B), and free proline (Figure 2C) in *L. davidii* in the

10.3389/fpls.2024.1470063

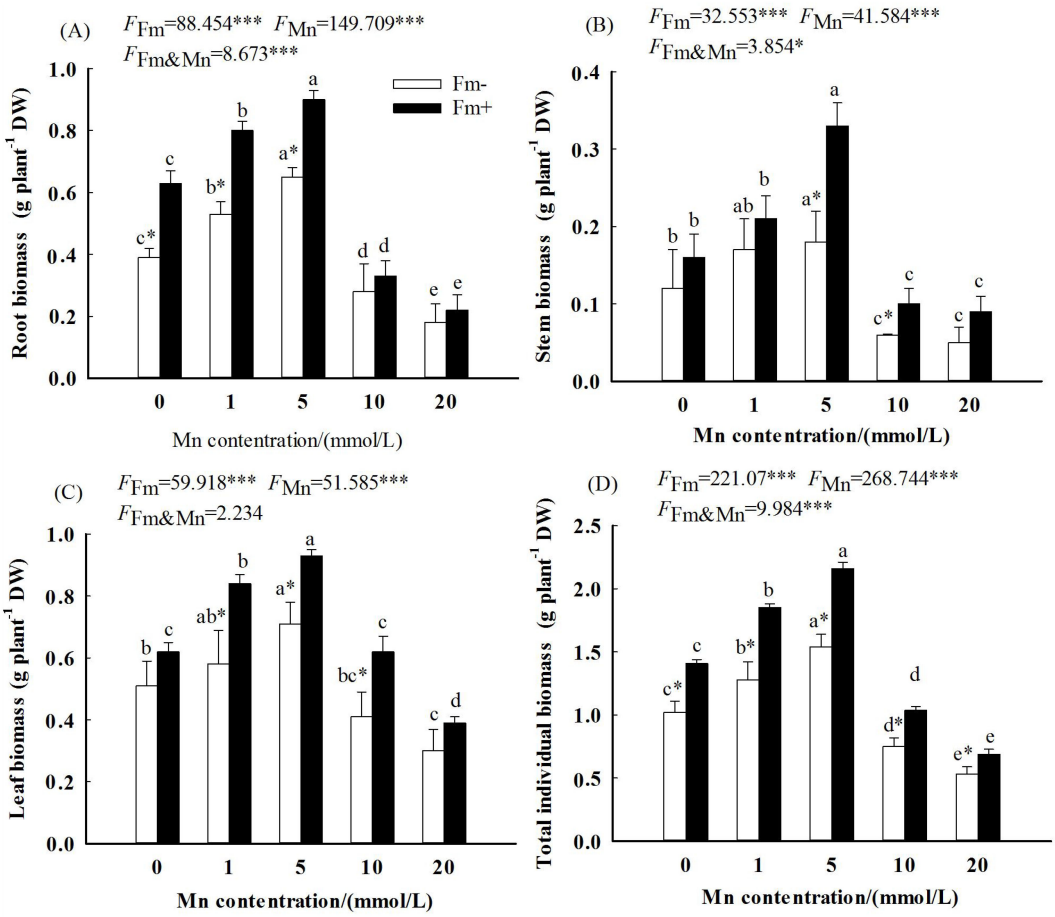

FIGURE 1
Effects of Mn treatments on stem biomass **(A)**, root biomass **(B)**, leaf biomass **(C)**, and total individual biomass **(D)** of *Lespedeza davidii* plants with AMF inoculation (Fm+) and non-inoculation (Fm–). All data show the means ± SE of 10 replicates. Values with different small letters within the same column indicate significant differences at the $p < 0.05$ level between Mn treatments. * indicates significant difference ($p < 0.05$) between AMF-inoculated plants and uninoculated plants. AMF, arbuscular mycorrhizal fungi. *** indicates highly significant difference (p<0.001).

inoculated group and the uninoculated group increased first and then decreased. The contents of soluble sugar (Figure 2A), soluble protein (Figure 2B), and free proline (Figure 2C) in the inoculated group were higher than those in the uninoculated group at the Mn concentration of 20 mmol/L, and the values of the inoculated group were respectively 2.25, 2.70, and 1.26 times those of the uninoculated group.

The two-way ANOVA showed that the effects of Mn stress and AMF inoculation on SOD, POD, and CAT activities reached a significant level ($p < 0.001$), the interaction between Mn stress and AMF inoculation on the effects on SOD activities reached a significant level ($p < 0.05$), and the effects on CAT activities reached a very significant level ($p < 0.001$), while the effects on POD activities did not reach a significant level. As the Mn concentration increased, the activities of SOD (Figure 3A), POD (Figure 3B), and CAT (Figure 3C) in the inoculated group and the uninoculated group increased first and then decreased with the increase of Mn concentration, and all decreased to the lowest values at the manganese concentration of 20 mmol/L ($p < 0.001$). The activities of SOD, POD, and CAT in the inoculated group were higher than those in the uninoculated group at the Mn concentration of 20 mmol/L. When the concentration of Mn was 20 mmol/L, the activities of SOD, POD, and CAT in the inoculated group were respectively 1.26, 1.33, and 2.94 times those of the uninoculated group.

The two-way ANOVA showed that the effects of Mn stress and whether or not to inoculate with AMF on the MDA content in *L. davidii* leaves reached a significant level ($p < 0.001$), while the interaction between Mn stress and AMF inoculation did not reach a significant level. With the increasing Mn concentration, the MDA content in *L. davidii* in the inoculated group and the uninoculated group increased (Figure 3D). When the Mn concentration was 20 mmol/L, the content of MDA in the inoculated group and the uninoculated group increased by 41.39% and 61.17%, respectively, compared with the control (Figure 3D; $p < 0.001$).

10.3389/fpls.2024.1470063

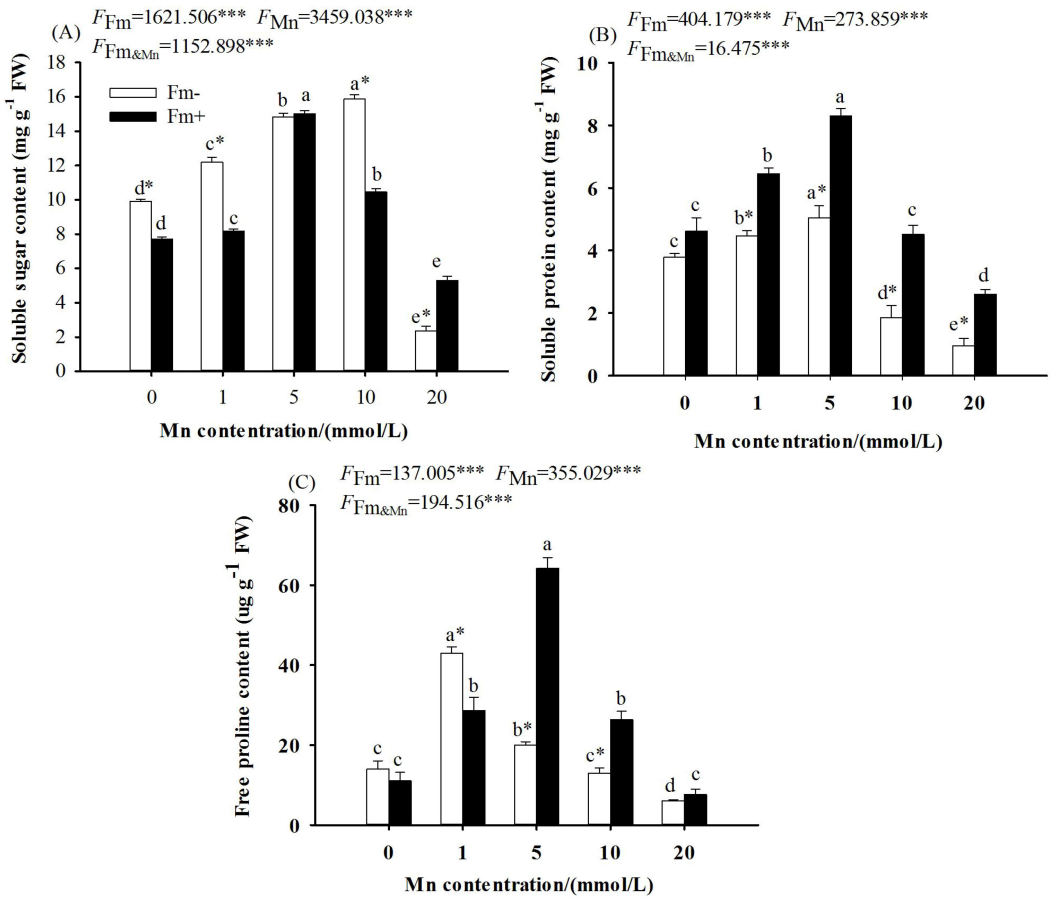

FIGURE 2
Effects of Mn treatments on the content of soluble sugar **(A)**, soluble protein **(B)**, and free proline **(C)** of *Lespedeza davidii* plants with AMF inoculation (Fm+) and non-inoculation (Fm−). Values with different small letters within the same column indicate significant differences at the $p < 0.05$ level between Mn treatments. * indicates significant difference ($p < 0.05$) between AMF-inoculated plants and uninoculated plants. AMF, arbuscular mycorrhizal fungi. *** indicates highly significant difference (p<0.001).

3.3 Mn accumulation

With the increasing Mn concentration, the Mn content of the roots (Figure 4A), stems (Figure 4B), leaves (Figure 4C), and total individual (Figure 4D) in the inoculated group and the uninoculated group increased. The two-way ANOVA showed that both Mn concentration and whether or not to inoculate with AMF had a significant effect on the Mn accumulation of the roots, stems, leaves, and total individual in *L. davidii* (Figure 4; $p < 0.001$). When the Mn concentration reached 20 mmol/L, the total Mn content in *L. davidii* in the inoculated group and the uninoculated group reached 15,199.81 mg/kg and 15,002.30 mg/kg, respectively. The content of Mn in the leaves of the inoculated group was lower than that of the uninoculated group when the concentration of Mn was 10 mmol/L and 20 mmol/L (Figure 4C; $p < 0.05$).

The two-way ANOVA showed that both Mn concentration and whether or not to inoculate with AMF had a significant effect on the BCF and TF of *L. davidii* (Table 1; $p < 0.001$). With the increasing Mn concentration, the BCF in both the inoculated and uninoculated groups decreased. At different Mn concentrations, the BCF of the inoculated group was higher than that of the uninoculated group.

With the increase of Mn concentration, the TF of the inoculated group increased, while that of the uninoculated group increased first and then decreased (Table 1; $p < 0.05$). At different concentrations, the TF of the inoculated group was higher than that of the uninoculated group.

3.4 Subcellular components of Mn

The two-way ANOVA showed that both Mn concentration and whether or not to inoculate with AMF had significant effects on the content of Mn in the cell wall components, soluble components (ribosomal fraction), mitochondrial components, and chloroplast and nuclear components of the roots, stems, and leaves of *L. davidii* ($p < 0.001$). With the increase of Mn concentration, the content of Mn in the cell wall components, chloroplast and nuclear components, mitochondrial components, and soluble components of the roots, stems, and leaves of *L. davidii* in the inoculated and uninoculated groups increased ($p < 0.05$). The Mn accumulations and distribution proportions in different subcellular fractions of the roots, stems, and

10.3389/fpls.2024.1470063

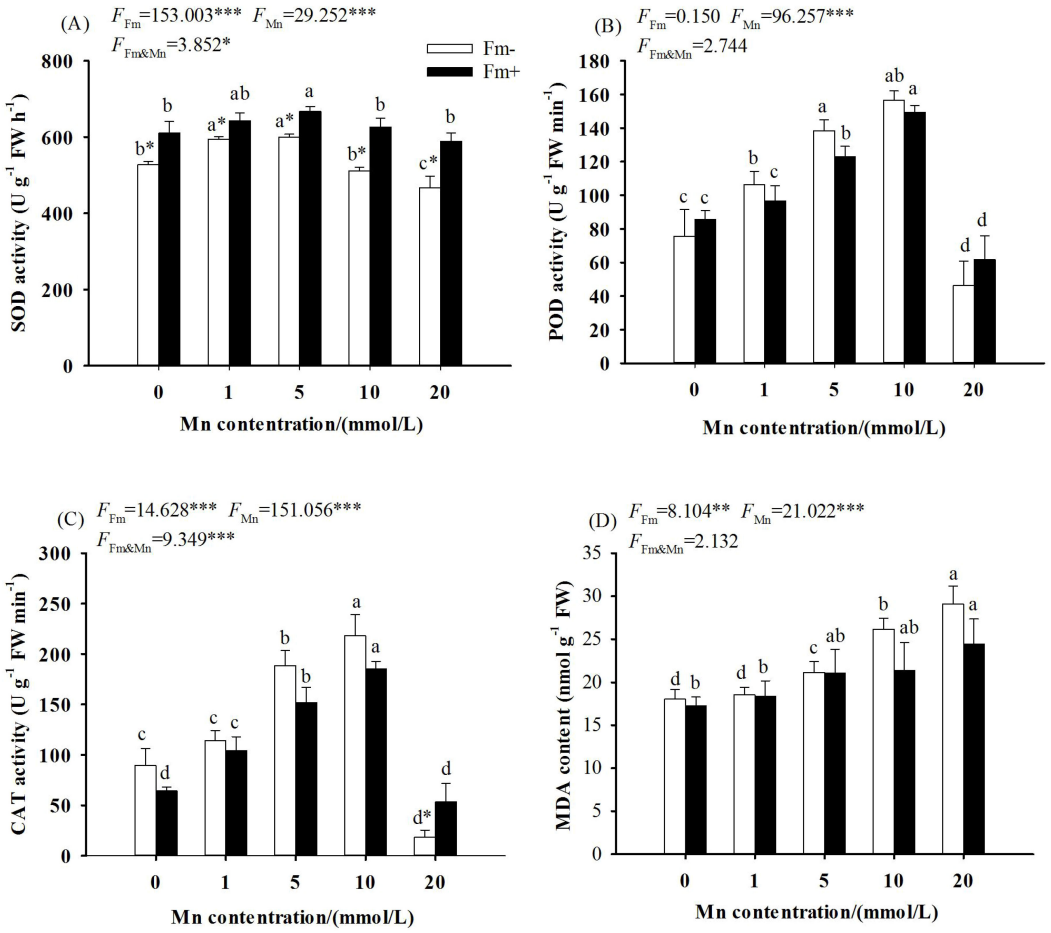

FIGURE 3
Effects of Mn treatments on superoxide dismutase (SOD; **A**), peroxidase (POD; **B**), catalase (CAT; **C**), and malondialdehyde (MDA; **D**) of *Lespedeza davidii* plants with AMF inoculation (Fm+) and non-inoculation (Fm–). Values with different small letters within the same column indicate significant differences at the $p < 0.05$ level between Mn treatments. * indicates significant difference ($p < 0.05$) between AMF-inoculated plants and uninoculated plants. AMF, arbuscular mycorrhizal fungi. ** indicates highly significant difference (p<0.01); *** indicates highly significant difference (p<0.001).

leaves are presented in Figure 5 and Supplementary Figures S1–S3, which showed that a large percentage of Mn (80%–90%) was accumulated in cell walls and the soluble fractions in the roots (Figures 5A, B), stems (Figures 5C, D), and leaves (Figures 5E, F), and a small portion of Mn presented in the cellular organelles (the chloroplast and nuclear components and mitochondrial components). Compared with that of the uninoculated group, the proportion of Mn content in the cell wall components and the soluble components in the leaves of the inoculated group was higher (Figures 5E, F).

3.5 Chemical forms of Mn

The effects of different treatments on the concentrations and proportions of Mn in different chemical forms in *L. davidii* are shown in Figure 6 and Supplementary Figures S4-S6. With the increasing Mn concentration, the contents of six chemical forms of Mn extracts in the roots (Supplementary Figure S4), stems (Supplementary Figure S5), and leaves (Supplementary Figure S6) of *L. davidii* in the uninoculated group and the inoculated group increased ($p < 0.05$). Chemical forms of Mn extracted using 80% ethanol (FE), deionized water (FW), and 1 M NaCl (FNaCl) were predominant (more than 90%) in both the uninoculated and inoculated plants (Figures 6A–F). The two-way ANOVA showed that the effects of Mn stress, inoculation and interaction of Mn stress, and inoculation on the contents of Mn ethanol extract, deionized water extract, sodium chloride extract, and acetic acid extract in the roots of *L. davidii* were extremely significant ($p < 0.001$). The proportions of Mn extracted using ethanol and deionized water in the uninoculated group in stems and roots were higher than those in the inoculated group (Figures 6C–F).

4 Discussion

4.1 The effects of AMF on plant biomass under Mn stress

Biomass variation under heavy metal stress is an important standard to determine plant tolerance and the phytoremediation

10.3389/fpls.2024.1470063

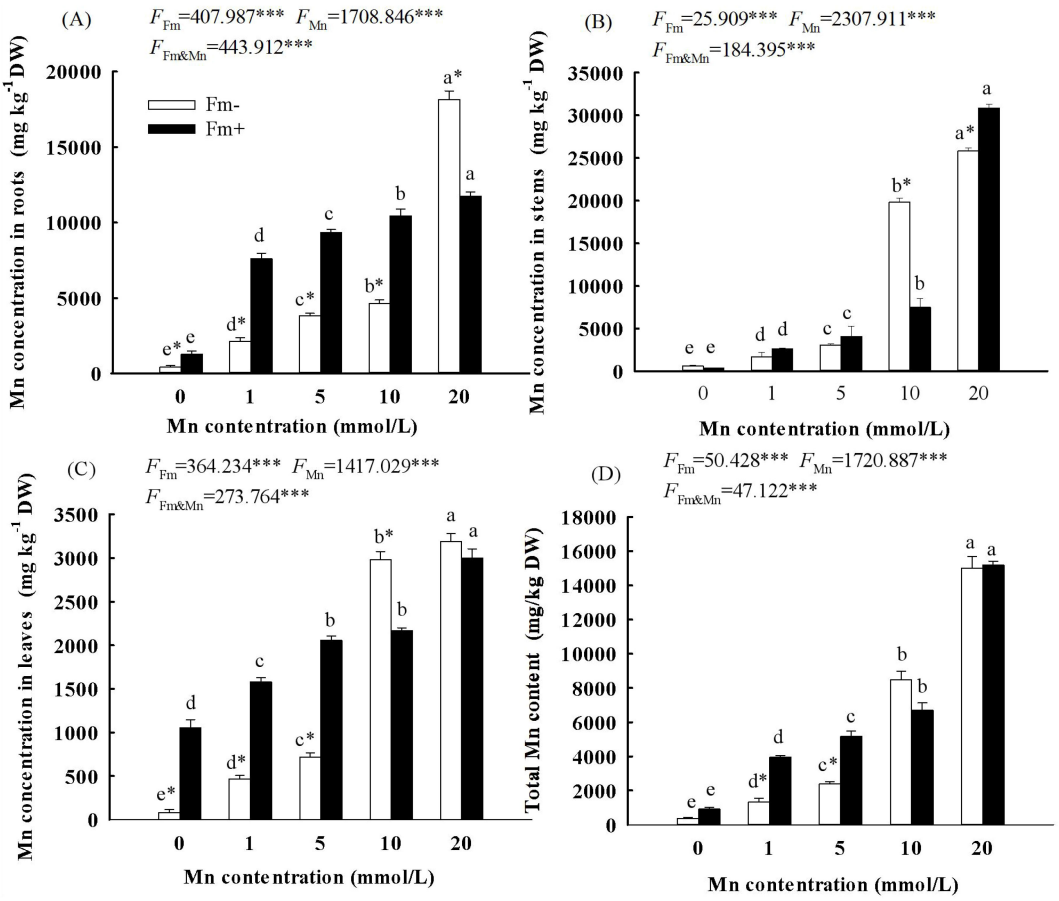

FIGURE 4
Effects of Mn treatments on the content of stems **(A)**, roots **(B)**, leaves **(C)**, and total individual **(D)** of *Lespedeza davidii* plants with AMF inoculation (Fm+) and non-inoculation (Fm–). Values with different small letters within the same column indicate significant differences at the $p < 0.05$ level between Mn treatments. * indicates significant difference ($p < 0.05$) between uninoculated plants and AMF-inoculated plants. AMF, arbuscular mycorrhizal fungi. *** indicates highly significant difference (p<0.001).

potential for plants (Han et al., 2021). In this study, the biomass of leaves, stems, roots, and the total individual of *L. davidii* increased first and then decreased with the increasing Mn concentration. This is consistent with the results on *Cleome viscosa* (Xiao et al., 2020) and *Rhus chinensis* (Pan et al., 2023a) under Mn stress. It showed that low promotion and high suppression are common phenomena for Mn in the growth of plants.

This study also showed that the inoculated plants of *L. davidii* had higher biomass than the uninoculated plants (Figure 1D). Chaturvedia et al. (2018) and Pan et al. (2023a) also found that the AMF-inoculated plants had higher plant height and biomass than the uninoculated counterparts. The present study is consistent with these studies. The reason lies in that AMFs are known to have the ability to change enzyme activity and increase the ability of host plants to resist heavy metal stress (Chen et al., 2019). In our study, the results showed that the contents of soluble sugar, soluble protein, free proline, SOD, POD, and CAT in the inoculated group were higher than those in the uninoculated group at the Mn concentration of 20 mmol/L. These would promote the growth of plants. In addition, previous studies also suggested that AMF can chelate Mn, thereby reducing the bioavailability of Mn. All of these would help plant growth under stress.

4.2 The effects of AMF on physiological characteristics under Mn stress

Osmotic regulation is an important mechanism for plants to cope with heavy metal stress. In order to resist the adverse environment, plants would produce and accumulate a large number of osmoregulation substances (such as soluble sugar, soluble protein, and free proline) to maintain the water balance and energy supply in cells, thereby reducing the stress damage caused by osmotic water loss and maintaining the normal life metabolism activities of cells. The present study showed that the contents of soluble sugar, soluble protein, and free proline in

TABLE 1 Effect of AMF on Mn bioconcentration coefficients (BCFs) and transport coefficients (TFs) of *Lespedeza davidii* leaves under Mn stress.

Mn concentration (mmol/L)	Bioconcentration coefficients/BCF		Transport coefficients/TF	
	+AMF	–AMF	+AMF	–AMF
CK			1.15 ± 0.20b	0.79 ± 0.15b
1	95.75 ± 2.78b*	32.06 ± 5.28b	0.56 ± 0.03d	0.50 ± 0.13c
5	25.01 ± 1.56b*	11.56 ± 0.58b	0.66 ± 0.14d	0.49 ± 0.02c
10	16.25 ± 1.05b*	20.56 ± 1.20b	0.92 ± 0.09c*	2.45 ± 0.08a
20	18.42 ± 0.26b	18.18 ± 0.83b	2.88 ± 0.05a*	0.80 ± 0.02b
F_{AMF}	78.926***		32.047***	
F_{Mn}	320.277***		189.731***	
$F_{Mn\times AMF}$	63.636***		206.837***	

* indicates significant difference ($p < 0.05$) between uninoculated plants and AMF-inoculated plants; ** indicates highly significant difference (p<0.01); *** indicates highly significant difference (p<0.001).
Values with different small letters within the same column indicate significant differences at the p < 0.05 levelbetween Mn treatments.

L. davidii in the inoculated and uninoculated groups increased first and then decreased with the increasing Mn concentration (Figure 3). Kuang et al. (2022) also found that osmoregulation substances increased first and then decreased with the increasing Mn concentration in *Daucus carota*. The reason is that Mn stress can activate the osmotic regulation system in *L. davidii* and resist Mn toxicity through the accumulation of osmotic regulation substances. When the Mn concentration is too high, the osmotic adjustment ability of *L. davidii* is insufficient to resist the toxicity of high Mn, the water balance mechanism is destroyed, and the plant resistance is weakened. The present study also showed that compared with those in the inoculated group, the contents of soluble protein (Figure 2B) and free proline (Figure 2C) in the inoculated group were higher when the Mn concentrations were 5 mmol/L, 10 mmol/L, and 20 mmol/L. This is the same as that in *Lolium perenne* (Xu et al., 2014) and *Tamarix chinensis* (Han et al., 2021) under salt stress, which suggested that AMF inoculation can effectively increase the content of osmoregulation substances. The reason is that AMF can regulate the osmotic regulation system to stabilize the physiological environment in plants to adapt to stress. AMF could change enzyme activity and increase the ability of host plants to resist oxidative stress (Pan et al., 2023b).

Mn stress would result in the accumulation of ROS such as H_2O_2, O_2, and MDA in the plant, which potentially leads to plasma membrane damage and a decrease in physiological activities related to membrane function. SOD, POD, and CAT are important components of plant antioxidant enzyme promotion systems. The synergistic effect of these three enzymes can effectively reduce the accumulation of ROS in plants and reduce the damage of stress to plants. In this study, the POD and CAT activities of *L. davidii* in the inoculated and uninoculated groups increased first and then decreased with the increase of Mn concentration. This showed that Mn stress can activate the antioxidant system of *L. davidii* and resist Mn toxicity by improving the activity of antioxidant enzymes. When the Mn concentration is too high, the antioxidant system of *L. davidii* may be destroyed, the activity of antioxidant enzymes is reduced, and the plant defense ability is weakened. Mn stress damages the cell membrane and destroys the original region of the metabolism of the protective enzyme system in the cell. Mn may also directly replace the trace elements in the activity of some enzymes to change or even destroy the enzyme activity. The present study also illustrated that when the Mn concentration was 20 mmol/L, the activities of SOD, POD, and CAT in the inoculated group were higher than those in the uninoculated group. This is the same as the results of marigold under cadmium stress (Liu et al., 2011), *Trifolium repens* in HM-contaminated soils (Azcón et al., 2009), and *Solanum lycopersicum* under salinization stress (Cao et al., 2022). This indicated that AMF inoculation can enhance the resistance of plants to high Mn toxicity by improving the activity of antioxidant enzymes and reducing lipid peroxidation, which would promote plant physiological metabolism and reduce the toxicity and damage of heavy metals to plants. Therefore, it appeared that it was an important mechanism for AMF to alleviate the damage of Mn by enhancing the activity of antioxidant enzymes and small molecular osmotic regulators.

MDA is the final product of membrane lipid peroxidation, which can measure the degree of damage to plant cell plasma membrane under stress. The level of MDA can reflect the degree of plant poisoning and also indicate the level of plant stress resistance. The present study showed that compared with that of the uninoculated group, the MDA content of the inoculated group was lower under the relevant Mn concentrations (Figure 3D). Similarly, AMF inoculation can effectively reduce the membrane lipid peroxidation of *Medicago sativa* under cadmium stress, reduce the MDA content in the host, and improve tolerance (Wang et al., 2022). This showed that excessive Mn makes the antioxidant enzyme system in the cells of *L. davidii* disordered, the balance between the production and elimination of ROS is broken, and the production of ROS in large quantities causes oxidative damage to plant cells, leading to a large MDA accumulation. AMF inoculation could weaken the damage of Mn toxicity to the leaf cells of *L. davidii* and make the physiological and biochemical environments in *L. davidii* relatively stable. Therefore, it appears that AMF can repair oxidative damage in membranes and maintain homeostasis in the internal environment.

10.3389/fpls.2024.1470063

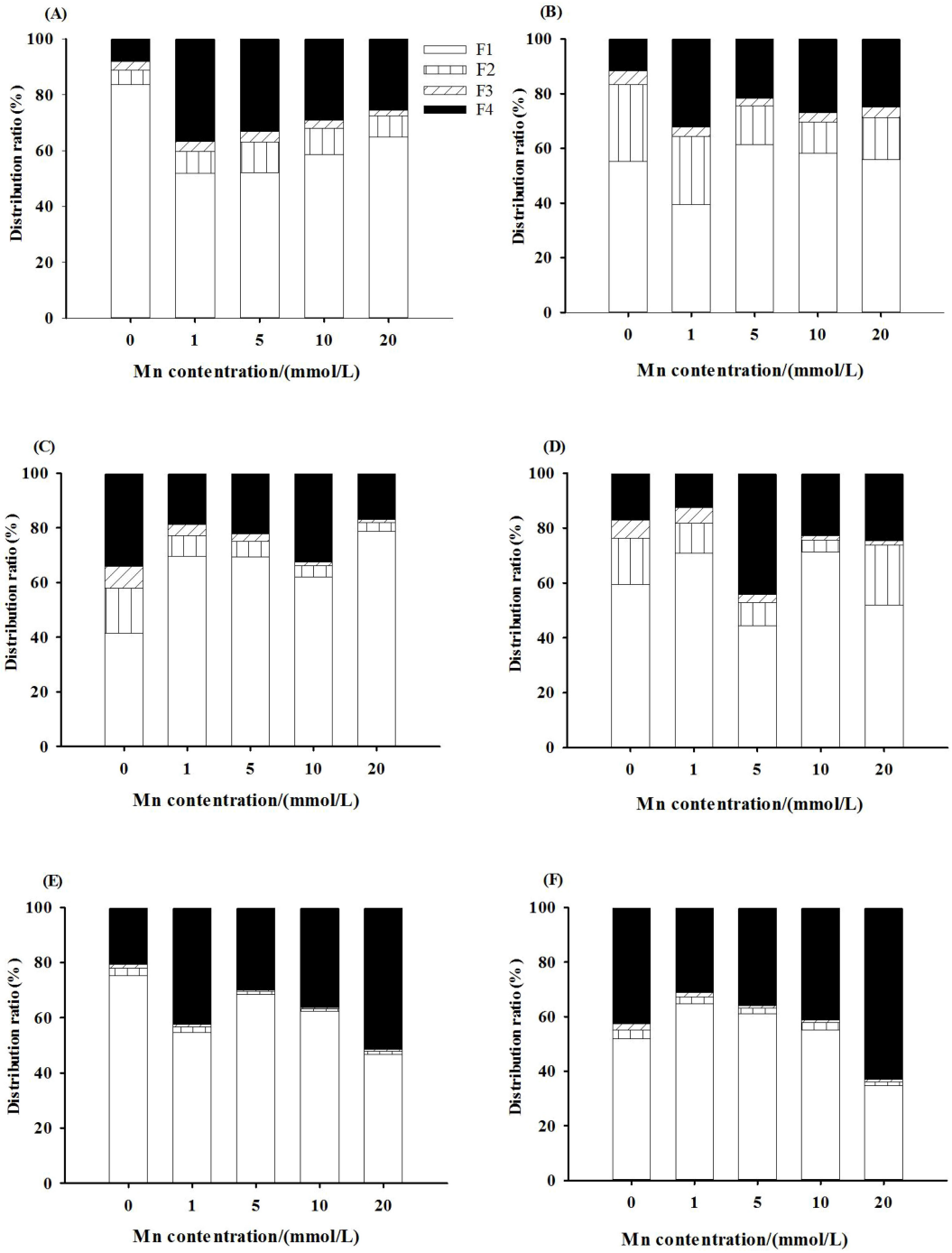

FIGURE 5
Manganese subcellular fraction distribution ratio of roots **(A, B)**, stems **(C, D)**, and leaves **(E, F)** of *Lespedeza davidii* in inoculated group and uninoculated group under Mn stress. **(A, C, E)** Uninoculated group. **(B, D, F)** Inoculated group. F1, cell wall fraction; F2, chloroplast and cell nuclear fraction; F3, mitochondrial fraction; F4, ribosomal fraction.

4.3 The effects of AMF on Mn accumulation under Mn stress

The enrichment characteristics of heavy metals in plants usually include three indicators, namely, heavy metal accumulation, bioaccumulation coefficient, and transport coefficient, which are the main factors determining whether they are tolerant to Mn stress. The present study showed that with the increasing Mn concentration, the Mn content in the roots, stems, and leaves of *L. davidii* in the inoculated group and the uninoculated group increased. Compared with that of the uninoculated group, the content of Mn in the leaves of the inoculated group was lower when the concentrations of Mn were 5 mmol/L and 20 mmol/L (Figure 4, $p < 0.05$). This indicated that inoculation with AMF significantly increased the uptake of Mn in soil by *L. davidii* roots and decreased the transportation to leaves. Similarly, mycorrhizal colonization significantly enhanced the fixation of

10.3389/fpls.2024.1470063

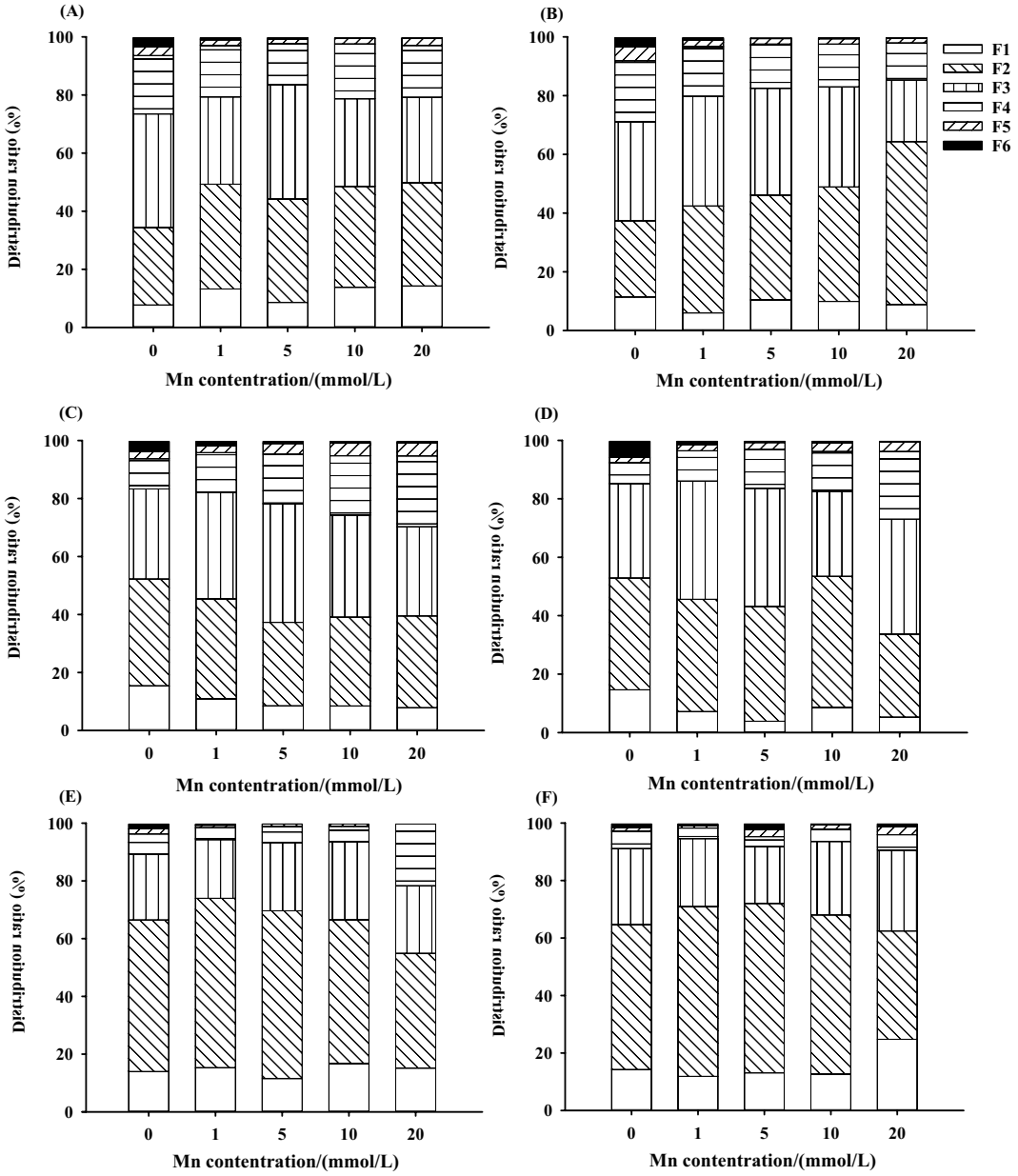

FIGURE 6
Manganese chemical form distribution ratio of roots **(A, B)**, stems **(C, D)**, and leaves **(E, F)** of *Lespedeza davidii* in inoculated group and uninoculated group under Mn stress. **(A, C, E)** Uninoculated group. **(B, D, F)** Inoculated group. F1, 80% ethanol; F2, deionized H_2O; F3, 1 M NaCl; F4, 2% HA; F5, 0.6 M HCl; F6, residue.

cadmium in the root system of *Lotus japonicus* (Chen et al., 2018), AMF inoculation significantly improved the absorption of cadmium in the soil by the root system of *Capsicum annuum* (Mou et al., 2021), and mycorrhizal infection increased the copper binding capacity of the cell wall of *M. sativa* (Wang et al., 2012). AMF inoculation often promotes the host plant and AMF to form a rhizobacterial structure. Plants can rely on this structure to expand the absorption range of nutrients and to improve the host's absorption of nutrients in the soil under adverse environments (Wipf et al., 2019). As a nutrient element of plants, Mn absorption by AMF will also increase, which will increase the Mn content in *L. davidii*. Comparing the inoculated group with the uninoculated group, the BCF and TF of the inoculated group were generally higher than those of the uninoculated group. Similarly, AMF inoculation significantly increased the enrichment coefficient and reduced the transport of heavy metals from roots to aboveground parts for *C. annuum* (Mou et al., 2021). Research found that when the concentration of heavy metals in the soil is high, AMF can fix most of the heavy metals in the roots or fungal rhizosphere of plants and inhibit their transfer to the aboveground parts, thus reducing the distribution ratio of heavy metals to the aboveground parts, reducing the toxic effect of heavy metals on important aboveground physiological organs of plants, and making plants have a higher tolerance to Mn stress.

4.4 The effects of AMF on subcellular components of Mn under Mn stress

Compartmentalization is a crucial strategy for detoxifying heavy metals in plant cells because after entering into plant cells, heavy metals can bind to different subcellular compartments (e.g., cell wall and soluble fraction), exhibiting different ecotoxicological significance. The present study showed that Mn in the roots, stems, and leaves of *L. davidii* is mainly distributed in the cell wall and soluble components. Compared with CK, the proportions of Mn in the cell wall and soluble components of the roots, stems, and leaves of *L. davidii* were higher, while the proportion of chloroplast and nuclear components, and mitochondrial components were lower. This showed that the cell wall components and soluble components are the main storage sites of Mn in various organs of *L. davidii*, and most of the Mn in *L. davidii* is fixed in the cell wall or isolated in vacuoles (the soluble fraction mainly exists in vacuoles). It is usually known that heavy metals are less toxic to plant cells when they are distributed in cell walls and vacuoles (the soluble fraction) but more toxic when they are distributed in chloroplasts, nuclei, mitochondria, and other organelles. Therefore, it is one of the growth strategies for tolerant plants to adapt to heavy metal stress environment to combine toxic or excessive heavy metal ions on plant cell walls or promote their separation in vacuoles, thus reducing the toxicity of Mn to organelles, which is one of the mechanisms of *L. davidii* for detoxifying Mn.

In addition, compared with that in the uninoculated group, it was found that the proportion of Mn content in the cell wall components and the soluble components in leaves in the inoculated group increased. This indicated that AMF enhanced the cell wall fixation and vacuole compartmentalization (the soluble fraction mainly composed in vacuoles) of *L. davidii* under Mn stress and reduced the toxicity of Mn to the organelles of *L. davidii*. Similarly, under cadmium stress, most cadmium (more than 90%) accumulated in the cell wall and soluble parts in *Zea mays*, while a small amount of cadmium exists in organelles, and AMF symbiosis promoted cadmium transfer to vacuoles (Zhang et al., 2019). Therefore, cell wall components may be the main site for Mn fixation in roots, which can reduce the transport of cadmium from roots to the upper ground (Gao et al., 2021).

4.5 The effects of AMF on chemical forms of Mn under Mn stress

The chemical forms of heavy metals are a major determinant of physiological functions and toxicity; different forms of heavy metals have different bioavailability and toxicity. Among them, ethanol and deionized water have the highest activity and mobility in the extracted state, which are the easiest to enter the plant symplast, and have the strongest toxicity to plants. The heavy metals extracted from sodium chloride (NaCl) are mainly combined with pectin and protein, and the solubility of heavy metals extracted from acetic acid (HAc) and hydrochloric acid (HCl) is low. The activity and mobility of these extracted heavy metals are low, and their toxicity to plants is weak. The residue state is the most stable, and the toxicity to plants is the most weak. The present study showed that, with the increasing Mn concentration, the content of different chemical forms of Mn in the stems of *L. davidii* in the uninoculated group and the inoculated group showed an increasing trend, and the Mn in the sodium chloride extract, acetic acid extract, and hydrochloric acid extract of *L. davidii* was more than that in the ethanol extract and deionized water extract. This illustrated that Mn stress made the activity and mobility of Mn ions in *L. davidii* lower, thus reducing the toxicity of Mn stress to *L. davidii*.

In addition, the present study showed that the Mn in *L. davidii* in the inoculated group had a higher ratio when extracted using sodium chloride, acetic acid, and hydrochloric acid than that in the uninoculated group. After inoculation with AMF, the proportion of sodium chloride extracted, acetic acid extracted, and residual Mn in *L. davidii* increased significantly, while the proportion of ethanol extracted and deionized water extracted Mn decreased significantly. This showed that AMF promoted the transformation of Mn ions in *L. davidii* from ethanol and deionized water extracts with strong activity to sodium chloride and acetic acid extracts with weak activity, thus reducing the damage of Mn ions to the cells and structures of *L. davidii*, maintaining its normal physiological and biochemical activities, and enhancing the Mn tolerance of *L. davidii*. Similarly, after inoculation with AMF, Li et al. (2016) also found that AMF may augment the tolerance to Cd of rice by decreasing the proportions of Cd in active forms (FE and FW) in 0.05–0.1 mM Cd solutions. AMF inoculation under cadmium stress increased the proportion of cadmium with weak active state in *M. sativa* (Wang et al., 2012). Therefore, AMF may also improve the resistance to Mn of *L. davidii* by converting Mn into inactive forms that are less toxic.

5 Conclusion

This study reports the effects of AMF inoculation and Mn stress on plant growth, physiological and biochemical characteristics, Mn uptake, subcellular distribution, and chemical forms of Mn in *L. davidii*. The results showed that the biomass of the AMF-inoculated plants was higher than that of the uninoculated plants, and the content of MDA in the inoculated plants was lower than that in the uninoculated plants, which showed that AMF can alleviate Mn toxicity. AMF inoculation enhanced the enrichment of Mn in *L. davidii* and enhanced the fixation of Mn in *L. davidii* roots so as to alleviate the damage of Mn stress to its aboveground parts. At low Mn substrate concentrations, the cell wall appears to play an important role in Mn retention, while the main subcellular fraction that contributed to Mn detoxification is the vacuoles at high Mn substrate concentrations (≥10 mM). Furthermore, the concentrations and proportions of Mn extracted by ethanol and

d-H_2O were also lower in the stems, and roots of the inoculated plants compared with the uninoculated plants at high substrate concentrations (≥10 mM), indicating that AMF can convert Mn into inactive forms, which are less toxic. The results of this study illustrated that inoculation with AMF could adjust the osmotic regulation system and antioxidant system to stabilize the physiological environment and accumulate more Mn in cell walls and soluble fractions to improve the tolerance of *L. davidii* to manganese stress.

Data availability statement

The original contributions presented in the study are included in the article/Supplementary Material. Further inquiries can be directed to the corresponding authors.

Author contributions

GP: Writing – original draft. JH: Writing – original draft. ZZ: Writing – original draft. WW: Writing – original draft, Data curation. XL: Writing – original draft. XX: Writing – original draft. WL: Writing – review & editing, Writing – original draft.

Funding

The author(s) declare financial support was received for the research, authorship, and/or publication of this article. This research was jointly supported by the National Natural Science Foundation of China (No.42177018).

Conflict of interest

The authors declare that the research was conducted in the absence of any commercial or financial relationships that could be construed as a potential conflict of interest.

Publisher's note

Supplementary material

The Supplementary Material for this article can be found online at: https://www.frontiersin.org/articles/10.3389/fpls.2024.1470063/full#supplementary-material

SUPPLEMENTARY FIGURE S1
Effect of AMF on Mn content in subcellular fractions of *L. davidii* root under Mn stress. Note: F1, cell wall fraction; F2, chloroplasts and cell nuclei fraction; F3, mitochondria fraction; F4, ribosomes fraction.

SUPPLEMENTARY FIGURE S2
Effect of AMF on Mn content in subcellular fractions of *L. davidii* stems under Mn stress. Note: F1, cell wall fraction; F2, chloroplasts and cell nuclei fraction; F3, mitochondria fraction; F4, ribosomes fraction.

SUPPLEMENTARY FIGURE S3
Effect of AMF on Mn content in subcellular fractions of *L. davidii* leaves under Mn stress.Note: F1, cell wall fraction; F2, chloroplasts and cell nuclei fraction; F3, mitochondria fraction; F4, ribosomes fraction.

SUPPLEMENTARY FIGURE S4
Effect of AMF on manganese chemical forms of manganese of *L. davidii* root under Mn stress. Note: F1, 80% ethanol; F2, deionized H_2O; F3, 1 M NaCl; F4, 2% HA; F5, 0.6 M HCl; F6, residue.

SUPPLEMENTARY FIGURE S5
Effect of AMF on manganese chemical forms of manganese of *L. davidii* stems under Mn stress. Note: F1, 80% ethanol; F2, deionized H_2O; F3, 1 M NaCl; F4, 2% HA; F5, 0.6 M HCl; F6, residue.

SUPPLEMENTARY FIGURE S6
Effect of AMF on manganese chemical forms of manganese of *L. davidii* leaves under Mn stress. Note: F1, 80% ethanol; F2, deionized H_2O; F3, 1 M NaCl; F4, 2% HA; F5, 0.6 M HCl; F6, residue.

References

Amir, H., Cavaloc, Y., Laurent, A., Pagand, P., Gunkel, P., Lemestre, M., et al. (2019). Arbuscular mycorrhizal fungi and sewage sludge enhance growth and adaptation of Metrosideros laurifolia on ultramafic soil in New Caledonia: A field experiment. *Sci. Total Environ.* 651, 334–343. doi: 10.1016/j.scitotenv.2018.09.153

Azcón, R., Perálvarez, M., del, C., Biró, B., Roldán, A., and Ruíz-Lozano, J. M. (2009). Antioxidant activities and metal acquisition in mycorrhizal plants growing in a heavy-metal multicontaminated soil amended with treated lignocellulosic agrowaste. *Appl. Soil Ecol.* 41, 168–177. doi: 10.1016/j.apsoil.2008.10.008

Bai, Y. X., Zhou, Y. C., and Gong, J. F. (2021). Physiological mechanisms of the tolerance response to manganese stress exhibited by Pinus massoniana, a candidate plant for the phytoremediation of Mn-contaminated soil. *Environ. Sci. pollut. Res. Int.* 28, 45422–45433. doi: 10.1007/s11356-021-13912-8

Boorboori, M. R., and Zhang, H. Y. (2022). Arbuscular mycorrhizal fungi are an influential factor in improving the phytoremediation of arsenic, cadmium, lead, and chromium. *J. Fungi* 8, 176. doi: 10.3390/jof8020176

Bradford, M. N. (1976). A rapid and sensitive method for the quantitation of microgram quantities of protein utilizing the principle of protein-dye binding. *Analytical Biochem.* 72, 248–254. doi: 10.1016/0003-2697(76)90527-3

Cao, L., Li, Y. W., Ling, K. J., Wang, J. Q., Yan, H., Mou, I. J., et al. (2022). Effects of arbuscular mycorrhizal fungi inoculation on salt-tolerance of tomato plants. *Fujian J. Agric. Sci.* 37, 188–196. doi: 10.19303/j.issn.1008-0384.2022.002.008

Chaturvedia, R., Favas, P., Pratasc, J., Varuna, M., and Paula, M. S. (2018). Assessment of edibility and effect of arbuscular mycorrhizal fungi on *Solanum melongena* L. grown under heavy metal(loid) contaminated soil. *Ecotoxicol. Environ. Saf.* 148, 318–326. doi: 10.1016/j.ecoenv.2017.10.048

Chen, B. D., Nayuki, K., Kuga, Y., Zhang, X., Wu, S. L., and Ohtomo, R. (2018). Uptake and intraradical immobilization of cadmium by arbuscular mycorrhizal fungi as revealed by a stable isotope tracer and synchrotron radiation μX-Ray fluorescence analysis. *Microbes Environ.* 33, 257–263. doi: 10.1264/jsme2.ME18010

Chen, X. W., Wu, L., Luo, N., Mo, C. H., Wong, M. H., and Li, H. (2019). Arbuscular mycorrhizal fungi and the associated bacterial community influence the uptake of cadmium in rice. *Geoderma* 337, 749–757. doi: 10.1016/j.geoderma.2018.10.029

Doty, S. L. (2008). Enhancing phytoremediation through the use of transgenics and endophytes. *New Phytol.* 179, 318–333. doi: 10.1111/j.1469-8137.2008.02446.x

Fu, X., Dou, C., Chen, Y., Chen, X., Shi, J., Yu, M., et al. (2011). Subcellular distribution and chemical forms of cadmium in Phytolacca americana L.. *J. Hazard. Mater.* 186 (1), 103–107. doi: 10.1016/j.jhazmat.2010.10.122

Gao, J. F. (2000). *Experimental Techniques of Plant Physiology* (Xi'an, China: World Publishing Corporation).

Gao, M. Y., Chen, X. W., Huang, W. X., Wu, L., Yu, Z. S., Xiang, L., et al. (2021). Cell wall modification induced by an arbuscular mycorrhizal fungus enhanced cadmium fixation in rice root. *J. Hazard. Mater.* 416, 125894. doi: 10.1016/j.jhazmat.2021.125894

Garcia, K. G. V., Gomes, V. F. F., Filho, P. F. M., Martins, C. M., Silva, J. J. M. T., Cunha, C. S. M., et al. (2018). Arbuscular mycorrhizal fungi in the phytostabilization of soil degraded by manganese mining. *J. Agric. Sci.* 10, 192–202. doi: 10.5539/jas.v10n12p192

Giovannetti, M., and Mosse, B. (1980). An evaluation of techniques for measuring vesicular arbuscular mycorrhizal infection in roots. *New Phytol.* 84, 489–500. doi: 10.1111/j.1469-8137.1980.tb04556.x

Han, Y., Zveushe, O. K., Dong, F. Q., Ling, Q., Chen, Y., Sajid, S., et al. (2021). Unraveling the effects of arbuscular mycorrhizal fungi on cadmium uptake and detoxification mechanisms in perennial ryegrass (*Lolium perenne*). *Sci. Total Environ.* 798, 149222. doi: 10.1016/j.scitotenv.2021.149222

Hu, J. Y., Wang, W. M., Kuang, X. S., and Liu, W. S. (2022). Effects of manganese stress on seed germination and seedling physiological and biochemical characteristics of *Lespedeza davidii*. *J. Anhui Univ. (Natural Sci. Edition)* 46, 84–92. doi: 10.3969/j.issn.1000-2162.2022.06.012

Kaya, C., Ugurlar, F., Ashraf, M., AlYemeni, M. N., Bajguz, A., and Ahmad, P. (2022). The involvement of hydrogen sulphide in melatonin-induced tolerance to arsenic toxicity in pepper (*Capsicum annuum* L.) plants by regulating sequestration and subcellular distribution of arsenic, and antioxidant defense system. *Chemosphere* 309, 136678. doi: 10.1016/j.chemosphere.2022.136678

Kuang, X. S., Wang, W. M., Hu, J. M., Liu, W. S., and Zeng, W. B. (2022). Subcellular distribution and chemical forms of manganese in *Daucus carota* in relation to its tolerance. *Front. Plant Sci.* 13. doi: 10.3389/fpls.2022.947882

Li, H., Luo, N., Zhang, L. J., Zhao, H. M., Li, Y. W., Cai, Q. Y., et al. (2016). Do arbuscular mycorrhizal fungi affect cadmium uptake kinetics, subcellular distribution and chemical forms in rice? *Sci. Total Environ.* 571, 1183–1190. doi: 10.1016/j.scitotenv.2016.07.124

Li, J. R., and Wang, M. S. (1989). Two flavanones from the root bark of *Lespedeza davidii*. *Phytochemistry* 28, 3564–3566. doi: 10.1016/0031-9422(89)80398-X

Liang, S. L., and Yan, F. G. (2018). Screening of the anti-inflammatory and analgesic active fractions from the root bark of Lespedeza davidii and its mechanism. *Natural Product Res. Dev.* 30, 1706–1713. doi: 10.16333/j.1001-6880.2018.10.008

Lin, Y., Jiao, Y., Zhao, M. F., Wang, G. J., Wang, D. M., Xiao, W., et al. (2021). Ecological restoration of wetland polluted by heavy metals in Xiangtan Manganese Mine Area. *Processes* 9, 1702. doi: 10.3390/pr9101702

Liu, L. Z., Gong, Z. Q., Zhang, Y. L., and Li, P. J. (2011). Growth, cadmium accumulation and physiology of marigold (Tagetes erecta L.) as affected by arbuscular mycorrhizal fungi. *Pedosphere* 21, 319–327. doi: 10.1016/S1002-0160(11)60132-X

Luo, X., Ren, B. Z., Hursthouse, A. S., Jiang, F., and Deng, R. J. (2020). Potentially toxic elements (PTEs) in crops, soil, and water near Xiangtan manganese mine, China: potential risk to health in the foodchain. *Environ. Geochem. Health* 42, 1965–1976. doi: 10.1007/s10653-019-00454-9

Marro, N., Grilli, G., Soteras, F., Caccia, M., Longo, S., Cofré, N., et al. (2022). The effects of arbuscular mycorrhizal fungal species and taxonomic groups on stressed and unstressed plants: a global meta-analysis. *New Phytol.* 235, 320–332. doi: 10.1111/nph.v235.1

Mou, Y. M., Xing, D., Zhou, P., Song, L. L., Wu, K. Y., Hu, M. W., et al. (2021). Effects of the arbuscular mycorrhizal fungi on cadmium accumulation and transport in *Capsicum annum* L. *J. South. Agric.* 52, 172–179. doi: 10.3969/j.issn.2095-1191.2021.01.021

Pan, J., Cao, S., Xu, G. F., Rehman, M., Li, X., Luo, D. J., et al. (2023b). Comprehensive analysis reveals the underlying mechanism of arbuscular mycorrhizal fungi in kenaf cadmium stress alleviation. *Chemosphere* 314, 137566. doi: 10.1016/j.chemosphere.2022.137566

Pan, G., Wang, W. M., Li, X. H., Pan, D., and Liu, W. S. (2023a). Revealing the effects and mechanisms of arbuscular mycorrhizal fungi on manganese uptake and detoxification in *Rhus chinensis*. *Chemosphere* 339, 139768. doi: 10.1016/j.chemosphere.2023.139768

Phillips, J. M., and Hayman, D. S. (1970). Improved procedures for clearing and staining parasitic and vesicular-arbuscular mycorrhizal fungi for rapid assessment of infection. *Trans. Br. Mycological Soc.* 55, 158–161. doi: 10.1016/S0007-1536(70)80110-3

Rai, K. K., Pandey, N., Meena, R. P., and Rai, S. P. (2021). Biotechnological strategies for enhancing heavy metal tolerance in neglected and underutilized legume crops: A comprehensive review. *Ecotoxicol. Environ. Saf.* 208, 111750. doi: 10.1016/j.ecoenv.2020.111750

Rao, B. K. R., Bailey, J., and Wingwafi, R. W. (2011). Comparison of three digestion methods for total soil potassium estimation in soils of papua New Guinea derived from varying parent materials. *Commun. Soil Sci. Plant Anal.* 42 (11), 1259–1265. doi: 10.1080/00103624.2011.571740

Riaz, M., Kamran, M., Fang, Y. Z., Wang, Q. Q., Cao, H. Y., Yang, G. L., et al. (2021). Arbuscular mycorrhizal fungi-induced mitigation of heavy metal phytotoxicity in metal contaminated soils: A critical review. *J. Hazard. Mater.* 402, 123919. doi: 10.1016/j.jhazmat.2020.123919

Santos, E. F., Santini, J. M. K., Paixão, A. P., Júnior, E. F., Lavres, J., Campos, M., et al. (2017). Physiological highlights of manganese toxicity symptoms in soybean plants: Mn toxicity responses. *Plant Physiol. Biochem.* 113, 6–19. doi: 10.1016/j.plaphy.2017.01.022

Wang, H. R., Che, Y. H., Wang, Z. H., Zhang, B. N., Huang, D., Feng, F., et al. (2021a). The multiple effects of hydrogen sulfide on cadmium toxicity in tobacco may be interacted with CaM signal transduction. *J. Hazard. Mater.* 403, 123651. doi: 10.1016/j.jhazmat.2020.123651

Wang, Y. L., Geng, Q. Q., Huang, J. H., Wang, C. H., Li, L., Hasi, M., et al. (2021b). Effects of nitrogen addition and planting density on the growth and biological nitrogen fixation of Lespedeza davurica. *Chin. J. Plant Ecol.* 45, 13–22. doi: 10.17521/cjpe.2020.0185

Wang, Y. P., Huang, J., and Gao, Y. Z. (2012). Arbuscular mycorrhizal colonization alters subcellular distribution and chemical forms of cadmium in Medicago sativa L. and resists cadmium toxicity. *PloS One* 7, e48669. doi: 10.1371/journal.pone.0048669

Wang, Y., Shen, H., Xie, Y., Gong, Y., Xu, L., and Liu, L. (2015). Transport, ultrastructural localization, and distribution of chemical forms of lead in radish (*Raphanus sativus* L.). *Front. Plant Sci.* 6, 1–13. doi: 10.3389/fpls.2015.00293

Wang, H. R., Zhao, X. Y., Zhang, J. M., Lu, C., and Feng, F. J. (2022). Arbuscular mycorrhizal fungus regulates cadmium accumulation, migration, transport, and tolerance in Medicago sativa. *J. Hazard. Mater.* 435, 129077. doi: 10.1016/j.jhazmat.2022.129077

Wipf, D., Krajinski, F., van Tuinen, D., Recorbet, G., and Courty, P. E. (2019). Trading on the arbuscular mycorrhiza market: from arbuscules to common mycorrhizal networks. *New Phytol.* 223, 1127–1142. doi: 10.1111/nph.2019.223.issue-3

Xiao, Z. H., Pan, G., Li, X. H., Kuang, X. S., Wang, W. M., and Liu, W. S. (2020). Effects of exogenous manganese on its plant growth, subcellular distribution, chemical forms, physiological and biochemical traits in *Cleome viscosa* L. *Ecotoxicol. Environ. Saf.* 198, 110696. doi: 10.1016/j.ecoenv.2020.110696

Xu, Y., Fan, Y., Yu, Y. H., Xu, C. Y., and Ge, Y. (2014). Effects of arbuscular mycorrhizal fungus on the growth and physiological salt tolerance parameters of *Carthamus tinctorius* seedlings under salt stress. *Chin. J. Ecol.* 33, 3395–3402. doi: 10.13292/j.1000-4890.2014.0305

Yang, Y., Tang, M., Sulpice, R., Chen, H., Tian, S., and Ban, Y. (2014). Arbuscularmycorrhizal fungi alter fractal dimension characteristics of Robinia pseudoacacia L. seedlings through regulating plant growth, leaf water status, photosynthesis, and nutrient concentration under drought stress. *J. Plant Growth Regul.* 33, 612–625. doi: 10.1007/s00344-013-9410-0

Zhang, X. F., Hu, Z. H., Yan, T. X., Lu, R. R., Peng, C. L., Li, S. S., et al. (2019). Arbuscular mycorrhizal fungi alleviate Cd phytotoxicity by altering Cd subcellular distribution and chemical forms in *Zea mays*. *Ecotoxicol. Environ. Saf.* 171, 352–360. doi: 10.1016/j.ecoenv.2018.12.097

Zheng, L. J., Liu, X. M., Lütz-Meindl, U., and Peer, T. (2011b). Effects of Lead and EDTA-Assisted Lead on Biomass, Lead Uptake and Mineral Nutrients in *Lespedeza chinensis* and *Lespedeza davidii*. *Water Air Soil pollut.* 220, 57–68. doi: 10.1007/s11270-010-0734-0

Zheng, L. J., Peer, T., Seybold, V., and Lütz-Meindl, U. (2011a). Pb-induced ultrastructural alterations and subcellular localization of Pb in two species of Lespedeza by TEM-coupled electron energy loss spectroscopy. *Environ. Exp. Bot.* 77, 196–206. doi: 10.1016/j.envexpbot.2011.11.018

Zhong, W. L., Li, J. T., and Chen, Y. T. (2012). A study on the effects of lead, cadmium and phosphorus on the lead and cadmium uptake efficacy of Viola baoshanensis inoculated with arbuscular mycorrhizal fungi. *J. Environ. Monit.* 14, 2497–2504. doi: 10.1039/c2em30333g

frontiers | Frontiers in Plant Science

TYPE Review
PUBLISHED 29 November 2024
DOI 10.3389/fpls.2024.1471044

OPEN ACCESS

EDITED BY
Lu Gong,
Xinjiang University, China

REVIEWED BY
Matheus Aparecido Pereira Cipriano,
São Paulo State University, Brazil
Aarti Gupta,
Central University of Kashmir, India

*CORRESPONDENCE
Ziting Wang
zitingwang@gxu.edu.cn

RECEIVED 26 July 2024
ACCEPTED 11 November 2024
PUBLISHED 29 November 2024

CITATION
Chen M, Xing Y, Chen C and Wang Z (2024) Enhancing sugarcane's drought resilience: the influence of Streptomycetales and Rhizobiales.
Front. Plant Sci. 15:1471044.
doi: 10.3389/fpls.2024.1471044

Enhancing sugarcane's drought resilience: the influence of Streptomycetales and Rhizobiales

Mianhe Chen, Yuanjun Xing, Chunyi Chen and Ziting Wang*

State Key Lab for Conservation and Utilization of Subtropical Agri-Biological Resources, Guangxi Key Lab for Sugarcane Biology, College of Agriculture, Guangxi University, Nanning, China

Drought stress is a critical environmental factor affecting sugarcane yield, and the adaptability of the sugarcane rhizosphere bacterial community is essential for drought tolerance. This review examines the adaptive responses of sugarcane rhizosphere bacterial communities to water stress and explores their significant role in enhancing sugarcane drought tolerance. Under drought conditions, the sugarcane rhizosphere bacterial community undergoes structural and functional shifts, particularly the enrichment of beneficial bacteria, including Streptomycetales and Rhizobiales. These bacteria enhance sugarcane resilience to drought through various means, including nutrient acquisition and phytohormone synthesis. Furthermore, changes in the rhizosphere bacterial community were closely associated with the composition and levels of soil metabolites, which significantly influenced the physiological and biochemical processes of sugarcane during drought stress. This study deepens our understanding of rhizosphere bacterial communities and their interactions with sugarcane, laying a scientific foundation for developing drought-resistant sugarcane varieties, optimizing agricultural practices, and opening new avenues for agricultural applications.

KEYWORDS

sugarcane, rhizosphere bacterial community, drought tolerance, Streptomycetales, Rhizobiales, plant growth-promoting bacteria (PGPB)

1 Introduction

Sugarcane (*Saccharum officinarum* L.) cultivation is crucial for both sugar and bioenergy production. However, this cultivation faces significant challenges that can severely affect growth and yield, particularly in areas where drought is prevalent (Ferreira et al., 2017; Dlamini, 2021). Microorganisms are emerging as pivotal agents in mitigating the adverse effects of climate change, notably through their capacity to ameliorate the challenges posed by abiotic stressors, including water scarcity, which

plants frequently encounter (Zhang et al., 2022). Fungi, including genera such as *Trichoderma* and essential arbuscular mycorrhizal fungi, along with bacteria such as *Azospirillum*, *Bacillus*, and *Pseudomonas*, constitute a vital component of the Earth's microbial community. Their multifaceted functions in the natural world include decomposing organic matter, mediating the nitrogen cycle, and enhancing plant growth. These microorganisms contribute not only to ecological balance but are also emerging as potential mitigators of climate change (Hu et al., 2022; Qin et al., 2024). Recent scientific insights have revealed that they may also serve as climate change adapters, with certain fungi and bacteria capable of sequestering atmospheric carbon, thereby augmenting soil carbon reserves and slowing the pace of global warming (Zhu et al., 2024). Moreover, by ameliorating soil structure and increasing soil water retention, these microbes enhance the ability of plants to withstand extreme climatic conditions, including drought, thereby mitigating the impacts of such environmental stresses (Ahmed et al., 2019). The resilience of sugarcane in the face of adversity is closely related to the dynamics of its rhizosphere bacterial communities (Liu et al., 2021a). These communities are gaining increasing recognition for their indispensable roles in enhancing plant health and productivity (Backer et al., 2018) (Table 1). These communities are not only passive inhabitants of the soil; they also actively interact with plant root systems, forming a network of symbiotic relationships (Liu et al., 2021b). They significantly aid plant adaptations to water scarcity by influencing soil nutrient cycling and modulating stress responses (Rolli et al., 2015; Vejan et al., 2016; Vurukonda et al., 2016). This interplay is crucial for plant survival and optimal performance under drought-prone conditions.

Roots are essential for plants to absorb water from the soil. During drought, crop roots and rhizosphere soil microorganisms are the first to detect and respond to environmental changes. These rhizosphere microorganisms exhibit heightened sensitivity to changes in the soil environment and often respond more quickly than plants (Cai and Ahmed, 2022; Cai et al., 2022). Complex interactions among rhizosphere microorganisms are key factors in the rapid adaptation of plants to soil-borne environmental stresses (Giehl and von Wirén, 2014; Pascale et al., 2020). Ecological and evolutionary studies provide compelling evidence that, in the short to medium term, the resilience and productivity of plants in the face of global warming are likely to be significantly influenced by the intricate dynamics within host-associated microbiomes (Trivedi et al., 2022). In their quest to mitigate the adverse consequences of drought on agricultural productivity, researchers are pursuing a range of biotechnological strategies, from refining traditional breeding techniques to applying innovative genetic engineering to enhance sugarcane drought tolerance (Sugiharto, 2018; Misra et al., 2022). Rhizosphere bacteria are pivotal in the biotechnological exploration of drought tolerance in sugarcane. These microorganisms can significantly augment the adaptive capacity and resilience of plants under arid conditions through a spectrum of physiological and biochemical mechanisms (Chieb and Gachomo, 2023). In sugarcane breeding, understanding how various drought-tolerant root system architectures influence the rhizosphere microbial community is pivotal. This analysis not only underpins the theoretical framework for drought-tolerant breeding but also propels the development of new sugarcane varieties adapted to withstand arid conditions (Liu et al., 2021a). By integrating the selection of drought-resistant traits with an in-depth examination of rhizosphere microbial dynamics, breeders can develop novel sugarcane cultivars with superior adaptability to water-deficient environments. Similarly, the introduction of drought tolerance-related genes into the sugarcane genome can lead to the development of transgenic sugarcane varieties with enhanced drought tolerance (Kumar et al., 2024). For example, by expressing the betaine synthase gene in sugarcane, the accumulation of betaine is increased, and the osmoregulatory capacity of cells is improved, thereby enhancing the survival of sugarcane under drought conditions (Rahman et al., 2021). Moreover, the exploration of sugarcane drought resistance mechanisms through advanced gene editing techniques, including RNA interference (RNAi) or CRISPR/Cas9, targeting both transcription factors and genes with currently obscure functions, holds promise for further enhancement of these mechanisms (Mall et al., 2024). In addition, genetic engineering not only focuses on the genetic improvement of sugarcane itself but also involves the interaction of the rhizosphere bacterial community. Additionally, genetic engineering targets not only the enhancement of sugarcane genetic characteristics but also the interactions within the rhizosphere bacterial community. The alteration of the soil environment by transgenic sugarcane under drought stress conditions affects the composition of the rhizosphere bacterial community, which subsequently modulates the physiological responses of sugarcane (Zhao et al., 2020). These studies indicate that genetic engineering can enhance the drought tolerance of sugarcane through direct genetic intervention and concurrently bolster its adaptive capacity to drought stress indirectly by modulating the structure and functionality of the associated rhizosphere bacterial community.

Variations in the diversity and abundance of sugarcane rhizosphere bacterial communities are pivotal in modulating soil nutrient availability and physiological responses of sugarcane to drought (Pereira et al., 2022) (Figure 1). Under drought stress, the structure and function of these bacterial communities undergo significant shifts and profoundly influence soil nutrient dynamics and plant interactions (Naylor and Coleman-Derr, 2018; Ling et al., 2022; Bandopadhyay et al., 2024). Particularly, under drought conditions, plants can alter the profile of soil metabolites in the rhizosphere via root exudation, effectively promoting the proliferation of specific bacteria capable of mitigating stress (Canarini and Dijkstra, 2015; Song et al., 2020). As a perennial crop, sugarcane exhibits a lengthy growth cycle and a sustained root system, establishing a long-lasting rhizosphere and a reliable source of nutrients for its bacterial community, which typically results in a more stable symbiotic interaction (Tayyab et al., 2022). Plant growth-promoting bacteria (PGPB) enhance the chemical properties of the rhizosphere soil and enzyme activity, improve the efficiency of nitrogen utilization in sugarcane, and facilitate water conservation by effectively regulating stomatal closure (Pereira et al., 2019). This management of stomata helps maintain leaf water potential and relative water content (Wei et al., 2013; Aguiar et al., 2016; Wang et al., 2023c) (Table 1). Current research has predominantly focused on the drought resistance of

TABLE 1 Mechanisms employed by rhizosphere bacteria to ameliorate drought stress in plants.

Bacteria	Plants	Description	Reference
Bacillus amyloliquefaciens	*Mentha piperita* L.	Increased total phenol content, enhanced DPPH free radical scavenging, and reduced membrane lipid peroxidation	Chiappero et al. (2019)
Bacillus amyloliquefaciens	*Cicer arietinum* L.	Biofilm formation, produced siderophores, and reduced oxidative stress	Kumar et al. (2016)
Bacillus rugosus	*Triticum aestivum* L.	Biofilm formation, produced siderophores, and increased nitrogen fixation capacity	Salem et al. (2024)
Bacillus subtilis	*Saccharum officinarum* L.	Improved nutrient uptake, accumulated osmoregulatory compounds, and improved water use efficiency	Fonseca et al. (2022)
Streptomyces albidoflavus and *Streptomyces rochei*	*Avena nuda* L.	Removal of excess ROS, improved root morphology, and accumulated osmoregulatory compounds	Qiao et al. (2024)
Streptomyces chartreusis and *Streptomyces griseorubiginosus*	*Saccharum officinarum* L.	Production of indole-3-acetic acid (IAA), regulation of root morphology, and improvement of water use efficiency	Wang et al. (2018b; 2023c)
Streptomyces pseudovenezuelae	*Solanum lycopersicum*	Produced 1-aminocyclopropane-1-carboxylate (ACC) deaminase, increased total sugar content, regulated expression of transcription factors, and increased antioxidant enzyme activity	Abbasi et al. (2020)
Arthrobacter arilaitensis and *Streptomyces pseudovenezuelae*	*Zea mays* L.	Phytohormonal modifications, production of exopolysaccharides, and accumulation of osmolytes	Chukwuneme et al. (2020)
Streptomyces pactum	*Triticum aestivum* L.	Increased osmoregulatory compounds, produced ACC deaminase, reduced membrane damage, and increased efficiency of photosynthesis	Yang et al. (2024)
Mesorhizobium huakuii	*Astragalus sinicus* L.	Accumulated solutes and increased nitrogen fixation and ammonia assimilation	Liu et al. (2022b)
Azospirillum sp.	*Triticum aestivum* L.	Production of plant hormones and promotion of root elongation	Moutia et al. (2010)
Rhizobium japonicum, *Azotobacter chroococcum*, and *Azospirillum brasilense*	*Glycine max* (L.) Merr.	Reduced electrolyte leakage, increased nitrogen fixation, and ammonia assimilation	Abbasi et al. (2013)
Sphingomonas sp.	*Zea mays* L.	Regulated osmotic compounds and increased antioxidant enzyme activity	Wang et al. (2022)
Sphingomonas sp.	*Arabidopsis thaliana* (L.) Heynh.	Promoted growth of lateral roots and root hairs, influenced levels of plant hormones, and increased proline content	Luo et al. (2019)
Sphingomonas panaciterrae	*Spinacia oleracea* L.	Improved nutrient uptake and increased antioxidant and vitamin C content	Sultana et al. (2024)
Rhizophagus spp. and *Burkholderia seminalison*	*Lycopersicon esculatum* and *Capsicum annuum*	Increased antioxidant enzyme activity, improved root structure, improved water use efficiency, and enhanced colonization by mycorrhizal fungi	Tallapragada et al. (2016)
Mitsuaria sp. and *Burkholderia* sp.	*Zea mays* L.	Reduced membrane damage and increased antioxidant enzyme activity	Huang et al. (2017)
Burkholderia sp.	*Cucumis sativus* L.	Regulation of gene expression and increases proline synthesis	Wang et al. (2023a)
Burkholderia sp.	*Saccharum officinarum* L.	Regulation of carotenoid biosynthesis, terpenoid skeleton formation, starch and sucrose metabolism, and phytohormone signaling	Nong et al. (2023)
Pseudomonas fluorescens	*Catharanthus roseus* (L.) G. Don	Promoted root system development, produced phytohormones, and increased alkaloid content	Jaleel et al. (2007)
Pseudomonas sp.	*Andropogon gerardii*	Produced ACC deaminase and regulated nitrogen transformation gene expression	Sarkar et al. (2022)

sugarcane, examining physiological and biochemical impacts, morphological changes in the rhizosphere and leaves, transgenic breeding, and cultivation practices (Liu et al., 2022a). Nonetheless, a significant gap persists in systematic research that integrates the role of root system bacterial communities in conferring drought resistance to sugarcane. Plants can modulate the activity of soil microorganisms under diverse drought conditions by altering the constituents and profiles of their root exudates (Hassan et al., 2019; Williams and de Vries, 2020). However, much of our understanding of plant–PGPB interactions under drought comes from noncrop species, with

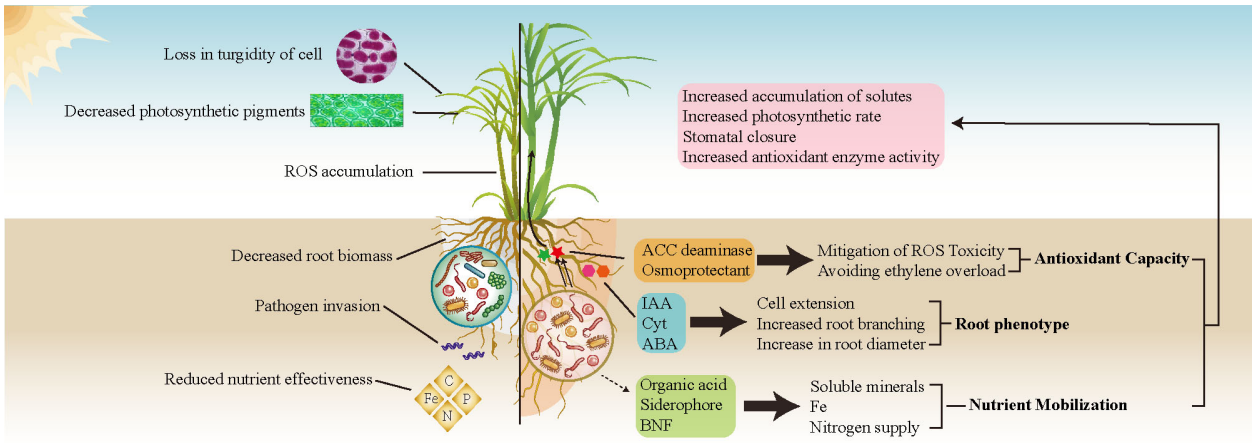

FIGURE 1
A comparison between water-deficient sugarcane without drought-resistant bacterial communities (left) and that with such communities (right). In the absence of a drought-resistant bacterial community, sugarcane is adversely affected, with reduced nutrient acquisition due to decreased water uptake, leading to stunted growth, an increase in reactive oxygen species (ROS), and impaired root development. Conversely, the recruitment of a drought-resistant bacterial community in sugarcane results in the production of essential phytohormones, including cytokinins (Cyt), indole-3-acetic acid (IAA), and abscisic acid (ABA). These phytohormones promote root growth and enhance the capacity for water and nutrient absorption by plants under drought stress. Furthermore, these beneficial bacteria also produce 1-aminocyclopropane-1-carboxylate (ACC) deaminase and osmoprotectants, which help to counteract the negative effects of ROS and mitigate membrane damage caused by drought conditions. Beyond their direct influence on sugarcane, these bacterial communities also increase soil nutrient availability through biological nitrogen fixation (BNF) and the secretion of secondary metabolites, including organic acids and iron-chelating compounds.

crop species potentially selected for traits that may inherently reduce drought tolerance and beneficial interactions with the rhizosphere microbiota (de Vries et al., 2020). In summary, we investigated the adaptive capacities of sugarcane rhizosphere bacterial communities under diverse drought stress scenarios, aiming to enhance our understanding of the mechanisms governing sugarcane–rhizosphere bacterial interactions during drought. We synthesized the effects of multiomics factors, such as sugarcane root architecture, soil metabolites, and nutrients, on rhizosphere bacterial community structure under different levels of drought stress. This exploration holds significant potential, offering novel pathways to enhance our understanding of these interactions and proposing avenues to deepen our insight into the interplay between sugarcane and rhizosphere bacteria in response to drought.

2 Rhizosphere environmental changes and adaptive responses of bacterial communities in sugarcane under the influence of drought

2.1 Rhizosphere soil nutrient changes

Significant alterations in soil nutrient levels substantially affect the rhizosphere environment of sugarcane plants during drought stress. Under such conditions, the total carbon, nitrogen, and phosphorus contents in soil may diminish because of the constraints imposed on microbial activity, which in turn decelerates the decomposition of organic matter and the mineralization of nutrients (Siebert et al., 2019; Gao et al., 2020; Deng et al., 2021). This reduction in nutrient availability directly impairs the ability of sugarcane roots to assimilate nutrients, thereby restricting plant growth and yield (Siebert et al., 2019; Deng et al., 2021). However, the effectiveness of soil nutrients in the sugarcane rhizosphere might not be severely compromised under mild drought conditions. Several studies have indicated that sugarcane initiates the recruitment of specific rhizosphere bacteria by altering root exudates, thereby enhancing its resilience to drought (Liu et al., 2021a, 2021b; Dao et al., 2023; Xing et al., 2023).

This recruitment process is a critical mechanism of adaptation for sugarcane in drought environments and enhances soil nutrient availability. Root exudates serve as nutrient sources for rhizosphere bacteria, fostering their growth and metabolic activities, which may, in turn, improve the availability of nutrients within the soil (Zhao et al., 2021; Balyan and Pandey, 2024). A significant shift in the rhizosphere bacterial community of sugarcane was observed when the field water-holding capacity of the soil fell below a critical threshold of 50%, indicating a transition from a reliance on the effectiveness of soil nutrients to a dependence on the rhizosphere bacterial community to enhance drought tolerance (Dao et al., 2023). At this juncture, sugarcane increasingly relies on microorganisms capable of thriving under drought conditions, including Streptomycetales and Rhizobiales, which may assist in coping with drought by producing plant growth regulators, enhancing soil structure, and improving nutrient uptake capacity (Ebrahimi-Zarandi et al., 2023; Nong et al., 2023; Yang et al., 2024) (Table 1). As drought intensifies, nutrient availability in sugarcane rhizosphere soils becomes increasingly critical. Under these circumstances, sugarcane may need to increasingly rely on changes in root secretions to enlist the aid of drought-tolerant

rhizosphere bacteria, which can facilitate access to and utilization of less-soluble nutrients in the soil. This adaptation is essential for sustaining plant vitality and productivity during water scarcity.

Changes in soil enzyme activity are key bioindicators of soil nutrient dynamics. The rhizosphere of sugarcane is notably influenced by drought conditions, with changes in soil enzyme activity significantly influencing nutrient cycling and plant growth (Jamir et al., 2019; Bogati and Walczak, 2022). Enzymes such as acid phosphatase, urease, and catalase facilitate the mineralization and transformation of nutrients in the soil, thereby directly affecting the availability of nutrients to sugarcane (Neemisha and Sharma, 2022). In drought environments, reduced soil moisture leads to a decline in enzyme activity, which in turn slows down the decomposition of organic matter and reduces the nutrient supply available to sugarcane, thereby affecting growth and productivity (Liu et al., 2021b). Moreover, soil enzymatic activity is closely linked to the structure and function of the rhizosphere microbial community. Changes in the rhizosphere bacterial community structure under drought conditions can modify the composition and activity of soil enzymes, which then influence nutrient dynamics within the sugarcane rhizosphere (Schimel, 2018; Bogati and Walczak, 2022). Additionally, a reduction in soil enzyme activity during drought may affect plant drought tolerance. Certain soil enzymes participate in the synthesis or degradation of organic substances related to drought resistance, such as proline, which plays a protective role in plants facing water scarcity (Deng et al., 2015). The effect of soil enzyme activity on the rhizosphere environment of sugarcane under drought conditions is multifaceted and encompasses soil nutrient cycling, microbial community structure, plant nutrient uptake, and plant drought resistance. Delving deeper into these processes will enhance our understanding of how drought affects sugarcane production and aid in the formulation of more effective strategies to mitigate its effects.

In conclusion, the effect of drought stress on soil nutrients is characterized by a complex interplay of factors, including a reduction in nutrient content, a decline in nutrient availability, and a decrease in soil enzyme activity. These elements, when combined, significantly influence the growth and health of sugarcane in the rhizosphere. A thorough understanding of these precise shifts in soil nutrient dynamics is imperative for a more nuanced appraisal of the alterations within the sugarcane rhizosphere under drought conditions. Furthermore, it is crucial to understand the adaptive mechanisms of rhizosphere bacterial communities that play a critical role in plant resilience and the overall response to water scarcity. This knowledge will inform the development of more precise and effective strategies to enhance the sustainability and productivity of sugarcane cultivation in drought environments.

2.2 Rhizosphere soil metabolite composition

Within the sugarcane rhizosphere, the sources of soil metabolites are multifaceted. The formation of these metabolites results not only from secretions by the sugarcane root system but also from the metabolic processes of rhizosphere microorganisms (Ponomarova et al., 2017). Marked variations characterize the composition and content of rhizosphere soil metabolites in sugarcane subjected to varying degrees of stress (Zhao et al., 2020). The types and contents of soil metabolites (fatty acids, carboxylic acids, carbohydrates, and amino acids) in sugarcane increased significantly under mild drought conditions, while long-chain organic acids (oleic acid and linoleic acid) increased under moderate drought conditions, and long-chain organic acids (oleic acid, monopalmitin, and monoolein) increased under severe drought conditions, compared to well-watered conditions (Xing et al., 2023). These metabolic changes are associated with the selective enrichment of specific bacterial communities within the sugarcane rhizosphere under drought stress. This enrichment is believed to act as an adaptive mechanism that enhances plant drought resilience (Cesari et al., 2019; Woo et al., 2020). As drought severity progresses, carbon uptake by sugarcane decreases, concurrently diminishing carbon flux in rhizosphere exudates. This reduction restricts interactions between sugarcane and its associated rhizosphere bacteria (Ingrisch et al., 2018; Karlowsky et al., 2018). Since rhizosphere bacteria rely on organic exudates from the sugarcane root system for their carbon supply, their activities may be concurrently constrained by carbon scarcity and water scarcity under severe drought conditions (Dijkstra et al., 2013). In conclusion, although drought stress can hinder the physiological metabolism of sugarcane, this species exhibits resilience by adjusting its photosynthetic allocation, metabolic pathways, and production of osmotic protectants. These adaptive responses reflect the intrinsic physiological mechanisms of the plant, which are further influenced by its interactions with root-associated bacterial communities. Through their metabolic activities and symbiotic relationships, these communities support the strategies plant's strategies for adapting and thriving under drought conditions. They aid in nutrient acquisition, boost stress tolerance, and improve water-use efficiency, thereby reinforcing the overall response of plants to drought.

3 Changes in the rhizosphere bacterial community of sugarcane under drought stress

3.1 Influencing factors and adaptability of sugarcane rhizosphere bacterial community diversity

The diversity and composition of sugarcane rhizosphere bacterial communities are intricately shaped by a dynamic equilibrium, influenced by various factors. Under drought stress, soil metabolites, soil nutrients, sugarcane genotypes, and root system traits have emerged as pivotal determinants of rhizosphere bacterial community structure (Zhao et al., 2020; Liu et al., 2021a, 2021b; Dao et al., 2023; Xing et al., 2023). Under drought conditions, a general decline in the diversity of sugarcane rhizosphere soil bacteria has been observed. However, the specific impacts of varying drought intensities reveal a

complex and variable response to water stress (Liu et al., 2021a; Xing et al., 2023). Under mild drought conditions, sugarcane and its associated rhizosphere bacterial communities exhibit a degree of tolerance. Adaptive alterations in root exudates, particularly increases in organic acids, sugars, and amino acids, may lead to increased bacterial diversity (Zhalnina et al., 2018; Chen et al., 2022). However, under moderate to severe drought conditions, a significant reduction in the alpha diversity of sugarcane rhizosphere bacterial communities has been observed, suggesting that the stress may have surpassed the tolerance limits of certain bacterial species, resulting in pronounced shifts in community composition (Xing et al., 2023). Streptomycetales and Rhizobiales bacteria have been shown to play a crucial role in the response to drought stress in the sugarcane rhizosphere (Liu et al., 2021a; Dao et al., 2023). These bacterial strains become more abundant under drought stress and are positively associated with key sugarcane root characteristics, including the number of root tips and total root length. This finding suggests that these strains may play a vital role in promoting the development of sugarcane roots and enhancing the efficiency of water and nutrient uptake (Maia Júnior et al., 2019; Liu et al., 2021b; Xing et al., 2023). In addition, soil nutrient status, particularly the levels of available phosphorus (P) and soil acid phosphatase activity, is correlated with the alpha diversity of sugarcane rhizosphere bacterial communities, underscoring the regulatory role of soil nutrients in shaping bacterial diversity (Zhao et al., 2020; Liu et al., 2021a, 2021b). Comparative analyses across sugarcane varieties have revealed that drought-tolerant varieties harbor a higher abundance of drought-associated bacteria, even under non-drought conditions, whereas these bacterial populations only increase under stress conditions in drought-sensitive varieties. Furthermore, significant differences in rhizosphere soil nutrient composition and enzyme activities have been observed among drought-tolerant varieties, highlighting the close relationship between sugarcane drought tolerance and the adaptive capabilities of rhizosphere bacterial communities (Zhao et al., 2020; Liu et al., 2021b; Dao et al., 2023). The diversity of sugarcane rhizosphere bacterial communities therefore represents a complex ecosystem influenced by multiple factors. A thorough understanding of the interplay between these factors and the establishment and function of rhizosphere bacterial communities is essential to guide the development of drought-tolerant sugarcane varieties, optimize agricultural practices, and enhance sugarcane yield and quality. Comprehensive analyses of soil metabolites, soil nutrients, sugarcane genotypes, and root characteristics can offer a more holistic understanding of the adaptive mechanisms of rhizosphere bacterial communities, thereby providing evidence to inform the sustainable cultivation of sugarcane under drought conditions.

3.2 Effect of Streptomycetales on the drought performance of sugarcane

Streptomycetales is the bacterial strain most responsive to drought stress in sugarcane and the relative abundance of this bacterial strain increases significantly under moderate and severe drought conditions (Liu et al., 2021a; Xing et al., 2023). Xu et al. (2018) reported a significant correlation between the relative abundance of Streptomycetales in plant root systems and host drought resistance. The mycelial and spore-forming properties of Streptomycetales enable these bacteria to survive in harsh environmental conditions compared to other PGPBs (Vurukonda et al., 2018). Streptomycetales can also produce many secondary metabolites and volatile metabolites (Olanrewaju and Babalola, 2019), and these metabolites can alter the structure of the rhizosphere bacterial community and influence crop root conformation (Chukwuneme et al., 2020; Zhang et al., 2024) (Figure 2).

Streptomycetales is a group of Actinobacteria belonging to the order Actinomycetales. These bacteria thrive in less hydrated soil environments and readily metabolize recalcitrant carbon sources typically found in such soils (Ebrahimi-Zarandi et al., 2023). Actinomycetes have also been associated with an inhibitory effect on soil fungal pathogen infestation, which increases with drought stress (Varela et al., 2016; Fallah et al., 2023). The survival of Streptomycetales under drought conditions can be attributed to its characteristic high substrate affinity coupled with a relatively slow growth rate compared to other sugarcane rhizosphere bacteria, enabling it to persist under limited moisture conditions (Acosta-Martinez et al., 2014; Nazari et al., 2023). Gram-positive bacteria, including Streptomycetales, are particularly adept at harnessing a diverse range of carbon sources more effectively than their Gram-negative counterparts. They possess the metabolic versatility to assimilate inorganic N from nutrient-poor, drought-affected soils, thereby facilitating the enzymatic breakdown of organic matter. In contrast, Gram-negative bacteria, such as Aspergillus and Acidobacteria, are primarily reliant on the immediate availability of carbon and N from root exudates (Reinsch et al., 2014; Martiny et al., 2017). Studies have indicated a positive correlation between drought severity and the presence of genes encoding carbohydrases in actinomycetes (Zhalnina et al., 2018). This genetic predisposition may underlie the increased carbohydrate content of soil metabolites, potentially enhancing the attraction and colonization of Streptomycetales in the rhizosphere of sugarcane, particularly during periods of prolonged drought stress.

Streptomycetales are crucial in the rhizosphere of sugarcane for maintaining plant health and enhancing drought resilience. Drought resistance is achieved through exudation of 1-aminocyclopropane-1-carboxylate (ACC) deaminase and secondary metabolites, such as antibiotics and indole-3-acetic acid (IAA) (Barnawal et al., 2013; Kour et al., 2024). The metabolites produced by Streptomycetales, such as antibiotics, vitamins, amino acids, and extracellular hydrolases, counter nutrient limitations arising from reduced enzymatic activity during drought, thereby stimulating enhanced nutrient absorption by sugarcane roots (Selim et al., 2019; Chaiharn et al., 2020; Borah et al., 2022). Warrad et al. (2020) observed that a cell-free extract (F2.7) of *Streptomyces* sp. Ac3 significantly increased the levels of total soluble sugars, proline, and betaine in maize, thereby improving its growth and quality under water-scarce conditions. Streptomycetales elevates proline levels by producing ACC deaminase, which aids in the stabilization of subcellular structures, maintenance of cellular redox balance, and mitigation of osmotic stress (Wang et al., 2018b; Chandra et al., 2019; Kour et al., 2022). Streptomycetales contribute to the stability of bacterial diversity of the rhizosphere under severe drought conditions by solubilizing complex compounds and providing carbon

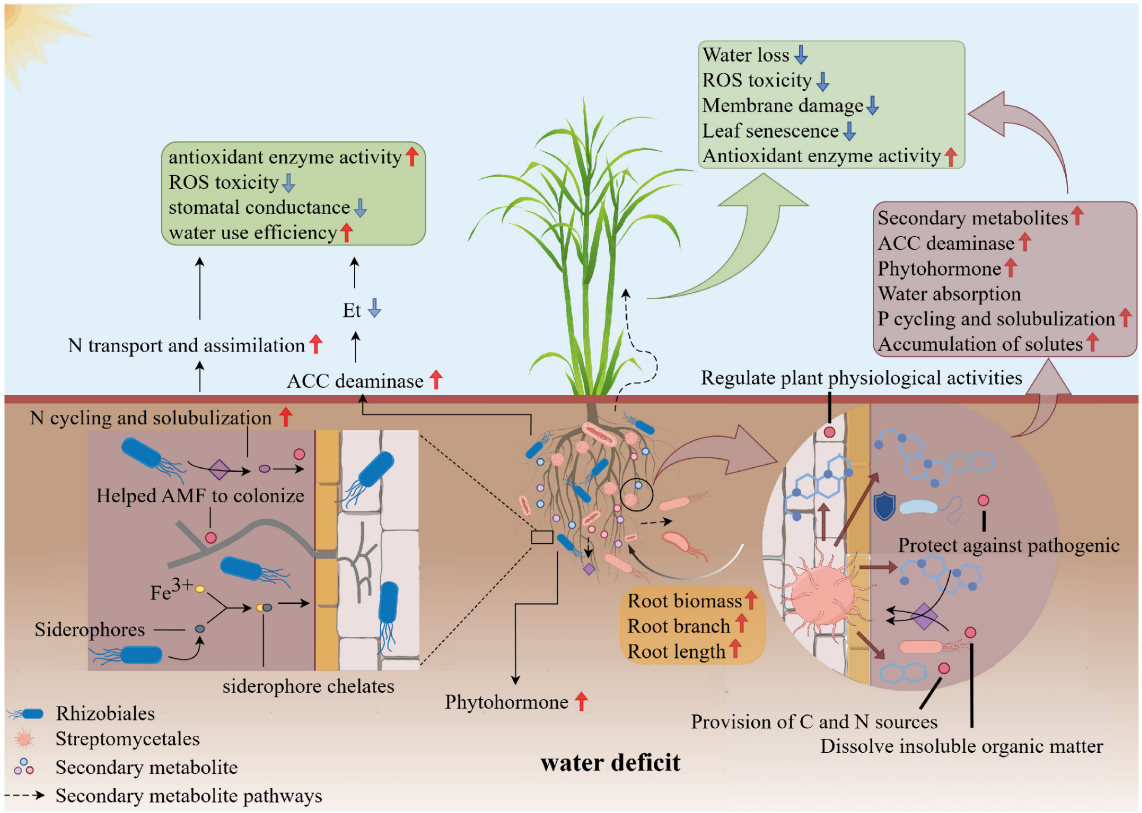

FIGURE 2
Effects of Streptomycetales and Rhizobiales on drought tolerance of sugarcane under drought conditions. The abundance of Streptomycetales and Rhizobiales increased in the inter-root of sugarcane under drought conditions. Streptomycetales can secrete a variety of secondary metabolites, which can enhance the drought resistance of sugarcane by protecting against pathogens, dissolving insoluble organic matter to improve plant root morphology, and enhancing root water and nutrient uptake, thereby improving drought tolerance. Rhizobiales, on the other hand, form a symbiotic relationship with the sugarcane root system, fixing atmospheric nitrogen and providing an essential nitrogen source. This symbiotic relationship enhances the growth and survival of sugarcane under drought conditions. Additionally, Rhizobiales can produce a variety of phytohormones that regulate physiological responses in sugarcane. Streptomycetales and Rhizobiales work together through different mechanisms to enhance the drought resistance of sugarcane under drought conditions.

and N sources for other bacteria (Viaene et al., 2016; Wang et al., 2018a). Drought affects the availability of effective P in the rhizosphere soil by impeding the decomposition of organic P and the release of inorganic P (Fan et al., 2021). However, Streptomycetales mobilizes soil phosphatases to accelerate the degradation of organic P substrates and enhance phosphate production, thereby supplying plants with essential P (Martín and Liras, 2021). During periods of drought, an increase in soil coverage by the crop root system is associated with more fine roots, thereby enhancing accessibility to essential resources (Gargallo-Garriga et al., 2018). Xing et al. (2023) reported a significant association between the relative abundance of Streptomycetales in the rhizosphere bacterial community and root phenotypes. This association is linked to the ability of Streptomycetales to produce IAA, an organic compound that fosters the proliferation of lateral roots and root hairs. The enhanced development of the root system helps sugarcane locate supplementary water resources in drought environments (Yandigeri et al., 2012; Kurepa and Smalle, 2022; Etesami and Glick, 2024). In addition, the abundance of Streptomycetales is positively associated with the abundance of other rhizosphere bacteria, including Streptosporangiales, Jiangellales, Micrococcales, and Rhizobiales (Xing et al., 2023). Streptomycetales may, therefore, enhance the role of other rhizosphere bacteria in promoting sugarcane growth and drought resistance by producing metabolites that mediate interbacterial communication.

3.3 Effect of Rhizobiales on the drought performance of sugarcane

The abundance of Rhizobiales in the sugarcane rhizosphere decreases under mild drought conditions but increases as the severity of drought increases (Xing et al., 2023). In addition to their essential role in promoting plant growth, Rhizobiales can trigger a range of physiological and biochemical stress responses in sugarcane plants. Specifically, PGPB enhance the production of osmoprotectants, which are crucial for maintaining cellular integrity during drought stress. Rhizobiales activate antioxidant enzymes that neutralize the harmful effects of reactive oxygen species, thereby bolstering sugarcane resistance to drought stress (Ahemad and Khan, 2012; Wang et al., 2018a).

Rhizobiales are highly abundant in the sugarcane rhizosphere. During drought events, alterations in soil physicochemical properties

and root exudates can create inhospitable conditions for some members of the Rhizobiales community (Liu et al., 2013; Dao et al., 2023). Nonetheless, certain Rhizobiales are adept at capitalizing on sugarcane rhizosphere exudates, thereby ameliorating the rhizosphere environment under drought stress. These adaptable rhizobiales may even dominate the bacterial community in the sugarcane rhizosphere (Gopalakrishnan et al., 2015; Trivedi et al., 2021; del Carmen Orozco-Mosqueda et al., 2022). This capability is attributed to the fact that, as part of the Alphaproteobacteria, Rhizobiales can efficiently metabolize the carbon found in sugarcane rhizosphere exudates (Da Costa et al., 2018). Furthermore, the abundance of *Streptomyces* is positively correlated with that of Rhizobiales (Xing et al., 2023). We propose that Rhizobiales can exploit metabolites from *Streptomyces* and synergistically interact with them to ameliorate soil physicochemical properties and regulate the physiological and biochemical responses of sugarcane.

Under drought conditions, Rhizobiales augment the nutrient response and enhance the drought tolerance of sugarcane through multiple mechanisms (Figure 2). Although Rhizobiales are recognized as plant growth-promoting bacteria and for their contribution to stress tolerance, there is a relative scarcity of literature on their specific impact on the drought resilience of non-leguminous plants, such as sugarcane. These bacteria can ameliorate the detrimental effects of drought on plants by modulating leaf stomatal conductance, photosynthetic capacity, and root morphology in non-leguminous species (Moutia et al., 2010). For instance, Chen et al. (2024) demonstrated that inoculation with *Rhizobium rhizogenes* led to an elevation in endogenous abscisic acid (ABA) levels in *Arabidopsis*, bolstering the sensitivity and adaptive response of the plant to drought stress. N and P are acknowledged as significant limiting factors in agroecosystems (Zuluaga and Sonnante, 2019; Bihari et al., 2022), and the acquisition of these elements by plants is closely connected with the availability of water. N must be dissolved in water to be absorbed by plant roots (Araus et al., 2020). During periods of drought, water accessibility is compromised, restricting the uptake of various nutrients (Osakabe et al., 2014). Furthermore, numerous genes involved in N transport and assimilation are suppressed at the transcriptional level under drought stress (Ristova et al., 2016). It has been observed that *Arabidopsis thaliana* employs a common set of genes to respond to N and drought signals (Cerda and Alvarez, 2024). Although Rhizobiales are often associated with legumes, providing N to their host plants through symbiosis, they have also been reported to replenish soil N in a saprophytic state and function as endophytes, thereby increasing the uptake of essential mineral elements such as N and P in sugarcane (Li Ting et al., 2013; Fallah et al., 2023). Conversely, the regulation of water channel proteins by different N levels influences hydraulic conductance (Araus et al., 2020). The availability of N in the soil facilitates water entry into cellular spaces by affecting the hydraulic properties of the cell membrane and intracellular nitrate concentration (Zheng et al., 2018). N availability also plays a role in stomatal regulation, affecting transpiration and water-use efficiency (Matimati et al., 2014). Rhizobiales may contribute to the demineralization of soil organic matter by modulating the activity of extracellular enzymes involved in soil nutrient cycling. This process increases total N and available P contents in the rhizosphere soil, creating conditions conducive to plant growth under drought stress (Ahluwalia et al., 2021; Wang et al., 2023b). Elevated levels of available P can effectively mitigate P stress caused by an imbalanced soil nitrogen-phosphorus ratio, promoting the growth of underground plant parts (Huang et al., 2018; Liu et al., 2021b). In addition, Rhizobiales produce phytohormones, including IAA and abscisic acid, which regulate root conformation in sugarcane and facilitate nutrient exploration (Barquero et al., 2022; Lopes et al., 2023).

3.4 Effect of other rhizosphere bacteria on drought performance of sugarcane

The rhizosphere bacterial community composition is generally consistent across different sugarcane varieties, but it differs under drought stress. For example, in the Zhongzhe 1 sugarcane variety, the bacteria Streptosporangiales and Sphingomonadales were enriched under drought conditions (Dao et al., 2023). Streptosporangiales, an order within Actinomycetes, has been observed to increase in abundance under drought conditions. However, there is a lack of research substantiating their growth-promoting effects on plants, specifically sugarcane, and their roles in enhancing drought tolerance. Conversely, Sphingomonadales are recognized for their superior adaptation to arid soils as oligotrophic bacteria and their proficiency in degrading organic pollutants (Roy et al., 2012; Kunihiro et al., 2013; Luo et al., 2019). *Sphingomonas* has been identified as a PGPB that emits volatile organic compounds (VOCs), which stimulate plant growth and mitigate the effects of plant pathogens, thereby improving drought resistance (Farag et al., 2013; Luo et al., 2020; Poudel et al., 2021). *Gluconacetobacter diazotrophicus* PAL5, an endophytic nitrogen-fixing bacterium associated with sugarcane, enhances the drought tolerance of sugarcane (Vargas et al., 2014). Nong et al. (2023) demonstrated upregulation of the biosynthesis of carotenoids and the terpenoid backbone by *Burkholderia* in sugarcane. The Guangxi sugarcane variety GT42D has been shown to harbor Burkholderiaceae as its core flora under drought stress (Liu et al., 2021a) (Table 1). Despite these findings, there is a scarcity of studies investigating the growth promotion and drought resistance properties of *Sphingomonas*, *Burkholderia*, and *Gluconacetobacter* in sugarcane. Further research is required to understand the mechanisms of action and to explore the potential applications of these bacteria in agriculture. Of note, *Bacillus* species are widely distributed across dynamic agroecosystems due to their robust tolerance to stress, which is facilitated by spore formation (Vardharajula et al., 2011; Radhakrishnan et al., 2017; Gowtham et al., 2020). *Bacillus* species have also been shown to enhance the drought tolerance of sugarcane (Chandra et al., 2018; Fonseca et al., 2022), even under severe drought stress. Almeida et al. (2024) demonstrated that inoculation with *Bacillus licheniformis* and *Bacillus subtilis* significantly enhanced the survival of presprouted sugarcane seedlings under water-limited conditions. These bacteria also improved the water-use efficiency of presprouted seedlings under severe drought conditions by nearly 200%. Furthermore, the abundance of *Bacillus* in sugarcane appears to remain stable under mild and moderate drought conditions and may decrease under

severe stress. These observations highlight the potentially important role of *Bacillus* as a bioregulator for improving crop drought tolerance. Nevertheless, the variation in *Bacillus* abundance under different drought intensities may be influenced by a multitude of ecological factors and plant–microbe interactions. Furthermore, in-depth studies are needed to fully understand the mechanism of its action in dynamic agroecosystems.

4 Conclusions

Sugarcane, a vital cash and energy crop worldwide, is acutely sensitive to water deficit throughout the growth cycle. Rhizosphere bacterial communities are crucial for crop growth and development. Our review evaluated the abundance of rhizosphere bacterial communities under crop water stress and examined evidence of plant–bacteria dynamics. Diversity within the bacterial community in the rhizosphere soil of sugarcane significantly changes when soil water-holding capacity reaches 50%. The abundance of some bacterial groups diminishes as the severity of drought stress increases, whereas the abundance of Streptomycetales and Rhizobiales increases with increasing drought stress. Streptomycetales enhance drought resistance in sugarcane by producing various secondary metabolites. They also support nutrient availability in the rhizosphere by supplying carbon or nitrogen to other microbes, thereby improving soil fertility. Rhizobiales, on the other hand, support nitrogen acquisition in sugarcane and produce siderophores to assist with iron uptake under drought conditions. There are differences in the response of bacterial rhizosphere communities to drought stress across sugarcane varieties. For example, during drought stress, Burkholderiaceae was prominent in the rhizosphere bacterial communities of the Guangxi sugarcane variety GT42D. Despite considerable advances in knowledge, our understanding of the interactions between PGPB and sugarcane under drought stress requires further investigation. Framework modeling of sugarcane rhizosphere bacterial communities and their productivity under varying levels of drought stress could provide important theoretical support and guidance for sugarcane cultivation and production practices.

Author contributions

MC: Writing – review & editing, Writing – original draft, Visualization, Software, Methodology, Formal analysis, Conceptualization. YX: Writing – review & editing, Validation, Supervision, Conceptualization. CC: Writing – review & editing, Validation, Supervision. ZW: Writing – review & editing, Visualization, Validation, Supervision, Resources, Project administration, Methodology, Investigation, Funding acquisition, Conceptualization.

Funding

The author(s) declare financial support was received for the research, authorship, and/or publication of this article. This study was supported by the National Natural Science Foundation of China (Grant No. 32260546), Guangxi Natural Science Foundation (Grant No. 2021AC19060), and Guangxi Natural Science Foundation (Grant No. 2020JJB130008). This study was also supported by the Sugarcane Research Foundation of Guangxi University (Grant No. 202200743).

Conflict of interest

The authors declare that the research was conducted in the absence of any commercial or financial relationships that could be construed as a potential conflict of interest.

Publisher's note

References

Abbasi, S., Sadeghi, A., and Safaie, N. (2020). *Streptomyces alleviate* drought stress in tomato plants and modulate the expression of transcription factors ERF1 and WRKY70 genes. *Scientia Hortic.* 265, 9. doi: 10.1016/j.scienta.2020.109206

Abbasi, S., Zahedi, H., Sadeghipour, O., and Akbari, R. (2013). Effect of plant growth promoting rhizobacteria (PGPR) on physiological parameters and nitrogen content of soybean grown under different irrigation regimes. *Res. Crops* 14, 798–803.

Acosta-Martinez, V., Cotton, J., Gardner, T., Moore-Kucera, J., Zak, J., Wester, D., et al. (2014). Predominant bacterial and fungal assemblages in agricultural soils during a record drought/heat wave and linkages to enzyme activities of biogeochemical cycling. *Appl. Soil Ecol.* 84, 69–82. doi: 10.1016/j.apsoil.2014.06.005

Aguiar, N. O., Medici, L. O., Olivares, F. L., Dobbss, L. B., Torres-Netto, A., Silva, S. F., et al. (2016). Metabolic profile and antioxidant responses during drought stress recovery in sugarcane treated with humic acids and endophytic diazotrophic bacteria. *Ann. Appl. Biol.* 168, 203–213. doi: 10.1111/aab.12256

Ahemad, M., and Khan, M. S. (2012). Productivity of greengram in tebuconazole-stressed soil, by using a tolerant and plant growth-promoting *Bradyrhizobium* sp. MRM6 strain. *Acta physiologiae plantarum* 34, 245–254. doi: 10.1007/s11738-011-0823-8

Ahluwalia, O., Singh, P. C., and Bhatia, R. (2021). A review on drought stress in plants: Implications, mitigation and the role of plant growth promoting rhizobacteria. *Resources Environ. Sustainability* 5, 100032. doi: 10.1016/j.resenv.2021.100032

Ahmed, A. A. Q., Odelade, K. A., and Babalola, O. O. (2019). Microbial inoculants for improving carbon sequestration in agroecosystems to mitigate climate change. *Handb. Climate Change resilience* 1-21. doi: 10.1007/978-3-319-93336-8_119

Almeida, L. C. O., Santos, H. L., de Casrto Nogueira, C. H., Carnietto, M. R. A., da Silva, G. F., Boaro, C. S. F., et al. (2024). Plant growth-promoting bacteria enhance survival, growth, and nutritional content of sugarcane propagated through pre-sprouted seedlings under water deficit. *Agriculture* 14, 189. doi: 10.3390/agriculture14020189

Araus, V., Swift, J., Alvarez, J. M., Henry, A., and Coruzzi, G. M. (2020). A balancing act: how plants integrate nitrogen and water signals. *J. Exp. Bot.* 71, 4442–4451. doi: 10.1093/jxb/eraa054

Backer, R., Rokem, J. S., Ilangumaran, G., Lamont, J., Praslickova, D., Ricci, E., et al. (2018). Plant growth-promoting rhizobacteria: context, mechanisms of action, and roadmap to commercialization of biostimulants for sustainable agriculture. *Front. Plant Sci.* 9. doi: 10.3389/fpls.2018.01473

Balyan, G., and Pandey, A. K. (2024). Root exudates, the warrior of plant life: revolution below the ground. *South Afr. J. Bot.* 164, 280–287. doi: 10.1016/j.sajb.2023.11.049

Bandopadhyay, S., Li, X., Bowsher, A. W., Last, R. L., and Shade, A. (2024). Disentangling plant-and environment-mediated drivers of active rhizosphere bacterial community dynamics during short-term drought. *Nat. Commun.* 15, 6347. doi: 10.1038/s41467-024-50463-1

Barnawal, D., Maji, D., Bharti, N., Chanotiya, C. S., and Kalra, A. (2013). ACC deaminase-containing *Bacillus subtilis* reduces stress ethylene-induced damage and improves mycorrhizal colonization and rhizobial nodulation in *Trigonella foenum-graecum* under drought stress. *J. Plant Growth Regul.* 32, 809–822. doi: 10.1007/s00344-013-9347-3

Barquero, M., Poveda, J., Laureano-Marín, A. M., Ortiz-Liébana, N., Brañas, J., and González-Andrés, F. (2022). Mechanisms involved in drought stress tolerance triggered by rhizobia strains in wheat. *Front. Plant Sci.* 13, 1036973. doi: 10.3389/fpls.2022.1036973

Bihari, B., Singh, Y. K., Shambhavi, S., Mandal, J., Kumar, S., and Kumar, R. (2022). Nutrient use efficiency indices of N, P, and K under rice-wheat cropping system in LTFE after 34th crop cycle. *J. Plant Nutr.* 45, 123–140. doi: 10.1080/01904167.2021.1943674

Bogati, K., and Walczak, M. (2022). The impact of drought stress on soil microbial community, enzyme activities and plants. *Agronomy* 12, 189. doi: 10.3390/agronomy12010189

Borah, A., Hazarika, S. N., and Thakur, D. (2022). Potentiality of actinobacteria to combat against biotic and abiotic stresses in tea [*Camellia sinensis* (L) O. Kuntze. *J. Appl. Microbiol.* 133, 2314–2330. doi: 10.1111/jam.15734

Cai, G. C., and Ahmed, M. A. (2022). The role of root hairs in water uptake: recent advances and future perspectives. *J. Exp. Bot.* 73, 3330–3338. doi: 10.1093/jxb/erac114

Cai, G. C., Ahmed, M. A., Abdalla, M., and Carminati, A. (2022). Root hydraulic phenotypes impacting water uptake in drying soils. *Plant Cell Environ.* 45, 650–663. doi: 10.1111/pce.14259

Canarini, A., and Dijkstra, F. A. (2015). Dry-rewetting cycles regulate wheat carbon rhizodeposition, stabilization and nitrogen cycling. *Soil Biol. Biochem.* 81, 195–203. doi: 10.1016/j.soilbio.2014.11.014

Cerda, A., and Alvarez, J. M. (2024). Insights into molecular links and transcription networks integrating drought stress and nitrogen signaling. *New Phytol.* 241, 560–566. doi: 10.1111/nph.v241.2

Cesari, A., Paulucci, N., López-Gómez, M., Hidalgo-Castellanos, J., Plá, C. L., and Dardanelli, M. S. (2019). Restrictive water condition modifies the root exudates composition during peanut-PGPR interaction and conditions early events, reversing the negative effects on plant growth. *Plant Physiol. Biochem.* 142, 519–527. doi: 10.1016/j.plaphy.2019.08.015

Chaiharn, M., Theantana, T., and Pathom-Aree, W. (2020). Evaluation of biocontrol activities of *Streptomyces* spp. against rice blast disease fungi. *Pathogens* 9, 126. doi: 10.3390/pathogens9020126

Chandra, D., Srivastava, R., Gupta, V. V., Franco, C. M., and Sharma, A. K. (2019). Evaluation of ACC-deaminase-producing rhizobacteria to alleviate water-stress impacts in wheat (*Triticum aestivum* L.) plants. *Can. J. Microbiol.* 65, 387–403. doi: 10.1139/cjm-2018-0636

Chandra, P., Tripathi, P., and Chandra, A. (2018). Isolation and molecular characterization of plant growth-promoting *Bacillus* spp. and their impact on sugarcane (*Saccharum* spp. hybrids) growth and tolerance towards drought stress. *Acta Physiologiae Plantarum* 40, 15. doi: 10.1007/s11738-018-2770-0

Chen, X., Favero, B. T., Nardy, R., He, J., de Godoy Maia, I., Liu, F., et al. (2024). Rhizobium rhizogenes rol C gene promotes leaf senescence and enhances osmotic stress resistance in Arabidopsis: the positive role of abscisic acid. *Physiologia Plantarum* 176, e14142. doi: 10.1111/ppl.v176.1

Chen, Y., Yao, Z., Sun, Y., Wang, E., Tian, C., Sun, Y., et al. (2022). Current studies of the effects of drought stress on root exudates and rhizosphere microbiomes of crop plant species. *Int. J. Mol. Sci.* 23, 2374. doi: 10.3390/ijms23042374

Chiappero, J., Cappellari, L., Sosa Alderete, L. G., Palermo, T. B., and Banchio, E. (2019). Plant growth promoting rhizobacteria improve the antioxidant status in *Mentha piperita* grown under drought stress leading to an enhancement of plant growth and total phenolic content. *Ind. Crops Products* 139, 9. doi: 10.1016/j.indcrop.2019.111553

Chieb, M., and Gachomo, E. W. (2023). The role of plant growth promoting rhizobacteria in plant drought stress responses. *BMC Plant Biol.* 23 (1), 408.

Chukwuneme, C. F., Babalola, O. O., Kutu, F. R., and Ojuederie, O. B. (2020). Characterization of actinomycetes isolates for plant growth promoting traits and their effects on drought tolerance in maize. *J. Plant Interact.* 15, 93–105. doi: 10.1080/17429145.2020.1752833

Da Costa, D. P., Dias, A. C., Cotta, S. R., Vilela, D., De Andrade, P. A., Pellizari, V. H., et al. (2018). Changes of bacterial communities in the rhizosphere of sugarcane under elevated concentration of atmospheric CO_2. *GCB Bioenergy* 10, 137–145. doi: 10.1111/gcbb.2018.10.issue-2

Dao, J., Xing, Y., Chen, C., Chen, M., and Wang, Z. (2023). Adaptation of rhizosphere bacterial communities of drought-resistant sugarcane varieties under different degrees of drought stress. *Microbiol. Spectr.* 11, e01184–e01123. doi: 10.1128/spectrum.01184-23

del Carmen Orozco-Mosqueda, M., Fadiji, A. E., Babalola, O. O., Glick, B. R., and Santoyo, G. (2022). Rhizobiome engineering: unveiling complex rhizosphere interactions to enhance plant growth and health. *Microbiological Res.* 263, 127137. doi: 10.1016/j.micres.2022.127137

Deng, L., Peng, C., Kim, D.-G., Li, J., Liu, Y., Hai, X., et al. (2021). Drought effects on soil carbon and nitrogen dynamics in global natural ecosystems. *Earth-Science Rev.* 214, 103501. doi: 10.1016/j.earscirev.2020.103501

Deng, F., Yang, S., and Gong, M. (2015). Regulation of cell signaling molecules on proline metabolism in plants under abiotic stress. *Plant Physiol. J.* 51, 1573–1582. doi: 10.13592/j.cnki.ppj.2015.1015

de Vries, F. T., Griffiths, R. I., Knight, C. G., Nicolitch, O., and Williams, A. (2020). Harnessing rhizosphere microbiomes for drought-resilient crop production. *Science* 368, 270–274. doi: 10.1126/science.aaz5192

Dijkstra, F. A., Carrillo, Y., Pendall, E., and Morgan, J. A. (2013). Rhizosphere priming: a nutrient perspective. *Front. Microbiol.* 4, 216. doi: 10.3389/fmicb.2013.00216

Dlamini, P. J. (2021). Drought stress tolerance mechanisms and breeding effort in sugarcane: A review of progress and constraints in South Africa. *Plant Stress* 2, 100027. doi: 10.1016/j.stress.2021.100027

Ebrahimi-Zarandi, M., Etesami, H., and Glick, B. R. (2023). Fostering plant resilience to drought with actinobacteria: unveiling perennial allies in drought stress tolerance. *Plant Stress* 10, 18. doi: 10.1016/j.stress.2023.100242

Etesami, H., and Glick, B. R. (2024). Bacterial indole-3-acetic acid: a key regulator for plant growth, plant-microbe interactions, and agricultural adaptive resilience. *Microbiological Res.* 281, 21. doi: 10.1016/j.micres.2024.127602

Fallah, N., Tayyab, M., Yang, Z., Pang, Z., Zhang, C., Lin, Z., et al. (2023). Free-living bacteria stimulate sugarcane growth traits and edaphic factors along soil depth gradients under contrasting fertilization. *Sci. Rep.* 13, 6288. doi: 10.1038/s41598-022-25807-w

Fan, Y. X., Lu, S. X., He, M., Yang, L. M., Hu, W. F., Yang, Z. J., et al. (2021). Long-term throughfall exclusion decreases soil organic phosphorus associated with reduced plant roots and soil microbial biomass in a subtropical forest. *Geoderma* 404, 10. doi: 10.1016/j.geoderma.2021.115309

Farag, M. A., Zhang, H. M., and Ryu, C. M. (2013). Dynamic chemical communication between plants and bacteria through airborne signals: induced resistance by bacterial vlatiles. *J. Chem. Ecol.* 39, 1007–1018. doi: 10.1007/s10886-013-0317-9

Ferreira, T. H., Tsunada, M. S., Bassi, D., Araújo, P., Mattiello, L., Guidelli, G. V., et al. (2017). Sugarcane water stress tolerance mechanisms and its implications on developing biotechnology solutions. *Front. Plant Sci.* 8, 1077. doi: 10.3389/fpls.2017.01077

Fonseca, M. C. D., Bossolani, J. W., de Oliveira, S. L., Moretti, L. G., Portugal, J. R., Scudeletti, D., et al. (2022). *Bacillus subtilis* inoculation improves nutrient uptake and physiological activity in sugarcane under drought stress. *Microorganisms* 10, 18. doi: 10.3390/microorganisms10040809

Gao, D., Bai, E., Li, M., Zhao, C., Yu, K., and Hagedorn, F. (2020). Responses of soil nitrogen and phosphorus cycling to drying and rewetting cycles: a meta-analysis. *Soil Biol. Biochem.* 148, 107896. doi: 10.1016/j.soilbio.2020.107896

Gargallo-Garriga, A., Preece, C., Sardans, J., Oravec, M., Urban, O., and Peñuelas, J. (2018). Root exudate metabolomes change under drought and show limited capacity for recovery. *Sci. Rep.* 8, 1–15. doi: 10.1038/s41598-018-30150-0

Giehl, R. F., and von Wirén, N. (2014). Root nutrient foraging. *Plant Physiol.* 166, 509–517. doi: 10.1104/pp.114.245225

Gopalakrishnan, S., Sathya, A., Vijayabharathi, R., Varshney, R. K., Gowda, C. L., and Krishnamurthy, L. (2015). Plant growth promoting rhizobia: challenges and opportunities. *3 Biotech.* 5, 355–377. doi: 10.1007/s13205-014-0241-x

Gowtham, H., Singh, B., Murali, M., Shilpa, N., Prasad, M., Aiyaz, M., et al. (2020). Induction of drought tolerance in tomato upon the application of ACC deaminase producing plant growth promoting rhizobacterium *Bacillus subtilis* Rhizo SF 48. *Microbiological Res.* 234, 126422. doi: 10.1016/j.micres.2020.126422

Hassan, M. K., McInroy, J. A., and Kloepper, J. W. (2019). The interactions of rhizodeposits with plant growth-promoting rhizobacteria in the rhizosphere: a review. *Agriculture* 9, 142. doi: 10.3390/agriculture9070142

Hu, A., Choi, M., Tanentzap, A. J., Liu, J., Jang, K.-S., Lennon, J. T., et al. (2022). Ecological networks of dissolved organic matter and microorganisms under global change. *Nat. Commun.* 13, 3600. doi: 10.1038/s41467-022-31251-1

Huang, J., Yu, H., Liu, J., Luo, C., Sun, Z., Ma, K., et al. (2018). Phosphorus addition changes belowground biomass and C: N: P stoichiometry of two desert steppe plants under simulated N deposition. *Sci. Rep.* 8, 3400. doi: 10.1038/s41598-018-21565-w

Huang, X.-F., Zhou, D., Lapsansky, E. R., Reardon, K. F., Guo, J., Andales, M. J., et al. (2017). *Mitsuaria* sp. and Burkholderia sp. from *Arabidopsis* rhizosphere enhance drought tolerance in *Arabidopsis thaliana* and maize (*Zea mays* L.). *Plant Soil* 419, 523–539. doi: 10.1007/s11104-017-3360-4

Ingrisch, J., Karlowsky, S., Anadon-Rosell, A., Hasibeder, R., König, A., Augusti, A., et al. (2018). Land use alters the drought responses of productivity and CO_2 fluxes in mountain grassland. *Ecosystems* 21, 689–703. doi: 10.1007/s10021-017-0178-0

Jaleel, C. A., Manivannan, P., Sankar, B., Kishorekumar, A., Gopi, R., Somasundaram, R., et al. (2007). *Pseudomonas fluorescens* enhances biomass yield and ajmalicine production in *Catharanthus roseus* under water deficit stress. *Colloids Surfaces B: Biointerfaces* 60, 7–11. doi: 10.1016/j.colsurfb.2007.05.012

Jamir, E., Kangabam, R. D., Borah, K., Tamuly, A., Deka Boruah, H., and Silla, Y. (2019). Role of soil microbiome and enzyme activities in plant growth nutrition and ecological restoration of soil health. *Microbes enzymes Soil Health bioremediation*, 99–132.

Karlowsky, S., Augusti, A., Ingrisch, J., Hasibeder, R., Lange, M., Lavorel, S., et al. (2018). Land use in mountain grasslands alters drought response and recovery of carbon allocation and plant-microbial interactions. *J. Ecol.* 106, 1230–1243. doi: 10.1111/jec.2018.106.issue-3

Kour, D., Khan, S. S., Kaur, T., Kour, H., Singh, G., Yadav, A., et al. (2022). Drought adaptive microbes as bioinoculants for the horticultural crops. *Heliyon* 8, 14. doi: 10.1016/j.heliyon.2022.e09493

Kour, D., Khan, S. S., Kour, H., Kaur, T., Devi, R., Rai, A. K., et al. (2024). ACC deaminase producing phytomicrobiomes for amelioration of abiotic stresses in plants for agricultural sustainability. *J. Plant Growth Regul.* 43, 963–985. doi: 10.1007/s00344-023-11163-0

Kumar, M., Mishra, S., Dixit, V., Kumar, M., Agarwal, L., Chauhan, P. S., et al. (2016). Synergistic effect of *Pseudomonas putida* and *Bacillus amyloliquefaciens* ameliorates drought stress in chickpea (*Cicer arietinum* L.). *Plant Signal Behav.* 11, e1071004. doi: 10.1080/15592324.2015.1071004

Kumar, T., Wang, J.-G., Xu, C.-H., Lu, X., Mao, J., Lin, X.-Q., et al. (2024). Genetic engineering for enhancing sugarcane tolerance to biotic and abiotic stresses. *Plants* 13, 1739. doi: 10.3390/plants13131739

Kunihiro, M., Ozeki, Y., Nogi, Y., Hamamura, N., and Kanaly, R. A. (2013). Benz[a] anthracene biotransformation and production of ring fission products by *Sphingobium* sp. strain KK22. *Appl. Environ. Microbiol.* 79, 4410–4420. doi: 10.1128/AEM.01129-13

Kurepa, J., and Smalle, J. A. (2022). Auxin/cytokinin antagonistic control of the shoot/root growth ratio and its relevance for adaptation to drought and nutrient deficiency stresses. *Int. J. Mol. Sci.* 23, 15. doi: 10.3390/ijms23041933

Ling, N., Wang, T., and Kuzyakov, Y. (2022). Rhizosphere bacteriome structure and functions. *Nat. Commun.* 13, 836. doi: 10.1038/s41467-022-28448-9

Li Ting, L. T., He Lai, H. L., and Liang QuanFeng, L. Q. (2013). Progress in the study of *Rhizobium* associated with non-leguminous plants. *J. Agric. Sci. Technol.* 15, 97–102.

Liu, X. P., Gong, C. M., Fan, Y. Y., Eiblmeier, M., Zhao, Z., Han, G., et al. (2013). Response pattern of amino compounds in phloem and xylem of trees to soil drought depends on drought intensity and root symbiosis. *Plant Biol.* 15, 101–108. doi: 10.1111/j.1438-8677.2012.00647.x

Liu, S., Fan, X., Yang, S., Deng, J., Quan, Y., Li, R., et al. (2022a). Effects of drought stress on diurnal changes and related characteristics of sugarcane photosynthesis. *J. South. Argiculture* 53, 430–440. doi: 10.3969/j.issn.2095-1191.2022.02.016

Liu, Y. J., Guo, Z. F., and Shi, H. F. (2022b). *Rhizobium* symbiosis leads to increased drought tolerance in chinese milk vetch (*Astragalus sinicus* L.). *Agronomy-Basel* 12, 11. doi: 10.3390/agronomy12030725

Liu, Q., Xie, S., Zhao, X., Liu, Y., Xing, Y., Dao, J., et al. (2021a). Drought sensitivity of sugarcane cultivars shapes rhizosphere bacterial community patterns in response to water stress. *Front. Microbiol.* 12, 732989. doi: 10.3389/fmicb.2021.732989

Liu, Q., Zhao, X., Liu, Y., Xie, S., Xing, Y., Dao, J., et al. (2021b). Response of sugarcane rhizosphere bacterial community to drought stress. *Front. Microbiol.* 12, 716196. doi: 10.3389/fmicb.2021.716196

Lopes, L. D., Futrell, S. L., Bergmeyer, E., Hao, J. J., and Schachtman, D. P. (2023). Root exudate concentrations of indole-3-acetic acid (IAA) and abscisic acid (ABA) affect maize rhizobacterial communities at specific developmental stages. *FEMS Microbiol. Ecol.* 99, 12. doi: 10.1093/femsec/fiad019

Luo, Y., Wang, F., Huang, Y., Zhou, M., Gao, J., Yan, T., et al. (2019). *Sphingomonas* sp. Cra20 increases plant growth rate and alters rhizosphere microbial community structure of *Arabidopsis thaliana* under drought stress. *Front. Microbiol.* 10. doi: 10.3389/fmicb.2019.01221

Luo, Y., Zhou, M., Zhao, Q., Wang, F., Gao, J., Sheng, H., et al. (2020). Complete genome sequence of *Sphingomonas* sp. Cra20, a drought resistant and plant growth promoting rhizobacteria. *Genomics* 112, 3648–3657. doi: 10.1016/j.ygeno.2020.04.013

Maia Júnior, S., Endres, L., Silva, J. V., and de Andrade, J. R. (2019). An efficient antioxidant system is associated with lower photosynthesis photoinhibition and greater tolerance to drought in sugarcane cultivars. *Bioscience J.* 35. doi: 10.14393/BJ-v35n3a2019-39571

Mall, A., Manimekalai, R., Misra, V., Pandey, H., Srivastava, S., and Sharma, A. (2024). CRISPR/Cas-mediated genome editing for sugarcane improvement. *Sugar Tech*, 1–13. doi: 10.1007/s12355-023-01352-2

Martín, J. F., and Liras, P. (2021). Molecular mechanisms of phosphate sensing, transport and signalling in *streptomyces* and related actinobacteria. *Int. J. Mol. Sci.* 22, 1129. doi: 10.3390/ijms22031129

Martiny, J. B., Martiny, A. C., Weihe, C., Lu, Y., Berlemont, R., Brodie, E. L., et al. (2017). Microbial legacies alter decomposition in response to simulated global change. *ISME J.* 11, 490–499. doi: 10.1038/ismej.2016.122

Matimati, I., Verboom, G. A., and Cramer, M. D. (2014). Nitrogen regulation of transpiration controls mass-flow acquisition of nutrients. *J. Exp. Bot.* 65, 159–168. doi: 10.1093/jxb/ert367

Misra, V., Solomon, S., Mall, A., Abid, M., Abid Ali Khan, M., and Ansari, M. I. (2022). "Drought stress and sustainable sugarcane production," in *Microbial biotechnology for sustainable agriculture*, vol. 1. (Singapore: Springer), 353–368.

Moutia, J.-F. Y., Saumtally, S., Spaepen, S., and Vanderleyden, J. (2010). Plant growth promotion by *Azospirillum* sp. in sugarcane is influenced by genotype and drought stress. *Plant Soil* 337, 233–242. doi: 10.1007/s11104-010-0519-7

Naylor, D., and Coleman-Derr, D. (2018). Drought stress and root-associated bacterial communities. *Front. Plant Sci.* 8. doi: 10.3389/fpls.2017.02223

Nazari, M. T., Schommer, V. A., Braun, J. C. A., dos Santos, L. F., Lopes, S. T., Simon, V., et al. (2023). Using Streptomyces spp. as plant growth promoters and biocontrol agents. *Rhizosphere*. 27, 100741. doi: 10.1016/j.rhisph.2023.100741

Neemisha,, and Sharma, S. (2022). "Soil enzymes and their role in nutrient cycling," in *Structure and functions of Pedosphere* (Singapore: Springer), 173–188.

Nong, Q., Lin, L., Xie, J., Mo, Z., Malviya, M. K., Solanki, M. K., et al. (2023). Regulation of an endophytic nitrogen-fixing bacteria GXS16 promoting drought tolerance in sugarcane. *BMC Plant Biol.* 23, 573. doi: 10.1186/s12870-023-04600-5

Olanrewaju, O. S., and Babalola, O. O. (2019). *Streptomyces*: implications and interactions in plant growth promotion. *Appl. Microbiol. Biotechnol.* 103, 1179–1188. doi: 10.1007/s00253-018-09577-y

Osakabe, Y., Osakabe, K., Shinozaki, K., and Tran, L.-S. P. (2014). Response of plants to water stress. *Front. Plant Sci.* 5, 76566. doi: 10.3389/fpls.2014.00086

Pascale, A., Proietti, S., Pantelides, I. S., and Stringlis, I. A. (2020). Modulation of the root microbiome by plant molecules: the basis for targeted disease suppression and plant growth promotion. *Front. Plant Sci.* 10, 501717. doi: 10.3389/fpls.2019.01741

Pereira, L. B., Andrade, G. S., Meneghin, S. P., Vicentini, R., and Ottoboni, L. M. M. (2019). Prospecting plant growth-promoting bacteria isolated from the rhizosphere of sugarcane under drought stress. *Curr. Microbiol.* 76, 1345–1354. doi: 10.1007/s00284-019-01749-x

Pereira, L. B., Gambarini, V. M. D., de Menezes, A. B., Ottoboni, L. M. M., and Vicentini, R. (2022). Influence of sugarcane variety on rhizosphere microbiota under irrigated and water-limiting conditions. *Curr. Microbiol.* 79, 10. doi: 10.1007/s00284-022-02946-x

Ponomarova, O., Gabrielli, N., Sévin, D., Mülleder, M., Zirngibl, K., Bulyha, K., et al. (2017). Yeast creates a niche for symbiotic lactic acid bacteria through nitrogen overflow. *Cell Syst.* 5, 345–357.e6. doi: 10.1016/j.cels.2017.09.002

Poudel, M., Mendes, R., Costa, L. A. S., Bueno, C. G., Meng, Y. M., Folimonova, S. Y., et al. (2021). The role of plant-associated bacteria, fungi, and viruses in drought stress mitigation. *Front. Microbiol.* 12. doi: 10.3389/fmicb.2021.743512

Qiao, M., Lv, S., Qiao, Y., Lin, W., Gao, Z., Tang, X., et al. (2024). Exogenous Streptomyces spp. enhance the drought resistance of naked oat (*Avena nuda*) seedlings by augmenting both the osmoregulation mechanisms and antioxidant capacities. *Funct. Plant Biol.* 51, 13. doi: 10.1071/FP23312

Qin, S., Zhang, D., Wei, B., and Yang, Y. (2024). Dual roles of microbes in mediating soil carbon dynamics in response to warming. *Nat. Commun.* 15, 6439. doi: 10.1038/s41467-024-50800-4

Radhakrishnan, R., Hashem, A., and Abd Allah, E. F. (2017). *Bacillus*: a biological tool for crop improvement through bio-molecular changes in adverse environments. *Front. Physiol.* 8. doi: 10.3389/fphys.2017.00667

Rahman, M. A., Wu, W., Yan, Y. C., and Bhuiyan, S. A. (2021). Overexpression of *TERF1* in sugarcane improves tolerance to drought stress. *Crop Pasture Sci.* 72, 268–279. doi: 10.1071/cp20161

Reinsch, S., Michelsen, A., Sárossy, Z., Egsgaard, H., Schmidt, I. K., Jakobsen, I., et al. (2014). Short-term utilization of carbon by the soil microbial community under future climatic conditions in a temperate heathland. *Soil Biol. Biochem.* 68, 9–19. doi: 10.1016/j.soilbio.2013.09.014

Ristova, D., Carré, C., Pervent, M., Medici, A., Kim, G. J., Scalia, D., et al. (2016). Combinatorial interaction network of transcriptomic and phenotypic responses to nitrogen and hormones in the *Arabidopsis thaliana* root. *Sci. Signaling* 9, rs13–rs13.

Rolli, E., Marasco, R., Vigani, G., Ettoumi, B., Mapelli, F., Deangelis, M. L., et al. (2015). Improved plant resistance to drought is promoted by the root-associated microbiome as a water stress-dependent trait. *Environ. Microbiol.* 17, 316–331. doi: 10.1111/1462-2920.12439

Roy, M., Khara, P., and Dutta, T. K. (2012). meta-Cleavage of hydroxynaphthoic acids in the degradation of phenanthrene by *Sphingobium* sp. strain PNB. *Microbiol. (Reading)* 158, 685–695. doi: 10.1099/mic.0.053363-0

Salem, M. A., Ismail, M. A., Radwan, K. H., and Abd-Elhalim, H. M. (2024). Unlocking the potential of plant growth-promoting rhizobacteria to enhance drought tolerance in Egyptian wheat (*Triticum aestivum*). *Sustainability* 16, 17. doi: 10.3390/su16114605

Sarkar, S., Kamke, A., Ward, K., Hartung, E., Ran, Q., Feehan, B., et al. (2022). *Pseudomonas* cultivated from *Andropogon gerardii* rhizosphere show functional potential for promoting plant host growth and drought resilience. *BMC Genomics* 23, 784. doi: 10.1186/s12864-022-09019-0

Schimel, J. P. (2018). Life in dry soils: effects of drought on soil microbial communities and processes. *Annu. Rev. ecology evolution systematics* 49, 409–432. doi: 10.1146/annurev-ecolsys-110617-062614

Selim, S., Hassan, Y. M., Saleh, A. M., Habeeb, T. H., and AbdElgawad, H. (2019). Actinobacterium isolated from a semi-arid environment improves the drought

tolerance in maize (*Zea mays* L.). *Plant Physiol. Biochem.* 142, 15–21. doi: 10.1016/j.plaphy.2019.06.029

Siebert, J., Sünnemann, M., Auge, H., Berger, S., Cesarz, S., Ciobanu, M., et al. (2019). The effects of drought and nutrient addition on soil organisms vary across taxonomic groups, but are constant across seasons. *Sci. Rep.* 9, 639. doi: 10.1038/s41598-018-36777-3

Song, Y., Li, X., Yao, S., Yang, X., and Jiang, X. (2020). Correlations between soil metabolomics and bacterial community structures in the pepper rhizosphere under plastic greenhouse cultivation. *Sci. Total Environ.* 728, 138439. doi: 10.1016/j.scitotenv.2020.138439

Sugiharto, B. (2018). Biotechnology of drought-tolerant sugarcane. *Sugarcane–Technology Res.* doi: 10.5772/intechopen.72436

Sultana, R., Islam, S. M. N., Sriti, N., Ahmed, M., Shuvo, S. B., Rahman, M. H., et al. (2024). *Sphingomonas panaciterrae* PB20 increases growth, photosynthetic pigments, antioxidants, and mineral nutrient contents in spinach (*Spinacia oleracea* L.). *Heliyon* 10, e25596. doi: 10.1016/j.heliyon.2024.e25596

Tallapragada, P., Dikshit, R., and Seshagiri, S. (2016). Influence of *Rhizophagus* spp. and *Burkholderia seminalison* the growth of tomato (*Lycopersicon esculatum*) and Bell Pepper (*Capsicum annuum*) under drought stress. *Commun. Soil Sci. Plant Anal.* 47, 1975–1984. doi: 10.1080/00103624.2016.1216561

Tayyab, M., Islam, W., Noman, A., Pang, Z., Li, S., Lin, S., et al. (2022). Sugarcane cultivars manipulate rhizosphere bacterial communities' structure and composition of agriculturally important keystone taxa. *3 Biotech.* 12, 32. doi: 10.1007/s13205-021-03091-1

Trivedi, P., Batista, B. D., Bazany, K. E., and Singh, B. K. (2022). Plant–microbiome interactions under a changing world: responses, consequences and perspectives. *New Phytol.* 234, 1951–1959. doi: 10.1111/nph.v234.6

Trivedi, P., Mattupalli, C., Eversole, K., and Leach, J. E. (2021). Enabling sustainable agriculture through understanding and enhancement of microbiomes. *New Phytol.* 230, 2129–2147. doi: 10.1111/nph.v230.6

Vardharajula, S., Zulfikar Ali, S., Grover, M., Reddy, G., and Bandi, V. (2011). Drought-tolerant plant growth promoting *Bacillus* spp.: effect on growth, osmolytes, and antioxidant status of maize under drought stress. *J. Plant Interact.* 6, 1–14. doi: 10.1080/17429145.2010.535178

Varela, M. C., Arslan, I., Reginato, M. A., Cenzano, A. M., and Luna, M. V. (2016). Phenolic compounds as indicators of drought resistance in shrubs from Patagonian shrublands (Argentina). *Plant Physiol. Biochem.* 104, 81–91. doi: 10.1016/j.plaphy.2016.03.014

Vargas, L., Santa Brigida, A. B., Mota Filho, J. P., de Carvalho, T. G., Rojas, C. A., Vaneechoutte, D., et al. (2014). Drought tolerance conferred to sugarcane by association with *Gluconacetobacter diazotrophicus*: a transcriptomic view of hormone pathways. *PloS One* 9, e114744. doi: 10.1371/journal.pone.0114744

Vejan, P., Abdullah, R., Khadiran, T., Ismail, S., and Boyce, A. N. (2016). Role of plant growth promoting rhizobacteria in agricultural sustainability-a review. *Molecules* 21, 17. doi: 10.3390/molecules21050573

Viaene, T., Langendries, S., Beirinckx, S., Maes, M., and Goormachtig, S. (2016). *Streptomyces* as a plant's best friend? *FEMS Microbiol. Ecol.* 92, fiw119. doi: 10.1093/femsec/fiw119

Vurukonda, S. S. K. P., Giovanardi, D., and Stefani, E. (2018). Plant growth promoting and biocontrol activity of *Streptomyces* spp. as endophytes. *Int. J. Mol. Sci.* 19, 952. doi: 10.3390/ijms19040952

Vurukonda, S., Vardharajula, S., Shrivastava, M., and SkZ, A. (2016). Enhancement of drought stress tolerance in crops by plant growth promoting rhizobacteria. *Microbiological Res.* 184, 13–24. doi: 10.1016/j.micres.2015.12.003

Wang, C. Y., Cui, J. T., Yang, L., Zhao, C. A., Wang, T. Y., Yan, L., et al. (2018a). Phosphorus-release dynamics by phosphate solubilizing actinomycetes and its enhancement of growth and yields in maize. *Int. J. Agric. Biol.* 20, 437–444. doi: 10.17957/ijab/15.0554

Wang, Q., Hu, Z., Fu, W., Li, G., and Hao, L. (2023a). Regulation of *Burkholderia* sp. GD17 on the drought tolerance of cucumber seedlings. *Biotechnol. Bull.* 39, 163–175. doi: 10.13560/j.cnki.biotech.bull.1985.2022-0753

Wang, X., Liang, C., Mao, J., Jiang, Y., Bian, Q., Liang, Y., et al. (2023b). Microbial keystone taxa drive succession of plant residue chemistry. *ISME J.* 17, 748–757. doi: 10.1038/s41396-023-01384-2

Wang, Z., Solanki, M. K., Kumar, A., Solanki, A. C., Pang, F., Ba, Z. X., et al. (2023c). Promoting plant resilience against stress by engineering root microenvironment with *Streptomyces* inoculants. *Microbiological Res.* 277, 12. doi: 10.1016/j.micres.2023.127509

Wang, Z., Solanki, M. K., Yu, Z. X., Yang, L. T., An, Q. L., Dong, D. F., et al. (2018b). Draft genome analysis offers insights into the mechanism by which *Streptomyces chartreusis* WZS021 increases drought tolerance in sugarcane. *Front. Microbiol.* 9. doi: 10.3389/fmicb.2018.03262

Wang, F., Wei, Y., Yan, T., Wang, C., Chao, Y., Jia, M., et al. (2022). *Sphingomonas* sp. Hbc-6 alters physiological metabolism and recruits beneficial rhizosphere bacteria to improve plant growth and drought tolerance. *Front. Plant Sci.* 13. doi: 10.3389/fpls.2022.1002772

Warrad, M., Hassan, Y. M., Mohamed, M. S., Hagagy, N., Al-Maghrabi, O. A., Selim, S., et al. (2020). A bioactive fraction from Streptomyces sp. enhances maize tolerance against drought stress. *J. Microbiol. Biotechnol.* 30, 1156. doi: 10.4014/jmb.2003.03034

Wei, C.-Y., Lin, L., Luo, L.-J., Xing, Y.-X., Hu, C.-J., Yang, L.-T., et al. (2013). Endophytic nitrogen-fixing *Klebsiella variicola* strain DX120E promotes sugarcane growth. *Biol. Fertility Soils* 50, 657–666. doi: 10.1007/s00374-013-0878-3

Williams, A., and de Vries, F. T. (2020). Plant root exudation under drought: implications for ecosystem functioning. *New Phytol.* 225, 1899–1905. doi: 10.1111/nph.v225.5

Woo, O. G., Kim, H., Kim, J. S., Keum, H. L., Lee, K. C., Sul, W. J., et al. (2020). *Bacillus subtilis* strain GOT9 confers enhanced tolerance to drought and salt stresses in *Arabidopsis thaliana* and *Brassica campestris*. *Plant Physiol. Biochem.* 148, 359–367. doi: 10.1016/j.plaphy.2020.01.032

Xing, Y., Dao, J., Chen, M., Chen, C., Li, B., and Wang, Z. (2023). Multi-omics reveals the sugarcane rhizosphere soil metabolism-microbiota interactions affected by drought stress. *Appl. Soil Ecol.* 190, 104994. doi: 10.1016/j.apsoil.2023.104994

Xu, S., Wang, J., Shang, H., Huang, Y., Yao, W., Chen, B., et al. (2018). Transcriptomic characterization and potential marker development of contrasting sugarcane cultivars. *Sci. Rep.* 8, 1683. doi: 10.1038/s41598-018-19832-x

Yandigeri, M. S., Meena, K. K., Singh, D., Malviya, N., Singh, D. P., Solanki, M. K., et al. (2012). Drought-tolerant endophytic actinobacteria promote growth of wheat (*Triticum aestivum*) under water stress conditions. *Plant Growth Regul.* 68, 411–420. doi: 10.1007/s10725-012-9730-2

Yang, B., Wen, H., Wang, S., Zhang, J., Wang, Y., Zhang, T., et al. (2024). Enhancing drought resistance and yield of wheat through inoculation with *Streptomyces pactum* Act12 in drought field environments. *Agronomy* 14, 16. doi: 10.3390/agronomy14040692

Zhalnina, K., Louie, K. B., Hao, Z., Mansoori, N., Da Rocha, U. N., Shi, S., et al. (2018). Dynamic root exudate chemistry and microbial substrate preferences drive patterns in rhizosphere microbial community assembly. *Nat. Microbiol.* 3, 470–480. doi: 10.1038/s41564-018-0129-3

Zhang, J., Zhang, H., Luo, S., Ye, L., Wang, C., Wang, X., et al. (2024). Analysis and functional prediction of core bacteria in the *Arabidopsis* rhizosphere microbiome under drought stress. *Microorganisms* 12. doi: 10.3390/microorganisms12040790

Zhang, H., Zhu, J., Gong, Z., and Zhu, J.-K. (2022). Abiotic stress responses in plants. *Nat. Rev. Genet.* 23, 104–119. doi: 10.1038/s41576-021-00413-0

Zhao, X., Jiang, Y., Liu, Q., Yang, H., Wang, Z., and Zhang, M. (2020). Effects of drought-tolerant Ea-DREB2B transgenic sugarcane on bacterial communities in soil. *Front. Microbiol.* 11, 704. doi: 10.3389/fmicb.2020.00704

Zhao, M., Zhao, J., Yuan, J., Hale, L., Wen, T., Huang, Q., et al. (2021). Root exudates drive soil-microbe-nutrient feedbacks in response to plant growth. *Plant Cell Environ.* 44, 613–628. doi: 10.1111/pce.13928

Zheng, W., Zeng, S., Bais, H., LaManna, J. M., Hussey, D. S., Jacobson, D. L., et al. (2018). Plant growth-promoting rhizobacteria (PGPR) reduce evaporation and increase soil water retention. *Water Resour. Res.* 54, 3673–3687. doi: 10.1029/2018WR022656

Zhu, B., Chen, Z., Hu, H., Andrei, A.-S., and Li, Y. (2024). Greenhouse gas emissions and mitigation: microbes, mechanisms and modeling. *Front. Microbiol.* 15, 1363814. doi: 10.3389/978-2-8325-4967-4

Zuluaga, D. L., and Sonnante, G. (2019). The use of nitrogen and its regulation in cereals: Structural genes, transcription factors, and the role of miRNAs. *Plants* 8, 294. doi: 10.3390/plants8080294

frontiers | Frontiers in Plant Science

TYPE Original Research
PUBLISHED 23 December 2024
DOI 10.3389/fpls.2024.1504238

OPEN ACCESS

EDITED BY
Xiao-Dong Yang,
Ningbo University, China

REVIEWED BY
Xue-Wei Gong,
Chinese Academy of Sciences (CAS), China
Mingshan Xu,
Zhejiang Institute of Hydraulics and Estuary, China

*CORRESPONDENCE
Xue-ni Zhang
xnzhang@xju.edu.cn

†These authors have contributed equally to this work

RECEIVED 30 September 2024
ACCEPTED 11 December 2024
PUBLISHED 23 December 2024

CITATION
Wang Y-c, Zhang X-n, Yang J-f, Tian J-y, Song D-h, Li X-h and Zhou S-f (2024) Spatial heterogeneity of soil factors enhances intraspecific variation in plant functional traits in a desert ecosystem. *Front. Plant Sci.* 15:1504238. doi: 10.3389/fpls.2024.1504238

Spatial heterogeneity of soil factors enhances intraspecific variation in plant functional traits in a desert ecosystem

Yong-chang Wang[1,2,3†], Xue-ni Zhang[1,2,3*†], Ji-fen Yang[1,2,3], Jing-ye Tian[1,2,3], Dan-hong Song[1,2,3], Xiao-hui Li[1,2,3] and Shuang-fu Zhou[1,2,3]

[1]College of Ecology and Environment, Xinjiang University, Urumqi, China, [2]Key Laboratory of Oasis Ecology of Education Ministry, Urumqi, China, [3]Xinjiang Jinghe Observation and Research Station of Temperate Desert Ecosystem, Ministry of Education, Urumqi, China

Introduction: Functional traits of desert plants exhibit remarkable responsiveness, adaptability and plasticity to environmental heterogeneity.

Methods: In this study, we measured six crucial plant functional traits (leaf carbon, leaf nitrogen, leaf phosphorus, leaf thickness, chlorophyll concentration, and plant height) and employed exemplar analysis to elucidate the effects of soil environmental heterogeneity on intraspecific traits variation in the high-moisture-salinity and low-moisture-salinity habitats of the Ebinur LakeWetland National Nature Reserve.

Results: The results showed that (1) The soil moisture and electrical conductivity heterogeneity showed significant differences between the two moisture-salinity habitats. Moreover, soil nutrient in high moisture-salinity habitat exhibited higher heterogeneity than in low moisture-salinity habitat. The order of intraspecific trait variation among different life forms was herbs > shrubs > trees in both the soil moisture-salinity habitats. (2) At the community level, intraspecific variation of leaf carbon, nitrogen, plant height and chlorophyll content in high moisture-salinity habitat was higher than that in low moisture-salinity habitat, while the opposite was true for leaf thickness and leaf phosphorus content. (3) Our findings revealed a positive impact of soil heterogeneity on intraspecific traits variation. In high moisture-salinity habitat, the heterogeneity of soil organic carbon had the highest explanatory power for intraspecific traits variation, reaching up to 20.22%, followed by soil total nitrogen (9.55%) and soil total phosphorus (3.49%). By comparison, in low-moisture-salinity habitat, the heterogeneity of soil moisture alone contributes the highest explanatory power for intraspecific traits variation in community-level, reaching up to 13.89%, followed by the heterogeneity of soil total nitrogen (3.76%).

Discussion: This study emphasizes the differences in soil heterogeneity and intraspecific trait variation among plant life forms under various soil moisture-salinity habitats and confirms the significant promoting effect of soil heterogeneity on intraspecific trait variation of desert plant. Our findings provide valuable theoretical basis and reference for predicting plant adaptation strategies under environmental change scenarios.

KEYWORDS

plant functional traits, plant adaptation strategies, desert plants, soil moisture-salinity habitat, habitat filtering effect

1 Introduction

Intraspecific trait variation (ITV) depends on the available phenotypic trait plasticity of individuals within a population. Phenotypic plasticity, that is, the phenotypic variation expressed by a single genotype under different environmental conditions (Nicotra et al., 2010). ITV contributes significantly to the persistence of plants in variable environments, in which abiotic factors play a non-negligible role (Stanton et al., 2000; Valladares et al., 2007). Soil heterogeneity refers to the uneven distribution of soil resources, such as nutrients and water (Feeser et al., 2018). Soil heterogeneity significantly affects plant growth and species coexistence (Liu et al., 2021; Olagoke et al., 2023), thus it is an important driver of plant community structure and dynamics (Lundholm, 2009). Few previous studies have reported on the important effects of soil heterogeneity within habitats on ITV in plant communities, especially in arid zones with sparse vegetation and environmental extremes.

Ecologists have long used the mean trait values of species to infer ecological processes (McGill et al., 2006). Nonetheless, current researches have demonstrated a significant amount of ITV (Stojnic et al., 2022; Westerband et al., 2021). For example, a recent meta-analysis has provided a comprehensive insight into the matter, indicating that ITV is responsible for 25%–31% of the variation in commonly measured traits within plant communities (Siefert et al., 2015). For example, Hurtado et al. have showed that intraspecific trait variability explained most of the functional changes in lichen communities in response to the latitudinal gradient (Hurtado et al., 2020). These findings emphasize the significant role of ITV on community assembly and ecosystem processes (Hart et al., 2016; Pérez-Izquierdo et al., 2019; Siefert et al., 2015; Turcotte and Levine, 2016). Phenotypic plasticity, which refers to the variation in phenotype expressed by a single genotype under varying environmental conditions (Nicotra et al., 2010; Sultan, 2000), is considered one of the key mechanisms through which plants respond to environmental changes (Arnold et al., 2019; Gratani, 2014). As an illustration, the ITV observed in *Eremanthus erythropappus* in Brazil has been shown to enhance its capability to thrive in various habitats, including forests and savannas (Silva et al., 2019). Likewise, a study on *Brachypodium hybridum*, an annual grass species in California, has revealed that ITV in seed biomass promotes its successful colonization in water-limited environments (Liu et al., 2019). Ecological niche theory suggests that species in an ecosystem occupy different ecological niches and vary with environmental gradients, so their ecological strategies change accordingly (Kearney and Porter, 2006; Violle and Jiang, 2009). It has been proposed that ITV characterizes the maximum fitness of a species and fundamentally determines the ecological niche width of a plant; Jung et al (2010) argued that ITV accounted for 44% of the variation in species' traits and increased the chances of a species being unfiltered by the environment, thus facilitating the coexistence of species (Jung et al., 2010).

It is generally recognized that heterogeneous environments typically contain more ecological niches than homogeneous environments (Chesson, 2000) and thus drive variations in plant functional traits (Des Roches et al., 2021; Wan et al., 2019), improve plant adaptations and positively affect their growth, reproduction and survival (Karbstein et al., 2020). In this sense, soil environmental heterogeneity within habitats can potentially result in an augmentation of the diversity of functional phenotype, thus enhancing ITV in plant traits (Bloomfield et al., 2018; Stark et al., 2017). For example, it has been found that the increase in ITV in Qinghai-Tibetan alpine meadow communities under different altitude conditions was related to soil heterogeneity (Siefert and Ritchie, 2016). However, the effects of soil heterogeneity on plant ITV in other ecosystems is still poorly understood. Therefore, studying intraspecific traits variation in relation to environmental heterogeneity better reflects the effects of soil heterogeneity within habitats, such as nutrient limitation (Frederiksen et al., 2005; Tautenhahn et al., 2019) or drought and salt stress effects (Tusifujiang et al., 2021). At present, the relationship between ITV and soil environmental heterogeneity across different life forms and communities has not received sufficient attention.

Regional variation in plant functional traits is associated with climatic heterogeneity (Símová et al., 2015). Soil heterogeneity tends to be more important to ITV at the local scale. For example, habitats characterized by a pronounced level of microenvironmental heterogeneity at small spatial scales, such as forest understories and alpine meadows are usually more important for ITV than interspecific trait variation. Furthermore, their contribution to intercommunity trait variation decreases with increasing spatial scale (Benes and Bracken, 2020). At small or local scales, topographic and soil factors play a crucial role in shaping the variations of plant traits (Liu and Ma, 2015). For instance, a study has demonstrated the significance of soil depth and moisture heterogeneity in driving variations in plant functional traits (Price et al., 2017). Soil heterogeneity influences both abiotic and biotic screening processes by altering competitive relationships among plants, suggesting that its impact on plant trait differentiation might surpass the effects of resource availability alone. Theoretically, greater plants trait variation resulting from soil heterogeneity contribute to increased functional diversity (Price et al., 2017). However, empirical investigations focusing on the role of soil environmental heterogeneity in elucidating plants trait variation within localized regional environments are limited, particularly in arid desert ecosystems where soil heterogeneity is more pronounced (Li et al., 2014). The northwest of Jinghe County in Xinjiang, which is characterized by its dry climate within the North Temperate Continental zone, is home to the Ebinur Lake Wetland National Nature Reserve (ELWNNR). This reserve, is situated in a typical temperate arid desert ecosystem, experiences limited rainfall and strong evaporation. The desert plants within this region are vital components of global biodiversity and play a significant role in sustaining regional ecological equilibrium. Previous studies have demonstrated the substantial impact of soil moisture-salinity content on functional traits of the plant communities in this region, particularly noting a closer relationship between interspecific and intraspecific trait variability and soil factors in high soil moisture-salinity habitat (Tusifujiang et al., 2021). Nonetheless, it remains uncertain whether soil heterogeneity in

the region increased intraspecific variation in plant traits, and how this effect varies across different soil moisture-salinity habitats. To address this uncertainty, we conducted a field investigation and measured the morphological, chemometric and physiological traits of plants and soil heterogeneity in the ELWNNR, and tried to answer the following questions: (1) What's the differences of ITV among life forms and between different soil moisture-salinity habitats? (2) Does soil heterogeneity promote ITV, and does change of the soil moisture-salinity habitats affect the role of soil heterogeneity on ITV? This study aims to provide novel insights into the response of ITV and plant adaptation to environmental heterogeneity in drylands. Furthermore, it will serve as a valuable reference for the preservation and restoration of desert ecosystem.

2 Materials and methods

2.1 Overview of the study zone

The study area, ELWNNR is situated in the southwest of the Junggar Basin, Xinjiang. It is the lowest depression and moisture-salinity accumulation center in the southwest margin of the Junggar Basin. Its coordinates are 44°30' N-45°09' N and 82°36' E-83°50' E, encompassing an zone with a dry environment characterized by uneven intra-annual precipitation distribution, averaging 105.17 mm annually. The region also experiences a high average annual evaporation of 1,315 mm and an average annual temperature of 5°C. The Aqikesu River, a crucial water source for ELWNNR situated on its eastern side, has been significantly impacted by human activity and climate change, leading to the river's near-complete drying, posing a threat to the degradation of riparian vegetation (Supplementary Figure S1). Previous research has highlighted the variation in plant species as well as soil moisture and salinity along the transect vertical to the Aqikesu River, indicating changes in these factors with distance from the river (Zhang et al., 2016). In this study, we focused on intraspecific traits variation of the following species, which are found in both the soil moisture-salinity habitats: the tree specie *Populus euphratica*, the shrubby plants *Nitraria tangutorum*, *Apocynum venetum*, *Alhagi sparsifolia* and *Halimodendron halodendron*, as well as the herbaceous plants *Phragmites australis* and *Karelinia capsica* (Wang et al., 2017) (Supplementary Table S1). These species are selected because they are distributed across both soil moisture-salinity habitats, and their population sizes are sufficient to meet the requirements of the study.

2.2 Sample plot setting and sampling

To minimize the influence of seasonal plant renewal and metabolic variations, our survey and sampling activities were strategically scheduled to coincide with the peak of plant biomass (July–August). The sample strips and plots were specifically laid out as follows: three sample strips, spaced 1 km apart and running perpendicular to the river channel, were established. Each sample strip extended northward and was investigated at intervals of 0.1 km, resulting in a total of 10 sample sites per strip, covering approximately 1 km in length. At each sample site, three 10 m × 10 m plots were investigated, with a spacing of about 100 m between plots (Supplementary Figure S1). This method resulted in 30 sample sites across the three sample strips, totaling 90 sample plots (30×3) were investigated. In this study, GPS was utilized to record the latitude and longitude of the center of each sample plot. Additionally, the species, plant height, and frequency of occurrence within each sample plot were documented. In each sample plot, three healthy, undamaged, and similarly-sized mature leaves were collected from three individuals of the same species (with a frequency greater than 3%). The relative chlorophyll content of these leaves was measured using a SPAD-502 chlorophyll meter. The thickness of each leaf was measured with a vernier caliper, taking care to avoid the main leaf veins and focusing on the central area, with an accuracy of 0.01mm. After leaf thickness measurement, approximately 20 grams of leaf samples were collected from each individual and stored in envelopes for transportation back to the laboratory. There, the leaf samples were analyzed to determine their carbon (C), nitrogen (N), and phosphorus (P) content. To comprehensively reflect the conditions of soil moisture, salinity and nutrients within the sample plots, three soil samples were randomly and uniformly selected within each plot. After removing the litter layer, soil samples at 0-20 cm depth were collected, rapidly mixed, and then bagged as composite samples. In total, 90 soil samples were collected from all sample plots. All soil samples were brought back to the Key Laboratory of Oasis Ecology of Education Ministry in Xinjiang University for further analysis.

2.3 Measurement and experimental analysis

Six functional traits were selected for analysis, encompassing morphological traits (leaf thickness, plant height), chemical traits (leaf carbon C, nitrogen N, phosphorus P), and a physiological trait (chlorophyll). Leaf thickness impacts the rate of photosynthesis; as leaf thickness increases, so does the resistance to water diffusion from the leaf interior to the surface, which helps to prevent water evaporation from plant (Liu., 2018). Plant height constitutes an adaptive response to environmental changes, and generally correlated with a plant's competitive ability. In environments where resources are limited, taller plants may have easier access to essential resources, thereby gaining a competitive edge over other species. The chemical traits, leaf C, N, and P, are essential nutrients that underpin plant photosynthesis, especially leaf N and P concentrations are the most important leaf traits regulating physiological effects and plant growth (Wright et al., 2004). Chlorophyll is a pivotal indicator that influence plant nitrogen profile, photosynthetic capacity and plant growth characteristics (Liu., 2018).

All leaf samples were dried in an oven at 75°C for 48 hours. After drying, the leaves were crushed and sieved to facilitate the determination of leaf C, N, and P content. The specific indices and experimental methods are as follows: the potassium dichromate-sulfate oxidation method was employed to determine the carbon content of leaves. The Kjeldahl method, with H_2SO_4 accelerated digestion, was utilized to determined leaf nitrogen content. Total

phosphorus in leaves was measured using the H_2SO_4-H_2O_2 digestion followed by the molybdenum antimony resistance colorimetric method. Soil volumetric water content (SWVC) and electrical conductivity (EC, used to represent for soil salinity) were assessed using the drying method and conductometer (DDS-307, Shanghai INESA Scientific Instrument Co., Ltd., Shanghai, China), respectively. Soil organic carbon (SOC) was determined by the potassium dichromate sulfuric acid oxidation. Soil total nitrogen (TN) was determined by the Kjeldahl. Soil total phosphorus (TP) was measured using the $HClO_4$-H_2SO_4 molybdenum antimony colorimetric method. All measurement procedures were based on the methods described in (Dong., 1997).

2.4 Statistical analysis

2.4.1 High and low soil moisture-salinity habitats delineation

Based on the soil water content and electrical conductivity data of each sample site(n=30), the 90 sample plots were categorized into two groups using cluster analysis (Hierarchical Clustering, euclidean distance) with the "average" method: high soil moisture-salinity habitat(n=36), where soil electrical conductivity ranged from 7.26 to 14.06 mS/cm with a mean value of 10.53 mS/cm, and SWVC ranged from 6.37% to 11.03% with a mean value of 9.28%; low soil moisture-salinity habitat(n=54), where soil electrical conductivity ranged from 3.14 to 4.93 mS/cm with a mean value of 4.52 mS/cm, and SWVC ranged from 1.67% to 5.54% with a mean value of 4.74%. Differences between the two soil moisture-salinity habitats were highly significant ($P < 0.01$).

2.4.2 Soil Heterogeneity and Plant intraspecific trait variation

(1) We employed the coefficient of variation (CV) to measure soil heterogeneity (SH) of each sample site. The formula is:

$$CV = \frac{SD}{mean} \times 100 \quad (1)$$

Where SD and mean is the standard deviation and average of soil factor in the three plots from the sample site. We calculated CV for each soil factor and for all soil factors (i.e. SH), where the SH is the mean values of CV for soil water content, soil electrical conductivity, soil organic carbon, soil total nitrogen and soil total phosphorus (Helm et al., 2019).

(2) The coefficient of variation (CV_1) was utilized to characterize the degree of intraspecific traits variation at species level. Intraspecific functional trait variation (iFD_{CV}) at species level is the average of CV_1 in all traits of the species under the same habitat. The iFD_{CV} of life-forms was calculated as the product of the average of CV_1 of six traits of each species in a certain life form and the relative abundance of the species in the life form.

(3) ITV of life-form types is calculated by summing the products of the relative abundance and CV_1 of species, which belong to the same life-form type in each sample site.

(4) ITV at community level (CWV) was accessed by referencing the formula of community weighted mean trait (CWM). Specifically, CWV was calculated as the following formula:

$$CWV = \sum_{i=1}^{S} P_i \cdot CV_i \quad (2)$$

Where P_i is the relative abundance of species i in a given plot, $CV_i$is the coefficient of variation of species i in the plot, and S is the number of species in the plot. Sample site was calculated by taking the average of the plot.

2.4.3 Impact of soil heterogeneity on intraspecific trait variation

Detrended correspondence analysis (DCA) revealed that the gradient lengths of community functional traits across the two soil moisture-salinity habitats were less than 3. Consequently, based on redundancy analysis (RDA), exemplar analysis was conducted to ascertain the relative importance and quantify the individual impact of the heterogeneity of various soil factor on intraspecific traits variation (Lai et al., 2022). We employed the adjusted coefficient of determination (R^2_{adj}) instead of the conventional coefficient of determination (R^2) to determine the final analytical results. This method helps to prevent model overfitting in R^2 calculations, as discussed by Crawley (Crawley, 2007).

Data were organized and compiled using Excel vers. 2016, and one-way ANOVA was performed with SPSS Amos version 26. Plots were predominantly created with Origin vers. 2025, exemplar analysis and cluster analysis were carried out using R's ade4, UpSet VP, rdacca.hp and stats packages.

3 Results

3.1 Soil heterogeneity in different soil moisture-salinity habitats

Soil heterogeneity of HSW habitat was generally higher than that of LSW habitat. Specifically, the soil electrical conductivity and organic carbon heterogeneity in HSW habitat were significantly higher than those in LSW habitat ($p<0.05$). The soil TN, TP heterogeneity and SH in HSW habitat were slightly higher than those in LSW habitat ($p>0.05$). However, the soil SWVC heterogeneity in HSW habitat was significantly lower than that in LSW habitat ($p<0.05$). The SOC heterogeneity was the highest in HSW habitat, the soil SWVC heterogeneity was the highest in LSW habitat, and the soil TP heterogeneity was the lowest in both habitats (Figure 1).

3.2 Plant intraspecific trait variation across soil moisture-salinity habitats

Among the six plant functional traits of herb, shrub and tree plants, the ITV of leaf carbon (C) is the lowest in both the habitats, which ranging from 3.85% to 6.14%. In contrast, plant height was the highest ITV in the two habitats, with a range of 20.40% to 27.52% (Table 1). The high moisture-salinity habitat exhibited greater ITV in leaf nitrogen (N), plant height, and chlorophyll

10.3389/fpls.2024.1504238

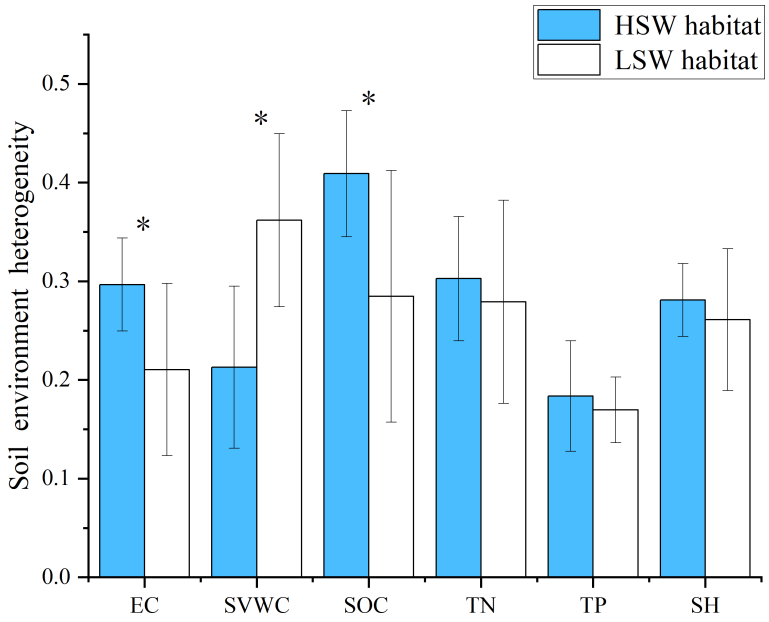

FIGURE 1
Blue and white represent the two distinct habitats, HSW (High Soil Moisture and Salinity) and LSW (Low Soil Moisture and Salinity), respectively. Each habitat exhibits differences in soil characteristics such as Soil volumetric water content (SVWC), electrical conductivity (EC), Soil organic carbon (SOC), total nitrogen (TN), total phosphorus (TP) and soil heterogeneity (SH). Bar heights indicate the average coefficient of variation (CV) for each soil characteristic. Error bars represent the standard error of the mean (SEM). Asterisks denote significant differences between the two habitats ($P < 0.05$).

among herbs, shrubs, and trees. When considering the ITV of the six functional traits, the order was herb > shrub > tree, but the ITV of leaf thickness (LT) and leaf phosphorus (P) are lower in HSW habitat compared to LSW habitat. Among different life forms, herbaceous plants demonstrated the highest ITV for functional traits other than chlorophyll.

In the HSW habitat, ITV among different life forms generally followed the order of herbs > shrubs > trees, with the exception of chlorophyll, showing a pattern of shrubs > herbs > trees. However, in the LSW habitat, ITV of all traits among life forms consistently followed the order of herbs > shrubs > trees.

At the community level, iFD_{CV} and ITV of C, N, LT, and CH did not vary significantly between the two habitats. The ITV of C, N, and H in the HSW habitat were slightly lower than those in the LSW habitat, while the ITV of LT and CH in the LSW habitat were slightly higher than those in the HSW habitat. Among all the traits at the community level, the ITV of C was the lowest under both habitats, but the higher ITV were H and P in the HSW habitat, and H and N in the LSW habitat.

3.3 Relationship between plant intraspecific trait variation and soil heterogeneity

There were significant positive correlations between plant ITV and the heterogeneity of various soil environmental factors (Supplementary Figure S2). Positive correlations were found

TABLE 1 Changes in ITV of life-forms and community traits in two soil moisture and salinity habitats (mean ± standard deviation).

Plant traits	High Soil Moisture and Salinity habitat				Low Soil Moisture and Salinity habitat			
	Tree	Shrub	Herb	Community	Tree	Shrub	Herb	Community
Leaf carbon	3.85 ± 1.75	4.50 ± 1.04	6.14 ± 1.78	5.26 ± 1.58	4.69 ± 2.62	4.72 ± 1.75	5.45 ± 2.11	5.03 ± 0.99
Leaf nitrogen	15.58 ± 11.50	15.69 ± 5.30	21.15 ± 8.73	18.48 ± 4.79	10.09 ± 7.54	12.45 ± 5.59	17.80 ± 8.82	17.30 ± 5.03
Leaf phosphorus	6.56 ± 3.78	13.62 ± 2.86	17.76 ± 9.22	15.91 ± 5.13	11.57 ± 4.54	15.25 ± 4.66	21.61 ± 10.44	23.24 ± 11.37
Leaf thickness	11.50 ± 5.12	11.74 ± 4.59	17.07± 4.46	15.84 ± 4.79	13.09 ± 5.58	12.06 ± 4.83	18.62 ± 8.92	16.06 ± 8.66
Chlorophyll	8.30 ± 3.80	10.96 ± 2.64	13.58 ± 3.20	10.83 ± 2.21	7.11 ± 5.01	13.55 ± 2.87	10.58 ± 3.15	11.12 ± 3.97
Plant height	24.42 ± 10.28	25.33 ± 9.65	27.52 ± 10.69	29.41 ± 9.48	20.40 ± 2.99	21.05 ± 8.67	23.87 ± 9.22	26.77 ± 8.37
iFD$_{CV}$	10.79 ± 2.83	14.79 ± 2.42	16.56 ± 3.91	15.84 ± 2.37	12.07 ± 1.51	13.47 ± 2.82	16.47 ± 3.79	15.06 ± 3.42

The bolded text indicate plant functional traits and index that were calculated for trait variation in this study.

between leaf N and leaf thickness variability and soil moisture heterogeneity, and between leaf N variability and soil salinity heterogeneity. Some other traits were positively correlated with soil nutrient heterogeneity. Namely, plant height variation was significantly correlated with soil total N and phosphorus heterogeneity, and chlorophyll variation was positively correlated with soil organic carbon heterogeneity.

The results of the linear regression modeling revealed a significant and positive correlation ($p<0.01$) between iFD_{CV} in trees, shrubs, herbs, and communities and soil heterogeneity (SH). In the HSW habitat, impacts of SH on ITV among different life forms showed a pattern of shrubs > herbs > trees. However, in the LSW habitat, the pattern shifted to herbs > shrubs > trees. Furthermore, the regression results for herbs and trees were higher in the low moisture-salinity environment, while the opposite trend was observed for shrubs and communities (Figure 2).

The results of exemplar analysis, which aimed to illustrate the impacts of soil heterogeneity on intraspecific plant trait variation at the community level, revealed that both hierarchical partitioning and variance breakdown of soil environmental heterogeneity made distinct contributions (Figure 3). In HSW habitat, SOC individually accounted for up to 20.22% of the variation in intraspecific traits at the community level, followed by soil TN (9.55%), soil TP (3.49%), and soil electrical conductivity (EC) (1.13%). In the LSW habitat, soil SVWC explained 13.89% of the total variation, with soil TN (3.76%), soil EC (1.76%), soil SOC (1.3%), and soil TP (0.17%) contributing subsequently.

4 Discussion

A notable ecological problem lies in understanding the effects of soil environmental heterogeneity on plant intraspecific trait variation (Stark et al., 2017; Vernham et al., 2024). This study provides compelling evidence that, in the arid zone, soil heterogeneity plays a substantial role in driving intraspecific trait variation at the community level and across different plant life forms. Furthermore, the study highlights that the degree to which individual components of soil environmental heterogeneity contribute to trait variation varies depending on soil moisture and salinity regimes. These findings shed light on the crucial role of soil heterogeneity in shaping plant intraspecific trait variation, emphasizing the significance of considering soil heterogeneity when studying plant traits in ecological contexts (Vernham et al., 2024).

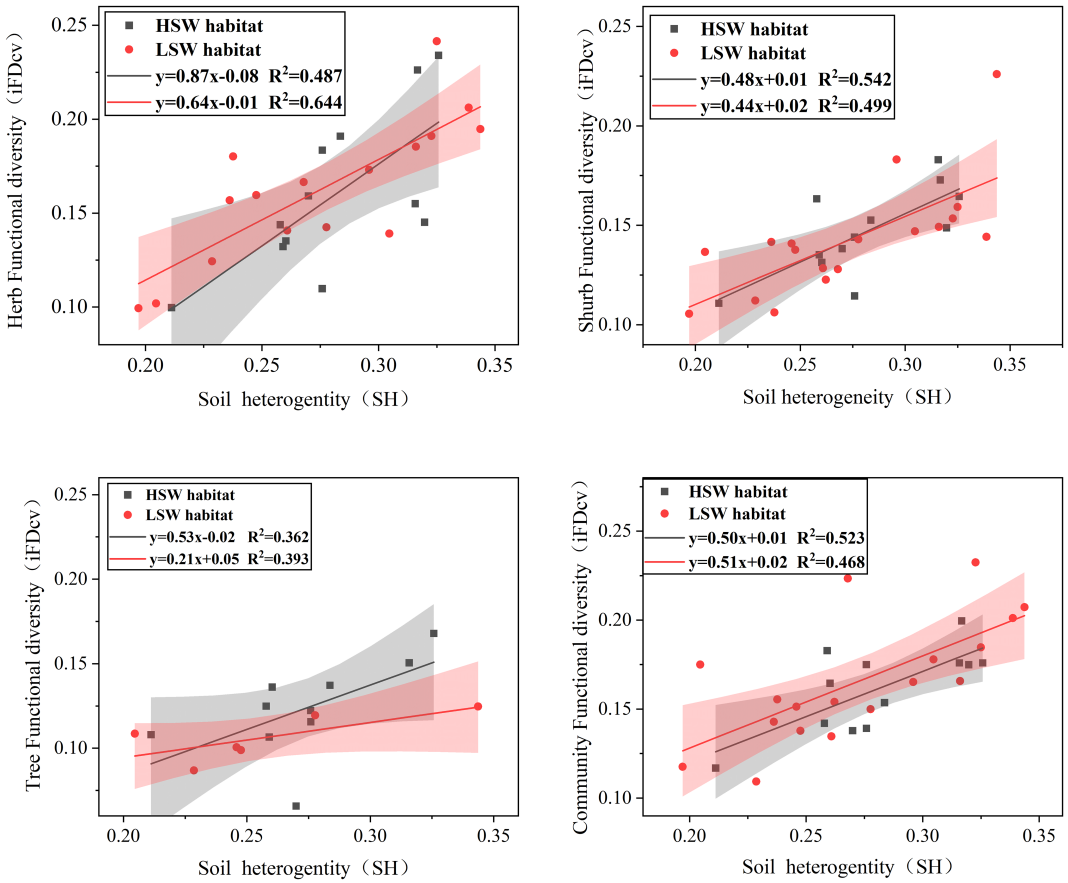

FIGURE 2
Regression analysis resulted in a significant positive correlation between intraspecific functional trait variation iFD_{CV} (trees, shrubs, herbs, and communities) and soil environmental heterogeneity. Confidence intervals (95%) were drawn. ($P<0.01$).

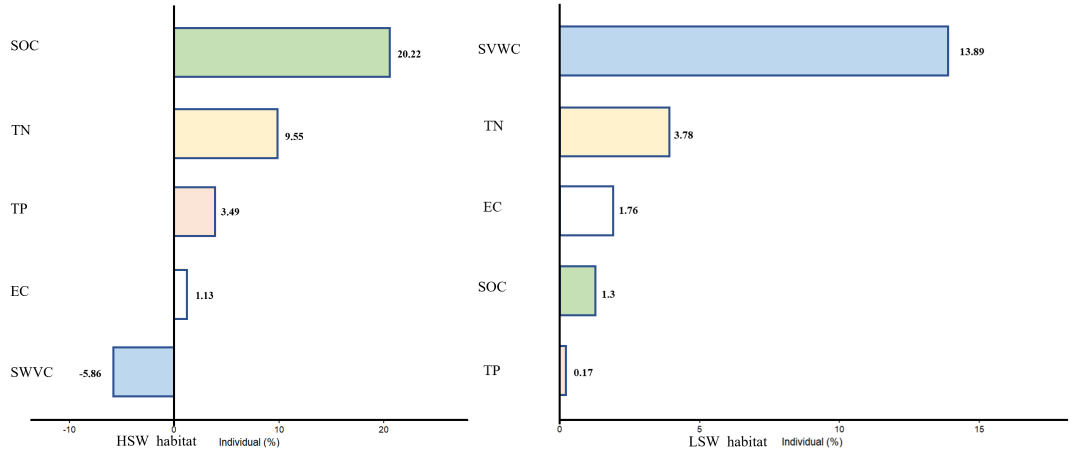

FIGURE 3
The effect of soil environmental heterogeneity on community traits is illustrated in the figure, which shows the results of variance decomposition and hierarchical partitioning, where the bars are the solitary effects of the variables and the numbers are the percentage of variance explained by the corresponding environmental factors.

4.1 Soil heterogeneity under different soil moisture-salinity habitats

In natural ecosystems, Zhang and Li (2019) proposed that the coefficient of variation of soil resources can be used to assess the geographical heterogeneity of soil environmental indicators in sample plots (Zhang and Li, 2019). Grading based on the coefficient of variation of soil environment (Hu et al., 1999), soil variables like SVWC, EC, SOC, TN, and TP exhibit moderate variability (10% < CV < 100%), indicating heterogeneity. In HSW habitat, the presence of abundant and unevenly distributed surface salt sources leads to increased salt aggregation in the topsoil layer of various plant communities. Consequently, soil EC heterogeneity is significantly higher in HSW habitat compared to LSW habitat. On the other hand, changes in soil surface water content are more pronounced in drier conditions with reduced vegetation cover, influenced by factors such as soil type and aridity. HSW habitat exhibit higher soil nutrient heterogeneity (SOC, TN, and TP) compared to LSW habitat due to the relative conditions for vegetation growth, resulting in a greater variety of plant species and higher vegetation cover. Increased litter contributes to organic matter accumulation in the soil. Nutrients in the soil are essential for plant growth, biomass accumulation, and tissue development (Ågren et al., 2012; Kerkhoff et al., 2006). The concentration of soil phosphorus is primarily influenced by the parent material and the extent of rock weathering. Our study site, situated in the arid region of northwest China, predominantly consists of calcareous and alkaline soils, which further shape the levels of phosphorus in the soil (Rezapour, 2014), soil phosphorus exists in the form of calcium phosphate, resulting in the least heterogeneity among different soil moisture-salinity habitats.

In smaller-scale research sites such as islands, depressions, and karst sinkholes, the response of abiotic elements to plant communities is more evident (Yang et al., 2021). The greater the habitat heterogeneity, influenced by factors like topography, soil moisture, and nutrients, the better it can support the growth requirements of various specie (Ma et al., 2017; Yang et al., 2017). For instance, Shui et al (2022) found that soil total nitrogen and water content had significant effects on plant functional trait variation at the sample site scale (Shui et al., 2022). Habitat heterogeneity plays a significant role in intraspecific trait variation, as confirmed by Yu et al. (2013), who found that soil heterogeneity controlled the pattern of species distribution at small scales and reflected its impact on plant adaptation (Yu et al., 2013). Soil environmental heterogeneity expands the ecological niche space for plants and improves the regulation of community functional traits through environmental filtration, as highlighted by Liu and Ma (2015), plants often adjust their morphological, physiological, and chemical traits to mitigate the adverse effects of environmental changes (Liu and Ma, 2015). Overall, HSW habitat exhibit higher soil heterogeneity compared to LSW habitat, indicating that ITV may higher and soil heterogeneity may have a greater influence on intraspecific trait variation in HSW habitat than in LSW habitat. This analysis serves as a theoretical basis and point of reference for forecasting plant adaptation strategies in the event of environmental change.

4.2 Intraspecific traits variation under different soil moisture-salinity habitats

Consistent with expectations, ITV in plant traits was higher in HSW than in LSW habitat. The coefficients of variation for intraspecific plant functional traits ranged from 3.85% to 29.41% in the HSW habitat, with a mean value of 15.84%; LSW habitat are from 4.69% to 26.77%, with a mean value of 15.02% (Table 1). Interestingly, this is different from Zhong et al (2018) finding of variation in functional traits of woody plants in the Qianzhong Karst (Zhong et al., 2018). This discrepancy may be attributed to the fact that different species are exposed to varying forms and

intensities of external biotic factors (such as species composition) and abiotic disturbances (such as moisture, salinity, and nutrient heterogeneity), leading to substantial variations in their effects on plant traits (Ding et al., 2011). Furthermore, Umaña and Zhang (2015) observed limited ITV in common species, suggesting a convergent strategy wherein plants adapt to their habitats to efficiently utilize available resources (Grime, 2006). The range of plant trait variation observed in different soil moisture-salinity habitats in our study can be explained by plants striving to strike a balance between costs and benefits. This phenomenon aligns with previous research demonstrating that species and trait composition exhibit variations along environmental gradients. Each plant's unique approach represents an optimal trade-off for its specific environmental conditions (Reich et al., 2003). In other words, ITV confers advantages to plants by enabling them to effectively adapt to their environmental conditions.

Plants of different life forms have adapted to their growing environments, exhibit variations in resource-use efficiency as reflected in the chemical, physiological, and morphological traits of leaves. The seven species selected in this study, originating from the life forms of trees, shrubs, and herbs, revealed significant ITV in leaf traits within the same soil moisture-salinity habitat (Table 2), underscoring the divergence of plant nutrient use strategies during species evolution (Niu et al., 2013). Intraspecific traits variation in the six functional traits of herbs, shrubs, and trees in the two soil moisture-salinity habitats were generally exhibited a trend of herbs > shrubs > trees. This suggests that herbaceous plants are more adaptable compared to shrubs and trees. Both within communities and within life forms, ITV was often greater in high soil moisture-salinity habitat than in low soil moisture-salinity habitat. It is noteworthy that the two soil moisture-salinity habitats showed the greatest change in plant height and the least change in leaf carbon content. A previous study found that different functional traits exhibited varying levels of ITV, with plant height accounting for 69% of the total variation, offering a potential explanation for the substantial intraspecific range in plant height across all life forms (Zhu et al., 2011). The C element, constituting the cytoskeleton of plants, is generally stable and internally robust, making it less susceptible to variations induced by changes in the external environment. This is consistent with the lower coefficient of variation of leaf C at the community level in our study (Table 1).

We observed that different habitats significantly influenced the ITV in leaf thickness. In arid environments with limited soil moisture, plants allocate more leaf photosynthetic products towards building protective tissues or increasing chloroplast density to mitigate leaf damage or water loss due to high temperatures, thereby enhancing water use efficiency (Dong et al., 2019). Leaf thickness is a particularly sensitive leaf trait for plants, as evidenced by the greater ITV in leaf thickness observed at the community level in LSW habitat compared to HSW habitat in our study. For instance, plants such as *Phragmites australis* thrive in moist habitats, explaining why herbs species dominate in HSW habitat, while shrubs like *Apocynum venetum*, with thicker leaves, are better adapted to more drier environments, leading to a predominance of shrub species in LSW habitat. This phenomenon may be attributed to the evolutionary development of ecological strategies by vegetation communities during natural succession, tailored to specific habitat conditions and resulting in more stable trait characteristics. Chlorophyll serves as a key indicator of a plant's photosynthetic capacity, and it has been

TABLE 2 Changes in ITV of species in two soil moisture and salinity habitats. leaf carbon(C), leaf nitrogen (N), leaf phosphorus (P), leaf thickness(LT), plant height(H), chlorophyll(CHl), intraspecific functional trait variation (iFD_{CV}).

Plant trait \ Species		*Populus euphratica*	*Alhagi sparsifolia*	*Apocynum venetum*	*Nitraria tangutorum*	*Halimodendron halodendron*	*Phragmites australis*	*Karelinia capsica*
C	HSW	3.85	4.32	4.80	4.77	4.13	5.27	7.01
	LSW	4.69	5.58	5.58	4.55	3.19	5.32	5.59
N	HSW	10.09	20.15	16.78	12.93	12.88	20.37	21.93
	LSW	15.58	17.62	11.37	13.11	7.70	20.59	15.02
P	HSW	6.56	16.68	13.29	11.10	13.43	17.20	18.32
	LSW	11.57	14.90	15.69	14.62	15.81	22.41	20.80
LT	HSW	11.50	11.82	17.50	10.78	6.86	14.53	19.61
	LSW	13.09	14.03	13.90	12.16	8.16	15.62	21.62
CHl	HSW	8.30	7.41	14.13	9.25	11. 24	9.41	17.75
	LSW	7.11	7.11	13.49	11.86	16.72	8.94	12.21
H	HSW	24.42	28.81	25.24	31.74	15.51	31.78	23.26
	LSW	20.40	24.92	18.91	26.69	13.68	26.19	21.55
iFD_{CV}	HSW	10.79	14.87	15.29	13.43	10.68	16.43	17.98
	LSW	12.07	14.03	13.16	13.83	10.88	16.51	16.13

noted that drought stress can alter chlorophyll content (Guan et al., 2003). This aligns with our findings of higher ITV in chlorophyll content in LSW habitat, suggesting that the community actively adapts to arid environments by modifying chlorophyll levels. Furthermore, previous studies have indicated that shrubs exhibit greater salt tolerance than trees, and both shrubs and herbs surpass trees in terms of water holding capacity (He et al., 2006; Holdaway et al., 2011). According to these results, plant functional traits variation is somewhat influenced by life form, and ITV among different life forms reflect differing environmental constraints and adaptive strategies (Símová et al., 2018). Overall, higher ITV could potentially strengthen plants' resilience to severe conditions and improve their adjustment to extreme environment (Niu et al., 2020), which may be a manifestation of desert plants' response to heterogeneous environments. Therefore, disregarding ITV may underestimate the response of community-level traits to environmental change.

4.3 Heterogeneity of soil factors enhances intraspecific trait variation of desert plant

Our investigation uncovered that soil environmental heterogeneity had a discernible impact on ITV across life forms, following a general pattern of herb > shrub > tree. This suggests that herbs may be more susceptible to the influence of soil heterogeneity and exhibit greater tolerance and resistance compared to shrubs and trees. The strong correlation between plant height variation and soil nitrogen and phosphorus heterogeneity suggests strong effects of soil nitrogen and phosphorus distribution on plant growth (Kerkhoff et al., 2006). The results were consistent with our expectations, namely, high soil heterogeneity in HSW habitat may promotes high ITV of plant height. The ITV of leaf N and P may partly depend on the content and distribution of N and P in the soil (Berman-Frank and Dubinsky, 1999). For example, a global analysis conducted by Ordonez revealed a positive correlation between the mass fraction of nitrogen and phosphorus in leaves and the availability of these elements in the soil. Therefore, the mass fraction of leaf nitrogen showed a positive correlation with soil phosphorus levels (Ordoñez et al., 2009). In addition, leaf nitrogen is directly related to water availability, storage and resource acquisition (Dong et al., 2019; Li et al., 2020).

Our study yields two main findings: (1) soil heterogeneity improve desert plant ITV; (2) The contribution of each soil factor heterogeneity to the ITV at community-level traits varies and changes with soil moisture and salinity conditions. Consistent with our expectations, soil heterogeneity had a higher effect on ITV in herbs and shrubs than in trees, suggesting that herbs and shrubs are more sensitive to soil heterogeneity. ITV increases with soil heterogeneity (Figure 2), conforming to the ecological niche theory, which illustrates the connection between plant species' environmental exposures and the diversity of their traits (Bucher et al., 2016; König et al., 2018). The ELWNNR, situated in a typical desert zone with infertile, arid soils and slow nutrient cycling, plant growth and distribution would be more obviously limited (Titus et al., 2002). At the community level, soil organic carbon heterogeneity in HSW habitat independently accounts for the highest percentage of plant functional traits variations (20.22%), followed by TN (9.55%) and TP (3.49%). Nutrient-deficient soils trigger a transition from species that are typically associated with rapid resource acquisition to those that are linked with resource preservation. This phenomenon, observed in our study, showed the adaptive response of plant communities to nutrient limitations in their environment. As nutrients become scarce, plants tend to prioritize conserving and efficiently utilizing available resources rather than investing in traits that promote rapid growth and resource acquisition (Diaz et al., 2004; Ordoñez et al., 2009). In LSW habitat, soil moisture and nitrogen heterogeneity are significant environmental factors influencing plant adaptation, with soil SVWC (13.89%) and TN (3.78%) heterogeneity explaining the highest rates of variation, respectively (Titus et al., 2002). This finding aligns with the observation that community chemical traits in typical grassland ecosystems respond to nitrogen and water enrichment and are dominated by ITV (Violle et al., 2007). Furthermore, plants in LSW habitat are more susceptible to drought stress than nutrient deficiency, as drought stress has been found to limit nutrient uptake, subsequently inhibiting photosynthesis and plant growth (Farooq et al., 2009; Jaleel et al., 2009; Pérez-Harguindeguy et al., 2016).

5 Conclusions

In summary, this study highlights the significant promoting influence of soil heterogeneity on ITV of desert plants in the ELWNNR, with this influence being more pronounced in herbs and shrubs, and varying with different soil moisture-salinity habitats. ITV of desert plant in the two habitats reflect both the habitat filtering effect of soil heterogeneity at small scales and the diverse adaptive mechanisms of plants to their habitats. Microhabitats provide the necessary space for these species to coexist. Consequently, soil heterogeneity plays a crucial role in enhancing trait variation in plant communities, and maximizing the survival efficiency of desert plant species in the ELWNNR. In summary, soil heterogeneity promotes multi-species coexistence in arid zones. Our findings provide a scientific foundation for conservation planning in arid land, it is essential to protect and enhance soil heterogeneity within habitats, which will serve as a buffer against extreme environmental impacts.

Data availability statement

The datasets presented in this study can be found in online repositories. The names of the repository/repositories and accession number(s) can be found in the article/Supplementary Material.

Author contributions

Y-cW: Data curation, Formal analysis, Methodology, Software, Visualization, Writing – original draft. X-nZ: Funding acquisition,

Project administration, Resources, Supervision, Validation, Writing – review & editing. J-fY: Data curation, Formal analysis, Investigation, Writing – review & editing. J-yT: Data curation, Investigation, Writing – review & editing. D-hS: Data curation, Software, Writing – review & editing. X-hL: Investigation, Writing – review & editing. S-fZ: Investigation, Writing – review & editing.

Funding

The author(s) declare that financial support was received for the research, authorship, and/or publication of this article. This research was supported by the National Natural Science Foundation of China (31700354, 32360277, 32360282).

Conflict of interest

The authors declare that the research was conducted in the absence of any commercial or financial relationships that could be construed as a potential conflict of interest.

Generative AI statement

The author(s) declare that no Generative AI was used in the creation of this manuscript.

Publisher's note

Supplementary material

The Supplementary Material for this article can be found online at: https://www.frontiersin.org/articles/10.3389/fpls.2024.1504238/full#supplementary-material

References

Ågren, G. I., Wetterstedt, J., and Billberger, M. F. K. (2012). Nutrient limitation on terrestrial plant growth - modeling the interaction between nitrogen and phosphorus. *New Phytol.* 194, 953–960. doi: 10.1111/j.1469-8137.2012.04116.x

Arnold, P. A., Kruuk, L. E. B., and Nicotra, A. B. (2019). How to analyse plant phenotypic plasticity in response to a changing climate. *New Phytol.* 222, 1235–1241. doi: 10.1111/nph.15656

Benes, K., and Bracken, M. E. S. (2020). Interactive effects of large- and local-scale environmental gradients on phenotypic differentiation. *Ecology.* 101, 10. doi: 10.1002/ecy.3078

Berman-Frank, I., and Dubinsky, Z. (1999). Balanced growth in aquatic plants: Myth or reality? Phytoplankton use the imbalance between carbon assimilation and biomass production to their strategic advantage. *Bioscience.* 49, 29–37. doi: 10.2307/1313491

Bloomfield, K. J., Cernusak, L. A., Eamus, D., Ellsworth, D. S., Prentice, I. C., Wright, I. J., et al. (2018). A continental-scale assessment of variability in leaf traits: Within species, across sites and between seasons. *Funct. Ecol.* 32, 1492–1506. doi: 10.1111/1365-2435.13097

Bucher, S. F., Auerswald, K., Tautenhahn, S., Geiger, A., Otto, J., Müller, A., et al. (2016). Inter- and intraspecific variation in stomatal pore area index along elevational gradients and its relation to leaf functional traits. *Plant Ecol.* 217, 229–240. doi: 10.1007/s11258-016-0564-2

Chesson, P. (2000). General theory of competitive coexistence in spatially-varying environments. *Theor. Popul. Biol.* 58, 211–237. doi: 10.1006/tpbi.2000.1486

Crawley, M. J. (2007). *The R book* (Chichester, UK: John Wiley & Sons, Ltd).

Des Roches, S., Pendleton, L. H., Shapiro, B., and Palkovacs, E. P. (2021). Conserving intraspecific variation for nature's contributions to people. *Nat. Ecol. Evol.* 5, 574–582. doi: 10.1038/s41559-021-01403-5

Diaz, S., Hodgson, J. G., Thompson, K., Cabido, M., Cornelissen, J. H. C., Jalili, A., et al. (2004). The plant traits that drive ecosystems: Evidence from three continents. *J. Veg. Sci.* 15, 295–304. doi: 10.1111/j.1654-1103.2004.tb02266.x

Ding, J., Wu, Q., Yan, H., and Zhang, S. (2011). Effects of topographic variations and soil characteristics on plant functional traits in a subtropical evergreen broad-leaved forest. *Biodiversity Science.* 19, 158–167. doi: 10.1007/s10255-011-0044-3

Dong., M. (1997). *Survey, observation and analysis of terrestrial biocommunities* (Beijing: China Standard Press).

Dong, X., Li, Y., Xin, Z., Liu, M., Hao, Y., Liu, D., et al. (2019). Variation in leaf traits and leaf δ^{13} C and δ^{15} N content in Nitraria tangutorum along precipitation gradient. *Acta Ecologica Sinica.* 39, 3700–3709. doi: 10.5846/stxb201804170873

Farooq, M., Wahid, A., Kobayashi, N., Fujita, D., and Basra, S. M. A. (2009). Plant drought stress: effects, mechanisms and management. *Agron. Sustain. Dev.* 29, 185–212. doi: 10.1051/agro:2008021

Feeser, K. L., Van Horn, D. J., Buelow, H. N., Colman, D. R., McHugh, T. A., Okie, J. G., et al. (2018). Local and regional scale heterogeneity drive bacterial community diversity and composition in a polar desert. *Front. Microbiol.* 9. doi: 10.3389/fmicb.2018.01928

Frederiksen, M., Harris, M. P., and Wanless, S. (2005). Inter-population variation in demographic parameters: a neglected subject? *Oikos.* 111, 209–214. doi: 10.1111/j.0030-1299.2005.13746.x

Gratani, L. (2014). Plant phenotypic plasticity in response to environmental factors. *Adv. Botany.* 2014, 1–17. doi: 10.1155/2014/208747

Grime, J. P. (2006). Trait convergence and trait divergence in herbaceous plant communities: mechanisms and consequences. *J. Veg. Sci.* 17, 255–260. doi: 10.1111/j.1654-1103.2006.tb02444.x

Guan, B., Ge, Y., Fan, M., Niu, X., and Lu, Y. (2003). Phenotypic plasticity of growth and morphology in Mosla chinensis responds to diverse relative soil water content. *Acta Ecologica Sinica.* 23, 259–263. doi: 10.1023/A:1022289509702

Hart, S. P., Schreiber, S. J., and Levine, J. M. (2016). How variation between individuals affects species coexistence. *Ecol. Lett.* 19, 825–838. doi: 10.1111/ele.12618

He, M., Wang, H., and Chen, Z. (2006). Water-retaining capability of desert plants. *J. Desert Res.* 26, 403–408.

Helm, J., Dutoit, T., Saatkamp, A., Bucher, S. F., Leiterer, M., and Römermann, C. (2019). Recovery of mediterranean steppe vegetation after cultivation: legacy effects on plant composition, soil properties and functional traits. *Appl. Veg. Sci.* 22, 71–84. doi: 10.1111/avsc.12415

Holdaway, R. J., Richardson, S. J., Dickie, I. A., Peltzer, D. A., and Coomes, D. A. (2011). Species- and community-level patterns in fine root traits along a 120 000-year soil chronosequence in temperate rain forest. *J. Ecol.* 99, 954–963. doi: 10.1111/j.1365-2745.2011.01821.x

Hu, K., Li, B., Lin, Q., Li, G., and Chen, D. (1999). Spatial variability of soil nutrient in wheat field. *Trans. CSAE.* 15, 33–38.

Hurtado, P., Prieto, M., Aragón, G., de Bello, F., and Martínez, I. (2020). Intraspecific variability drives functional changes in lichen epiphytic communities across Europe. *Ecology.* 101, 10. doi: 10.1002/ecy.3017

Jaleel, C. A., Manivannan, P., Wahid, A., Farooq, M., Al-Juburi, H. J., Somasundaram, R., et al. (2009). Drought stress in plants: a review on morphological characteristics and pigments composition. *Int. J. Agric. Biol.* 11, 100–105. doi: 10.3763/ijas.2009.0459

Jung, V., Violle, C., Mondy, C., Hoffmann, L., and Muller, S. (2010). Intraspecific variability and trait-based community assembly. *J. Ecol.* 98, 1134–1140. doi: 10.1111/j.1365-2745.2010.01687.x

Karbstein, K., Prinz, K., Hellwig, F., and Roemermann, C. (2020). Plant intraspecific functional trait variation is related to within-habitat heterogeneity and genetic diversity in Trifolium montanum L. *Ecol. Evol.* 10, 5015–5033. doi: 10.1002/ece3.6255

Kearney, M., and Porter, W. P. (2006). Ecologists have already started rebuilding community ecology from functional traits. *Trends Ecol. Evol.* 21, 481–482. doi: 10.1016/j.tree.2006.06.019

Kerkhoff, A. J., Fagan, W. F., Elser, J. J., and Enquist, B. J. (2006). Phylogenetic and growth form variation in the scaling of nitrogen and phosphorus in the seed plants. *Am. Nat.* 168, E103–E122. doi: 10.1086/507879

König, P., Tautenhahn, S., Cornelissen, J. H. C., Kattge, J., Bönisch, G., and Römermann, C. (2018). Advances in flowering phenology across the Northern Hemisphere are explained by functional traits. *Glob. Ecol. Biogeogr.* 27, 310–321. doi: 10.1111/geb.12696

Lai, J. S., Zou, Y., Zhang, J. L., and Peres-Neto, P. R. (2022). Generalizing hierarchical and variation partitioning in multiple regression and canonical analyses using the rdacca.hp R package. *Methods Ecol. Evol.* 13, 782–788. doi: 10.1111/2041-210x.13800

Li, C. J., Lei, J. Q., Shi, X., and Liu, R. (2014). Scale dependence of soil spatial variation in a temperate desert. *Pedosphere.* 24, 417–426. doi: 10.1016/s1002-0160(14)60028-x

Li, D., Si, J., Zhang, X., Gao, Y., Luo, H., Qin, J., et al. (2020). Ecological adaptation of *Populus euphratica* to drought stress. *J. Desert Res.* 40, 17–23. doi: 10.7522/j.issn.1000-694X.2019.00082

Liu., R. (2018). *Study on the variation of functional traits of woody plants in the Lijiang River terrestrial and aquatic zones* (Guilin: Guangxi Normal University).

Liu, Y. J., Li, G. E., Wang, M. X., Yan, W. J., and Hou, F. J. (2021). Effects of three-dimensional soil heterogeneity and species composition on plant biomass and biomass allocation of grass-mixtures. *Aob Plants.* 13, 8. doi: 10.1093/aobpla/plab033

Liu, X., and Ma, K. (2015). Plant functional traits—concepts, applications and future directions. *Chin. Sci. Life Sci.* 45, 325–339. doi: 10.1360/N052014-00244

Liu, S. S., Streich, J., Borevitz, J. O., Rice, K. J., Li, T. T., Li, B., et al. (2019). Environmental resource deficit may drive the evolution of intraspecific trait variation in invasive plant populations. *Oikos.* 128, 171–184. doi: 10.1111/oik.05548

Lundholm, J. T. (2009). Plant species diversity and environmental heterogeneity: spatial scale and competing hypotheses. *J. Veg. Sci.* 20, 377–391. doi: 10.1111/j.1654-1103.2009.05577.x

Ma, H., Yang, X., Lu, G., He, X., Zhang, X., Wang, X., et al. (2017). Water sources of dominant desert species in ebinur lake wetland nature reserve, Xinjiang, China. *Acta Ecologica Sinica.* 37, 829–840. doi: 10.5846/stxb201508311804

McGill, B. J., Enquist, B. J., Weiher, E., and Westoby, M. (2006). Rebuilding community ecology from functional traits. *Trends Ecol. Evol.* 21, 178–185. doi: 10.1016/j.tree.2006.02.002

Nicotra, A. B., Atkin, O. K., Bonser, S. P., Davidson, A. M., Finnegan, E. J., Mathesius, U., et al. (2010). Plant phenotypic plasticity in a changing climate. *Trends Plant Sci.* 15, 684–692. doi: 10.1016/j.tplants.2010.09.008

Niu, D., Li, Q., Jiang, S., Chang, P., and Fu, H. (2013). Seasonal variations of leaf C:N: P stoichiometry of six shrubs in desert of China's Alxa plateau. *Chin. J. Plant Ecology.* 37, 317–325. doi: 10.3724/SPJ.1258.2013.00031

Niu, K. C., Zhang, S., and Lechowicz, M. (2020). Harsh environmental regimes increase the functional significance of intraspecific variation in plant communities. *Funct. Ecol.* 34, 1666–1677. doi: 10.1111/1365-2435.13582

Olagoke, A., Jeltsch, F., Tietjen, B., Berger, U., Ritter, H., and Maass, S. (2023). Small-scale heterogeneity shapes grassland diversity in low-to-intermediate resource environments. *J. Veg. Sci.* 34, 14. doi: 10.1111/jvs.13196

Ordoñez, J. C., van Bodegom, P. M., Witte, J. P. M., Wright, I. J., Reich, P. B., and Aerts, R. (2009). A global study of relationships between leaf traits, climate and soil measures of nutrient fertility. *Glob. Ecol. Biogeogr.* 18, 137–149. doi: 10.1111/j.1466-8238.2008.00441.x

Pérez-Harguindeguy, N., Díaz, S., Garnier, E., Lavorel, S., Poorter, H., Jaureguiberry, P., et al. (2016). New handbook for standardised measurement of plant functional traits worldwide. *Aust. J. Bot.* 64, 715–716. doi: 10.1071/bt12225

Pérez-Izquierdo, L., Zabal-Aguirre, M., González-Martínez, S. C., Buée, M., Verdú, M., Rincón, A., et al. (2019). Plant intraspecific variation modulates nutrient cycling through its below ground rhizospheric microbiome. *J. Ecol.* 107, 1594–1605. doi: 10.1111/1365-2745.13202

Price, J., Tamme, R., Gazol, A., de Bello, F., Takkis, K., Uria-Diez, J., et al. (2017). Within-community environmental variability drives trait variability in species-rich grasslands. *J. Veg. Sci.* 28, 303–312. doi: 10.1111/jvs.12487

Reich, P. B., Wright, I. J., Cavender-Bares, J., Craine, J. M., Oleksyn, J., Westoby, M., et al. (2003). The evolution of plant functional variation: traits, spectra, and strategies. *Int. J. Plant Sci.* 164, S143–S164. doi: 10.1086/374368

Rezapour, S. (2014). Effect of sulfur and composted manure on SO_4-S, P and micronutrient availability in a calcareous saline-sodic soil. *Chem. Ecol.* 30, 147–155. doi: 10.1080/02757540.2013.841896

Shui, W., Guo, P., Zhu, S., Feng, J., Sun, X., and Li, H. (2022). Variation of plant functional traits and adaptive strategy of woody species in degraded karst tiankeng of Yunnan Province. *Scientia Geographica Sinica.* 42, 1295–1306. doi: 10.13249/j.cnki.sgs.2022.07.016

Siefert, A., and Ritchie, M. E. (2016). Intraspecific trait variation drives functional responses of old-field plant communities to nutrient enrichment. *Oecologia.* 181, 245–255. doi: 10.1007/s00442-016-3563-z

Siefert, A., Violle, C., Chalmandrier, L., Albert, C. H., Taudiere, A., Fajardo, A., et al. (2015). A global meta-analysis of the relative extent of intraspecific trait variation in plant communities. *Ecol. Lett.* 18, 1406–1419. doi: 10.1111/ele.12508

Silva, M. C., Teodoro, G. S., Bragion, E. F. A., and van den Berg, E. (2019). The role of intraspecific trait variation in the occupation of sharp forest-savanna ecotones. *Flora.* 253, 35–42. doi: 10.1016/j.flora.2019.03.003

Símová, I., Violle, C., Kraft, N. J. B., Storch, D., Svenning, J. C., Boyle, B., et al. (2015). Shifts in trait means and variances in North American tree assemblages: species richness patterns are loosely related to the functional space. *Ecography.* 38, 649–658. doi: 10.1111/ecog.00867

Símová, I., Violle, C., Svenning, J. C., Kattge, J., Engemann, K., Sandel, B., et al. (2018). Spatial patterns and climate relationships of major plant traits in the New World differ between woody and herbaceous species. *J. Biogeogr.* 45, 895–916. doi: 10.1111/jbi.13171

Stanton, M. L., Roy, B. A., and Thiede, D. A. (2000). Evolution in stressful environments. i. phenotypic variability, phenotypic selection, and response to selection in five distinct environmental stresses. *Evolution.* 54, 93–111. doi: 10.1111/j.0014-3820.2000.tb00011.x

Stark, J., Lehman, R., Crawford, L., Enquist, B. J., and Blonder, B. (2017). Does environmental heterogeneity drive functional trait variation? A test in montane and alpine meadows. *Oikos.* 126, 1650–1659. doi: 10.1111/oik.04311

Stojnic, S., Kovacevic, B., Kebert, M., Vasić, V., Vuksanović, V., Trudić, B., et al. (2022). Genetic differentiation in functional traits among wild cherry (*Prunus avium L.*) half-sib lines. *J. Forestry Res.* 33, 991–1003. doi: 10.1007/s11676-021-01390-0

Sultan, S. E. (2000). Phenotypic plasticity for plant development, function and life history. *Trends Plant Sci.* 5, 537–542. doi: 10.1016/s1360-1385(00)01797-0

Tautenhahn, S., Grün-Wenzel, C., Jung, M., Higgins, S., and Römermann, C. (2019). On the relevance of intraspecific trait variability-A synthesis of 56 dry grassland sites across Europe. *Flora.* 254, 161–172. doi: 10.1016/j.flora.2019.03.002

Titus, J. H., Nowak, R. S., and Smith, S. D. (2002). Soil resource heterogeneity in the Mojave Desert. *J. Arid. Environ.* 52, 269–292. doi: 10.1006/jare.2002.1010

Turcotte, M. M., and Levine, J. M. (2016). Phenotypic plasticity and species coexistence. *Trends Ecol. Evol.* 31, 803–813. doi: 10.1016/j.tree.2016.07.013

Tusifujiang, Y., Zhang, X. N., and Gong, L. (2021). The relative contribution of intraspecific variation and species turnover to the community-level foliar stoichiometric characteristics in different soil moisture and salinity habitats. *PloS One* 16, 16. doi: 10.1371/journal.pone.0246672

Umaña, M. N., Zhang, C. C., Cao, M., Lin, L. X., and Swenson, N. G. (2015). Commonnes s, rarity, and intraspecific variation in traits and performance in tropical tree seedlings. *Ecol. Lett.* 18(12), 1329–1337. doi: 10.1111/ele.12527

Valladares, F., Gianoli, E., and Gómez, J. M. (2007). Ecological limits to plant phenotypic plasticity. *New Phytol.* 176, 749–763. doi: 10.1111/j.1469-8137.2007.02275.x

Vernham, G., Bailey, J. J., Field, R., and Schrodt, F. (2024). What is the relationship between plant trait diversity and geodiversity? a plot-based, pan-European analysis. *Global. Ecol. Biogeogr.* 33, e13904. doi: 10.1111/geb.13904

Violle, C., and Jiang, L. (2009). Towards a trait-based quantification of species niche. *J. Plant Ecol.* 2, 87–93. doi: 10.1093/jpe/rtp007

Violle, C., Navas, M. L., Vile, D., Kazakou, E., Fortunel, C., Hummel, I., et al. (2007). Let the concept of trait be functional! *Oikos.* 116, 882–892. doi: 10.1111/j.2007.0030-1299.15559.x

Wan, J. Z., Wang, M. Z., Qin, T. J., Bu, X. Q., Li, H. L., and Yu, F. H. (2019). Spatial environmental heterogeneity may drive functional trait variation in Hydrocotyle vulgaris (Araliaceae), an invasive aquatic plant. *Aquat. Biol.* 28, 149–158. doi: 10.3354/ab00716

Wang, X. P., Zhang, F., Kung, H. T., and Yu, H. Y. (2017). Spectral response characteristics and identification of typical plant species in Ebinur lake wetland national nature reserve (ELWNNR) under a water and salinity gradient. *Ecol. Indic.* 81, 222–234. doi: 10.1016/j.ecolind.2017.05.071

Westerband, A. C., Funk, J. L., and Barton, K. E. (2021). Intraspecific trait variation in plants: a renewed focus on its role in ecological processes. *Ann. Botany.* 127, 397–410. doi: 10.1093/aob/mcab011

Wright, I. J., Reich, P. B., Westoby, M., Ackerly, D. D., Baruch, Z., Bongers, F., et al. (2004). The worldwide leaf economics spectrum. *Nature.* 428, 821–827. doi: 10.1038/nature02403

Yang, X. D., Long, Y. X., Sarkar, B., Li, Y., Lü, G. H., Ali, A., et al. (2021). Influence of soil microorganisms and physicochemical properties on plant diversity in an arid desert of Western China. *J. Forestry Res.* 32, 2645–2659. doi: 10.1007/s11676-021-01292-1

Yang, X. D., Lv, G. H., Ali, A., Ran, Q. Y., Gong, X. W., Wang, F., et al. (2017). Experimental variations in functional and demographic traits of Lappula semiglabra among dew amount treatments in an arid region. *Ecohydrology.* 10, 10. doi: 10.1002/eco.1858

Yu, M., Zhou, Z.-Y., Kang, F.-F., Ouyang, S., Mi, X.-C., and Sun, J.-X. (2013). Gradient analysis and environmental interpretation of understory herb-layer communities in Xiaoshegou of Lingkong Mountain, Shanxi, China. *Chin. J. Plant Ecology.* 37, 373–383. doi: 10.3724/sp.J.1258.2013.00039

Zhang, J., and Li, W. (2019). Study on the soil nutrient status of Huashan pine forest on the west slope of Erlang Mountain. *Agric. Technology.* 39, 10–11. doi: 10.19754/j.nyyjs.20190815004

Zhang, X., Yang, X., and Lv, G. (2016). Diversity patterns and response mechanisms of desert plants to the soil environment along soil water and salinity gradients. *Acta Ecologica Sinica*. 36, 3206–3215. doi: 10.5846/stxb201505291082

Zhong, Q.-L., Liu, L.-B., Xu, X., Yang, Y., Guo, Y.-M., Xu, H.-Y., et al. (2018). Variations of plant functional traits and adaptive strategy of woody species in a karst forest of central Guizhou Province, southwestern China. *Chin. J. Plant Ecology*. 42, 562–572. doi: 10.17521/cjpe.2017.0270

Zhu, B., Xu, B., and Zhang, D. (2011). Extent and sources of variation in plant functional traits in grassland. *J. Beijing Normal University(Natural Science)*. 47, 485–489. doi: CNKI:SUN:BSDZ.0.2011-05-012

frontiers | Frontiers in Plant Science

TYPE Original Research
PUBLISHED 11 February 2025
DOI 10.3389/fpls.2025.1511277

OPEN ACCESS

EDITED BY
Yanju Liu,
The University of Newcastle, Australia

REVIEWED BY
Quan Li,
Zhejiang Agriculture and Forestry University, China
Mingliang Zhao,
Chinese Academy of Sciences (CAS), China

*CORRESPONDENCE
Jinlong Wang
wangjl@xju.edu.cn
Guanghui Lv
ler@xju.edu.cn

RECEIVED 14 October 2024
ACCEPTED 20 January 2025
PUBLISHED 11 February 2025

CITATION
Wang J, Lv G, Yang J, He X, Wang H and Li W (2025) Impacts of plant root traits and microbial functional attributes on soil respiration components in the desert-oasis ecotone. *Front. Plant Sci.* 16:1511277. doi: 10.3389/fpls.2025.1511277

Impacts of plant root traits and microbial functional attributes on soil respiration components in the desert-oasis ecotone

Jinlong Wang[1,2,3]*, Guanghui Lv[1,2,3]*, Jianjun Yang[1,2,3], Xuemin He[1,2,3], Hengfang Wang[1,2,3] and Wenjing Li[1,2,3]

[1]College of Ecology and Environment, Xinjiang University, Urumqi, China, [2]Key Laboratory of Oasis Ecology of Education Ministry, Xinjiang University, Urumqi, China, [3]Xinjiang Jinghe Observation and Research Station of Temperate Desert Ecosystem, Ministry of Education, Jinghe, China

Dividing soil respiration (Rs) into autotrophic respiration (Ra) and heterotrophic respiration (Rh) represents a pivotal step in deciphering how Rs responds to environmental perturbations. Nevertheless, in arid ecosystems beset by environmental stress, the partitioning of Rs and the underlying mechanisms through which microbial and root traits govern the distinct components remain poorly understood. This study was strategically designed to investigate Rs and its components (Ra and Rh), soil properties, and root traits within the desert-oasis ecotone (encompassing the river bank, transitional zone, and desert margin) of northwest China. Employing metagenomics, we quantitatively characterized microbial taxonomic attributes (i.e., taxonomic composition) and functional attributes (specifically, functional genes implicated in microbial carbon metabolism). Field measurements during the growing season of 2019 unveiled a pronounced decline in soil respiration rates along the environmental gradient from the river bank to the desert margin. The mean soil respiration rate was recorded as 1.82 ± 0.41 μmol m^{-2} s^{-1} at the river bank, 0.49 ± 0.15 μmol m^{-2} s^{-1} in the transitional zone, and a meager 0.45 ± 0.12 μmol m^{-2} s^{-1} in the desert margin. Concomitantly, the Ra and Rh components exhibited a similar trend throughout the study period, with Rh emerging as the dominant driver of Rs. Utilizing random forest modeling, we unearthed significant associations between microbial taxonomic and functional features and Rs components. Notably, both Ra and Rh displayed robust positive correlations with the abundance of phosphatidylinositol glycan A, a key player in microbial carbon metabolism. Partial least squares path modeling further elucidated that soil properties and microbial functions exerted direct and positive influences on both Ra and Rh, whereas taxonomic features failed to register a significant impact. When considering the combined effects of biotic and abiotic factors, microbial

functional attributes emerged as the linchpin in dictating Rs composition. Collectively, these findings suggest that a trait-based approach holds great promise in more effectively revealing the response mechanisms of Rs composition to environmental changes, thereby offering novel vistas for future investigations into carbon cycling in terrestrial soils.

KEYWORDS

autotrophic respiration, heterotrophic respiration, microbial functional attributes, plant traits, desert-oasis ecotone

1 Introduction

In terrestrial ecosystems, the soil carbon pool represents the greatest carbon storage pool at about two to three times larger than the plant carbon pool or the atmospheric carbon pool (Chen et al., 2024; Huang et al., 2020). Soil respiration (Rs), being the primary carbon release mechanism in the terrestrial carbon cycle (Li et al., 2021), has garnered significant interest among ecologists over the past few decades, emerging as a crucial factor in global carbon cycle studies (Hashimoto et al., 2023). Rs serves as the principal conduit for transferring carbon from soil pools to the atmosphere (Huang et al., 2020), comprising two key elements: autotrophic respiration (Ra), involving CO_2 emissions from plant roots and associated microbial activity, and heterotrophic respiration (Rh), stemming from microbial breakdown of organic matter in soil. Ra contributes between 10% and 90% to the total Rs (Yan et al., 2015). A portion of the CO_2 captured annually via photosynthesis in terrestrial plants is immediately emitted back into the atmosphere as part of Ra, whereas the rest is temporarily sequestered in organic matter and later released through Rh (Hopkins et al., 2013). However, the complexity of the different sources of CO_2 produced by soils and the factors influencing them makes a comprehensive understanding of Rs uncertain (Bond-Lamberty, 2018), especially in more heterogeneous arid ecosystems (Kukumägi et al., 2017; Wang et al., 2021b). Consequently, it's essential to distinguish between the autotrophic and heterotrophic components of Rs and evaluate their responses to environmental shifts, along with their consistent contributions to Rs (Chu et al., 2023; Huang et al., 2015).

Rs variations are affected by various biotic and abiotic factors including soil microclimate (temperature and moisture), nutrients, microbes, and plant traits (Borden et al., 2021; Wang et al., 2022a, 2021b). In arid regions, soil moisture and temperature exhibit extreme variability, and the scarcity of water and nutrients makes the ecosystem highly fragile (Liu et al., 2024). For example, low rainfall and high temperatures can lead to significant fluctuations in soil water availability, which will have a major impact on soil microbial activity and root physiological processes (Furtak and Wolińska, 2023), and thus affect soil respiration (Han et al., 2024). Unlike humid regions, where soil respiration is often influenced by multiple factors such as high vegetation cover and abundant water supply (Li et al., 2024b), while the limited water resources and harsh environmental conditions make soil microclimate and nutrients the primary factors controlling soil respiration in arid areas (Ngaba et al., 2024). This difference in driving factors makes the study of soil respiration in arid areas unique and provides an opportunity to understand the specific responses of ecosystems to environmental stresses. Differences in how Rh and Ra respond to these factors may alter their roles in Rs, potentially leading to decreased water and nutrient availability (Huang et al., 2015; Zheng et al., 2021). Many studies indicate that Rh fluctuations are significantly influenced by external factors like soil microclimate, nutrient status, and soil microbes (Kang et al., 2022; Tang et al., 2020a), whereas Ra correlates more with soil's physical and chemical properties, root morphology, and chemical makeup (Paradiso et al., 2019). Root-mediated soil organic matter decomposition and the ensuing CO_2 release through respiration occur at the root level, involving both the plant root system and inter-root microorganisms (Adamczyk et al., 2019; Chari and Taylor, 2022). However, the microbial control over Rs components, particularly the role of inter-root microorganisms in Ra, remains largely unclear.

The vegetation in arid regions is predominantly comprised of drought-tolerant plant species, whose root structures and physiological characteristics are specifically adapted to the arid environment (Liu et al., 2024). For example, certain plants possess more developed root systems that can penetrate deeper into the soil in pursuit of water and nutrients (Li et al., 2024a). This distinctive vegetation structure exerts an impact on the sources contributing to soil respiration (Borden et al., 2021; Wang et al., 2021c), with the proportion of autotrophic respiration to heterotrophic respiration potentially differing from that in other ecosystems (Quoreshi et al., 2022). Traits or functional traits are measurable characteristics of organisms that have adapted and evolved over time in response to the external environment, affecting the organism's survival, growth, and reproduction and thus its adaptations to and functions in the environment (Shen et al., 2019). The biogeographical distribution of traits connects an organism's function to its habitat, enabling theoretical predictions of how organisms, communities, and ecosystems respond to environmental shifts through trait modifications (Vernham et al., 2023). Trait-based microbial ecology and plant ecology research focuses on identifying a core set of traits for microbial and plant

adaptations to environmental changes to predict changes in ecosystem function (Montoya, 2023; Violle et al., 2014). Root systems, crucial for plant water and nutrient absorption, adapt to various environmental conditions, making root traits vital for sustaining diverse ecosystem processes. These traits serve as key indicators for assessing plant resilience in challenging habitats (Cortois et al., 2016; Wang et al., 2021c). Research has shown that functional traits such as root morphology, chemical composition, and physiological activity have a significant impact on microbial community structure and activity (Furey and Tilman, 2023; Rathore et al., 2023; Wan et al., 2021). Most metabolic traits of microorganisms can directly affect nutrient and elemental cycling processes in ecosystems (Martiny et al., 2015). Microbial genetic traits primarily manifest through specific functional genes or metabolic pathways present in their genomes (Escalas et al., 2019). Genomic analyses, including metagenomics, facilitate comparisons between targeted gene sequences and databases annotating gene or protein functions (e.g., KEGG), aiding in deducing the roles of these sequences in carbon cycling and microbial functionality (Dai et al., 2021). Despite methods linking root trait and microbial data (including taxonomy and metabolism) to Rs (Trivedi et al., 2013), understanding of how these subterranean traits react to environmental shifts and influence Rs components remains limited.

Desert ecosystems, covering about 22% of Earth's land surface, significantly influence the global carbon cycle (Wang et al., 2022b). Desert-oasis ecotones, found in the extremely arid deserts of northwest China, are unique ecosystems known for their high biodiversity and primary productivity. Desert-oasis ecotones are crucial for combating wind erosion, stabilizing riverbeds, moderating local climates, preserving biodiversity, and ensuring regional ecological safety (An et al., 2023; Wang et al., 2019a, 2021a; Zhang et al., 2018c). Recently, changes in ecological processes and natural landscapes within desert-oasis ecotones, driven by regional climate shifts and escalating human activities, pose significant threats to both the ecological services of these oases and the sustainability of the regional economy (Ling et al., 2015). Desert-oasis ecotones encompass various habitats, typically transitioning from densely forested riparian zones to sparse desert vegetation (Wang et al., 2021b; Williams et al., 2006). Ecological processes shaping ecosystem structure and function can vary across these habitats (Bennett et al., 2009; Tianjiao et al., 2022). Differences in environmental habitat factors make desert-oasis ecotones ideal for assessing the response of Rs components to environmental stresses. This study employed root exclusion experiments on *Nitraria tangutorum* and *Alhagi sparsifolia*, common desert plants in the Ebinur Lake basin's desert-oasis ecotone, northwest China. The objectives were to assess (1) the proportional roles of Rh and Ra in Rs; (2) correlations between microbial taxonomy/functionality and Rs components; and (3) the impacts of soil properties, root traits, microbial diversity, and functionality on Rs components. The hypothesis posits that environmental stress decreases Rs yet enhances Rh's relative contribution, and that Rs components exhibit greater sensitivity to microbial functional genes compared to microbial taxonomic composition.

2 Materials and methods

2.1 Study sites and experimental design

The study site is situated in the Ebinur Lake Wetland National Nature Reserve, Xinjiang Uygur Autonomous Region, China (82° 36'–83°50'E, 44°30'–45°09'N), within the Ebinur Lake basin adjacent to the southwestern border of the Gurbantunggut Desert (Fu et al., 2021). The area experiences a characteristic temperate continental arid climate, marked by minimal rainfall and significant evaporation. Dominant plant communities consist primarily of saline- and drought-tolerant species including *Populus euphratica*, *A. sparsifolia*, and *N. tangutorum*. Plant distribution in the study area forms a patchy mosaic, interspersed with bare ground, offering an optimal natural setting for investigating Rs components (Zhao et al., 2011). In July 2018, a transect was set up in the Ebinur Wetland Nature Reserve, running from the Aqikesu River towards the Mutter Desert. Three habitats were identified based on their proximity to the riverbank: river bank (at a distance of 150 meters from the riverbank), transitional zone (at a distance of 3000 meters from the riverbank), and desert margin (at a distance of 5000 meters from the riverbank) (Figure 1) (Wang et al., 2021b).

In mid-August 2018, a randomized block experimental design method was used to set up three 5 m × 5 m blocks (replicates) in each of the three different habitats (Figure 1). Each habitat group included one *N. tangutorum* community and one *A. sparsifolia* community as control treatments, with each plot measuring 1 m × 1 m. Additionally, a root exclusion technique (trenching combined with gap analysis) was employed to create a 1 m × 1 m root excision plot in a bare area approximately 0.5 m from the control treatment. A trench, 0.2 m wide and 0.8 m deep, was excavated around the sample (with no root presence below 0.8 m of soil), followed by the placement of a polyvinyl chloride (PVC) sheet with a 0.2 mm mesh size in the trench to prevent root intrusion into the plot. Lastly, the excavated soil was returned to the trenches (Huang et al., 2015; Lavigne et al., 2003). Ultimately, 12 plots (comprising six control treatments and six root excision plots) were set up per habitat, totaling 36 plots across all treatments within the three habitats studied.

2.2 Measurements of Rs and its components

A PVC collar, 20 cm in inner diameter and 15 cm tall, was centrally positioned in each quadrat, exposing approximately 5 cm above ground. The positions of these 36 collars remained unchanged during the entire measurement period. Prior to each Rs measurement, new growth was cleared from the root cutting quadrat to exclude plant respiration from the Rs readings. Within the control treatment, only above-ground live plants within the PVC collar were removed. Rs and Rh were assessed using the LI-8100 automated soil CO_2 flux system (LI-COR, Lincoln, NE, USA) on calm, sunny days chosen mid-month from May to August 2019. All experimental measurements occurred between 10:00 and 12:00

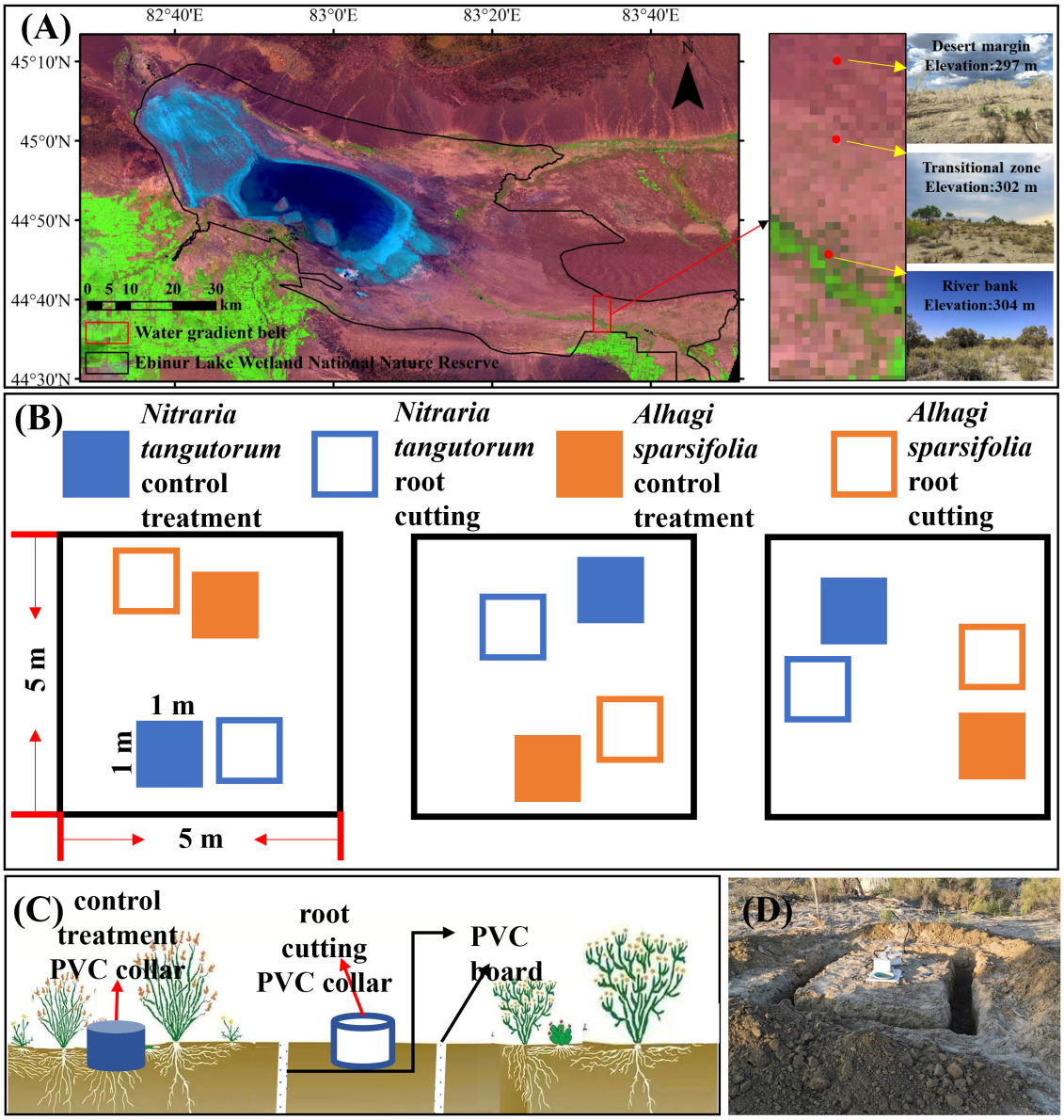

FIGURE 1
Soil respiration component partitioning experiment. **(A)** Study area and sampling point distribution; **(B)** plot layout; **(C)** schematic diagram of the root exclusion method (trenching + gap analysis) to differentiate soil respiration components. The polyvinyl chloride (PVC) collar (dark color) of the control quadrat was used to measure soil respiration, and the PVC collar (light color) of the root cutting quadrat was used to measure heterotrophic respiration. The difference between the two was autotrophic respiration. **(D)** Field *in-situ* trenching treatment.

local time on the same day, aiming to accurately reflect average daily CO_2 emissions (Wang et al., 2021b). Each PVC collar underwent three measurements, with the average serving as the respiration rate for that location. Respiration rates in control and root excision plots were designated as Rs and Rh, respectively. Ra was determined via subtraction (Rs−Rh), with autotrophic and heterotrophic respiration ratios expressed as Ra/Rs and Rh/Rs, respectively (Borden et al., 2021). Throughout each measurement session, soil temperature (ST) was recorded at a 10 cm depth adjacent to the PVC collar, utilizing a temperature sensor (MS-10, Rain Root Technology Co., Ltd., Beijing, China).

2.3 Sample collection and measurement

Soil sampling occurred in mid-June 2019, with separate collections of rhizosphere and bulk soil samples. For microbial analysis, rhizosphere soil samples were taken from depths of 0–30 cm within each control treatment plot, using sterile tweezers disinfected over an alcohol lamp flame and cooled with sterile water to extract roots and remove loose soil. Once loose soil was removed, it was sealed in a sterile bag and refrigerated. Samples were transported to the lab for rhizosphere soil collection (Li et al., 2022). Root samples were moved to a 50 mL sterile centrifuge tube containing 30 mL phosphate-buffered

saline (PBS) buffer (137 mmol L^{-1} NaCl, 2.7 mmol L^{-1} KCl, 8.5 mmol L^{-1} Na_2HPO_4, and 1.5 mmol L^{-1} KH_2PO_4 at pH 7.3) on a sterile operating table, where root surfaces were cleaned with sterile forceps (Edwards et al., 2015). Using sterile tweezers, the root system was extracted from the centrifuge tube, and the remaining suspension was centrifuged at −4°C (10,000 g, 1 min) to concentrate the rhizosphere soil sample. Roots extracted from the rhizosphere soil were cleaned with sterile water and dried with sterile filter paper for further root trait analysis. Surface soil was gathered from each root-cutting plot and placed in a 50 mL sterilized centrifuge tube as bulk soil. Due to insufficient DNA quantity and concentration in some bulk soil samples, metagenomic sequencing was ultimately conducted on 33 samples, comprising 18 rhizosphere and 15 bulk soils.

The soil with roots removed was split into thirds: one portion was kept in an aluminum box for soil water content (SWC) measurement via drying (105°C, 48h); another was refrigerated (4°C) for ammonium nitrogen (AN) and nitrate nitrogen (NN) content analysis; the last was air-dried for assessing soil pH, soil salinity content (SSC), soil organic carbon (SOC), available phosphorus (AP), total phosphorus (TP), and total nitrogen (TN). Total root surface area was determined with WinRhizo Pro.2013 (Reagent Instruments Inc., Canada), followed by drying roots at 65°C to a constant weight for root dry weight (RDW) calculation. Dried root samples were pulverized and sifted through a 100-mesh screen to measure plant root carbon content (RCC), root nitrogen content (RNC), and root phosphorus content (RPC). Specific root area (SRA) was computed by dividing total root surface area by RDW. Soil properties and root nutrient contents were measured according to Wang et al.' s method (2022a).

2.4 DNA extraction and sequencing

About 0.2 g of rhizosphere or bulk soil was placed in a 2-mL sterile centrifuge tube, and DNA was extracted using a PowerSoil® DNA extraction kit according to standard procedures. DNA integrity was assessed using a 1% agarose gel (200 V, 30 min), and DNA concentration was measured quantitatively with Qubit 2.0. DNA fragmentation was conducted with Covaris S220 based on operational parameters to create a paired-end (PE) library (Novogene Biotechnology Co., Ltd., Beijing, China). Paired-end sequencing was carried out on the Illumina Genome Analyzer (HiSeq PE150, Illumina Inc., San Diego, CA, USA). From the soil samples collected, 1,912,296,608 high-quality metagenomic DNA sequences were generated, and 17,590,216 sequences were derived through assembly and gene prediction (Supplementary Table S2). A total of 106 phyla, 737 families, 2,523 genera, and 16,981 species of microbial communities with definite classification information were detected. The data were submitted to the NCBI database repository under accession number PRJNA 664310.

2.5 Bioinformatics analysis

During data quality control, fastp software (Chen et al., 2018) was initially used to trim 3' and 5' adapter sequences from reads. Reads shorter than 50 bp, with an average base quality score below 20, or containing N bases were discarded, retaining only high-quality paired-end and single-end reads. For data assembly, Megahit software (Li et al., 2015), utilizing succinct de Bruijn graph principles, was used to splice and assemble optimized sequences, selecting contigs ≥ 300 bp for the final assembly outcomes. Gene prediction utilized Prodigal (Hyatt et al., 2010) to forecast open reading frames (ORFs) within contig mosaics. Genes with a nucleic acid length ≥ 100 bp were chosen and translated into amino acid sequences. All sample-predicted gene sequences were clustered with CD-HIT (Fu et al., 2012), selecting the longest gene per cluster as the representative sequence to form a non-redundant gene set. SOAPaligner (Li et al., 2008) was employed to quantify gene abundance in the relevant samples.

For taxonomic annotation of species, Diamond (Buchfink et al., 2015) compared the amino acid sequences of the non-redundant gene set against the NCBI non-redundant protein sequence (NR) database, setting the expected e-value for BLASTP comparisons at 1e-5. Taxonomic annotations for species were derived from the database matching the NR database, and species abundance was determined by summing gene abundances associated with each species. Subsequently, the abundance of carbohydrate-active enzymes was computed using the sum of gene abundances linked to these enzymes. Ultimately, 33 metagenomic data points from three locations were contrasted with the NR and carbohydrate-active enzyme databases.

2.6 Statistical analysis

Initially, the 'randomForest' package was used for random forest machine learning algorithm analysis to determine the most important microbial predictors of Rs components. The genus-level taxonomic composition and functional genes obtained using KEGG analyses based on the metagenomics of rhizosphere and bulk soil microorganisms were regressed with Rs components, and the genera or genes that contributed greatly to the prediction accuracy of the model were found by performing five rounds of 10-fold cross-validation (Zhang et al., 2018a). The 'rfPermute' and 'A3' packages enabled 1000 random permutations to assess predictor importance and overall model significance (Fortmann-Roe, 2015). Spearman correlation assessed the relationship between functional genes and Rs components. Subsequently, the 'vegan' package was employed for non-metric multidimensional scaling (NMDS) using Bray-Curtis distances to analyze genus-level microbial communities and functional genes, visualizing shifts in microbial taxonomy and functionality (Chen et al., 2020; Liu et al., 2019). Lastly, partial least squares path modeling (PLS-PM) was utilized to investigate the interconnections among microbial taxonomy and function (NMDS axes), root traits (SRA, RDW, RCC, RNC, RPC), soil properties (pH, SSC, SOC, TN, AN, NN, TP, AP, SWC, ST), and Rs components (Ra, Rh) via the "plspm" package (Zhou et al., 2022). A goodness of fit (GoF) index represented the overall predictive ability of the final PLS-PM model (Tenenhaus et al., 2005).

3 Results

3.1 Changes in Rs and soil properties

During the measurement process, soil respiration rates exhibited more pronounced fluctuations in the river bank habitat as compared to those in the transitional zone and the desert margin. Through one-way analysis of variance (ANOVA), it was ascertained that the rates were significantly elevated in the river bank habitat (P <0.05, Figure 2; Table 1). From May to August 2019, the mean value of Rs was 1.82 ± 0.41 μmol m^{-2} s^{-1} for the river bank, 0.49 ± 0.15 μmol m^{-2} s^{-1} for the transitional zone, and 0.45 ± 0.12 μmol m^{-2} s^{-1} for the desert margin (Table 1). Between May and August, the average contribution of Ra to Rs was 45% in river bank, 38% in the transitional zone, and 37% at the desert margin (Figure 2C). Compared with the river bank, the Ra in the transitional zone and the desert margin decreased by 77.8% and 79%, respectively, and the Rh decreased by 68.6% and 74.5%, respectively (Table 1). RCC, RNC, and RPC were the highest in the river bank plot, while SRA was the highest in the desert margin (Table 1). The soil in the study area had a high sand content but low silt and clay content (Supplementary Table S1). Sand content increased gradually from the river bank to the desert margin, while silt and clay content decreased (Supplementary Table S1). The environmental gradient observed primarily resulted from variations in soil properties, showing declining SWC and soil nutrients from the river bank to the desert margin as ST increased, suggesting greater environmental stress at the desert margin (Supplementary Table S1). Except for TN, AN, and AP, root exclusion treatment did not significantly affect other soil properties (P > 0.05, Supplementary Table S1).

3.2 Structure and function of soil microbial communities

Soil sample bacterial abundance varied, with rhizosphere > bulk, while archaeal abundance followed the opposite pattern, rhizosphere < bulk (P < 0.05, Table 2). Across all soil samples, the dominant phyla were Proteobacteria, Actinobacteria, Bacteroidetes, Gemmatimonadetes, Planctomycetes, Chloroflexi, Firmicutes, Cyanobacteria, and Euryarchaeota. These nine dominant phyla collectively made up 79.46% of the community, with Proteobacteria and Actinobacteria being the most abundant. Proteobacteria comprised 40.77% of rhizosphere soil and 17.99% of bulk soil, whereas Actinobacteria represented 21.54% of rhizosphere soil and 40.67% of bulk soil (Supplementary Figure S1).

Dominant genera in rhizosphere and bulk soil varied slightly across different habitats. These dominant genera all fell within the major bacterial phyla: Actinobacteria, Proteobacteria, Gemmatimonadetes, and Bacteroidetes (Figure 3). Dominant genera in rhizosphere samples included *Gemmatimonas* (3.08% ± 1.10%), *Streptomyces* (1.88% ± 0.41%), *Halomonas* (1.71% ± 1.12%), *Nitriliruptor* (1.68% ± 0.86%), *Gammaproteobacteria noname* (1.59% ± 0.29%), and *Nitriliruptor* (4.43% ± 3.40%). In contrast, bulk soil samples were dominated by *Rubrobacter* (4.22% ± 3.96%), *Gemmatimonas* (3.29% ± 2.37%), *Streptomyces* (3.07% ± 0.93%), and *Actinobacteria class noname* (2.18% ± 0.62%). The relative abundances of *Gracilimonas*, *Rhodothermaceae noname*, and *Gemmatirosa* exhibited a gradual decrease from the river bank to the desert margin in both rhizosphere and bulk soil samples (Figure 3).

Metagenomic sequencing revealed a substantial presence of genes encoding carbohydrate enzymes within the soil microbial genome (Supplementary Figure S2A). Specifically, these genes were categorized into 109 glycoside hydrolase (GH) families, 66 glycosyl transferase (GT) families, 19 polysaccharide lyase (PL) families, 16 carbohydrate esterase (CE) families, 12 auxiliary activity (AA) families, and 41 carbohydrate binding module (CBM) families, with respective counts of 340,862; 367,148; 39,947; 259,918; 88,806 genes (Supplementary Figure S2B). Gene abundances for AAs, CBMs, and PLs were notably higher in rhizosphere soil compared to bulk soil, whereas GHs exhibited an inverse pattern (P < 0.05). Furthermore, the abundance of carbohydrate enzyme genes varied across different environmental gradients (Figures 4G–L). Notably, the abundance of CBM and CE genes in river bank was significantly greater than in transitional zone and desert margin (Figures 4H–I).

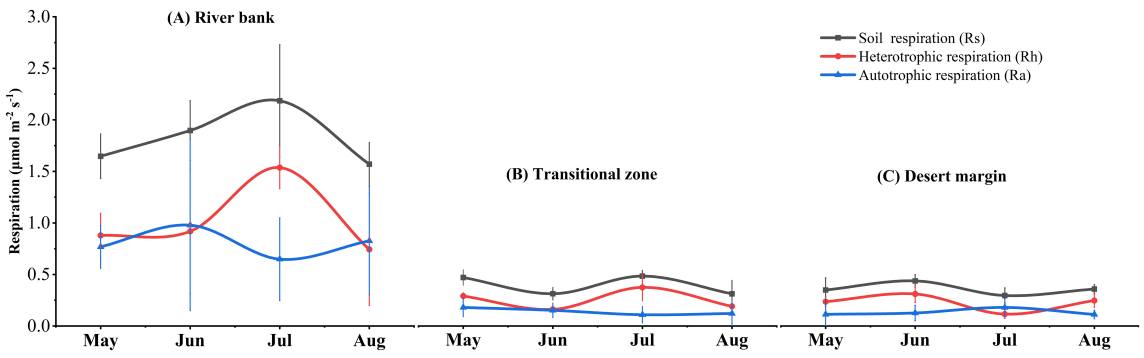

FIGURE 2
Dynamics of soil respiration and its components along the environmental gradient during the growing season (May–August). Data shown are the means ± SE of sampling plots (n = 6) from each habitat.

TABLE 1 One-way analysis of variance (ANOVA) for soil respiration and its components and root traits along the environmental gradient.

Plot	River bank	Transitional zone	Desert margin
Soil respiration (Rs; μmol m^{-2} s^{-1})	1.82 ± 0.41 a	0.49 ± 0.15 b	0.45 ± 0.12 b
Heterotrophic respiration (Rh; μmol m^{-2} s^{-1})	1.02 ± 0.48 a	0.32 ± 0.06 b	0.28 ± 0.04 b
Autotrophic respiration (Ra; μmol m^{-2} s^{-1})	0.81 ± 0.48 a	0.18 ± 0.10 b	0.17 ± 0.07 b
Specific root area (SRA; cm^2 g^{-1})	4.89 ± 2.22 a	2.72 ± 1.39 a	5.44 ± 4.56 a
Root dry weight (RDW; g g^{-1})	9.18 ± 4.06 b	13.86 ± 7.06 a	13.61 ± 6.16 a
Root carbon content (RCC; mg g^{-1})	246.37 ± 22.53 a	244.64 ± 15.30 a	242.48 ± 7.75 a
Root nitrogen content (RNC; mg g^{-1})	15.14 ± 3.43 a	13.31 ± 2.89 a	14.36 ± 1.74 a
Root phosphorus content (RPC; mg g^{-1})	0.85 ± 0.32 a	0.48 ± 0.09 b	0.54 ± 0.14 b

The same letters indicate no significant differences ($P > 0.05$) between different habitat types.

3.3 Identification of drivers related to Rs and its components

Utilizing a random forest model and five iterations of 10-fold cross-validation, we identified the optimal combination of 20 genera and 10 functional genes that encapsulate sample feature information ($P < 0.05$). These combinations accounted for variations in Rs components ranging from 0.329 to 0.486 ($P < 0.001$, Figure 5). The chosen carbon-degrading bacteria primarily consisted of bacterial communities, with certain selected genera and functional genes showing significant correlations with Rs components ($P < 0.05$, Supplementary Table S4).

The PLS-PM model revealed that soil properties and functional attributes exerted significant direct positive influences on both Ra and Rh (with Goodness-of-Fit values of 0.67 and 0.62, respectively), whereas taxonomic attributes did not show a statistically significant impact (Figure 4). Soil properties positively influenced root traits and functional attributes, indirectly affecting Ra through these pathways. Consequently, alterations in Rs components across environmental gradients were primarily achieved through modifications in root traits and microbial functional attributes.

4 Discussion

4.1 Relative contributions of Rh and Ra to Rs along the environmental gradient

Prior research indicates that Rs and soil physicochemical properties exhibit high variability within desert ecosystems (Wang et al., 2021b). Precisely categorizing observed Rs into various components and evaluating their environmental responsiveness is crucial for comprehending terrestrial ecosystem carbon balances (Chin et al., 2023). This study determined that Ra's contribution to Rs ranged from 37% to 45% at the research site, aligning with previously reported ranges for desert ecosystems (13%-94%) (Zhao et al., 2011). However, these figures differ from those in other ecosystems (Cahoon et al., 2016; Huang et al., 2015) due to variations in site-specific conditions and measurement methodologies affecting Ra's contribution to Rs (Hanson et al., 2000). Moreover, Rh accounted for over 50% of Rs in all three plots, clearly indicating Rh as the primary driver of Rs, corroborating earlier findings (Chen et al., 2015; Ma et al., 2019; Subke et al., 2006). Research in an alpine meadow on the Qinghai-Tibet Plateau revealed that warming decreased the Rh/Rs ratio, primarily attributed to minimal Rh variation and Ra augmentation induced by warming (Yan et al., 2022). Conversely, a study in a drier temperate evergreen broadleaf forest indicated that diminished rainfall resulted in a 40% reduction in root respiration, with no impact on Rh, thus elevating the Rh/Rs ratio (Hinko-Najera et al., 2015). Notably, this study discovered that environmental stress enhanced Rh's relative contribution to Rs (Table 1), typically explained by Ra experiencing a more pronounced reduction under drought stress compared to Rh (Balogh, 2016; Li et al., 2013). To sum up, these findings suggest that root activities are more suppressed in arid desert ecosystems (Zhou et al., 2019), leading to a higher percentage of carbon emissions originating from soil microbes rather than root and rhizosphere respiration (Wang et al., 2019b). As global climate change and drought frequency rise (Knapp et al., 2015), future climates in arid deserts could significantly alter Rs through shifts in component intensities and proportions (Liu et al., 2017). Soil moisture might also play a crucial role in the carbon cycle during the growing seasons in arid regions (Kannenberg et al., 2024).

TABLE 2 Distribution of different domains obtained using MetaPhlAn analysis according to metagenomic sequence samples.

Plot	River bank		Transitional zone		Desert margin	
	Rhizosphere soil	Bulk soil	Rhizosphere soil	Bulk soil	Rhizosphere soil	Bulk soil
Bacteria	98.51 ± 0.23a	96.75 ± 1.30b	98.10 ± 1.03a	97.37 ± 0.16b	98.26 ± 0.47a	97.45 ± 0.45b
Fungi	0.11 ± 0.01a	0.09 ± 0.02a	0.14 ± 0.06a	0.11 ± 0.01a	0.11 ± 0.01a	0.10 ± 0.01a
Viruses	0.09 ± 0.06a	0.08 ± 0.02a	0.08 ± 0.04a	0.06 ± 0.01a	0.06 ± 0.01a	0.04 ± 0.01a
Archaea	1.29 ± 0.29b	3.08 ± 1.31a	1.68 ± 1.03b	2.46 ± 0.16a	1.59 ± 0.48b	2.40 ± 0.45a

The same letters indicate that there are no significant differences (P > 0.05) between rhizosphere soil and bulk soil within the same habitat type.

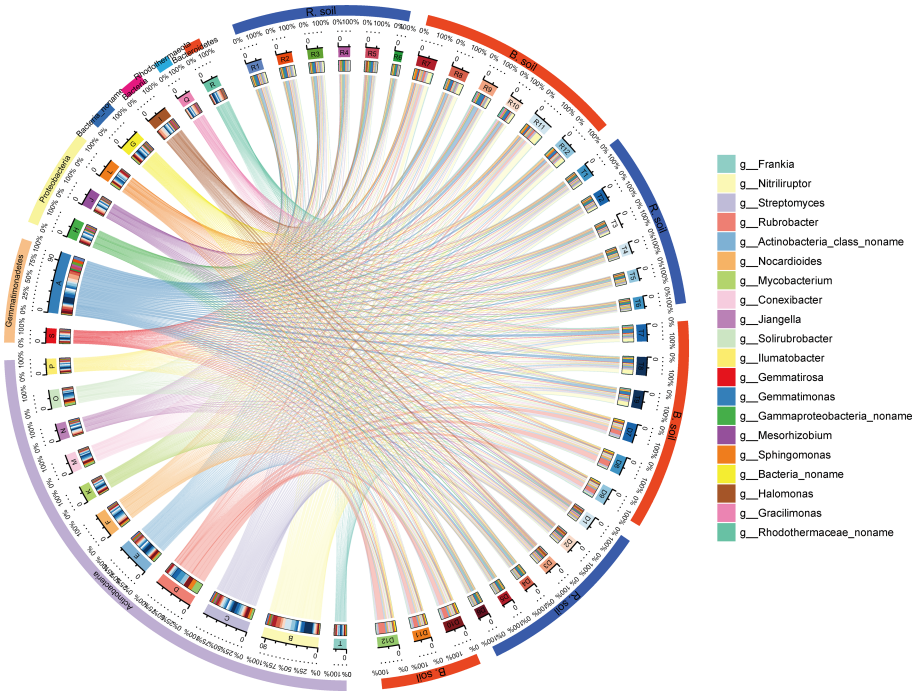

FIGURE 3
Relative abundances and proportions of dominant species in different soil samples at the genus level (showing the top 20 species with the highest relative abundances). The right semicircle represents the species abundance composition of the sample, and the left semicircle represents the distribution proportion of species in different samples. Circles from the outside to the inside depict the following: the first and second colored circles: the left half circle represents the distribution proportion of different samples in dominant species, different colors represent different samples, and the length represents the distribution proportion of the sample in a species (the percentage displayed in the second circle); the circle on the right half represents the species composition corresponding to different samples, different colors represent different species, and the length represents the abundance proportion of a species in the sample (the percentage shown in the second circle); the third circle: there is a colored band in the circle, with one end connecting the sample (right semicircle), where the end width of the band represents the abundance of species in the sample, and the other end connecting the species (left semicircle), where the end width of the band represents the distribution proportion of the sample in the corresponding species, and the value outside the circle represents the abundance value of the corresponding species. R1–R6, T1–T6, and D1–D6 are rhizosphere soil; R7–R12, T7–T9, and D7–D12 are bulk soils.

4.2 Changes in Ra driven by root traits and rhizosphere microorganisms

Consistent with the initial hypothesis, environmental stress can affect Ra by altering microbial activity and plant physiological structure (Vries et al., 2016). This study identified a diverse range of microorganisms, including bacteria, archaea, fungi, and viruses, in the rhizosphere (Table 2). Additionally, shifts in the microbial community's composition and structure were observed across different environmental gradients (Figure 3; Supplementary Figure S1). This may be due to the fact that these microorganisms are adjacent to plant roots, and their combination can obtain nutrients for plants to promote plant growth and health (Abraham and Babalola, 2019). Some researchers have pointed out that environmental stress can lead to strong changes in rhizosphere microbial community structure and functional genes (Argaw et al., 2021; Naseem et al., 2018; Sanaullah et al., 2011; Segovia et al., 2013). Microorganisms that occupy the rhizosphere and promote plant growth and tolerance can adopt certain adaptive life history strategies to cope with changes in resource availability and abiotic conditions (Aslam et al., 2022; Ju et al., 2020; Li et al., 2022), thereby affecting Ra mediated by rhizosphere microorganisms. Studies have shown that life history strategies that focus on the interaction between microorganisms and the environment can help to link microbial ecology with ecosystem functions (Malik et al., 2019a). Character-based microbial life history strategies can be divided into three categories: high yield (Y), resource acquisition (A), and stress tolerance (S) (Malik et al., 2019a). In soils from river bank habitats to desert marginal habitats, the abundance of PL and CE genes involved in polysaccharides and carbohydrate esters decreased gradually, while the abundance of GH genes involved in soil organic C decomposition increased gradually (Figure 4), which meant that the microbial life history strategy changed from stress tolerance (S) to resource acquisition-stress tolerance combination (S-A) (Naseem et al., 2018). This is because with the increase of environmental stress, microorganisms not only need to increase their investment in extracellular polysaccharide (EPS) to cope with drought stress (Naseem et al., 2018) but also need to increase investment in extracellular enzyme production to alleviate resource constraints (Allison and Vitousek, 2005; Lipson, 2015). However, this strategic shift reduces metabolism in other physiological processes (e.g., Ra) due to increased metabolic investment in resource acquisition, typically resulting in slower cell growth rates (Malik et al., 2019a).

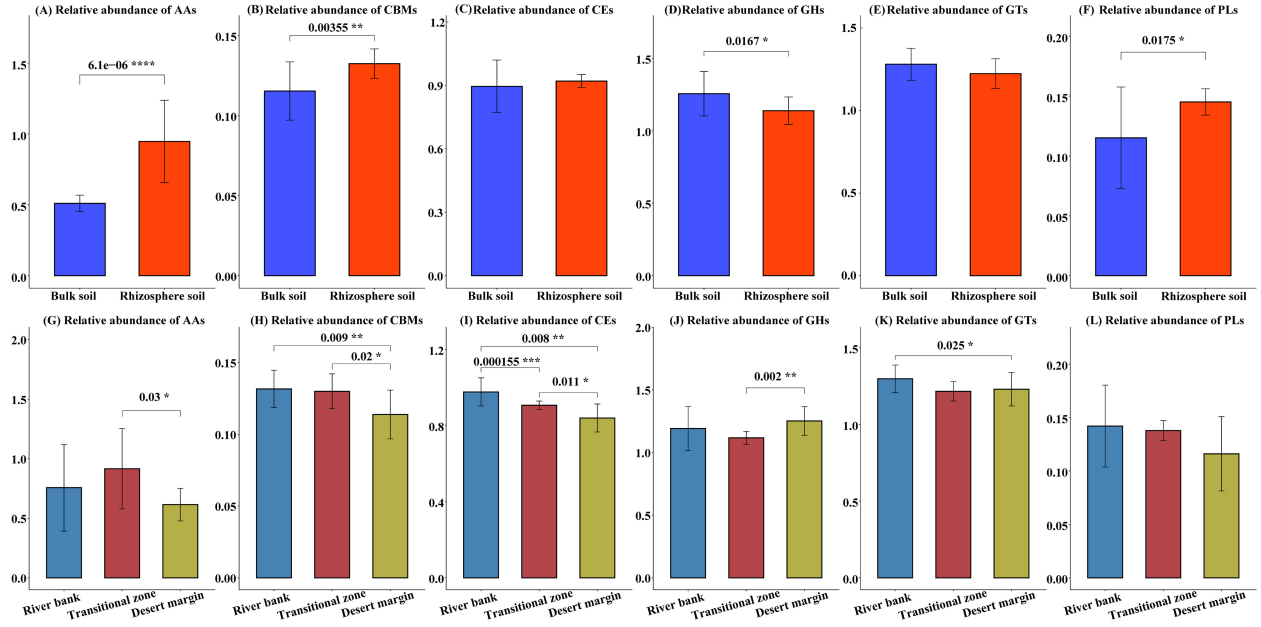

FIGURE 4
Differences in the carbohydrate enzyme gene abundance between different microhabitats **(A–F)** and plot types **(G–L)**. Glycoside hydrolases (GHs), glycosyl transferases (GTs), polysaccharide lyases (PLs), carbohydrate esterases (CEs), auxiliary activities (AAs), and carbohydrate binding modules (CBMs). GHs and GTs are involved in soil organic C decomposition and biosynthesis, respectively. PLs, CEs, and AAs are involved in the microbial decomposition of polysaccharides, carbohydrate esters, and lignin, respectively. The gene abundance of GHs, GTs, PLs, CEs, and AAs is the sum of the relative abundances of each specific gene belonging to a specific module. The numbers and asterisks above the horizontal line represent significant differences between the two groups, **P*<0.05, ***P*<0.01, ****P*<0.001, *****P*<0.0001.

In addition, the random forest model identified a new list of key microbial classification and functional attributes (Figure 5). These microbial attributes were significantly correlated with Ra ($P < 0.05$, Figure 5), and they were important Ra predictors along the environmental gradient. Among them, Ra was significantly positively correlated with related genera in Firmicutes (e.g., *Caldicellulosiruptor*, *Pediococcus*, *Succinispira*, and *Acetohalobium*) and significantly negatively correlated with related genera in Proteobacteria (e.g., *Paramesorhizobium*, *Pannonibacter*, and *Pelagibacterium*) (Supplementary Table S4). An increasing number of studies have shown that archaea exist in various environments on Earth (Flemming and Wuertz, 2019; Shu and Huang, 2022), and these microorganisms play important roles in biochemical processes such as carbon fixation, methane oxidation, methane production, and organic matter degradation (Adam et al., 2017). Although archaea are considered to be rare members of the microbial biosphere, some archaea have been shown to be major members of ecosystems (Spang et al., 2017). Among them, Methanobacteriales and Methanococcales, as methanogenic archaea, conduct the anaerobic fermentation of inorganic or organic compounds to convert them into methane and carbon dioxide (Evans et al., 2019; Kurth et al., 2021). In this study, a positive correlation was detected between the related genera of Euryarchaeota (*Methanomicrobia noname* and *Methanomicrobiales noname*) and Ra (Supplementary Table S4), which is consistent with previous research results (Zhang and Lv, 2020). This result indicates that archaea are also involved in the regulation of rhizosphere soil carbon metabolism, but the current research is still in its infancy. In the future, next-generation omics techniques (such as metatranscriptomics and metaproteomics) are needed to verify the ecological functions of these archaea, thereby increasing the understanding of carbon metabolism in arid desert ecosystems.

There is evidence that different microorganisms can perform similar metabolic functions due to horizontal gene transfer between microorganisms, and their communities usually exhibit high 'functional redundancy' (Louca et al., 2016). The research framework based on microbial taxonomy does not necessarily reflect the significant impact of species diversity reduction or community species composition changes on their mediated ecological processes or the response to environmental changes (Green et al., 2008). Interestingly, it was found that soil properties, root traits, and microbial functional attributes were closely related to Ra (Figure 6), which provides direct evidence that soil function is driven by soil properties, root traits, and microbial functional genes (Spitzer et al., 2021; Trivedi et al., 2016), and suggests that microbial functional attributes rather than taxonomic attributes may provide a more effective link between microorganisms and Ra (Chen et al., 2020). The gene abundances of starch synthase (K00703), phosphatidylinositol glycan A (K03857) encoding GTs and UDP-3-O-[3-hydroxymyristoyl] N-acetylglucosamine deacetylase (K16363), and heparan sulfate N-deacetylase/N-sulfotransferase1 (K02576) encoding CEs were significantly positively correlated with Ra ($P < 0.05$, Supplementary Table S4). The CAZy annotation results showed that these genes were key genes in carbohydrate metabolism and lipid metabolism (Kanehisa et al., 2015). Therefore, paying attention to

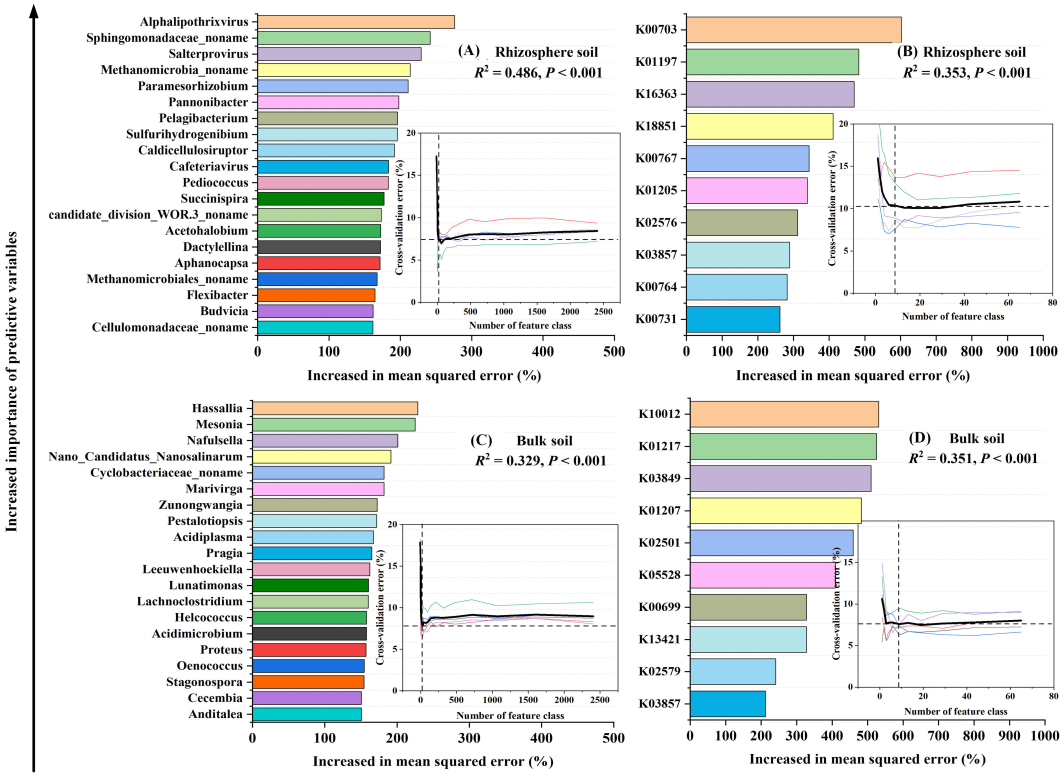

FIGURE 5
Random forest analysis identifying the significant (P < 0.05) microbial predictors of soil respiration components: the relative abundance of the soil microbial community at the genus level **(A, C)**, and the abundance of functional genes **(B, D)**. These functional genes were annotated according to the CAZy (carbohydrate active enzyme) database using metagenomic data derived from a subset of soil samples (Supplementary Table S3). Embedded in the figure are five 10-fold cross-validation results to assess the importance of microbial variables. When the cross-validation error is at the minimum (stable), the prediction model has the best performance. The importance of the variable is measured by the "percentage of increase of mean square error (Increase in MSE(%))" value in the random forest. Higher MSE% values mean more important variables. In the figure, the importance of microbial variables to model accuracy decreases in turn.

these genes may be of great significance for understanding the soil carbon cycle in desert ecosystems, and these genes may be involved in the related processes of microbial respiration and carbon metabolism in rhizosphere soil.

Environmental changes, altering soil water conditions and nutrient availability, directly or indirectly affect Ra (Bloor and Bardgett, 2012; Tang et al., 2020b). Typically, in natural environments, low SWC leads to high ST, restricting root and microbial metabolism (Liu et al., 2018; Luo and Zhou, 2006), and consequently suppressing root and rhizosphere respiration (Jarvi and Burton, 2013). Brunner et al. (2015) noted that during drought, tree species allocate significant carbon to defense and storage, like woody tissues, instead of acquiring external resources. This strategy enhances plant resilience to environmental stress, aligning with current findings. The study observed that SRA rises with drought stress, suggesting that more carbon is directed towards increasing underground biomass rather than respiration, significantly lowering Ra (Figure 2; Table 1). This can be attributed to the fact that under drought stress conditions, plants can preferentially allocate more carbon to root storage pools and osmotic adjustment, while the proportion used for their own metabolic consumption is relatively reduced, and the decline in Ra is due to the reduction of metabolic activity, which improves their adaptability (Hasibeder et al., 2014). In addition, because phosphorus is the main component of adenosine triphosphate (ATP), a product of root respiration, the decrease of phosphorus content in plant tissues inhibits the decrease of ATP synthesis and thus limits Ra (Jarvi and Burton, 2017). Overall, the results of this study highlight that in order to provide accurate information on future belowground carbon partitioning and carbon cycling, it may be effective to evaluate Ra patterns associated with soil properties, root traits, and rhizosphere microorganisms (especially functional genes) (Jia et al., 2013).

4.3 Revealing the subsurface driving factors of Rh

The bare soil environment is a typical oligotrophic environment, in which most of the microorganisms survive and grow slowly in the soil in an adaptive oligotrophic metabolic model (Chen et al., 2021). Evidence suggests that numerous oligotrophic microorganisms, such as actinomycetes, facilitate soil organic matter decomposition by aiding in the breakdown of challenging compounds like cellulose and lignin (Kanokratana et al., 2010; Li et al., 2016). Our findings reveal differences in microbial community structure and composition between the rhizosphere and bulk soils (Table 2). Bulk soil

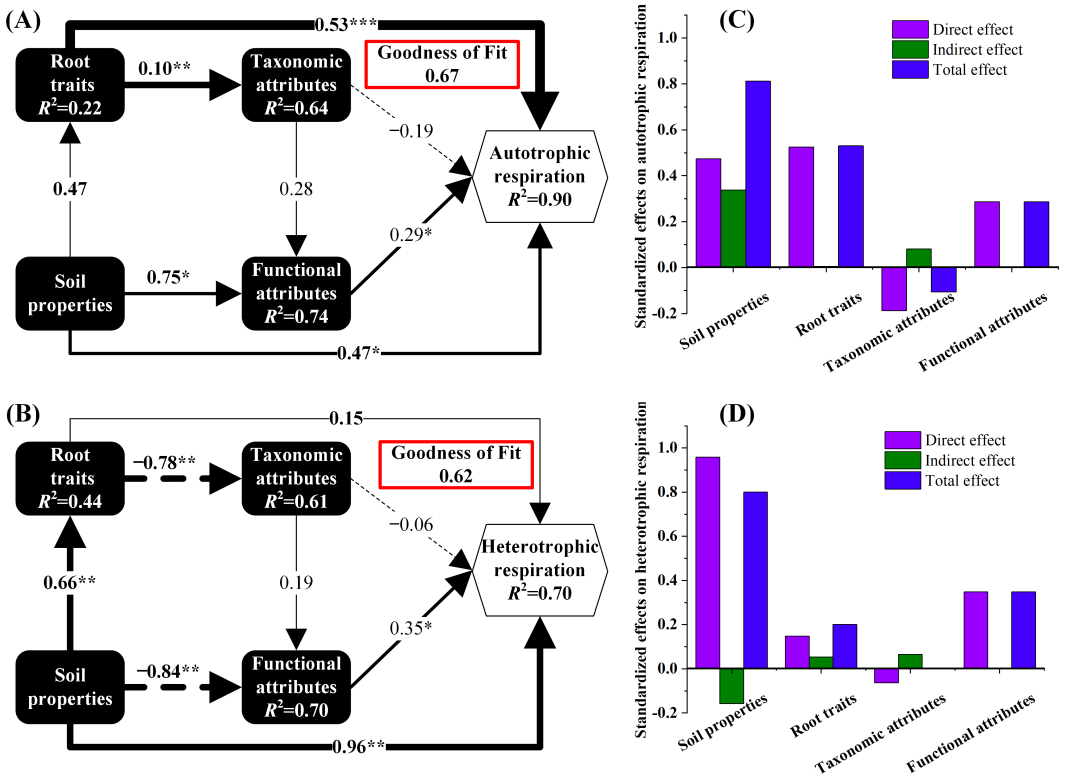

FIGURE 6
Partial least squares path modeling (PLS-PM) for determining the effects of soil properties, root traits, taxonomic attributes, and functional attributes on soil respiration components **(A, B)** and standardized path coefficients **(C, D)**. Arrow widths describe the magnitude of the path coefficients, and solid and dashed arrows indicate positive and negative effects, respectively. *$P < 0.05$, **$P < 0.01$. Microbial classification attributes and functional attributes are represented by the first and second axes of non-metric multidimensional scale ranking (NMDS) based on the Bray–Curtis distance, respectively. More information about NMDS is provided in Supplementary Figure S3.

microbiota was predominantly bacterial, with actinomycetes showing the greatest relative abundance (Figure 3; Supplementary Figure S1), aligning with prior research on alpine peatland microbial communities (Kang et al., 2022). This could stem from the selective pressure of the oligotrophic bare environment, favoring actinomycete groups adapted to prolonged oligotrophic metabolic conditions (Zhang et al., 2018b). Research indicates that over 90% of enzymes responsible for carbohydrate degradation originate primarily from Firmicutes and Bacteroidetes (Gong et al., 2020). We observed that environmental stress decreased the relative abundance of Bacteroidetes in bulk soil (Figure 3), potentially accounting for the reduction in Rh from river bank to desert margin. Furthermore, our analysis identified 20 microbial genera associated with Rh, including nine from Bacteroidetes. Consequently, we propose that Bacteroidetes could serve as a valuable biological indicator for estimating soil Rh variations across different environmental gradients.

It is worth noting that in the present study, a complex gene pool composed of diverse enzyme families was identified in bulk soil (Supplementary Figure S2), which can provide a variety of degradation capabilities for the utilization of various carbohydrate substrates (Gong et al., 2020). Compared with rhizosphere soil, bulk soil had a higher abundance of GH carbohydrate active genes (Figure 4), and these enzymes were assigned to 109 GH families (Supplementary Figure S2). This is because in bulk soils with low resource availability, microorganisms increase investment in extracellular enzyme production to break down complex resources (Allison et al., 2010), resulting in richer GH genes and higher GH enzyme activity (Malik et al., 2019b). In addition, beta-N-acetylhexosaminidase (K00703) and L-iduronidase (K01217) genes encoding GHs exhibited positive effects on Rh (Supplementary Table S4), which is consistent with other research results that these gene predictors are significantly correlated with soil C metabolic functioning (Yang et al., 2021). Surprisingly, the present study found that phosphatidylinositol glycan A (K03857) could also explain the change of Rh (Supplementary Table S4), which was consistent with Ra. Phosphatidylinositol glycan A is a gene encoding the catalytic subunit of GPI-N-glucosamine acetate transferase and a key enzyme in the biosynthesis of glycosylphosphatidylinositol (GPI) (Miyata et al., 1993). Therefore, we suggest that identifying this key functional gene is essential if microbial communities are to be used to predict patterns of changes in respiratory components in different environments. Although previous studies have thoroughly demonstrated that Rh, as a complex process, is closely related to the microbial community composition and soil properties (Whitaker et al., 2014; Zhang et al., 2021), this study also evaluated the effects of microbial functional attributes on Rh on the basis of previous studies. In PLS-PM, the relationship between Rh and microbial functional attributes was superior to the taxonomic attributes (Figure 6), which further

confirmed the importance of incorporating microbial functional genes into Rs models (Liu et al., 2019; Xu et al., 2018; Yang et al., 2021).

Among the three methods for distinguishing Ra and Rh, the root exclusion method stands out as the simplest and most dependable for extensive *in-situ* separation of Rs components (Borden et al., 2021; Zhao et al., 2011). Root exclusion methods commonly involve root removal, trenching, and gap analysis (Chin et al., 2023). To address the inherent limitations of the root exclusion method (Hopkins et al., 2013; Zhao et al., 2011) and given the ease of measuring multiple sampling points, this study integrated trenching and gap analysis to separate various Rs components. Despite performing the initial Rs measurement after 10 months of trenching to mitigate soil disturbance and dead root decomposition effects (Chin et al., 2023; Schiedung et al., 2023), it's important to acknowledge that this approach carries uncertainties. The fundamental premise of the root exclusion method is that Rh stays constant post-root and associated root exudate removal (Chin et al., 2023; Zhao et al., 2011). It's noteworthy that even though bare soil lacks inputs of readily decomposable organic matter like root exudates and plant residues, microbes can influence Rh by breaking down more recalcitrant soil carbon pools (Tian et al., 2024). To sum up, the root exclusion method alters microbial substrate availability by decreasing root exudates rich in labile carbon, potentially impacting the 'priming effect' on soil carbon mineralization (Chin et al., 2023). This influences soil organic carbon decomposition rates, possibly causing variations in Rh estimates (Classen et al., 2015). Obviously, future studies are required to investigate how the priming effect impacts Rh under prolonged root exclusion, aiming to resolve existing uncertainties.

5 Conclusion

In summary, our research represents an important step in unraveling the complex relationships between soil microbial communities, soil properties, root traits, and Rs components within the unique context of the desert-oasis ecotone in arid regions. Through a comprehensive field investigation and advanced metagenomic analysis, we have provided novel insights into the factors governing Rs and its autotrophic and heterotrophic components.

Our findings clearly demonstrate that environmental stress, manifested as a gradient from the relatively more favorable river bank to the harsher desert margin, exerts a significant negative impact on Rs and its constituent parts. This stress not only affects the biotic drivers, such as root and microbial traits, but also the abiotic drivers, including soil microclimate and nutrient levels (Figure 7). Importantly, we have discovered that the components of Rs are more responsive to microbial functional genes than to microbial taxonomic diversity. This indicates that the balance between microbial metabolic expenditure and the presence of carbon-degrading genes plays a crucial role in determining the contribution of microbial activities to Rs components.

These results have important implications for future research on the carbon cycle in desert ecosystems. We emphasize the need to distinguish between the autotrophic and heterotrophic components of Rs when evaluating their responses to environmental changes. Moreover, we recommend the utilization of traits, including microbial functional genes, root traits, and chemical properties, as essential regulatory elements in Rs modeling. This approach will enhance the precision of predicting soil carbon emissions and

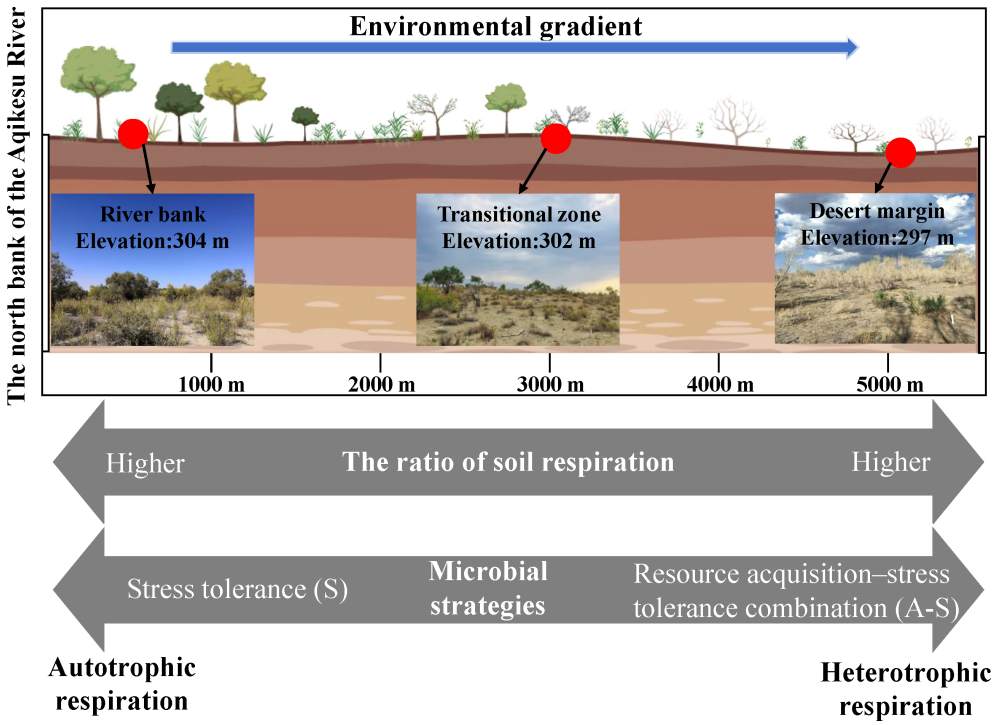

FIGURE 7
Underlying mechanisms of abiotic and biotic drivers on soil respiration components and their changes in a desert-oasis ecotone in an arid region.

carbon cycling in these arid regions, thereby providing a more accurate understanding of the role of desert ecosystems in the global carbon cycle. Our study thus serves as a foundation for further investigations aimed at developing effective strategies for carbon management and ecosystem conservation in arid and semi-arid regions.

Data availability statement

The original contributions presented in the study are included in the article/Supplementary Material. Further inquiries can be directed to the corresponding authors.

Author contributions

JW: Data curation, Funding acquisition, Investigation, Methodology, Resources, Software, Validation, Visualization, Writing – original draft, Writing – review & editing. GL: Conceptualization, Funding acquisition, Writing – review & editing. JY: Conceptualization, Writing – review & editing. XH: Funding acquisition, Writing – review & editing. HW: Funding acquisition, Writing – review & editing. WL: Data curation, Methodology, Software, Writing – review & editing.

Funding

The author(s) declare financial support was received for the research, authorship, and/or publication of this article. The author(s) declare financial support was received for the research, authorship, and/or publication of this article. This research was supported by the National Natural Science Foundation of China (42171026 and 32360282), the Special Project for Construction of Innovation Environment in Xinjiang Uygur Autonomous Region-Science and Technology Innovation Base Construction Project (PT2107), the Special Projects of the Central Government in Guidance of Local Science and Technology Development (ZYYD2023A03), the Tianchi Talent Program of Xinjiang Uygur Autonomous Region (5105240150h).

Conflict of interest

The authors declare that the research was conducted in the absence of any commercial or financial relationships that could be construed as a potential conflict of interest.

Generative AI statement

The author(s) declare that no Generative AI was used in the creation of this manuscript.

Publisher's note

All claims expressed in this article are solely those of the authors and do not necessarily represent those of their affiliated organizations, or those of the publisher, the editors and the reviewers. Any product that may be evaluated in this article, or claim that may be made by its manufacturer, is not guaranteed or endorsed by the publisher.

Supplementary material

The Supplementary Material for this article can be found online at: https://www.frontiersin.org/articles/10.3389/fpls.2025.1511277/full#supplementary-material

References

Abraham, O., and Babalola, O. (2019). Bacteria, fungi and archaea domains in rhizospheric soil and their effects in enhancing agricultural productivity. *Int. J. Environ. Res. Public Health* 16, 3873. doi: 10.3390/ijerph16203873

Adam, P., Borrel, G., Brochier-Armanet, C., and Gribaldo, S. (2017). The growing tree of Archaea: New perspectives on their diversity, evolution and ecology. *ISME J.* 11, 2407–2425. doi: 10.1038/ismej.2017.122

Adamczyk, B., Sietiö, O.-M., Straková, P., Prommer, J., Wild, B., Hagner, M., et al. (2019). Plant roots increase both decomposition and stable organic matter formation in boreal forest soil. *Nat. Commun.* 10, 3982. doi: 10.1038/s41467-019-11993-1

Allison, S., and Vitousek, P. (2005). Responses of extracellular enzymes to simple and complex nutrient inputs. *Soil Biol. Biochem.* 37, 937–944. doi: 10.1016/j.soilbio.2004.09.014

Allison, S., Wallenstein, M., and Bradford, M. (2010). Soil-carbon response to warming dependent on microbial physiology. *Nat. Geosci.* 3, 336–340. doi: 10.1038/ngeo846

An, Z., Zhang, K., Tan, L., Niu, Q., Zhang, H., and Liu, B. (2023). Quantifyting research on the protection effect of a desert–oasis ecotone in Dunhuang, Northwest China. *J. Wind Eng. Ind. Aerodynamics* 236, 105400. doi: 10.1016/j.jweia.2023.105400

Argaw, A., Zhou, Y., Ryder, M., and Denton, M. (2021). Soil environment influences plant growth-promotion traits of isolated rhizobacteria. *Pedobiologia* 90, 150785. doi: 10.1016/j.pedobi.2021.150785

Aslam, M., Okal, E., Idris, A., Zhang, Q., Xu, W., Jk, K., et al. (2022). Rhizosphere microbiomes can regulate plant drought tolerance. *Pedosphere* 32, 61–74. doi: 10.1016/S1002-0160(21)60061-9

Balogh, J. (2016). Autotrophic component of soil respiration is repressed by drought more than the heterotrophic one in dry grasslands. *Biogeosciences* 13, 5171–5182. doi: 10.5194/bg-13-5171-2016

Bennett, A., Haslem, A., Cheal, D., Clarke, M., Jones, R., Koehn, J., et al. (2009). Ecological processes: A key element in strategies for nature conservation. *Blackwell Sci. Asia Pty Ltd* 10, 192–199. doi: 10.1111/j.1442-8903.2009.00489.x

Bloor, J., and Bardgett, R. (2012). Stability of above-ground and below-ground processes to extreme drought in model grassland ecosystems: Interactions with plant species diversity and soil nitrogen availability. *Perspect. Plant Ecol. Evol. Systematics* 14, 193–204. doi: 10.1016/j.ppees.2011.12.001

Bond-Lamberty, B. (2018). New techniques and data for understanding the global soil respiration flux. *Earth's Future* 6, 1176–1180. doi: 10.1029/2018EF000866

Borden, K., Mafa-Attoye, T., Dunfield, K., Thevathasan, N., Gordon, A., and Isaac, M. (2021). Root functional trait and soil microbial coordination: implications for soil respiration in riparian agroecosystems. *Front. Plant Sci.* 12, 681113. doi: 10.3389/fpls.2021.681113

Brunner, I., Herzog, C., Dawes, M., Arend, M., and Sperisen, C. (2015). How tree roots respond to drought. *Front. Plant Sci.* 6, 547. doi: 10.3389/fpls.2015.00547

Buchfink, B., Xie, C., and Huson, D. H. (2015). Fast and sensitive protein alignment using DIAMOND. *Nat. Methods* 12, 59–60. doi: 10.1038/nmeth.3176

Cahoon, S., Sullivan, P., Gamm, C., Welker, J., Eissenstat, D., Post, E., et al. (2016). Limited variation in proportional contributions of auto- and heterotrophic soil respiration, despite large differences in vegetation structure and function in the Low Arctic. *Biogeochemistry* 127, 339–351. doi: 10.1007/s10533-016-0184-x

Chari, N. R., and Taylor, B. N. (2022). Soil organic matter formation and loss are mediated by root exudates in a temperate forest. *Nat. Geosci.* 15, 1011–1016. doi: 10.1038/s41561-022-01079-x

Chen, Q., Ding, J., Li, C., Yan, Z.-Z., He, J.-Z., Hu, H., et al. (2020). Microbial functional attributes, rather than taxonomic attributes, drive top soil respiration, nitrification and denitrification processes. *Sci. Total Environ.* 734, 139479. doi: 10.1016/j.scitotenv.2020.139479

Chen, D., li, J., Zhichun, L., Hu, S., and Bai, Y. (2015). Soil acidification exerts a greater control on soil respiration than soil nitrogen availability in grasslands subjected to long-term nitrogen enrichment. *Funct. Ecol.* 30, 658-669. doi: 10.1111/1365-2435.12525

Chen, Y., Neilson, J. W., Kushwaha, P., Maier, R.M., and Barberán, A. (2021). Life-history strategies of soil microbial communities in an arid ecosystem. *ISME J.* 15, 649–657. doi: 10.1038/s41396-020-00803-y

Chen, Y., Qin, W., Zhang, Q., Wang, X., Feng, J., Han, M., et al. (2024). Whole-soil warming leads to substantial soil carbon emission in an alpine grassland. *Nat. Commun.* 15, 4489. doi: 10.1038/s41467-024-48736-w

Chen, S., Zhou, Y., Chen, Y., and Gu, J. (2018). fastp: an ultra-fast all-in-one FASTQ preprocessor. *Bioinformatics (Oxford, England)* 34, i884-i890. doi: 10.1093/bioinformatics/bty560

Chin, M.-Y., Lau, S. Y. L., Midot, F., Jee, M. S., Lo, M. L., Sangok, F. E., et al. (2023). Root exclusion methods for partitioning of soil respiration: Review and methodological considerations. *Pedosphere* 33, 683–699. doi: 10.1016/j.pedsph.2023.01.015

Chu, H., Ni, H., Ma, J., and Shen, Y. (2023). Contrary responses of soil heterotrophic and autotrophic respiration to spring and summer drought in alfalfa on the Loess Plateau. *Geoderma* 440, 116722. doi: 10.1016/j.geoderma.2023.116722

Classen, A. T., Sundqvist, M. K., Henning, J. A., Newman, G. S., Moore, J. A. M., Cregger, M. A., et al. (2015). Direct and indirect effects of climate change on soil microbial and soil microbial-plant interactions: What lies ahead? *Ecosphere* 6, art130. doi: 10.1890/ES15-00217.1

Cortois, R., Schroeder-Georgi, T., Weigelt, A., Putten, W., and Deyn, G. B. (2016). Plant–soil feedbacks: role of plant functional group and plant traits. *J. Ecol.* 104, 1608-1617. doi: 10.1111/1365-2745.12643

Dai, Z., Zang, H., Chen, J., Fu, Y., Wang, X., Liu, H., et al. (2021). Metagenomic insights into soil microbial communities involved in carbon cycling along an elevation climosequences. *Environ. Microbiol.* 23, 4631–4645. doi: 10.1111/1462-2920.15655

Edwards, J., Johnson, C., Santos-Medellín, C., Lurie, E., Podishetty, N. K., Bhatnagar, S., et al. (2015). Structure, variation, and assembly of the root-associated microbiomes of rice. *Proc. Natl. Acad. Sci.* 112, E911–E920. doi: 10.1073/pnas.1414592112

Escalas, A., Hale, L., Voordeckers, J., Yang, Y., Firestone, M., Alvarez-Cohen, L., et al. (2019). Microbial functional diversity: From concepts to applications. *Ecol. Evol.* 9, 12000-12016. doi: 10.1002/ece3.5670

Evans, P. N., Boyd, J. A., Leu, A. O., Woodcroft, B. J., Parks, D. H., Hugenholtz, P., et al. (2019). An evolving view of methane metabolism in the Archaea. *Nat. Rev. Microbiol.* 17, 219–232. doi: 10.1038/s41579-018-0136-7

Flemming, H.-C., and Wuertz, S. (2019). Bacteria and archaea on Earth and their abundance in biofilms. *Nat. Rev. Microbiol.* 17, 247–260. doi: 10.1038/s41579-019-0158-9

Fortmann-Roe, S. (2015). Consistent and clear reporting of results from diverse modeling techniques: the A3 method. *J. Stat. Software* 66, 1–23. doi: 10.18637/jss.v066.i07

Fu, A., Li, W., Yaning, C., Wang, Y., Hao, H., Peng, L., et al. (2021). The effects of ecological rehabilitation projects on the resilience of an extremely drought-prone desert riparian forest ecosystem in the Tarim River Basin, Xinjiang, China. *Sci. Rep.* 11, 18485. doi: 10.1038/s41598-021-96742-5

Fu, L., Niu, B., Zhu, Z., Wu, S., and Li, W. (2012). CD-HIT: accelerated for clustering the next-generation sequencing data. *Bioinf. (Oxford England)* 28, 3150–3152. doi: 10.1093/bioinformatics/bts565

Furey, G. N., and Tilman, D. (2023). Plant chemical traits define functional and phylogenetic axes of plant biodiversity. *Ecol. Lett.* 26, 1394–1406. doi: 10.1111/ele.14262

Furtak, K., and Wolińska, A. (2023). The impact of extreme weather events as a consequence of climate change on the soil moisture and on the quality of the soil environment and agriculture – A review. *CATENA* 231, 107378. doi: 10.1016/j.catena.2023.107378

Gong, G., Zhou, S., Luo, R., Gesang, Z., and Suolang, S. (2020). Metagenomic insights into the diversity of carbohydrate-degrading enzymes in the yak fecal microbial community. *BMC Microbiol.* 20, 302. doi: 10.1186/s12866-020-01993-3

Green, J., Bohannan, B., and Whitaker, R. (2008). Microbial biogeography: from taxonomy to traits. *Sci. (New York N.Y.)* 320, 1039–1043. doi: 10.1126/science.1153475

Han, Y., Wang, G., Xiong, L., Xu, Y., and Li, S. (2024). Rainfall effect on soil respiration depends on antecedent soil moisture. *Sci. Total Environ.* 926, 172130. doi: 10.1016/j.scitotenv.2024.172130

Hanson, P. J., Edwards, N. T., Garten, C. T., and Andrews, J. A. (2000). Separating root and soil microbial contributions to soil respiration: A review of methods and observations. *Biogeochemistry* 48, 115–146. doi: 10.1023/A:1006244819642

Hashimoto, S., Ito, A., and Nishina, K. (2023). Divergent data-driven estimates of global soil respiration. *Commun. Earth Environ.* 4, 460. doi: 10.1038/s43247-023-01136-2

Hasibeder, R., Fuchslueger, L., Richter, A., and Bahn, M. (2014). Summer drought alters carbon allocation to roots and root respiration in mountain grassland. *New Phytol.* 205, 1117–1127. doi: 10.1111/nph.13146

Hinko-Najera, N., Fest, B., Livesley, S., and Arndt, S. (2015). Reduced throughfall decreases autotrophic respiration, but not heterotrophic respiration in a dry temperate broadleaved evergreen forest. *Agric. For. Meteorol.* 200, 66–77. doi: 10.1016/j.agrformet.2014.09.013

Hopkins, F., Gonzalez-Meler, M. A., Flower, C. E., Lynch, D. J., Czimczik, C., Tang, J., et al. (2013). Ecosystem-level controls on root-rhizosphere respiration. *New Phytol.* 199, 339–351. doi: 10.1111/nph.12271

Huang, W., Han, T., Liu, J., Wang, G., and Zhou, G. (2015). Changes in soil respiration components and their specific respiration along three successional forests in subtropics. *Funct. Ecol.* 30, 1466–1474. doi: 10.1111/1365-2435.12624

Huang, N., Wang, L., Song, X.-P., Black, T. A., Jassal, R. S., Myneni, R. B., et al. (2020). Spatial and temporal variations in global soil respiration and their relationships with climate and land cover. *Sci. Adv.* 6, eabb8508. doi: 10.1126/sciadv.abb8508

Hyatt, D., Chen, G.-L., Locascio, P. F., Land, M. L., Larimer, F. W., Hauser, L. J., et al. (2010). Prodigal: prokaryotic gene recognition and translation initiation site identification. *BMC Bioinf.* 11, 119. doi: 10.1186/1471-2105-11-119

Jarvi, M., and Burton, A. (2013). Acclimation and soil moisture constrain sugar maple root respiration in experimentally warmed soil. *Tree Physiol.* 33, 949-959. doi: 10.1093/treephys/tpt068

Jarvi, M., and Burton, A. (2017). Adenylate control contributes to thermal acclimation of sugar maple fine-root respiration in experimentally warmed soil: Thermal acclimation of maple root respiration. *Plant Cell Environ.* 41. doi: 10.1111/pce.13098

Jia, S., McLaughlin, N., Gu, J., Li, X., and Wang, Z. (2013). Relationships between root respiration rate and root morphology, chemistry and anatomy in Larix gmelinii and Fraxinus mandshurica. *Tree Physiol.* 33, 579–589. doi: 10.1093/treephys/tpt040

Ju, W., Jin, X., Liu, L., Shen, G., Zhao, W., and Duan, C. (2020). Rhizobacteria inoculation benefits nutrient availability for phytostabilization in copper contaminated soil: Drivers from bacterial community structures in rhizosphere. *Appl. Soil Ecol.* 150, 103450. doi: 10.1016/j.apsoil.2019.103450

Kanehisa, M., Sato, Y., Kawashima, M., Furumichi, M., and Tanabe, M. (2015). KEGG as a reference resource for gene and protein annotation. *Nucleic Acids Res.* 44, D457-62. doi: 10.1093/nar/gkv1070

Kang, E., Li, Y., Zhang, X., Zhongqing, Y., Zhang, W., Zhang, K., et al. (2022). Extreme drought decreases soil heterotrophic respiration but not methane flux by modifying the abundance of soil microbial functional groups in alpine peatland. *CATENA* 212, 106043. doi: 10.1016/j.catena.2022.106043

Kannenberg, S. A., Anderegg, W. R. L., Barnes, M. L., Dannenberg, M. P., and Knapp, A. K. (2024). Dominant role of soil moisture in mediating carbon and water fluxes in dryland ecosystems. *Nat. Geosci.* 17, 38–43. doi: 10.1038/s41561-023-01351-8

Kanokratana, P., Uengwetwanit, T., Rattanachomsri, U., Bunterngsook, B., Nimchua, T., Tangphatsornruang, S., et al. (2010). Insights into the phylogeny and metabolic potential of a primary tropical peat swamp forest microbial community by metagenomic analysis. *Microbial. Ecol.* 61, 518–528. doi: 10.1007/s00248-010-9766-7

Knapp, A., Hoover, D., Wilcox, K., Avolio, M., Koerner, S., La Pierre, K., et al. (2015). Characterizing differences in precipitation regimes of extreme wet and dry years: Implications for climate change experiments. *Global Change Biol.* 21, 2624-2633. doi: 10.1111/gcb.12888

Kukumägi, M., Ostonen, I., Uri, V., Helmisaari, H.-S., Kanal, A., Kull, O., et al. (2017). Variation of soil respiration and its components in hemiboreal Norway spruce stands of different ages. *Plant Soil* 414, 265–280. doi: 10.1007/s11104-016-3133-5

Kurth, J. M., Nobu, M. K., Tamaki, H., de Jonge, N., Berger, S., Jetten, M. S. M., et al. (2021). Methanogenic archaea use a bacteria-like methyltransferase system to demethoxylate aromatic compounds. *ISME J.* 15, 3549–3565. doi: 10.1038/s41396-021-01025-6

Lavigne, M., Boutin, R., Foster, R., Goodine, G., Bernier, P., and Robitaille, G. (2003). Soil respiration responses to temperature are controlled more by roots than by decomposition in Balsam fir ecosystems. *Can. J. For. Research-revue Can. Recherche Forestiere - Can. J. For. Res.* 33, 1744–1753. doi: 10.1139/x03-090

Li, R., Li, Y., Kristiansen, K., Wang, J., and Wang, J. (2008). SOAP: short oligonucleotide alignment program. *Bioinf. (Oxford England)* 24, 713–714. doi: 10.1093/bioinformatics/btn025

Li, W., Li, Y., Lv, J., He, X., Wang, J., Teng, D., et al. (2022). Rhizosphere effect alters the soil microbiome composition and C, N transformation in an arid ecosystem. *Appl. Soil Ecol.* 170, 104296. doi: 10.1016/j.apsoil.2021.104296

Li, M., Liu, T., Duan, L., Ma, L., Wang, Y., Zhou, Y., et al. (2021). Hydrologic gradient changes of soil respiration in typical steppes of Eurasia. *Sci. Total Environ.* 794, 148684. doi: 10.1016/j.scitotenv.2021.148684

Li, D., Liu, C.-M., Luo, R., Sadakane, K., and Lam, T.-W. (2015). MEGAHIT: an ultra-fast single-node solution for large and complex metagenomics assembly via succinct de Bruijn graph. *Bioinf. (Oxford England)* 31, 1674–1676. doi: 10.1093/bioinformatics/btv033

Li, W., Qin, T., Liu, S., Yang, Y., Liu, H., and Xu, S. (2024b). Driving factors analysis of soil respiration in China ecosystems. *Plant Soil*, 1–21. doi: 10.1007/s11104-024-06962-7

Li, X., Sun, M., Zhang, H., Xu, N., and Sun, G. (2016). Use of mulberry-soybean intercropping in salt-alkali soil impacts the diversity of the soil bacterial community. *Microbial. Biotechnol.* 9, 293-304. doi: 10.1111/1751-7915.12342

Li, B., Wang, X., and Li, Z. (2024a). Plants extend root deeper rather than increase root biomass triggered by critical age and soil water depletion. *Sci. Total Environ.* 914, 169689. doi: 10.1016/j.scitotenv.2023.169689

Li, D., Zhou, X., Wu, L., Zhou, J., and Luo, Y. (2013). Contrasting responses of heterotrophic and autotrophic respiration to experimental warming in a winter annual-dominated prairie. *Global Change Biol.* 19, 3553-3564. doi: 10.1111/gcb.12273

Ling, H., Zhang, P., Xu, H., and Zhao, X. (2015). How to regenerate and protect desert riparian populus euphratica forest in arid areas. *Sci. Rep.* 5, 15418. doi: 10.1038/srep15418

Lipson, D. A. (2015). The complex relationship between microbial growth rate and yield and its implications for ecosystem processes. *Front. Microbiol.* 6. doi: 10.3389/fmicb.2015.00615

Liu, Y.-R., Delgado-Baquerizo, M., Yang, Z., Feng, J., Zhu, J., and Huang, Q. (2019). Microbial taxonomic and functional attributes consistently predict soil CO_2 emissions across contrasting croplands. *Sci. Total Environ.* 702, 134885. doi: 10.1016/j.scitotenv.2019.134885

Liu, L., Gou, X., Wang, X., Yang, M., Qie, L., Pang, G., et al. (2024). Relationship between extreme climate and vegetation in arid and semi-arid mountains in China: A case study of the Qilian Mountains. *Agric. For. Meteorol.* 348, 109938. doi: 10.1016/j.agrformet.2024.109938

Liu, Y., Li, J., Jin, Y., Zhang, Y., Sha, L., Grace, J., et al. (2018). The influence of drought strength on soil respiration in a woody savanna ecosystem, Southwest China. *Plant Soil* 428, 321-333. doi: 10.1007/s11104-018-3678-6

Liu, Z., Zhang, Y.-Q., Fa, K., Qin, S., and She, W. (2017). Rainfall pulses modify soil carbon emission in a semiarid desert. *CATENA* 155, 147–155. doi: 10.1016/j.catena.2017.03.011

Louca, S., Jacques, S., Pires, A., Leal, J., Srivastava, D., Wegener Parfrey, L., et al. (2016). High taxonomic variability despite stable functional structure across microbial communities. *Nat. Ecol. Evol.* 1, 0015. doi: 10.1038/s41559-016-0015

Luo, Y., and Zhou, X. (2006). *Soil respiration and the environment*. Elsevier Inc. doi: 10.1016/B978-0-12-088782-8.X5000-1

Ma, M., Zang, Z., Xie, Z., Chen, Q., Xu, W., Zhao, C., et al. (2019). Soil respiration of four forests along elevation gradient in northern subtropical China. *Ecol. Evol.* 9, 12846–12857. doi: 10.1002/ece3.5762

Malik, A., Martiny, J., Brodie, E., Martiny, A., Treseder, K., Allison, S., et al. (2019a). Defining trait-based microbial strategies with consequences for soil carbon cycling under climate change. *ISME J.* 14, 1–9. doi: 10.1038/s41396-019-0510-0

Malik, A., Puissant, J., Goodall, T., Allison, S., and Griffiths, R. (2019b). Soil microbial communities with greater investment in resource acquisition have lower growth yield. *Soil Biol. Biochem.* 132, 36-39. doi: 10.1016/j.soilbio.2019.01.025

Martiny, J., Jones, S., Lennon, J., and Martiny, A. (2015). Microbiomes in light of traits: A phylogenetic perspective. *Science* 350, aac9323–aac9323. doi: 10.1126/science.aac9323

Miyata, T., Takeda, J., Iida, Y., Yamada, N., Inoue, N., Takahashi, M., et al. (1993). The cloning of PIG-A, a component in the early step of GPI-anchor biosynthesis. *Science* 259, 1318–1320. doi: 10.1126/science.7680492

Montoya, D. (2023). Variation in diversity–function relationships can be explained by species interactions. *J. Anim. Ecol.* 92, 226–228. doi: 10.1111/1365-2656.13836

Naseem, H., Ahsan, M., Shahid, M. A., and Khan, N. (2018). Exopolysaccharides producing rhizobacteria and their role in plant growth and drought tolerance. *J. Basic Microbiol.* 58, 1009–1022. doi: 10.1002/jobm.201800309

Ngaba, M. J. Y., Uwiragiye, Y., Hu, B., Zhou, J., Dannenmann, M., Calanca, P., et al. (2024). Effects of environmental changes on soil respiration in arid, cold, temperate, and tropical zones. *Sci. Total Environ.* 952, 175943. doi: 10.1016/j.scitotenv.2024.175943

Paradiso, E., Jevon, F., and Matthes, J. (2019). Fine root respiration is more strongly correlated with root traits than tree species identity. *Ecosphere* 10, e02944. doi: 10.1002/ecs2.2944

Quoreshi, A. M., Kumar, V., Adeleke, R., Qu, L., and Atangana, A.R (2022). Editorial: Soils and vegetation in desert and arid regions: Soil system processes, biodiversity and ecosystem functioning, and restoration. *Front. Environ. Sci.* 10. doi: 10.3389/fenvs.2022.962905

Rathore, N., Hanzelková, V., Dostálek, T., Semerád, J., Schnablová, R., Cajthaml, T., et al. (2023). Species phylogeny, ecology, and root traits as predictors of root exudate composition. *New Phytol.* 239, 1212–1224. doi: 10.1111/nph.19060

Sanaullah, M., Blagodatskaya, E., Chabbi, A., Rumpel, C., and Kuzyakov, Y. (2011). Drought effects on microbial biomass and enzyme activities in the rhizosphere of grasses depend on plant community composition. *Appl. Soil Ecol.* 48, 38–44. doi: 10.1016/j.apsoil.2011.02.004

Schiedung, M., Don, A., Beare, M. H., and Abiven, S (2023). Soil carbon losses due to priming moderated by adaptation and legacy effects. *Nat. Geosci.* 16, 909–914. doi: 10.1038/s41561-023-01275-3

Segovia, E., Reuben, S., and Han, P. (2013). Effect of drought on microbial growth in plant rhizospheres. *Microbiol. Res.* 3, 83. doi: 10.5923/j.microbiology.20130302.04

Shen, Y., Gilbert, G. S., Li, W., Fang, M., Lu, H., and Yu, S. (2019). Linking aboveground traits to root traits and local environment: implications of the plant economics spectrum. *Front. Plant Sci.* 10. doi: 10.3389/fpls.2019.01412

Shu, W.-S., and Huang, L.-N. (2022). Microbial diversity in extreme environments. *Nat. Rev. Microbiol.* 20, 219–235. doi: 10.1038/s41579-021-00648-y

Spang, A., Caceres, E., and Ettema, T. (2017). Genomic exploration of the diversity, ecology, and evolution of the archaeal domain of life. *Science* 357, eaaf3883. doi: 10.1126/science.aaf3883

Spitzer, C., Wardle, D., Lindahl, B., Sundqvist, M., Gundale, M., Fanin, N., et al. (2021). Root traits and soil microorganisms as drivers of plant-soil feedbacks within the sub-arctic tundra meadow. *J. Ecol.* 110, 466-478. doi: 10.1111/1365-2745.13814

Subke, J.-A., Inglima, I., and Cotrufo, M. F. (2006). Trends and methodological impacts in soil CO_2 efflux partitioning: A metaanalytical review. *Global Change Biol.* 12, 921–943. doi: 10.1111/j.1365-2486.2006.01117.x

Tang, X., Du, J., Shi, Y., Lei, N., Chen, G., Cao, L., et al. (2020a). Global patterns of soil heterotrophic respiration – A meta-analysis of available dataset. *CATENA* 191, 104574. doi: 10.1016/j.catena.2020.104574

Tang, X., Pei, X., Lei, N., Luo, X., Liu, L., Shi, L., et al. (2020b). Global patterns of soil autotrophic respiration and its relation to climate, soil and vegetation characteristics. *Geoderma* 369, 114339. doi: 10.1016/j.geoderma.2020.114339

Tenenhaus, M., Vinzi, V. E., Chatelin, Y.-M., and Lauro, C. (2005). PLS path modeling. *Comput. Stat Data Anal.* 48, 159–205. doi: 10.1016/j.csda.2004.03.005

Tian, J., Dungait, J. A. J., Hou, R., Deng, Y., Hartley, I.P., Yang, Y., et al. (2024). Microbially mediated mechanisms underlie soil carbon accrual by conservation agriculture under decade-long warming. *Nat. Commun.* 15, 377. doi: 10.1038/s41467-023-44647-4

Tianjiao, F., Dong, W., Ruoshui, W., Yixin, W., Zhiming, X., Fengmin, L., et al. (2022). Spatial-temporal heterogeneity of environmental factors and ecosystem functions in farmland shelterbelt systems in desert oasis ecotones. *Agric. Water Manage.* 271, 107790. doi: 10.1016/j.agwat.2022.107790

Trivedi, P., Anderson, I., and Singh, B. (2013). Microbial modulators of soil carbon storage: Integrating genomic and metabolic knowledge for global prediction. *Trends Microbiol.* 21, 641-651. doi: 10.1016/j.tim.2013.09.005

Trivedi, P., Delgado-Baquerizo, M., Trivedi, C., Hu, H., Anderson, I., Jeffries, T., et al. (2016). Microbial regulation of the soil carbon cycle: evidence from gene–enzyme relationships. *ISME J.* 10, 2593–2604. doi: 10.1038/ismej.2016.65

Vernham, G., Bailey, J. J., Chase, J. M., Hjort, J., Field, R., and Schrodt, F. (2023). Understanding trait diversity: the role of geodiversity. *Trends Ecol. Evol.* 38, 736–748. doi: 10.1016/j.tree.2023.02.010

Violle, C., Reich, P., Pacala, S., Enquist, B., and Kattge, J. (2014). The emergence and promise of functional biogeography. *Proc. Natl. Acad. Sci. U. S. A.* 111, 13690-13696. doi: 10.1073/pnas.1415442111

Vries, F., Brown, C., and Stevens, C. (2016). Grassland species root response to drought: consequences for soil carbon and nitrogen availability. *Plant Soil* 409, 297–312. doi: 10.1007/s11104-016-2964-4

Wan, X., Chen, X., Huang, Z., and Chen, H. Y. H. (2021). Contribution of root traits to variations in soil microbial biomass and community composition. *Plant Soil* 460, 483–495. doi: 10.1007/s11104-020-04788-7

Wang, H., Cai, Y., Yang, Q., Gong, Y., and Lv, G. (2019a). Factors that alter the relative importance of abiotic and biotic drivers on the fertile island in a desert-oasis ecotone. *Sci. Total Environ.* 697, 134096. doi: 10.1016/j.scitotenv.2019.134096

Wang, H., Lv, G., Cai, Y., Zhang, X., Jiang, L., Yang, X.-D., et al. (2021a). Determining the effects of biotic and abiotic factors on the ecosystem multifunctionality in a desert-oasis ecotone. *Ecol. Indic.* 128, 107830. doi: 10.1016/j.ecolind.2021.107830

Wang, J., Song, B., Ma, F., Tian, D., Li, Y., Yan, T., et al. (2019b). Nitrogen addition reduces soil respiration but increases the relative contribution of heterotrophic component in an alpine meadow. *Funct. Ecol.* 33, 2239–2253. doi: 10.1111/1365-2435.13433

Wang, J., Teng, D., He, X., Qin, L., Yang, X., Lv, G., et al. (2021b). Spatial non-stationarity effects of driving factors on soil respiration in an arid desert region. *CATENA* 207, 105617. doi: 10.1016/j.catena.2021.105617

Wang, J., Teng, D., He, X., Li, Z., Chen, Y., Ma, W., et al. (2022a). Spatial variation in the direct and indirect effects of plant diversity on soil respiration in an arid region. *Ecol. Indic.* 142, 109288. doi: 10.1016/j.ecolind.2022.109288

Wang, R., Yu, G., and He, N. (2021c). Root community traits: scaling-up and incorporating roots into ecosystem functional analyses. *Front. Plant Sci.* 12. doi: 10.3389/fpls.2021.690235

Wang, X., Geng, X., Liu, B., Cai, D., Li, D., Xiao, F., et al. (2022b). Desert ecosystems in China: Past, present, and future. *Earth-Science Rev.* 234, 104206. doi: 10.1016/j.earscirev.2022.104206

Whitaker, J., Ostle, N., Nottingham, A., Ccahuana, A., Salinas, N., Bardgett, R., et al. (2014). Microbial community composition explains soil respiration responses to changing carbon inputs along an Andes-to-Amazon elevation gradient. *J. Ecol.* 102, 1058-1071. doi: 10.1111/1365-2745.12247

Williams, J., O'Farrell, M., and Riddle, B. (2006). Habitat use by bats in a riparian corridor of the Mojave desert in Southern Nevada. *J. Mammal.* 87, 1145–1153. doi: 10.1644/06-MAMM-A-085R2.1

Xu, Y., Seshadri, B., Sarkar, B., Rumpel, C., Sparks, D., and Bolan, S. N. (2018). Microbial Control of Soil Carbon Turnover. in T. H. P Nannipieri *The Future of Soil Carbon*. Academic Press, pp. 165–194. doi: 10.1016/b978-0-12-811687-6.00006-7

Yan, M., Guo, N., Ren, H., Zhang, X., and Zhou, G. (2015). Autotrophic and heterotrophic respiration of a poplar plantation chronosequence in northwest China. *For. Ecol. Manage.* 337, 119–125. doi: 10.1016/j.foreco.2014.11.009

Yan, Y., Wang, J., Tian, D., Zhang, R., Song, L., Li, Z., et al. (2022). Heterotrophic respiration and its proportion to total soil respiration decrease with warming but increase with clipping. *CATENA* 215, 106321. doi: 10.1016/j.catena.2022.106321

Yang, C., Lv, D., Jiang, S., Lin, H., Sun, J., Li, K., et al. (2021). Soil salinity regulation of soil microbial carbon metabolic function in the Yellow River Delta, China. *Sci. Total Environ.* 790, 148258. doi: 10.1016/j.scitotenv.2021.148258

Zhang, L., and Lv, J. (2020). Metagenomic analysis of microbial community and function reveals the response of soil respiration to the conversion of cropland to plantations in the Loess Plateau of China. *Global Ecol. Conserv.* 23, e01067. doi: 10.1016/j.gecco.2020.e01067

Zhang, M., Niu, Y., Wang, W., Hosseini Bai, S., Luo, H., Tang, L., et al. (2021). Responses of microbial function, biomass and heterotrophic respiration, and organic carbon in fir plantation soil to successive nitrogen and phosphorus fertilization. *Appl. Microbiol. Biotechnol.* 105, 1–14. doi: 10.1007/s00253-021-11663-7

Zhang, J., Zhang, N., Liu, Y.-X., Zhang, X., Hu, B., Qin, Y., et al. (2018a). Root microbiota shift in rice correlates with resident time in the field and developmental stage. *Sci. China Life Sci.* 61, 613–621. doi: 10.1007/s11427-018-9284-4

Zhang, Y., Zhang, M., Tang, L., and Fu, L. (2018b). Long-term harvest residue retention could decrease soil bacterial diversities probably due to favouring oligotrophic lineages. *Microbial. Ecol.* 76, 771–781. doi: 10.1007/s00248-018-1162-8

Zhang, Y., Zhao, W., He, J., and Fu, L. (2018c). Soil susceptibility to macropore flow across a desert-oasis ecotone of the hexi corridor, Northwest China. *Water Resour. Res.* 54, 1281–1294. doi: 10.1002/2017WR021462

Zhao, C., Zhimin, Z., Yilihamu,, Hong, Z., and Jun, L. (2011). Contribution of root and rhizosphere respiration of Haloxylon ammodendron to seasonal variation of soil respiration in the Central Asian desert. *Quaternary Int. - QUATERN Int.* 244, 304–309. doi: 10.1016/j.quaint.2010.11.004

Zheng, P., Wang, D., Yu, X., Jia, G., Liu, Z., Wang, Y., et al. (2021). Effects of drought and rainfall events on soil autotrophic respiration and heterotrophic respiration. *Agriculture Ecosyst. Environ.* 308, 107267. doi: 10.1016/j.agee.2020.107267

Zhou, L., Liu, Y., Zhang, Y., Sha, L., Song, Q., Zhou, W., et al. (2019). Soil respiration after six years of continuous drought stress in the tropical rainforest in Southwest China. *Soil Biol. Biochem.* 138, 107564. doi: 10.1016/j.soilbio.2019.107564

Zhou, J., Zhang, J., Lambers, H., Wu, J., Qin, G., Li, Y., et al. (2022). Intensified rainfall in the wet season alters the microbial contribution to soil carbon storage. *Plant Soil* 476, 337–351. doi: 10.1007/s11104-022-05389-2

frontiers | Frontiers in Plant Science

TYPE Original Research
PUBLISHED 24 March 2025
DOI 10.3389/fpls.2025.1544893

OPEN ACCESS

EDITED BY
Xiao-Dong Yang,
Ningbo University, China

REVIEWED BY
Hongmei Cai,
Huazhong Agricultural University, China
Jianping Liu,
Fujian Agriculture and Forestry University, China

*CORRESPONDENCE
Zhihai Wu
wuzhihai@jlau.edu.cn

RECEIVED 13 December 2024
ACCEPTED 28 February 2025
PUBLISHED 24 March 2025

CITATION
Jiang H, Li W, Jiang Z, Li Y, Shen X, Nuo M, Zhang H, Xue B, Zhao G, Tian P, Yang M and Wu Z (2025) Silicon enhanced phosphorus uptake in rice under dry cultivation through root organic acid secretion and energy distribution in low phosphorus conditions. *Front. Plant Sci.* 16:1544893. doi: 10.3389/fpls.2025.1544893

Silicon enhanced phosphorus uptake in rice under dry cultivation through root organic acid secretion and energy distribution in low phosphorus conditions

Hao Jiang[1,2], Wanchun Li[1], Zixian Jiang[1], Yunzhe Li[3], Xinru Shen[1], Min Nuo[1], Hongcheng Zhang[1], Bei Xue[1], Guangxin Zhao[1], Ping Tian[1], Meiying Yang[4] and Zhihai Wu[1,2]*

[1]Faculty of Agronomy, Jilin Agricultural University, Changchun, Jilin, China, [2]Jilin Province Green and High Quality Japonica Rice Engineering Research Center, Jilin Agricultural University, Changchun, Jilin, China, [3]Changchun Farmers Vocational Education Center, Changchun Agriculture and Rural Bureau, Changchun, Jilin, China, [4]College of Life Sciences, Jilin Agricultural University, Changchun, Jilin, China

Dry cultivation of rice (DCR) is one of the important rice cultivation practices aimed at addressing freshwater resource shortages. However, the non-renewable nature of phosphate resources constrains agricultural development. In the context of the contradiction between rice, water, and phosphorus, there is little research on using the silicon phosphorus relationship to improve the phosphorus availability and uptake of DCR. This experiment used field soil and established five fertilization treatments: no phosphorus application, low phosphorus and normal phosphorus (0, 25, 75 kg·ha^{-1} P_2O_5) (0P, 25P, 75P), along with two silicon levels (0, 45kg·ha^{-1} SiO_2), resulting in the treatments 0P, 0PSi, 25P, 25PSi, and 75P. The soil phosphorus components and plant phosphorus uptake were analyzed. The results showed that adding silicon to 25P increased the Olsen-P content (14.37%) by increasing Ca_8-P (9.04%) and Al-P (19.31%). Additionally, root and leaf phosphorus content increased by 7.6% and 5.8%, respectively, comparable to the levels observed in the 75P treatment. On one hand, adding silicon increases malate (40.48%) and succinate (49.73%) content, enhances acid phosphatase activity, and increases the abundance of *Bradyrhizobium*, *Paenibacillus*, and *Bacillus*, as well as the proportion of *Fusarium*, forming an "organic acid microbial" activated phosphorus system. On the other hand, the addition of silicon alleviated phosphorus limitations by reducing ATP consumption in roots through a decrease in ATPase and P-ATPase content. This also minimized excessive NSC transport to roots, thereby promoting shoot growth by downregulating *SUT1*, *SWEET11*, *SUS2*, and *CIN2*. In addition to optimizing root-to-shoot ratio and providing sufficient energy, silicon addition also increases root volume and upregulates *OsPT2*, *OsPT4*, and

OsPT8, thereby promoting phosphorus uptake. In summary, 25PSi optimizes the root-to-shoot ratio and promotes phosphorus conversion and uptake through organic acid, microbial, and energy pathways. Applying silicon is beneficial for the sustainable and efficient management of phosphorus in DCR.

KEYWORDS

phosphorus, silicon, rice, dry cultivation, root architecture, organic acid, microorganism, energy metabolism

Introduction

The International Food Policy Research Institute predicts that by 2050, climate change will cause a 20% decrease in irrigated rice production in developing countries, while available freshwater resources are expected to decline by 50% (Aditi et al., 2020). Insufficient moisture significantly impacts crop yields and threatens global food security (Maryam, 2021). Rice is a food crop with high water consumption, and addressing the "rice-water contradiction" is a pressing issue in rice-growing regions worldwide. In recent years, dry farming of rice has gradually become a research hotspot in the field of agricultural ecology. The 'blue revolution' concept for food security through water-saving and drought-resistant rice has been proposed, leading to the cultivation and widespread promotion of water-saving and drought-resistant rice varieties (Xia et al., 2022). Significant progress has been made in variety screening (Wei et al., 2022), quality assessment (Wang et al., 2023), and yield enhancement strategies (Jiang et al., 2023a) for rice cultivation under drought conditions. Numerous studies on the exploration of drought-resistant germplasm resources and drought-resistant mechanisms have demonstrated that dry rice cultivation has outstanding advantages, including water conservation, saving costs and labor, adapting to mechanization, and simplifying rice cultivation (Jiang et al., 2023b; Bi et al., 2021; Guo et al., 2024. As a result, it is currently a research hotspot in the field of water-saving cultivation of rice.

Phosphorus (P) is a key nutrient element for crop growth. Increased food production may drive the demand for phosphorus input in farmland, but phosphate ore is a non-renewable resource. The total amount of phosphorus fertilizer application in global farmland continues to increase, reaching 18 TgP yr^{-1} in 2013, which has exceeded the boundary value (6-12 TgP yr^{-1} to TgP yr^{-1}). This figure is projected to increase to 22-27 TgP yr^{-1} by 2050 (Zou et al., 2022). Improper use of phosphorus in crop production leads to excessive leaching of phosphorus into water bodies, posing a threat to aquatic organisms and human health (Bouwman et al., 2017). In order to meet the growing demand for food, address the rice-water-phosphorus contradiction, and solve the multiple challenges of exacerbating phosphorus pollution and depleting phosphate rock reserves, it is essential to improve the phosphorus utilization efficiency in rice under dry cultivation production, particularly in low phosphorus environments.

There are various strategies plants use to improve soil phosphorus availability and uptake: (1) "P-mining", which utilizes root exudates such as organic anions (carboxylates) and phosphatases to mineralize difficult to utilize inorganic and organic phosphorus pools (Wen et al., 2020); (2) Root foraging ", where plants alter their root system configuration to obtain more effective soil phosphorus (Liu, 2021); (3) Symbiotic relationships, such as root colonization with arbuscular mycorrhizal and ectomycorrhizal fungi (Song et al., 2021); (4) Metabolic adaptation, such as replacing phospholipids with non-phospholipids (such as galactolipids and thiolipids) (Hans et al., 2012); (5) Improved internal phosphorus utilization efficiency, which increases plant yield per unit of phosphorus uptake (Liao et al., 2020). We discovered that silicon can increase rice yield under dry cultivation under normal phosphorus conditions (Jiang et al., 2023a). However, the relationship between silicon and phosphorus under low phosphorus conditions remains to be explored, and the effects of silicon on the soil phosphorus environment and root phosphorus uptake are not yet clear.

The relationship between rhizosphere microbial communities and root exudates has become one of the research hotspots in root-soil interaction (Sreejata et al., 2024). However, the impact of silicon-phosphorus interaction in the rhizosphere of rice under dry cultivation on root exudates and microbial communities remains unclear. Phosphorus is well known to play a critical role in essential life processes such as respiration and energy metabolism. Plant metabolic activities, ion transport, ineffective cycling, sucrose transport, and response to abiotic stress require a significant amount of energy (Jeffrey et al., 2019). In cases of phosphorus deficiency, the root-to-shoot ratio of crops often increases (Xiao et al., 2022; Hermans et al., 2006). However, the role of energy metabolism in root development of rice under dry cultivation induced by phosphorus scarcity remains unclear. Therefore, we propose two scientific questions (1) What is the root-soil microbial relationship of silicon-phosphorus interaction under dry cultivation? (2) How does silicon regulate phosphorus absorption and development through root energy metabolism in response to changes in phosphorus environment? This experiment aims to develop a "water-saving, phosphorus-reducing, and

efficiency-enhancing" technology model for rice while also elucidating the root-soil-microbial interaction mechanism of silicon phosphorus interaction. This will provide new solutions to address the rice-water-phosphorus contradiction.

Materials and methods

Site description

The experiment was conducted from 2023 to 2024 at the National Crop Variety Approval Characteristic Appraisal Station (125°39 E, 44°46 N) of Jilin Agricultural University in Changchun, Jilin Province, China. The 0-20 cm soil layer has a clay loam structure with a pH value of 6.3, organic matter of 16.5 $g{\cdot}kg^{-1}$, available silicon of 96.45 $mg{\cdot}kg^{-1}$, alkaline nitrogen of 92.3 $mg{\cdot}kg^{-1}$, available phosphorus of 9.6 $mg{\cdot}kg^{-1}$, and available potassium of 208.46 $mg{\cdot}kg^{-1}$. Over the past three years, the accumulated temperature and rainfall during the entire growth period in the region were 2873°C and 674.6 mm, respectively.

Experimental design and crop management

This experiment uses the rice variety 'Suigeng 18' (China Rice Data Center, No. 2014021, https://www.ricedata.cn/variety/varis/614593.htm) as the material. Research indicates that 'Suigeng 18' is a rice variety suitable for dry farming in the central region of Jilin Province (Jiang et al., 2021; Wei et al., 2022).

Potted experiments were conducted in 2023 and 2024, while field experiments were conducted in 2024. This experiment included three levels of phosphorus (P_2O_5) fertilizer (0 $kg{\cdot}ha^{-1}$、25 $kg{\cdot}ha^{-1}$、75 $kg{\cdot}ha^{-1}$) and two levels of silicon (SiO_2) fertilizer (0 $kg{\cdot}ha^{-1}$、45 $kg{\cdot}ha^{-1}$), resulting in five treatments: 0P, 0PSi, 25P, 25PSi, and 75P. The soil for the pot experiment was sourced from the field, with 8.5 kg of soil used per pot. Three holes were sown per pot, with eight seeds per hole. Each treatment was repeated three times. The field experimental plot covers an area of 25 m^2 and is sown using the dry broadcasting method with a seeding rate of 150 $kg{\cdot}ha^{-1}$. The strip sowing method is used with a row spacing of 30 cm, and each treatment is repeated three times.

Silicon, phosphorus, and potassium fertilizers are applied simultaneously as base fertilizers. The silica fertilizer is derived from Russian mineral silica (Biotronik, Berlin, Germany), with an effective silica content of ≥ 72% (Supporting Information, Supplementary Figure S1). The phosphate fertilizer is composed of superphosphate (P_2O_5 12%). The potassium fertilizer consists of 75 $kg{\cdot}ha^{-1}$ potassium chloride (K_2O 60%). The nitrogen fertilizer consists of urea (pure N 46%) applied at a rate of 160 $kg{\cdot}ha^{-1}$, with a distribution ratio of 5:3:2 for base fertilizer, tiller fertilizer, and spike fertilizer. The entire growth period is mainly rain-fed, and a soil water potential analyzer (SYS-TSS1, Sayas Technology Co., Ltd, Liaoning, China) is used to monitor changes in water potential in the experimental field. When the soil water potential at a depth of 10-15 cm falls below -35 kPa, a fixed spray 360° atomizing rotary sprinkler is used, with a spraying radius of 8 m and a water output of 0.7 $m^3{\cdot}h^{-1}$. After replenishment, the soil water potential reaches -10 kPa. Water control in the potted plant experiment is consistent with that in the field experiment. Other measures are implemented according to the requirements for high-yield cultivation.

Plant and soil sampling

45 days after sowing, the rhizosphere soil attached to the surface of the root system was collected, visible plant materials were removed, and the soil was sieved (2 mm). The soil was then analyzed for microorganisms, acid phosphatase activity, available phosphorus content, and inorganic phosphorus grading. Fresh root systems were collected for quantitative analysis of root architecture, carboxylates, energy metabolism, and gene fluorescence. Biomass, root phosphorus content, and non-structural carbohydrates were measured after separating plant roots, stems, and leaves.

Morphological indicators and plant biomass

Root system architecture

Root images were scanned using a root morphology scanner (Epson Perfection V800 photo; EPSON, Tokyo, Japan) and stored on a computer. Root length, root surface area, and root volume were analyzed using the root analysis system software WinRhizo PRO 2016 (Regent Instruments, Quebec, Canada).

Leaf area and biomass

Leaf area was measured using a leaf area analyzer (CID-203; CID Bioscience, Camas, WA, USA). The plant was decomposed into three parts: roots, stems, and leaves, and placed in sulfuric acid paper bags. This process was repeated three times. The drying process was carried out at 105 °C for 30 minutes, then at 80 °C until constant weight was reached. The weight was recorded. Root/shoot ratio=root weight/stem and leaf weight.

Plant phosphorus content and physicochemical properties

Plant phosphorus content

The dried samples were crushed by a powder machine and mixed well. 0.05 g of the sample was weighed and placed in a digestion tube, and then mixed and boiled with H_2SO_4-H_2O_2. Repeat three times. After cooling, adjust the volume and determine the total phosphorus content using the molybdenum antimony colorimetric method (Siddiqi and Glass, 1981).

Non-structural carbohydrates

The soluble sugar and starch content were determined using an improved sulfuric acid anthrone colorimetric method (DuBois et al.,

2002). The content of total non-structural carbohydrates (NSC) was calculated as the sum of soluble sugars and starch content. NSC root/shoot ratio= (NSC×root weight)/(NSC×shoot weight).

Root energy metabolism

The content of ATP, ATPase, plasma membrane H^+-ATPase (P-ATPase), V-ATPase, alternative oxidase (AOX) was measured. Frozen roots (0.01g) were ground into fine powder in liquid nitrogen, homogenized in 0.01M PBS (pH 7.2), and centrifuged at 2000g for 20 minutes. The content of ATP, ATPase, P-ATPase, as well as the activity of V-ATPase and AOX were measured using the supernatant, following the manufacturer's instructions (Shanghai Enzyme-Linked Biotechnology Co., Ltd.).

Measurements of mitochondrial complex activities. Frozen root systems (0.01g) were ground and mitochondria were extracted in an ice bath using reagents from the mitochondrial complex activity assay kit. The extract underwent 30 cycles of ultrasound treatment (power, 20%; ultrasound time, 3s; interval time, 10s). The activity of complex I and complex V was measured according to the manufacturer's instructions (Comin Biotechnology Co., Ltd.) using a mitochondrial complex activity assay kit (Li et al., 2023).

Root gene expression level

The root system was frozen with liquid nitrogen and transferred to a -80°C freezer. After grinding the tissue in liquid nitrogen, total RNA was extracted using TriPure reagent (Aidlab Biotechnologies). RNA was reverse transcribed into single-stranded cDNA using ReverTra Ace qPCR RT Master Mix (TOYOBO). Real-time fluorescent quantitative PCR amplification was carried out using cDNA as a template. The reaction system consisted of a 20 μL reaction system, 10 μL of 2×SuperReal PreMix Plus, 8 μL ddH_2O, 0.5 μL of upstream and downstream primers, and 1 μL of cDNA template. The PCR amplification reaction system was pre-denatured at 95°C for 15 minutes. The following 40 cycles were performed: pre-denaturation at 95°C for 20 seconds, annealing at 60 °C for 20 seconds, extension at 72 °C for 20 seconds, and melting for 6 seconds. Relative gene expression was analyzed using the $2^{-\Delta\Delta CT}$ method. Primer information is shown in Supplementary Table S1.

Collection of root exudates and soil analysis

Soil available phosphorus and inorganic phosphorus components

The crop roots were excavated, and the "shaking soil method" was used to remove residual non-rhizosphere soil from the roots while retaining rhizosphere soil. The rhizosphere soil was sealed in plastic bags, transported to the laboratory for air drying, and stored at room temperature (25°C). Effective phosphorus was extracted using 0.5 mol·L^{-1} $NaHCO_3$ (Olsen et al., 1954) and measured by spectrophotometry at 700 nm (T3202, Youke Instrument, Shanghai, China). Six types of soil inorganic phosphorus components were extracted from soil samples using a sequential extraction program, including dicalcium phosphate (Ca_2-P), octacalcium phosphate (Ca_8-P), aluminum phosphate (Al-P), iron phosphate (Fe-P), occluded phosphate (O-P) and apatite (Ca_{10}-P). The measurement of inorganic phosphorus components follows the method of Liu et al (Liu et al., 2022).

Root exudates

The roots and attached rhizosphere soil were soaked in a beaker containing 100 mL of $CaCl_2$ solution (0.2 μmol·L^{-1}) (Yu et al., 2023). After soaking the roots for 60 seconds, the root sheath soil was removed as much as possible to reduce root damage. 10 ml of supernatant was transferred to a centrifuge tube containing 2 drops of microbial inhibitor and 3 drops of concentrated phosphoric acid. The sample was stored at 20 °C until it passed through a 0.22 μm filter and analyzed for tartrate, succinate, malate, and citrate content by HPLC-MS/MS. The measurement of carboxylate salts follows the method of Fiori et al. (2018). The remaining soil in the beaker was dried and weighed to calculate the concentration of carboxylate based on the weight of the root sheath soil.

Soil acid phosphatase and microorganisms

A portion of the rhizosphere soil was stored at 4°C for acid phosphatase measurement, while another portion was stored at -80°C for microbial analysis. Soil acid phosphatase was determined using the colorimetric method with sodium phenylene phosphate.

Genomic DNA of microbial communities was extracted from soil samples using the magnetic bead soil DNA assay kit (RT 405-02; TIANGEN, Beijing, China). DNA extract was detected by 2% agarose gel electrophoresis, and DNA concentration and purity were determined by NanoDrop 2000 (Thermo Fisher Scientific, Waltham, MA, USA). Using a 10 ng DNA template, 0.2 μM forward and reverse primers, and 15 μL Phusion ® High fidelity PCR Master Mix (New England Biolabs, Ipswich, MA, USA), the highly variable region ITS 1 of the fungal ITS rRNA gene was amplified. The samples were processed on the NovaSeq 6000 platform (Novogene Technology Co, Ltd., Tianjin, China) and clustered into operational taxonomic units (OTUs) at the 97% threshold. The DADA2 module in QIIME2 software was used to denoise and filter out sequences with an abundance less than 5, yielding the final amplicon sequence variations (ASVs) and feature table.

Statistical analysis

Microsoft Excel 2021 (Microsoft, Redmond, United States) was used to organize the data. All experiments were conducted in triplicate (n = 3). One-way analysis of variance (ANOVA) and statistical analysis were performed to determine statistically significant differences between the control and other treatments using SPSS 27 software (SPSS, Chicago, United States). At $P<0.05$, the difference was considered statistically significant. Origin 2022

software (OriginLab, Northampton, USA) was used to generate figures.

Results

Soil phosphorus components and root phosphorus uptake under different silicon and phosphorus conditions

Regarding the soil phosphorus environment, the addition of silicon significantly increased the Olsen-P content in the 0P and 25P treatments ($P<0.05$) (Figure 1A), with increases of 11.36% and 14.37%, respectively. In terms of the proportion of phosphorus components. Adding silicon increased the proportion of circulating phosphorus components (Ca_8-P, Al-P), which were 17.98% and 24.58% higher than the 0P treatment and 9.75% and 20.09% higher than the 25P treatment. Silicon addition reduces the proportion of refractory phosphorus component (Ca_{10}-P), which is less than 0P and 25P, respectively, by 6.78% and 4.94% (Figure 1B). In terms of different phosphorus component contents. The easily absorbable Ca_2-P content showed a significant increase trend ($P<0.05$) among different phosphorus dosages (Figure 1C). The addition of silicon significantly increased the content of Ca_8-P and Al-P components in the medium cycle phosphorus treated with 0P and 25P ($P<0.05$), while the addition of silicon under the 25P treatment increased Ca8-P and Al-P contents by 9.04% and 19.31%, respectively (Figures 1D, E). Conversely, silicon addition significantly reduced the Fe-P content ($P<0.05$). However, no significant difference was observed between 25PSi and 75P ($P>0.05$) (Figure 1F). The content

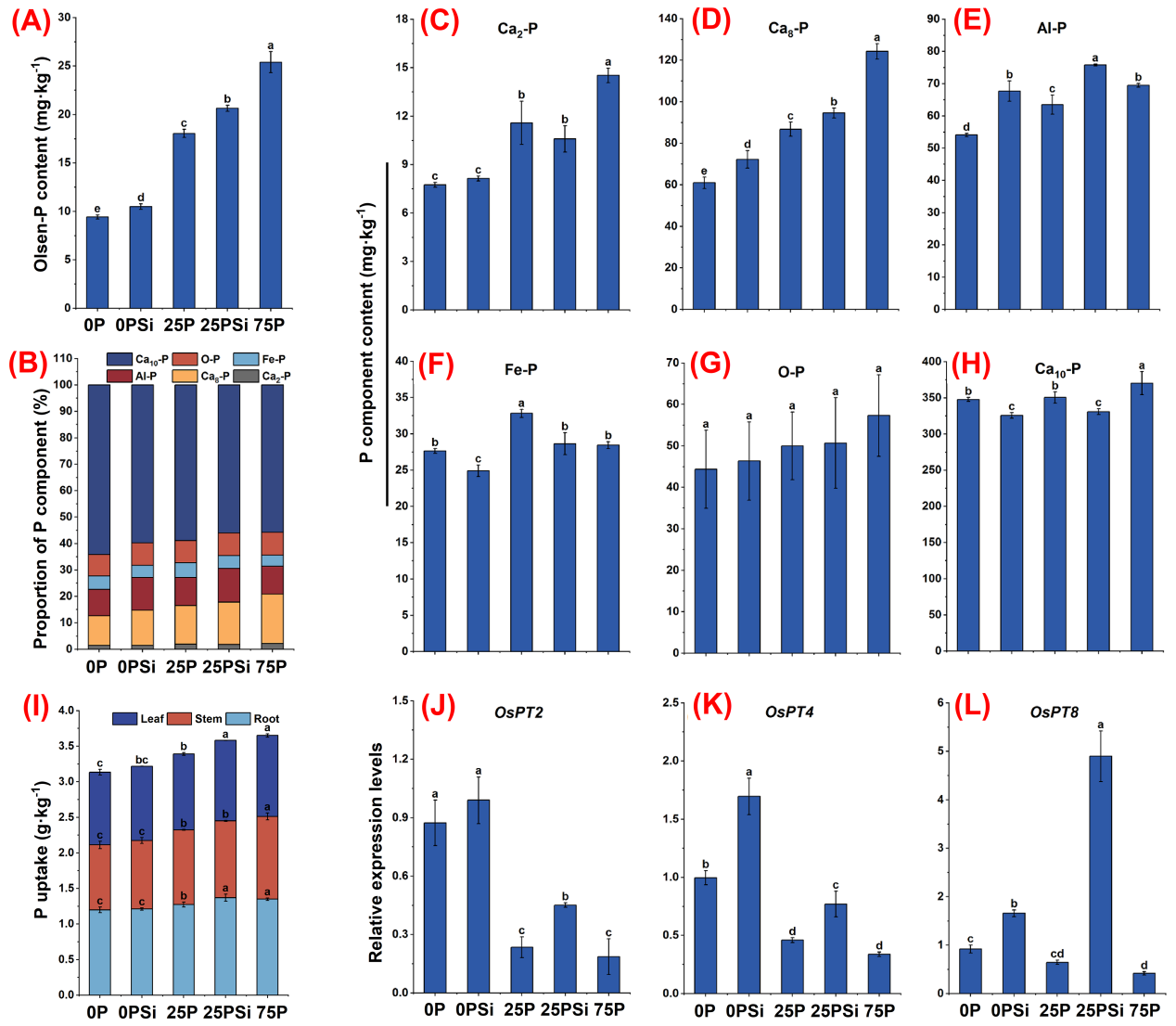

FIGURE 1
The effect of silicon and phosphorus on the phosphorus environment and root phosphorus uptake in rice under dry cultivation. **(A)**, Olsen-P content. **(B)**, Proportion of phosphorus (P) components. **(C–H)**, Phosphorus component content, **(C)**, Ca_2^-P; **(D)**, Ca_8^-P; **(E)**, Al-P; **(F)**, Fe-P; **(G)**, O-P; **(H)**, Ca_{10}^-P. **(I)**, Plant phosphorus uptake. **(J–L)**, Relative expression levels, **(J)**, *OsPT2*; **(K)**, *OsPT4*; **(L)**, *OsPT8*. Different letters represent significant differences in the same indicator between different treatments ($P<0.05$).

of refractory phosphorus components O-P and Ca_{10}-P, was highest in the 75P treatment. O-P exhibited an increasing trend across the treatments, but there was no significant difference (*P>0.05*) (Figure 1G). The addition of silicon significantly reduced the Ca_{10}-P content in 0P and 25P treatments by 6.34% and 5.55%, respectively (*P<0.05*) (Figure 1H). It is evident that silicon addition increases the proportion of circulating phosphorus components, reduces Ca_{10}-P content, and increases the soil Olsen-P content.

Silicon addition significantly increased phosphorus content in the roots and leaves of 25P by 7.6% and 5.8%, respectively (*P<0.05*) (Figure 1I), but there was no significant difference between 25PSi and 75P (*P>0.05*). From the overall perspective of roots, stems, and leaves, adding silicon increased the phosphorus content of 0P and 25P plants by 2.65% and 5.58%, respectively. Silicon addition significantly increased the expression levels of phosphorus transport genes *OsPT4* and *OsPT8* in the 0P and 25P treatments (Figures 1K, L). There was no significant change in the expression level of *OsPT2* with silicon addition at 0P; however, silicon addition at 25P significantly upregulated the expression level of *OsPT2* (Figure 1J). It is evident that silicon addition upregulates the expression levels of phosphorus transporters in 0P and 25P treatments, significantly increasing the phosphorus content in 25P.

Plant growth and RSA under different silicon and phosphorus conditions

The plant height was significantly lower in the 0P treatment than in other treatments, and reached its highest at 25PSi (Figures 2A, B). The addition of silicon increased the leaf area in the 0P and 25P treatments by 9.31% (*P>0.05*) and 21.93% (*P<0.05*), respectively, with no significant difference between 25PSi and 75P (Figures 2C, F). The biomass of various parts of the plant increased after silicon addition (Figure 2D). There was no significant difference in root weight among the treatments (Figure 2G). However, there was a significant difference in stem and leaf weight between 25P and 25PSi *(P<0.05)*, while no significant difference was observed between 25PSi and 75P (*P>0.05*). Compared with 0P, the root shoot ratio of 25PSi decreased by 27.29%, and decreased by 15.43% compared to 25P (Figure 2E). After adding silicon, the total root length, volume, and surface area of 0P and 25P treatments increased (Figures 2H-J), with silicon significantly increasing the root volume of 25P treatment *(P<0.05)* (Figure 2I). It is evident that silicon addition increased plant height, leaf area, and biomass of roots, stems, and leaves in the 0P and 25P treatments, with the 25PSi treatment showing the highest levels.

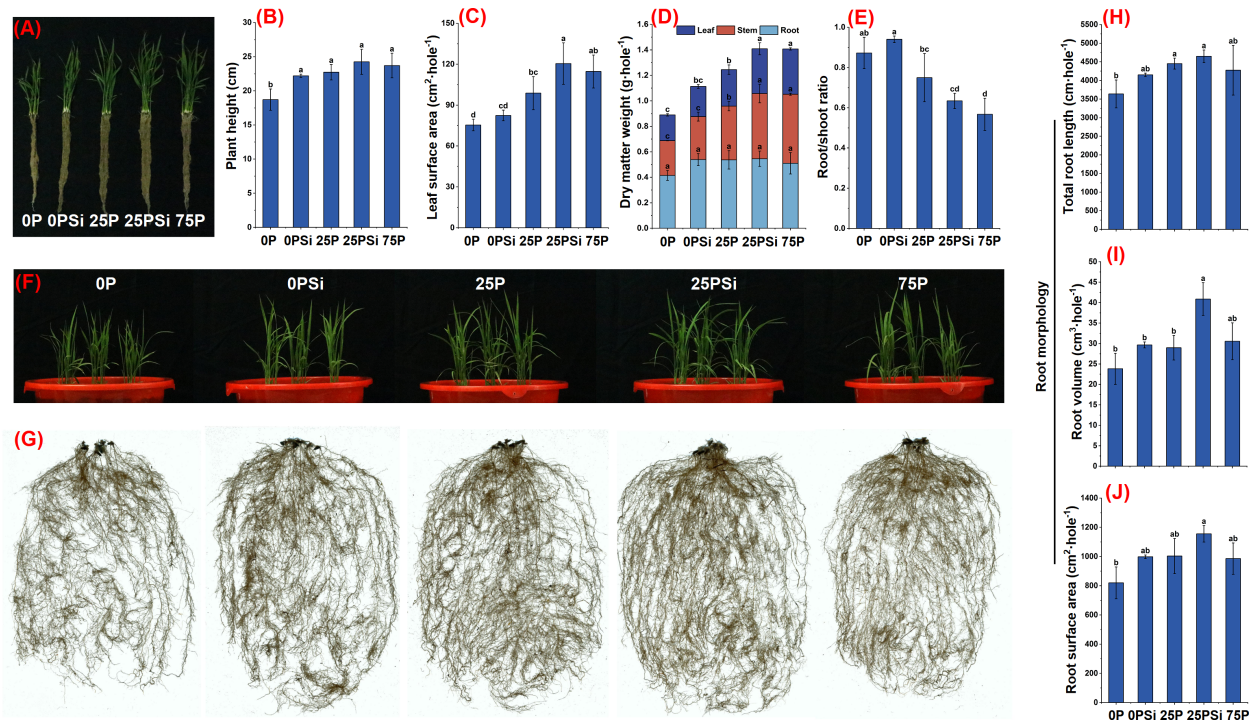

FIGURE 2
Effects of silicon and phosphorus on plant growth and RSA of rice under dry cultivation. **(A)**, Photos of plants; **(B)**, plant height; **(C)**, leaf surface area; **(D)**, dry matter weight; **(E)**, root/shoot ratio; **(F)**, photos of aboveground parts of plants; **(G)**, root photo. **(H–J)**, Root morphology with different diameters, **(H)**, root length; **(I)**, root volume; **(J)**, root surface area. Different letters represent significant differences in the same indicator between different treatments (*P*<0.05).

The promotion effect of silicon on aboveground growth is accompanied by a decrease in root-to-shoot ratio. The two-year pot experiment and field experiment showed the same trend (Supporting Information, Supplementary Figures S2, S3).

Carboxylate secretion by roots under different silicon and phosphorus conditions

Silicon addition promotes carboxylate secretion, with the root system treated with 25PSi exhibiting the highest carboxylate secretion content (Figure 3A). Silicon addition significantly promoted the content of malate and citrate in 0P and 25P treatments ($P<0.05$). Malate content increased by 40.98% and 40.48%, while citrate content increased by 73.26% and 36.52%, respectively, with the 25PSi treatment showing higher values than the 75P treatment. Additionally, silicon addition significantly increased the tartrate content in the 0P treatment ($P<0.05$) and significantly promoted the succinate content in the 25P treatment (P<0.05). The tartrate content in the 0PSI treatment and the succinate content in the 25PSi treatment were significantly higher than those in other treatments ($P<0.05$). Across all treatments, citrate accounted for the highest proportion, while tartrate had the lowest proportion (Figure 3B). These findings indicate that the 25PSi treatment resulted in the highest carboxylate secretion. Silicon addition primarily increased the content and proportion of citrate and tartrate in the 0P treatment, while enhancing the content and proportion of malate and succinate in the 25P treatment.

Soil acid phosphatase activity exhibited a decreasing trend among different phosphorus dosages. Silicon addition increased enzyme activity in 0P and 25P treatments by 2.38% ($P>0.05$) and 8.79% ($P<0.05$), respectively (Figure 3C).

Soil microbial diversity under different silicon and phosphorus conditions

This experiment uses 16S rRNA and ITS rRNA to examine changes in microbial communities. The larger the chao1 index, the more low-abundance species there are in the community. Similarly, the larger the pielou-e index and shannon index, the more evenly distributed the species. For bacterial communities, the addition of silicon increased the chao1 indices in the 0P and 25P treatments (Figure 4A). The pielou-e and shannon indices were similar between the 0P and 0PSi treatments, but showed a successive decline in the 25P, 25PSi, and 75P treatments (Figures 4B, C). PCoA analysis revealed that PC1 explained 16% of the variation, while PC2 explained 10.07% of the variation (Figure 4G). These results indicates differences in bacterial composition in soil after silicon addition. Furthermore, compared with the 25P treatment, the bacterial community composition in the 25PSi treatment was more extensive.

For fungal communities, silicon addition reduced the chao1 indices in the 0P and 25P treatments, with the 75P treatment showing the lowest values (Figure 4D). The addition of silicon significantly decreased the pielou-e and shannon index of the 25P treatment by 15.37% and 16.33%, respectively (Figures 4E, F). PC1 accounted for 14.19% of the fungal community variation in the sample, while PC2 accounted for 10.31% of the fungal community variation in the sample (Figure 4H). Significant group segregation was observed under different phosphorus dosages. Compared with the 0P treatment, the soil fungal composition in the 25P, 25PSi, and 75P treatments differed, leading to distinct fungal community structures in the soil. These findings suggest that silicon addition increases the number of bacterial species, whereas the combination of silicon and 25P reduces fungal diversity.

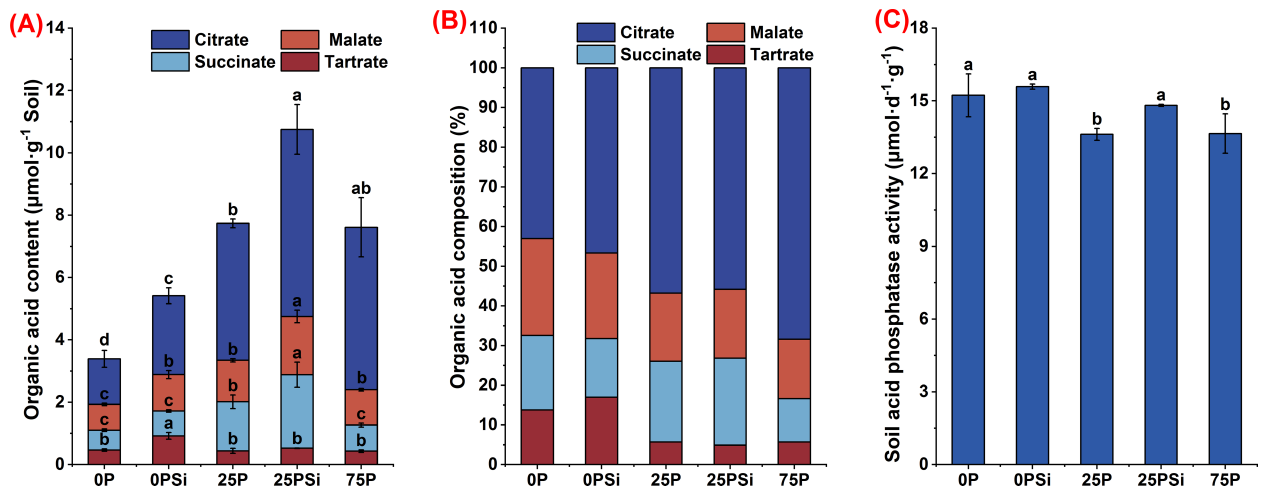

FIGURE 3
Effects of silicon and phosphorus on carboxylate secretion by the rice root system under dry cultivation and soil acid phosphatase activity. **(A)**, Carboxylates content. **(B)**, Carboxylate composition. **(C)**, Activity of soil acid phosphatase. Different letters represent significant differences in the same indicator between different treatments ($P<0.05$).

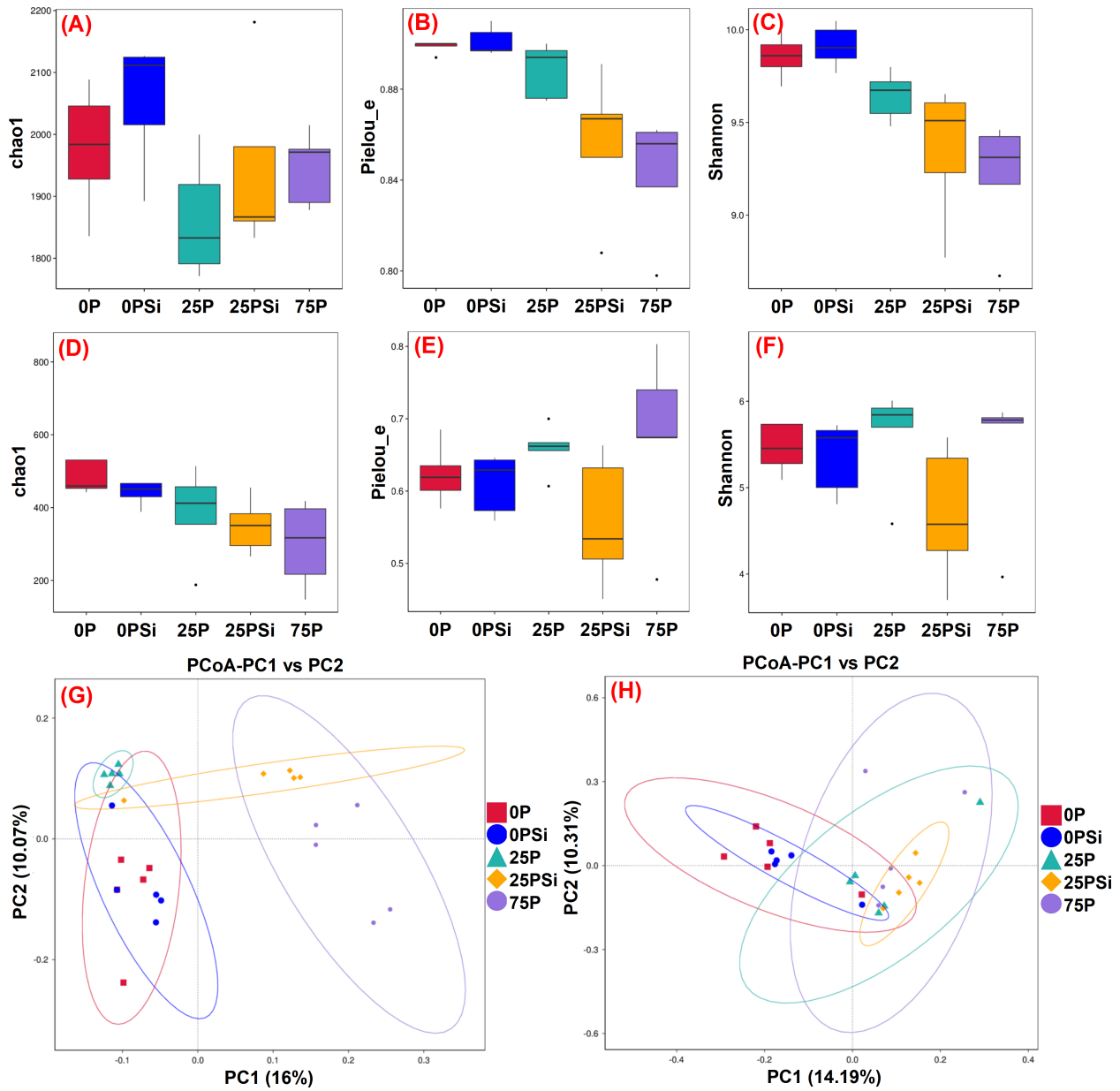

FIGURE 4
Effects of silicon and phosphorus on the α-diversity and β-diversity of soil microorganisms in rice under dry cultivation. **(A–C)** and **(D-F)**, α-diversity of bacteria and fungi, **(A, D)**, chao1; **(B, E)**, pielou_e; **(C, F)**, shannon. **(G, H)**, β-diversity of bacteria and fungi.

Soil microbial community structure and composition under different silicon and phosphorus conditions

The abundance of bacterial communities at the phylum level is shown in Figure 5A. The top 10 most abundant phyla across all samples are *Myxococcota*、*Chloroflexi*、*Verrucomicrobiota*、*Bacteroidota*、*Cyanobacteria*、*Gemmatimonadota*、*Acidobacteriota*、*Actinobacteriota*、*Firmicutes* and *Proteobacteria*. Silicon addition promotes the abundance of *Acidobacteriota* and *Verrucomicrobota* under 0P and 25P treatments. Silicon addition promotes the abundance of *Gemmatimonadota* and *Myxococcata* under 0P conditions and increases the abundance of *Cyanobacteria*, *Bacteroidota*, and *Chloroflexi* treated under 25P conditions. Conversely, the abundance of *Actinobacteriota*, which is associated with phosphorus solubilization, showed a decreasing trend after silicon addition.

The abundance of fungal communities at the phylum level is shown in Figure 5B. *Glomeromycota*、*Mortierellomycota*、*Chytridiomycota*、*Basidiomycota* and *Ascomycota* are the top 5 most abundant phyla among all samples. Adding silicon increases the abundance of *Basidiomycota* by 0P and 25P treatments, and also increases the abundance of *Mortierellomycota* by 0P treatment. The abundance of *Glomeromycota* associated with arbuscular mycorrhizal fungi (AMF) showed a decreasing trend after adding silicon addition.

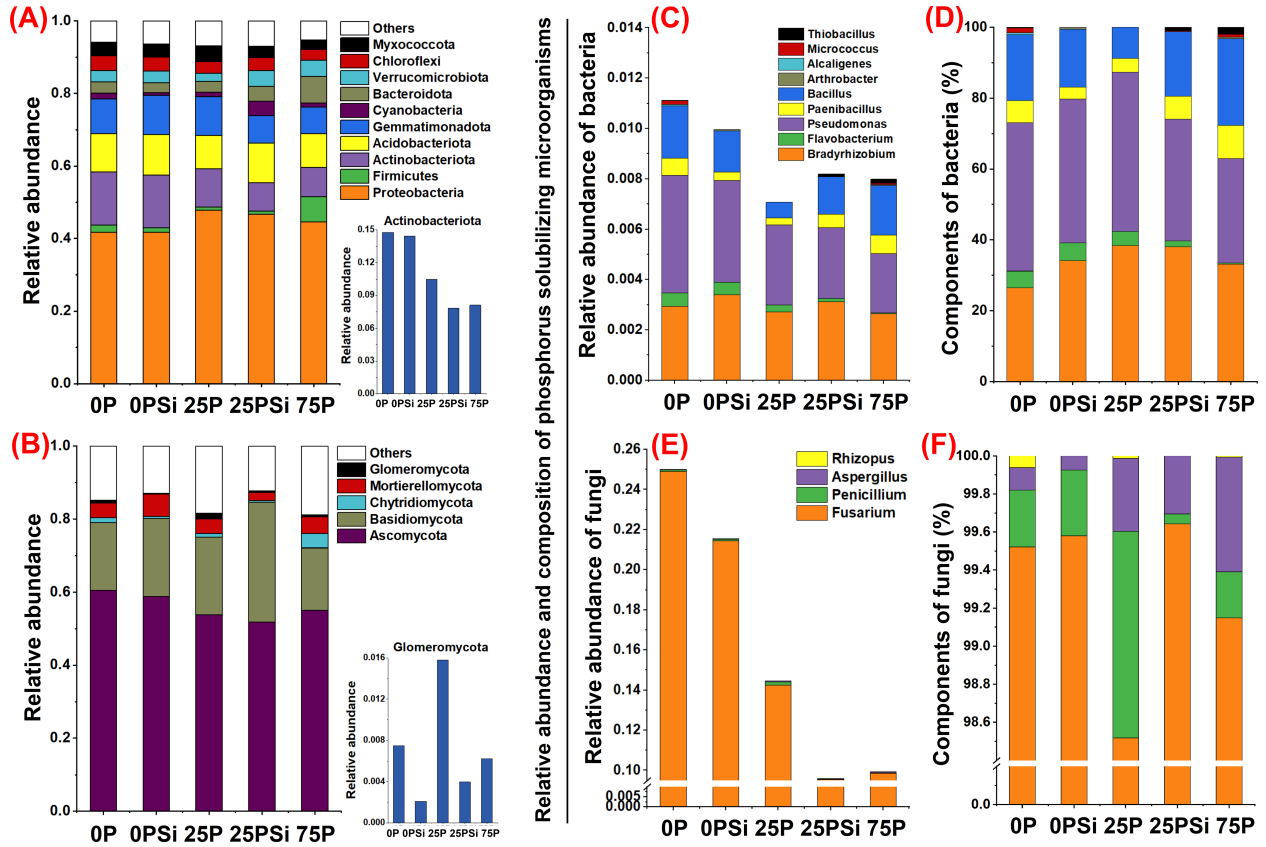

FIGURE 5
Effects of silicon and phosphorus on the abundance of soil microbial phyla and phosphorus solubilizing microbial genera in rice under dry cultivation. **(A, B)**, Relative abundance of bacteria and fungi. **(C–F)**, Relative abundance and composition of phosphorus solubilizing microorganisms, **(C, D)**, phosphate solubilizing bacteria; **(E, F)**, phosphate solubilizing fungi.

Thirteen phosphorus solubilizing microorganisms were identified, including nine phosphorus solubilizing bacteria (Figure 5C) and four phosphorus solubilizing fungi (Figure 5E). In terms of bacteria, silicon addition promoted the abundance of *Bradyrhizobium* under 0P and 25P treatments, while reducing the abundance of *Flavobacteria* and *Pseudomonas*. Among most phosphorus-solubilizing bacteria, it was found that silicon addition also increased the abundance and proportion of *Paenibacillus* and Bacillus under 25P treatment. Additionally, it increased the abundance and proportion of *Arthrobacter* under 0P and *Microcystis* and *Thiobacillus* under 25P, although these three bacteria accounted for a relatively small proportion of the phosphate solubilizing bacteria (Figures 5C, D). In terms of fungi, silicon addition reduced fungal abundance under 0P and 25P treatments, increased the proportion of *Fusarium* and *Penicillium* under 0P treatment, and increased the proportion of *Fusarium* under 25P treatment (Figures 5E, F). In summary, silicon addition induced distinct microbial changes under 0P and 25P treatments, notably decreasing *Actinobacteriota* and *Glomeromycota* abundance at the phylum level. The specific recruitment effect of silicon on phosphate-solubilizing bacteria is primarily reflected in the increased abundance of *Bradyrhizobium* and the proportion of fungi *Fusarium* and *Penicillium* under 0P treatment, and in the increased abundance of *Bradyrhizobium*, *Paenibacillus*, and *Bacillus*, along with the proportion of fungi *Fusarium* under 25P treatment.

Root sugar transport and metabolism under different silicon and phosphorus conditions

As the phosphorus dosage increased, starch, soluble sugar, and NSC showed a decreasing trend. NSC and soluble sugar showed significant differences among different phosphorus dosages ($P<0.05$). Silicon addition significantly reduced the soluble sugar content in the 0P treatment and the starch and soluble sugar content in the 25P treatment ($P<0.05$) (Figures 6B, C). Silicon addition significantly reduced the NSC content in both the 0P and 25P treatments ($P<0.05$) (Figure 6A), and decreased the NSC root-to-shoot ratio (Figure 6D). However, there was no significant difference in the root-to-shoot ratio between 25PSi and 75P treatments ($P>0.05$).

SUTs and SWEETs are involved in the allocation of assimilates in plants, and several genes involved in sucrose transport were studied. Silicon addition downregulated the expression levels of *SUT1* and

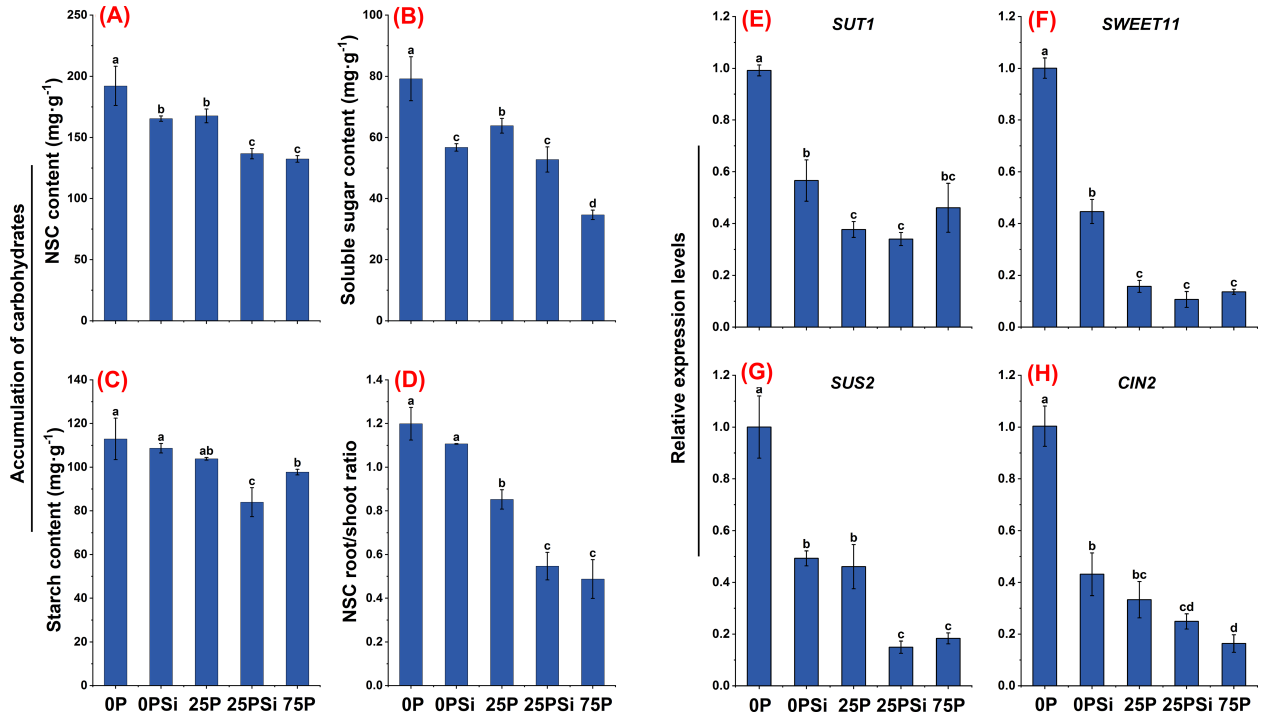

FIGURE 6
Effects of silicon and phosphorus on root sugar transport and metabolism in rice under dry cultivation. **(A–D)**, Accumulation of carbohydrates, **(A)**, non-structural carbohydrate (NSC) content; **(B)**, soluble sugar content; **(C)**, starch content; **(D)**, NSC root/shoot ratio. **(E–H)**, Relative expression levels, **(E)**, *SUT1*; **(F)**, *SWEET11*; **(G)**, *SUS2*; **(H)**, *CIN2*. Different letters represent significant differences in the same indicator between different treatments ($P<0.05$).

SWEET11 in both the 0P and 25P treatments, reaching significant levels between 0P and 0PSi ($P<0.05$). No significant difference was found between 25PSi and 75P ($P>0.05$) (Figures 6E, F). SUS and CIN play key roles in sucrose metabolism. The expression levels of *SUS2* and *CIN2* were downregulated with increasing phosphorus and silicon addition. Silicon addition significantly downregulated the expression levels of *SUS2* and *CIN2* in the 0P treatment ($P<0.05$), and significantly reduced the expression level of *SUS2* in the 25P treatment ($P<0.05$). There was no significant difference between 25PSi and 75P ($P>0.05$) (Figures 6G, H). In summary, compared to 75P, 0P and 25P allocate more NSC to the roots, while silicon addition reduces the allocation of sugar to the roots.

Root energy metabolism under different silicon and phosphorus conditions

We investigated the mitochondrial respiratory electron transport chain complex to elucidate the role of silicon in affecting root energy production. Silicon addition increased the ATP content in the 25P treatment, which was similar to the 75P treatment (Figure 7A). The activity of complex V showed significant differences among different phosphorus dosages ($P<0.05$). The addition of silicon significantly reduced the activity of complex V in the treatments with 0P and 25P (Figure 7B). The activity of complex I was highest in the 0P treatment and lowest in the 75P treatment, with no significant change after silicon addition (Figure 7C). AOX is an important factor influencing the energy production efficiency in plants. Silicon addition increased the AOX activity in the 0P and 25P treatments, although the difference was not significant ($P>0.05$) (Figure 7D).

In terms of energy utilization, the content of ATPase, P-ATPase, and V-ATPase activity decreased with increasing phosphorus dosage and silicon addition. Silicon addition significantly reduced ATPase, P-ATPase content, and V-ATPase activity in 0P and 25P treatments (Figures 7E-G). In summary, compared to the 75P treatment, the 0P and 25P treatments promote energy generation and increase energy consumption, while adding silicon reduces energy consumption (Figure 7H).

Discussion

The effect of silicon addition on plant growth and RSA under low phosphorus conditions in rice under dry cultivation

Plant growth relies on water and mineral nutrients, and the RSA is crucial for obtaining these resources from the soil (Hans et al., 2006). The morphology and distribution of root systems play a crucial role in phosphorus uptake and vary with changes in soil phosphorus levels (Liu, 2021). This study found that the addition of silicon did not significantly affect root weight, but it reduced root branching strength and root length density (Supporting

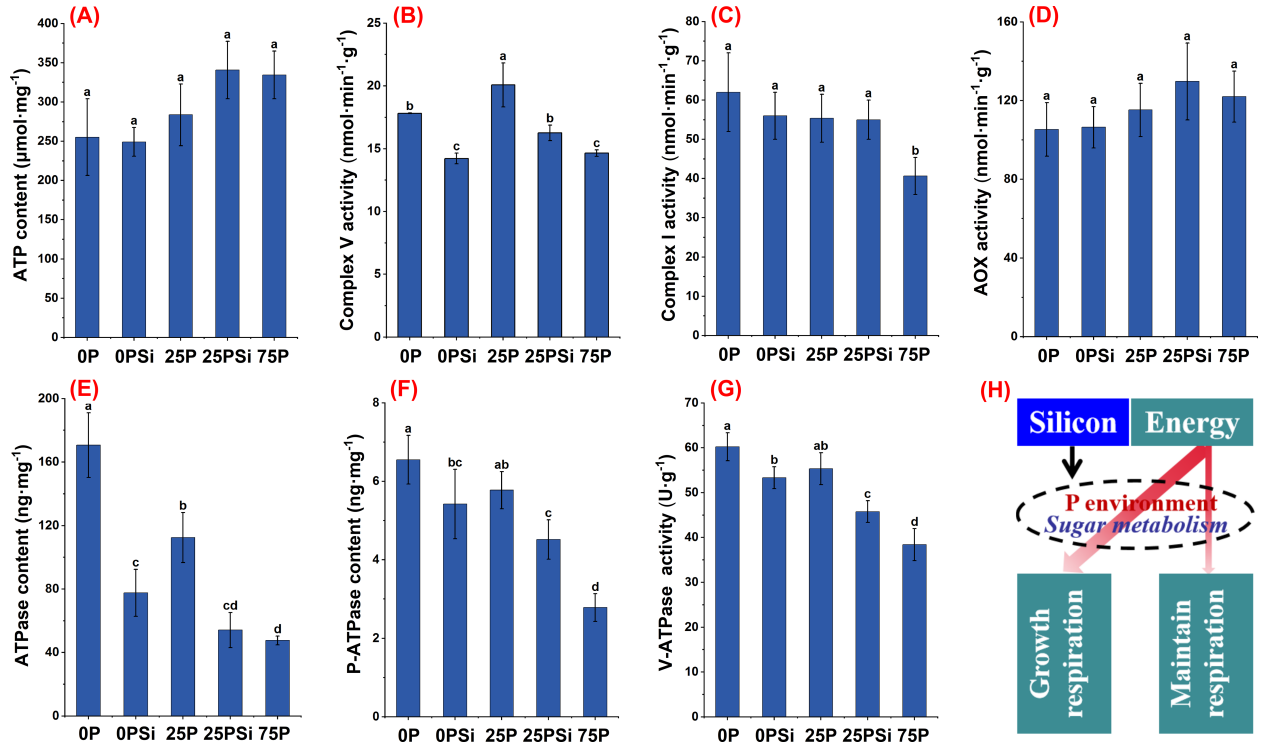

FIGURE 7
Effects of silicon and phosphorus on energy metabolism of rice under dry cultivation. **(A)**, ATP content; **(B)**, Complex V activity; **(C)**, Complex I activity; **(D)**, Alternative oxidase (AOX) activity; **(E)**, ATPase content; **(F)**, Plasma membrane H^+-ATPase (P-ATPase) content; **(G)**, V-ATPase activity; **(H)**, Schematic diagram of silicon affecting energy distribution. Different letters represent significant differences in the same indicator between different treatments ($P<0.05$).

Information, Supplementary Figure S4) and increased root diameter. This suggests that silicon primarily influences root diameter development rather than branching. Shallow roots are beneficial for phosphorus absorption when phosphorus is low, as crops inhibit the elongation of the main root and the growth of root diameter, thereby promoting lateral root development (Sun et al., 2018; Hans et al., 2006). When phosphorus is abundant, crops will inhibit the growth of lateral roots and allocate nutrients for main root elongation and increased root diameter (Lynch, 1995). The author previously found that adding silicon under phosphorus-sufficient conditions can promote root growth and increase root hair quantity in rice under dry cultivation (Jiang et al., 2022, 2023a). This experiment found that adding silicon mainly promotes root volume under low phosphorus conditions. In the case of phosphorus deficiency, the increase in the root-to-shoot ratio is primarily due to the decrease in stem growth and an increase in carbon distribution from stem to root (Hermans et al., 2006). Plant development in this experiment under different phosphorus dosages is consistent with previous conclusions. There is a significant positive correlation between root NSC and root shoot ratio (Figure 8). Further investigation revealed that silicon addition promoted leaf area and plant biomass under both 0P and 25P conditions. The addition of silicon significantly promoted aboveground development under the 25P treatment, accompanied by a decrease in the root-to-shoot ratio. The key finding is that the increase in the root-to-shoot ratio under low phosphorus treatment results from enhanced root respiration, which mobilizes NSC transport to the root system, influencing the development of stems and leaves.

Silicon addition enhances soil phosphorus availability through carboxylate and microbial pathways

There are various forms of phosphorus with different bioavailability in soil (Wei et al., 2020; Liu et al., 2019). In this experiment, the addition of silicon had a greater phosphorus activation effect on the 25P treatment than on the 0P treatment. The decrease in Fe-P after silicon addition may be due to the reduction and dissolution of trivalent iron, which is key to the increase in Olsen-P. Silicon addition simultaneously increases the intermediate cycle phosphorus components (Ca_8-P and Al-P) as reserves, and Olsen-P and P uptake are significantly positively correlated with Ca_8-P and Al-P (Figure 8). Ca_{10}-P and O-P are relatively stable and refractory phosphorus components that are difficult for plants to absorb and utilize (Cao et al., 2020). Excessive phosphorus application leads to the accumulation of significant amounts of excess phosphorus (residual phosphorus) in the soil, which pollutes surface water (Bouwman et al., 2017). We found that adding silicon decreases the content of Ca_{10}-P in soil, offering a new approach to addressing phosphorus pollution. This study presents a

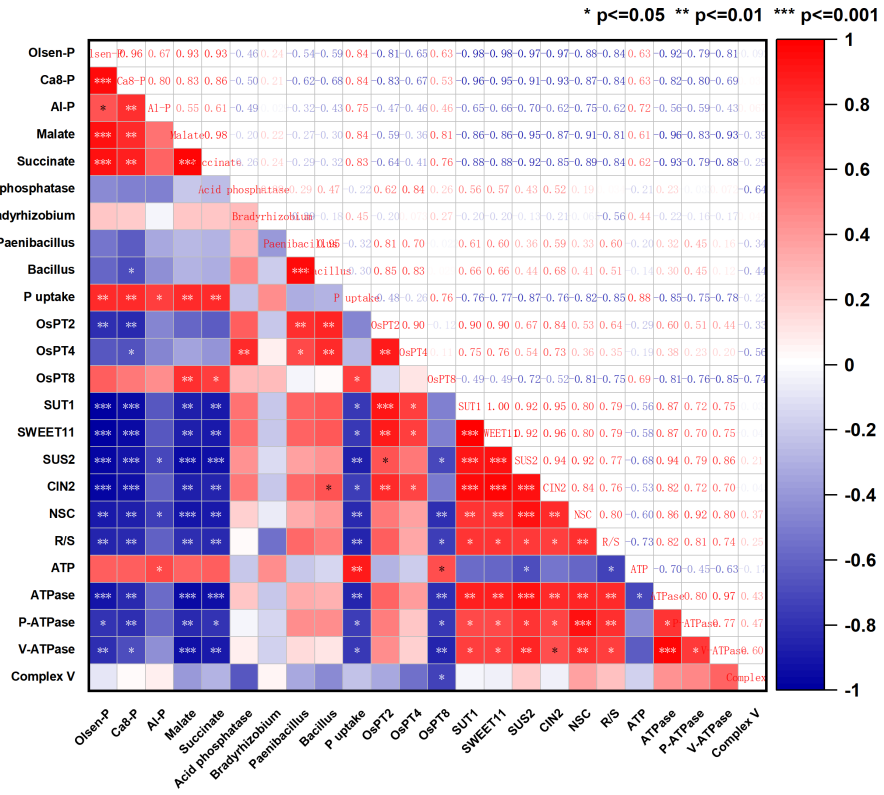

FIGURE 8
Correlation analysis.

novel approach to reducing phosphorus application. Farmers may not necessarily need to apply more phosphorus fertilizer when practicing water-saving rice cultivation; however, this does not imply that silicon fertilizer can be used without restrictions. Therefore, further research is required to optimize the nutrient efficiency of silicon-phosphorus interactions.

P deficiency triggers the release of root exudates, including acid phosphatases and RNases (Wang and Liu, 2018), carboxylates, and protons (Wang and Lambers, 2019), which aid in dissolving phosphorus and releasing it from organic phosphorus compounds, thereby increasing phosphorus availability. Organic anions enhance the soil phosphorus effectiveness by competing with both inorganic and organic phosphorus for adsorption sites, promoting mineral dissolution, and stimulating plant growth and microbial growth (Liao et al., 2020). This experiment found that adding silicon promotes the secretion of carboxylate in the roots of rice under dry cultivation, and also leads to an increase in the Mn concentration in the leaves (Figure 3A; Supporting information, Supplementary Figure S5). This aligns with the finding by Yu et al. (2023) that using leaf Mn concentration can reflect the phosphorus promoting effect mediated by rhizosphere organic acids. We further discovered that the phosphorus release mechanism of silicon through the carboxylate pathway varies under different phosphorus conditions. The addition of silicon to the 0P treatment primarily increases the content and proportion of citrate and tartrate, whereas the addition of silicon to the 25P treatment mainly increases the content and proportion of malate and succinate. Correlation analysis showed a significant positive correlation between malate, succinate, Olsen-P, and P uptake (Figure 8). The promotion effect of silicon on soil acid phosphatase activity is more significant in the 25P treatment.

Currently, the influence of root exudates on the structure of rhizosphere microbial communities has become one of the research hotspots in plant-soil microorganism interactions (Afridi et al., 2024; Bandopadhyay et al., 2024). We found that compared to the 25P treatment, the community composition in the 25Psi treatment was more diverse. The recruitment effect of silicon on phosphate solubilizing bacteria was most evident in *Bradyrhizobium* bacteria and *Fusarium* and *Penicillium* fungi under the 0P treatment. In the 25P treatment, it was mainly reflected in bacteria *Bradyrhizobium*, *Paenibacillus*, *Bacillus*, and fungi *Fusarium*. This indicates that the increased secretion of organic acid anions from the root system stimulates the formation of beneficial microbial communities capable of activating phosphorus. It is interesting to note that this experiment found a decrease in the abundance of *Actinobacteriota* after adding silicon, as well as a decrease in soil fungal density (Supporting information, Supplementary Figure S6). Previous studies have shown that organic acids may promote phosphorus uptake through direct mobilization or selection of phosphorus solubilizing microorganisms (Zhang et al., 2023; Bandopadhyay et al., 2024). However, there are multiple phosphorus solubilizing bacteria in the soil that work independently or cross over, and *Actinobacteriota* is just one of them. Silicon addition promotes the secretion of organic acids under low phosphorus conditions in rice

under dry cultivation and increases the abundance of phosphorus solubilizing bacteria *Bradyrhizobium*, *Paenibacillus*, and *Bacillus*, thereby increasing available phosphorus. Although silicon alleviates low phosphorus limitation, which may weaken the effect and abundance of *Actinobacteriota*, it does not affect plant regulation of root shoot ratio and energy metabolism to absorb phosphorus from the soil and increase phosphorus content. We found that the hydrolysis of phosphorus by silicon is neither an acid phosphatase process driven by actinomycetes nor an AMF driven process. The potential of silicon addition to promote AMF colonization in roots remains to be explored. This experiment indicates that the hydrolysis of phosphorus by silicon is achieved through the selection of phosphorus-solubilizing microorganisms by organic acids.

Silicon addition regulates phosphorus absorption and glucose metabolism through energy metabolism

Plants obtain phosphorus from the soil in the form of orthophosphate ($H_2PO_4^-$) through phosphorus transporters located on the cytoplasmic membrane of their roots (Raghothama and Karthikeyan, 2005). This experiment found that the addition of silicon upregulated the expression levels of phosphorus transporters in the 0P and 25P treatments, significantly increasing the root phosphorus content in the 25P treatment. Plants often adjust their respiration to adapt to stressful conditions such as low temperature (Yu et al., 2020), high temperature (Li et al., 2021), and low light (Li et al., 2023), primarily using energy to sustain respiration rather than growth respiration. This study found that compared to normal phosphorus, the 0P and 25P treatments promote energy production and increase energy consumption, whereas silicon addition reduces energy consumption. This occurs because rice under dry cultivation enhances root respiration and increases the activity of complex V and complex I in response to low phosphorus. The decrease in ATP content during low phosphorus is due to an increase in ATPase, which is primarily activated in response to low phosphorus and helps sustain plant growth. Plasma membrane H^+-ATPase (P-ATPase) generates energy by hydrolyzing ATP to actively pump H^+ out of the cell, creating a proton driving force that facilitates the transport of nutrient ions into the cell (Palmgren, 2001). Adding silicon increases soil phosphorus availability, reduces phosphorus uptake and energy consumption, decreases P-ATPase content and V-ATPase activity, reduces energy consumption for sustaining respiration, and allocates more energy to growth and respiration,

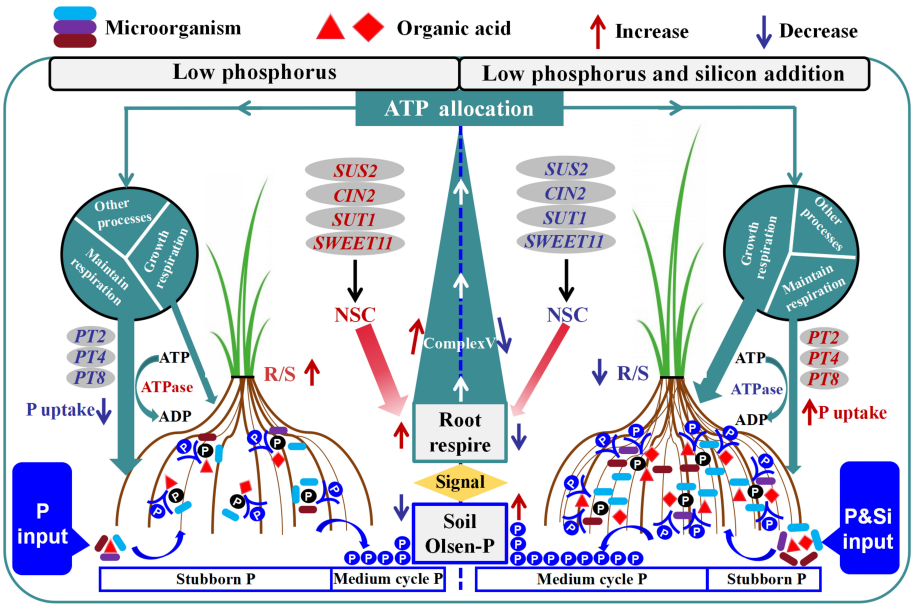

FIGURE 9
Functional description model of silicon phosphorus interaction in phosphorus conversion and absorption in rice under dry cultivation. (Left) Under low phosphorus conditions, there are fewer root exudates and phosphorus solubilizing microorganisms, with a higher proportion of stubborn phosphorus and less Olsen-P. Root perception of low phosphorus environment enhances respiration and increases Complex V activity. NSC distributes to the roots under the action of *SUT1*, *SWEET11*, *SUS2*, and *CIN2* to supply respiration. Resulting in an increase in R/S. A low phosphorus environment leads to an increase in ATPase, which mainly distributes energy to maintain respiration. Phosphorus transport genes (*OsPT2*, *OsPT4*, *OsPT8*) are downregulated, resulting in lower phosphorus uptake. (Right) After adding low phosphorus and silicon, root exudates recruit phosphorus solubilizing microorganisms to form phosphorus solubilizing groups, increasing the proportion of medium cycle phosphorus and Olsen-P. The activity of Complex V decreased. The increase of NSC in the aboveground part leads to a decrease in R/S. After the improvement of phosphorus environment, ATPase decreases, energy mainly supplies growth respiration, phosphorus transport genes are upregulated, and phosphorus absorption increases. In the figure, red font indicates activation, blue font indicates inhibition. NSC, non-structural carbohydrates; R/S, root/shoot ratio.

thereby promoting plant development. Respiration consumes glucose, and when phosphorus is deficient, the aboveground parts of the plant allocate more sucrose to the roots (John and Philip, 2011). Correlation analysis showed that root *SUT1*, *SWEET11*, *SUS2*, *CIN2* were significantly positively correlated with NSC and ATPase (Figure 8). We found that compared to the 75P treatment, the 0P and 25P treatments allocated more NSC to the roots. Silicon addition down regulated the sucrose transport genes *SUT1* and *SWEET11* in the 25P treatment, reducing sucrose allocation to roots and promoting aboveground development. The root-to-shoot ratio of NSC significantly decreased (Figure 6D). Conversion enzymes promote sucrose metabolism and ATP production, primarily responsible for breaking down sucrose into two monosaccharides (Jiang et al., 2020). The downregulation of the sucrose metabolism gene *SUS2* and invertase gene *CIN2* after silicon addition indirectly proves that a phosphorus rich environment reduces the sugar required for root respiration, aligning with changes in energy. In summary, adding silicon regulates energy allocation, facilitates sugar transport, and balances phosphorus uptake, energy consumption, and plant growth in response to changes in phosphorus environment. We found that adding silicon increased the accumulation of phosphorus in roots, but the absorption and utilization of phosphorus in aboveground parts of the plant, along with their underlying mechanisms, require further experimental verification and research.

Conclusion

We have discovered a crucial production technology—the "silicon-phosphorus partnership" (Figure 9)—to enhance phosphorus efficiency and mitigate phosphorus levels in rice under dry cultivation. Silicon addition in low phosphorus conditions can enhance the proportion of circulating phosphorus components in rhizosphere soil, reduce recalcitrant phosphorus components, and thereby increase Olsen-P by 14.37% and root phosphorus content by 7.6%. Silicon addition promotes root volume, phosphatase activity, and carboxylate production, facilitating the targeted recruitment of phosphorus-solubilizing microorganisms. This process improves soil phosphorus availability, and helps regulate energy allocation to maintain a balance between phosphorus uptake and plant growth under fluctuating phosphorus conditions. These findings provide new solutions for efficient cultivation in low phosphorus conditions and enhance our understanding of the role of root-soil-microbe interactions within the silicon-phosphorus partnership in improving the phosphorus environment and regulating phosphorus uptake in rice under dry cultivation. Future research should focus on developing products that integrate silicon-phosphorus composite granulation with phosphorus-solubilizing engineered microbial agents, optimizing nutrient release rates, and exploring the relationship between nutrient release rates of silicon phosphorus partners and nutrient utilization at the plant-root-soil interface.

Data availability statement

The original contributions presented in the study are included in the article/Supplementary Material. Further inquiries can be directed to the corresponding author/s.

Author contributions

HJ: Formal Analysis, Methodology, Writing – original draft. WL: Methodology, Software, Writing – original draft. ZJ: Conceptualization, Data curation, Writing – original draft. YL: Conceptualization, Writing – original draft. XS: Software, Writing – original draft. MN: Investigation, Writing – original draft. HZ: Data curation, Writing – original draft. BX: Investigation, Writing – original draft. GZ: Writing – review & editing. PT: Writing – review & editing. MY: Supervision, Writing – review & editing. ZW: Funding acquisition, Supervision, Writing – review & editing.

Funding

The author(s) declare that financial support was received for the research and/or publication of this article. This work was supported by the Jilin Science and technology development plan project (20240303024NC).

Acknowledgments

We would like to express our gratitude to Professor Guanfu Fu and his team members from the China Rice Research Institute for providing experimental guidance and assistance.

Conflict of interest

The authors declare that the research was conducted in the absence of any commercial or financial relationships that could be construed as a potential conflict of interest.

Generative AI statement

The author(s) declare that no Generative AI was used in the creation of this manuscript.

Publisher's note

Supplementary material

The Supplementary Material for this article can be found online at: https://www.frontiersin.org/articles/10.3389/fpls.2025.1544893/full#supplementary-material

SUPPLEMENTARY TABLE 1
Design of RT-qPCR reaction primer.

SUPPLEMENTARY FIGURE 1
Silicon fertilizer information.

SUPPLEMENTARY FIGURE 2
Plant growth indicators for potted experiment in 2024.

SUPPLEMENTARY FIGURE 3
Plant growth indicators for field experiments in 2024.

SUPPLEMENTARY FIGURE 4
Root system architecture of potted plant experiment in 2023.

SUPPLEMENTARY FIGURE 5
Leaf Mn content.

SUPPLEMENTARY FIGURE 6
Hyphal abundance.

References

Aditi, G., Andrés, R., and Caño-Delgado, I. A. (2020). The physiology of plant responses to drought. *Science* 368, 266–269. doi: 10.1126/science.aaz7614

Afridi, M. S., Kumar, A., Javed, M. A., Dubey, A., De Medeiros, F. H. V., and Santoyo, G. (2024). Harnessing root exudates for plant microbiome engineering and stress resistance in plants. *Microbiol. Res.* 279, 127564. doi: 10.1016/j.micres.2023.127564

Bandopadhyay, S., Li, X. X., Bowsher, A. W., Last, R. L., and Shade, A. (2024). Disentangling plant- and environment-mediated drivers of active rhizosphere bacterial community dynamics during short-term drought. *Nat. Commun.* 15, 6347. doi: 10.1038/S41467-024-50463-13

Bi, J. G., Hou, D. P., Zhang, X. X., Tan, J. S., Bi, Q. Y., Zhang, K. K., et al. (2021). A novel water-saving and drought-resistance rice variety promotes phosphorus absorption through root secreting organic acid compounds to stabilize yield under water-saving condition. *J. Clean. Prod.* 315, 127992. doi: 10.1016/J.JCLEPRO.2021.127992

Bouwman, F. A., Beusen, W. H. A., Lassaletta, L., Apeldoorn, D. F. A., Grinsven, H. J. M. V., Zhang, J., et al. (2017). Lessons from temporal and spatial patterns in global use of N and P fertilizer on cropland. *Sci. Rep.* 7, 40366. doi: 10.1038/SREP40366

Cao, D. Y., Lan, Y., Liu, Z. Q., Yang, X., Liu, S. N., He, T. Y., et al. (2020). Responses of organic and inorganic phosphorus fractions in brown earth to successive maize stover and biochar application: a 5-year field experiment in Northeast China. *J. Soils Sediments.* 20, 1–10. doi: 10.1007/s11368-019-02508-y

DuBois, M., Gilles, K. A., Hamilton, J. K., Rebers, P. A., and Smith, F. (2002). Colorimetric method for determination of sugars and related substances. *Anal. Chem.* 28, 350–356. doi: 10.1021/ac60111a017

Fiori, J., Amadesi, E., Fanelli, F., Tropeano, C. V., Rugolo, M., and Gotti, R. (2018). Cellular and mitochondrial determination of low molecular mass organic acids by LC–MS/MS. *J. Pharm. Biomed. Anal.* 150, 33–38. doi: 10.1016/j.jpba.2017.11.071

Guo, Z. L., Wang, S. C., Zhang, F., Xiang, D. H., Yang, J., Li, D., et al. (2024). Common and specific genetic basis of metabolite-mediated drought responses in rice. *Stress. Biol.* 4, 6. doi: 10.1007/S44154-024-00150-4

Hans, L., Gregory, R. C., Patrick, G., John, K., Etienne, L., Stuart, J. P., et al. (2012). Proteaceae from severely phosphorus-impoverished soils extensively replace phospholipids with galactolipids and sulfolipids during leaf development to achieve a high photosynthetic phosphorus-use-efficiency. *New Phytol.* 196, 1098–1108. doi: 10.1111/j.1469-8137.2012.04285.x

Hans, L., Michael, W. S., Michael, D. C., Stuart, J. P., and Erik, J. V. (2006). Root structure and functioning for efficient acquisition of phosphorus: Matching morphological and physiological traits. *Ann. Bot.* 9, 693–713. doi: 10.1093/AOB/MCL114

Hermans, C., Hammond, J. P., White, P. J., and Verbruggen, N. (2006). How do plants respond to nutrient shortage by biomass allocation? *Trends Plant Sci.* 11, 610–617. doi: 10.1016/j.tplants.2006.10.007

Jeffrey, S. A., Arren, B., Andrew, D. H., Harvey, M. A., Mark, S., Lee, J. S., et al. (2019). Engineering strategies to boost crop productivity by cutting respiratory carbon loss. *Plant Cell* 31, 297–314. doi: 10.1105/tpc.18.00743

Jiang, H., Song, Z., Su, Q. W., Wei, Z. H., Li, W. C., Jiang, Z. X., et al. (2022). Transcriptomic and metabolomic reveals silicon enhances adaptation of rice under dry cultivation by improving flavonoid biosynthesis, osmoregulation, and photosynthesis. *Front. Plant Sci.* 13. doi: 10.3389/FPLS.2022.967537

Jiang, H., Thobakgale, T., Li, Y. Z., Liu, L. W., Su, Q. W., Cang, B. F., et al. (2021). Construction of dominant rice population under dry cultivation by seeding rate and nitrogen rate interaction. *Sci. Rep.* 11, 7189. doi: 10.1038/S41598-021-86707-Z

Jiang, H., Xing, X., Meng, X., Chen, J. L., Yu, K., Xu, X. T., et al. (2023b). Research progress in water-saving cultivation of rice in China. *Crop Sci.* 63, 2623–2635. doi: 10.1002/CSC2.21068

Jiang, H., Xu, X. T., Sun, A. R., Bai, C. Y., Li, Y. Z., Nuo, M., et al. (2023a). Silicon nutrition improves the quality and yield of rice under dry cultivation. *J. Sci. Food Agric.* 104, 1897–1908. doi: 10.1002/JSFA.13098

Jiang, N., Yu, P. H., Fu, W. M., Li, G. Y., Feng, B. H., Chen, T. T., et al. (2020). Acid invertase confers heat tolerance in rice plants by maintaining energy homoeostasis of spikelets. *Plant Cell Environ.* 43, 1273–1287. doi: 10.1111/pce.13733

John, P. H., and Philip, J. W. (2011). Sugar signaling in root responses to low phosphorus availability. *Plant Physiol.* 156, 1033–1040. doi: 10.1104/pp.111.175380

Li, G. Y., Chen, T. T., Feng, B. H., Peng, S. B., Tao, L. X., and Fu, G. F. (2021). Respiration, rather than photosynthesis, determines rice yield loss under moderate high-temperature conditions&. *Front. Plant Sci.* 12. doi: 10.3389/FPLS.2021.678653

Li, H. B., Feng, B. H., Li, J. C., Fu, W. M., Wang, W. T., Chen, T. T., et al. (2023). RGA1 alleviates low-light-repressed pollen tube elongation by improving the metabolism and allocation of sugars and energy. *Plant Cell Environ.* 46, 1363–1383. doi: 10.1111/pce.14547

Liao, D., Zhang, C. C., Li, H. J., Lambers, H., and Zhang, F. S. (2020). Changes in soil phosphorus fractions following sole cropped and intercropped maize and faba bean grown on calcareous soil. *Plant Soil* 448, 1–15. doi: 10.1007/s11104-020-04460-0

Liu, D. (2021). Root developmental responses to phosphorus nutrition. *JIPB* 63, 1065–1090. doi: 10.1111/JIPB.13090

Liu, H. Y., Wang, R. Z., Wang, H. Y., Cao, Y. Z., Dijkstra, F. A., Shi, Z., et al. (2019). Exogenous phosphorus compounds interact with nitrogen availability to regulate dynamics of soil inorganic phosphorus fractions in a meadow steppe. *Biogeosciences* 16, 4293–4306. doi: 10.5194/bg-16-4293-2019

Liu, P., Yan, H. H., Xu, S. G., Lin, X., Wang, W. Y., and Wang, D. (2022). Moderately deep banding of phosphorus enhanced winter wheat yield by improving phosphorus availability, root spatial distribution, and growth. *Soil Till Res.* 220, 105388. doi: 10.1016/J.STILL.2022.105388

Lynch, J. (1995). Root architecture and plant productivity. *Plant Physiol.* 109, 7–13. doi: 10.1104/pp.109.1.7

Maryam, S. (2021). Global water shortage and potable water safety; Today's concern and tomorrow's crisis. *Environ. Int.* 158, 106936. doi: 10.1016/J.ENVINT.2021.106936

Olsen, S., Cole, C., Watanabe, F., and Dean, L. (1954). Estimation of available phosphorus in soils by extraction with sodium bicarbonate. *USDA Circ.* 939, 1–19.

Palmgren, M. G. (2001). Plant plasma membrane H+-atpases: powerhouses for nutrient uptake. *Annu. Rev. Plant Physiol. Plant Mol. Biol.* 52, 817–845. doi: 10.1146/annurev.arplant.52.1.817

Raghothama, G. K., and Karthikeyan, S. A. (2005). Phosphate acquisition. *Plant Soil* 274, 37–49. doi: 10.1007/1-4020-4099-72

Siddiqi, M. Y., and Glass, A. D. M. (1981). Utilization index: A modified approach to the estimation and comparison of nutrient utilization efficiency in plants. *J. Plant Nutr.* 4, 289–302. doi: 10.1080/01904168109362919

Song, C., Sarpong, C. K., Zhang, X. F., Wang, W. W. J., Wang, L. F., Gan, Y. F., et al. (2021). Mycorrhizosphere bacteria and plant-plant interactions facilitate maize P acquisition in an intercropping system. *J. Clean. Prod.* 314, 127993. doi: 10.1016/J.JCLEPRO.2021.127993

Sun, B. R., Gao, Y. Z., and Lynch, J. P. (2018). Large crown root number improves topsoil foraging and phosphorus acquisition. *J. Plant Physiol.* 177, 90–104. doi: 10.1104/pp.18.00234

Wang, Y., and Lambers, H. (2019). Root-released organic anions in response to low phosphorus availability: recent progress, challenges and future perspectives. *Plant Soil* 447, 135–156. doi: 10.1007/s11104-019-03972-8

Wang, L. S., and Liu, D. (2018). Functions and regulation of phosphate starvation-induced secreted acid phosphatases in higher plants. *Plant Sci.* 271, 108–116. doi: 10.1016/j.plantsci.2018.03.013

Wang, G., Shen, X. R., Bai, C. Y., Zhuang, Z. X., Jiang, H., Yang, M. Y., et al. (2023). Metabolomic study on the quality differences and physiological characteristics between rice cultivated in drought and flood conditions. *Food Chem.* 425, 135946. doi: 10.1016/J.FOODCHEM.2023.135946

Wei, X. S., Cang, B. F., Yu, K., Li, W. C., Tian, P., Han, X., et al. (2022). Physiological characterization of drought responses and screening of rice varieties under dry cultivation. *Agron. J.* 12, 2849–2849. doi: 10.3390/AGRONOMY12112849

Wei, W. L., Zhang, S. R., Wu, L. P., Cui, D. J., and Ding, X. D. (2020). Biochar and phosphorus fertilization improved soil quality and inorganic phosphorus fractions in saline-alkaline soils. *Arch. Agron. Soil Sci.* 67, 1177–1190. doi: 10.1080/03650340.2020.1784879

Wen, Z. H., Pang, J. Y., Tueux, G., Liu, Y. F., Shen, J. B., Ryan, M. H., et al. (2020). Contrasting patterns in biomass allocation, root morphology and mycorrhizal symbiosis for phosphorus acquisition among 20 chickpea genotypes with different amounts of rhizosheath carboxylates. *Funct. Ecol.* 34, 1311–1324. doi: 10.1111/1365-2435.13562

Xia, H., Zhang, X. X., Liu, Y., Bi, J. G., Ma, X. S., Zhang, A. N., et al. (2022). Blue revolution for food security under carbon neutrality: A case from the water-saving and drought-resistance rice. *Mol. Plant* 15, 1401–1404. doi: 10.1016/J.MOLP.2022.07.014

Xiao, X. L., Zhang, J. Q., Satheesh, V., Meng, F. X., Gao, W. L., Dong, J. S., et al. (2022). SHORT-ROOT stabilizes PHOSPHATE1 to regulate phosphate allocation in Arabidopsis. *Nat. Plants.* 8, 1074–1081. doi: 10.1038/S41477-022-01231-W

Yu, P. H., Jiang, N., Fu, W. M., Zheng, G. J., Li, G. Y., Feng, B. H., et al. (2020). ATP hydrolysis determines cold tolerance by regulating available energy for glutathione synthesis in rice seedling plants. *Rice* 13, 23. doi: 10.1186/s12284-020-00383-7

Yu, R. P., Su, Y., Lambers, H., van Ruijven, J., An, R., Yang, H., et al. (2023). A novel proxy to examine interspecific phosphorus facilitation between plant species. *New Phytol.* 239, 1637–1650. doi: 10.1111/NPH.19082

Zhang, F. B., Hou, Y. X., Zed, R., Mauchline, T. H., Shen, J. B., Zhang, F. S., et al. (2023). Root exudation of organic acid anions and recruitment of beneficial actinobacteria facilitate phosphorus uptake by maize in compacted silt loam soil. *SBB* 184, 109074. doi: 10.1016/j.soilbio.2023.109074

Zou, T., Zhang, X., and Davidson, E. A. (2022). Global trends of cropland phosphorus use and sustainability challenges. *Nature* 611, 81–87. doi: 10.1038/S41586-022-05220-Z

frontiers | Frontiers in Plant Science

TYPE Original Research
PUBLISHED 27 March 2025
DOI 10.3389/fpls.2025.1522534

OPEN ACCESS

EDITED BY
Xiao-Dong Yang,
Ningbo University, China

REVIEWED BY
Qiangbo Liu,
Shandong Agricultural University, China
Zhoukang Li,
Xinjiang Agricultural University, China

*CORRESPONDENCE
Haijiang Wang
wanghaijiang@shzu.edu.cn

†These authors have contributed equally to this work and share first authorship

RECEIVED 04 November 2024
ACCEPTED 28 February 2025
PUBLISHED 27 March 2025

CITATION
Li W, Zhong M, Wang H, Shi X, Song J, Wang J and Zhang W (2025) Exogenous carbon inputs alleviated salt-induced oxidative stress to cotton in salinized field by improving soil aggregate structure and microbial community. *Front. Plant Sci.* 16:1522534. doi: 10.3389/fpls.2025.1522534

Exogenous carbon inputs alleviated salt-induced oxidative stress to cotton in salinized field by improving soil aggregate structure and microbial community

Weidi Li[1,2†], Mingtao Zhong[1,2†], Haijiang Wang[1,2*], Xiaoyan Shi[1,2], Jianghui Song[1,2], Jingang Wang[1,2] and Wenxu Zhang[1,2]

[1]Agricultural College, Shihezi University, Shihezi, Xinjiang, China, [2]Key Laboratory of Oasis Ecological Agriculture of Xinjiang Production and Construction Corps, Shihezi University, Shihezi, Xinjiang, China

High concentrations of salt ions in salinized soils not only destroy soil structure, but also inhibit crop growth. Straw and straw-derived biochar have great potential in improving soil structure, reducing soil salinity, improving soil environment, and alleviating salt stress. However, the effects and mechanisms of exogenous addition of different carbon sources on the aggregate structure and microbial community of soils with different salinization degrees in cotton fields as well as the antioxidant defense system of cotton are still unclear. In this column experiment since 15 March, 2023, three soil salt contents (1.5 (S1), 5 (S2), and 10 (S3) g/kg) and five carbon treatments (straw incorporation: 6 t/hm^2 (C1), 12 t/hm^2 (C2); biochar incorporation: 2.25 t/hm^2 (B1), 4.5 t/hm^2 (B2); CK: no straw and biochar incorporation) were designed. Then, the effects of straw and biochar incorporation on the particle size distribution of soil aggregates, bacterial and fungal communities, and cotton leaf antioxidant system in S1, S2, and S3 soils were explored. The results showed that straw and biochar incorporation, especially B2, significantly reduced the salt content of S1, S2, and S3 soils, but increased the proportion of macroaggregates by 7.01%–13.12%, 5.03%–10.24%, and 4.16%–8.31%, respectively, compared with those of CK. Straw and biochar incorporation, especially C2, increased the abundances of Actinobacteria, Acidobacteria, and Enterobacteriaceae, but decreased that of Proteobacteria, compared with CK. Besides, straw and biochar incorporation significantly increased the superoxide dismutase (SOD) and catalase (CAT) activities in salt-stressed cotton leaves, and decreased the malondialdehyde (MDA) content and peroxidase (POD) activity, compared with CK. It should be noted that the alleviating effect of straw and biochar incorporation on salt stress gradually decreased with the growth of cotton and the increase of soil salinity. In

summary, straw and biochar incorporation could significantly reduce the salt content of salinized soils, increase the proportion of soil macroaggregates and microbial diversity, and alleviate the salt stress in cotton. This study will provide a scientific basis for the improvement and utilization of salinized soils.

KEYWORDS

biochar, cotton physiology, straw, salt gradient, soil aggregates

1 Introduction

Soil salinization is a global environmental problem that needs to be solved urgently. About 25% of arable land worldwide is affected by soil salinization. The accumulation of large amounts of salt ions such as Na^+ and Cl^- in salinized soils leads to reduced soil cohesion and stability (Xie et al., 2020), soil aggregate disintegration (Rengasamy and Olsson, 1991), and soil compaction, decreasing soil permeability (Tang et al., 2020). Soil microorganisms play an important role in soil nutrient cycling and ecosystem function (Sahu et al., 2019). However, the increase of soil salinity changes the soil microbial ecological function and metabolic pathways (Haj Amor et al., 2022), causing decreases in the ability of soil microorganisms to utilize substrates as well as the diversity and abundance of bacterial and fungal communities (Feng et al., 2024; Wei et al., 2024; Kumawat et al., 2022). Soil microbial communities have a close relationship with soil aggregates (Luo et al., 2018; Zhang et al., 2021). However, differences in the effects of different soil salinity on soil aggregate structure and microbial community and their interactions are still unclear.

Massive accumulation of base cations in the soil causes osmotic stress, ionic toxicity, and physiological drought in crops (Liu et al., 2018; Arif et al., 2020). At the same time, crops adsorb large amounts of Na^+ from soil, and the Ca^{2+} on crop cell membrane is replaced by Na^+ (Jin et al., 2017), causing membrane leakage and limited crops' absorption of mineral elements. In addition, salt stress leads to the production of excessive reactive oxygen species (ROS), causing oxidative damage to crops' cell structure and suppression on the nutrient synthesis and transport (Liu et al., 2018; Arif et al., 2020). Crops could resist salt stress through regulating its redox system, i.e., the activities of superoxide dismutase (SOD), catalase (CAT), and POD (Nefissi Ouertani et al., 2021). However, under high soil salinity conditions, the negative impacts on crops remains significant (Zhao et al., 2021).

Straw and straw-derived biochar have great potential in improving soil structure and alleviate salt stress in crops (Cen et al., 2021; Singh et al., 2021). Straw incorporation can improve soil aeration porosity, cut off soil capillaries, and prevent salt aggregation (Bai et al., 2024). In addition, straw incorporation promotes the dissolution of soluble salts in salinized soils, reducing the accumulation of salts in the soils (Ran C, et al., 2023). Biochar, with characteristics of large pores and specific surface area, can increase soil aeration and permeability, promoting salt leaching (Da Silva Mendes et al., 2021). Biochar can also adsorb salt ions on its surface or in its pores, reducing the salts in the soil (Siedt et al., 2021). The stable, loose, and porous structure and strong adsorption capacity of biochar can significantly promote the polymerization and cementation of soil particles and nutrients, promoting the formation of aggregates (Ghorbani and Amirahmadi, 2024). Duan et al. (2021) showed that Ca^{2+} and Mg^{2+} contained in biochar could replace Na^+ in salinized soils, stimulate the combination of polyvalent cations and soil particles, increase soil aggregates, and reduce salt content. Zhao et al. (2020) reported that straw and biochar incorporation significantly increased the Shannon and Simpson diversity indexes of soil microbial communities by increasing the soil C/N ratio compared with the control. Wang et al. (2021) reported that straw incorporation significantly increased the relative abundances of Proteobacteria and Actinobacteria, while biochar incorporation significantly increased the relative abundances of Acidobacteria and Nitrospira, compared with the control. In addition, Zhu et al. (2022) found that straw and biochar incorporation significantly reduced the malondialdehyde (MDA) content and relative conductivity in crops, increased the activity of leaf antioxidant enzymes, and maintained the stability of cell membrane structure and function.

In summary, high soil salinity damages soil structure (Tang et al., 2020), inhibits soil microbial activity (Feng et al., 2024), and causes adverse impacts on plants such as metabolic disorders (Zhang W, et al., 2019). Straw and biochar incorporation can improve the physicochemical properties of salinized soils. However, it is not clear whether straw and biochar incorporation for soils with different salinization degrees can improve the physiological responses of crops to salt stress by adjusting soil aggregate structure and microbial community. Especially, the interaction effect of crops, aggregates, and microorganisms in different salinized soils mediated by straw and biochar application also needs to be further explored. In this study, straw and straw-derived biochar were incorporated into salinized soils with different salt contents, aiming to clarify their effects on the soil salinity and salt stress in cotton. The following hypotheses were proposed: (1) Straw and biochar incorporation might improve the aggregate structure and microbial community structure of soils with different salinization degrees; (2) The improved soil aggregate structure and microbial community might regulate the antioxidative system of cotton,

alleviating the salt stress; (3) There might be a specific interaction between salinized soil aggregates, microorganisms, and crops mediated by straw and biochar application. This study will provide a scientific basis for the remediation and utilization of salinized soils in arid and semi-arid areas.

2 Materials and methods

2.1 Test materials

2.1.1 Study area

This study was carried out in 2023 at the experimental field of Agricultural College of Shihezi University (44°19′N, 86°58′E) in Shihezi, Xinjiang, China. The region had a temperate continental climate. The average annual precipitation was only about 220 mm, while the average annual evaporation was about 1500 mm. The average annual precipitation was only about 220 mm, while the average annual evaporation was about 1500 mm (Figure 1). The soil type was calcareous soil, and the texture was loam. For the soil used in this experiment, one part was collected from the nearby cotton fields under continuous cropping for more than 10 years (salt content of the 0–30 cm layer: 1.50 $g{\cdot}kg^{-1}$). The other part was collected from the salinized wasteland of Beiwucha in Manas County, Xinjiang, China (salt content of the 0–30 cm layer: 22.35 $g{\cdot}kg^{-1}$). The salt ions in the two soils were similar, mainly including Na^+, Ca^{2+}, K^+, SO_4^{2-}, and Cl^-. The wasteland soil and the cotton field soil were mixed in different proportions to obtain soils with different salt contents (Table 1).

2.1.2 Biochar preparation

Cotton straw was collected from the cotton fields in the study area after the cotton harvest. After removing the roots and impurities on the surface of the straw with deionized water, the straw was air-dried, crushed, and passed through a 2 mm sieve for later use. The crushed cotton straw was pyrolyzed in a muffle furnace under oxygen limiting condition. The temperature was raised to 450 ℃ at a uniform rate for 6-hour continuous pyrolysis. After cooling to room temperature, the straw was dried at 75 ℃ for 24 h, crushed, and passed through a 2 mm sieve. Finally, the prepared cotton straw-derived biochar was collected.

2.2 Experimental design

This column experiment began on 15 March, 2023. Experimental plots were arranged in a randomized block design. By mixing the soils from the above two sources, three soil salt contents were obtained, namely non-salinization (S1): 1.5 $g{\cdot}kg^{-1}$, mild salinization (S2): 5 $g{\cdot}kg^{-1}$, and moderate salinization (S3): 10 $g{\cdot}kg^{-1}$. Cotton straw and biochar were used as exogenous carbons, and five carbon treatments were designed, including no carbon (CK), 6 $t{\cdot}hm^{-2}$ of straw incorporation (C1), 12 $t{\cdot}hm^{-2}$ of straw incorporation (C2), 2.25 $t{\cdot}hm^{-2}$ of biochar incorporation (B1, equal to C1 in carbon content), 4.5 $t{\cdot}hm^{-2}$ of biochar incorporation (B2, equal to C2 in carbon content). There were a total of 15 treatments, and each treatment had three replicates/columns. The pre-processed straw and biochar were evenly mixed into the 0–30 cm soil layer. Cotton seeds (variety Xinluzao 43) were sown after thirty days (16 April, 2023). The soil columns were 36 cm in diameter and 80 cm in height (Figure 2). To avoid the leaching of water and salts, the bottom of the soil columns was sealed with an impermeable membrane. One month before planting, the prepared straw and biochar were evenly mixed with the 0–30 cm soil layer. The mixed soils were layered into the soil columns while keeping the bulk density at 1.42 $g{\cdot}cm^{-3}$. Then, the columns were buried into the field, keeping the soil column top flush with the ground surface. Film mulching and drip irrigation were adopted. Four cotton were planted under one film, and each drip tape supplied water for two rows of cotton. Eight cotton seeds were evenly sown in each soil column, and four seedlings were retained in each soil column after emergence. During the whole growth period of cotton, cotton plants were irrigated every 15 days (10 times in total), and the total irrigation volume was 5400 $m^3{\cdot}hm^{-2}$. The irrigation volume was controlled by water meters. According to the local fertilization scheme, 360 $kg{\cdot}hm^{-2}$ of urea (N, 46.2%), 105 $kg{\cdot}hm^{-2}$ of calcium superphosphate (P_2O_5, 46%), and 75 $kg{\cdot}hm^{-2}$ of potassium sulfate (K_2O, 50%) were applied. Two-fifths of the fertilizers were applied before sowing, and the remaining were topdressed through the drip irrigation system after dissolving in water. Other management measures were consistent with those in the local fields.

2.3 Sampling

2.3.1 Collection and preservation of soil samples

At the bolling stage (18 July, 2023), 200 g of soil (0–30 cm layer) was collected from each treatment by a ring cutter. After removing the soil sample part contacting with the shovel, the time, place, and amount of sampling were recorded in detail. Then, the samples were taken back to the laboratory, and shaking and tipping over were avoided when transporting samples. In the laboratory, the impurities such as roots and stones were removed from the soil samples. Then, the soil samples were placed in a ventilated place to dry naturally for the determination of soil aggregates.

In addition, soil drills were used to collect soil samples of the 0–30 cm layer (three replicates per treatment). About 100 g of soil was collected from each column. A total of 45 soil samples were collected. The soil samples were put into sealed bags, air-purged, sealed, and stored in an ice box, to prevent moisture evaporation and ensure sample activity. After taking back to the laboratory, the soil samples were divided into two parts. One part was subjected to impurity (stones and animal residues) removing and sieving (2 mm). Then, the samples were stored in sterile sealed bags for the determination of soil moisture content (SMC) and soil microbial composition. The other part was air-dried, ground, and sieved through a 2 mm sieve for the determination of soil conductivity, cation exchange capacity (CEC), and pH.

2.3.2 Cotton plant sampling

In the budding (1 June, 2023), flowering (20 June), and bolling (18 July) stages of cotton, three cotton plants were randomly selected from each treatment for destructive sampling. The third and fourth leaves on the plant top were put into an ice box and brought back to the laboratory. The samples were washed separately with water, 1% hydrochloric acid, and deionized water. After drying with absorbent paper, the samples were wrapped with silver paper and stored in an ultra-low temperature refrigerator at −80°C for the determination of oxidative stress-related indicators.

2.4 Determination methods

2.4.1 Determination of soil properties

The weight of each particle-size fraction of soil aggregates was determined by drying-sieving method. Specifically, 100 g of air-dried soil samples were sequentially sieved with sieves with pore sizes of 1, 0.5, and 0.25 mm (the sieves had a bottom and cover), to obtained the aggregates larger than 1 mm ($AGG_{>1}$) and in the range of 1–0.5 mm ($AGG_{1-0.5}$) and 0.5–0.25 mm ($AGG_{0.5-0.25}$) in diameter. After sieving, the aggregates on each sieve and the soil particles with a particle size smaller than 0.25 mm ($AGG_{<0.25}$) were separately weighed, to obtain the weight of the aggregates of different particle sizes. Then, the proportion of the aggregates of each particle size was calculated, followed by the calculation of geometric mean diameter (GMD) (Equation 1), mean weight diameter (MWD) (Equation 2), and proportion of soil aggregates greater than 0.25 mm ($AGG_{>0.25}$) in the total aggregates ($R_{0.25}$) (Equation 3) (Wan et al., 2024). Soil pH was determined by a pH meter (Shilu Instrument Co. Ltd, Shanghai, China) (soil: water = 1: 2.5). Soil electrical conductivity (EC) (soil: water = 1: 5) was determined by a conductivity meter (Mettler Toledo, Shanghai, China). Soil CEC was determined by ammonium acetate extraction (Bao, 2000). The SMC was determined by drying method.

$$GMD = \exp\left(\frac{\sum_{i=1}^{n} Wi \times \ln di}{\sum_{i=1}^{n} Wi}\right) \quad (1)$$

$$MWD = \sum_{i=1}^{n} \bar{R}_i W_i \quad (2)$$

$$R_{0.25} = (M_{>0.25}/M_T) \times 100\,\% \quad (3)$$

Where $\bar{R}_i$ is the average diameter (mm) of the aggregates in any particle size range, Wi is the fraction of the mass of aggregates in any particle size range to the dry mass of soil samples (%), $M_{>0.25}$ is the weight of the aggregates greater than 0.25 mm, M_T is the total weight of soil samples of each treatment, di is the average diameter of the ith-size aggregates, Wi is the proportion of the mass of the ith-size aggregates in the total mass, and n is the number of aggregates of each size.

2.4.2 Determination of antioxidant enzyme activities of cotton plant samples

The content of MDA was determined by the thiobarbituric acid method. The activity of superoxide dismutase (SOD) was determined by NBT photoreduction method. The activity of peroxidase (POD) was determined by the guaiacol method. The activity of catalase (CAT) was determine by ultraviolet absorption (Li et al., 2016).

2.4.3 Determination of soil microbial composition

According to the results of a pre-test, the S1 and S3 treatments had significant differences. Therefore, the composition of soil microbial community of the two treatments were determined. The DNA extraction kit (Shanghai Meiji Biotechnology Co., Ltd., China) was used to extract microbial DNA from soil samples. The extracted DNA was used as a template, and 338F/806R and ITS1F/ITS2R were used as primers to amplify the gene sequence of soil bacterial 16S rRNA and fungal ITS. The PCR products of each sample were mixed and detected by 2% agarose gel electrophoresis. The qualified PCR library was subjected to double-end sequencing by Shanghai Meiji Biotechnology Co., Ltd. using the Illumina NovaSeq sequencing platform.

2.5 Statistical analysis

SPSS 26.0 (Statistical, Product and Service Solutions, Chicago, USA) was used for one-way ANOVA. Duncan's multiple range test was used to analyze the significance of differences between means of different treatments at $p< 0.05$. Pearson correlation coefficients were calculated to analyze the correlation between indicators. Origin 2023 (Origin Lab, Massachusetts, USA) was use for charting.

3 Results

3.1 Effects of exogenous carbon addition on the physicochemical properties of different salinized soils

3.1.1 Soil aggregation and stability

Straw and biochar incorporation had a significant effect on the number of aggregates of different particle sizes in different salinized soils (Figure 3). The number of $AGG_{>1}$ and $AGG_{1-0.5}$ decreased with the increase of soil salinity, while that of $AGG_{0.5-0.25}$ and $AGG_{<0.25}$ increased. Straw (C1, C2) and biochar (B1, B2) incorporation increased the number of $AGG_{>1}$, $AGG_{1-0.5}$, and $AGG_{0.5-0.25}$ in the S1, S2 and S3 soils, compared with CK, and the effect of biochar incorporation was stronger than that of straw incorporation. At each soil salinity level, biochar incorporation (B1, B2) significantly increased the number of $AGG_{>1}$, $AGG_{1-0.5}$, and $AGG_{0.5-0.25}$ compared with CK, with the most significant increase in the number of $AGG_{0.5-0.25}$. Among the straw treatments, only the C2 significantly increased the number of $AGG_{>0.25}$ compared with CK. There was no significant difference between CK and C1 treatments.

The GMD, MWD, and $R_{0.25}$ decreased with the increase of soil salinity (Figure 3). The GMD, MWD, and $R_{0.25}$ of the S2CK

10.3389/fpls.2025.1522534

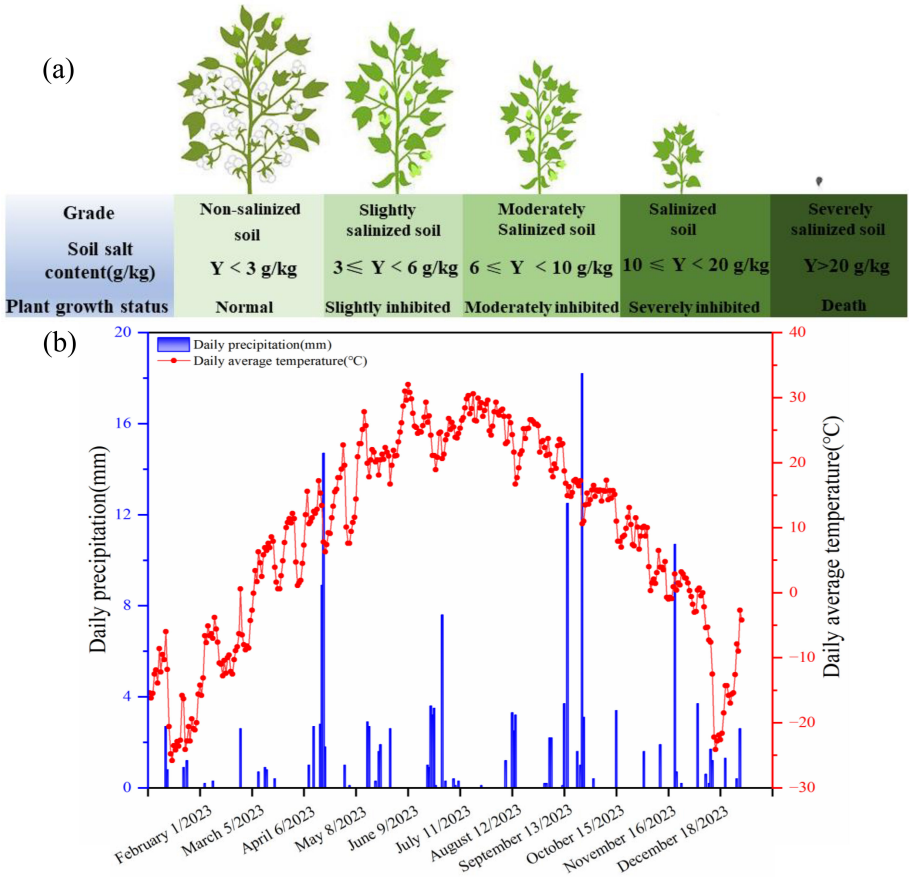

FIGURE 1
Salinized soil classifications **(a)**, precipitation and temperature **(b)** in the study area.

treatment significantly decreased by 7.75%, 5.79%, and 5.22%, respectively, and those of the S3CK treatment significantly decreased by 13.24%, 11.17%, and 9.19%, respectively, compared with those of the S1CK treatment. Straw and biochar incorporation increased the GMD, MWD, and $R_{0.25}$ of the S1, S2, and S3 soils compared with the CK (B2 > B1 > C2 > C1 > CK). The GMD, MWD, and R0.25 of the B2 treatments (S1B2, S2B2, S3B2) significantly increased by 9.31%–11.63%, 6.75%–7.35%, and 12.42%–13.24%, respectively compared with those of the corresponding CK treatment.

3.1.2 Soil moisture content, electrical conductivity, and cation exchange capacity

Straw and biochar incorporation significantly impacted soil physicochemical properties (Table 2). Without straw and biochar incorporation, soil EC increased significantly with the increase of soil salinity, SMC and CEC decreased significantly, and soil pH did not change significantly (Table 2). At each soil salinity level, soil CEC and SMC increased with the increase of straw and biochar application rate, and B2 treatments had the highest CEC and SMC, followed by C2, B1, C1, and CK. Straw and biochar incorporation significantly reduced the soil EC at each soil salinity level, and the effect of biochar incorporation was more significant (B2 > B1 > C2 > C1 > CK).

3.2 Effects of exogenous carbon addition on antioxidant defense system in cotton

3.2.1 Malondialdehyde content and peroxidase activity

Under the conditions without straw and biochar incorporation, the MDA content and POD activity of cotton leaves increased with the increase of soil salinity, and showed an increasing trend with the growth of cotton, reaching the peak at the bolling stage. At each soil salinity level, the leaf MDA content of the straw and biochar treatments showed an increasing trend during the whole growth period, while the POD content increased first and then decreased. Under straw and biochar incorporation, at each soil salinity level, the MDA content and POD activity decreased with the growth of cotton. The MDA content and POD activity of the B2 treatments were significantly lower than those of the other treatments (CK > C1 > B1 > C2 > B2), and the MDA content and POD activity of the

10.3389/fpls.2025.1522534

TABLE 1 Soil physical and chemical properties.

Soil source	pH	Total salt content	Total nitrogen content	Organic matter content	Available phosphorus content	Available potassium content	Salinized soil type
		g·kg^{-1}	g·kg^{-1}	g·kg^{-1}	mg·kg^{-1}	mg·kg^{-1}	
Salinized wasteland	8.86	22.35	0.43	8.46	10.53	136.79	Chloride-sulfate type
Cotton field	7.91	1.5	0.78	15.12	22.26	235.16	Chloride-sulfate type

C2 treatments (S1C2, S2C2, S3C2) were significantly lower than those of CK (Figure 4).

3.2.2 Superoxide dismutase and catalase activities

Under the conditions without straw and biochar incorporation, the activity of SOD and CAT in cotton leaves increased with the increase of soil salinity. The SOD activity of the S1CK, S2CK, and S3CK treatments continued to increase with the growth of cotton, reaching the maximum at the bolling stage (increasing by 61.01% – 85.8% compared with that of the budding stage). However, the CAT activity of the S1CK, S2CK, and S3CK treatments showed a trend of increasing first and then decreasing, reaching the peak at the flowering stage (increasing by 56.50% – 58.62% compared with that of the budding stage). Straw and biochar incorporation increased the leaf SOD and CAT activities of cotton in salinized soils. At each salinity level, the activity of SOD and CAT increased significantly with the increase of straw and biochar application rates (CK< C1< B1< C2< B2). The activity of SOD and CAT of the B2 treatments were significantly higher than those of the other treatments, and the activity of SOD and CAT of the C2 treatments were significantly higher than those of the C1 (S1C1, S2C1, S3C1) and CK (S1CK, S2CK, S3CK) treatments. Interestingly, after the flowering stage of cotton, the activity of SOD and CAT of the S3B1 and S3B2 treatments were higher than those of S3C1 and S3C2 treatments (CK< C1< C2< B1< B2) (Figure 5).

3.3 Effects of straw and biochar incorporation on microbial activity in different salinized soils

3.3.1 Changes of soil microbial diversity

The number of bacterial Operational Taxonomic Units (OTUs) shared by all treatments was 2021, and the number of bacterial OUTs specific to S1CK, S1C2, S1B2, S3CK, S3C2, and S3B2 treatments were 279 (accounting for 12.13%), 525 (20.62%), 431 (17.58%), 218 (9.74%), 428 (17.48%), and 316 (13.52%), respectively. The number of fungal OTUs shared by all treatments was 194, and the number of fungal OTUs specific to S1CK, S1C2, S1B2, S3CK, S3C2, and S3B2 treatments were 59 (23.32%), 89 (31.45%), 84 (30.21%), 50 (20.49%), 74 (27.61%), and 66 (23.66%), respectively. The number of bacterial and fungal OUTs in each treatment decreased with the increase of soil salinity. At each soil salinity level, the effect of the straw treatments on soil bacterial and fungal communities was more significant than that of the biochar treatments (C2 > B2 > CK) (Figure 6).

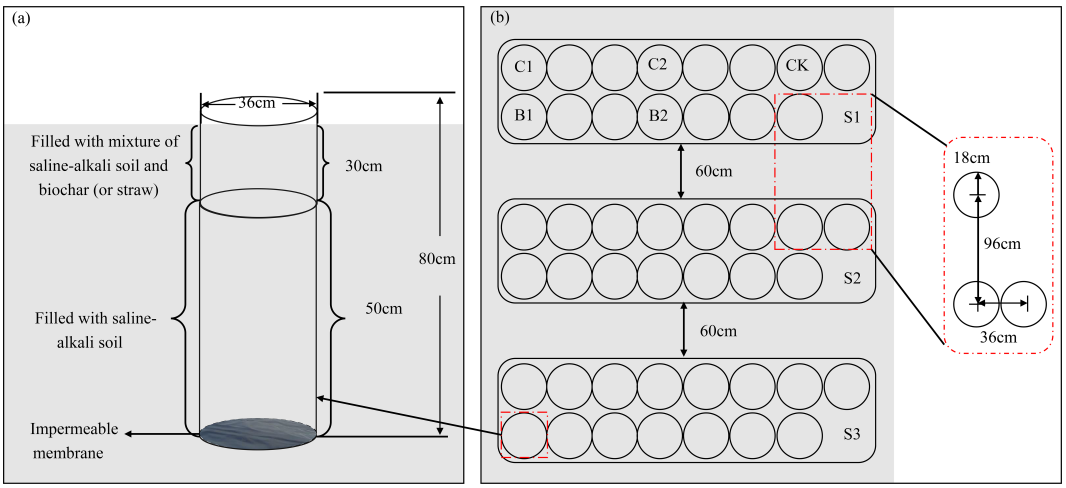

FIGURE 2
Soil column design **(a)** and layout **(b)**. S1, S2, and S3 represent soil salt content of 1.5, 5, and 10 g·kg^{-1}, respectively. CK, no carbon addition; C1, 6 t·hm^{-2} of straw incorporation; C2, 12 t·hm^{-2} of straw incorporation; B1 (equal to C1), 2.25 t·hm$_{-2}$ of biochar incorporation; B2 (equal to C2), 4.5 t·hm^{-2} of biochar incorporation. The same below.

10.3389/fpls.2025.1522534

TABLE 2 Changes of soil moisture content, electrical conductivity, pH, and cation exchange capacity in different salinized soils under straw and biochar incorporation.

Index	Treatment	S1	S2	S3
Soil moisture content (%)	CK	14.81 ± 0.74e	16.04 ± 0.79d	17.3 ± 0.87bc
	C1	16.51 ± 0.82cd	16.85 ± 0.85c	17.64 ± 0.93bc
	C2	17.27 ± 0.85bc	17.92 ± 0.9b	18.37 ± 0.93ab
	B1	16.81 ± 0.85cd	17.42 ± 0.87bc	18.22 ± 0.87ab
	B2	18.47 ± 0.93ab	18.68 ± 0.95a	18.85 ± 0.94a
Electrical conductivity (mS/cm)	CK	0.85 ± 0.10i	1.61 ± 0.13e	2.52 ± 0.13a
	C1	0.56 ± 0.11j	1.41 ± 0.14f	2.37 ± 0.12b
	C2	0.51 ± 0.11j	1.32 ± 0.13f	2.28 ± 0.11c
	B1	0.42 ± 0.10j	1.24 ± 0.12g	2.10 ± 0.12d
	B2	0.29 ± 0.08k	1.15 ± 0.11h	2.05 ± 0.11d
pH	CK	7.88 ± 0.07ab	8.00 ± 0.09ab	7.93 ± 0.18ab
	C1	7.82 ± 0.13ab	7.75 ± 0.13ab	7.84 ± 0.09ab
	C2	7.72 ± 0.08ab	7.67 ± 0.16a	7.81 ± 0.13ab
	B1	7.95 ± 0.17ab	7.97 ± 0.14ab	8.02 ± 0.15ab
	B2	8.05 ± 0.11ab	8.07 ± 0.13ab	8.17 ± 0.20b
Cation exchange capacity ($cmol \cdot kg^{-1}$)	CK	2.3 ± 0.14f	2.23 ± 0.16f	2.22 ± 0.13f
	C1	2.63 ± 0.16e	2.83 ± 0.17de	2.53 ± 0.15e
	C2	2.99 ± 0.19cd	3.16 ± 0.21bc	2.73 ± 0.16de
	B1	2.74 ± 0.15de	2.87 ± 0.18de	2.97 ± 0.16cd
	B2	3.42 ± 0.22ab	3.56 ± 0.22a	3.25 ± 0.23ab

S1: non-salinization (1.5 $g \cdot kg^{-1}$), S2: mild salinization (5 $g \cdot kg^{-1}$), S3: moderate salinization (10 $g \cdot kg^{-1}$). CK: no carbon, C1: 6 $t \cdot hm^{-2}$ of straw incorporation, C2:12 $t \cdot hm^{-2}$ of straw incorporation, B1: 2.25 $t \cdot hm^{-2}$ of biochar incorporation (B1, equal to C1), B2:4.5 $t \cdot hm^{-2}$ of biochar incorporation (B2, equal to C2). All values are means ± SD (n = 3). Different lowercase letters indicate significant differences between different biochar application rates at $p < 0.05$.

3.3.2 Changes of soil microbial community composition

At the phylum level (Figure 7a), the top five bacterial phyla by relative abundance in all treatments were Actinobacteria (25.74%), Proteobacteria (22.94%), Chloroflexi (15.11%), Acidobacteria (9.18%), and Gemmatimonadetes (5.31%), accounting for 78.28% in total. The relative abundances of Proteobacteria and Bacteroidete of the S1CK, S2CK, and S3CK treatments increased with the increase of soil salinity, while those of Chloroflexi and Acidobacteria showed an opposite variation trend. At each soil salinity level, the relative abundances of Actinobacteria and Acidobacteria of the C2 (S1C2, S2C2, S3C2) and B2 (S1B2, S2B2, and S3B2) treatments increased compared with those of the CK treatments, while the relative abundances of Gemmatimonadetes and Bacteroidetes decreased. Besides, there was no significant change in the relative abundances of Proteobacteria and Chloroflexi. In general, the effect of the C2 treatments on the relative abundances of soil bacteria was stronger than that of the B2 treatments.

At the genus level (Figure 7b), the top five dominant bacterial genera by relative abundance were *Arthrobacter* (11.61%), *JG30-KF-CM45* (5.95%), *Vicinamibacterales* (3.38%), *Vicinamibacteraceae* (2.86%), and *Sphingomonas* (1.98%), accounting for 25.33% in total. The relative abundances of *Arthrobacter*, *JG30-KF-CM45*, *Aicinamibacterales*, and *Vicinamibacteraceae* of the S1CK, S2CK, and S3CK treatments reduced with the increase of soil salinity, while that of *Sphingomonas* increased. The relative abundance of *Arthrobacter* of the C2 (S1C2, S3C2) and B2 (S1B2, S3B2) treatments increased (S1C2 > S1B2; S3C2 > S3B2) compared with that of the S1CK treatment. The relative abundance of *Vicinamibacterales* of the S3C2 and S3B2 treatments increased, while that of *Sphingomonas* decreased, compared with those of the S3CK treatment. There was no significant change in the relative abundance of *JG30-KF-CM45*.

At the phylum level (Figure 8a), the top five fungal phyla by relative abundance in all treatments were Ascomycota (89.75%), Mortierella (7.23%), Chytridiomycota (1.33%), Basidiomycota (1.02%), and unclassified_k_Fungi (0.55%), accounting for about 90% in total. The relative abundance of Ascomycota of the S1CK, S2CK, and S3CK treatments increased with the increase of soil salinity, while that of Ascomycota, Chytridiomycota, Basidiomycota, and unclassified_k_Fungi decreased. The relative abundances of Ascomycota and Chytridiomycota of the S1C2 treatment and Mortierella and Chytridiomycota of the S1B2

10.3389/fpls.2025.1522534

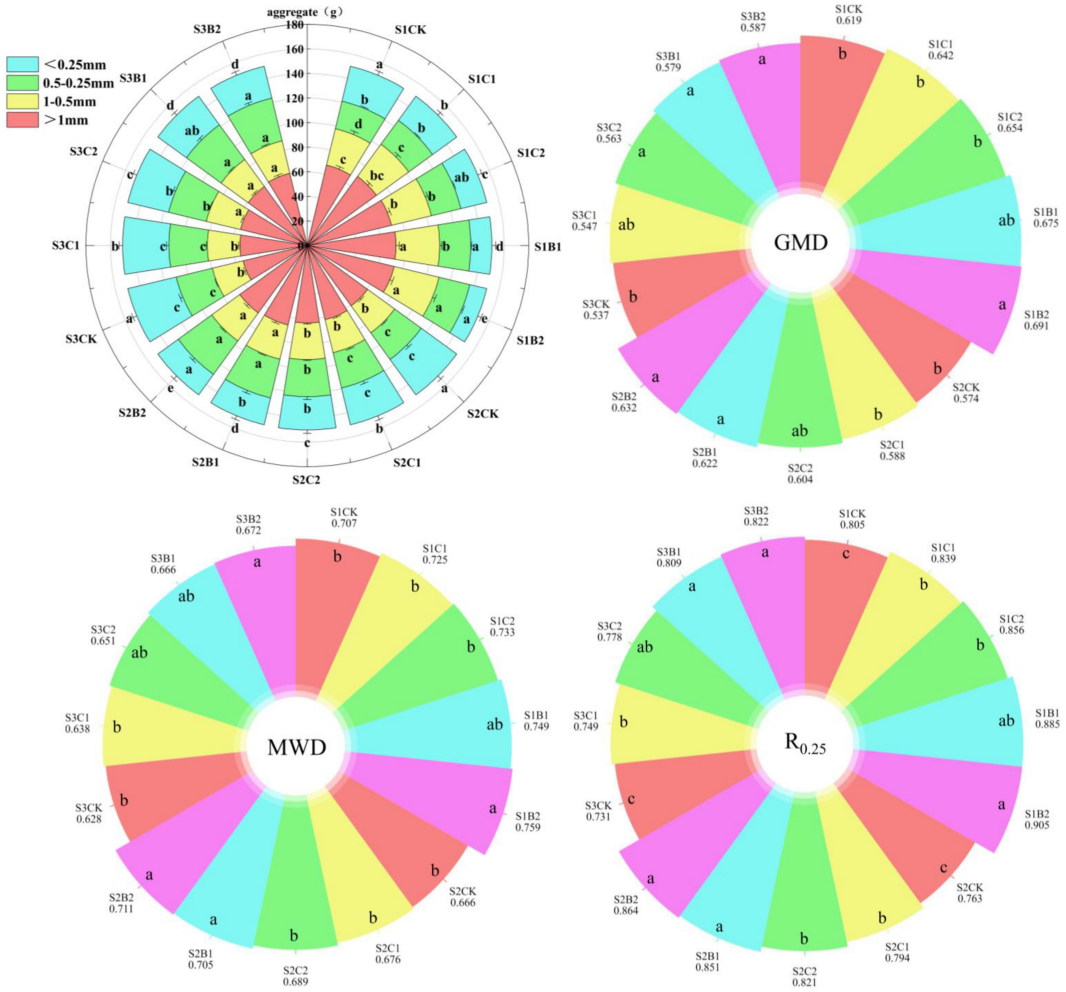

FIGURE 3
Changes of particle size distribution of aggregates in different degrees of salinized soil induced by straw and biochar incorporation. GMD, Geometric mean diameter of soil aggregates; MWD, The average weight diameter of soil aggregates R0.25: Proportion of 0.25mm particle size aggregates. Different lowercase letters in the same column indicate significant difference between groups ($p < 0.05$).

treatment increased, while the relative abundance of Basidiomycetes of the S1C2 treatment decreased, compared with those of the S1CK treatment. The relative abundance of Basidiomycetes of the S3C2 and S3B2 treatments increased compared with that of the S3CK treatment, while that of Ascomycota did not change significantly.

At the genus level (Figure 8b), the top five dominant genera by relative abundance were *Lectera* (15.68%), *Cladosporium* (12.18%), *Alternaria* (10.81%), *Chactomium* (9.36%) and *Fusarium* (8.15%), accounting for 56.24% in total. The relative abundances of *Lectera* and *Fusarium* of the S1CK, S2CK, and S3CK treatments reduced with the increase of soil salinity, while those of *Alternaria* and *Chactomium* increased. The relative abundances of *Cladosporium* and *Chactomium* of the S1C2 and S1B2 treatments increased (S1C2 > S1B2) compared with those of the S1CK treatment, while the relative abundance of *Lectera* decreased. The relative abundances of *Cladosporium* and *Fusarium* of the S3C2 and S3B2 treatments increased (S3B2 > S3C2), while the relative abundance of *Lectera* decreased, compared with those of the S3CK treatment. The relative abundance of *Alternaria* of the S3B2 treatment reduced compared with that of the S3CK treatment, while there was no significant difference between S3C2 treatment and S3CK treatment.

3.3.3 Microbial species differences

At the phylum level (Figure 9a), the relative abundances of Actinobacteria (19%), Chloroflexi (20%), and Acidobacteria (24%) were significantly higher in the S1C2 treatment than in other treatments (S1C2 > S3C2 > S1B2 > S1CK > S3B2 > S3CK). However, the relative abundances of Proteobacteria (20%) and Blastomonas (23%) were significantly higher in the S3CK treatment than in other treatments. At the genus level (Figure 9b), the relative abundances of *Arthrobacter* (20%) and *Vicinamibacteraceae* (27%) were significantly higher in the S1C2 treatment than in other treatments. The relative abundances of *Vicinamibacterales* (26%) and *JG30-KF-CM45* (21%) were significantly higher in the S1CK treatment than in other treatments. The relative abundance of *Sphingomonas* (26%) was significantly higher in the S3CK treatment than in other treatments. In general, straw incorporation treatments had a more significant effect on soil bacterial community structure than biochar incorporation treatments.

10.3389/fpls.2025.1522534

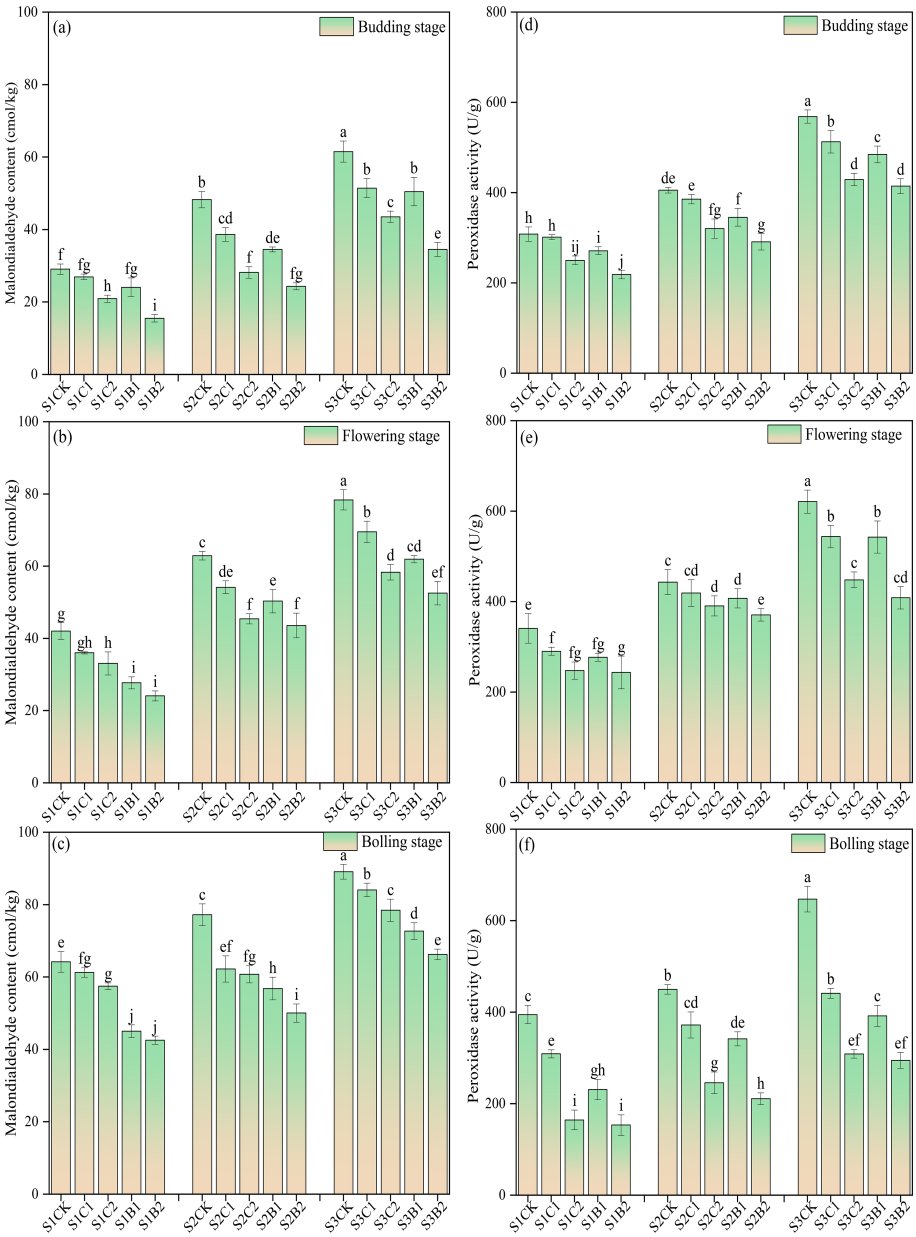

FIGURE 4
Changes of malondialdehyde (MDA) content **(a)**, budding stage; **(b)** flowering stage; **(c)** boll-forming stage) and peroxidase (POD) activity **(d)**, budding stage; **(e)** flowering stage; **(f)** boll-forming stage) with the growth of cotton in salinized soils under straw and biochar incorporation. Different lowercase letters in the same column indicate significant difference between groups ($p< 0.05$).

At the phylum level (Figure 9c), the relative abundances of Proteobacteria ($p = 0.0014$) and Bacteroidetes ($p = 0.0268$) of the S3 treatments (S3C1, S3C2, S3B1, S3B2) were significantly higher than those of the S1 treatments (S1C1, S1C2, S1B1, S1B2), while the relative abundances of Chloroflexi ($p = 0.0019$), Acidobacteria ($p = 0.008$), and Gemmatimonadetes ($p = 0.0422$) were significantly lower than those of the S1 treatments. At the genus level (Figure 9d), the relative abundances of *Arthrobacter* ($p = 0.0422$), *Subgroup_10* ($p = 0.0242$), *Microvirga* ($p = 0.0080$), *Massilia* ($p = 0.0272$), *AKIW781* ($p = 0.0007$), and *Ramlibacter* ($p = 0.0104$) of the S3 treatments were significantly higher than those of the S1 treatments. However, the relative abundances of *G30-KF-CM45* ($p = 0.0026$), *Vicinamibacterales* ($p = 0.0216$), *Gemmatimonadaceae* ($p = 0.0242$), *KD4-96* ($p = 0.0422$), *RB41* ($p = 0.0080$), *Soilrubrobacter* ($p = 0.0104$), and *Stenotrophobacter* ($p = 0.0468$) of the S3 treatments were significantly lower than those of the S1 treatments.

At the phylum level (Figure 10a), the relative abundances of Mortierellomycota (31%), unclassified_k_Fungi (29%), and Basidiomycota (29%) were significantly higher in the S1C2 treatment than in other treatments. The relative abundance of Chytridiomycota (20%) was significantly higher in the S3C2 treatment than in other treatments. The relative abundance of Ascomycetes (19%) was significantly higher in the S3CK treatment than in other treatments. At the genus level

10.3389/fpls.2025.1522534

(Figure 10b), the relative abundance of *Lectera* (32%) was significantly higher in the S1C2 treatment than in other treatments. The relative abundance of *Cladosporium* (34%) was significantly higher in the S3CK treatment than in other treatments. The relative abundances of *Alternaria* (36%), *Chactomium* (40%), and *Fusarium* (24%) was significantly higher in the S3C2 treatment than in other treatments. In general, the effect of straw incorporation treatment on soil fungal community structure was more significant than that of biochar incorporation treatment.

At the phylum level (Figure 10c), there were significant differences in the relative abundances of Ascomycota and Rhodomycota between S1, S2, and S3 treatments, and the relative abundances of Ascomycota (p = 0.0017) and Rhodomycota (p = 0.0214) of the S3 treatment were significantly higher than those of the S1 treatments. At the genus level (Figure 10d), the relative abundances of *Penicillium* (p = 0.0014), *Vishniacozyma* (p = 0.0047), and *Ochroconis* (p = 0.0339) of the S3 treatments were significantly higher than those of the S1 treatments, while the relative abundances of *Alternaria* (p = 0.0272), *Retroconis* (p = 0.0019), *Cephalotrichum* (p = 0.0104), *Acaulium* (p = 0.0340), and *Sordariales* (p = 0.0104) were significantly lower than those of the S1 treatments.

At the phylum level (Figure 11a), there were significant correlations between dominant soil bacterial phyla (i.e.,

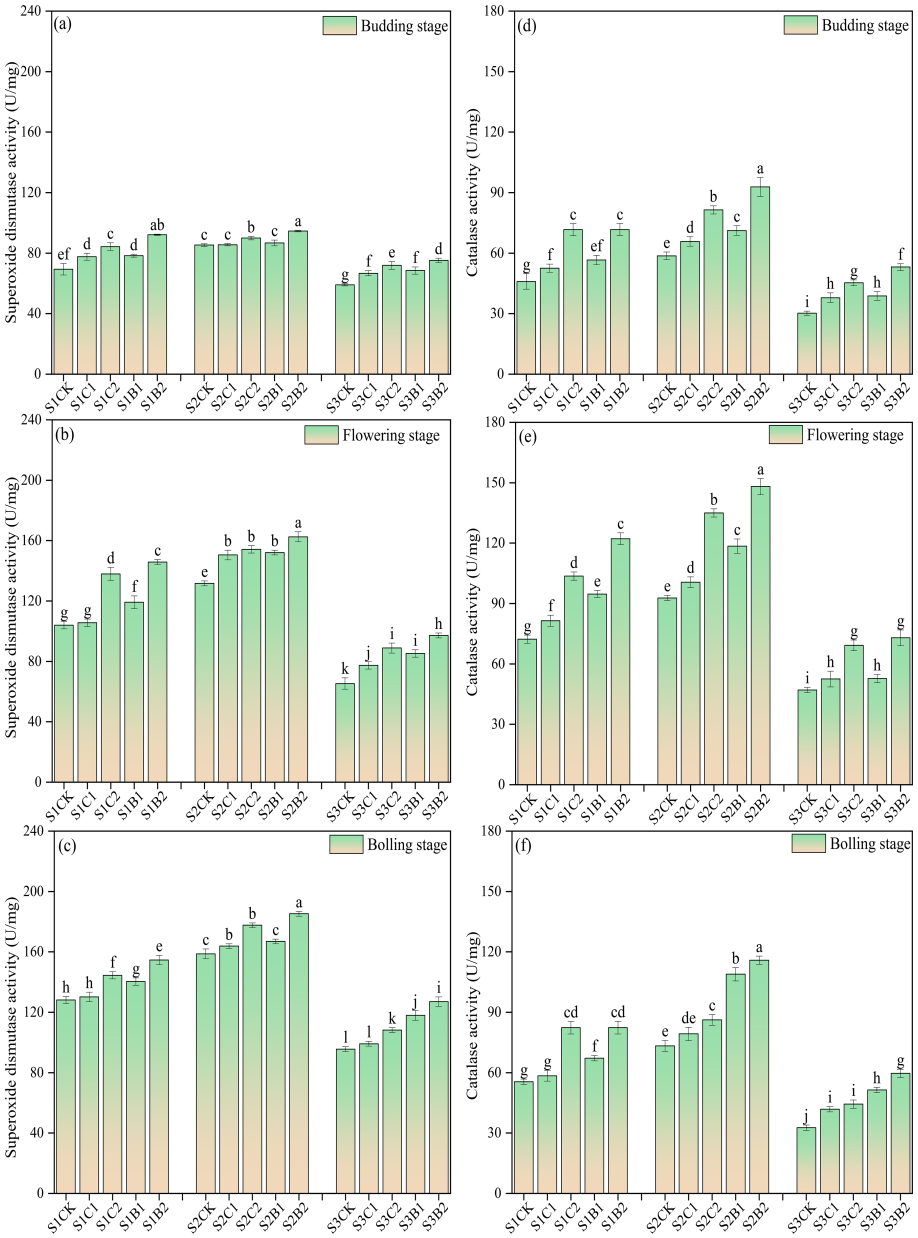

FIGURE 5
Changes of superoxide dismutase (SOD) **(a)**, budding stage; **(b)** flowering stage; **(c)** boll-forming stage) and catalase (CAT) **(d)**, budding stage; **(e)** flowering stage; **(f)** boll-forming stage) activities with the growth of cotton in salinized soils under straw and biochar incorporation. Different lowercase letters in the same column indicate significant difference between groups (p< 0.05).

10.3389/fpls.2025.1522534

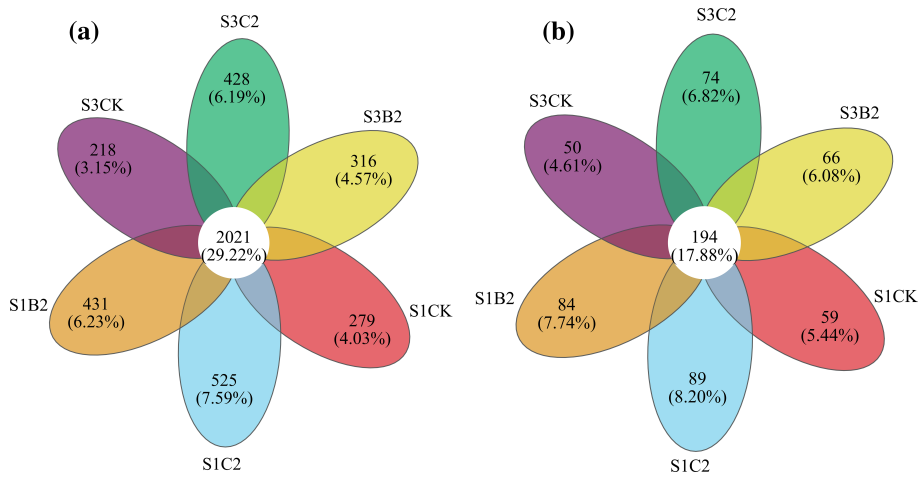

FIGURE 6
Venn diagram of bacterial **(a)** and fungal **(b)** operational taxonomic units (OTUs).

Acidobacteria, Abditibacteriot, Strangeococcus, Actinobacteria, Chloroflexi, and Proteobacteria) and environmental factors (soil factors and cotton parameters). Specifically, the relative abundance of Acidobacteria was positively correlated with $AGG_{>1}$ number, $AGG_{1-0.5}$ number, leaf SOD activity, and leaf CAT activity ($p< 0.05$), and negatively correlated with $AGG_{<0.25}$ number, soil EC, and leaf MDA content ($p< 0.05$). The relative abundance of Abditibacteriot was positively correlated with the number of $AGG_{>1}$ and $AGG_{1-0.5}$ ($p< 0.01$), and negatively correlated with soil EC ($p< 0.01$) and leaf MDA content ($p< 0.05$). The relative abundance of Strangeococcus was negatively correlated with soil EC ($p< 0.05$), and positively correlated with the number of $AGG_{>1}$ and $AGG_{1-0.5}$, leaf SOD activity, and CAT activity. The relative abundances of Actinobacteria and Chloroflexi were positively correlated with the number of $AGG_{>1}$ and $AGG_{1-0.5}$ ($p< 0.05$), and negatively correlated with $AGG_{<0.25}$ number, soil EC, and leaf MDA content ($p< 0.05$). The relative abundance of Proteobacteria was negatively correlated with the number of $AGG_{>1}$ and $AGG_{1-0.5}$ ($p< 0.01$), and positively correlated with soil EC and leaf MDA content ($p< 0.01$). At the genus level (Figure 11b), the relative abundances of dominant bacterial genera *Ramlibacter*, *Roseiflexaceae*, *AKIW781*, *AKYG1722*, *RB41*, *Microvinga*, *Subgroup_10*, *Blastococcus*, *Vicinamibacterales*, and *JG30-KF-CM45* were significantly correlated with environmental factors. Among them, the relative abundance of *AKIW781* was positively correlated with the number of $AGG_{<0.25}$ ($p< 0.001$). The relative abundance of *Microvinga* was negatively correlated with the number of $AGG_{>1}$ and $AGG_{1-0.5}$, and positively correlated with leaf MDA content. The relative abundance of *Ubgroup_10* was negatively correlated with the number of $AGG_{>1}$ and $AGG_{1-0.5}$ ($p< 0.01$), and positively correlated with leaf MDA content ($p< 0.001$). The relative abundance of *Vicinamibacterales* was positively correlated with the number of $AGG_{>1}$ and $AGG_{1-0.5}$. The relative abundance of *JG30-KF-CM45* was positively correlated with the number of $AGG_{>1}$ and $AGG_{1-0.5}$ ($p< 0.05$), and negatively correlated with the number of $AGG_{<0.25}$ ($p< 0.001$).

At the phylum level (Figure 12a), there were significant correlations between dominant soil fungi (i.e, Ascomycota, Calcosporangia, and Basidiomycetes) and environmental factors. Among them, the relative abundances of Ascomycota and

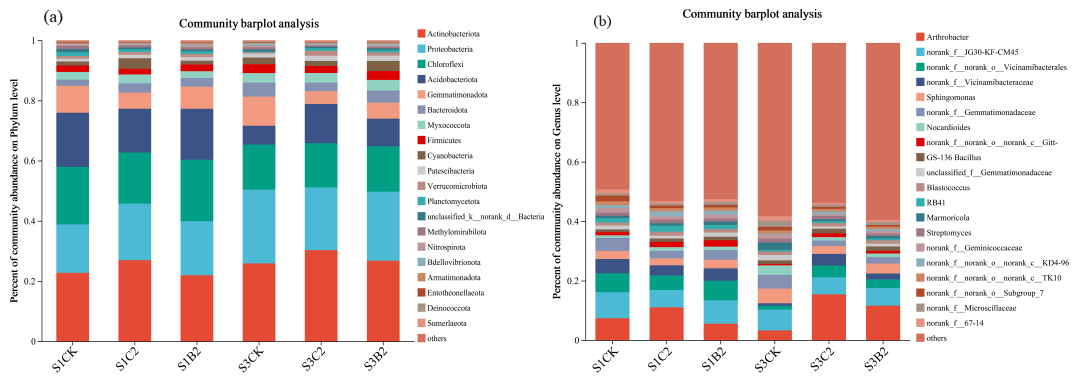

FIGURE 7
Changes of phylum-level **(a)** and genus-level **(b)** bacterial community composition in different salinized soils under straw and biochar incorporation.

10.3389/fpls.2025.1522534

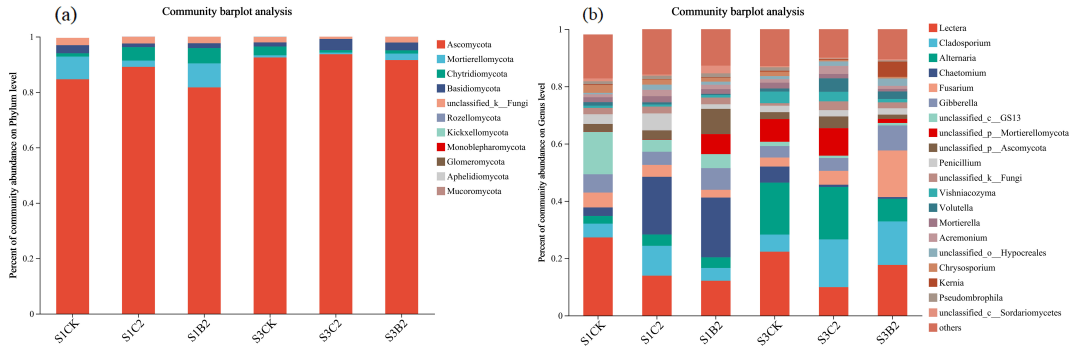

FIGURE 8
Changes of phylum-level **(a)** and genus-level **(b)** fungal community composition in different salinized soils under straw and biochar incorporation.

Calcosporangia were negatively correlated with $AGG_{>1}$ number, $AGG_{1-0.5}$ number and leaf CAT activity ($p< 0.01$), and positively correlated with $AGG_{0.5-0.25}$ number, soil EC, and leaf POD activity ($p< 0.01$). The relative abundance of Roselle was negatively correlated with $AGG_{>1}$ number, $AGG_{1-0.5}$ number and leaf CAT activity ($p< 0.05$), and positively correlated with $AGG_{0.5-0.25}$ number, soil EC, and leaf POD activity ($p< 0.05$). The relative abundance of Basidiomycota was positively correlated with CEC and SMC ($p< 0.01$), and negatively correlated with leaf POD activity ($p< 0.05$).

At the genus level (Figure 12b), there were significant correlations between dominant soil fungal genera (i.e.,

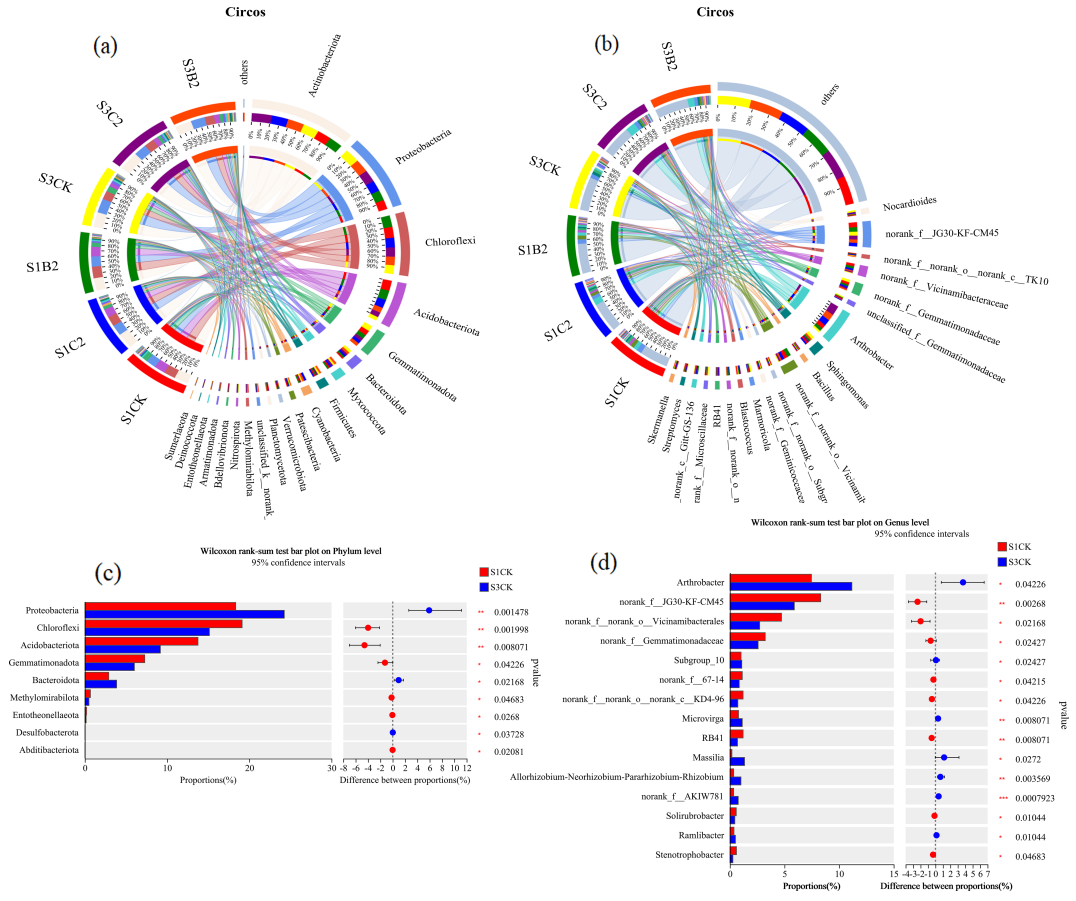

FIGURE 9
Analysis of differences in bacterial abundance in different salinized soils under straw and biochar incorporation. **(a)** Differences in the relative abundances of bacterial phyla under straw and biochar incorporation; **(b)** Differences in the relative abundances of bacterial genera under straw and biochar incorporation; **(c)** Differences in the relative abundances of bacterial phyla under salt treatments; **(d)** Differences in the relative abundances of bacterial genera under salt treatments.

10.3389/fpls.2025.1522534

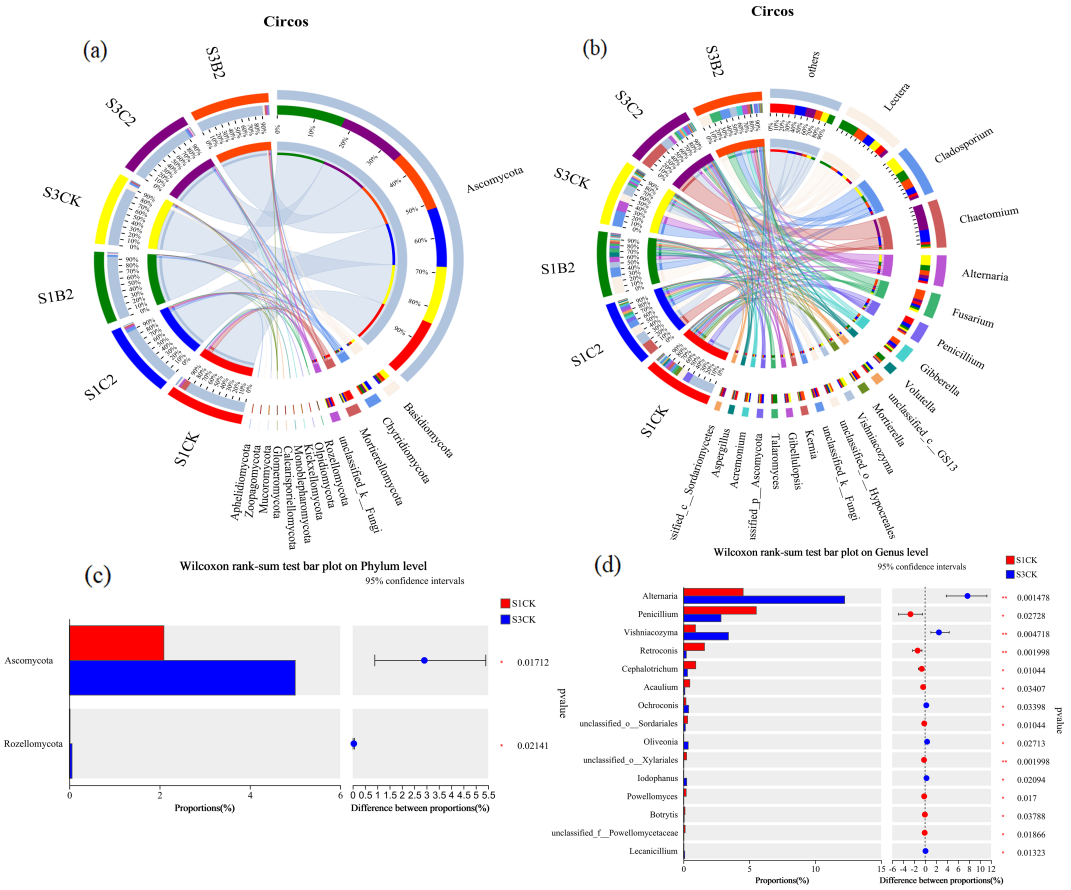

FIGURE 10
Analysis of differences in fungal abundance in different salinized soils under straw and biochar incorporation. **(a)** Differences in the relative abundances of fungal phyla under straw and biochar incorporation; **(b)** Differences in the relative abundances of fungal genera under straw and biochar incorporation; **(c)** Differences in the relative abundances of fungal phyla under salt treatments; **(d)** Differences in the relative abundances of fungal genera under salt treatments.

Chytridiomycota, *Ochroconis*, *Cladosporium*, *Purpureoclilium*, *Microascus*, *Vishniacozyma*, *Retroconis*, and *Alternaria*) and environmental factors. Among them, the relative abundances of *Chytridiomycota* and *Retroconis* were positively correlated with $AGG_{>1}$ number, $AGG_{1-0.5}$ number and CEC ($p< 0.01$), and negatively correlated with leaf MDA content ($p< 0.01$). The relative abundance of *Chytridiomycota* was negatively correlated with the number of $AGG_{0.5-0.25}$ ($p< 0.01$). The relative abundance of *Retroconis* was negatively correlated with the number of $AGG_{<0.25}$($p< 0.05$). The relative abundance of *Ochroconis* was positively correlated with soil EC ($p< 0.01$), $AGG_{0.5-0.25}$ number ($p< 0.05$), and leaf MDA content ($p< 0.05$), and negatively correlated with leaf SOD activity ($p< 0.01$). The relative abundances of *Purpureoclilium* and *Microascus* were positively correlated with $AGG_{0.5-0.25}$ number and leaf POD activity ($p< 0.01$), and negatively correlated with CEC and CAT activity ($p< 0.01$). The relative abundance of *Vishniacozyma* was negatively correlated with $AGG_{>1}$ number, $AGG_{1-0.5}$ number, leaf SOD activity, and CAT activity ($p< 0.01$), and positively correlated with $AGG_{0.5-0.25}$ number, soil EC, and leaf MDA content ($p< 0.01$).

4 Discussion

4.1 Effects of straw and biochar incorporation on the physicochemical properties of different salinized soils

Soil salinization greatly affects the productivity of cultivated lands. High soil salinity damages soil aggregate structure, leading to soil compaction and reduced permeability (Wong et al., 2010). This may ultimately lead to the abandonment of cultivated lands. Previous studies have shown that straw and biochar incorporation can significantly reduce soil salinity, improve soil environment, and promote the leaching of base ions in salinized soils (Yue et al., 2016; Xie et al., 2017). Similarly, this study found that straw and biochar incorporation significantly reduced soil EC, but increased soil CEC (Table 2). This may be due the fact that (1) straw and biochar incorporation increase soil porosity and aeration (Artiola et al., 2012) and accelerate the leaching of Na^+. (2) Biochar has a large surface area and strong adsorption capacity, thus it can adsorb base ions and reduce salt content in salinized soils (Yang

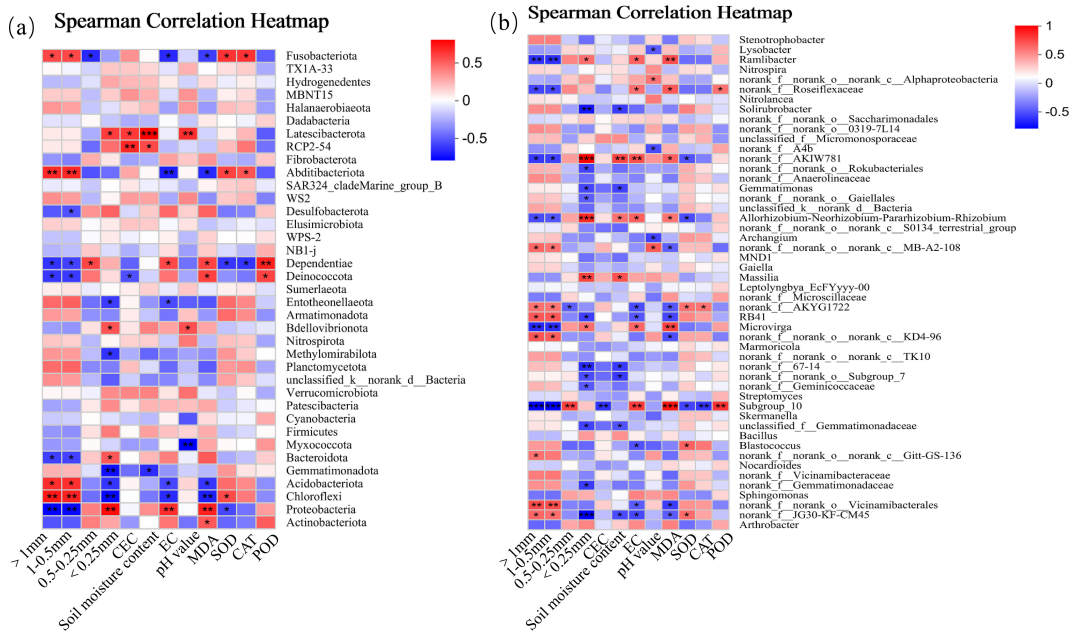

FIGURE 11
Correlation analysis of soil bacterial community ((**a**) bacterial phyla; **(b)** bacterial genera) and environmental factors.

et al., 2024). (3) Straw and biochar have a large number of oxygen-containing functional groups such as hydroxyl and carboxyl groups, which can combined with Ca^{2+}, Mg^{2+}, K^{+}, and Al^{3+} to stabilize in the soil. This may be the main reason for the increase of CEC. This study also found that straw incorporation reduced soil pH compared with CK, while biochar incorporation had no significant impact on soil pH. This may be due to that the soil pH (8.35) in the study area is high causing an insignificant effect of biochar incorporation on soil pH.

Soil aggregate is not only a fundamental unit of soil structure, but also an important carrier of soil moisture, organic matter, and nutrients. Its stability and the proportion of each size of particles largely determine the soil structure, water and fertilizer retention capacity (Guidi et al., 2017). In this study, the number of soil macroaggregates in high-salinity soil was significantly lower than that in low- and medium-salinity soils, and the GMD, MWD, and $R_{0.25}$ were smaller. This is consistent with the results of Duan et al. (2021). This may be due to the fact that the Na^{+} content of high-salinity soil is higher than that of low- and medium-salinity soils, and the larger hydration radius of Na^{+} weakens the force between soil particles, thus reducing the number of macroaggregates in the soil (Shen et al., 2024). In addition, the large accumulation of Na^{+} reduces the soil osmotic potential, resulting in loose aggregate structure and soil compaction (Guo et al., 2019). Straw and biochar incorporation can increase the number and average diameter of macroaggregates and the stability of soil aggregates by reducing the soil Na^{+} content and increasing organic and inorganic cementing substances (Zheng et al., 2018). In this study, straw and biochar incorporation increased the number of soil macroaggregates in low-, medium-, and high-salinity soils by 7.01%–13.12%, 5.03%–10.24%, and 4.16%–8.31%, respectively, compared with CK (Figure 3). Among them, the increase in the soil macroaggregates in low-salinity soil was the largest, and the effect of biochar incorporation was better than that of straw incorporation. However, the mechanisms of action of straw and biochar incorporation are different. Lignin and protein released during straw decomposition are important factors to maintain the stability of aggregates (Xie et al., 2020). The surface of biochar is rich in divalent cations such as Ca^{2+} and Mg^{2+}, which can replace excess Na^{+} in salinized soil and inhibit the Na^{+}-induced cohesion reduction of soil aggregates (Duan et al., 2021). In addition, biochar can also act as an intermediate between soil organic matter and soil minerals, promoting the formation of an organic matter-biochar-mineral complex through adsorption and cationic bridging (Kim et al., 2016). This ultimately enhances the stability of aggregates.

4.2 Response of antioxidant defense system of cotton to salt stress and exogenous carbon addition

Soil salinization causes salt stress, which limits crop growth by inducing physiological drought, ion toxicity, and oxidative damage (Bose et al., 2014; Nefissi Ouertani et al., 2021). Kesawat et al. (2023) found that salt stress led to excess accumulation of reactive oxygen species (ROS) in crop organelles (i.e., mitochondria and peroxisomes), and disrupted cell membrane integrity and functional molecules such as nucleic acids, proteins, and lipids. In this study, the MDA content in cotton leaves continued to increase under high salinity treatment. This is due to the fact that under salt

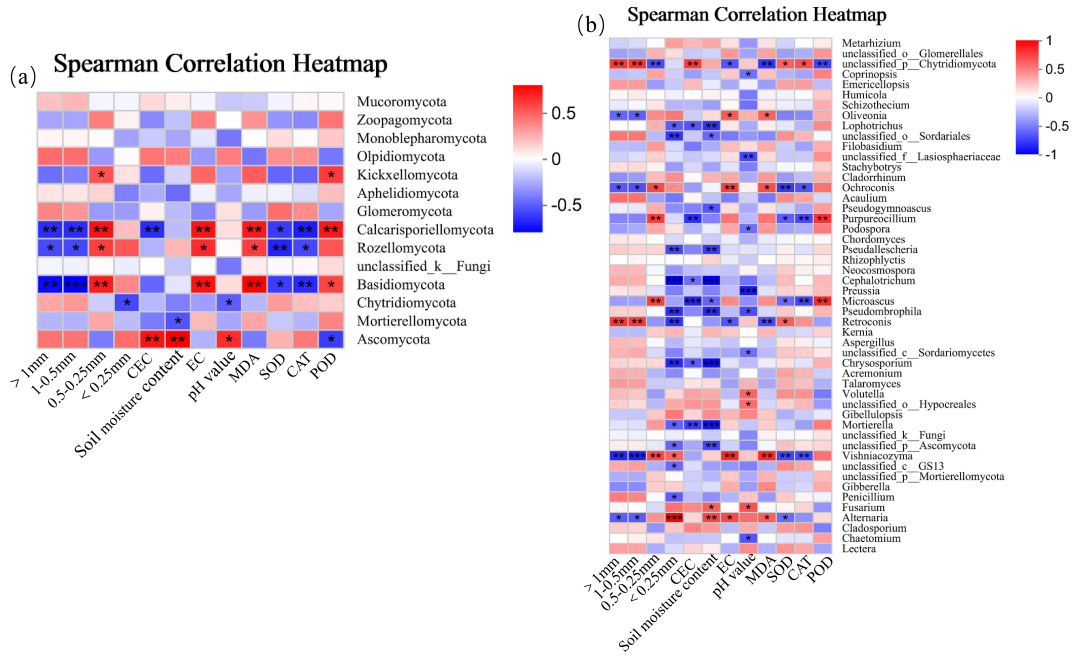

FIGURE 12
Correlation analysis of soil fungal community ((**a**) fungal phyla; (**b**) fungal genera) and environmental factors.

stress, the reaction of excess ROS with unsaturated fatty acids on the cell membrane causes increasing membrane lipid peroxidation in cotton leaves (Zhao et al., 2023). In addition, excess Na^+ competes with K^+ and Ca^{2+} to destroy the ion balance in crops, leading to a large accumulation of MDA (Hussain et al., 2021). In this study, the activities of POD, SOD, and CAT in cotton of the straw and biochar incorporation treatments significantly increased compared with those of the CK treatment. This indicates that crops can resist salt stress by regulating the antioxidant defense system to remove excess ROS and reduce the damage of oxidative stress to cells (Hossain and Dietz, 2016).

In this study, the straw and biochar incorporation significantly increased the leaf SOD and CAT activities in cotton in salinized soils (Figure 5), and decreased the MDA content and POD activity, compared with CK (Figure 4). This is consistent with the results of previous studies (Abbas et al., 2022; Hamoud et al., 2022; Zhang J, et al., 2019). This may be due to the fact that straw and biochar contains rich nutrients, which can promote the nutrient absorption of cotton roots and provide a material basis for the synthesis of SOD and CAT. SOD catalyzes superoxide anions to undergo dismutation reaction and decomposes superoxide anions (O_2^-) into H_2O_2 and water, and CAT further decomposes H_2O_2 into H_2O and (O_2). The two synergistically alleviate the oxidative stress caused by excess ROS under salt stress (Hossain and Dietz, 2016; Muchate et al., 2016). In addition, straw and biochar incorporation can promote the leaching of soil base ions (especially Na^+) by improving soil physical properties (Huang et al., 2023; Jin et al., 2024), reduce the absorption of Na^+ by cotton, thus alleviating the inhibition of soil salts on the synthesis of SOD and CAT. It should be noted that in this study, the leaf SOD and POD activities continued to increase with the growth of cotton, while the CAT activity increased first and then decreased (Figures 4d-f and 5). This may be due to the continuous accumulation of ROS in cotton caused by salt stress. Excess Na^+ intake in cotton affects the molecular structure and active site of CAT, resulting in a decrease in CAT activity (Mishra et al., 2013).

4.3 Effects of straw and biochar incorporation on microbial community in different salinized soils

Soil salts greatly impact the composition and diversity of soil microbial communities (Rath and Rousk, 2015). Straw and biochar incorporation can regulate the microbial community structure by reducing soil salinity and increasing soil fertility. This study found that the relative abundances of Proteobacteria (p = 0.0014) and Bacteroidetes (p = 0.0268) increased with the increase of soil salinity, while those of Chloroflexi (p = 0.0019), Acidobacteria (p = 0.008), and Gemmatimonadetes (p = 0.0422) decreased (Figure 9c). This may be due to the fact that Proteobacteria can absorb and accumulate compatible solutes such as glycine betaine, and maintain normal metabolic activity under salt stress by changing osmotic balance and antioxidant defense system. Bacteroidetes is an aerobic organism, which can cooperate with other bacteria to increase nutrient uptake by using the matrix in salinized soil (Li et al., 2021) to resist salt stress. Besides, soil

microbial competition is also one of the important reasons. High soil salinity inhibits the activity of non-salt-tolerant microorganisms, thus enabling salt-tolerant microorganisms (such as Proteobacteria and Bacteroidetes) to obtain greater living space and more resources (Zheng et al., 2017).

Actinobacteria and Ascomycota, as the main bacterial and fungal phyla, play a very important role in carbon and nitrogen cycling in soil ecosystems (Chen et al., 2023; Xu et al., 2012). Acidobacteria and Chytridiomycota can decompose organic matters such as cellulose and chitin (Ran T, et al., 2023). Mortierella significantly affects the contents of available nitrogen and available phosphorus in soil. Song et al. (2017) and Guan et al. (2022) showed that the total carbon content, total nitrogen content, and C/N ratio in the soil under straw and biochar incorporation significantly increased by 31.3%, 40%, and 44%, respectively compared with the control. In this study, straw and biochar incorporation increased the relative abundances of beneficial bacterial (i.e., Actinobacteria and Acidobacteria) and fungal (i.e., Enterobacteriaceae) phyla in salinized soils (Figures 6-8). This may be due to that straw and biochar incorporation regulate carbon and nitrogen cycles and C/N ratio in salinized soils (Dong et al., 2023). Importantly, the relative abundance of Ascomycota in high-salinity soil (p = 0.0017) increased compared with that in the low-salinity soil in this study (Figure 10c). This may be due to the fact that salt-tolerant bacteria such as Ascomycota can resist Na^+ stress through special mechanisms (Egidi et al., 2019), that is, they can use ion pumps (such as H^{+-}ATPASE and Na^+/H^+ retrotransporters) and ion channels to regulate the ion concentration difference inside and outside the cell, and excrete Na^+ out of the cell, to adapt to the high-salinity environment. In summary, under stress conditions, soil microbial communities adapt to the environment by adjusting the community structure, while straw and biochar incorporation can enhance the stability of soil ecosystems to help to resist the stresses.

It has been found that biochar incorporation leads to a wider and higher intensity in the absorption peak of polysaccharides (Wang et al., 2024), and increases the accumulation of chlorophyll and photosynthetic metabolites (such as soluble sugar, sucrose, fructose, and starch) in crop leaves, enhancing the photosynthetic capacity of crops (Zahra et al., 2022). Zhang et al. (2023) showed that biochar incorporation increased the net photosynthetic rate of crops by improving stomatal restriction and intercellular carbon dioxide concentration in crop leaves compared with the control. Wang et al. (2021) showed that exogenous carbon addition significantly improved the structure, growth, and photosynthetic capacity of crop canopy, i.e., leaf number, leaf area expansion, leaf area duration, and canopy openness, which further leads to an increase in photosynthetic rate, leaf area index, chlorophyll content, and other photosynthetic traits of crops. Therefore, straw and biochar can enhance the photosynthetic capacity of crops, but how exogenous carbon incorporation improve soil physical, chemical, and biological properties and the accumulation of photosynthetic metabolites in crops needs to be further explored. In the follow-up research, we will further explore the effects of straw and biochar incorporation on the photosynthetic processes of cotton.

5 Conclusion

Straw and biochar incorporation, especially 4.5 $t{\cdot}hm^{-2}$ of biochar incorporation (B2), significantly reduced the salt content of soils with different salinization degrees, and increased the proportion of macroaggregates, compared with the control. Straw and biochar incorporation, especially 12 $t{\cdot}hm^{-2}$ of straw incorporation (C2), significantly increased the relative abundance of dominant bacteria such as Actinomycetes and Acidobacteria, and the diversity of soil microorganisms, compared with the control. Besides, straw and biochar incorporation significantly alleviated the salt stress by regulating the antioxidant defense system of cotton leaves (increasing the activities of SOD and CAT as well as decreasing the MDA content and POD activity). In conclusion, straw and biochar incorporation could significantly reduce the salt content of salinized soils by improving soil structure and regulating soil microbial community structure and abundance. Therefore, straw and biochar incorporation are effective strategies to remediate salinized soils, alleviate the salt stress in cotton, and achieve the efficient utilization of salinized soils by cotton planting.

Apart from biochar, modified biochar also shows good performance in the remediation of salinized soils. Therefore, more types of exogenous carbon will be combined to achieve better performance in the future.

Data availability statement

The data analyzed in this study is subject to the following licenses/restrictions: Confidentiality for a certain period of time. Requests to access these datasets should be directed to WL, 1048481036@qq.com.

Author contributions

WL: Conceptualization, Investigation, Methodology, Writing – original draft, Writing – review & editing. MZ: Conceptualization, Investigation, Methodology, Writing – original draft. HW: Conceptualization, Funding acquisition, Supervision, Writing – review & editing. XS: Investigation, Writing – review & editing. JS: Investigation, Writing – review & editing. JW: Investigation, Visualization, Writing – review & editing. WZ: Investigation, Writing – review & editing.

Funding

The author(s) declare that financial support was received for the research and/or publication of this article. This work is supported by the National Natural Science Foundation of China (42161042), the Core Agricultural Technology Research Project of Xinjiang Production and Construction Corps (2023AA601, 2023AA303), the Leading Talents Project of Science and Technology Innovation of Xinjiang Production and Construction Corps (2023CB008-10), and "Tianchi Yingcai" Program of the Xinjiang Uygur Autonomous Region - Young Doctor (CZ006047).

Acknowledgments

The authors are grateful for the help of providing experiment condition by Shihezi University. In addition, we should also like to thank the reviewer for the constructive comments.

Conflict of interest

The authors declare that the research was conducted in the absence of any commercial or financial relationships that could be construed as a potential conflict of interest.

Generative AI statement

The author(s) declare that no Generative AI was used in the creation of this manuscript.

Publisher's note

All claims expressed in this article are solely those of the authors and do not necessarily represent those of their affiliated organizations, or those of the publisher, the editors and the reviewers. Any product that may be evaluated in this article, or claim that may be made by its manufacturer, is not guaranteed or endorsed by the publisher.

References

Abbas, G., Abrar, M. M., Naeem, M. A., Siddiqui, M. H., Ali, H. M., Li, Y., et al. (2022). Biochar increases salt tolerance and grain yield of quinoa on saline-sodic soil: multivariate comparison of physiological and oxidative stress attributes. *J. Soils Sediments* 22, 1446–1459. doi: 10.1007/s11368-022-03159-2

Arif, Y., Singh, P., Siddiqui, H., Bajguz, A., and Hayat, S. (2020). Salinity induced physiological and biochemical changes in plants: An omic approach towards salt stress tolerance. *Plant Physiol. Biochem.* 156, 64–77. doi: 10.1016/j.plaphy.2020.08.042

Artiola, J. F., Rasmussen, C., and Freitas, R. (2012). Effects of a biochar-amended alkaline soil on the growth of romaine lettuce and Bermudagrass. *Soil Sci.* 177, 561–570. doi: 10.1097/SS.0b013e31826ba908

Bai, T., Ran, C., Ma, Q., Miao, Y., Li, S., Lan, H., et al. (2024). The application of straw return with nitrogen fertilizer increases rice yield in saline–sodic soils by regulating rice organ ion concentrations and soil leaching parameters. *Agronomy* 14, 2807. doi: 10.3390/agronomy14122807

Bao, S. D. (2000). *Soil and Agricultural Chemistry Analysis. 3rd edn* (Beijing: China Agriculture Press).

Bose, J., Rodrigo-Moreno, A., and Shabala, S. (2014). ROS homeostasis in halophytes in the context of salinity stress tolerance. *J. Exp. Bot.* 65, 1241–1257. doi: 10.1093/jxb/ert430

Cen, R., Feng, W., Yang, F., Wu, W., Liao, H., and Qu, Z. (2021). Effect mechanism of biochar application on soil structure and organic matter in semi-arid areas. *J. Environ. Manage.* 286, 112198. doi: 10.1016/j.jenvman.2021.112198

Chen, Y., Qiu, Y., Hao, X., Tong, L., Li, S., and Kang, S. (2023). Does biochar addition improve soil physicochemical properties, bacterial community and alfalfa growth for saline soils? *Land Degrad. Dev.* 34, 3314–3328. doi: 10.1002/ldr.4685

Da Silva Mendes, J., Fernandes, J. D., Chaves, L. H. G., Guerra, H. O. C., Tito, G. A., and de Brito Chaves, I. (2021). Chemical and physical changes of soil amended with biochar. *Water Air Soil pollut.* 232, 338. doi: 10.1007/s11270-021-05289-8

Dong, X., Wang, J., Tian, L., Lou, B., Zhang, X., Liu, T., et al. (2023). Review of relationships between soil aggregates, microorganisms and soil organic matter in salt-affected soil. *Chin. J. Eco-Agric.* 31, 364–372. doi: 10.12357/cjea.20220752

Duan, M., Liu, G., Zhou, B., Chen, X., Wang, Q., Zhu, H., et al. (2021). Effects of modified biochar on water and salt distribution and water-stable macro-aggregates in saline-alkaline soil. *J. Soils Sediments* 21, 2192–2202. doi: 10.1007/s11368-021-02913-2

Egidi, E., Delgado-Baquerizo, M., Plett, J. M., Wang, J., Eldridge, D. J., Bardgett, R. D., et al. (2019). A few Ascomycota taxa dominate soil fungal communities worldwide. *Nat. Commun.* 10, 2369. doi: 10.1038/s41467-019-10373-z

Feng, G., Wu, Y., Yang, C., Zhang, Q., Wang, S., Dong, M., et al. (2024). Effects of coastal saline-alkali soil on rhizosphere microbial community and crop yield of cotton at different growth stages. *Front. Microbiol.* 15. doi: 10.3389/fmicb.2024.1359698

Ghorbani, M., and Amirahmadi, E. (2024). Insights into soil and biochar variations and their contribution to soil aggregate status–A meta-analysis. *Soil Tillage Res.* 244, 106282. doi: 10.1016/j.still.2024.106282

Guan, F. Y., Liu, C., Fu, Q. L., Li, P., Lin, Y. C., and Guo, B. (2022). Effects of straw addition on rice yield, soil carbon, nitrogen, and microbial community. *Trans. Chin. Soc. Agric. Eng.* 38, 223–230. doi: 10.11975/j.issn.1002-6819.2022.02.025

Guidi, P., Vittori Antisari, L., Marè, B. T., Vianello, G., and Falsone, G. (2017). Effects of alfalfa on aggregate stability, aggregate preserved-C and nutrients in region mountain agricultural soils 1 year after its planting. *Land Degrad. Dev.* 28, 2408–2417. doi: 10.1002/ldr.2771

Guo, Z., Zhang, J., Fan, J., Yang, X., Yi, Y., Han, X., et al. (2019). Does animal manure application improve soil aggregation? Insights from nine long-term fertilization experiments. *Sci. Total Environ.* 660, 1029–1037. doi: 10.1016/j.scitotenv.2019.01.051

Haj-Amor, Z., Araya, T., Kim, D. G., Bouri, S., Lee, J., Ghiloufi, W., et al. (2022). Soil salinity and its associated effects on soil microorganisms, greenhouse gas emissions, crop yield, biodiversity and desertification: A review. *Sci. Total Environ.* 843, 156946. doi: 10.1016/j.scitotenv.2022.156946

Hamoud, Y. A., Shaghaleh, H., Wang, R., Gouertoumbo, W. F., Hamad, A. A. A., Sheteiwy, M. S., et al. (2022). Wheat straw burial improves physiological traits, yield and grain quality of rice by regulating antioxidant system and nitrogen assimilation enzymes under alternate wetting and drying irrigation. *Rice Sci.* 29, 473–488. doi: 10.1016/j.rsci.2022.07.007

Hossain, M. S., and Dietz, K. J. (2016). Tuning of redox regulatory mechanisms, reactive oxygen species and redox homeostasis under salinity stress. *Front. Plant Sci.* 7. doi: 10.3389/fpls.2016.00548

Huang, K., Li, M., Li, R., Rasul, F., Shahzad, S., Wu, C., et al. (2023). Soil acidification and salinity: the importance of biochar application to agricultural soils. *Front. Plant Sci.* 14. doi: 10.3389/fpls.2023.1206820

Hussain, S., Ali, B., Ren, X., Chen, X., Li, Q., and Ahmad, N. (2021). Recent progress in understanding salinity tolerance in plants: Story of Na+/K+ balance and beyond. *Plant Physiol. Biochem.* 160, 239–256. doi: 10.1016/j.plaphy.2021.01.029

Jin, J., Cui, H., Lv, X., Yang, Y., Wang, Y., and Lu, X. (2017). Exogenous CaCl2 reduces salt stress in sour jujube by reducing Na^+ and increasing K^+, Ca^{2+}, and Mg^{2+} in different plant organs. *J. Hortic. Sci. Biotechnol.* 92, 98–106. doi: 10.1080/14620316.2016.1228435

Jin, F., Piao, J., Miao, S., Che, W., Li, X., Li, X., et al. (2024). Long-term effects of biochar one-off application on soil physicochemical properties, salt concentration, nutrient availability, enzyme activity, and rice yield of highly saline-alkali paddy soils: based on a 6-year field experiment. *Biochar* 6, 1–22. doi: 10.1007/s42773-024-00332-3

Kesawat, M. S., Satheesh, N., Kherawat, B. S., Kumar, A., Kim, H. U., Chung, S. M., et al. (2023). Regulation of reactive oxygen species during salt stress in plants and their crosstalk with other signaling molecules—Current perspectives and future directions. *Plants* 12, 864. doi: 10.3390/plants12040864

Kim, H. S., Kim, K. R., Yang, J. E., Ok, Y. S., Owens, G., Nehls, T., et al. (2016). Effect of biochar on reclaimed tidal land soil properties and maize (Zea mays L.) response. *Chemosphere* 142, 153–159. doi: 10.1016/j.chemosphere.2015.06.041

Kumawat, C., Kumar, A., Parshad, J., Sharma, S. S., Patra, A., Dogra, P., et al. (2022). Microbial diversity and adaptation under salt-affected soils: a review. *Sustainability* 14, 9280. doi: 10.3390/su14159280

Li, X., Wang, A., Wan, W., Luo, X., Zheng, L., He, G., et al. (2021). High salinity inhibits soil bacterial community mediating nitrogen cycling. *Appl. Environ. Microbiol.* 87, e01366–e01321. doi: 10.1128/aem.01366-21

Li, X. F., and Zhang, Z. L. (2016). *Guide to experiment in plant physiology*. Beijing: Higher Education Press.

Liu, Z., Zhu, J., Yang, X., Wu, H., Wei, Q., Wei, H., et al. (2018). Growth performance, organ-level ionic relations and organic osmoregulation of Elaeagnus angustifolia in response to salt stress. *PloS One* 13, e0191552. doi: 10.1371/journal.pone.0191552

Luo, S., Wang, S., Tian, L., Shi, S., Xu, S., Yang, F., et al. (2018). Aggregate-related changes in soil microbial communities under different ameliorant applications in saline-sodic soils. *Geoderma* 329, 108–117. doi: 10.1016/j.geoderma.2018.05.023

Mishra, P., Bhoomika, K., and Dubey, R. S. (2013). Differential responses of antioxidative defense system to prolonged salinity stress in salt-tolerant and salt-sensitive Indica rice (Oryza sativa L.) seedlings. *Protoplasma* 250, 3–19. doi: 10.1007/s00709-011-0365-3

Muchate, N. S., Nikalje, G. C., Rajurkar, N. S., Suprasanna, P., and Nikam, T. D. (2016). Plant salt stress: adaptive responses, tolerance mechanism and bioengineering for salt tolerance. *Bot. Rev.* 82, 371–406. doi: 10.1007/s12229-016-9173-y

Nefissi Ouertani, R., Abid, G., Karmous, C., Ben Chikha, M., Boudaya, O., Mahmoudi, H., et al. (2021). Evaluating the contribution of osmotic and oxidative stress components on barley growth under salt stress. *AoB Plants* 13, plab034. doi: 10.1093/aobpla/plab034

Ran, C., Gao, D., Bai, T., Geng, Y., Shao, X., and Guo, L. (2023). Straw return alleviates the negative effects of saline sodic stress on rice by improving soil chemistry and reducing the accumulation of sodium ions in rice leaves. *Agric. Ecosyst. Environ.* 342, 108253. doi: 10.1016/j.agee.2022.108253

Ran, T., Li, J., Liao, H., Zhao, Y., Yang, G., and Long, J. (2023). Effects of biochar amendment on bacterial communities and their function predictions in a microplastic-contaminated Capsicum annuum L. soil. *Environ. Technol. Innov.* 31, 103174. doi: 10.1016/j.eti.2023.103174

Rath, K. M., and Rousk, J. (2015). Salt effects on the soil microbial decomposer community and their role in organic carbon cycling: a review. *Soil Biol. Biochem.* 81, 108–123. doi: 10.1016/j.soilbio.2014.11.001

Rengasamy, P., and Olsson, K. A. (1991). Sodicity and soil structure. *Soil Res.* 29, 935–952. doi: 10.1071/sr9910935

Sahu, P. K., Singh, D. P., Prabha, R., Meena, K. K., and Abhilash, P. C. (2019). Connecting microbial capabilities with the soil and plant health: Options for agricultural sustainability. *Ecol. Indic.* 105, 601–612. doi: 10.1016/j.ecolind.2018.05.084

Shen, J., Wang, Q., Chen, Y., Zhang, X., Han, Y., and Liu, Y. (2024). Experimental investigation into the salinity effect on the physicomechanical properties of carbonate saline soil. *J. Rock Mech. Geotech. Eng.* 16, 1883–1895. doi: 10.1016/j.jrmge.2023.09.024

Siedt, M., Schäffer, A., Smith, K. E., Nabel, M., Roß-Nickoll, M., and Van Dongen, J. T. (2021). Comparing straw, compost, and biochar regarding their suitability as agricultural soil amendments to affect soil structure, nutrient leaching, microbial communities, and the fate of pesticides. *Sci. Total Environ.* 751, 141607. doi: 10.1016/j.scitotenv.2020.141607

Singh, G., Mavi, M. S., Choudhary, O. P., Gupta, N., and Singh, Y. (2021). Rice straw biochar application to soil irrigated with saline water in a cotton-wheat system improves crop performance and soil functionality in north-west India. *J. Environ. Manage.* 295, 113277. doi: 10.1016/j.jenvman.2021.113277

Song, D. L., Xi, X. Y., Huang, S. M., Zhang, S. Q., Yuan, X. M., Huang, F. S., et al. (2017). Effects of combined application of straw biochar and nitrogen on soil carbon and nitrogen contents and crop yields in a fluvo-aquic soil. *J. Plant Nutr. Fertil.* 23, 369–379. doi: 10.11674/zwyf.16399

Tang, S., She, D., and Wang, H. (2020). Effect of salinity on soil structure and soil hydraulic characteristics. *Can. J. Soil Sci.* 101, 62–73. doi: 10.1139/cjss-2020-0018

Wan, X., Zhang, S. W., Zhang, R. Q., Li, Z. P., Chen, P., Xing, S. L., et al. (2024). Soil aggregate stability of different land use pattern on the Qinghai-Tibetan Plateau. *Research of Soil & Water Conservation* 91 (01), 53–60. doi: 10.13869/j.cnki.rswc.2024.01.047

Wang, C., Chen, D., Shen, J., Yuan, Q., Fan, F., Wei, W., et al. (2021). Biochar alters soil microbial communities and potential functions 3–4 years after amendment in a double rice cropping system. *Agric. Ecosyst. Environ.* 311, 107291. doi: 10.1016/j.agee.2020.107291

Wang, X., Riaz, M., Xia, X., Babar, S., El-Desouki, Z., Li, Y., et al. (2024). Alleviation of cotton growth suppression caused by salinity through biochar is strongly linked to the microbial metabolic potential in saline-alkali soil. *Sci. Total Environ.* 92, 171407. doi: 10.1016/j.scitotenv.2024.171407

Wei, Y., Chen, L., Feng, Q., Xi, H., Zhang, C., Gan, K., et al. (2024). Structure and assembly mechanism of soil bacterial community under different soil salt intensities in arid and semiarid regions. *Ecol. Indic.* 158, 111631. doi: 10.1016/j.ecolind.2024.111631

Wong, V. N., Greene, R. S. B., Dalal, R. C., and Murphy, B. W. (2010). Soil carbon dynamics in saline and sodic soils: a review. *Soil Use Manag.* 26, 2–11. doi: 10.1111/j.1475-2743.2009.00251.x

Xie, W., Chen, Q., Wu, L., Yang, H., Xu, J., and Zhang, Y. (2020). Coastal saline soil aggregate formation and salt distribution are affected by straw and nitrogen application: A 4-year field study. *Soil Tillage Res.* 198, 104535. doi: 10.1016/j.still.2019.104535

Xie, W., Wu, L., Zhang, Y., Wu, T., Li, X., and Ouyang, Z. (2017). Effects of straw application on coastal saline topsoil salinity and wheat yield trend. *Soil Tillage Res.* 169, 1–6. doi: 10.1016/j.still.2017.01.007

Xu, L., Ravnskov, S., Larsen, J., Nilsson, R. H., and Nicolaisen, M. (2012). Soil fungal community structure along a soil health gradient in pea fields examined using deep amplicon sequencing. *Soil Biol. Biochem.* 46, 26–32. doi: 10.1016/j.soilbio.2011.11.010

Yang, K., Jing, W., Wang, J., Zhang, K., Li, Y., Xia, M., et al. (2024). Structure–activity mechanism of sodium ion adsorption and release behaviors in biochar. *Agriculture* 14, 1246. doi: 10.3390/agriculture14081246

Yue, Y., Guo, W. N., Lin, Q. M., Li, G. T., and Zhao, X. R. (2016). Improving salt leaching in a simulated saline soil column by three biochars derived from rice straw (Oryza sativa L.), sunflower straw (Helianthus annuus), and cow manure. *J. Soil Water Conserv.* 71, 467–475. doi: 10.2489/jswc.71.6.467

Zahra, N., Al Hinai, M. S., Hafeez, M. B., Rehman, A., Wahid, A., Siddique, K. H., et al. (2022). Regulation of photosynthesis under salt stress and associated tolerance mechanisms. *Plant Physiology and Biochemistry* 178, 55–69. doi: 10.1016/j.plaphy.2022.03.003

Zhang, J., Bai, Z., Huang, J., Hussain, S., Zhao, F., Zhu, C., et al. (2019). Biochar alleviated the salt stress of induced saline paddy soil and improved the biochemical characteristics of rice seedlings differing in salt tolerance. *Soil Tillage Res.* 195, 104372. doi: 10.1016/j.still.2019.104372

Zhang, J., Liu, X., Wu, Q., Qiu, Y., Chi, D., Xia, G., et al. (2023). Mulched drip irrigation and maize straw biochar increase peanut yield by regulating soil nitrogen, photosynthesis and root in arid regions. *Agricultural Water Management* 289, 108565. doi: 10.1016/j.agwat.2023.108565

Zhang, W. W., Chong, W. A. N. G., Rui, X. U. E., and Wang, L. J. (2019). Effects of salinity on the soil microbial community and soil fertility. *J. Integr. Agric.* 18, 1360–1368. doi: 10.1016/S2095-3119(18)62077-5

Zhang, Y., Liu, Q., Zhang, W., Wang, X., Mao, R., Tigabu, M., et al. (2021). Linkage of aggregate formation, aggregate-associated C distribution, and microorganisms in two different-textured ultisols: A short-term incubation experiment. *Geoderma* 394, 114979. doi: 10.1016/j.geoderma.2021.114979

Zhao, M., Anayatullah, S., Irfan, E., Hussain, S. M., Rizwan, M., Sohail, M. I., et al. (2023). Nanoparticles assisted regulation of oxidative stress and antioxidant enzyme system in plants under salt stress: A review. *Chemosphere* 314, 137649. doi: 10.1016/j.chemosphere.2022.137649

Zhao, C., Zhang, Y., Liu, X., Ma, X., Meng, Y., Li, X., et al. (2020). Comparing the effects of biochar and straw amendment on soil carbon pools and bacterial community structure in degraded soil. *J. Soil Sci. Plant Nutr.* 20, 751–760. doi: 10.1007/s42729-019-00162-4

Zhao, S., Zhang, Q., Liu, M., Zhou, H., Ma, C., and Wang, P. (2021). Regulation of plant responses to salt stress. *Int. J. Mol. Sci.* 22, 4609. doi: 10.3390/ijms22094609

Zheng, H., Wang, X., Luo, X., Wang, Z., and Xing, B. (2018). Biochar-induced negative carbon mineralization priming effects in a coastal wetland soil: Roles of soil aggregation and microbial modulation. *Sci. Total Environ.* 610, 951–960. doi: 10.1016/j.scitotenv.2017.08.166

Zheng, W., Xue, D., Li, X., Deng, Y., Rui, J., Feng, K., et al. (2017). The responses and adaptations of microbial communities to salinity in farmland soils: a molecular ecological network analysis. *Appl. Soil Ecology.* 120, 239–246. doi: 10.1016/j.apsoil.2017.08.019

Zhu, Y., Lv, X., Li, T., Zhong, M., Song, J., and Wang, H. (2022). Cotton straw biochar and compound Bacillus biofertilizer reduce Cd stress on cotton root growth by regulating root exudates and antioxidant enzymes system. *Front. Plant Sci.* 13. doi: 10.3389/fpls.2022.1051935

frontiers | Frontiers in Plant Science

TYPE Original Research
PUBLISHED 01 April 2025
DOI 10.3389/fpls.2025.1549173

OPEN ACCESS

EDITED BY
Xiao-Dong Yang,
Ningbo University, China

REVIEWED BY
Mika Tapio Tarkka,
Helmholtz Association of German Research Centers (HZ), Germany
Wenjing Li,
Xinjiang University, China

*CORRESPONDENCE
Xueli He
xlh3615@126.com
Yuxing Zhang
jonsonzhyx@163.com

RECEIVED 20 December 2024
ACCEPTED 17 March 2025
PUBLISHED 01 April 2025

CITATION
Liu Y, Wang Z, Sun X, He X and Zhang Y (2025) Specific soil factors drive the differed stochastic assembly of rhizosphere and root endosphere fungal communities in pear trees across different habitats.
Front. Plant Sci. 16:1549173.
doi: 10.3389/fpls.2025.1549173

Specific soil factors drive the differed stochastic assembly of rhizosphere and root endosphere fungal communities in pear trees across different habitats

Yunfeng Liu[1,2], Zhenzhou Wang[2], Xiang Sun[2], Xueli He[2*] and Yuxing Zhang[1*]

[1]College of Horticulture, Hebei Agricultural University, Baoding, China, [2]College of Life Sciences, Hebei University, Baoding, China

Introduction: *Pyrus betulifolia* is tolerant to diverse environmental conditions and is commonly planted in infertile habitats (such as beaches and ridges) to conserve arable land for cereal crops. Symbiotic fungi in the rhizosphere and root endosphere benefit host plants by enhancing their resilience to nutritional deficiencies under stressful conditions. However, the mechanisms underlying the assembly of these symbiotic fungal communities in the roots of *P. betulifolia* across different habitats remain poorly understood.

Methods: *Pyrus betulifolia* of 30-year-old were selected from five sites in northern China to investigate the assembly of fungal communities in the rhizosphere and root endosphere. Soil samples were collected to assess the heterogeneity of the environment surrounding each plant. Procrustes analysis, variance partitioning analysis, and ordination regression analysis were employed to explore the ecological relationships between soil factors and fungal community composition.

Results: The rhizosphere fungal community exhibited higher richness, greater diversity and lower structural variability compared to the root endosphere. Additionally, the rhizosphere supported a fungal network with higher abundance and stronger connectivity than the root endosphere. The composition of fungal communities varies significantly among different regions. In both the rhizosphere and root endosphere fungal communities, the number of genera specific to mountainous regions was larger than those in plain areas and saline-alkali areas. Null model-based analyses indicated that the assembly of rhizosphere and root endosphere fungal communities in *P. betulifolia* was mainly governed by stochastic processes. Specifically, in non-saline-alkali soils, the assembly of rhizosphere fungi was primarily driven by dispersal limitation, whereas the assembly of root endosphere fungi was dominated by ecological drift. In saline-alkali soils, both rhizosphere and root endosphere fungal communities were primarily influenced by ecological drift.

Conclusion: The assembly of root-associated fungal communities in *P. betulifolia* is not only driven by soil physicochemical properties but also influenced by root compartment niche and topography. Moreover, the impact

intensity of the root compartment niche is greater than topography. Specifically, the assembly of the rhizosphere fungal community was primarily influenced by alkaline nitrogen (AN) and alkaline phosphatase (ALP), while the root endosphere fungal community was more strongly affected by pH and sucrase (SUC). These findings could provide valuable insights for the design of beneficial root-associated microbiomes to enhance fruit tree performance.

KEYWORDS

fungal community, rhizosphere, root endosphere, assembly, ecological relationship

1 Introduction

The soil-root interface is a hotspot for microbial activity, where plant roots provide abundant organic compounds, attracting a diverse array of microorganisms. These microorganisms establish complex symbiotic relationships with plant roots. Along the soil-root continuum, plant roots organize soil microorganisms into three distinct microhabitats, based on differences in the plant-inhabiting niches: the rhizosphere (the microbial community surrounding the roots), the rhizoplane (the epiphytic microbial community on the root surface), and the root endosphere (the microbial community living inside the roots) (Lee et al., 2019). Among plant-associated microbial communities, fungi dominate and play a crucial role in plant health and functionality (Trivedi et al., 2020). In recent years, significant progress has been made in understanding the characteristics and assembly mechanisms of microbial communities in the rhizosphere and root endosphere. Different root niches support distinct microbial communities, and the process of community assembly is a key mechanism that determines microbial composition. This process is influenced either by the filtering effects of environmental parameters or by stochastic processes, such as random dispersal. While research on root-associated microorganisms has predominantly focused on grasses and crops (Latz et al., 2021), studies on woody plants, particularly pears, remain limited. Therefore, understanding the assembly rules of fungal communities in pears and their ecological relationships with soil physicochemical properties is crucial for advancing our knowledge of fruit trees ecosystem structure and function.

Rhizosphere fungi form symbiotic relationships with plants, directly influencing plant growth and health (Bakker et al., 2013). These fungi convert nutrients that are difficult for plant roots to absorb, such as organic phosphorus, into more accessible forms, thereby enhancing nutrient utilization efficiency in plants. The assembly of rhizosphere fungi is shaped by multiple factors, including soil environmental conditions and root compartment niches. On one hand, changes in the physicochemical properties of the soil can directly or indirectly alter the living conditions of rhizosphere fungi, affecting their assembly patterns. On the other hand, host plants interact with rhizosphere fungi through root exudates and other mechanisms, exerting either inducing or inhibitory effects on fungal assembly (Hassani et al., 2018). However, the primary factors influencing the assembly of rhizosphere fungi remain unclear.

The biological relationship between plants and root endophytes is symbiotic and co-evolutionary. These endophyte taxa are considered the "second genome" of plants and play a crucial role in the health of multicellular hosts (Trivedi et al., 2020). For example, mycorrhizal fungi expand the root system's absorption area, enhancing water and phosphorus uptake (Basiru et al., 2023). Endophytic fungi such as *Paraphoma* sp. derived from the root system can help plants neutralize heavy metal toxicity and improve stress resistance. Investigating the composition and assembly process of fungal communities in the root endosphere of pear trees under different habitats, as well as their interrelationships with soil physicochemical properties, is crucial for comprehensively understanding the plant-microbe symbiotic system.

Pyrus betulifolia belongs to the deciduous trees of Rosaceae. As a wild species widely distributed in northern China, it is native to the deciduous forest areas in northern, central China and Tibet. Its root system is well-developed with numerous fibrous roots, and it has excellent abilities of drought tolerance, cold tolerance and salt-alkali stress tolerance (Li et al., 2016). Moreover, it can tolerate lime-induced iron chlorosis (Zhao et al., 2020). Due to its excellent grafting compatibility, *P. betulifolia* is the main rootstock in the commercial pear production in northern China, and also a crucial parental material in the cultivation of dwarf pear rootstocks and the resistance breeding work. Although *P. betulifolia* can adapt to various extreme soil types such as mountainous areas and saline -alkali lands, it is extremely sensitive to the changes in soil fertility. Therefore, regulating the soil physicochemical properties is of great significance for the growth and development of *P. betulifolia* plants and even the improvement of the pear yields above-ground. Traditional soil improvement methods, such as deep plowing and the application of organic fertilizers, are effective but costly. Adjusting the structure of the fungal community in the rhizosphere and endosphere, as a "green" strategy, can enhance the rhizosphere micro-ecological environment and optimize soil properties (Edwards et al., 2015). Previous studies have reported the soil physicochemical properties and fungal community composition of pear trees in different regions, but the research remains relatively superficial. For example, Huang et al. reported the effects of soil chemical properties

and geographical distance on the composition of arbuscular mycorrhizal fungal communities in pear orchards (Huang et al., 2019). Currently, the role of the holobiome system composed of *P. betulifolia* and its microbial symbionts has received little attention. In this study, 30-year-old *P. betulifolia* pear trees were selected from five sites in Northern China to investigate the composition of rhizosphere and root endosphere fungal communities and their assembly processes. We formulated three hypotheses: (1) The root compartment niches (rhizosphere and root endosphere) of pear trees significantly influence the diversity and composition of fungal communities. (2) The assembly of rhizosphere and root endosphere fungal communities in pear trees is primarily governed by stochastic processes and is influenced by soil physicochemical factors. (3) Fungal community composition varied significantly across regions, with topography influencing fungal assembly. This study contributes to a better understanding of the relationship between plants and their microbiota, providing a foundation for engineering beneficial plant microbiota in sustainable agricultural production.

2 Materials and methods

2.1 Experimental sites

Pear's root and rhizosphere soil samples were collected in May 2023 from five pear-growing regions in Hebei Province, China: WX, XJ, BT, QY, and YT. At the regional scale, topography is a crucial determinant of the patterns of species diversity and species composition within forest communities. Moreover, various habitat types have often been proven to be defined by topographic features, such as altitude (Wang et al., 2022). According to the geomorphic features and altitudes, five regions were classified into two types: the mountainous type, which includes YT and QY regions, and the plain type, which encompasses BT region, WX region, and XJ region. Since *P. betulaefolia* plants in YT region mostly grow in valley areas, while a large number of pear trees in QY region are planted at relatively high altitudes, the altitudes of the sampling sites in YT region are relatively low, and those in QY region are relatively high. As the samples in this study were collected from the salinized soil area of BT region, and according to the measurement results of soil pH, which were significantly higher than those of other regions, BT region was classified as a saline-alkali land type. Finally, these three different types of ecological environments were uniformly defined as habitat types, namely the mountainous type, the plain type, and the saline-alkali land type. These regions share a temperate semi-arid monsoon climate with distinct seasonal variations. Detailed regional information was provided in Supplementary Table S1.

2.2 Collection strategy and laboratory process of samples

Three plots of 30 m × 20 m were established at each site (WX, XJ, QY, and BT), and two plots were set up at YT, for a total of 14 plots, in May, 2023. Nine healthy 30-year-old pear trees at the full fruiting stage were randomly selected in each plot (126 individuals in total). Dead branches and leaves around each tree were removed. Root and rhizosphere soil samples were collected from each selected tree using a shovel that was sprayed with 75% ethanol and wiped with sterilized paper before use. Fine roots (approximately 50 g) were carefully picked from a hole 30 cm deep, 30–50 cm away from the main trunk with sterile plastic bags. Rhizosphere soil (approximately 1000 g) was gently shaken off the roots and collected with sterile plastic bags. The root and soil samples were labeled and transported to the laboratory on ice immediately. Rhizosphere soil for DNA extraction was gently brushed off the roots with a fine brush, collected into 5 mL centrifuge tubes, and stored at -80°C. Root samples were brushed and washed with deionized water, then surface-sterilized with 70% ethanol for 5 minutes and 5% sodium hypochlorite for 2 minutes, followed by rinsing with sterile distilled water. These samples were then frozen in liquid nitrogen and stored at -80°C for DNA extraction. Fifty grams of bagged rhizosphere soil were stored at 4°C for subsequent enzyme activity assays. The remaining soil was air-dried, sieved through a 2-mm mesh, and used for physical and chemical property measurements.

2.3 Extraction of total DNA and high-throughput sequencing

Root and rhizosphere soil samples of 0.1 g each were used for DNA extraction. Total genomic DNA was extracted using the E.Z.N.A.®Soil DNA Kit (Omega Bio-tek) following the manufacturer's instructions. DNA concentration and purity were assessed using a NanoDrop 2000 (Thermo Fisher Scientific, USA) and checked for quality by 1% agarose gel electrophoresis. PCR amplification of the fungal ITS1 region was performed using barcoded primers ITS1F (5'-CTTGGTCATTTAGAGGAAGTAA-3') and ITS2R (5'-GCTGCGTTCTTCATCGATGC-3'). The PCR mixture contained 4 μL of 5×TransStart FastPfu buffer, 2 μL of 2.5 mM dNTPs, 0.8 μL of each primer (5 μM), 0.4 μL of TransStart FastPfu DNA polymerase, 10 ng of DNA, and nuclease-free water to a final volume of 20 μL. Amplification conditions were as follows: 95°C for 3 min, followed by 27 cycles of 95°C for 30 s, 55°C for 30 s, and 72°C for 30 s, with a final extension at 72°C for 10 min. PCR products were purified by 2% agarose gel electrophoresis and extracted using the AxyPrep DNA Gel Extraction Kit (Axygen Biosciences, Union City, CA, USA). The purified products were quantified using the Quantus™ Fluorometer (Promega, USA). Library construction was performed using the NEXTFLEX Rapid DNA-Seq Kit, including adapter ligation, magnetic bead selection, PCR enrichment, and bead recovery. Sequencing was conducted on the Illumina PE300 platform (Shanghai Meiji Biomedical Technology Co., Ltd.), and raw data were uploaded to the NCBI SRA database (PRJNA1161009, PRJNA1160469).

Quality control of paired-end raw sequencing reads was conducted using fastp (Chen et al., 2018) (https://github.com/OpenGene/fastp, version 0.19.6). Read merging was performed

with FLASH (http://www.cbcb.umd.edu/software/flash, version 1.2.11), filtering out bases with a quality score below 20 at read tails using a 50 bp sliding window. Reads shorter than 50 bp or containing N bases were discarded. Paired reads were merged with a minimum overlap of 10 bp and a maximum allowed mismatch ratio of 0.2. Sequences were filtered based on barcode (0 mismatches) and primer mismatches (up to 2 mismatches). Quality-controlled and merged sequences were clustered into Operational Taxonomic Units (OTUs) with 97% similarity using UPARSE v7.1 (Edgar, 2013) (http://drive5.com/uparse/), and chimeric sequences were removed. Sequences annotated as non-fungi organisms were excluded. Samples were rarefied to the minimum sequence count. OTU taxonomic classification was conducted using the RDP classifier (http://rdp.cme.msu.edu/, version 2.11) against UNITE database (version 8.0). Functional guild annotation was performed using FUNGuild software v1.0 (http://www.funguild.org/).

2.4 Soil physicochemical properties analysis

SM was measured using a FieldScout TDR 350 (Spectrum, Aurora, Illinois, US) soil moisture meter. Soil pH was determined with a portable pH meter (pH 3000, STEP Systems GmbH, Germany). OC was assessed by loss-on-ignition in a TMF-4-10 T muffle furnace (Gemtop, Shanghai, China) at 550°C for 4 h (Heiri et al., 2001). TN was measured using the semi-micro Kjeldahl method, and TP was quantified by sulfuric acid-hypochlorite digestion (Valderrama, 1981). Alkaline nitrogen (AN) and AP were measured using the alkaline diffusion method and sodium bicarbonate extraction-molybdenum antimony colorimetric method, respectively (Bever et al., 1996; Tarafdar and Marschner, 1994). AK was determined by NH_4OAc extraction-flame photometry. EC was measured with a DDS-307W conductivity meter (Lida Instruments, Shanghai, China). The C/N ratio was calculated from soil OC and TN. ALP activity was measured using the modified Bremner and Tabatabai method (Tarafdar and Marschner, 1994), assessing the conversion of pNPP (μg/g) per gram of soil per hour. UR activity was assessed by the method described by Kandeler and Gerber (1988), measuring NH_3-N production (μg) from urea decomposition per gram of soil per hour. SUC activity was assessed using the 3,5-dinitrosalicylic acid method, measuring glucose (mg/g) produced from sucrose hydrolysis per gram of soil. Altitude and latitude-longitude data were obtained from a GPS device. MAT and MAP were sourced from the China Meteorological Data Network (http://cdc.cma.gov.cn).

2.5 Statistical analysis

Alpha diversity was calculated using mothur (Rzehak et al., 2024) software (http://www.mothur.org/wiki/Calculators), with differences analyzed using the Wilcoxon rank-sum test ($P < 0.05$). PCoA based on Bray-Curtis distance was used to assess the similarity in fungal community structure, while Beta diversity analysis evaluated within-group dispersion of rhizosphere and root endosphere fungal communities. PERMANOVA non-parametric tests and ANOSIM similarity analysis were conducted to explore differences between rhizosphere and root endosphere fungi, as well as variations across different regions. Based on the results of the taxonomic analysis, the species compositions at the phylum and class levels of different groups were analyzed. The Wilcoxon rank-sum test was used to analyze whether microbial community relative abundances were significantly different between rhizosphere and root endosphere ($P < 0.05$). Differences among regions were analyzed using a Kruskal-Wallis H test ($P < 0.05$). R (version 3.3.1) software was used to achieve the Venn diagram at the genus level. Circos software (Circos-0.67-7, http://circos.ca/) was used to visualize the relationships between rhizocompartment types or regions types and the relative abundances of fungal trophic modes. Soil physicochemical properties were analyzed using SPSS 24.0, and mean values were compared using Duncan's test ($P < 0.05$). Procrustes analysis via PCA plots was used to assess correlations between fungal communities and soil properties. VPA investigated the effects of soil, geographical, and climatic factors on fungal communities. Mantel analysis in R 3.3.1 with the vegan package (version 2.4.3) examined the influence of soil physicochemical properties on microbial structure. Spearman correlation was used to assess the association between soil physicochemical properties and fungal phyla.

Network parameters were analyzed using R packages (igraph, psych, Hmisc, vegan, dplyr, reshape2), and network modularity was assessed in Gephi. Microbial diversity and ecological evolution were studied within a deterministic versus stochastic framework. The βNTI index (based on βMNTD and phylogenetic quantification) was used to determine process dominance: $|\beta NTI| \geq 2$ indicated deterministic processes, while $|\beta NTI| < 2$ indicated stochastic processes. The relative contributions of deterministic (homogeneous and heterogeneous selection) and stochastic processes (dispersal limitation, homogeneous dispersal, ecological drift) were quantified using βNTI and RCBray.

3 Results

3.1 Analysis of rhizosphere soil physicochemical properties

Analysis of the physicochemical properties of rhizosphere soil across regions revealed that YT had the highest levels of soil TN (1.56 mg/g), AN (156.14 μg/g), and OC (31.92 mg/g), but the lowest TP (0.19 mg/g) (Figures 1A–C, F). The C/N ratio was highest in XJ (37.42), significantly exceeding that of WX, BT, and YT, with no significant difference from QY (Figure 1G). WX had the highest TP and AP at 0.25 mg/g and 38.59 μg/g, respectively (Figure 1B, D). Soil AK was significantly higher in WX and YT, at 124.83 μg/g and 129 μg/g, respectively, compared to other regions (Figure 1E). Soil pH was the highest in BT at 8.22 and lowest in QY at 6.79 (Figure 1H). Soil EC was the highest in BT (486.67 μS/cm) and lowest in QY (162.25 μS/cm) (Figure 1I). Soil ALP activity was the highest in YT at 249.87 μg/g/h (Figure 1J). Soil UR activity was the

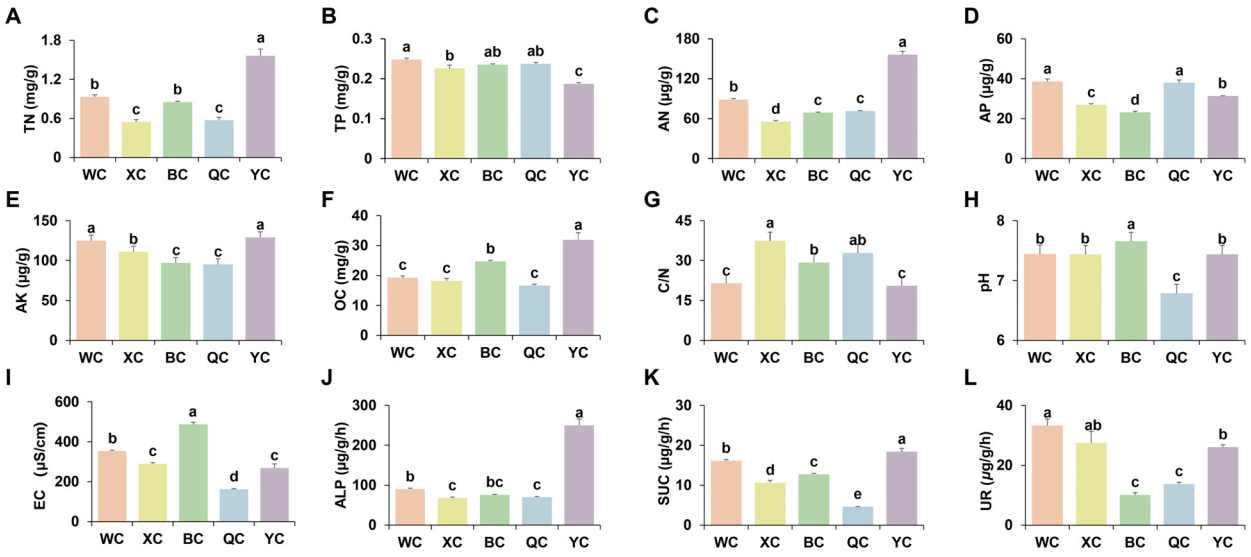

FIGURE 1
Characteristics of physicochemical properties and enzyme activity of the pear trees rhizospheric soil among different regions. The error bars illustrate the standard error of the mean. Different lowercase letter above the error bars indicates significant difference at $P < 0.05$. **(A)** TN. **(B)** TP. **(C)** AN. **(D)** AP. **(E)** AK. **(F)** OC. **(G)** C/N: OC/TN. **(H)** pH. **(I)** EC. **(J)** ALP. **(K)** SUC. **(L)** UR. The WC, XC, BC, QC and YC represent rhizosphere soils from WX, XJ, BT, QY and YT regions, respectively.

highest in WX (33.28 μg/g/h) and XJ (27.44 μg/g/h), followed by YT (26.09 μg/g/h), with BT and QY having the lowest values at 10.11 μg/g/h and 13.74 μg/g/h, respectively (Figure 1L). SUC activity was the highest in YT at 18.41 μg/g/h and lowest in QY at 4.61 μg/g/h (Figure 1K). SM was highest in BT (144.29%vwc) and lowest in QY (77.98%vwc) (Supplementary Figure S1).

3.2 Diversity and symbiotic patterns of rhizosphere and root endosphere fungi

Alpha and Beta diversity metrics were used to assess fungal community heterogeneity. The abundance and Shannon index (α-diversity) of rhizosphere fungi were significantly higher than those of root endosphere fungi ($P < 0.001$). Specifically, the Sobs index for rhizosphere fungi in YT was significantly higher than in other regions ($P < 0.001$). The Shannon index of rhizosphere fungi in BT was significantly higher than in XJ, QY and YT ($P < 0.001$). For root endosphere fungi, the Sobs index in QY was the highest, significantly greater than in WX ($P < 0.05$) and YT ($P < 0.001$). The Shannon index of root endosphere fungi was significantly higher in BT than in WX ($P < 0.01$) and QY ($P < 0.001$). Additionally, the Shannon index of root endosphere fungi was significantly higher in YT than in QY ($P < 0.01$) (Figures 2A–C).

PCoA based on Bray-Curtis distance revealed that rhizosphere and root endosphere fungal communities formed two distinct clusters along the first coordinate axis, which explained 25.66% of the total variation, indicating distinct spatial differentiation (Permutational multivariate analysis of variance (PERMANOVA): $R^2 = 0.16$, $P < 0.001$; ANOSIM: $R = 0.64$, $P < 0.001$). Root endosphere fungal communities exhibited significantly higher variation in sample classification compared to rhizosphere fungi ($P < 0.001$). PCoA analysis of rhizosphere fungi across regions showed significant compositional differences (PERMANOVA: $R^2 = 0.36$, $P < 0.001$; ANOSIM: $R = 0.82$, $P < 0.001$). Rhizosphere fungal communities in QY, YT, and WX did not significantly separate along the first coordinate axis but were clearly distinct from those in BT and XJ. Rhizosphere fungi in BT and XJ formed independent clusters along the second coordinate axis, indicating differences from other regions. For root endosphere fungi, PCoA analysis also revealed significant compositional differences among regions (PERMANOVA: $R^2 = 0.23$, $P < 0.001$; ANOSIM: $R = 0.40$, $P < 0.001$) (Figures 2D–F). PERMANOVA of fungal data showed that variations in microbial communities were influenced by both region types and root compartment niches ($R^2 = 0.40$, $P < 0.001$). In addition, niches ($R^2 = 0.16$, $P < 0.001$) explained more differences in the microbial community than region type ($R^2 = 0.14$, $P < 0.001$). Particularly, region types ($R^2 = 0.14$, $P < 0.001$) explained more differences in the microbial community than topography ($R^2 = 0.08$, $P < 0.001$). All regions rendered rhizosphere and root endosphere fungal microbiota significantly dissimilar from each other (P values listed in Table 1).

Co-occurrence networks analysis revealed that the rhizosphere fungal community formed a highly interconnected network with a larger scale (nodes = 351) and higher connectivity (edges = 1171) (Supplementary Table S2). Positive correlations dominated in both networks, accounting for 87.36% and 99.19%, respectively, while negative correlations were less common (12.64% and 0.81%) (Figure 2G). Comparative analysis across regions showed notable differences in network structures, despite high connectivity of rhizosphere and root endosphere fungi in various regions (Supplementary Figure S2). In BT, the rhizosphere fungal

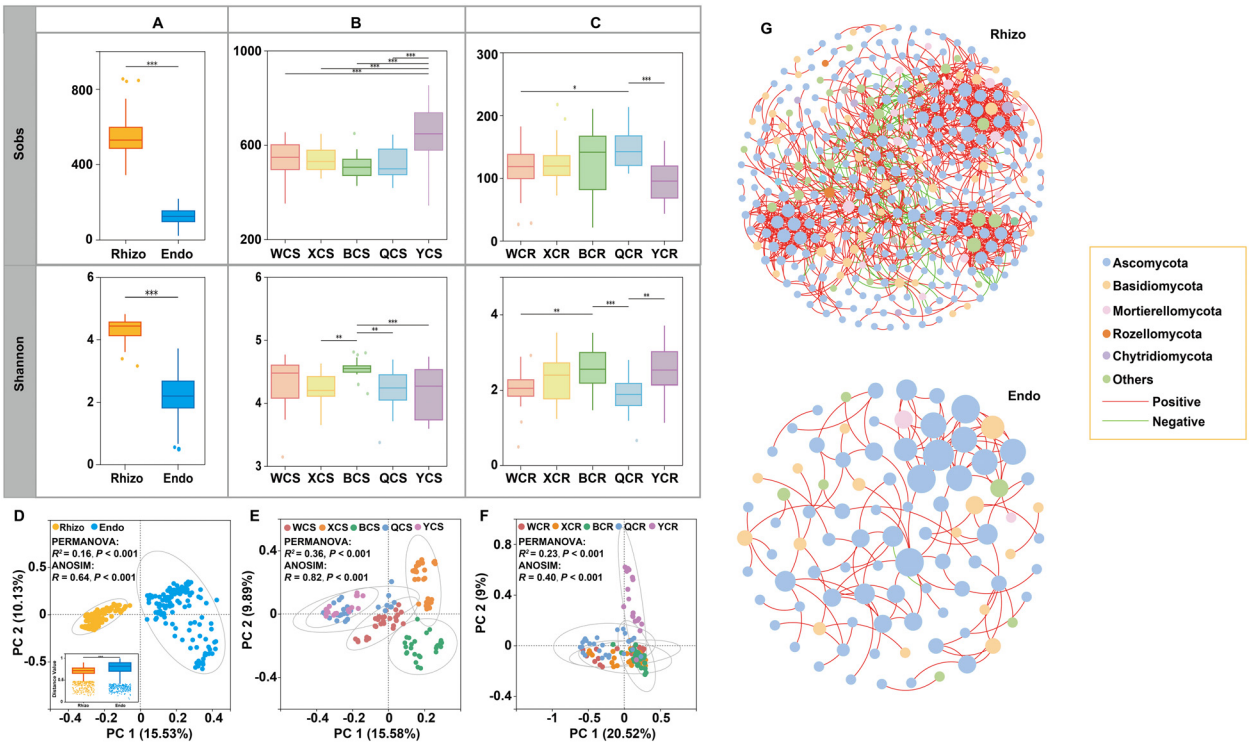

FIGURE 2
The α diversity and β diversity of fungal communities inhabiting the rhizosphere (Rhizo) and root endosphere (Endo). **(A)** Sobs and Shannon indices of fungal communities in the rhizosphere and root endosphere. **(B)** Sobs and Shannon indices of fungal communities in the rhizosphere of different regions. **(C)** Sobs and Shannon indices of fungal communities in the root endosphere of different regions. **(D)** PCoA plot depicting the β diversity patterns of rhizospheric and root endospheric fungal communities. **(E)** PCoA plot depicting the β diversity patterns of rhizospheric fungal communities of different regions. **(F)** PCoA plot depicting the β diversity patterns of root endospheric fungal communities of different regions. **(G)** Co-occurrence networks of fungal communities in the rhizosphere (Rhizo) and root endosphere (Endo). Nodes represent fungal OTUs. Edges represent significant interactive correlations between pairs of OTUs. Node colors represent fungal OTUs species information (phylum level) and the size of nodes corresponds to the relative abundances of specific fungus. Red edges indicate positive relationships, and green edges indicate negative relationships. *$P < 0.05$; **$P < 0.01$; ***$P < 0.001$. WCS (WCR), XCS (XCR), BCS (BCR), QCS (QCR) and YCS (YCR) represent rhizosphere (root endosphere) fungi in WX, XJ, BT, QY, and YT regions, respectively.

network had the most nodes (nodes = 279), whereas XJ had the highest number of edges, clustering coefficient, and network density (edges = 4434; clustering coefficient = 0.575; network density = 0.146), but the lowest modularity (modularity = 0.228). Conversely, YT's rhizosphere fungal network had the fewest nodes but the highest modularity (nodes = 175; modularity = 0.424). WX's rhizosphere fungal network showed lower connectivity and clustering coefficient (edges = 1401; clustering coefficient = 0.399). For root endosphere fungi, YT's network had the most nodes (nodes = 97), while XJ led in edges, clustering coefficient, and network density (edges = 548; clustering coefficient = 0.663; network density = 0.173). WX's root endosphere fungal network had the lowest node connectivity but the highest modularity (nodes = 38; edges = 38; modularity = 0.798) (Supplementary Table S2).

3.3 Taxonomic and functional composition of rhizosphere and root endosphere fungi

Taxonomic analysis revealed the OTUs were classified into 14 phyla, 46 classes, 111 orders, 249 families, and 560 genera. The dominant fungal phyla were *Ascomycota* (70.63–93.58%), *Basidiomycota* (5.43–25.61%) and *Mortierellomycota* (8.04–15.66%) (Figure 3A). At the class level, the dominant classes were *Sordariomycetes* (36.98–51.42%) and *Dothideomycetes* (8.72–22.46%). Notably, *Dothideomycetes* (54.82%) was the most abundant in the root endosphere of QY (Figure 3B). Fungal taxonomic distributions showed significant differences between the rhizosphere and root endosphere microhabitats. *Ascomycota* was significantly ($P < 0.05$) enriched in the root endosphere, while *Mortierellomycetes* was depleted in this compartment compared to the rhizosphere (Figure 3C). *Dothideomycetes*, *Agaricomycetes*, and *Leotiomycetes* were significantly ($P < 0.05$) enriched in the root endosphere, whereas *Mortierellomycetes*, *Eurotiomycetes*, *Tremellomycetes* and *Pezizomycetes* were depleted, as compared to the rhizosphere (Figure 3D). Region-specific patterns were observed, with *Leotiomycetes* (29.17%) being significantly ($P < 0.05$) enriched in the root endosphere of Yutian (YT), and *Tremellomycetes* (15.70%) enriched in the rhizosphere of YT. *Agaricomycetes* was significantly ($P < 0.05$) enriched in the root endosphere of XJ and BT (Supplementary Figure S3).

Venn analysis revealed that the rhizosphere and root endosphere fungal genera numbered 411 and 544, respectively, with 395 shared genera, representing 53.55% of the total. The

TABLE 1 R^2 and *P* values calculated by PERMANOVA for the variance of fungal communities among different regions.

Factors	Results by factor		Results by regions/niche		
	R^2	*P* value[a]		R^2	*P* value[a]
Root compartment niche (Rhizo *vs* Endo)	0.16	0.001	WX	0.28	0.001
			XJ	0.25	0.001
			BT	0.29	0.001
			QY	0.30	0.001
			YT	0.35	0.001
region type	0.14	0.001	Rhizo	0.36	0.001
			Endo	0.23	0.001
Topography	0.08	0.001	Rhizo	0.20	0.001
			Endo	0.11	0.001
Compartment niche×region type	0.40	0.001			
Compartment niche×topography	0.28	0.001			

Rhizo, rhizosphere; Endo, root endosphere.

rhizosphere contained 149 unique genera, while the root endosphere had only 16 unique genera, indicating substantial differences in community composition. Regional comparisons revealed that 298 genera were shared across regions in the rhizosphere (30.13% of total), while the number of unique genera varied across regions: YT and QY had 21 and 7 unique genera (5.64% and 3.80%, respectively); BT had 6 unique genera (2.63%); WX and XJ had 3 and 5 unique genera (1.57% and 1.88%, respectively). For root endosphere fungi, 101 unique genera were shared across regions (10.14% of total), with YT and QY having the most unique genera (29 and 23, respectively), followed by WX (21), XJ (18), and BT (15) (Supplementary Figure S4).

Functional annotation of fungal taxa using the FunGuild database categorized fungi into three primary trophic modes: pathotrophs, symbiotrophs, and saprotrophs. The major trophic modes were further divided into specific guilds, including arbuscular mycorrhizal fungi, plant pathogens, and animal pathogens (Schmidt et al., 2019). In terms of trophic modes, saprotrophs (38.49%) and pathotroph-saprotroph-symbiotrophs (29.4%) dominated both rhizosphere and root endosphere fungal assemblages (Supplementary Figure S5A). No significant differences in trophic modes were observed among rhizosphere fungi across regions (Supplementary Figure S5B). Notably, pathotroph-saprotrophs accounted for a larger proportion (32%) in the composition of root endophytic fungi in YT compared to other regions (Supplementary Figure S5C). From the perspective of fungal guilds, undefined saprotrophs (22.00%–29.97%) and unknown fungi (10.52%–32.98%) were predominant in both the rhizosphere and root endosphere across the five regions. Unknown fungi (32.98%) were the most abundant in the root endosphere of BT, while wood saprotrophs (37.92%) were most abundant in the root endosphere of QY. The Endophyte-Plant Pathogen-Undefined Saprotroph guild (26.92%) was a prominent category in the root endosphere of YT. Ectomycorrhizal fungi and endophytes were found in both rhizosphere and root endosphere across the five regions but in small quantities. Ericoid Mycorrhizal fungi were present in the rhizosphere and root endosphere of YT,

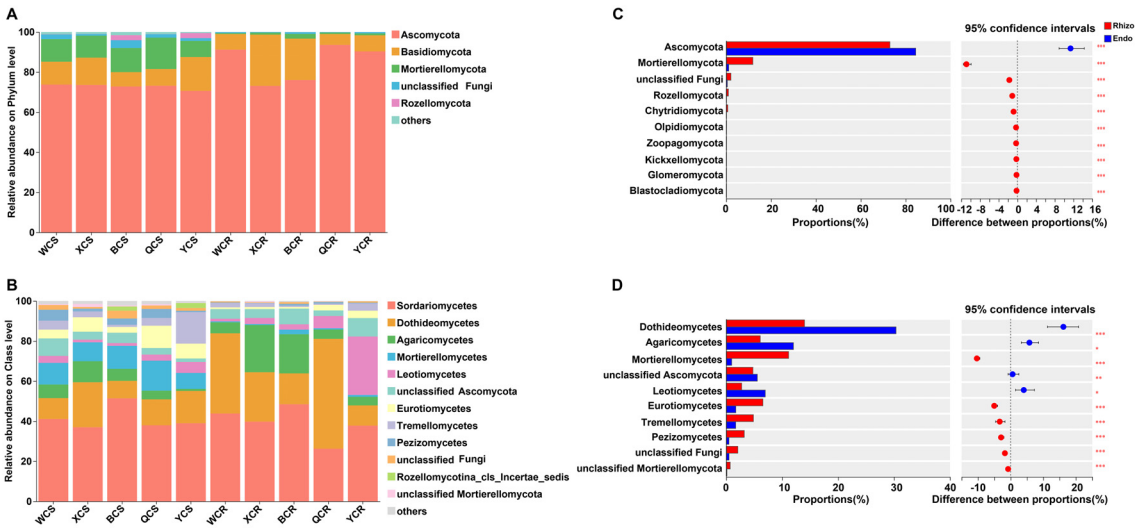

FIGURE 3
Fungal composition of the rhizosphere (S) and root endosphere (R) of *P. betulifolia*: relative abundances of fungal community structure at the phyla **(A)** and class **(B)** levels. **(C)** and **(D)** show taxa differences of fungi between the rhizosphere and root endosphere at the phyla and class levels, respectively. The vertical axis shows taxa at class level with mean sums in the top 10, and different colored boxes indicate different groups. The horizontal axis represents the average relative abundance of taxa. *$P < 0.05$; **$P < 0.01$; ***$P < 0.001$, Rhizo and Endo, Rhizosphere and root endosphere, respectively.

WX, and QY, particularly in the QY root endosphere (Supplementary Figures S5D, E).

3.4 Ecological evolution of fungal community assemblage aggregation in the rhizosphere and root endosphere

The ecological and evolutionary mechanisms driving the assembly of rhizosphere and root endosphere fungal communities were explored using the βNTI and Raup-Crick (RC-Bray) models based on Bray-Curtis dissimilarity. The results revealed that stochastic processes predominated in both community types. Specifically, rhizosphere fungi were mainly influenced by dispersal limitation (72.68%), while root endosphere fungi were primarily shaped by ecological drift (84.24%) (Figures 4A–C). Regional analysis showed that the assembly of rhizosphere fungi in WX, XJ, QY, and YT was primarily controlled by dispersal limitation, contributing 52.67%, 53.50%, 68.04%, and 67.28%, respectively, to microbial community structure. In contrast, the assembly of rhizosphere fungi in BT was mainly driven by ecological drift (39.37%) (Figure 4D). For root endosphere fungi, ecological drift dominated across all regions, contributing 69.82%, 60.77%, 76.41%, 48.42%, and 58.64% in WX, XJ, BT, QY, and YT, respectively. Notably, in the QY region, dispersal limitation played a significant role, contributing 43.07%, which was nearly equivalent to the effect of ecological drift. Compared with other regions, homogeneous selection occupied a larger proportion (about 37.65%) of the root endosphere fungal assemblage in YT (Figure 4E).

3.5 Relationship between fungal assemblages in rhizosphere and root endosphere, and rhizosphere soil physicochemical properties

Procrustes analysis was used to compare the alignment between rhizosphere and root endosphere fungal community structures and environmental factors (e.g. soil properties, geography, and climate), revealing significant correlations with environmental factors ($P < 0.001$) (Figures 5A, B). Variance partitioning analysis (VPA) further indicated that rhizosphere soil physicochemical properties were key determinants of fungal community composition in both rhizosphere and root endosphere, explaining 32.86% and 37.12% of the variance, respectively (Figures 5C, D). Mantel analysis demonstrated significant relationships between fungal communities and rhizosphere soil physicochemical properties (Supplementary Figure S6). To reveal potential relationships, ordination regression analysis showed significant correlations ($P < 0.05$) between rhizosphere fungal composition and rhizosphere soil factors (TN, TP, AN, AP, OC, C/N, pH, ALP, SUC, and AK), except UR and SM. Similarly, root endosphere fungi displayed significant correlations ($P < 0.05$) with TN, TP, AN, AP, OC, C/N, pH, ALP, SUC, and SM, excluding UR and AK. In specific, the assembly of rhizosphere fungi community was mainly affected by AN (44.6%) and ALP (31.9%), while the assembly of root endosphere fungi was primarily affected by pH (42.3%) and SUC (27.7%) (Figure 6).

Spearman correlation analysis revealed that rhizosphere soil physicochemical properties had a stronger association with the

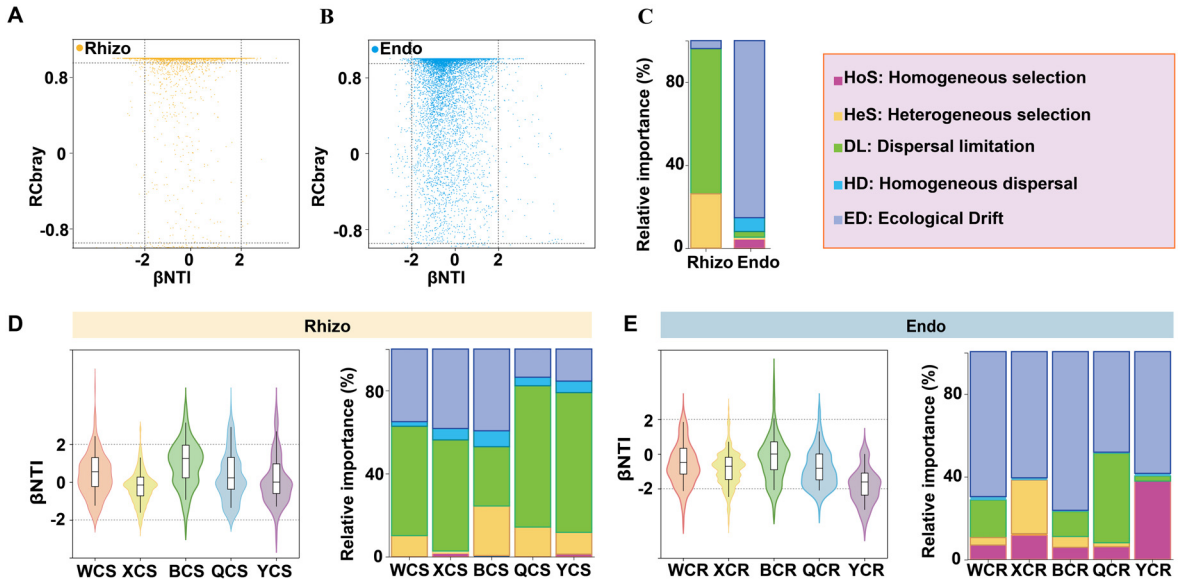

FIGURE 4
The relative importance of ecological processes that determine fungal community assembly in the rhizosphere (Rhizo) and root endosphere (Endo). **(A)** Variation in the βNTI and RCBray for fungal communities in the rhizosphere. **(B)** Variation in the βNTI and RCBray for fungal communities in the root endosphere. **(C)** The percentages depicted in stacked bar charts represent the proportions at which homogeneous selection, heterogeneous selection, dispersal limitation, homogenizing dispersal and ecological drift contribute to fungal community assembly. **(D)** Variation in the βNTI and RCBray for fungal communities in the rhizosphere of different regions. **(E)** Variation in the βNTI and RCBray for fungal communities in the root endosphere of different regions. βNTI > 2 indicates variable selection, and βNTI < −2 indicates homogenous selection. |βNTI| < 2 and RCBray < −0.95 indicate homogenous dispersal. |βNTI| < 2 and RCBray > 0.95 indicate dispersal limitation. |βNTI| < 2 and |RCBray| < 0.95 mainly indicate ecological drift.

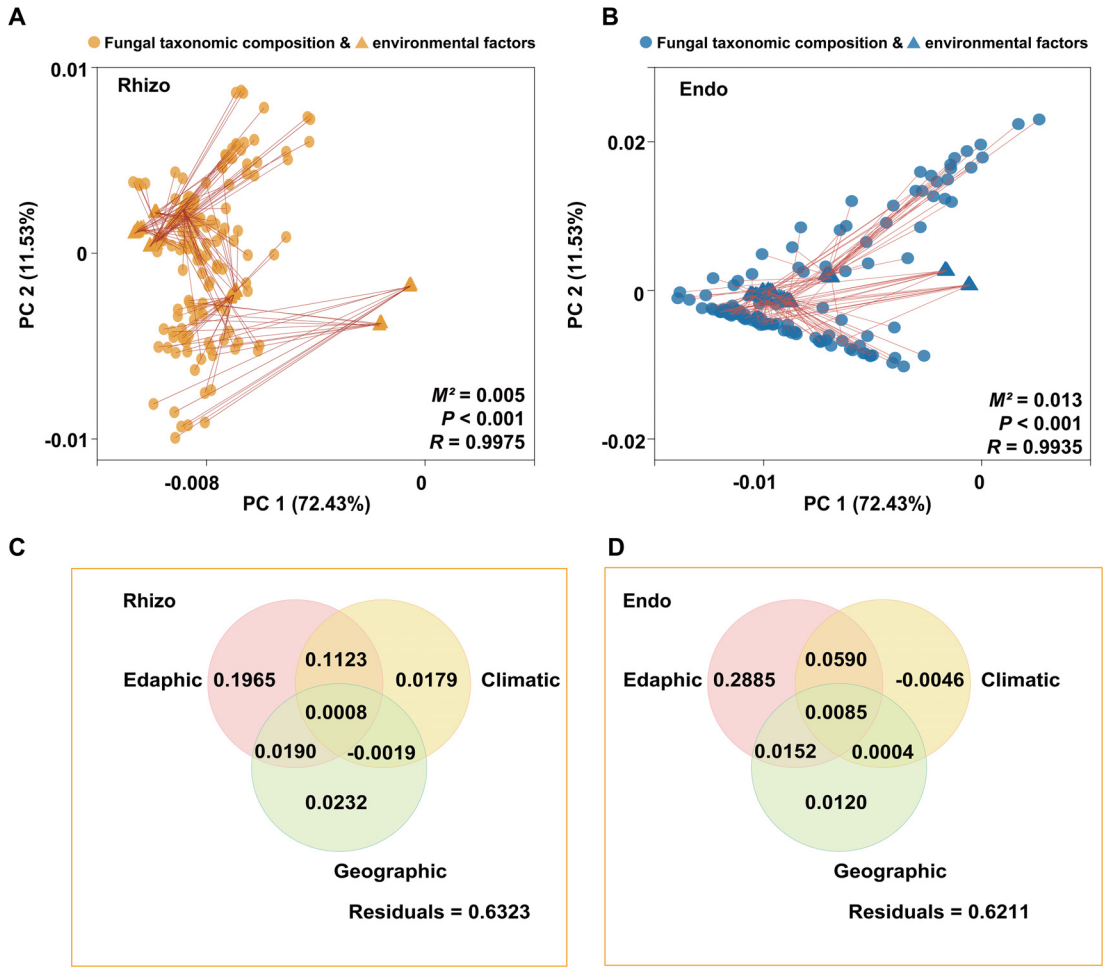

FIGURE 5
Analysis of correlation between the rhizospheric (Rhizo) and root endospheric (Endo) fungal taxonomic compositions and environmental factors. **(A)** Procrustes analysis of the rhizosphere fungal taxonomic compositions and environmental factors. **(B)** Procrustes analysis of the root endosphere fungal taxonomic compositions and environmental factors. M^2 indicates the sum of the squared distances between matched sample pairs. *R* represents the correlation in a symmetric Procrustes rotation; the *P* value is determined from 999 labeled permutations. **(C)** Variance partitioning analysis (VPA) of the relative contributions of edaphic (TN, TP, AN, AP, AK, OC, C/N, pH, EC, ALP, SUC, UR, SM), geographic (Altitude), and climatic (MAT and MAP) variables to the rhizosphere fungal taxonomic compositions. **(D)** Variance partitioning analysis (VPA) of the relative contributions of edaphic (TN, TP, AN, AP, AK, OC, C/N, pH, EC, ALP, SUC, UR, SM), geographic (Altitude), and climatic (MAT and MAP) variables to the root endosphere fungal taxonomic compositions.

relative abundances of major fungal orders in the rhizosphere community compared to the root endosphere. Correlation heatmap showed that pH was significantly positively correlated with the relative abundances of *Tubeufiales*, *Glomerellales*, and *Capnodiales*, but was negatively related to the relative abundances of *Pleosporales*, *Sebacinales*, *Cystofilobasidiales*, and *Chaetothyriales* in root endosphere of pear trees. In addition, pH was also significantly negatively correlated with the relative abundances of *Filobasidiales*, *Eurotiales*, and Microascales, but was positively related to the relative abundances of *Hypocreales* in rhizosphere of pear trees. These results indicated that the above-mentioned fungal taxa prefer the pH of the habitat. Furthermore, in terms of root endosphere of pear trees, the relative abundances of *Glomerellales*, *Tubeufiales*, and *Capnodiales* had a negative relationship with the contents of AP and UR, but had a positive relationship with the content of OC, pH and SM. Interestingly, *Pleosporales* showed an opposite correlation pattern with the above-mentioned taxa. In terms of rhizosphere of pear trees, the relative abundances of *Cystofilobasidiales*, and *Filobasidiales* had a positive relationship with the contents of AK, UR, SUC, ALP, TN, AN, and AP, but had a negative relationship with the content of pH and C/N (Supplementary Figure S7).

4 Discussion

4.1 Diversity and community structure of fungal communities in the rhizosphere and root endosphere

Fungal communities in the rhizosphere and root endosphere form a diverse micro-ecosystem surrounding and inhabiting plant roots, playing a critical role in assessing rhizosphere soil health and

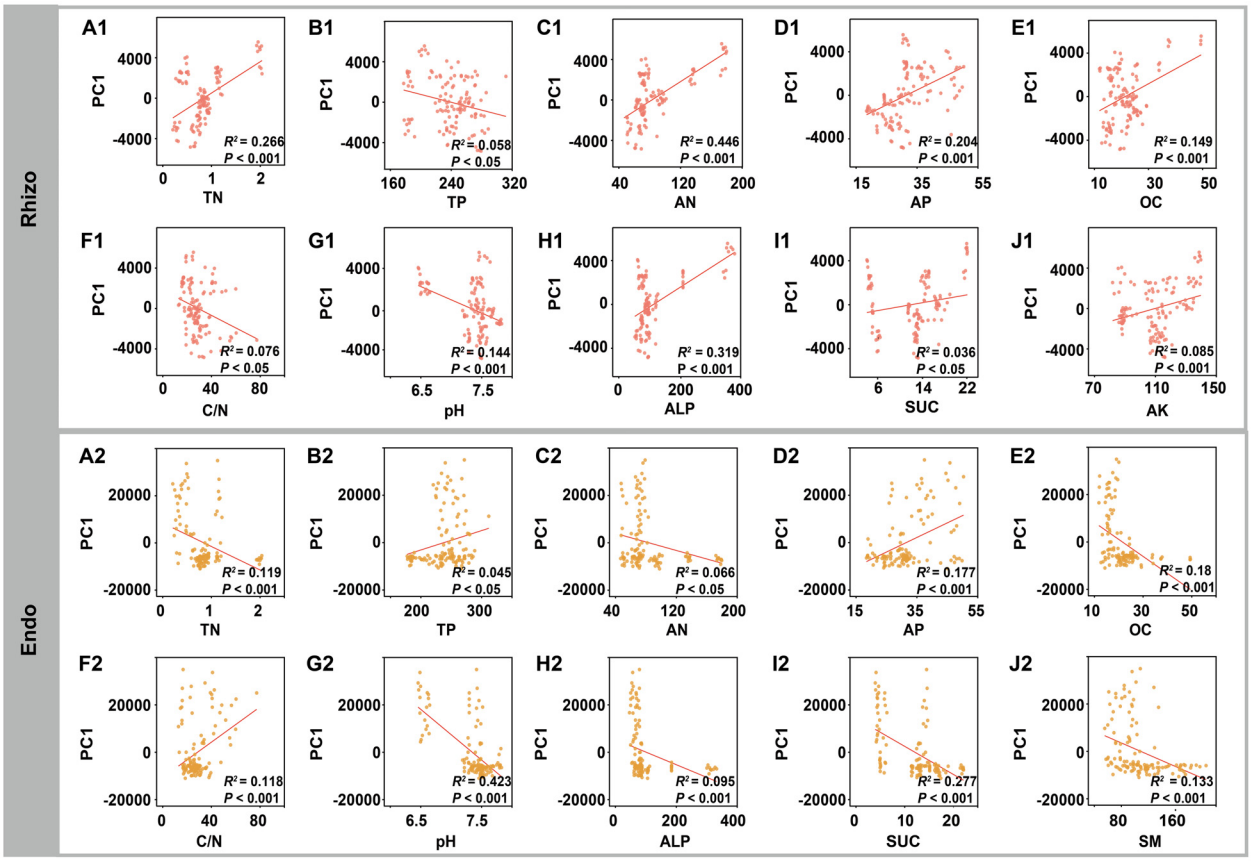

FIGURE 6
Relationships between the rhizosphere (Rhizo) and root endosphere (Endo) fungal taxonomic compositions and specific soil physicochemical properties. Linear regression model fittings illustrated significant relationships between the rhizosphere fungal taxonomic compositions and **(A1)** TN, **(B1)** TP, **(C1)** AN, **(D1)** AP, **(E1)** OC, **(F1)** C/N ratio, **(G1)** pH, **(H1)** ALP, **(I1)** SUC, and **(J1)** AK. Linear regression model fittings illustrated significant relationships between the root endosphere fungal taxonomic compositions and **(A2)** TN, **(B2)** TP, **(C2)** AN, **(D2)** AP, **(E2)** OC, **(F2)** C/N ratio, **(G2)** pH, **(H2)** ALP, **(I2)** SUC, and **(J2)** SM. R^2 represents the deviance explained by the linear regression model.

crop growth (Tan et al., 2017). A significant decline in the Sobs and Shannon indices of fungal communities from the rhizosphere to the root endosphere indicated that the barrier between these two compartments in pear trees exerts a strong filtering effect on the recruitment of specific microorganisms (Figure 2A) (Lumibao et al., 2020). This finding aligned with the theory of plant-microbiota coevolution, which posited that plants attract and select beneficial microbiota through the release of signaling molecules, immune system activation, and the provision of specialized nutrients and habitat types, thereby exerting selective pressure. Microbiota capable of recognizing signaling molecules and colonizing specific niches are preferentially enriched, while others are filtered out (Boyno and Demir, 2022). The structural variability of fungal communities in the root endosphere was greater than that in the rhizosphere, suggesting that the processes of colonization and community formation in the root endosphere are more variable (Figure 2D) (Zhang et al., 2023). Co-occurrence network analysis revealed that rhizosphere fungal networks exhibited higher connectivity, reflecting greater stability, functionality, and adaptability (Figure 2G). The rhizosphere, with its abundant resources, supports extensive fungal cooperation and complex networks, whereas the more isolated environment of the root endosphere reduces diversity and limits innately specific taxa to thrive (Wu et al., 2024a).

The results indicated that *Asc*ractions, thus allowing on*omycota* were dominant in the root-associated fungal communities of pear trees across all regions (Figure 3A). The prevalence of *Ascomycota* in most plants can be attributed to their strong spore production and rapid growth, which enable them to quickly establish dominance under favorable conditions. Moreover, *Ascomycota* are saprophytes that decomposed recalcitrant organic matter, playing a crucial role in nutrient cycling in the rhizosphere and maximizing nutrient recovery for pear trees *in situ*. In the rhizosphere of YT, many *Leotiomycetes* were present (Figure 3B), exhibiting rich species diversity. Some of these groups could produce secondary metabolites with complex structures and broad activities, which have significant potential for development in plant pest control and other applications (Fujita et al., 2021). Furthermore, fungal species identification revealed that 0.8–3.92% of the fungal taxa in the rhizosphere and 0.12–0.83% in the root endosphere were unidentified across the five regions, underscoring a substantial reservoir of undiscovered fungal taxa.

In the rhizosphere of pear trees, undefined and unknown saprotrophic fungi predominated, constituting a significant proportion of the fungal community (Supplementary Figure S5D). These fungi contribute to soil nutrient enhancement and fertility by decomposing organic matter. Similarly, in the root endosphere fungal communities across the five regions, saprotrophs and pathotrophs were also dominant (Supplementary Figure S5E). This may be due to improper agricultural practices or the fact that pear trees, aged approximately 30 years, have gradually entered a stage of decline, leading to weakened resistance in the root systems of these trees to pathogenic fungi. Under favorable environmental conditions, these pathogens may proliferate rapidly, potentially inducing diseases in pear trees (Hardoim et al., 2015). However, numerous probiotic fungi, such as Ericoid, Mycorrhizal, and Ectomycorrhizal fungi (Supplementary Figure S5D), also inhabit the rhizosphere, indicating that this ecosystem retains a certain degree of adaptability and self-regulation (Ward et al., 2021).

4.2 Stochastic processes govern the assembly of rhizospheric and root endospheric fungal microbiota at the full-fruiting stage of pear

The assembly of plant fungal communities is crucial for plant adaptability and ecological functions (Xu et al., 2023). βNTI analysis revealed that the composition of fungal communities in the rhizosphere and root endosphere of pear trees was predominantly shaped by stochastic processes (Figures 4A–C), aligning with previous studies on the mechanisms underlying the construction of rhizosphere fungal communities in *Phoebe bournei* plantations (Yan et al., 2024). The abundance of nutrients can enhance ecological randomness and reduce competitive pressures, leading to stochastic dominance in fungal assembly under anthropogenic disturbances (Dini-Andreote et al., 2015). Additionally, the stochastic processes governing fungal community assembly varied across different regions of the pear roots. Although fungi produce numerous spores, their limited dispersal constrains the spread of the rhizosphere community, making its assembly more influenced by dispersal limitations (Li et al., 2021). In contrast, the root endosphere, with its smaller and less diverse community, was more susceptible to ecological drift, resulting in greater stochasticity (Fitzpatrick et al., 2020). The assembly process of the fungal community is significantly influenced by the habitat type (R^2 = 0.08, P < 0.001), and the response of the rhizosphere fungal community to the habitat type is stronger than that of the endosphere (Rhizo: R^2 = 0.20, P < 0.001; Endo: R^2 = 0.11, P < 0.001) (Table 1). For example, the assembly processes of the rhizosphere fungal communities in YT and QY exhibit remarkable similarities (Figure 4D). It is speculated that it may be attributed to the fact that the terrain significantly affects the structure of the rhizosphere fungal community through driving rhizosphere sedimentation, and then regulates its ecological functions. Specifically, the differences in hydrothermal conditions caused by different altitude gradients may prompt changes in the secretion patterns of plant roots, leading to the differentiation of carbon metabolic functions and the ecological filtering effect of allelochemicals in root exudates. Eventually, a spatially heterogeneous community structure is formed, thus promoting the adaptive evolution of plants and the stability of ecosystem functions (Yang et al., 2023). Studies have shown that plant roots can recruit rhizosphere microorganisms in a targeted manner by secreting specific metabolites (Bi et al., 2021), and these microorganisms promote nutrient cycling in the root zone through nutritional interactions (Zhao et al., 2022). In mountainous ecosystems, microbial diversity has been confirmed to maintain the stability of soil organic carbon decomposition (Xu et al., 2021). The YT area, situated in the Yanshan Mountains, may experience geographical isolation and hinder the free migration of species, resulting in a relatively limited species pool. Consequently, during root endosphere community assembly, this limitation allows species with similar characteristics to dominate, leading to a significant contribution of homogeneous selection, second only to ecological drift (Fitzpatrick et al., 2020) (Figure 4E).

4.3 Effects of rhizosphere soil factors on the assembly of fungal communities in pear trees within different habitats

An increasing number of studies have indicated that various soil characteristics, including soil pH (Naz et al., 2022), soil texture (Girvan et al., 2003), and soil nitrogen availability (Frey et al., 2004), may be related to the changes in the composition of fungal communities (Qiu et al., 2022). Similarly, correlation analysis revealed that the physicochemical properties of the soil were the primary factors driving the assembly of rhizosphere and root endosphere fungal communities in pear trees across regions (Figure 6). YT exhibited the highest rhizosphere fungal richness (Figure 2B), likely due to its abundant organic matter, which promoted fungal growth. In contrast, BT showed the lowest rhizosphere fungal abundance (Figure 2B), possibly due to high soil pH and EC, which may stress fungi and limit their growth (Zhang et al., 2016). Co-occurrence networks analysis of rhizosphere soil fungi demonstrated high connectivity and notable regional differences (Figure 2G). For example, rhizosphere fungal network in XJ displayed increased competition, potentially attributed to a high C/N ratio that favors nitrogen-efficient fungi (Yang et al., 2017). The study also revealed significant regional differences in the Sobs and Shannon indices of root endosphere fungi. QY exhibited the highest abundance of root endosphere fungi (Figure 2C), likely due to its high AP, high C/N ratio, and weakly acidic environment, which were favorable for saprophytic fungi (Yang et al., 2017). BT showed the highest Shannon index for both rhizosphere and root endosphere fungi (Figures 2B, C), potentially reflecting the presence of diverse fungal communities that were

adapted to high soil pH stress. Co-occurrence network analysis of root endosphere fungi across regions confirmed high connectivity among species and highlighted regional differences in community structures (Supplementary Figures S2A, B). The network structure of endophytic fungi in WX was relatively simple, which may be due to the traditional agricultural management practices in WX, which often involve the extensive use of chemical fertilizers and pesticides. These practices may reduce the diversity of endophytic fungi, leading to a more simplified network structure (Wu et al., 2024b; Ye et al., 2021). Venn diagram analysis revealed that more unique genera were found in the rhizosphere and root endosphere of pear trees in the YT and QY regions, respectively (Supplementary Figures S4B, C). This may be due to the variable terrain, altitude, and complex soil types that provide diverse habitats for fungi (Siles and Margesin, 2016). Overall, these findings confirmed that fungal community composition varied significantly across regions, and that the effect of topography on fungal community assembly was less pronounced than the effects of regional types and root compartment niches.

5 Conclusions

Stochastic processes dominate the assembly of both rhizosphere and root endosphere fungal communities at the soil-root interface during the full fruiting stage of perennial fruit trees. The composition of fungal communities varies significantly among different regions. In both the rhizosphere and root endosphere fungal communities, the number of genera specific to mountainous regions was larger than those in plain areas and saline-alkali areas. The assembly of root-associated fungal communities in *P. betulifolia* is not only driven by soil physicochemical properties but also influenced by root compartment niche and topography. Moreover, the impact intensity of the root compartment niche is greater than topography. Specifically, the assembly of rhizosphere fungal communities primarily driven by AN and ALP, while the assembly of root endophytic fungi was mainly influenced by pH and SUC. The barrier between the rhizosphere-root endosphere in pear trees exerted a strong filtering effect on the recruitment of specific microorganisms. Our study not only describes the diversity of fungal microbiota in the rhizosphere and endosphere of perennial woody fruit trees, but also elucidates the assembly mechanisms of these microbiota and clarifies the impacts of rhizosphere soil factors on fungal community assembly. These findings provide fundamental data for designing beneficial root-associated microbiomes to enhance fruit tree performance.

Data availability statement

The datasets presented in this study can be found in online repositories. The names of the repository/repositories and accession number(s) can be found below: https://www.ncbi.nlm.nih.gov/, PRJNA1161009, https://www.ncbi.nlm.nih.gov/, PRJNA1160469.

Author contributions

YL: Data curation, Formal Analysis, Investigation, Visualization, Writing – original draft, Writing – review & editing. ZW: Investigation, Resources, Writing – review & editing. XS: Supervision, Writing – review & editing. XH: Conceptualization, Funding acquisition, Supervision, Writing – review & editing. YZ: Conceptualization, Funding acquisition, Supervision, Writing – review & editing.

Funding

The author(s) declare that financial support was received for the research and/or publication of this article. This research was funded by the Pear Industrial Technology Engineering Research Center of the Ministry of Education and Hebei Pear Technology Innovation Center. This work was also supported by the Natural Science Foundation of Hebei Province of China (No. H2022201056).

Acknowledgments

We thank Minghui Xu, Yuepeng Xi, Xiaojian Guo and Shuai Yuan for sampling and laboratory work.

Conflict of interest

The authors declare that the research was conducted in the absence of any commercial or financial relationships that could be construed as a potential conflict of interest.

Generative AI statement

The author(s) declare that no Generative AI was used in the creation of this manuscript.

Publisher's note

Supplementary material

The Supplementary Material for this article can be found online at: https://www.frontiersin.org/articles/10.3389/fpls.2025.1549173/full#supplementary-material

References

Bakker, P. A. H. M., Berendsen, R. L., Doornbos, R. F., Wintermans, P. C. A., and Pieterse, C. M. J. (2013). The rhizosphere revisited: Root microbiomics. *Front. Plant Sci.* 4. doi: 10.3389/fpls.2013.00165

Basiru, S., Mhand, K. A. S., and Hijri, M. (2023). Disentangling arbuscular mycorrhizal fungi and bacteria at the soil-root interface. *Mycorrhiza* 33, 119–137. doi: 10.1007/s00572-023-01107-7

Bever, J. D., Morton, J. B., Antonovics, J., and Schultz, P. A. (1996). Host dependent sporulation and species diversity of arbuscular mycorrhizal fungi in a mown grassland. *J. Ecol.* 84, 71–82. doi: 10.2307/2261701

Bi, B., Wang, K., Zhang, H., Wang, Y., Fei, H. Y., Pan, R. P., et al. (2021). Plants use rhizosphere metabolites to regulate soil microbial diversity. *Land Degrad. Dev.* 32, 5267–5280. doi: 10.1002/ldr.4107

Boyno, G., and Demir, S. (2022). Plant-mycorrhiza communication and mycorrhizae in inter-plant communication. *Symbiosis* 86, 155–168. doi: 10.1007/s13199-022-00837-0

Chen, S., Zhou, Y., Chen, Y., and Gu, J. (2018). Fastp: An ultra-fast all-in-one FASTQ preprocessor. *Bioinformatics* 34, 884–890. doi: 10.1093/bioinformatics/bty560

Dini-Andreote, F., Stegen, J. C., van Elsas, J. D., and Salles, J. F. (2015). Disentangling mechanisms that mediate the balance between stochastic and deterministic processes in microbial succession. *Proc. Natl. Acad. Sci. U.S.A.* 112, E1326–E1332. doi: 10.1073/pnas.1414261112

Edgar, R. C. (2013). UPARSE: Highly accurate OTU sequences from microbial amplicon reads. *Nat. Methods* 10, 996–998. doi: 10.1038/nmeth.2604

Edwards, J., Johnson, C., Santos-Medellín, C., Lurie, E., Podishetty, N. K., Bhatnagar, S., et al. (2015). Structure, variation, and assembly of the root-associated microbiomes of rice. *Proc. Natl. Acad. Sci.* 112, E911–E920. doi: 10.1073/pnas.1414592112

Fitzpatrick, C. R., Salas-González, I., Conway, J. M., Finkel, O. M., Gilbert, S., Russ, D., et al. (2020). The plant microbiome: from ecology to reductionism and beyond. *Annu. Rev. Microbiol.* 74, 81–100. doi: 10.1146/annurev-micro-022620-014327

Frey, S. D., Knorr, M., Parrent, J. L., and Simpson, R. T. (2004). Chronic nitrogen enrichment affects the structure and function of the soil microbial community in temperate hardwood and pine forests. *For. Ecol. Manage.* 196, 159–171. doi: 10.1016/j.foreco.2004.03.018

Fujita, K., Ikuta, M., Nishimura, S., Sugiyama, R., Yoshimura, A., and Kakeya, H. (2021). Amphiol, an antifungal fungal pigment from Pseudogymnoascus sp. PF1464. *J. Nat. Prod.* 84, 986–992. doi: 10.1021/acs.jnatprod.0c01010

Girvan, M. S., Bullimore, J., Pretty, J. N., Osborn, A. M., and Ball, A. S. (2003). Soil type is the primary determinant of the composition of the total and active bacterial communities in arable soils. *Appl. Environ. Microbiol.* 69, 1800–1809. doi: 10.1128/AEM.69.3.1800-1809.2003

Hardoim, P. R., van Overbeek, L. S., Berg, G., Pirttilä, A. M., Compant, S., Campisano, A., et al. (2015). The hidden world within plants: ecological and evolutionary considerations for defining functioning of microbial endophytes. *Microbiol. Mol. Biol. Rev.* 79, 293–320. doi: 10.1128/mmbr.00050-14

Hassani, M. A., Durán, P., and Hacquard, S. (2018). Microbial interactions within the plant holobiont. *Microbiome* 6, 58. doi: 10.1186/s40168-018-0445-0

Heiri, O., Lotter, A. F., and Lemcke, G. (2001). Loss on ignition as a method for estimating organic and carbonate content in sediments: Reproducibility and comparability of results. *J. Paleolimnol.* 25, 101–110. doi: 10.1023/A:1008119611481

Huang, Z., Zhao, F., Wang, M., Qi, K., Wu, J., and Zhang, S. (2019). Soil chemical properties and geographical distance exerted effects on arbuscular mycorrhizal fungal community composition in pear orchards in Jiangsu Province, China. *Appl. Soil Ecol.* 142, 18–24. doi: 10.1016/j.apsoil.2019.05.017

Kandeler, E., and Gerber, H. (1988). Short-term assay of soil urease activity using colorimetric determination of ammonium. *Biol. Fertil. Soils* 6, 68–72. doi: 10.1007/BF00257924

Latz, M. A., Kerrn, M. H., Sørensen, H., Collinge, D. B., Jensen, B., Brown, J. K., et al. (2021). Succession of the fungal endophytic microbiome of wheat is dependent on tissue-specific interactions between host genotype and environment. *Sci. Total Environ.* 759, 143804. doi: 10.1016/j.scitotenv.2020.143804

Lee, S. J., Morse, D., and Hijri, M. (2019). Holobiont chronobiology: Mycorrhiza may be a key to linking aboveground and underground rhythms. *Mycorrhiza* 29, 403–412. doi: 10.1007/s00572-019-00903-4

Li, K. Q., Xu, X. Y., and Huang, X. S. (2016). Identification of differentially expressed genes related to dehydration resistance in a highly drought-tolerant pear, *Pyrus betulaefolia*, as through RNA-Seq. *PloS One* 11, e0149352. doi: 10.1371/journal.pone.0149352

Li, Y. M., Yang, Y., Wu, T. E., Zhang, H., Wei, G. H., and Li, Z. F. (2021). Rhizosphere bacterial and fungal spatial distribution and network pattern of Astragalus mongholicus in representative planting sites differ the bulk soil. *Appl. Soil Ecol.* 168, 104114. doi: 10.1016/j.apsoil.2021.104114

Lumibao, C. Y., Kimbrough, E. R., Day, R. H., Conner, W. H., Krauss, K. W., and Van Bael, S. A. (2020). Divergent biotic and abiotic filtering of root endosphere and rhizosphere soil fungal communities along ecological gradients. *FEMS Microbiol. Ecol.* 96, fiaa124. doi: 10.1093/femsec/fiaa124

Naz, M., Dai, Z. C., Hussain, S., Tariq, M., Danish, S., Khan, I. U., et al. (2022). The soil pH and heavy metals revealed their impact on soil microbial community. *J. Environ. Manage.* 321, 115770. doi: 10.1016/j.jenvman.2022.115770

Qiu, Y. F., Zhou, S. L., Zhang, C. C., Zhou, Y. J., and Qin, W. D. (2022). Soil microplastic characteristics and the effects on soil properties and biota: A systematic review and meta-analysis. *Environ. pollut.* 313, 120183. doi: 10.1016/j.envpol.2022.120183

Rzehak, T., Praeg, N., Galla, G., Seeber, J., Hauffe, H. C., and Illmer, P. (2024). Comparison of commonly used software pipelines for analyzing fungal metabarcoding data. *BMC Genomics* 25, 1085. doi: 10.1186/s12864-024-11001-x

Siles, J. A., and Margesin, R. (2016). Abundance and diversity of bacterial, archaeal, and fungal communities along an altitudinal gradient in alpine forest soils: What are the driving factors? *Microb. Ecol.* 72, 207–220. doi: 10.1007/s00248-016-0748-2

Tan, Y., Cui, Y., Li, H., Kuang, A., Li, X., Wei, Y., et al. (2017). Diversity and composition of rhizospheric soil and root endogenous bacteria in Panax notoginseng during continuous cropping practices. *J. Basic Microbiol.* 57, 337–344. doi: 10.1002/jobm.201600464

Tarafdar, J. C., and Marschner, H. (1994). Phosphatase activity in the rhizosphere and hyphosphere of VA mycorrhizal wheat supplied with inorganic and organic phosphorus. *Soil Biol. Biochem.* 26, 387–395. doi: 10.1016/0038-0717(94)90288-7

Trivedi, P., Leach, J. E., Tringe, S. G., Sa, T. M., and Singh, B. K. (2020). Plant-microbiome interactions: From community assembly to plant health. *Nat. Rev. Microbiol.* 18, 607–621. doi: 10.1038/s41579-020-0412-1

Valderrama, J. C. (1981). The simultaneous analysis of total nitrogen and total phosphorus in natural waters. *Mar. Chem.* 10, 109–122. doi: 10.1016/0304-4203(81)90027-X

Wang, Y. H., Li, S. F., Lang, X. D., Huang, X. B., and Su, J. R. (2022). Effects of microtopography on soil fungal community diversity, composition, and assembly in a subtropical monsoon evergreen broadleaf forest of Southwest China. *Catena* 211, 106025. doi: 10.1016/j.catena.2022.106025

Ward, E. B., Duguid, M. C., Kuebbing, S. E., Lendemer, J. C., Warren, R. J., and Bradford, M. A. (2021). Ericoid mycorrhizal shrubs alter the relationship between tree mycorrhizal dominance and soil carbon and nitrogen. *J. Ecol.* 109, 3524–3540. doi: 10.1111/1365-2745.13734

Wu, C. C., Song, X. P., Wang, D., Ma, Y. J., Shan, Y. P., Ren, X. L., et al. (2024b). Combined effects of mulch film-derived microplastics and pesticides on soil microbial communities and element cycling. *J. Hazard. Mater.* 466, 133656. doi: 10.1016/j.jhazmat.2024.133656

Wu, C. Y., Zhang, X. Q., Liu, Y. X., Tang, X., Li, Y., Sun, T., et al. (2024a). Drought stress increases the complexity of the bacterial network in the rhizosphere and endosphere of rice (*Oryza sativa* L.). *Agronomy* 14, 1662. doi: 10.3390/agronomy14081662

Xu, M., Li, X. L., Kuyper, T. W., Xu, M., Li, X. L., and Zhang, J. L. (2021). High microbial diversity stabilizes the responses of soil organic carbon decomposition to warming in the subsoil on the Tibetan plateau. *Glob. Change Biol.* 27, 2061–2075. doi: 10.1111/gcb.15553

Xu, P., Stirling, E., Xie, H., Li, W., Lv, X., Matsumoto, H., et al. (2023). Continental-scale deciphering of microbiome networks untangles the phyllosphere homeostasis in tea plants. *J. Adv. Res.* 44, 13–22. doi: 10.1016/j.jare.2022.04.002

Yan, H., Wu, Y., He, G., Wen, S., Yang, L., and Ji, L. (2024). Fertilization regime changes rhizosphere microbial community assembly and interaction in Phoebe bournei plantations. *Appl. Microbiol. Biot.* 108, 417. doi: 10.1007/s00253-024-13106-5

Yang, L., Gong, J., Liu, M., Yang, B., Zhang, Z., Luo, Q., et al. (2017). Advances in the effect of nitrogen deposition on grassland litter decomposition. *Chin. J. Plant Ecol.* 41, 894–913. doi: 10.17521/cjpe.2017.0023

Yang, Y., Qiu, K. Y., Xie, Y. Z., Li, X. C., Zhang, S., Liu, W. S., et al. (2023). Geographical, climatic, and soil factors control the altitudinal pattern of rhizosphere microbial diversity and its driving effect on root zone soil multifunctionality in mountain ecosystems. *Sci. Total Environ.* 904, 166932. doi: 10.1016/j.scitotenv.2023.166932

Ye, Z. C., Li, J., Wang, J., Zhang, C., Liu, G. B., and Dong, Q. G. (2021). Diversity and co-occurrence network modularization of bacterial communities determine soil fertility and crop yields in arid fertigation agroecosystems. *Biol. Fertil. Soils* 57, 809–824. doi: 10.1007/s00374-021-01571-3

Zhang, Y., Ding, C. T., Jiang, T., Liu, Y. H., Wu, Y., Zhou, H. W., et al. (2023). Community structure and niche differentiation of endosphere bacterial microbiome in *Camellia oleifera*. *Microbiol. Spectr.* 11, e0133523. doi: 10.1128/spectrum.01335-23

Zhang, T., Wang, N. F., Liu, H. Y., Zhang, Y. Q., and Yu, L. Y. (2016). Soil pH is a key determinant of soil fungal community composition in the Ny–Ålesund region, Svalbard (High Arctic). *Front. Microbiol.* 7. doi: 10.3389/fmicb.2016.00227

Zhao, Y. Y., Sun, M. D., Liang, Z. X., Li, H. G., Yu, F. T., and Liu, S. Z. (2020). Analysis of contrast iron chlorosis tolerance in the pear cv. 'Huangguan' grafted onto *pyrus betulifolia* and quince A grown in calcareous soils. *Sci. Hortic.* 271, 109488. doi: 10.1016/j.scienta.2020.109488

Zhao, X. C., Tian, P., Sun, Z. L., Liu, S. E., Wang, Q. K., and Zeng, Z. Q. (2022). Rhizosphere effects on soil organic carbon processes in terrestrial ecosystems: a meta-analysis. *Geoderma.* 412, 115739. doi: 10.1016/j.geoderma

Glossary

WX	Weixian
XJ	Xinji
BT	Botou
QY	Quyang
YT	Yutian
WCS	Rhizosphere fungi in WX
XCS	Rhizosphere fungi in XJ
BCS	Rhizosphere fungi in BT
QCS	Rhizosphere fungi in QY
YCS	Rhizosphere fungi in YT
WCR	Root endosphere fungi in WX
XCR	Root endosphere fungi in XJ
BCR	Root endosphere fungi in BT
QCR	Root endosphere fungi in QY
YCR	Root endosphere fungi in YT
SM	Soil moisture
OC	Organic carbon
TN	Total nitrogen
TP	Total phosphorus
AN	Alkaline nitrogen
AP	Available phosphorus
AK	Available potassium
EC	Electrical conductivity
C/N	Soil organic carbon/Total nitrogen
ALP	Alkaline phosphatase
UR	Urease
SUC	Sucrase
MAT	Mean annual temperature
MAP	Mean annual precipitation
OTUs	Operational Taxonomic Units
PCoA	Principal Coordinates Analysis
pNPP	p-nitrophenyl phosphate
PCoA	Principal Coordinates Analysis
PERMANOVA	Permutational multivariate analysis of variance
VPA	Variance partitioning analysis

frontiers | Frontiers in Plant Science

TYPE Original Research
PUBLISHED 27 June 2025
DOI 10.3389/fpls.2025.1518846

OPEN ACCESS

EDITED BY
Yanju Liu,
The University of Newcastle, Australia

REVIEWED BY
Hongxia Zhang,
Chinese Academy of Sciences (CAS), China
Muhammad Arif,
Guilin Tourism University, China

*CORRESPONDENCE
Yan Luo
luoyan505@xju.edu.cn

†These authors have contributed equally to this work

RECEIVED 29 October 2024
ACCEPTED 26 May 2025
PUBLISHED 27 June 2025

CITATION
Luo Y, Wei W, Wang Y, Xue T and Du K (2025) Soil and climate factors affect the nutrient resorption characteristics of desert shrub roots in Xinjiang, China. *Front. Plant Sci.* 16:1518846. doi: 10.3389/fpls.2025.1518846

Soil and climate factors affect the nutrient resorption characteristics of desert shrub roots in Xinjiang, China

Yan Luo[1,2,3*†], Wenya Wei[1†], Yaxuan Wang[1], Tianai Xue[1] and Kaijuan Du[1]

[1]College of Ecology and Environment, Xinjiang University, Urumqi, China, [2]Key Laboratory of Oasis Ecology, Ministry of Education, Xinjiang University, Urumqi, China, [3]Xinjiang Jinghe Observation and Research Station of Temperate Desert Ecosystem, Ministry of Education, Xinjiang University, Urumqi, China

Introduction: Nutrient resorption is a vital nutrient utilization strategy in desert plants and is essential for understanding desert ecosystems and addressing climate change. Although the resorption characteristics in plants have been studied extensively, those of desert plant roots remain insufficiently explored.

Methods: This study investigated the concentrations of nitrogen, phosphorus, and potassium, as well as their resorption efficiencies, in 21 shrubs within a desert ecosystem in Xinjiang, Northwest China. Our study was designed to compare nutrient resorption efficiency patterns among shrub species and assess how the these patterns respond to variations in climatic conditions and edaphic properties.

Results: The results indicated that nitrogen resorption efficiency (NRE), phosphorus resorption efficiency (PRE), and potassium resorption efficiency (KRE) for all plants were 29.14 ± 0.98%, 37.58 ± 0.92%, and 42.20 ± 0.93%, respectively. Among functional groups, angiosperms exhibited higher PRE (36.31 ± 1.00%) and KRE (41.85 ± 0.98%) than gymnosperms. C_4 plants (44.88 ± 1.53%) had significantly higher KRE than C_3 plants (40.85 ± 1.17%). Among different families, *Tamaricaceae* had significantly higher NRE (33.84 ± 2.07%) and PRE (46.23 ± 1.72%) compared to others, while *Solanaceae* had the lowest KRE (33.84 ± 2.07%). Plant nutrient resorption efficiency is regulated by multiple environmental factors. Specifically, soil total phosphorus (STP) and total potassium (STK) serve as the primary drivers of NRE, while electrical conductivity (EC) and aridity index (AI) play critical roles in modulating PRE. Climate factors exhibit distinct influences: AI shows positive correlations with PRE in C_3 plants and with NRE in C4 plants. MAT negatively affects KRE in C4 plants, whereas MAP exerts a positive effect on it. Notably, *Polygonaceae* plants demonstrate unique response patterns: NRE is jointly regulated by MAP and MAT, PRE is predominantly influenced by MAT and AI, and KRE depends on the combined influence of MAP and AI.

Discussion: Our research further explores the mechanisms of nutrient cycling in desert ecosystems by analyzing the root nutrient resorption strategies of desert plants. This provides theoretical support for understanding how plants in desert ecosystems efficiently utilize limited nutrient resources under extreme drought conditions.

KEYWORDS

desert shrub, root, nutrient resorption efficiency, nutrient limitation, environmental factors

1 Introduction

Nitrogen (N), phosphorus (P), and potassium (K) are three essential nutrients for plant growth and play crucial roles in various physiological functions (Chapin, 1980; Elser et al., 2007; Du et al., 2020; Lopez et al., 2023). N and P are typically regarded as the primary limiting factors in terrestrial ecosystems (Sardans et al., 2014; Liao et al., 2024), while K not only plays a crucial role in key processes such as photosynthesis, water regulation, and stress resistance, but it is also vital for plant growth and development. Especially in arid ecosystems, the demand for K in plants is actually higher than for P (Sardans and Peñuelas, 2015; Jungová et al., 2023; Das and Mondal, 2024). When nutrient supplies are limited, plants have evolved nutrient resorption strategies to enhance nutrient use efficiency and reduce reliance on external sources. This process involves resorbing nutrients from senesced tissues and transferring them to green tissues, thereby enhancing their adaptation to nutrient-poor environments (Killingbeck, 1996; Reed et al., 2012; Brant and Chen, 2015; Zhang J. et al., 2024). Nutrient resorption efficiency (NuRE), as a measure of nutrient resorption, is defined as the nutrient difference between mature and senescent leaves and the ratio of nutrients in mature leaves (Reich and Oleksyn, 2004). Desert ecosystems exhibit extremely low soil nutrient concentrations, prompting plants to depend on internal recycling and resorption to adapt to nutrient-poor conditions (Lambers, 2022; Tariq et al., 2024; Gao et al., 2025). By maximizing nutrient reclamation, these plants can enhance their utilization efficiency. To gain a deeper understanding of nutrient cycling and resource-use strategies, studying nutrient resorption in desert areas is essential.

Nutrient resorption is a vital strategy used by desert plants to thrive in arid, low-nutrient environments (Drenovsky and Richards, 2006; Reichert et al., 2022; Zhao et al., 2024). Desert plants mitigate nutrient limitation by improving nutrient resorption efficiency. For instance, shrub leaves in the Chihuahua Desert exhibit significantly higher NRE and PRE compared to other regions (Killingbeck, 1993). However, studies suggest that the nitrogen resorption efficiency (NRE) and phosphorus resorption efficiency (PRE) of shrub leaves in the Chihuahua and Gurbantunggut deserts are not significantly higher than those in other areas (Killingbeck and Whitford, 2001; Zhang et al., 2018). Additionally, studies have shown that the PRE in desert plant leaves is generally higher than the NRE. This phenomenon is consistent with the relative resorption hypothesis, which posits that plants tend to preferentially absorb limiting nutrients (Han et al., 2013). K is of crucial significance, under drought-stress conditions, it maintains ion homeostasis and regulates osmotic balance, enabling plants to better adapt to water deficits, thereby enhancing their survival and ecological adaptability (Lebaudy et al., 2007; Sardans and Peñuelas, 2015; Gupta et al., 2020; Johnson et al., 2022). The potassium resorption efficiency (KRE) of leaves in the Xinjiang Desert is lower than that of global woody plants, likely due to soil nutrient scarcity and the adaptation strategies of the plants (Luo et al., 2020). Previous studies on plant nutrient resorption have predominantly focused on leaf tissues, with limited research on nutrient resorption characteristics of roots (Zheng et al., 2018). Roots are vital structures for water and nutrient absorption in plants and play crucial roles in nutrient acquisition and storage (Bardgett et al., 2014; Weemstra et al., 2016; Freschet and Roumet, 2017; Liu et al., 2022, 2024). Some studies have reported minimal or no significant changes in nutrient concentrations between live and dead roots (Aerts, 1996). Gordon and Jackson (2000) emphasized that roots function as sites for nutrient accumulation and as potential sources of nutrients. Desert plants enhance their ability to absorb limited water and nutrients by increasing root hair density and length and accumulating osmoregulatory substances, which helps maintain cellular osmotic pressure, prevents dehydration, and ensures normal nutrient resorption (Freschet et al., 2010; Gao et al., 2024; Wang et al., 2025). Additionally, they often form symbiotic relationships with arbuscular mycorrhizal fungi, significantly improving their efficiency in absorbing soil nutrients, especially phosphorus (Tariq et al., 2024). However, the extent to which roots contribute to nutrient resorption remains inadequately documented, primarily because of challenges in collection methods and associated costs. Further investigation into root nutrient resorption characteristics will deepen our understanding of plant resource utilization strategies in nutrient-poor environments and provide insights into their performance and ecological adaptation mechanisms.

The climate, soil nutrients, and plant characteristics are among the key driving forces of nutrient resorption (Reed et al., 2012; Yan et al., 2018; Huang et al., 2018). Climate, soil nutrients, and plant characteristics drive nutrient resorption (She et al., 2024; Wang

et al., 2025). Key climatic factors include temperature, precipitation, and the aridity index. Suitable temperatures boost enzyme and transporter activities, enhancing nutrient absorption and transport, and increase fine root biomass and absorption area (Zhang S. et al., 2024). Precipitation enhances soil moisture, aeration, and microbial activity, promoting nutrient availability and root zone access. Under drought, plants adapt by increasing root hairs and accumulating osmoregulatory substances to maintain osmotic pressure and prevent dehydration (Li et al., 2025a). High temperatures in deserts can both enhance and inhibit enzyme activity, depending on thresholds, and induce stress hormones like ABA, affecting nutrient uptake and distribution (Beugnon et al., 2024). Plants also adapt to water stress by adjusting root architecture, leaf morphology, and physiological metabolism (Li et al., 2025b). Studies indicate that plants adapt to water stress through various strategies, including adjusting root architecture to increase water uptake capacity, changing leaf morphology to reduce transpiration, and regulating physiological metabolic processes (Delgado-Baquerizo et al., 2013; Williams and de Vries, 2020). These response mechanisms help plants to more efficient nutrient acquisition and utilization in nutrient-poor environments. Resorption efficiency may decrease due to drought (Zhang et al., 2018). However, some studies have indicated that drought does not inhibit resorption but rather plays a positive role in this process (Lobo-do-Vale et al., 2019; Luo et al., 2024). Soil nutrients directly influence resorption efficiency and are fundamental for plant growth (He et al., 2015). Studies have demonstrated that reduced soil moisture in arid regions adversely affects the resorption capacity of plants. This limitation occurs primarily because the soil nutrient diffusion is restricted. Moreover, the activities of soil and root enzymes decrease simultaneously, contributing to a nutrient-limiting ecological state (Sardans et al., 2017; Li et al., 2022). In arid regions, soil salinity is a major limiting factor for plant growth (James et al., 2005; Zhang S. et al., 2024). Conversely, some studies have shown that soil salinity has a minimal effect on the nutrient resorption of desert plant leaves (Wang L. et al., 2020). Desert plants employ various strategies to manage drought stress and the efficiency of nutrient resorption varies among species. Previous studies have demonstrated that the NRE of *Lycium ruthenicum* surpasses that of other elements, whereas the PRE of *Halostachys caspica* is greater than that of other shrubs in desert environments (Luo et al., 2020). Angiosperms and gymnosperms differ in their adaptations to high temperatures and drought stress. Angiosperms have complex roots and metabolic regulation, enhancing nutrient absorption through root hair density and organic acid secretion (Langguth et al., 2024). In contrast, gymnosperms have drought-resistant features like thick cuticles and low stomatal density, reducing water loss. Under prolonged drought, they optimize stomatal closure and root growth via ABA signaling (Kim et al., 2024; Rizzuto et al., 2024). Investigating the nutrient resorption mechanisms of desert plants and their responses to environmental changes will elucidate how these plants adapt to extreme conditions and provide a scientific basis for the restoration and management of desert ecosystems.

Desert plants are able to adapt to poor environments for a long time, so they have developed unique nutrient utilization strategies including optimized root architecture, efficient nutrient recovery mechanisms, and special photosynthesis mechanisms. Although the resorption of nutrients from the leaves has been extensively studied, the mechanisms underlying root nutrient resorption remain

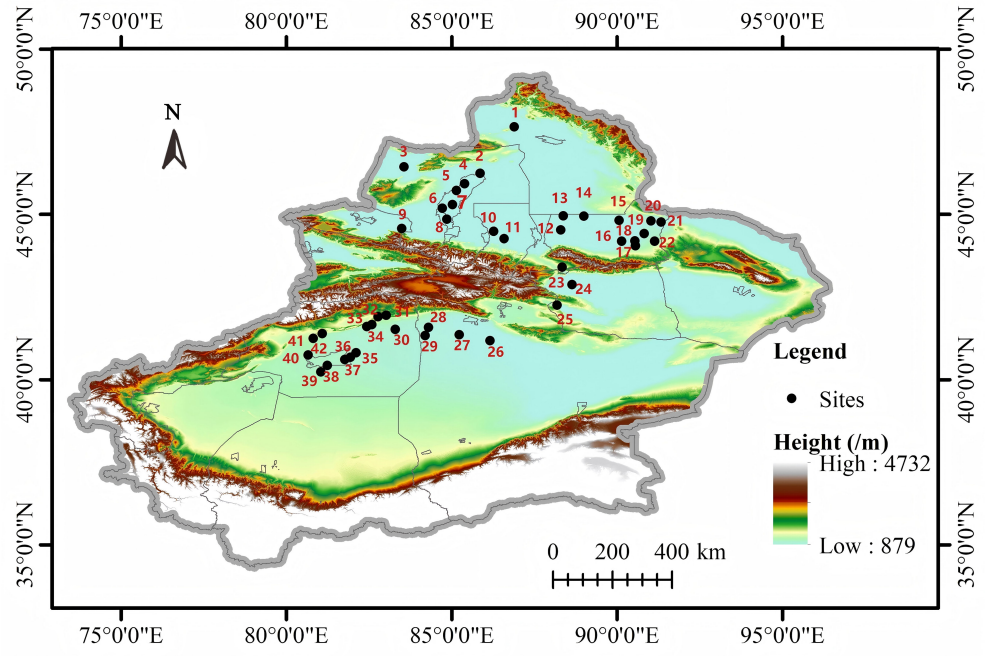

FIGURE 1
Overview of the study area.

unclear. Xinjiang is the most widely distributed desert province in China, where shrubs occupy a significant ecological niche. In this study, we selected 21 shrub species from the Xinjiang desert region to analyze the concentration of N, P, and K in their roots. Aims to answer the following scientific questions: (1) What are the N, P and K stoichiometric characteristics of desert shrub plant roots and what is the relationship between these characteristic and nutrient resorption? (2) how do climate and soil factors affect the nutrient resorption characteristics of desert shrub roots? Our study aimed to elucidate nutrient utilization strategies for shrub roots in arid desert ecosystems. Understanding how desert shrubs optimize resorption of essential nutrients will improve our knowledge of plant adaptation to extreme environments.

2 Materials and methods

2.1 Study area

This study was conducted across 42 field sites located in the desert region of Xinjiang (38.86-48.19°N, 77.06-93.44°E), with altitudes ranging from 270 to 1451 m (Figure 1; Supplementary Table S1). The study area is characterized by a temperate, continental arid climate featuring high temperatures and drought conditions during the summer months and low temperatures in winter. The mean annual temperature (MAT) ranged from 5.29 to 14.35 °C, while the mean annual precipitation (MAP) varied from 38 to 226 mm. The precipitation levels were higher during the summer months and lower in the winter, exhibiting a significant disparity in distribution throughout the year. The shrub species in the area include plants such as *Lycium ruthenicum*, *Nitraria tangutorum*, *Tamarix ramosissima*, and *Reaumuria soongorica* (Supplementary Table S2). According to the soil classification system established by the United States Department of Agriculture, the predominant soil types in the region are grey desert soil, gray-brown desert soil, and aeolian sandy soil. Soil salt concentration was assessed by electrical conductivity (EC), and the soil salt concentration in the study area was relatively high, as shown in Supplementary Tables S3, S4.

2.2 Sampling and measurement

We collected plant samples in mid-to-late July and mid-September in 2021. These specific sampling time periods were selected based on the phenological characteristics of desert plants in Xinjiang. In mid-to-late July, plants in Xinjiang desert areas are usually in their peak growth period. By mid-September, many desert plants in Xinjiang began to show signs of decline. Our study was conducted at 42 sampling sites in the desert region of Xinjiang. At each sampling point, we set a 20×20m quadrat. In each plot, 3 to 5 dominan plants with vigorous growth and consistent morphology were randomly selected, and 3–5 replicate icates were performed for each plant to ensure sample representativeness and reliability of ecological data. Coarse roots with diameters greater than 2 mm and a depth of approximately 50 cm below the surface were excavated. Soil particles and other substances were removed from the root surfaces. The roots were carefully rinsed with deionized water to remove any adhering soil particles and debris. Dried at 105 °C for 30 min and subsequently dried at 65 °C until a constant weight was achieved. They were then ground and stored for chemical analysis. Five soil samples at a depth of 0–50 cm were collected from each block using a soil sampler (XDB-Y, Jiangsu Xindacheng Instrument Co., Ltd, China.), and these samples were pooled together and fully mixed to remove organic debris and stones. Then a "four section" was used to spread the pooled soil into a thin layer, divided into four equal parts, and the four samples were recombined and mixed again. After screening, the samples were stored separately, transported to the laboratory, and spread the soil samples on a clean, non-reactive surface and placed them in a well-ventilated, cool, and shaded environment to ensure that the samples were protected from direct sunlight, dust, and chemical contamination. The dried soil was ground and then stored for chemical analysis.

At each sampling point, we collected 3–5 replicates based on the actual distribution. For the statistical analysis of the original dataset, we collected a total of 55 plants, 3 replicates, 58 plants, and 5 replicates for a total of 455 plant samples. The N concentration was determined using an Alpkem autoanalyzer (Kjektec System 1026 distillation unit, Sweden). Plant and soil samples were dried and ground to ensure uniformity. Subsequently, the N in the sample was distilled using the Kjeldahl method. After sulfuric acid digestion, the N was released as ammonia, and its concentration was determined by acid titration. The P content was determined using the molybdate/ascorbate blue colorimetric method with a ICP-OES instrument (7300 DV, PerkinElmer, United States). After chemical treatment, molybdate was added under specific pH conditions to generate a phosphorus-molybdenum blue complex. Using ascorbic acid as a reducing agent, this complex was further reduced to a blue compound, which was quantified by colorimetry. The method for determining potassium (K) concentration is described as follows: Accurately weigh 0.5 g of plant powder sample and place it into a polytetrafluoroethylene (PTFE) digestion vessel. Add 10 mL of concentrated nitric acid (HNO_3, 65%) and 3 mL of hydrogen peroxide (H_2O_2, 30%). Seal the digestion vessel and place it into the microwave digestion system (Mars Xpress, CEM Corporation, USA) for digestion. After digestion, the sample is analyzed using inductively coupled plasma-optical emission spectrometry (ICP-OES). The instrument used is the Optima 7000 DV (PerkinElmer Inc., USA). The sample solution is nebulized and introduced into the plasma torch, where it is ionized into a plasma state at high temperature. Potassium emits characteristic spectra at a specific wavelength (766.49 nm), and its concentration is quantitatively determined by measuring the emission intensity (Ebrahim et al., 2014).

10.3389/fpls.2025.1518846

2.3 Meteorological data acquisition

MAT (°C) and MAP (mm) data were derived from WorldClim version 2.0 (http://worldclim.org/version2), and the drought index (AI) was derived from the meteorological database of the International Centre for Agricultural Research Spatial Information Consortium (http://www.cgiar-csi.org).

2.4 Nutrient resorption efficiency

Nutrient resorption efficiency (NuRE) was calculated as described by Vergutz et al. (2012):

$$\mathbf{NuRE} = \frac{\mathbf{Nu_{mature}} - \mathbf{Nu_{senesced}}}{\mathbf{Nu_{mature}}} \times 100\,\% \quad (1)$$

where, NuRE is the nutrient resorption efficiency, Nu_{mature} is the nutrient concentration in the roots during summer, and $Nu_{senesced}$ is the nutrient concentration in the roots during autumn.

Relative nutrient resorption (RNuR) is calculated as described by Han et al. (2013):

$$RNuR1 = NRE - PRE \quad (2)$$

$$RNuR2 = NRE - KRE \quad (3)$$

$$RNuR3 = KRE - PRE \quad (4)$$

where, NRE, PRE, and KRE are the nutrient resorption efficiencies of N, P, and K, respectively.

2.5 Statistical analyses

One-way analysis of variance was employed to determine the differences in N, P, and K stoichiometry and nutrient resorption efficiency among the course roots of the sampled individuals. Tukey's HSD test was used to assess significant differences between multiple groups ($p < 0.05$). The relative nutrient resorption proportion between N and P was quantified as the difference between NRE and PRE, i.e., NRE-PRE. The stoichiometric ratio N:P was used to indicate the relative limitation of N versus P in plants. To identify critical thresholds, we performed regression analysis between the relative resorption efficiency (NRE-PRE) and the N:P ratio (log-transformed), with the results visualized in Figure 2. In the figure: The horizontal dashed line marks the equilibrium point where NRE equals PRE (NRE-

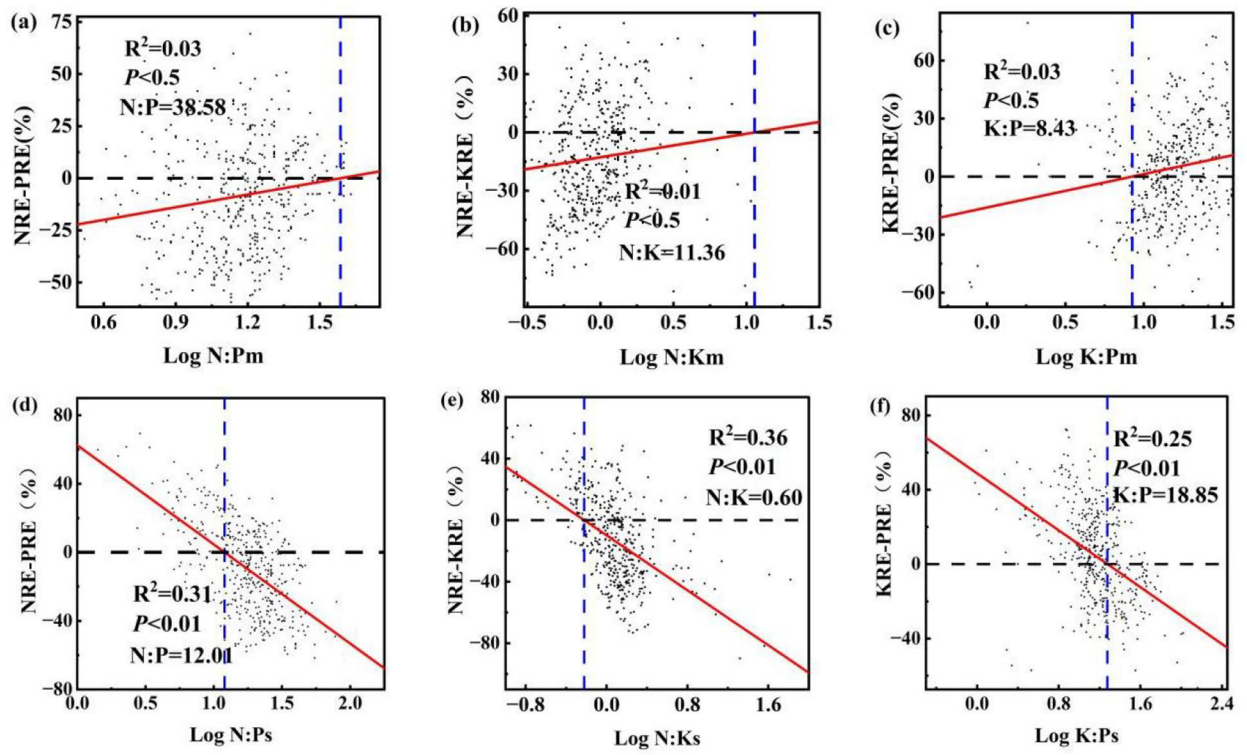

FIGURE 2
Ratios of N, P, K and relative resorption efficiency in summer and autumn roots Note: **(a)** N: P_m and NRE-KRE; **(b)** N: K_m and NRE-KRE; **(c)** K: P_m and KRE-PRE; **(d)** N: P_s and NRE-KRE; **(e)** N: K_s and NRE-KRE; **(f)** K: P_s and KRE-PRE. Horizontal black dashed line indicates the NRE equal to the critical N: P ratio of the PRE. The vertical blue dashed line crosses the black dashed line and the intersection of the red fitted curve is the corresponding ratio.

PRE=0). The vertical dashed line indicates the critical N:P ratio derived from the regression model after logarithmic transformation (Han et al., 2013).

The impact of environmental variables on NRE, PRE, and KRE was investigated using a linear mixed model (LMM). Regression analysis of environmental factors was performed using the restricted maximum likelihood estimation method, with the model constructed using the nlme package in R version 4.3.3. The LMM was designed using NRE, PRE, and KRE as response variables. The analysis incorporated various plant types as random effects and climatic (MAT, MAP, and AI) and soil factors (STN, STP, STK, pH, EC, and K_{soil}) as fixed effects. The RDA analysis of climate and nutrient reabsorption efficiency was performed using the "vegan" package in R. All data processing, analyses, and visualizations were performed using Microsoft Excel 2013, Origin 2024, and R version 4.3.3.

3 Results

3.1 Stoichiometric characteristics of N, P and K in roots of desert shrubs

The concentrations and stoichiometric ratios of N, P, and K were analyzed in the roots of the entire shrub population during summer and autumn using classical statistical methods (Figures 3, 4). The N, P, and K content in the roots of shrub plants in summer were 11.20 ± 0.20 mg g^{-1}, 0.81 ± 0.02 mg g^{-1}, and 12.26 ± 0.24 mg g^{-1}, respectively. In autumn, the root content was 7.91 ± 0.17 mg g^{-1} for N, 0.49 ± 0.01 mg g^{-1} for P, and 6.93 ± 0.16 mg g^{-1} for K. The ratios of N:P, N:K, and K:P for summer roots were 16.47 ± 0.37, 1.21 ± 0.08, and 13.61 ± 0.98, respectively, while the ratios for autumn roots were 20.04 ± 0.64, 2.04 ± 0.32, and 18.64 ± 0.89.

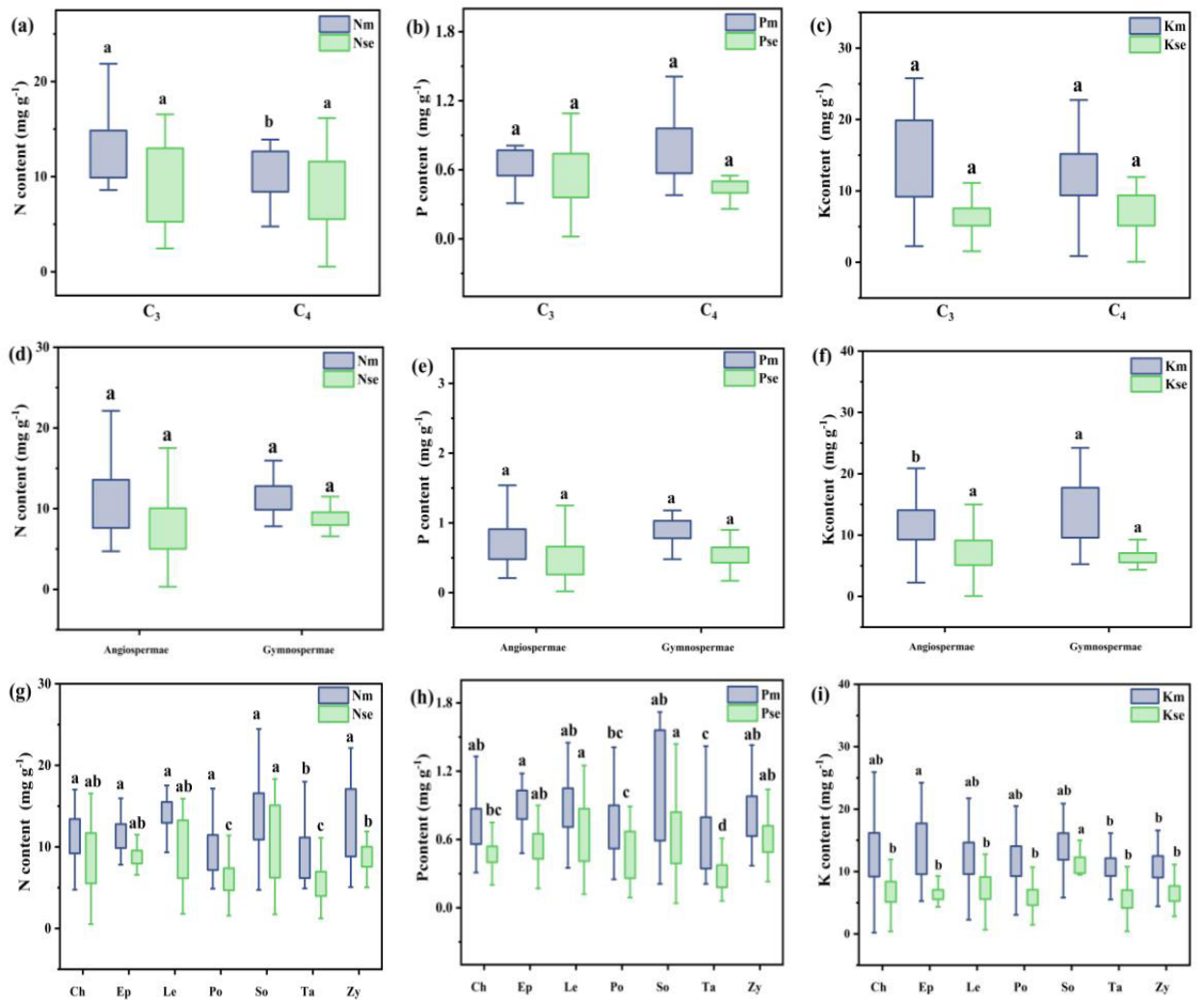

FIGURE 3
Root N, P, and K contents in different photosynthetic pathway plants in Xinjiang deserts across summer and autumn Note: Figures **(a-c)** show N, P, and K contents in roots of C_3 and C_4 plants; **(d-f)** in roots of gymnosperms and angiosperms; and **(g-i)** in roots of different families. m and se represent summer and autumn, respectively. Where C_3 and C_4 represent different photosynthetic pathway. CH, Chenopodiaceae; EP, Ephedraceae; LE, Leguminosae; PO, Polygonaceae; SO, Solanaceae; TA, Tamaricaceae; ZY, Zygophyllaceae. Different lowercase letters for different groups in the same column indicate a significant difference in element content (Turkey's HSD test, ANOVA: $p<0.05$).

10.3389/fpls.2025.1518846

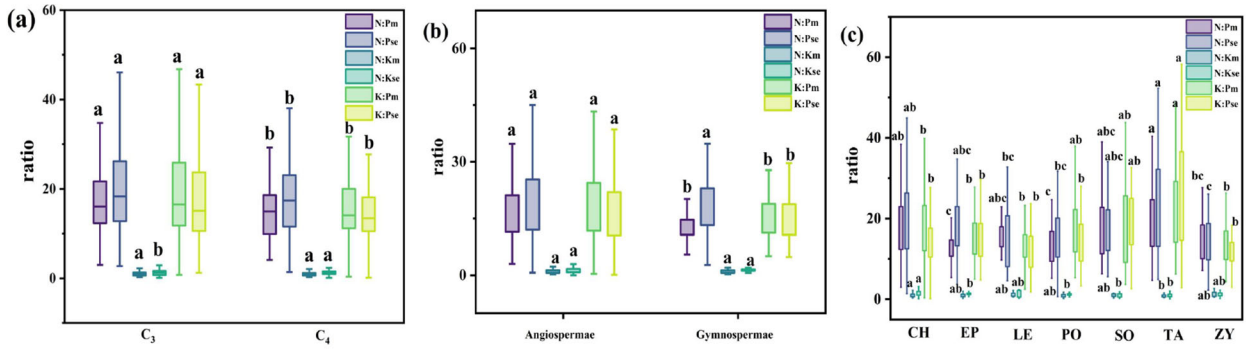

FIGURE 4
Root N, P, and K ratio of shrubs in different families in Xinjiang desert in summer and autumn Note: Figure **(a-c)** show the ratio of nutrient content in different light and pathway plants, gymnosperms and angiosperms, and plants in different families. Different lowercase letters for different groups in the same column indicate a significant difference in element content (Turkey's HSD test, ANOVA: $p<0.05$).

For different functional groups of plants, the mean N, P, and K content in the summer roots of C_3 plants were 11.47 ± 0.24 mg g^{-1}, 0.81 ± 0.03 mg g^{-1}, and 12.44 ± 0.30 mg g^{-1}, respectively. In contrast, the mean N, P, and K content in the summer roots of C_4 plants were 10.66 ± 0.35 mg g^{-1}, 0.79 ± 0.03 mg g^{-1}, and 11.89 ± 0.42 mg g^{-1}, respectively. The N and K content in the summer roots of C_3 plants were significantly higher than those in C_4 plants. In autumn, the mean N, P, and K content in the roots of C_3 plants were 8.02 ± 0.22 mg g^{-1}, 0.49 ± 0.02 mg g^{-1}, and 7.11 ± 0.20 mg g^{-1}, respectively. For C_4 plants in autumn, the mean content values were 7.70 ± 0.26 mg g^{-1} for N, 0.49 ± 0.07 mg g^{-1} for P, and 6.54 ± 0.25 mg g^{-1} for K. There were no significant differences in N, P, and K content between the autumn roots of C_3 and C_4 plants. Additionally, the ratios of N:P and K:P in the summer roots of C_3 plants were significantly higher than those of C_4 plants. Conversely, the N:P ratio in autumn was significantly lower in C_3 plants compared to C_4 plants.

The mean N, P, and K content in the summer roots of angiosperms were 11.10 ± 0.22 mg g^{-1}, 0.78 ± 0.02 mg g^{-1}, and 11.96 ± 0.25 mg g^{-1}, respectively. For gymnosperms, the mean values were 11.93 ± 0.39 mg g^{-1} for N, 1.00 ± 0.06 mg g^{-1} for P, and 14.41 ± 0.89 mg g^{-1} for K. The P and K content in the summer roots of angiosperms were significantly lower than those in gymnosperms. In autumn, the mean N, P, and K content in the roots of angiosperms were 7.81 ± 0.19 mg g^{-1}, 0.49 ± 0.05 mg g^{-1}, and 6.89 ± 0.17 mg g^{-1}, respectively, while the mean values for gymnosperms were 8.58 ± 0.30 mg g^{-1} for N, 0.53 ± 0.03 mg g^{-1} for P, and 7.21 ± 0.43 mg g^{-1} for K. There were no significant differences in nutrient content between the autumn roots of angiosperms and gymnosperms. The ratios of N:P, N:K, and K:P for the summer roots of angiosperms were 16.47 ± 0.37, 1.21 ± 0.08, and 13.61 ± 0.98, respectively, while in autumn, the ratios were 20.04 ± 0.64, 2.04 ± 0.32, and 18.64 ± 0.89. The N:P ratio in summer and the K:P ratios in both summer and autumn were significantly higher in angiosperms compared to gymnosperms.

For different plant families, the N, P, and K content in the autumn roots of *Solanaceae* plants was significantly higher than that of other families. The N content in the summer and autumn roots, as well as the P content in the autumn roots of *Polygonaceae* and *Tamaricaceae* plants, was significantly lower than that of plants from other families. The N:P and K:P ratios in the summer and autumn roots of *Tamaricaceae* plants were significantly higher compared to other families. In contrast, the N:P ratio in the summer roots of *Ephedraceae* and *Polygonaceae* was significantly lower than that observed in other families.

3.2 Nutrient resorption efficiency of the desert shrub roots

3.2.1 Root nutrient resorption characteristics of desert shrub plants

The analysis of N, P, and K nutrient resorption efficiencies in the summer and autumn roots of different functional groups revealed average resorption efficiencies of 29.14 ± 0.98% for NRE, 37.58 ± 0.92% for PRE, and 42.20 ± 0.93% for KRE (Figure 5, the resorption characteristics of specific species are shown in Supplementary Table S3) (Equation 1). Notably, KRE was significantly higher than PRE and NRE. Among the plant functional groups, C_3 plants exhibited significantly higher NRE and PRE than C_4 plants, whereas C_4 plants had a significantly higher KRE (Figure 5B). For angiosperms, the NRE, PRE, and KRE were 29.46 ± 1.06%, 36.31 ± 1.00%, and 41.85 ± 0.98%, respectively, with gymnosperms showing a significantly higher PRE than angiosperms (Figure 5C).

The results of N, P and K nutrient resorption efficiencies in the roots of shrubs from different families during summer and autumn are presented in Figure 5D, Significant differences in NRE, PRE, and KRE were observed among families ($p< 0.05$). NRE ranged from 24.45% to 33.84%, PRE from 28.20% to 46.41%, and KRE from 22.22% to 47.08%. Notably, *Tamaricaceae* had a significantly higher NRE (33.84%) than *Chenopodiaceae* (24.45%). The PRE of *Ephedraceae* (46.41%) and *Tamaricaceae* (46.23%) were significantly higher than those of other families. In contrast, *Solanaceae* had a significantly lower KRE (22.22%) compared to other families.

3.2.2 Relative resorption efficiency and nutrient limitation of desert shrub roots

The stoichiometric ratio and relative resorption efficiencies are crucial indicators for assessing the nutrient limitations of N and P, and their effectiveness. In summer, the relative resorption efficiency of the roots positively correlated with the ratios N:P_m, N:K_m, and K:P_m (NRE-PRE (Equation 2) and N:P_m: r^2 = 0.03, p< 0.5 (Figure 2A); NRE-KRE (Equation 3) and N:K_m: r^2 = 0.01, p< 0.5 (Figure 2B); and KRE-PRE (Equation 4) and K:P_m: r^2 = 0.03, p< 0.5 (Figure 2C)). Conversely, in autumn, the relative resorption efficiency in roots demonstrated a consistent negative correlation with the N:P_{se}, N:K_{se}, and K:P_{se} ratios (NRE-PRE and N:P_{se}: r^2 = 0.31, p< 0.01; NRE-KRE and N:K_{se}: r^2 = 0.36, p< 0.01 (Figure 2E); and KRE-PRE and K:P_{se}: r^2 = 0.25, p< 0.01 (Figure 2F)). The horizontal black dotted line indicates the position where the NRE equals PRE, and the vertical blue dotted line indicates the corresponding critical N:P ratio. The critical N:P, N:K, and K:P ratios for the summer roots were 38.58, 11.36, and 8.43, respectively, while for the autumn roots were 12.01, 0.60, and 18.85, respectively.

3.3 Effects of environmental factors on nutrient resorption efficiency of shrub roots

LMM results (Table 1) indicated that both soil total phosphorus (STP) and soil total potassium (STK) had a significant impact on the response variable NRE. Specifically, STP was negatively correlated with NRE, whereas STK was positively correlated. Additionally, pH significantly affected NRE. For PRE, Electrical conductivity (EC), and aridity index (AI) demonstrated highly significant effects, with EC showing a positive correlation and AI a negative correlation. Soil water stress coefficient (K_{soil}) also influenced the PRE. For KRE, only STK had a significant effect.

For plants in different functional groups (Table 2), K_{soil} and AI significantly influenced NRE of C_4 plants. K_{soil} was negatively correlated with NRE, whereas AI was positively correlated. Additionally, K_{soil} positively affected the NRE of angiosperms. Both K_{soil} and AI significantly affected the PRE of C_3 plants, with K_{soil} negatively correlated and AI positively correlated. Furthermore, MAT and MAP had significant effects on KRE of C_4 plants, with negative and positive correlations, respectively.

Among different families (Table 3) NRE of *Chenopodiaceae* and *Polygonaceae* families exhibited significant responses to various environmental factors. Among these, K_{soil}, Soil total nitrogen (STN), and MAT had the most pronounced effects on the NRE of *Chenopodiaceae* plants. In contrast, pH, K_{soil}, STN, STK, MAP, and MAT significantly affected the NRE of *Polygonaceae* plants. In addition, K_{soil}, STK, MAT, and AI had the most significant effects on the PRE of *Polygonaceae* plants. MAP and AI significantly affected the KRE of *Polygonaceae* plants.

The relationship between climate and nutrient resorption efficiency was illustrated in Figure 6. The RDA results showed that the first axis (RDA 1) explained 82.32% of the variation, while the second axis (RDA 2) explained 15.75% of the variation. Overall, the first two axes accounted for over 98% of the ecological data variation, indicating that the selected environmental variables significantly explained species distribution. RDA 1 was primarily driven by MAP and MAT, suggesting that under warm and humid conditions, plants exhibited significantly higher PRE and KRE. RDA 2 was closely related to the AI, implying that high soil nitrogen availability reduced NRE.

4 Discussion

4.1 Stoichiometric characteristics and stoichiometric ratios of N, P, and K in desert shrub roots

N and P are essential components of important biomolecules such as proteins, nucleic acids, and amino acids in plants. K plays important physiological regulatory functions in plant cells (Lopez

TABLE 1 Responses of all plants' NRE, PRE, and KRE to climate and soil variables.

	Estimate	NRE Std	*p*	Estimate	PRE Std	*p*	Estimate	KRE Std	*p*
pH	-2.86	2.82	0.03*	3.13	2.87	0.28	3.86	2.92	0.89
EC	0.09	0.08	0.31	0.26	0.08	0.0009***	3.51	7.93	0.66
K_{soil}	0.98	1.66	0.23	4.04	1.69	0.017*	3.06	1.73	0.08
STN	-0.90	0.88	0.56	-0.56	0.90	0.53	-2.80	9.07	0.76
STP	-3.20	0.84	0.0002***	-0.76	0.85	0.37	1.25	8.32	0.14
STK	0.82	0.21	0.0002***	0.05	0.22	0.83	4.90	2.22	0.03*
MAP	-0.07	0.04	0.09	0.06	0.04	0.20	-6.08	4.05	0.89
MAT	-1.76	1.01	0.08	0.26	1.03	0.80	-1.64	1.03	0.11
AI	-109.40	169.79	0.52	-458.93	172.85	0.008**	-2.94	1.77	0.09

Note: Estimate and *p* represent the model regression coefficient and significance level for each explanatory variable, respectively. K_{soil} (%): soil water stress coefficient, defined as the ratio of actual evapotranspiration to potential evapotranspiration; AI (no unit): arid index, calculated as the ratio of precipitation to potential evapotranspiration; drought zone (AI > 0.2), transition zone (0.2< AI< 0.65) and wet zone (AI> 0.65).*p< 0.05;**p< 0.01;***p< 0.001.

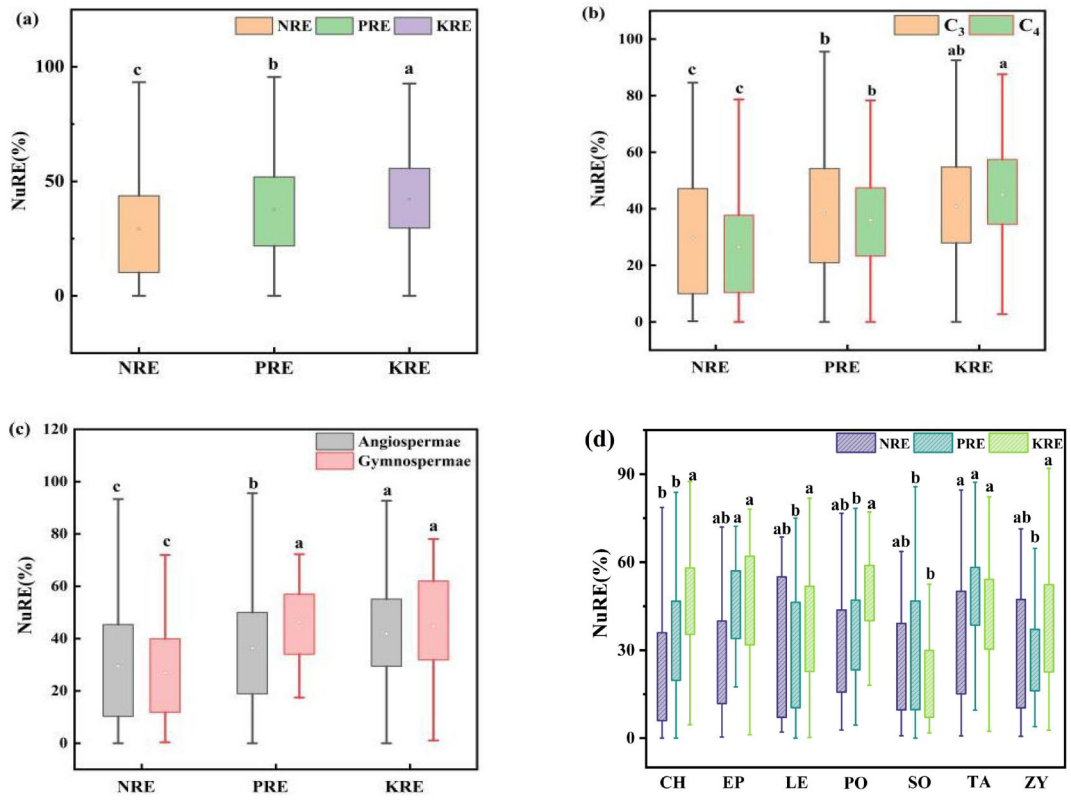

FIGURE 5
NRE, PRE, and KRE of desert shrub plant roots: **(a)** all plants; **(b)** different light and pathways; **(c)** gymnosperms and angiosperms, **(d)** different families. Where C_3 and C_4 represent different photosynthetic pathway. The lowercase letters in the figure indicate significant differences between NRE, PRE, and KRE (Turkey's HSD test, ANOVA: $p<0.05$).

et al., 2023; Das and Mondal, 2024). The concentrations of these elements not only reflect the inherent physiological characteristics of plants but also illustrate their adaptive capacity and response mechanisms to environmental conditions (Han et al., 2011; An et al., 2021). In the present study, the average concentrations of N, P, and K in the roots of all shrub species during summer were significantly higher than in the roots during autumn. This difference is primarily attributed to the active growth and metabolism of roots during summer, in the summer high temperature and drought conditions, plants through a series of adaptive mechanisms to maintain growth, these mechanisms include the adaptability of root changes, antioxidant defense and metabolic regulation, hormone signal regulation and microbial interaction (Gupta et al., 2021; Zhang et al., 2022), leading to an increased demand for nutrients and enhanced ability to absorb nutrients from the soil (Moreau et al., 2019). With root senescence, metabolic activity declines, nutrient demand decreases, and elemental concentrations diminish. The concentration of N and P in the roots of desert plants in summer was higher than both global (8.8 mg g^{-1}, 0.69 mg g^{-1}) and national levels (4.87 mg g^{-1}, 0.47 mg g^{-1}) (Yuan et al., 2011; Yang et al., 2018). Desert plants sustain their normal physiological functions by absorbing sufficient water and nutrients, allowing them to adapt to arid and nutrient-poor environments (Schenk and Jackson, 2002; Kautz et al., 2013; Mahdieh et al., 2021; Tariq et al., 2024). In summer, the K concentration in roots was lower than that in other regions, which may be attributed to the specific characteristics of desert habitats. Drought and saline conditions limit K uptake by plants. C_3 plants rely heavily on ribulose-1,5-bisphosphate carboxylase/oxygenase (Rubisco) for photosynthesis, an enzyme that is nitrogen-rich. This reliance means C_3 plants need higher nitrogen levels to support Rubisco synthesis and function. However, Rubisco's susceptibility to oxygen inhibition during CO_2 fixation leads to photorespiration, which reduces photosynthetic efficiency. To compensate, C_3 plants require more nitrogen (Paulus et al., 2013; Li et al., 2024a; Wang F. et al., 2020). Additionally, C_3 plants often have a higher specific root length, allowing them to explore soil more extensively for nutrients like N and K, which are essential for photosynthesis and maintaining cell osmotic pressure (Mukundan et al., 2024). In contrast, C_4 plants use the more efficient enzyme phosphoenolpyruvate carboxylase (PEP carboxylase) for initial CO_2 fixation, reducing their dependence on Rubisco and lowering their nitrogen requirements. Consequently, C_4 plants have relatively lower nitrogen concentrations in their roots compared to C_3 plants (Huang et al., 2022), C_4 plants are generally more adaptable to high temperatures and drought conditions, which may contribute to the observed differences in physiological and ecological performance between C_4 and C_3 plants (Ozeki et al., 2022). C_4 plants often exhibit greater

TABLE 2 Responses of climate and soil variables to NRE, PRE and KRE in different functional groups.

		Estimate								
		pH	EC	K_{soil}	STN	STP	STK	MAP	MAT	AI
NRE	C_3	-5.85	0.16	3.81*	-2.03	-2.68**	0.54*	-0.02	-2.46*	-449.14*
	C_4	13.71*	-0.48*	-16.71***	4.15*	-2.57	0.75	-0.07	-2.83	1689.60***
	An	-3.33	0.05	1.90	-2.04*	-2.38**	0.81***	-0.01	-1.64	-261.27
	Gy	-12.72	0.58	-18.46	4.73	-0.69	-0.78	-0.22	-3.46	2060.58
PRE	C_3	1.60	0.16	5.43**	0.76	-1.05	0.26	0.10*	0.17	-689.01***
	C_4	4.68	0.39	0.39	-2.02	0.52	-0.51	-0.07	-0.81	740.90
	An	2.47	2.48**	3.47*	-2.32*	3.48	1.27	9.48	1.17	-4.14*
	Gy	-2.01	2.89	-3.10	6.38	2.39	-1.58	-1.41	-1.70	2.91
KRE	C_3	-7.68*	5.72	3.69*	9.68	1.15	6.14*	1.24*	-2.97*	-4.72*
	C_4	1.42*	2.15	-2.69	-4.03*	6.61	2.28	-7.75***	9.01***	6.38
	An	2.32	5.88	2.30	-1.41	1.80*	4.30	-1.23	-1.14	-2.00
	Gy	-1.84	-2.43	5.07	7.90	-8.61	6.78	1.14	-9.32	-4.69

C_3 and C_4 represent plants with different light and pathway, respectively; An and Gy represent Angiospermae and Gymnospermae, respectively. *p< 0.05; **p< 0.01; ***p< 0.001.

productivity and resilience in extreme environments, thereby giving them a competitive advantage over C_3 plants in certain habitats (Guidi et al., 2019). Gymnosperms preferentially utilize available N, P, and K during biosynthesis, leading to higher concentrations of these essential nutrients in their tissues. This selective uptake can be attributed to the phosphoenolpyruvate (PEP) synthesis pathway and adaptive changes in the cell wall, Under drought conditions, lignin and phenolic compounds content in gymnosperm cell walls increase, which contribute to cell wall hardening and lignification, thus improving plant drought resistance, which optimize nutrient assimilation and utilization (Wang et al., 2019; Langguth et al., 2024). In resource-limited environments, *Only Tamariaceae* shows the preferential absorption of K^+ to support osmotic regulation and water retention, and this adaptability is mainly attributed to its efficient K^+ absorption mechanism. *Tamariaceae* plants absorb and transport K^+ through high-affinity K^+ transporters (e. g., HAK 5) and K^+ channels (such as AKT 1). These transporters exhibit efficient absorption under low K conditions, thus helping plants maintain cellular osmotic pressure and water balance in drought and salt stress environments (Chen et al., 2023). Conversely, *Chenopodiaceae* plants can adjust the osmotic levels in their cells by regulating the concentrations of N and P, thereby enhancing their adaptability to extreme environment (He et al., 2024).

The nitrogen to phosphorus (N:P) ratio in terrestrial vegetation serves as an indicator of soil nitrogen and phosphorus availability, highlighting nutrient limitations and the overall health of plant growth (Güsewell, 2004). Compared to leaves, the N:P ratio of stems and roots can serve as a more effective indicator of soil nutrient availability (Schreeg et al., 2014; Zeng et al., 2016). This study found that the N:P ratio of mature roots of all shrubs was 16.47 ± 0.37, while that of senescent roots was 20.04 ± 0.64. Both ratios exceeded 16, suggesting that the growth of desert shrub roots in Xinjiang may be limited by P. With limited water and nutrients, desert plants have reduced resource absorption, leading to decreased nutrient cycling and metabolic activity (Li et al., 2024a). The K:P ratio of the desert shrub roots was 18.41, further indicating that the growth of desert shrubs in Xinjiang was limited by P, which is consistent with the results of our previous study in this region (Luo et al., 2020). Because of their complex metabolic pathways, angiosperms can absorb and utilize N and K from the soil more effectively, resulting in higher N:P and K:P ratios. For example, they can dissolve the P in the soil through root exudates (such as organic acids and phosphatases), thus improving phosphorus availability (Ma et al., 2022; Pang et al., 2024). The root structure of angiosperms and microbial symbiosis (such as mycorrhizal fungi) also enhance N and K resorption. In addition, Angiosperms are more efficient in absorbing N and K by optimizing root architecture and increasing nutrient uptake efficiency (Langguth et al., 2024). *Tamarixaceae* plants exhibit high K:P ratios and possess well-developed roots that can penetrate deep into the soil to access water and nutrients, particularly in arid saline environments where their capacity for K uptake is enhanced (Hussain et al., 2022; Islam et al., 2024).

4.2 Changes in nutrient resorption characteristics of desert shrub roots

4.2.1 Characteristics of NuRE

In desert ecosystems, the harsh environmental conditions typically lead to lower rates of nutrient resorption and utilization compared to other ecosystems. As a result, desert plants are more reliant on internal nutrient cycling for their survival (Reichert et al., 2022; Tariq et al., 2024). In the present study, we found that the nutrient resorption efficiencies of the desert shrub roots were 29.14% for nitrogen (NRE), 37.58% for phosphorus (PRE), and 42.20% for potassium (KRE), as shown in Figure 1. These values are

TABLE 3 Responses of climate and soil variables to NRE, PRE and KRE of different families.

	Family	Estimate								
		pH	EC	K_{soil}	STN	STP	STK	MAP	MAT	AI
NRE	CH	7.05	-2.65	1.83***	-6.19***	5.78	1.14***	-1.04	8.47***	1.59**
	EP	-2.31*	6.69*	-3.48*	8.87*	-3.66	-1.11	-1.31*	-1.35*	3.38**
	LE	2.93	7.12	-1.15**	4.80	-3.08	3.21	-1.11**	-3.20**	1.03**
	PO	-5.15***	-1.73	-3.51***	8.93***	-7.27**	-2.92***	4.43***	-2.86***	2.47**
	SO	-4.53	-1.51	1.53	-7.38	3.75***	-5.82	5.54	5.75	-4.36
	TA	-8.89	3.89	-8.68	-7.55	3.16	-1.27	6.12***	-2.44***	-4.71
	ZY	6.36*	-2.03	-1.15***	2.91	-2.33	1.84	-1.13	2.29	1.23***
PRE	CH	4.54	1.77	1.41*	-3.47*	-4.52	-6.36	7.25	2.34	-1.26*
	EP	-1.13	3.60	-4.17**	7.53*	3.19	-1.39	8.17	-1.81*	3.75**
	LE	2.40	3.09	-6.77	5.92	-2.06	2.14	9.15	-2.20	5.25
	PO	-3.14*	5.44	-4.41***	7.19**	-3.52	-3.05***	-2.50	-1.78***	4.18***
	SO	-5.62	-6.08**	3.87	3.61	1.58	-9.27**	6.00	4.85	-1.11*
	TA	2.21*	5.24	-1.63**	5.99	-1.51	1.91*	-5.74	5.17	1.73**
	ZY	-2.40	-3.66	4.48	-2.06	1.90	-1.43	1.20	-1.23	-1.03
KRE	CH	3.06	2.99	1.42*	-2.89	2.37	7.59	-1.30	1.51	-1.30*
	EP	-1.92	-4.84	-1.14	9.38*	-9.17	-2.60	2.32	-1.19	6.32
	LE	-3.51	1.41	-8.33	-3.21	-3.44	-5.04	9.26	1.09	6.05
	PO	-2.13	2.71	-2.22*	2.20	-1.22	-2.60	-6.53**	2.64	2.75**
	SO	-4.54	-2.51	2.75	-7.67	2.23*	-8.90*	9.58*	8.55*	-6.61
	TA	1.44	-2.45	-1.48*	1.14	3.89	4.57	3.86*	8.51	1.36
	ZY	-2.15	3.92*	-1.78	-7.89	8.44	-1.74	-1.47	-9.03	1.45

CH, Chenopodiaceae; EP, Ephedraceae; LE, Leguminosae; PO, Polygonaceae; SO, Solanaceae; TA, Tamaricaceae; ZY, Zygophyllaceae. *$p< 0.05$; **$p< 0.01$; ***$p< 0.001$.

higher than the global average NRE of 27% for roots but lower than the global average PRE of 57% (Freschet et al., 2010). This discrepancy may be attributed to the fact that desert plants thrive in arid, nutrient-poor soils, and are developmentally and physiologically adapted to low-nutrient conditions (Suseela and Tharayil, 2018). In a study of root P levels, Yuan et al. (2011) reported that senescing roots reabsorbed 27% of P on average. Additionally, in a study involving 40 subarctic species, Freschet et al. (2010) found that 57% of P was resorbed in the roots, which was comparable to the 63% resorption rate observed in the leaves. The higher KRE value may reflect the need for plants in desert ecosystems to adapt to drought and water scarcity. To cope with these conditions, plants enhance their K resorption mechanisms, thereby improving K use efficiency.

The NRE and PRE in C_3 plants were generally higher than those of C_4 plants, a phenomenon that is attributable to the relatively low photosynthetic efficiency of C_3. This inherent inefficiency coerces C_3 plants to invest greater amounts of N and P to sustain their photosynthetic processes and metabolic functions (Kubásek et al., 2013; Guidi et al., 2019; Tanigawa et al., 2024). The structural simplicity of the xylem vascular bundle in gymnosperms enhances their ability to efficiently resorb and transport essential nutrients, optimizing nutrient resorption and retention, thereby facilitating their adaptability to various environmental conditions (Gleason et al., 2016; Langguth et al., 2024). *Tamaricaceae* plants exhibited a stronger absorption capacity for N and P, probably because their roots form symbiotic relationships with N-fixing bacteria (Cavagnaro, 2016). These bacteria convert N into a form that can be readily absorbed by plants, thereby enhancing the N utilization efficiency. In addition, organic acids secreted by *Tamaricaceae* plants, such as citric and oxalic acids, converts P in the soil into a form that can be absorbed by plants (Kumar and Rai, 2020), thereby increasing the effective uptake and utilization of P. In contrast, the K absorption efficiency of *Solanaceae* plants was significantly lower than that of other families. This may be attributed to the higher degree of lignification in their roots and increased rigidity of their cell walls, which adversely affects the extension and branching capabilities of the roots, consequently affecting their efficiency in absorbing water and nutrients (Basak et al., 2024).

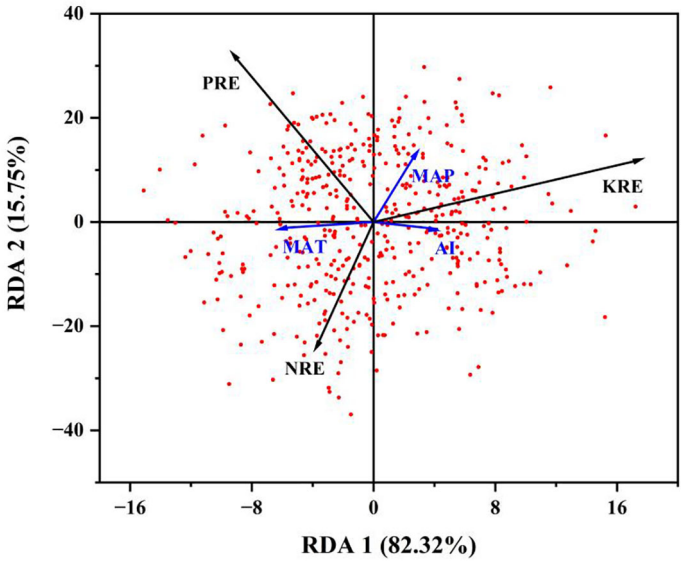

FIGURE 6
The influence of climatic factors on nutrient resorption efficiency (RDA analyse). Note: The direction of the blue arrows in the figure indicates the changing trend of the environmental factor, and the length of the arrows indicates the degree to which this environmental factor explains the sample distribution. The longer the arrow indicates that the greater the influence of this environmental factor on the sample distribution. The angles between the arrows and the sorting axes indicate the correlation between the environmental factors and the sorting axes. The smaller the clip angle, the higher the correlation. The quadrant in which the arrow indicates the positive or negative correlation of environmental factors with the sorting axis. The points in the plot represent species at different sampling points. The locations of the dots shows their relative positions in the RDA analysis.

4.2.2 Relative resorption efficiency and nutrient limitation

Nutrient ratios and relative nutrient resorption are important indicators for assessing plant nutritional status and understanding potential mechanisms of nutrient resorption (Güsewell, 2005; Schreeg et al., 2014). In the present study, the root PRE of desert shrub plants was higher than the NRE. Specifically, the relative resorption efficiencies of N and P (NRE-PRE< 0) were negative, which aligns with the prediction of the relative resorption hypothesis and suggests that plants tend to absorb limiting nutrients more than other nutrients (Han et al., 2013). The NRE-PRE, NRE-KRE, and KRE-PRE of all shrub roots were positively correlated with the N:P, N:K, and K:P ratios in roots during summer, whereas they were negatively correlated with these ratios in autumn (Figure 3), which is also consistent with our previous research results. When the N:P, N:K, and K:P ratios were 12.01, 0.60, and 18.85, respectively, the absorption efficiencies of all shrub roots in autumn reached equilibrium (NRE = PRE, NRE = KRE, and KRE = PRE), indicating that these plant groups were limited by N and P, N and K, and K and P near these critical ratios.

4.3 Relationship between nutrient resorption characteristics and environmental factors

Changes in the nutrient resorption efficiency reflect the response and adaptation of plants to their environment (Hartley et al., 2007; Liu et al., 2010; Takahashi et al., 2020). Desert plants have developed specialized survival and nutrient utilization strategies, through long-term adaptation, to cope with drought and high-salinity conditions (Gao et al., 2023). LMM results showed an inverse relationship between NRE and increased STP and STK in all plants. Soil N concentration in desert areas, characterized by low precipitation and high evaporation rates, is typically low. This limitation inhibits vegetation growth and intensifies rock weathering, increasing P concentration (Delgado-Baquerizo et al., 2013). Soil erosion further reduces plant coverage, which in turn inhibits the N mineralization process in the soil, decreasing the available N concentration. Excessive P occupies a significant number of absorption sites in plant roots, thereby affecting N uptake (McCulley et al., 2004). Soil K exerts a strong influence on N uptake by plant roots. As STK levels increase, the activity and absorption capacity of plant roots also increases, potentially enhancing NRE. The NRE of C_4 plants decreased with increasing K_{soil} and increased with increasing AI. This phenomenon may be attributed to the inhibition of photosynthesis and growth in C_4 plants as drought conditions intensify and soil moisture decreases, leading to reduced absorption capacity (Guidi et al., 2019). The NRE of *Chenopodiaceae* and *Polygonaceae* families exhibited the most significant responses to environmental factors. These two families dominate desert alkaline and arid regions and possess strong salt and drought tolerances (Gross et al., 2024). Plants accumulate compatible solutes, such as proline and betaine, in cells under high-salt and drought conditions. Proline is an important osmotic regulator that increases the osmotic pressure of cells, enabling them to absorb water from the outside environment under low-water-potential conditions (Li et al., 2024b). Their specialized survival and nutrient utilization

strategies enable them to respond rapidly to environmental changes and sustain their growth under water-scarce conditions.

PRE in all plants roots increased with increasing EC but decreased with increasing drought severity. An increase in EC elevates the ion concentration in the soil solution, allowing plants to access various nutrients necessary for adaptation to their growth environment more readily (Zhao et al., 2015). Conversely, plants experience water deficiency stress as drought conditions worsens. The limited mobility of nutrients in arid soils affects the concentration of nutrients absorbed by plants (Gao et al., 2022). The PRE of C_3 plants decreased with increasing K_{soil} and increased with increasing AI. Under water stress, C_3 plants close their stomata to reduce water evaporation, which negatively affects photosynthesis and metabolic activities of cells (Mukundan et al., 2024). Consequently, the entire plant reduces the demand and utilization of P. Under water stress conditions, P exhibits poor mobility in the soil, primarily exists in the form of insoluble compounds (Salim et al., 2024), its uptake by plant roots is restricted, and resorption efficiency reduces. Unique physiological structure and characteristics of *Polygonaceae* plants make them highly sensitive to variations in soil and climatic conditions. Their root systems are well-developed in arid and saline–alkaline environments, with extensive root hairs and a complex branching structure, which can effectively explore a larger soil volume to absorb water and nutrients (Vries et al., 2019). All these factors, including the root system, stomatal regulation, photosynthetic efficiency, and physiological adaptability, together enhance the nutrient and water resorption efficiency of *Polygonaceae* plants, thereby improving their survival and ecological competitiveness in harsh environments (McCulley et al., 2004; Freschet and Roumet, 2017; Moreau et al., 2019).

STK plays a crucial role in predicting the changes in the potassium resorption efficiency (KRE) of entire plants, encompassing both the soluble forms that plants can directly absorb and the insoluble forms released from soil minerals. In desert soils, the high potassium availability promotes plant growth and enhances interactions with microorganisms, leading to improved potassium utilization efficiency by plants (Cavagnaro, 2016). MAP and AI significantly influenced the KRE in *Polygonaceae* plants. Precipitation and drought conditions affect plant growth and nutrient uptake by affecting soil moisture and nutrient availability (Luo et al., 2024). Excessive precipitation can result in K loss, whereas moderate drought conditions can enhance K absorption by plants (Lebaudy et al., 2007). The key factors that have a significant impact on KRE in *Polygonaceae* plants are adaptability and regulatory mechanisms under diverse water conditions (Yang et al., 2020). Under arid or water-limited conditions, these plants have evolved specific morphological and physiological traits to cope with water scarcity. For instance, they may develop more efficient water-absorbing root systems or adjust their stomatal conductance to minimize water loss while maintaining essential physiological processes related to K uptake and utilization (Adame et al., 2021). Root branching and extension are key features of plant adaptation to drought stress (Zhang et al., 2021). In drought environments with limited resources, the branching structure of the roots can significantly increase the contact area between the roots and the soil, thereby allowing for more effective exploration of soil nutrients (Gao et al., 2024). Studies have shown that moderate drought stress can promote the formation of root branches and the lateral extension of roots (Shafi et al., 2024). This change in root architecture enables plants to more efficiently absorb potassium ions from the soil under drought conditions, especially when potassium availability in the soil is low.

Drought stress significantly constrains the physiological and ecological processes of desert plants. Redundancy analysis (RDA) revealed that MAP, MAT, and AI collectively explained over 98% of the variation in nutrient resorption efficiency, underscoring the pivotal role of water availability in regulating plant nutrient cycling under extreme environmental conditions. This study demonstrates distinct response mechanisms among different nutrient elements in terms of resorption efficiency. Phosphorus resorption efficiency (PRE) exhibited a precipitation-driven response signature. Episodic rainfall events in arid environments temporarily alleviated soil water deficits, significantly enhancing phosphorus uptake during the growth period (Zhao M. et al., 2024). Elevated MAT prolonged the root nutrient resorption and enzymatic reaction cycles, enabling plants to accumulate phosphorus reserves in mature leaves, thereby forming a vital allocation mechanism for scarce phosphorus resources. This adaptive strategy manifested as a marked increase in PRE under warm and humid conditions (Cao et al., 2024). Potassium resorption efficiency (KRE) reflected drought adaptation strategies. The enhancement of KRE was directly linked to osmotic regulation demands, as plants under drought stress intensified potassium resorption to maintain cell membrane integrity (Lee et al., 2024). The negative correlation between AI and NRE highlighted the inhibitory effects of prolonged drought on nitrogen conservation. High AI values exacerbated soil water deficits, suppressing microbial-mediated nitrogen mineralization processes and forcing plants to prioritize metabolic resource allocation (Shafi et al., 2024; Li et al., 2024b). Our results show that the efficiency of nutrient resorption is influenced by both soil and climatic factors. Temperature affects nutrient resorption by impacting soil nutrient availability, the rate of plant senescence, and nutrient resorption by altering soil moisture conditions and nutrients levels (Yuan et al., 2011; Cao et al., 2020). The nutrient cycling process of plants in desert ecosystems is complex, and the primary factors that influence nutrient resorption warrant further investigation.

5 Conclusion

This study comprehensively analyzes the variations in nutrient stoichiometry and resorption patterns of desert shrub roots in Xinjiang and their responses to climate and soil factors. The results indicate that nitrogen (N) and phosphorus (P) concentrations in desert shrub roots are significantly higher than those in other regions, while potassium (K) concentrations are significantly lower. The N:P ratio exceeds 16, suggesting that growth may be limited by P availability. Additionally, KRE in desert shrub roots significantly surpasses both NRE and PRE, highlighting the

importance of K in their nutrient resorption strategies. Soil moisture, nutrient content and its chemical form will affect the nutrient absorption and utilization of desert plants, and climatic factors such as temperature and precipitation will affect soil moisture, nutrient availability and plant metabolic process, thereby affecting the efficiency of plant nutrient resorption. The findings provide important insights into the resorption patterns and utilization strategies of root nutrients in desert shrubs, as well as the relationship between plants and their environment within desert ecosystems.

Data availability statement

The raw data supporting the conclusions of this article will be made available by the authors, without undue reservation.

Author contributions

YL: Investigation, Writing – original draft. WW: Writing – original draft. YW: Writing – review & editing. TX: Investigation, Writing – review & editing. KD: Investigation, Writing – review & editing.

Funding

The author(s) declare that financial support was received for the research and/or publication of this article. This project was funded by the Youth fund of Natural Science Foundation of Xinjiang Uygur Autonomous Region (No. 2024D01C218), the Research projects of basic scientific research business fees of colleges and universities in Xinjiang Uygur Autonomous Region (No. XJEDU2024P017), the Light of West China Program of the Chinese Academy of Sciences, the Special Project of Introducing High-level Talents to Xinjiang Uygur Autonomous Region, China.

Conflict of interest

The authors declare that the research was conducted in the absence of any commercial or financial relationships that could be construed as a potential conflict of interest.

Generative AI statement

The author(s) declare that no Generative AI was used in the creation of this manuscript.

Publisher's note

Supplementary material

The Supplementary Material for this article can be found online at: https://www.frontiersin.org/articles/10.3389/fpls.2025.1518846/full#supplementary-material

References

Adame, M. F., Reef, R., Santini, N. S., Najera, E., Turschwell, M. P., Hayes, M. A., et al. (2021). Mangroves in arid regions: Ecology, threats, and opportunities. *Estuar. Coast. Shelf Sci.* doi: 10.1016/j.ecss.2020.106796

Aerts, R. (1996). Nutrient resorption from senescing leaves of perennials: Are there general patterns? *J. Ecol.* 84, 597–608. doi: 10.2307/2261481

An, N., Lu, N., Fu, B., Wang, M., and He, N. (2021). Distinct responses of leaf traits to environment and phylogeny between herbaceous and Woody angiosperm species in China. *Front. Plant Sci.* 2875. doi: 10.3389/fpls.2021.799401

Bardgett, R. D., Mommer, L., and De Vries, F. T. (2014). Going underground: root traits as drivers of ecosystem processes. *Trends Ecol. Evol.* 29, 692–699. doi: 10.1016/j.tree.2014.10.006

Basak, H., Cimrin, K., and Turan, M. (2024). Effects of mycorrhiza on plant nutrition, enzyme activities, and lipid peroxidation in pepper grown under salinity stress. *J. Agric. Sci. Technol.* 26, 359–369. doi: 10.22034/JAST.26.2.359

Beugnon, R., Le Guyader, N., Milcu, A., Lenoir, J., Puissant, J., Morin, X, et al. (2024). Microclimate modulation: An overlooked mechanism influencing the impact of plant diversity on ecosystem functioning. *Glob. Change Biol.* 30, e17214. doi: 10.1111/gcb.17214

Brant, A., and Chen, H. (2015). Patterns and mechanisms of nutrient resorption in plants. *Crit. Rev. Plant Sci.* 34, 471–486. doi: 10.1111/j.1466-8238.2008.00425.x

Cao, Q., Zhou, Y., Bai, Y., and Han, Z. (2024). Available nitrogen and enzyme activity in rhizosphere soil dominate the changes in fine-root nutrient foraging strategies during plantation development. *Geoderma*. 446, 116901. doi: 10.1016/j.geoderma.2024.116901

Cao, Q., Yang, B., Li, J., Wang, R., Liu, T., and Xiao, H. (2020). Characteristics of soil water and salt associated with Tamarix ramosissima communities during normal and dry periods in a semi-arid saline environment. *Catena.* 193, 104661. doi: 10.1016/j.catena.2020.104661

Cavagnaro, T. R. (2016). Soil moisture legacy effects: impacts on soil nutrients, plants and mycorrhizal responsiveness. *Soil Biol. Biochem.* 95, 173–179. doi: 10.1016/j.soilbio.2015.12.016

Chapin, III, F.S. (1980). The mineral nutrition of wild plants. *Annu. Rev. Eco. Evo.* S. 11, 233–260. doi: 10.1146/annurev.es.11.110180.001313

Chen, X., Zhao, Y., Zhong, Y., Chen, J., and Qi, X. (2023). Deciphering the functional roles of transporter proteins in subcellular metal transportation of plants. *Planta*. 258, 17. doi: 10.1007/s00425-023-04170-8

Das, C., and Mondal, N. (2024). A case study of nutrient retranslocation in four deciduous tree species of West Bengal tropical forest, India. *Trop. Ecol.* 65, 580–591. doi: 10.1007/s42965-024-00352-x

Delgado-Baquerizo, M., Maestre, F., Gallardo, A., Bowker, M., Wallenstein, M., Quero, J., et al. (2013). Decoupling of soil nutrient cycles as a function of aridity in global drylands. *Nature.* 502, 672–676. doi: 10.1038/nature12670

Drenovsky, R., and Richards, J. (2006). Low leaf N and P resorption contributes to nutrient limitation in two desert shrubs. *Plant Ecol.* 183, 305–314. doi: 10.1007/s11258-005-9041-z

Du, E. Z., Terrer, C., Pellegrini, A., Ahlström, A., Caspar, J., Zhao, X., et al. (2020). Global patterns of terrestrial nitrogen and phosphorus limitation. *Nat. Geosci.* 13, 221–226. doi: 10.1038/s41561-019-0530-4

Ebrahim, N. A., Abd El-Mageed, T. A., and Shaker, A. (2014). Determination of potassium in high salinity water samples using flame photometry. *Am. J. Anal. Chem.* 5, 547–552. doi: 10.4236/ajac.2014.59065

Elser, J. J., Bracken, M. E., Cleland, E. E., Gruner, D. S., Harpole, W. S., Hillebrand, H., et al. (2007). Global analysis of nitrogen and phosphorus limitation of primary producers in freshwater, marine and terrestrial ecosystems. *Ecol. Lett.* 10, 1135–1142. doi: 10.1111/j.1461-0248.2007.01113.x

Freschet, G., Cornelissen, J., Van-Logtestijn, R., and Aerts, R. (2010). Substantial nutrient resorption from leaves, stems and roots in a subarctic flora: what is the link with other resource economics traits? *New Phytol.* 186, 879–889. doi: 10.1111/j.1469-8137.2010.03228.x

Freschet, G. T., and Roumet, C. (2017). Sampling roots to capture plant and soil functions. *Funct. Ecol.* 31, 1506–1518. doi: 10.1111/1365-2435.12883

Gao, H., Song, Y., and Li, M. (2025). Nutrient availability shapes the resistance of soil bacterial community and functions to disturbances in desert ecosystem. *Environ. Microbiol.* 27, e70081. doi: 10.1111/1462-2920.70081

Gao, Y., Su, Y., and Chao, D. (2024). Exploring the function of plant root diffusion barriers in sealing and shielding for environmental adaptation. *Nat. Plants.* 10, 1865–1874. doi: 10.1038/s41477-024-01842-5

Gao, Y., Tariq, A., Zeng, F., Zhang, Z., Sardans, J., Peuelas, J., et al. (2022). Allocation of foliar-P fractions of Alhagi sparsifolia and its relationship with soil-P fractions and soil properties in a hyperarid desert ecosystem. *Geoderma.* 407, 115546. doi: 10.1016/j.geoderma.2021.115546

Gao, Y. J., Zeng, F. J., Islam, W., Zhang, Z. Z., Du, Y., Zhang, Y. L., et al. (2023). Coexistence desert plants respond to soil phosphorus availability by altering the allocation patterns of foliar phosphorus fractions and acquiring different forms of soil phosphorus. *J. Plant Growth Regul.* 42, 3770–3784. doi: 10.1007/s00344-022-10836-6

Gleason, S. M., Westoby, M., Jansen, S., Choat, B., Hacke, U. G., Pratt, R. B., et al. (2016). Weak tradeoff between xylem safety and xylem-specific hydraulic efficiency across the world's woody plant species. *New Phytol.* 209, 123–136. doi: 10.1111/nph.13646

Gordon, W. S., and Jackson, R. B. (2000). Nutrient concentrations in fine roots. *Ecology* 81, 275–280. doi: 10.1890/0012-965

Gross, N., Maestre, F., Liancourt, P., Berdugo, M., Martin, R., Gozalo, B., et al. (2024). Unforeseen plant phenotypic diversity in a dry and grazed world. *Nature.* 632, 808–814. doi: 10.1038/s41586-024-07731-3

Guidi, L., Lo Piccolo, E., and Landi, M. (2019). Chlorophyll fluorescence, photoinhibition and abiotic stress: does it make any difference the fact to be a C_3 or C_4 species? *Front. Plant Sci.* 10. doi: 10.3389/fpls.2019.00174

Gupta, S., Kaushal, R., Sood, G., Bhardwaj, S., and Chauhan, A. (2021). Indigenous plant growth promoting rhizobacteria and chemical fertilizers: Impact on soil health and productivity of capsicum (Capsicum annuum L.) in North Western Himalayan Region. *Commun. Soil Sci. Plant Anal.* 52(6), 948–963. doi: 10.1080/00103624.2021.1872595

Gupta, A., Rico-Medina, A., and Caño-Delgado, A. I. (2020). The physiology of plant responses to drought. *Science* 368, 266–269. doi: 10.1126/science.aaz7614

Güsewell, S. (2004). N:P ratios in terrestrial plants: variation and functional significance. *New Phytol.* 164, 243–266. doi: 10.1111/j.1469-8137.2004.01192.x

Güsewell, S. (2005). Nutrient resorption of wetland graminoids is related to the type of nutrient limitation. *Funct. Ecol.* 19, 344–354. doi: 10.1111/j.0269-8463.2005.00967.x

Han, W. X., Fang, J. Y., Reich, P. B., Woodward, F. I., and Wang, Z. H. (2011). Biogeography and variability of eleven mineral elements in plant leaves across gradients of climate, soil and plant functional type in China. *Ecol. Lett.* 14, 788–796. doi: 10.1111/j.1461-0248.2011.01641.x

Han, W. X., Tang, L. Y., Chen, Y. H., and Fang, J. Y. (2013). Relationship between the relative limitation and resorption efficiency of nitrogen vs phosphorus in woody plants. *PloS One* 8, e83366. doi: 10.1371/journal.pone.0094515

Hartley, A., Barger, N., Belnap, J., and Okin, G. S. (2007). Dryland ecosystems. *Soil Biol* 10, 271–307. doi: 10.1007/978-3-540-68027-7-10

He, M., Feike, A., Zhang, K., Tan, H., Zhao, Y., and Li, X. (2015). Influence of life form, taxonomy, climate, and soil properties on shoot and root concentrations of 11 elements in herbaceous plants in a temperate desert. *Plant Soil.* 398, 339–350. doi: 10.1007/s11104-015-2669-0

He, R., Liu, Y., Song, C., Feng, G., and Song, J. (2024). Osmotic regulation beyond nitrate nutrients in plant resistance to stress: a review. *Plant Growth Regul.* 103, 1–8. doi: 10.1007/s10725-023-01093-y

Huang, G., Su, Y. G., Mu, X. H., and Li, Y. (2018). Foliar nutrient resorption responses of three life-form plants to water and nitrogen additions in a temperate desert. *Plant Soil.* 424, 479–489. doi: 10.1007/s11104-017-3551-z

Huang, W., Zhang, L., Columbus, T. J., Hu, Y., Zhao, Y., Tang, L., et al. (2022). A well-supported nuclear phylogeny of Poaceae and implications for the evolution of C_4 photosynthesis. *Mol. Plant* 4, 755–777. doi: 10.1016/j.molp.2022.01.015

Hussain, T., Asrar, H., Li, J., Feng, X., Gul, B., and Liu, X. (2022). The presence of salts in the leaf exudate improves the photosynthetic performance of a recreto-halophyte, Tamarix chinensis. *Environ. Exp. Bot.* 199, 104896. doi: 10.1016/j.envexpbot.2022.104896

Islam, W., Zeng, F. J., Dar, A. A., and Yousaf, M. S. (2024). Dynamics of soil biota and nutrients at varied depths in a Tamarix ramosissima-dominated natural desert ecosystem: Implications for nutrient cycling and desertification management. *J. Environ. Manage* 354, 120217. doi: 10.1016/j.jenvman.2024.120217

James, J., Tiller, R., and Richards, J. (2005). Multiple resources limit plant growth and function in a saline-alkaline desert community. *J. Ecol.* 93, 113–126. doi: 10.1111/j.0022-0477.2004.00948.x

Johnson, R., Vishwakarma, K., Hossen, M., Kumar, V., and Hasanuzzaman, M. (2022). Potassium in plants: growth regulation, signaling, and environmental stress tolerance. *Plant Physiol. Biochem.* 172, 56–69. doi: 10.1016/j.plaphy.2022.01.001

Jungová, M., Asare, M. O., Michal, H., Hakl, J., and Pavlu, V. (2023). Distribution and resorption efficiency of macroelements (N, P, K, ca, and mg) in organs of *rumex alpinus L.* in the alps and the giant (Krkonoše) mountains. *J. Soil Sci. Plant Nutr.* 23, 469–484. doi: 10.1007/s42729-022-01059-5

Kautz, T., Amelung, W., Ewert, F., Gaiser, T., Horn, R., Jahn, R., et al. (2013). Nutrient acquisition from arable subsoils in temperate climates: A review. *Soil Biol. Biochem.* 57, 1003–1022. doi: 10.1016/j.soilbio.2012.09.014

Killingbeck, K. T. (1993). Nutrient resorption in desert shrubs. *Rev. Chil. Hist. Nat.* 66, 345–355. doi: 10.1080/00222939300770711

Killingbeck, K. T. (1996). Nutrients in senesced leaves: keys to the search for potential resorption and resorption proficiency. *Ecology.* 77, 1716–1727. doi: 10.2307/2265777

Killingbeck, K. T., and Whitford, W. G. (2001). Nutrient resorption in shrubs growing by design, and by default in Chihuahuan Desert arroyos. *Oecologia.* 128, 351–359. doi: 10.1007/s004420100668

Kim, J., Kidokoro, S., Yamaguchi-Shinozaki, K., and Shinozaki, K. (2024). Regulatory networks in plant responses to drought and cold stress. *Plant Physiol.* 195, 170–189. doi: 10.1093/plphys/kiae105

Kubásek, J., Urban, O., and Šantrůček, J. (2013). C_4 plants use fluctuating light less efficiently than do C_3 plants: a study of growth, photosynthesis and carbon isotope discrimination. *Physiol. Plant* 149, 528–539. doi: 10.1111/ppl.12057

Kumar, A., and Rai, L. (2020). Soil organic carbon and phosphorus availability regulate abundance of culturable phosphate-solubilizing bacteria in paddy fields. *Pedosphere.* 30, 405–413. doi: 10.1016/S1002-0160(17)60403-X

Lambers, H. (2022). Phosphorus acquisition and utilization in plants. *Annu. Rev. Plant Biol.* 73, 11–126. doi: 10.1146/annurev-arplant-102720-125738

Langguth, J. R., Zadworny, M., Andraczek, K., Lo, M., Tran, N., Patrick, K., et al. (2024). Gymnosperms demonstrate patterns of fine-root trait coordination consistent with the global root economics space. *J. Ecol.* 112, 1425–1439. doi: 10.1111/1365-2745.14315

Lebaudy, A., Véry, A., and Sentenac, H. (2007). K^+ channel activity in plants: Genes, regulation and functions. *FEBS Lett.* 25, 2357–2366. doi: 10.1016/j.febslet.2007.03.058

Lee, D., Park, T., Lim, K., Jeong, M., Nam, G., Kim, W, et al. (2024). Biofumigation-Derived Soil Microbiome Modification and Its Effects on Tomato (Solanum lycopersicum L.) Health under Drought>. *Agronomy*. 14(10), 2225. doi: 10.3390/agronomy14102225

Li, C., He, H., Zhang, X., Ren, X., Shi, L., Zhang, L., et al. (2025a). Long-term leaf nitrogen and phosphorus dynamics and drivers in China's forests under global change. *Front. Plant Sci.* 13, 100325. doi: 10.1016/j.fecs.2025.100325

Li, Y., Li, Y., Lai, Q., Yao, Z., Zhou, K., and Niu, D. (2024a). Proline metabolism and its osmotic regulatory role in enhancing hypersalinity tolerance of the razor clam (Sinonovacula constrict a). *Aquaculture* 589, 741019. doi: 10.1016/j.aquaculture.2024.741019

Li, W., Migliavacca, M., Forkel, M., Denissen, J. M. C., Reichstein, M., Yang, H., et al. (2022). Widespread increasing vegetation sensitivity to soil moisture. *Nat. Commun.* 13, 3959. doi: 10.1038/s41467-022-31667-9

Li, W., Wang, H., Lv, G., Wang, J., and Li, J. (2024b). Regulation of drought stress on nutrient cycle and metabolism of rhizosphere microorganisms in desert riparian forest. *Sci. Total Environ.* 954, 176148. doi: 10.1016/j.scitotenv.2024.176148

Li, G., Wei, N., and Hou, H. (2025b). Uncovering the secrets of how plants adapt to water stress. *Plant Cell Environment*. doi: 10.1111/pce.15571

Liao, L., Wang, J., Dijkstra, F. A., Lei, S., Zhang, L., Wang, X., et al. (2024). Nitrogen enrichment stimulates rhizosphere multi-element cycling genes via mediating plant biomass and root exudates. *Soil Biol. Biochem.* 190, 109306. doi: 10.1016/j.soilbio.2023.109306

Liu, G., Freschet, G. T., Pan, X., Cornelissen, J. C., Li, Y., and Dong, M. (2010). Coordinated variation in leaf and root traits across multiple spatial scales in Chinese semi-arid and arid ecosystems. *New Phytol.* 188, 543–553. doi: 10.1007/s11104-015-2669-0

Liu, C., Hao, Y., Wu, X., Dai, F., Abd-Allah, E., Wu, Q., et al. (2024). Arbuscular mycorrhizal fungi improve drought tolerance of tea plants via modulating root architecture and hormones. *Plant Growth Regul.* 102, 13–22. doi: 10.1007/s10725-023-00972-8

Liu, S., He, F., Kuzyakov, Y., Xiao, H., Hoang, D. T., Pu, S., et al. (2022). Nutrients in the rhizosphere: A meta-analysis of content, availability, and influencing factors. *Sci. Total Environ.* 826, 153908. doi: 10.1016/j.scitotenv.2022.153908

Lobo-do-Vale, R., Besson, C., Caldeira, M., Chaves, M., and Pereira, J. (2019). Drought reduces tree growing season length but increases nitrogen resorption efficiency in a Mediterranean ecosystem. *Biogeosciences.* 16, 1265–1279. doi: 10.5194/bg-16-1265-2019

Lopez, G., Ahmadi, S., Amelung, W., Athmann, M., Ewert, F., Gaiser, T., et al. (2023). Nutrient deficiency effects on root architecture and root-to-shoot ratio in arable crops. *Front. Plant Sci.* 13. doi: 10.3389/fpls.2022.1067498

Luo, Y., Peng, Q., He, M., Zhang, M., Liu, Y., Gong, Y., et al. (2020). N, P and K stoichiometry and resorption efficiency of nine dominant shrub species in the deserts of Xinjiang, China. *Ecol. Res.* 35, 625–637. doi: 10.1111/1440-1703.12111

Luo, Y., Shen, Y., Elrys, A. S., Du, L., Mahmood, M., Zhang, J., et al. (2024). Drought and nitrogen deposition regulate plant nutrient resorption in a typical steppe. *Agric. Ecosyst. Environ.* 374, 109160. doi: 10.1016/j.agee.2024.109160

Ma, W., Tang, S., Deng, Z., Zhang, D., Zhang, T., and Ma, X. (2022). Root exudates contribute to belowground ecosystem hotspots: A review. *Front. Microbiol.* 13. doi: 10.3389/fmicb.2022.937940

Mahdieh, S., Hosseyni, M., Naser, S., Jalal, S., and Niloufar, H. (2021). Desert-adapted fungal endophytes induce salinity and drought stress resistance in model crops. *Plant Physiol. Biochem.* 160, 225–238. doi: 10.1016/j.plaphy.2021.01.022

McCulley, R. L., Jobbágy, E. G., Pockman, W. T., and Jackson, R. B. (2004). Nutrient uptake as a contributing explanation for deep rooting in arid and semi-arid ecosystems. *Oecologia.* 141, 620–628. doi: 10.1007/s00442-004-1687-z

Moreau, D., Bardgett, R. D., Finlay, R. D., Jones, D. L., and Philippot, L. (2019). A plant perspective on nitrogen cycling in the rhizosphere. *Funct. Ecol.* 33, 540–552. doi: 10.1111/1365-2435.13303

Mukundan, N., Satyamoorthy, K., and Sankar, V. (2024). Investigating photosynthetic evolution and the feasibility of inducing C_4 syndrome in C_3 plants. *Plant Biotechnol. Rep.* 18, 449–463. doi: 10.1007/s11816-024-00908-2

Ozeki, K., Miyazawa, Y., and Sugiura, D. (2022). Rapid stomatal closure contributes to higher water use efficiency in major C_4 compared to C_3 Poaceae crops. *Plant Physiol.* 189, 188–203. doi: 10.1093/plphys/kiac040

Pang, F., Li, Q., Solanki, M., Wang, Z., Xing, Y., and Dong, D. (2024). Soil phosphorus transformation and plant uptake driven by phosphate-solubilizing microorganisms. *Front. Microbiol.* 15. doi: 10.3389/fmicb.2024.1383813

Paulus, J., Schlieper, D., and Groth, G. (2013). Greater efficiency of photosynthetic carbon fixation due to single amino-acid substitution. *Nat. Commun.* 4, 1518. doi: 10.1038/ncomms2504

Reed, S. C., Townsend, A. R., Davidson, E. A., and Cleveland, C. C. (2012). Stoichiometric patterns in foliar nutrient resorption across multiple scales. *New Phytol.* 196, 173–180. doi: 10.1111/j.1469-8137.2012.04249.x

Reich, P. B., and Oleksyn, J. (2004). Global patterns of plant leaf N and P in relation to temperature and latitude. *Proc. Natl. Acad. Sci.* 101, 11001–11006. doi: 10.1073/pnas.0403588101

Reichert, T., Rammig, A., Fuchslueger, L., Lugli, L. F., Quesada, C. A., and Fleischer, K. (2022). Plant phosphorus-use and acquisition strategies in Amazonia. *New Phytol.* 234, 1126–1143. doi: 10.1111/nph.17985

Rizzuto, G., Wang, D., Chen, J., Hung, T., Fitzky, A., Flashman, E., et al. (2024). Contrasted NCED gene expression across conifers with rising and peaking abscisic acid responses to drought. *Plant Stress.* 14, 100574. doi: 10.1016/j.stress.2024.100574

Salim, M., Chen, Y., Solaiman, Z. M., Zaka, M., and Kadambot, H. M. (2024). Phosphorus fertilisation differentially affects morpho-physiological traits and yield in soybean exposed to water stress. *Plant Soil* 504, 779–797. doi: 10.1007/s11104-024-06657-z

Sardans, J., Grau, O., Chen, H., Janssens, I., Ciais, P., Piao, S., et al. (2017). Changes in nutrient concentrations of leaves and roots in response to global change factors. *Glob Change Biol.* 23, 3849–3856. doi: 10.1111/gcb.13721

Sardans, J., Janssens, I. A., Alonso, R., Veresoglou, S. D., and Peñuelas, J. (2014). Foliar elemental composition of European forest tree species associated with evolutionary traits and present environmental and competitive conditions. *Glob. Ecol. Biogeogr.* 24, 240–255. doi: 10.1111/geb.12253

Sardans, J., and Peñuelas, J. (2015). Potassium: a neglected nutrient in global change. *Glob. Ecol. Biogeogr.* 24, 261–275. doi: 10.1111/geb.12259

Schenk, H. J., and Jackson, R. B. (2002). Rooting depths, lateral root spreads and below-ground/above-ground allometries of plants in water-limited ecosystems. *J. Ecol.* 90, 480–494. doi: 10.1046/j.1365-2745.2002.00682.x

Schreeg, L. A., Santiago, L. S., and Wright, S. J. (2014). Stem, root, and older leaf N:P ratios are more responsive indicators of soil nutrient availability than new foliage. *Ecology* 95, 2062–2068. doi: 10.1890/13-1671

Shafi, I., Gautam, M., and Kariyat, R. (2024). Integrating ecophysiology andomics to unlock crop response to drought and herbivory stress. *Front. Plant Sci.* 15. doi: 10.3389/fpls.2024.1500773

She, W., Zhou, Y., Luo, W., Bai, Y, Feng, W, Lai, Z, et al. (2024). Precipitation and plant functional composition mediate desert canopy nutrient responses to water and nitrogen addition. *Plant Soil.* 496, 609–621. doi: 10.1007/s11104-023-06384-x

Suseela, V., and Tharayil, N. (2018). Decoupling the direct and indirect effects of climate on plant litter decomposition and terrestrial nutrient cycling. *Glob Change Biol.* 24, 1428–1451. doi: 10.1111/gcb.13923

Takahashi, F., Kuromori, T., Urano, K., Yamaguchi-Shinozaki, K., and Shinozaki, K. (2020). Drought stress responses and resistance in plants: from cellular responses to long-distance intercellular communication. *Front. Plant Sci.* 11. doi: 10.3389/fpls.2020.556972

Tanigawa, K., Yuchen, Q., Katsuhama, N., Sakoda, K., Wakabayashi, Y., Tanaka, Y., et al. (2024). C_4 monocots and C_4 dicots exhibit rapid photosynthetic induction response in contrast to C_3 plants. *Physiol. Plant* 176, e14431. doi: 10.1111/ppl.1443

Tariq, A., Graciano, C., Sardans, J., Zeng, F., Hughes, A., Ahmed, Z., et al. (2024). Plant root mechanisms and their effects on carbon and nutrient accumulation in desert ecosystems under changes in land use and climate. *New Phytol.* 242, 916–934. doi: 10.1111/nph.19676

Vergutz, L., Manzoni, S., Porporato, A., Novais, R. F., and Jackson, R. B. (2012). Global resorption efficiencies and concentrations of carbon and nutrients in leaves of terrestrial plants. *Ecol. Monogr.* 82, 205–220. doi: 10.1890/11-0416.1

Vries, F. T., Williams, A., Stringer, F., Willcocks, R., Mcewing, R., Langridge, H., et al. (2019). Changes in root-exudate-induced respiration reveal a novel mechanism through which drought affects ecosystem carbon cycling. *New Phytol.* 224, 132–145. doi: 10.1111/nph.16001

Wang, D., Freschet, G., McCormack, M., Lambers, H., and Gu, J. (2025). Nutrient resorption of leaves and roots coordinates with root nutrient-acquisition strategies in a temperate forest. *New Phytol.* 246, 515–527. doi: 10.1111/nph.70001

Wang, F., Gao, J., Yong, J., Wang, Q., Ma, J., and He, X. (2020). Higher atmospheric CO_2 levels favor C_3 plants over C_4 plants in utilizing ammonium as a nitrogen source. *Front. Plant Sci.* 11. doi: 10.3389/fpls.2020.537443

Wang, C., McCormack, M. L., Guo, D., and Li, J. (2019). Global meta-analysis reveals different patterns of root tip adjustments by angiosperm and gymnosperm trees in response to environmental gradients. *J. Biogeogr.* 46, 123–133. doi: 10.1111/jbi.13472

Wang, L., Zhang, X., and Xu, S. (2020). Is salinity the main ecological factor that influences foliar nutrient resorption of desert plants in a hyper-arid environment? *BMC Plant Biol.* 20, 461. doi: 10.1186/s12870-020-02680-1

Weemstra, M., Mommer, L., Visser, E., Van Ruijven, J., Kuyper, T., Mohren, G., et al. (2016). Towards a multidimensional root trait framework: a tree root review. *New Phytol.* 211, 1159–1169. doi: 10.1111/nph.14003

Williams, A., and de Vries, F. (2020). Plant root exudation under drought: implications for ecosystem functioning. *New Phytol.* 225, 1899–1905. doi: 10.1111/nph.16223

Yan, T., Zhu, J., and Yang, K. (2018). Leaf nitrogen and phosphorus resorption of woody species in response to climatic conditions and soil nutrients: a meta-analysis. *J. For. Res.* 29, 905–913. doi: 10.1007/s11676-017-0519-z

Yang, Y., Liu, B. R., and An, S. S. (2018). Ecological stoichiometry in leaves, roots, litters and soil among different plant communities in a desertified region of Northern China. *Catena.* 166, 328–338. doi: 10.1016/j.catena.2018.04.018

Yang, M., Lu, J., Liu, M., Lu, X. Y., and Yang, H. M. (2020). Leaf nutrient resorption in lucerne decreases with relief of relative soil nutrient limitation under phosphorus and potassium fertilization with irrigation. *Sci. Rep.* 10, 10525. doi: 10.1038/s41598-020-65484-1

Yuan, Z., Chen, H., and Reich, P. (2011). Global-scale latitudinal patterns of plant fine-root nitrogen and phosphorus. *Nat. Commun.* 2, 344. doi: 10.1038/ncomms1346

Zeng, Q., Li, X., Dong, Y., An, S., and Darboux, F. (2016). Soil and plant components ecological stoichiometry in four steppe communities in the Loess Plateau of China. *Catena.* 147, 481–488. doi: 10.1016/j.catena.2016.07.047

Zhang, S., Deng, Q., Kallenbach, R., and Yuan, Z. (2024). Soil pH and drought affect nutrient resorption of Leymus chinensis in the Inner Mongolian grasslands along a 1200-km transect. *Plant Soil*. doi: 10.1007/s11104-024-07035-5

Zhang, M., Luo, Y., Yan, Z., Chen, J., Anwar, E., and Li, K. (2018). Resorptions of ten mineral elements in leaves of desert shrubs and their contrasting responses to aridity. *Plant Ecol.* 12, 358–366. doi: 10.1093/jpe/rty034

Zhang, M., Wang, Y., Chen, X., Xu, F., Ding, M., Ye, W., et al. (2021). Plasma membrane H^+-ATPase overexpression increases rice yield via simultaneous enhancement of nutrient uptake and photosynthesis. *Nat. Commun.* 12, 735. doi: 10.1038/s41467-021-20964-4

Zhang, J., Yu, W., Wang, Y., Huang, Z., and Liu, G. (2024). Effects of climate, soil, and leaf traits on nutrient resorption efficiency and proficiency of different plant functional types across arid and semiarid regions of northwest China. *BMC Plant Biol.* 24, 1093. doi: 10.1186/s12870-024-05794-y

Zhang, H., Zhu, J., Gong, Z., and Zhu, J. (2022). Abiotic stress responses in plants. *Nat. Rev. Genet.* 23, 104–119. doi: 10.1038/s41576-021-00413-0

Zhao, F., Kang, D., Han, X., Yang, G., Feng, Y., and Ren, G. (2015). Soil stoichiometry and carbon storage in long-term afforestation soil affected by understory vegetation diversity. *Ecol. Eng.* 74, 415–422. doi: 10.1016/j.ecoleng.2014.11.010

Zhao, M., Mills, B., Poulton, S., Wan, B., Xiao, K., Guo, M., et al. (2024). Drivers of the global phosphorus cycle over geological time. *Nat. Rev. Earth Environ.* 5, 873–889. doi: 10.1038/s43017-024-00603-4

Zhao, Q., Zhang, Y., Wang, Y., and Han, G. (2024). Different responses of foliar nutrient resorption efficiency in two dominant species to grazing in the desert steppe. *Sci. Rep.* 14, 4090. doi: 10.1038/s41598-024-53574-3

Zheng, J., She, W., Zhang, Y., Bai, Y., Qin, S., and Wu, B. (2018). Nitrogen enrichment alters nutrient resorption and exacerbates phosphorus limitation in the desert shrub artemisia ordosica. *Ecol. Evol.* 8, 9998–10007. doi: 10.1002/ece3.4407

frontiers | Frontiers in Plant Science

TYPE Original Research
PUBLISHED 04 July 2025
DOI 10.3389/fpls.2025.1554879

OPEN ACCESS

EDITED BY
Xiao-Dong Yang,
Ningbo University, China

REVIEWED BY
Weiwei She,
Beijing Forestry University, China
Mingshan Xu,
Zhejiang Institute of Hydraulics & Estuary, China

*CORRESPONDENCE
Zhaobin Mu
muzhaobin@ms.xjb.ac.cn
Waqar Islam
waqarislam@ms.xjb.ac.cn
Fanjiang Zeng
fjzeng@ms.xjb.ac.cn

†These authors have contributed equally to this work

RECEIVED 03 January 2025
ACCEPTED 16 June 2025
PUBLISHED 04 July 2025

CITATION
Zhang Y, Du Y, Mu Z, Islam W, Zeng F, Gonzalez NCT and Zhang Z (2025) Impact of seasonal changes on root-associated microbial communities among phreatophytes of three basins in desert ecosystem. *Front. Plant Sci.* 16:1554879. doi: 10.3389/fpls.2025.1554879

Impact of seasonal changes on root-associated microbial communities among phreatophytes of three basins in desert ecosystem

Yulin Zhang[1,2,3,4†], Yi Du[1,2,3,5†], Zhaobin Mu[1,2,3,6*], Waqar Islam[1,2,3*], Fanjiang Zeng[1,2,3,4,5*], Norela C. T. Gonzalez[7] and Zhihao Zhang[1,2,3]

[1]Xinjiang Key Laboratory of Desert Plant Roots Ecology and Vegetation Restoration, Xinjiang Institute of Ecology and Geography, Chinese Academy of Sciences, Urumqi, China, [2]State Key Laboratory of Ecological Safety and Sustainable Development in Arid Lands, Xinjiang Institute of Ecology and Geography, Chinese Academy of Sciences, Urumqi, China, [3]Cele National Station of Observation and Research for Desert-Grassland Ecosystems, Hotan, China, [4]College of Ecology and Environmental, Xinjiang University, Urumqi, China, [5]University of Chinese Academy of Sciences, Beijing, China, [6]State Key Laboratory of Advanced Environmental Technology and Guangdong Key Laboratory of Environmental Protection and Resources Utilization, Guangzhou Institute of Geochemistry, Chinese Academy of Sciences, Guangzhou, China, [7]College of Forestry, Central South University of Forestry and Technology, Changsha, Hunan, China

Seasons often alter climate conditions and affect nutrient cycling by altering plant physiology and microbial dynamics. Plant growth and health depend on a symbiotic relationship with root microbes, however, the root-associated microbiota is key to plant evolution and ecosystem function. Seasonal changes in root-associated microbiome diversity and composition of desert plants are vital for understanding plant adaptation in desert ecosystems. We employed high-throughput sequencing to investigate the seasonal dynamics of root-associated microbial communities, including the root endosphere (RE), rhizosphere soil (RS), and bulk soil (BS), across three basins in Xinjiang, China: Turpan, Tarim, and Dzungaria. *Proteobacteria* dominated bacterial communities in different seasons, while *Ascomycota* prevailed in fungi. The spring and summer conditions favor greater microbial differentiation. The RE, RS, and BS bacterial communities in May (spring) showed a noticeable absence of highly connected nodes within and between modules. However, the opposite trend was observed in July (summer) and September (autumn). The community assembly of root-associated microbiome (bacteria and fungi) in different seasons primarily followed a random process. Random forest analysis found that seasonal variations in RE bacterial communities were primarily influenced by scattered radiation, while fungal communities were mainly affected by soil available potassium. Environmental factors affect the BS bacterial community more than the fungal community across different seasons. A structural equation model revealed temperature and precipitation's direct effects on microbial communities, mediated by soil and root nutrient availability. Soil pH and EC predominantly affected root bacterial communities, not fungal communities. The fungal community within the RE was found to be directly influenced by seasonal shifts, whereas the RS fungal community composition was significantly impacted by changes in precipitation patterns driven by seasonal variation. The climate

seems to be a crucial factor in influencing the dynamic of the root microbiome in desert plants, surpassing the influence of soil and root nutrient availability. This study underscores seasonal root-associated microbiome variations and their important roles in desert ecosystem functions.

KEYWORDS

seasonal dynamics, desert plants, soil nutrients, microbial composition, soil microbiome

1 Introduction

Plant roots harbor a distinctive microbiome comprising soil-derived microorganisms (Chen et al., 2019; Zhang et al., 2018). These microorganisms form a symbiotic relationship with the plant, which is significant for the plant because it affects its growth and nutrient absorption throughout its life cycle (Domeignoz-Horta et al., 2020; Oldroyd and Leyser, 2020). Although seasonal climate changes can influence plant communities (Fraterrigo and Rusak, 2008), there is a lack of studies investigating seasonal variations in root-associated microbiomes (Hannula et al., 2019). Microbial seasonality has not been fully understood due to neglect of various microbial groups (Regan et al., 2014; Wang et al., 2018). Furthermore, few studies concurrently investigate microbial variations across different root compartments (Monson et al., 2006; Wu et al., 2016). Recent studies have illuminated root-associated microbiomes as sensitive bioindicators to environmental changes, exhibiting seasonal community shifts across diverse ecosystems (Manzoni et al., 2012). These changes may affect soil biogeochemical cycles (Siles et al., 2016). The impact of elevated temperatures on soil microbial physiology and community composition has been extensively explored through short-term warming experiments over the past few decades (Jansson and Hofmockel, 2020). However, soil microbial communities do not simply respond passively to temperature fluctuations; they also exhibit adaptive responses to prolonged warming (Bradford et al., 2008). Consequently, delving into the seasonal dynamics of root-associated microbiomes promises a comprehensive comprehension of how climate change impacts biogeochemical processes in desert ecosystems.

Despite numerous research studies into the seasonal fluctuations of root-associated microbiome, a coherent understanding remains elusive, lacking consensus on influencing factors (Tan et al., 2014; Hannula et al., 2019). Seasonality is common in natural ecosystems, indicating the concurrent fluctuation of different environmental elements like temperature, rainfall, and soil characteristics (Zhang et al., 2023; Howe et al., 2023). Studies have demonstrated that late-season precipitation significantly increases the biomass of arbuscular mycorrhizal fungi (AMF) and markedly alters the relative abundance of dominant genera within AMF and protist community (Yu et al., 2024). In addition, the relative abundance of major bacterial phyla such as Actinobacteria, Firmicutes, and Proteobacteria has been found to correlate strongly with annual mean temperature and precipitation at the watershed scale. However, seasonal variation—rather than spatial heterogeneity—emerged as the primary driver of the composition of soil antibiotic resistance genes (Xiang et al., 2021). Despite the widely recognized impact of seasonality on ecological processes, our understanding of how it fully affects the assembly of root microbial communities remains inadequate (White and Hastings, 2020). Previous studies have shown notable variations throughout the seasons in microbial populations and their functional categories (He et al., 2021), especially in agricultural and water environments (Grady et al., 2019; He et al., 2020; Maurice et al., 2024a). A comparison between ecological floating beds planted with *Cyperus involucratus* Rottb., *Thalia dealbata* Fraser, and *Iris tectorum* Maxim, and a control group (static water) revealed that root-associated microbial communities exhibited their highest abundance and diversity in autumn. These communities were dominated by taxa such as *Proteobacteria, Actinobacteriota, Cyanobacteria, Chloroflexi, Firmicutes, Bacteroidota*, and *Acidobacteriota*, highlighting a distinct seasonal pattern of microbial proliferation (Felipe et al., 2021; Zhang et al., 2022a). Distinct soil fungal community composition differences were found among forest types and seasons (Xie and Yin, 2022). Nevertheless, the impact of seasonal fluctuations on the structure of root-associated microbial communities in arid ecosystems has not been widely explored (Eilers et al., 2010). These microbial communities are affected by a mixture of climatic, soil physicochemical, and biological factors, among which temperature and precipitation are of vital importance (Ibekwe et al., 2020). Seasonal shifts influence soil physicochemical attributes and resource quality, resulting in variations in microbial composition (Sharhabil et al., 2023; Fan et al., 2023). Several studies have investigated the relationship between environmental factors and soil bacterial diversity across 90 different habitats in China's temperate desert region. These studies indicate that soil bacterial α and beta diversity are primarily driven by abiotic and spatial factors, followed by plant-related influences (Wang et al., 2020). Among these abiotic factors, soil pH has emerged as a key determinant of bacterial diversity and community composition. It has a stronger influence than spatial and climatic (biome-related) variables in shaping microbial patterns (Zhou et al., 2024). In a separate study conducted in Michigan, USA, soils were sampled monthly from May to November across replicated plots of three land-use types: conventional row-crop agriculture, reduced-input row-crop agriculture, and early successional grasslands. Results showed that

α-diversity exhibited stronger temporal variability driven by sampling month than by land-use type. In contrast, β-diversity patterns remained relatively stable across land-use types throughout the 7-month period, suggesting that the timing of sampling is less critical when assessing community composition across different land uses (Rasche et al., 2011; Lauber et al., 2013). Furthermore, the structure of soil microbial communities can also vary in response to seasonal fluctuations in plant activity and carbon inputs (Islam et al., 2023; Gao et al., 2024). Mostly, Plants selectively cultivate specific microbial communities in the rhizosphere through root exudates, influencing the surrounding soil's physical and chemical characteristics (Wang et al., 2022). Microbial responses to seasonal changes differ between the rhizosphere and bulk soil, with significant differences among different microbial categories (Xu et al., 2023; Markus et al., 2024).

Desert ecosystems, found in arid and semi-arid regions, are defined by extreme water scarcity, high temperatures, and limited nutrients (Ibáñez et al., 2007; Tariq et al., 2022; Islam et al., 2024a). Desert vegetation has evolved special adaptation mechanisms to cope with these extreme circumstances (Zhang et al., 2022b; Islam et al., 2024b; Gao et al., 2024). *Calligonum caput-medusae* Schrenk., *Alhagi sparsifolia* Shap., and *Tamarix ramosissima* Ledeb., are key desert plants that contribute to ecological stability by preventing wind erosion and stabilizing sand, while also serving as valuable forage to support regional animal husbandry (Zhang et al., 2020; Islam et al., 2024c). The study collected root endosphere (RE), rhizosphere soil (RS), and bulk soil (BS) samples from three key desert plants—*C. caput-medusae*, *A. sparsifolia*, and *T. ramosissima*—in Xinjiang, China. These species are crucial for the stability and sustainability of the desert ecosystem. We investigated and analyzed how seasonal changes affect the bacterial and fungal communities associated with the roots using high-throughput amplicon sequencing on the Illumina HiSeq platform. This study investigated the composition and diversity of root-associated microbiomes to uncover their distinct seasonal dynamics and the underlying influences of soil and plant nutrients. We hypothesized that: (i) the community composition, diversity, co-occurrence patterns, and assembly processes of root-associated microbiomes—including root endosphere (RE), rhizosphere (RS), and bulk soil (BS) compartments—would vary across seasons; and (ii) specific environmental factors would significantly influence the composition and diversity of these microbiomes in different seasons. Our findings shed light on the seasonal shifts in microbial communities associated with key desert plants and the environmental drivers shaping these patterns. This research provides critical insights into microbially mediated ecological adaptations, supporting strategies for enhancing the resilience and sustainable management of desert ecosystems under arid and stressful conditions.

2 Materials and methods

2.1 Study area overview, experimental design, and sample collection

The experiment was carried out at three long-term desert locations {Xinjiang Institute of Ecology and Geography, Chinese Academy of Sciences (XIEG, CAS)}: Cele and Mosuowan desert research station (CL and MSW) and Turpan desert botanical garden (TLF). The climate data are from the Cele, Turpan, and Mosuowan desert research stations. For detailed information, see Tables 1, 2; Supplementary Figure S1.

Four homogeneous quadrats, each measuring approximately 30 m × 30 m, were selected at each of the three study fields (stations). Each quadrat included three representative desert plant species—*C. caput-medusae*, *A. sparsifolia*, and *T. ramosissima*—that thrive naturally. In total, twelve research blocks were chosen. Fieldwork was conducted at three long-term observation stations in May (spring), July (summer), and September (autumn) of 2022. The samples were divided into RE, RS, and BS compartments (Edwards et al., 2015). Root and soil samples representing RE, RS, and BS were collected from a range of desert plant species at depths of 0 to 2 meters. Both soil and root samples were collected at corresponding depths to ensure consistent sampling across compartments. The BS, which was loosely adhered to fine roots, was used for evaluating its physical and chemical properties. We used a sterile brush to gather RS, closely associated with fine roots (≤ 2 mm), by collecting soil from the roots. The collected soil was then placed in individual sterile

TABLE 1 Geographic and climatic characteristics in the three study sites.

Characteristics		Site		
		Cele (CL)	Mosuowan (MSW)	Turpan (TLF)
Geographic	Latitude (°N)	35°00′57″	45°07′27″	42°51′59″
	Longitude (°E)	80°43′45″	86°01′31″	89°12′01″
	Altitude (m)	1318	346	-105 m ~ -76 m
Climatic	MAT (°C)	11.9	6.6	13.9
	MAP (mm)	35.1	117.0	16.4
	PEP (mm)	2595.3	1979.5	3000
	AI	0.01	0.06	0.005
Soil type	ST	aeolian sandy soil	grey desert soil	grayish brown desert soil

MAT, mean annual temperature; MAP, mean annual precipitation; PEP, potential evapotranspiration; AI, aridity index, calculated as AI = MAP/PEP. ST, soil type.

10.3389/fpls.2025.1554879

TABLE 2 Climate factors in three years (mean).

Site	Season	Temp (°C)	Prep (mm)	Atm (hPa)	WS (m/s)	WD (°)	DR (w/m^2)	SR (w/m^2)	HR (w/m^2)	Hum (%)
Cele	May	23.64	0.0015	854.99	4.13	213.63	288.37	94.73	306.46	26. 20
	July	29.90	0.0055	851.74	3.46	195.02	293.75	92.55	307.92	23.66
	September	23.55	0.00012	857.97	3.06	208.06	308.12	63.34	253.50	24.58
Mosuowan	May	27.08	0.015	969.79	4.21	186.71	261.38	99.84	281.16	27.64
	July	30.31	0.0060	964.89	4.04	199.54	249.55	107.84	284.32	27.36
	September	23.19	0.018	973.43	3.38	169.83	239.25	64.30	197.62	31.99
Turpan	May	29.89	0.00096	1011.62	2.37	196.76	252.62	103.63	281.20	20.76
	July	34.00	0.0011	1005.56	2.49	203.89	238.97	110.22	281.27	23.27
	September	27.98	0.00056	1014.75	1.68	197.45	295.64	63.48	228.22	21.45

Temp, temperature; Prep, precipitation; Atm, atmospheric pressure; WS, wind speed; WD, wind direction; DR, direct radiation; SR, scattered radiation; HR, horizontal radiation; Hum, air relative humidity.

centrifuge tubes. The root samples were immersed in 75% alcohol, oscillating them for three rounds, each lasting 15 secondsRoots were thoroughly cleaned by washing with sterile water on a vortex oscillator for three one-minute intervals to remove adhering soil particles. The cleaned roots were then cut into small fragments and placed into sterile containers. In total, 324 samples were collected throughout 2022, encompassing three plant species, three compartments (RE, RS, and BS), multiple basins, and three seasons, with four biological replicates per group. All samples were immediately stored at −80 °C in an ultra-low temperature freezer to preserve microbial integrity prior to DNA extraction.

2.2 DNA extraction, polymerase chain reaction, and Illumina sequencing

To extract total soil genomic DNA from 0.5 g of BS and RS, the DNA extraction kit manufactured by Qiagen, Inc. in the Netherlands was utilized. RE samples were prepared by pulverizing 0.4 g with liquid nitrogen, followed by extracting total microbial DNA using the DNeasy Plant Maxi Kit (Qiagen, Netherlands). PCR amplification targeted the bacterial 16S rRNA gene V3-V4 region {341F (5'-CCTAYGGGRBGCASCAG-3') and 806R (5'-GGACTACNNGGGTATCTAAT-3')}and the fungal ITS (Internal Transcribed Spacer) 1–5 F region {5-1737F (5'-GGAAGTAAAAGTCGTAACAAGG-3') and 2-2043R (5'-GCTGCGTTCTTCATCGATGC-3')}. Each sample was distinguished from the dismounting data using its Barcode and PCR primer sequences. After removing barcode and primer sequences, the reads for each sample were merged using FLASH (v1.2.11) (Magoč and Steven, 2011), generating raw tag sequences. These raw tags were then processed using FASTP (v0.23.1) with stringent quality filtering parameters to produce high-quality clean tags (Bokulich et al., 2013). o further improve sequence quality, chimeric sequences were identified and removed using VSEARCH (v2.16.0) by aligning the tags to a reference species annotation database. The resulting high-quality, non-chimeric sequences were designated as effective tags for downstream analysis (Rognes et al., 2016).

Additional sequence filtering was performed using the QIIME-II software (v202202) (Caporaso et al., 2010). DADA2 plugin was used to control the quality, denoise, splicing, and removal of chimerism to generate amplicon sequence variants (ASVs) (Callahan et al., 2016). Using the RDP (Ribosomal Database Project) classifier at a 70% confidence threshold, the Mothur method, and SSUrRNA database from Silva version 138.1 with a 0.8–1 threshold range, bacterial ASVs were identified (Wang et al., 2007; Quast et al., 2013). Fungal ASVs were classified using the UNITE database (Altschul et al., 1990). The original sequencing data was stored at the National Center for Biotechnology Information (NCBI) under the number PRJNA1024038. The dilution curve is shown in Supplementary Figure S2.

2.3 Soil's physical and chemical properties

The oxidation method using $K_2Cr_2O_7$-H_2SO_4 was employed to analyze the contents of root and soil organic carbon (ROC and SOC), whereas the total nitrogen (TN) contents were quantified

using the Kjeldahl Nitrogen Analyzer (K1160, produced by Jinan Hanon Instruments Co. Ltd., China) (Hooper and Vitousek, 1998; Bao, 2000). Available nitrogen (AN) was assessed through the alkali hydrolysis method, while total phosphorus (TP) and total potassium (TK) were analyzed with the Inductively Coupled Plasma-Optical Emission Spectrometer (iCAP 6300, Thermo Elemental, USA) following sample dissolution in concentrated nitric acid (Neff et al., 2005; Warra et al., 2015; Lu et al., 2015). Available phosphorus (AP) was extracted by combining hydrochloric acid and ammonium fluoride, followed by analysis using colorimetric method with ascorbic acid molybdate on a continuous-flow auto-analyzer manufactured by Bran and Luebbe in Germany (Olsen and Sommer, 1982). The NH_4OAc extraction method was applied to ascertain the available potassium (AK) content (Warra et al., 2015). Soil pH levels were measured using a pH meter (PHSJ-6 L, INESA Scientific Instrument Co. Ltd., China) with a 1:2.5 soil-to-water ratio, and electrical conductivity (EC) was assessed with an EC meter (DDSJ-319 L, INESA Scientific Instrument Co. Ltd., China) at a 1:5 soil to water ratio (Bao, 2000).

2.4 Metrological/climate data

Meteorological data were collected from the National Meteorological Science Data Center (https://data.cma.cn/) for three sites—Cele, Turpan, and Mosuowan—managed by the Chinese Academy of Sciences. The dataset included temperature (Temp), precipitation (Prep), relative humidity (Hum), atmospheric pressure (Atm), wind speed (WS), wind direction (WD), direct radiation (DR), horizontal radiation (HR), and scattered radiation (SR) (Table 2).

2.5 Statistical analyses

Statistical analysis was performed using R version 4.1.0 (R Core Team, 2021). The Shapiro-Wilk normality test was used to check the normality of the raw data. The findings were primarily presented using packages like 'ggplot2', 'microeco', 'vegan', 'corrplot', 'randomForest', 'rfPermute', and 'iCAMP' (Hahsler et al., 2008; Wei and Simko, 2013; Archer, 2016; Oksanen et al., 2017). A one-way ANOVA was conducted to assess the seasonal impact on the physical and chemical properties of roots and soil. The α-diversity (Chao1, Shannon-Wiener, Pielou_e, and Simpson index) at the ASVs level was calculated using QIIME2. For the calculation of β diversity, the vectorized ASVs matrix based on the Bray-Curtis distance was adopted. The impact of season on the top 10 relative abundances, Observed_OTUs number, and both α-diversity and β-diversity was assessed using one-way and two-way ANOVA. The agricolae package was employed to analyze sources of variation through the least significant difference (LSD) test (Mendiburu, 2020).

To assess community assembly processes, we employed a phylogenetic bin-based null model analysis framework using the iCAMP package (Stegen et al., 2015; Ning et al., 2020). This framework quantifies the relative contributions of deterministic and stochastic processes, with higher absolute values of the standardized effect size (SES) indicating a stronger influence of deterministic forces. First, phylogenetic signals were assessed using a phylogenetic Mantel correlogram to determine whether phylogenetic turnover could reliably inform ecological inference within the system (Dini-Andreote et al., 2015). Second, the beta mean nearest taxon distance (βMNTD) was recalculated to generate a null distribution, obtained through 999 random permutations. The deviation of the observed βMNTD from the mean of this null distribution, expressed in standard deviation units, was calculated as the beta nearest taxon index (βNTI). The βNTI value less than –2 or greater than +2 indicates significantly lower or higher phylogenetic turnover than expected by chance, respectively, suggesting the dominance of deterministic processes (Stegen et al., 2012).

Co-occurrence networks were constructed using Gephi software based on Spearman's correlation matrices, retaining only correlations with an absolute coefficient above 0.7 and a false discovery rate (FDR)-adjusted p-value below 0.001. The topological features of microbial network modules, including within-module connectivity (Zi) and among-module connectivity (Pi), were used to classify nodes into four categories: module hubs (high connectivity within modules; $Zi > 2.5$, $Pi < 0.62$), connectors (high connectivity between modules; $Zi < 2.5$, $Pi > 0.62$), network hubs (high connectivity both within and across modules; $Zi > 2.5$, $Pi > 0.62$), and peripherals (low connectivity; $Zi < 2.5$, $Pi < 0.62$) (Deng et al., 2012).

To identify key environmental drivers influencing root microbial community composition, random forest analysis was performed using the first principal coordinate axis derived from principal coordinate analysis (PCoA) of amplicon sequence variant (ASV)-level data as the response variable. The 'randomForest' and 'rfPermute' R packages were employed to assess variable importance, measured by the percentage increase in mean squared error (%IncMSE), with significance levels calculated accordingly.

Structural equation modeling (SEM) was applied to explore the pathways through which climate, soil, and plant factors affect microbial communities in desert plant roots. PCoA was used to reduce dimensionality of soil available nutrients (nitrogen, phosphorus, potassium), root nutrients (organic carbon, total nitrogen, total phosphorus, total potassium), and microbial community composition across root compartments (root endosphere, rhizosphere soil, and bulk soil), with the first axis scores serving as variables in SEM analyses conducted in Amos-24 software. Model fit was evaluated based on multiple criteria: chi-square (χ^2) with $P > 0.05$ indicating good fit; chi-square/degrees of freedom (χ^2/df) between 1 and 3; root mean square error of approximation (RMSEA) below 0.05; comparative fit index (CFI) and goodness of fit index (GFI) both exceeding 0.90; and Akaike information criterion (AIC), where lower values indicate better fit and facilitate model comparison (Lange et al., 2015; Fan et al., 2016).

3 Results

3.1 Effects of seasonal changes on soil and root physical and chemical properties

In May, the soil TK content was significantly lower than that in July and September. The root ROC in May was also significantly lower than that in July. Throughout the growth seasons of May, July, and September, there was no significant difference between the soil properties (pH, EC, SOC, TN, TP, AN, AP, and AK) and root nutrient contents (TN, TP, and TK) (Table 3).

3.2 Seasonal variations influence the abundance and Observed_OTUs number in root microbial communities

Seasons significantly affected the root bacterial Observed_OTUs number ($p < 0.01$). Root partitioning significantly affected the root bacterial and fungal Observed_OTUs number ($p < 0.001$). Season and root partitioning interaction significantly influenced fungal Observed_OTUs number ($p < 0.01$) (Table 4). The RS bacterial Observed_OTUs number in September was significantly greater than in May and July ($p < 0.05$) (Figure 1A). The RS fungal Observed_OTUs number was significantly higher in July compared to May and September, while the BS fungal Observed_OTUs number were significantly more numerous in May than in September ($p < 0.05$) (Figure 1B).

For bacteria, seasons significantly affected the relative abundance of *Proteobacteria*, *Actinobacteriota*, *Bacteroidota*, *Chloroflexi*, and *Deinococcota* ($p < 0.05$). Root partitioning significantly affected the relative abundance of *Proteobacteria*, *Cyanobacteria*, *Verrucomicrobiota*, *Acidobacteriotaota*, *Deinococcota*, *Gemmatimonadota*, *Chloroflexi*, *Bacteroidota*, *Firmicutes*, and *Actinobacteriota* ($p < 0.001$). Season and root partitioning interaction significantly influenced the relative abundance of *Proteobacteria*, *Chloroflexi*, *Gemmatimonadota*, *Deinococcota*, *Acidobacteriotaota*, and *Verrucomicrobiota* ($p < 0.05$) (Supplementary Table S1). In RE, bacterial *Proteobacteria* show reduced relative abundance in July compared to May and September. In RS, the relative abundance of bacterial *Proteobacteria* exhibits a contrasting pattern. The relative abundance of BS bacterial *Proteobacteria* is greater in September compared to May and July (Figure 2A). The relative abundance of RE bacterial *Actinobacteriota* is lower in September compared to May and July (Figure 2A; Supplementary Table S1).

For fungi, seasons significantly affected the relative abundance of *Basidiomycota* and *Mortierellomycota* ($p < 0.05$). Root partitioning significantly affected the relative abundance of *Ascomycota*, *Fungi_phy_Incertae_sedis*, *Basidiomycota*, *Chytridiomycota*, *Mortierellomycota*, *Aphelidiomycota*, and *Rozellomycota* ($p < 0.01$). Season and root partitioning interaction significantly influenced the relative abundance of *Fungi_phy_Incertae_sedis*, *Basidiomycota*, and *Mortierellomycota* ($p < 0.05$) (Supplementary Table S1). For *Ascomycota* in RE and RS fungi, its relative abundance in July was lower than that in May and September. In BS fungi, *Ascomycota* showed a higher relative abundance in September compared to May and July (Figure 2B). For *Basidiomycota* in root compartments (RE, RS, and BS) compartments fungi, its relative abundance in September was higher than that in May and July (Figure 2B; Supplementary Table S1).

3.3 Seasonal variations influence the community assembly processes of root microbial communities

The mantel correlogram revealed that both the RE, RS, and BS bacterial and fungal communities had significant phylogenetic signals (Supplementary Figure S3). The community assembly of root bacteria and fungi in different seasons primarily followed a random process. The BS bacterial community assembly in different seasons was primarily governed by a deterministic process. For fungi (BS), the community construction in May and July was dominated by a deterministic process, while in September, it was dominated by a random process (Figures 3A, B; Table 5).

For RE bacteria, deterministic processes in spring and summer were primarily driven by homogeneous selection (HOS), while stochastic processes were mainly dominated by dispersal limitation (DL). For RS bacteria, deterministic processes in spring and autumn were mainly governed by heterogeneous selection (HES), whereas random processes across spring, summer, and autumn were predominantly influenced by DL. In BS bacteria, deterministic processes in spring and autumn were largely attributed to HOS, with DL being the main random process throughout spring, summer, and autumn. For fungi in the RE, RS, and BS compartments, deterministic processes across all three seasons (spring, summer, and autumn) were primarily associated with HOS, while random processes were mainly driven by DL (Table 5).

The deterministic processes of bacteria (RE and RS) and fungi (RE) contributed more in July compared to May and September. For bacteria (BS), the deterministic process contributed less in July compared to May and September. For fungi (RS and BS), the deterministic process's relative contribution in different seasons was highest in September, followed by July, and lowest in May (Supplementary Figure S4).

3.4 Seasonal variations influence the root microbial α and β diversity

Seasons significantly affected the root bacterial and fungal Chao1, Pielou_e, and Simpson indices ($p < 0.05$). Root partitioning significantly affected the root bacterial and fungal Chao1, Shannon-Wiener, Pielou_e, and Simpson indices ($p < 0.05$). Season and root partitioning interaction significantly influenced bacterial (Shannon-Wiener, Pielou_e, and Simpson) and fungal diversity (Chao1, Shannon-Wiener, and Pielou_e) ($p < 0.05$) (Table 4).

The RS bacterial diversity (Chaol, Shannon-Wiener, and Pielou e) was notably higher in September when compared to May and July

10.3389/fpls.2025.1554879

TABLE 3 Seasonal changes of soil physicochemical properties and root nutrient content of desert plants.

Factor	Index	Spring	Summer	Autumn
Soil	SOC (g•kg^{-1})	2.81 ± 0.30a	2.8 ± 0.26a	2.62 ± 0.30a
	TN (g•kg^{-1})	0.23 ± 0.03a	0.23 ± 0.03a	0.22 ± 0.03a
	TP (g•kg^{-1})	0.75 ± 0.04a	0.75 ± 0.03a	0.75 ± 0.04a
	TK (g•kg^{-1})	18.97 ± 0.29b	20.59 ± 0.34a	20.21 ± 0.36a
	AN (mg•kg^{-1})	14.37 ± 1.62a	16.56 ± 1.61a	14.9 ± 1.51a
	AP (mg•kg^{-1})	3.25 ± 0.36a	3.57 ± 0.37a	3.39 ± 0.31a
	AK (mg•kg^{-1})	265.67 ± 20.8a	294.83 ± 29.93a	286.42 ± 21.92a
	pH	8.72 ± 0.04a	8.74 ± 0.06a	8.69 ± 0.05a
	EC (uS•cm^{-1})	969.55 ± 188.87a	1252.46 ± 235.13a	1089.86 ± 181.74a
Root	ROC (g•kg^{-1})	453.53 ± 3.82b	465.26 ± 3.66a	462.07 ± 1.92ab
	TN (g•kg^{-1})	9.05 ± 0.61a	7.65 ± 0.50a	7.15 ± 0.71a
	TP (g•kg^{-1})	0.5 ± 0.08a	0.44 ± 0.04a	0.41 ± 0.05a
	TK (g•kg^{-1})	4.54 ± 0.44a	3.88 ± 0.27a	4.33 ± 0.37a

Different lowercase letters (a, b, and c) indicate that the different seasons have significant differences (LSD test, $P < 0.05$). SOC, soil organic carbon (g•kg^{-1}); ROC, root organic carbon (g•kg^{-1}); TN, total nitrogen (g•kg^{-1}); TP, total phosphorus (g•kg^{-1}); TK, total potassium (g•kg^{-1}); AN, available nitrogen (mg•kg^{-1}); AP, available phosphorus (mg•kg^{-1}); AK, available potassium (mg•kg^{-1}); EC, electrical conductivity (uS•cm^{-1}). Spring (May), Summer (July), and Autumn (September).

($p < 0.05$). (Figures 4A–C). The bacterial Simpson index in RS was notably lower in July compared to May and September ($p < 0.05$) (Figure 4D). In July, the RS fungal Chaol index was significantly greater than in May and September ($p < 0.05$) (Figure 4E). Additionally, the RE fungal Shannon-Wiener index was notably higher in September relative to July ($p < 0.05$), and the Simpson index was significantly higher in September than in May ($p < 0.05$) (Figures 4F, H). TheRS fungal diversity (Shannon-Wiener, Pielou e, and Simpson) was significantly lower in May than in both July and September ($p < 0.05$). For BS fungi, the Chao1 index was notably higher in May compared to September ($p < 0.05$) (Figures 4E–H).

The β diversity of RE, RS, and BS bacteria was significantly greater in May than in September ($p < 0.05$) (Figure 5A). In contrast, the β diversity of RE, RS, and BS fungi was significantly higher in July than in September ($p < 0.05$) (Figure 5B).

3.5 Seasonal variations influence the co-occurrence network of root microbial communities

In September, the RE, RS, and BS bacterial communities exhibited increased numbers of nodes, edges, and average degrees compared to May and July (Figure 6). In the fungal community, the number of nodes, edges, and average degree of RE and BS in September exceeded those recorded in May and July. The RS fungal

TABLE 4 Variance analysis of α diversity in typical desert plants by different seasons and root partitioning.

Factor	Index	Season	Root partitioning	Season×Root partitioning
Bacteria	Observed_OTUs number	5.90**	97.42***	1.75
	Chao1	5.72**	95.81***	1.72
	Shannon-Wiener	3.86*	152.74***	2.80*
	Pielou_e	3.26*	148.76***	2.83*
	Simpson	3.26*	84.37***	2.45*
Fungi	Observed_OTUs number	2.45	57.59***	3.90**
	Chao1	3.18*	57.52***	3.81**
	Shannon-Wiener	2.61	147.33***	3.66**
	Pielou_e	4.99**	137.81***	2.68*
	Simpson	6.98***	108.81***	2.20

*$P < 0.05$; **$P < 0.01$; ***$P < 0.001$.

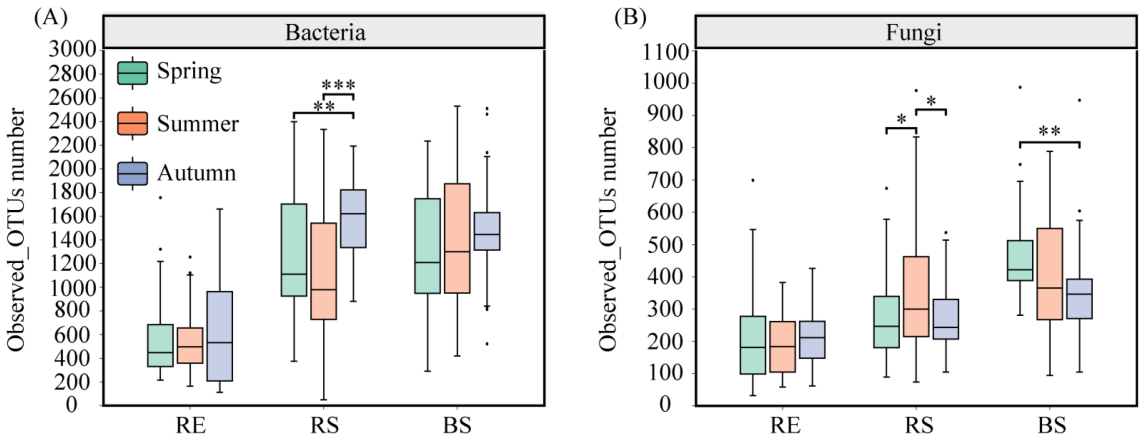

FIGURE 1
The Observed_OTUs number of root-associated dominant bacterial and fungal of desert plants. **(A)** the Observed_OTUs number of root-associated dominant bacterial of desert plants. **(B)** the Observed_OTUs number of root-associated dominant fungal of desert plants. RE, root endosphere; RS, rhizosphere soil; BS, bulk soil. Spring (May); Summer (July); and Autumn (September). Significance codes, *P < 0.05; **P < 0.01; ***P< 0.001.

nodes, edges, and average degree exhibited higher values in July compared to May and September (Supplementary Figure S5).

In May, the bacterial module connectivity mainly belongs to peripherals, and most of the fungal module connectivity belongs to connectors. In July, the bacterial modular connectivity includes peripherals and connectors, while the fungal modular connectivity includes peripherals. In September, both the bacteria and fungi module connectivity belong to peripherals and connectors (Supplementary Figure S6).

3.6 Effects of abiotic environmental factors on root microbial communities

Random forest analysis revealed that the variation of the RE bacterial community across different seasons was predominantly affected by SR (Figure 7A). The seasonal variation in the BS bacterial community was primarily influenced by WS, Prep, Hum, Atm, SR, WD, Temp, DR, soil properties (EC, TP, TK, AN, AP, and AK), and root nutrients (SOC, TN, TP, and TK), all of which had significant effects (Figure 7C). Seasonal changes in the RE fungal community were primarily affected by soil AK (Figure 7D). The seasonal variation in the BS fungal community was primarily affected by atmospheric pressure and soil TK (Figure 7F). The seasonal variation in the RS bacterial and fungal community has no significant influence factors (Figures 7B, E).

3.7 Pathway analysis of root microbial communities and abiotic factors

Season exerted a notable negative direct influence on the RS bacterial community. It also had a significant negative direct effect

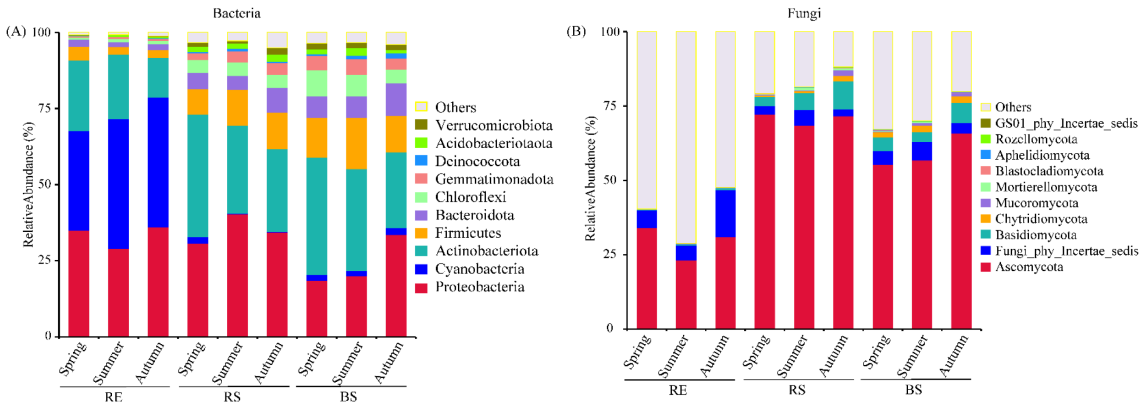

FIGURE 2
The abundances of root-associated dominant bacterial and fungal of desert plants. **(A)** the relative abundance of dominant bacteria (top 10 phyla) from different seasons. **(B)** the relative abundance of dominant fungi (top 10 phyla) from different seasons. RE, root endosphere; RS, rhizosphere soil; BS, bulk soil. Spring (May); Summer (July); and Autumn (September).

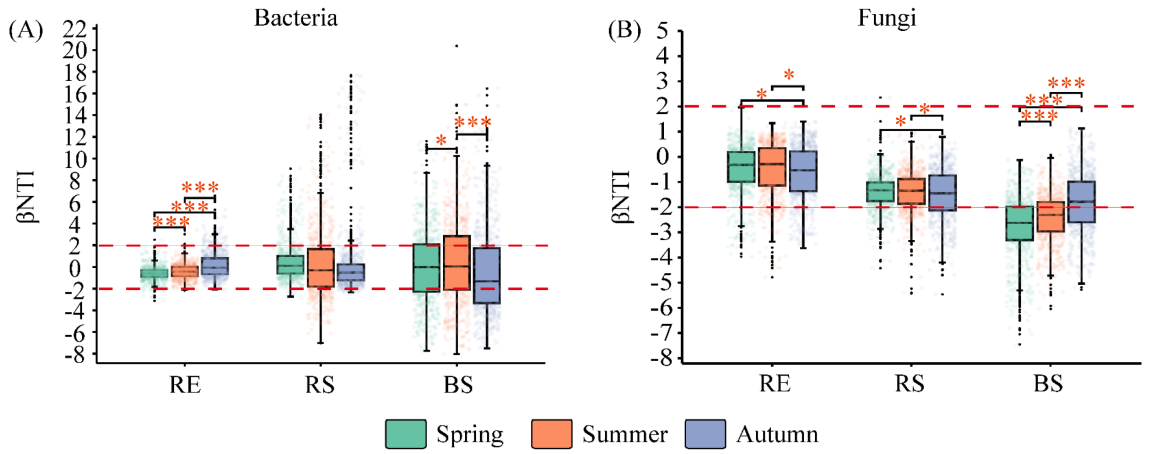

FIGURE 3
The β nearest taxon index (βNTI) of bacterial and fungal communities among season in desert plants. **(A)** the βNTI of bacterial communities among season in desert plants. **(B)** the βNTI of fungal communities among season in desert plants. RE, root endosphere; RS, rhizosphere soil; BS, bulk soil. Spring (May); Summer (July); and Autumn (September). Significance codes, *P < 0.05; ***P < 0.001.

on temperature, which in turn affected soil nutrient availability, consequently impacting microbial populations in both RS and BS compartments (Figure 8A). Similarly, season significantly and negatively affected the RS fungal community, while precipitation had a significant negative impact on the BS fungal community. Additionally, season directly and negatively influenced temperature, which significantly affected both precipitation and soil nutrients, thereby influencing fungal communities in RS and BS (Figure 8B). Regarding environmental drivers, the direct effect of precipitation on the RE bacterial community was stronger than that of temperature, soil nutrients, and root nutrients. Conversely, the total effect of precipitation on the RS fungal community surpassed those of temperature, soil nutrients, and root nutrients. For BS bacterial and fungal communities, temperature had a greater total effect than precipitation, soil nutrients, and root nutrients (Table 6).

4 Discussion

4.1 Effects of seasonal variation on the composition and stability of root bacterial and fungal community

This study found that *Proteobacteria* and *Cyanobacteria* were the core bacterial phyla in the root communities of typical desert plants across seasonal changes, while *Ascomycota* was the dominant fungal phylum. Notably, the RE bacterial community contained a higher abundance of *Cyanobacteria*, whereas its fungal community exhibited a lower proportion of *Ascomycota*. Due to the arid climate, infrequent precipitation, low soil moisture content, and poor nutrients in desert areas (Zhang et al., 2022b; Islam et al., 2024a), plant roots provide suitable living places and nutrients for *Cyanobacteria*, in turn, they provide nitrogen and other nutritional support for plants (Zhang et al., 2024a; Zhao et al., 2024). This mutually beneficial symbiotic relationship is conducive to the colonization and reproduction of the *Cyanobacteria*, however, desert plants are also more inclined to establish close ties with *Cyanobacteria*, which provides favorable conditions for its survival in roots (Zhang et al., 2024a; Zhao et al., 2024). Studies indicate that fungal communities in roots are vital for grass resource acquisition, particularly in arid grasslands where *Ascomycota* predominates (Green et al., 2008; Porras-Alfaro et al., 2008). *Ascomycota* is vital for collaborating with other microbes to decompose soil litter, increase nutrient availability, support plant growth, and adapt to harsh environments (Glassman et al., 2017; Islam et al., 2024b).

In this study, the relative abundance of *Ascomycota* in RE was lower than that in RS and BS. It indicates that the selection of microorganisms within the RE has a strong host selection effect that root epidermis providing a more stable and buffered habitat (Maestre et al., 2015; Bahram et al., 2018; Xiong et al., 2021). Numerous studies have found that certain microorganisms in the rhizosphere attach to and are filtered by the roots, ultimately influencing the aggregation of the microbial community in the roots (Edwards et al., 2018). Additionally, roots not only attract microorganisms nearby but also possess genetically determined factors that contribute to the stability of specific microbial species (Bulgarelli et al., 2013). Our study also found that the community assembly of bacteria and fungi in both RE and RS associated with desert plants across different seasons primarily followed a stochastic process, mainly driven by dispersal limitation. In desert regions, frequent high temperatures during July (summer) and September (autumn) lead to elevated soil surface temperatures (Zhang et al., 2022b; Islam et al., 2024c). To protect themselves from such environmental stresses, desert plant roots release exudates that recruit specialized microorganisms, which bind tightly to the roots forming protective complexes (Haichar et al., 2008; Reinhold-Hurek et al., 2015). While our results confirm that environmental factors influence the recruitment of soil microbes to the rhizosphere (Fitzpatrick et al., 2018; Wu et al., 2021), it is

TABLE 5 Community construction process of desert plant root microbial communities in different seasons.

Factor	Assembly process	Properties	RE			RS			BS		
			Spring	Summer	Autumn	Spring	Summer	Autumn	Spring	Summer	Autumn
Bacteria	Deterministic	HES (%)	0.16	0.63	7.14	12.70	22.38	9.37	26.19	31.90	22.70
		HOS (%)	2.06	0.63	0.16	0.63	22.70	4.44	29.05	26.83	42.22
		Sum (%)	2.22	1.27	7.30	13.33	45.08	13.81	55.24	58.73	64.92
	Stochastic	DL (%)	65.56	49.84	40.32	73.49	35.24	72.70	41.11	39.37	33.49
		HD (%)	0.79	1.75	0.63	2.86	1.27	2.54	0.63	0.48	0.32
		Drift (and other) (%)	31.43	47.14	51.75	10.32	18.41	10.95	3.02	1.43	1.27
		Sum (%)	97.78	98.73	92.70	86.67	54.92	86.19	44.76	41.27	35.08
Fungi	Deterministic	HES (%)	0.16	0.00	0.00	0.16	0.00	0.00	0.00	0.00	0.00
		HOS (%)	8.57	10.63	12.54	17.14	20.32	28.73	74.76	65.24	42.54
		Sum (%)	8.73	10.63	12.54	17.30	20.32	28.73	74.76	65.24	42.54
	Stochastic	DL (%)	36.19	51.75	58.10	71.43	62.70	55.87	24.76	26.67	55.24
		HD (%)	3.33	4.13	2.54	0.32	0.16	0.16	0.16	0.16	0.32
		Drift (and other) (%)	51.75	33.49	26.83	10.95	16.83	15.24	0.32	7.94	1.90
		Sum (%)	91.27	89.37	87.46	82.70	79.68	71.27	25.24	34.76	57.46

RE, root endosphere; RS, rhizosphere soil; BS, bulk soil. HES, Heterogeneous Selection; HOS, Homogeneous Selection; DL, Dispersal Limitation; HD, Homogenizing Dispersal. Spring (May), Summer (July), and Autumn (September).

10.3389/fpls.2025.1554879

10.3389/fpls.2025.1554879

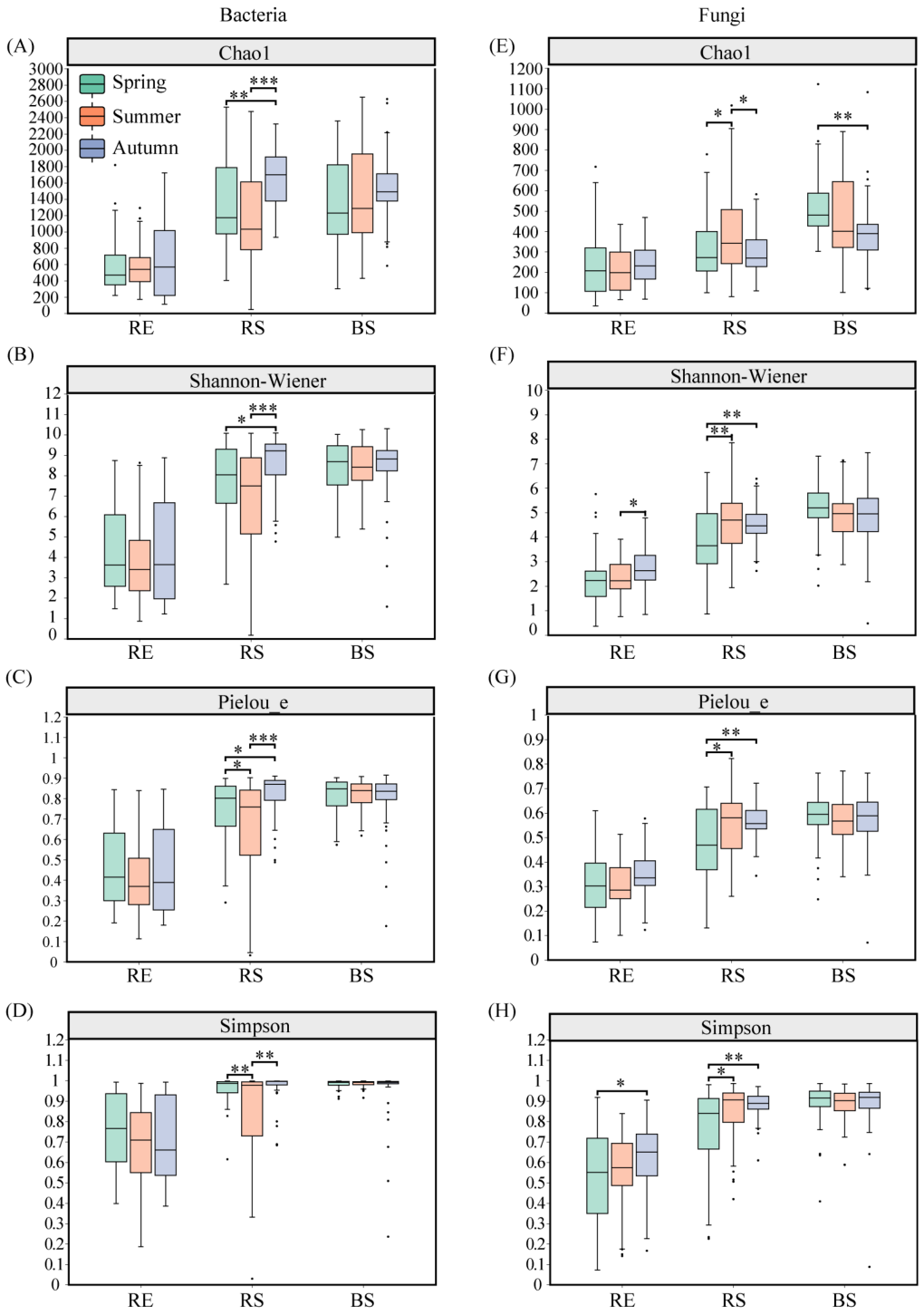

FIGURE 4
The α diversity of bacterial and fungal communities among season in desert plants. **(A–D)** the α diversity (Chao1, Shannon-Wiener, Pielou_e, and Simpson index) of bacterial communities among season in desert plants. **(E–H)** the α diversity (Chao1, Shannon-Wiener, Pielou_e, and Simpson index) of fungal communities among season in desert plants. RE, root endosphere; RS, rhizosphere soil; BS, bulk soil. Spring (May); Summer (July); and Autumn (September). Significance codes, *P < 0.05; **P < 0.01; ***P< 0.001.

crucial to recognize the importance of host-specific inheritance in maintaining microbial community stability in desert plants.

Co-occurrence network analysis revealed that in May (spring), root bacterial communities lacked highly connected nodes both within and between modules. In contrast, such highly connected nodes were present in July (summer) and September (autumn). This observed pattern could potentially be attributed to the seasonal variations in temperature and precipitation, as well as the pronounced micro-environmental gradient from the RE to BS, which is mainly influenced by soil pH, water availability, and

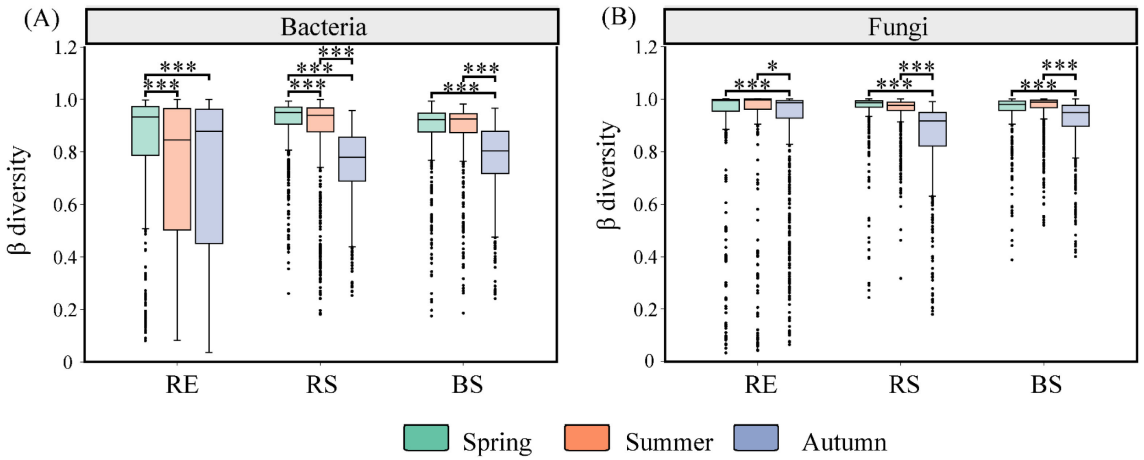

FIGURE 5
The β diversity of bacterial and fungal communities among season in desert plants. **(A)** the β diversity of bacterial communities among season in desert plants. **(B)** the β diversity of fungal communities among season in desert plants. RE, root endosphere; RS, rhizosphere soil; BS, bulk soil. Spring (May);Summer (July); and Autumn (September). Significance codes, *P < 0.05; ***P < 0.001.

nutrients (Hinsinger et al., 2009; Ali et al., 2024; Zhang et al., 2024b). Except as microbial co-occurrence networks, which can characterize the complexity and stability of microbial communities, the microbial diversity index can indicate the degree of complexity among them (Coyte et al., 2015; de Vries et al., 2018; Maurice et al., 2024b). Seasons had a significant influence on the α diversity of root bacteria and fungi. However, the β diversity of root bacteria and fungi in desert plants decreased significantly in autumn. Phreatophytes in desert ecosystems exhibit long-term adaptability to external conditions, leading to varied outcomes (Hernandez et al., 2021; Islam et al., 2024a). Our findings showed that the RS bacterial diversity (Chao1, Shannon-Wiener, and Pielou_e) was significantly higher in September (autumn) compared to May (spring) and July (summer). On the one hand, the plants grow vigorously in summer, and rhizosphere microorganisms compete with each other to obtain limited carbon sources, nitrogen sources, and other nutrients. The preferential elimination by rhizosphere microorganisms decreases their β diversity (Lai et al, 2025). On the other hand, the high temperature and arid environment in autumn may destroy the established symbiotic relationship between rhizosphere microorganisms, which may not only affect the types of microorganisms involved in symbiosis but also hurt the structure and diversity of the entire rhizosphere microbial community (Berendsen et al., 2012; Durán et al., 2018; Xie and Yin, 2022).

4.2 Influence of environmental factors on root bacterial and fungal community composition and diversity

Our study revealed that soil total potassium content was significantly higher in July (summer) and September (autumn) compared to May (spring), likely due to increased plant growth and accumulation of plant residues during these seasons, which are returned than in spring. These plant residues contain a certain amount of potassium, which reenters the soil after decomposition (Dawson and Goldsmith, 2018; Gao et al., 2023). The root organic carbon content in July (summer) is significantly higher than in May (spring). This is because there is less precipitation in desert areas in July (summer) (Gao et al., 2023; Zhang et al., 2024b). To absorb and store water more effectively, plants tend to develop more developed roots, which also promotes the increase of root organic carbon content (Körner, 2015; Ledo et al., 2020). In this study, the RE bacterial communities were mainly influenced by scattered radiation in different seasons. For the BS bacterial community, its seasonal variation was mainly caused by climate and was significantly affected by soil physicochemical properties and root nutrients. Regarding the RE and BS fungal communities, their seasonal variations were mainly influenced by soil nutrients. Therefore, it can be concluded that the root microbial composition and diversity (RE, RS, and BS) in deep-rooted desert plants are influenced by factors beyond just soil and root nutrients. Instead, climatic factors from the external environment are likely to have the most direct impact on these microbial communities (Trivedi et al., 2022).

Environmental changes influence the spatial heterogeneity of microbial communities, with environmental factors playing a significant role in shaping the assembly processes of rhizosphere and root endosphere microbial communities (Chase and Myers, 2011; Zhong et al., 2022). Seasonal variations in precipitation have a direct positive effect on the composition of the RS fungal community. Conversely, these precipitation changes indirectly inhibit the composition of the BS fungal community by reducing the availability of soil nutrients. Season, temperature, and precipitation indirectly impact RE and BS fungal communities by affecting soil and root nutrient availability. Many studies have demonstrated that climate factors contribute substantially, accounting for 65% of soil fungal community fluctuations in the biogeography of gramineous root-associated fungi in the North American Plains (Hawkins et al., 2003; Jennifer et al., 2022). Studies

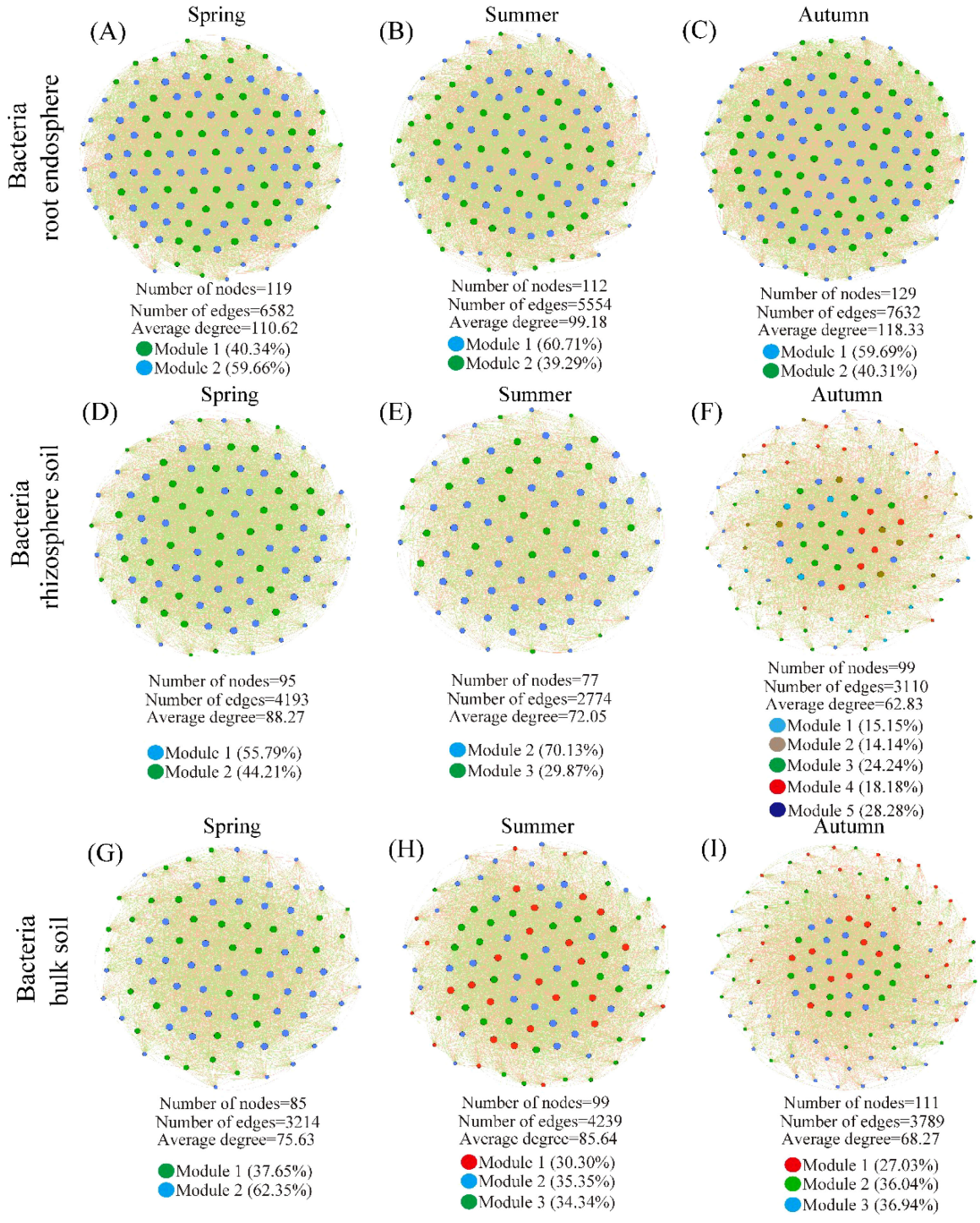

FIGURE 6
Co-occurrence network of root endosphere, rhizosphere soil, and bulk soil bacteria of desert plants. **(A–C)** theco-occurrence network of root endosphere bacteria of desert plants. **(D–F)** the co-occurrence network of rhizosphere soil bacteria of desert plants. **(G–I)** the co-occurrence network of bulk soil bacteria of desert plants. Spring (May); Summer (July); and Autumn (September).

have shown that the relationship between the fungal communities in plant roots and soil is not close but rather dispersed across plant and soil compartments, which helps maintain microenvironmental stability (Chase, 2007; Glynou et al., 2018). The changes in precipitation and temperature caused by seasonal variations can indirectly and significantly inhibit the community composition of RS and BS bacteria by significantly altering soil pH and available nutrients. Previous studies have confirmed that precipitation and soil pH have a significant influence on the diversity and structure of soil microbial communities at both regional and global levels

10.3389/fpls.2025.1554879

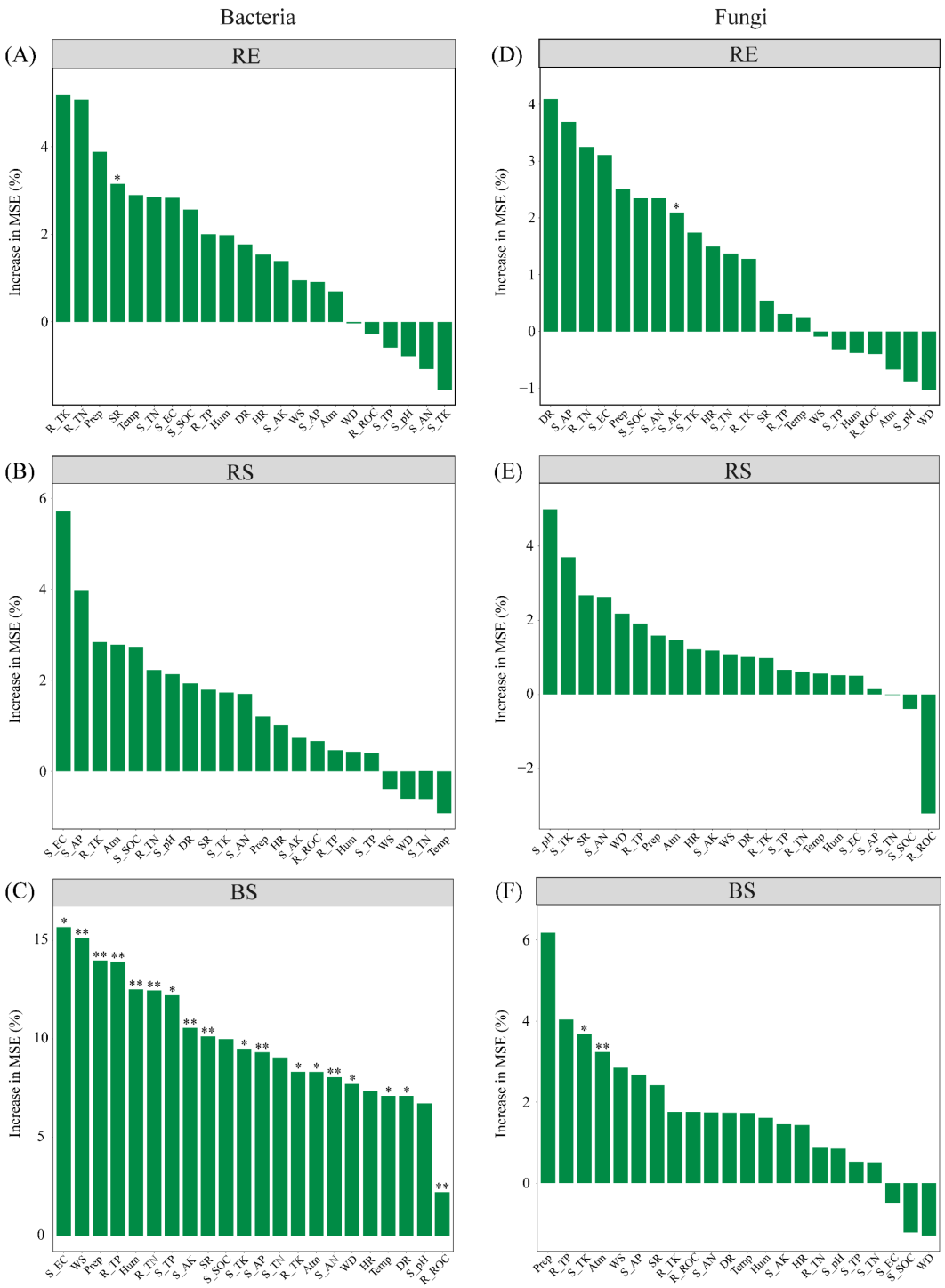

FIGURE 7
The random forest analyses between bacterial and fungal communities and environmental factors. **(A–C)** the random forest analyses between bacterial communities (RE, RS, and BS) and environmental factors. **(D–F)** the random forest analyses between fungal communities (RE, RS, and BS) and environmental factors. RE, root endosphere; RS, rhizosphere soil; BS, bulk soil; S_SOC, soil organic carbon (g•kg^{-1}); R_ROC, root organic carbon (g•kg^{-1}); TN, total nitrogen (g•kg^{-1}); TP, total phosphorus (g•kg^{-1}); TK, total potassium (g•kg^{-1}); AN, available nitrogen (mg•kg^{-1}); AP, available phosphorus (mg•kg^{-1}); AK, available potassium (mg•kg^{-1}); EC, electrical conductivity (mS•cm^{-1}); Temp, temperature; Prep, precipitation; Atm, atmospheric pressure; WS, wind speed; WD, wind direction; DR, direct radiation; SR, scattered radiation; HR, horizontal radiation; Hum, air relative humidity. Significance codes, *P < 0.05; **P < 0.01.

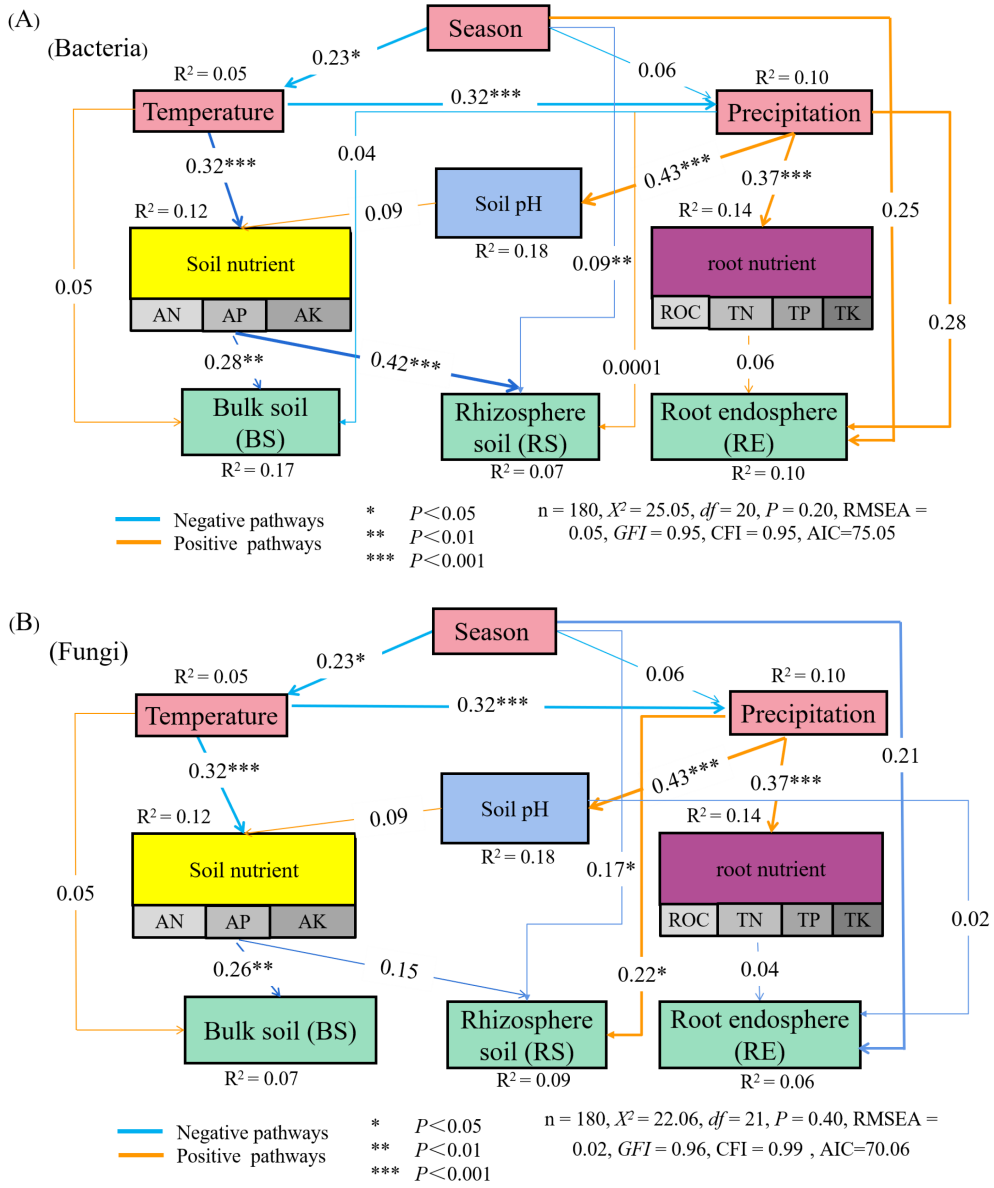

FIGURE 8
The structural equation model of effects of theenvironmental factors and soil or root nutrients on bacterial and fungal communities. **(A)** the structuralequation model of effects of theenvironmental factors and soil or root nutrients on bacterial communities. **(B)** the structural equation model of effects of theenvironmental factors and soil or root nutrients on fungal communities. ROC, root organic carbon (g•kg^{-1}); TN, total nitrogen (g•kg^{-1}); TP, total phosphorus (g•kg^{-1}); TK, total potassium (g•kg^{-1}); AN, available nitrogen (mg•kg^{-1}); AP, available phosphorus (mg•kg^{-1}); AK, available potassium (mg•kg^{-1}).

(Maestre et al., 2015; Bahram et al., 2018; Delgado-Baquerizo et al., 2018). Climatic and soil factors affect the composition of soil microbiota and the attraction of microorganisms to the rhizosphere via plant roots (Philippot et al., 2013; Edwards et al., 2015; Makhalanyane et al., 2015).

5 Conclusion

Seasonal variation exerted a significant influence on the α diversity of both bacterial and fungal communities in desert plant-associated environments. Specifically, within the root endosphere (RE), rhizosphere soil (RS), and bulk soil (BS), the β diversity of bacterial and fungal communities was markedly higher during May (spring) and July (summer) compared to September (autumn), indicating a pronounced seasonal shift in microbial composition. This pattern suggests that spring and summer conditions favor greater microbial differentiation, possibly due to more dynamic environmental changes and plant activity during these periods. The diversity and structure of root-associated microbial communities were shaped by a complex interplay of factors, including soil physicochemical properties, plant-derived nutrient inputs, and external climatic variables such as temperature and precipitation. Notably, the fungal community

TABLE 6 Path analysis of the root microbial community, physicochemical properties (of both root and soil), and climatic environmental factors.

Factor	Index	Root endosphere (RE)			Rhizosphere soil (RS)			Bulk soil (BS)		
		Direct effect	Indirect effect	Total effect	Direct effect	Indirect effect	Total effect	Direct effect	Indirect effect	Total effect
Bacteria	Season	0.25	0.0041	0.2541	-0.09	-0.031	-0.1211	0.00	-0.0323	-0.0323
	Temperature	0.00	0.00	0.00	0.00	0.00	0.00	0.05	0.00	0.05
	Precipitation	0.28	0.00	0.28	0.0001	0.00	0.0001	-0.04	0.00	-0.04
	Soil nutrient	0.00	0.00	0.00	-0.42	0.00	-0.42	-0.28	0.00	-0.28
	Root nutrient	0.06	0.00	0.06	0.00	0.00	0.00	0.00	0.00	0.00
	Soil pH	0.00	0.00	0.00	0.00	0.00	0.00	0.00	0.00	0.00
Fungi	Season	-0.21	-0.0003	-0.2103	-0.17	-0.0243	-0.1943	0.00	-0.0308	-0.0308
	Temperature	0.00	0.00	0.00	0.00	0.00	0.00	0.05	0.00	0.05
	Precipitation	0.00	0.00	0.00	0.22	0.00	0.22	0.00	0.00	0.00
	Soil nutrient	0.00	0.00	0.00	-0.15	0.00	-0.15	-0.26	0.00	-0.26
	Root nutrient	-0.04	0.00	-0.04	0.00	0.00	0.00	0.00	0.00	0.00
	Soil pH	-0.02	0.00	-0.02	0.00	0.00	0.00	0.00	0.00	0.00

10.3389/fpls.2025.1554879

within the RE was found to be directly influenced by seasonal shifts, whereas the RS fungal community composition was significantly impacted by changes in precipitation patterns driven by seasonal variation. In contrast, temperature showed only a limited effect on fungal community composition across the three compartments (RE, RS, and BS), highlighting the stronger role of moisture availability and nutrient cycling. These findings contribute important insights into the seasonal dynamics of microbial assemblages in desert ecosystems and help address existing knowledge gaps concerning the ecological roles and habitat specificity of microbes associated with deep-rooted desert plants.

Data availability statement

The datasets presented in this study can be found in online repositories. The names of the repository/repositories and accession number(s) can be found in the article/Supplementary Material.

Author contributions

YZ: Conceptualization, Data curation, Investigation, Methodology, Software, Writing – original draft. YD: Conceptualization, Data curation, Investigation, Methodology, Software, Writing – original draft. ZM: Conceptualization, Investigation, Methodology, Writing – review & editing, Funding acquisition. WI: Conceptualization, Methodology, Writing – review & editing. FZ: Conceptualization, Funding acquisition, Project administration, Writing – review & editing. NG: Conceptualization, Methodology, Writing – review & editing. ZZ: Investigation, Software, Writing – review & editing.

Funding

The author(s) declare that financial support was received for the research and/or publication of this article. The research was funded by the Tianshan Talents Program of Xinjiang Autonomous Region (2023TSYCLJ0046), the Startup Foundation for Introducing Talent of Xinjiang Institute of Ecology and Geography (E4500109), Chinese Academy of Sciences, the Natural Science Foundation of Xinjiang Uygur Autonomous Region (2024D01B86), the National Natural Science Foundation of China (42271071), and the National Key Research and Development Project of China (2022YFF1302504) supported this work.

Conflict of interest

The authors declare that the research was conducted in the absence of any commercial or financial relationships that could be construed as a potential conflict of interest.

Generative AI statement

The author(s) declare that no Generative AI was used in the creation of this manuscript.

Publisher's note

All claims expressed in this article are solely those of the authors and do not necessarily represent those of their affiliated organizations, or those of the publisher, the editors and the reviewers. Any product that may be evaluated in this article, or claim that may be made by its manufacturer, is not guaranteed or endorsed by the publisher.

Supplementary material

The Supplementary Material for this article can be found online at: https://www.frontiersin.org/articles/10.3389/fpls.2025.1554879/full#supplementary-material

References

Ali, R., Chaluvadi, S. R., Wang, X. W., Hazzouri, K. M., Sudalaimuthuasari, N., Rafi, M., et al. (2024). Microbiome properties in the root nodules of *Prosopis cineraria*, a leguminous desert tree. *Microbiol. Spectr.* 12, e0361723. doi: 10.1128/spectrum.03617-23

Altschul, S. F., Gish, W., Miller, W., Myers, E. W., and Lipman, D. J. (1990). Basic local alignment search tool. *J. Mol. Biol.* 215, 403–410. doi: 10.1016/S0022-2836(05)80360-2

Archer, E. (2016). RfPermute: Estimate permutation p-values for random forest importance metrics. R Package Version 1. Available online at: https://CRAN.R-project.org/package=rfPermute.

Bahram, M., Hildebrand, F., Forslund, S. K., Anderson, J. L., Soudzilovskaia, N. A., Bodegom, P. M., et al. (2018). Structure and function of the global topsoil microbiome. *Nature* 560, 233–237. doi: 10.1038/s41586-018-0386-6

Bao, S. D. (2000). *Analysis of Soil and Agrochemistry. 3 ed* (Beijing: China Agriculture Press).

Berendsen, R. L., Pieterse, C. M., and Bakker, P. A. (2012). The rhizosphere microbiome and plant health. *Trends. Plant Sci.* 17, 478–486. doi: 10.1016/j.tplants.2012.04.001

Bokulich, N. A., Subramanian, S., Faith, J. J., Gevers, D., Gordon, J. I., Knight, R., et al. (2013). Quality-filtering vastly improves diversity estimates from Illumina amplicon sequencing. *Nat. Methods* 10, 57–59. doi: 10.1038/nmeth.2276

Bradford, M. A., Davies, C. A., Frey, S. D., Maddox, T. R., Melillo, J. M., Mohan, J. E., et al. (2008). Thermal adaptation of soil microbial respiration to elevated temperature. *Ecol. Lett.* 11, 1316–1327. doi: 10.1111/j.1461-0248.2008.01251.x

Bulgarelli, D., Schlaeppi, K., Spaepen, S., Ver Loren van Themaat, E., and Schulze-Lefert, P. (2013). Structure and functions of the bacterial microbiota of plants. *Annu. Rev. Plant Biol.* 64, 807–838. doi: 10.1146/annurev-arplant-050312-120106

Callahan, B. J., McMurdie, P. J., Rosen, M. J., Han, A. W., Johnson, A. J., and Holmes, S. P. (2016). DADA2: High-resolution sample inference from Illumina amplicon data. *Nat. Methods* 13, 581–583. doi: 10.1038/nmeth.3869

Caporaso, J. G., Kuczynski, J., Stombaugh, J., Bittinger, K., Bushman, F. D., Costello, E. K., et al. (2010). QIIME allows analysis of high-throughput community sequencing data. *Nat. Methods* 7, 335–336. doi: 10.1038/nmeth.f.303

Chase, J. M. (2007). Drought mediates the importance of stochastic community assembly. *Proc. Natl. Acad. Sci. U.S.A.* 104, 17430–17434. doi: 10.1073/pnas.0704350104

Chase, J. M., and Myers, J. A. (2011). Disentangling the importance of ecological niches from stochastic processes across scales. *Philos. T. R. Soc B.* 366, 2351–2363. doi: 10.1098/rstb.2011.0063

Chen, S. M., Waghmode, T. R., Sun, R. B., Kuramae, E. E., Hu, C. S., and Liu, B. B. (2019). Root-associated microbiomes of wheat under the combined effect of plant development and nitrogen fertilization. *Microbiome* 7, 136. doi: 10.1186/s40168-019-0750-2

Coyte, K. Z., Jonas, S., and Kevin, R. F. (2015). The ecology of the microbiome: Networks, competition, and stability. *Science* 350, 663–666. doi: 10.1126/science.aad2602

Dawson, T. E., and Goldsmith, G. R. (2018). The value of wet leaves. *New. Phytol.* 219, 1156–1169. doi: 10.1111/nph.15307

Delgado-Baquerizo, M., Oliverio, A. M., Brewer, T. E., Benavent-González, A., Eldridge, D. J., Bardgett, R. D., et al. (2018). A global atlas of the dominant bacteria found in soil. *Science* 359, 320–325. doi: 10.1126/science.aap9516

Deng, Y., Jiang, Y. H., Yang, Y. F., He, Z. L., Luo, F., and Zhou, J. Z. (2012). Molecular ecological network analyses. *BMC. Bioinf.* 13, 113. doi: 10.1186/1471-2105-13-113

de Vries, F. T., Griffiths, R. I., Bailey, M., Craig, H., Girlanda, M., Gweon, H. S., et al. (2018). Soil bacterial networks are less stable under drought than fungal networks. *Nat. Commun.* 9, 3033. doi: 10.1038/s41467-018-05516-7

Dini-Andreote, F., Stegen, J. C., van Elsas, J. D., and Salles, J. F. (2015). Disentangling mechanisms that mediate the balance between stochastic and deterministic processes in microbial succession. *Proc. Natl. Acad. Sci. U.S.A.* 112, E1326–E1332. doi: 10.1073/pnas.1414261112

Domeignoz-Horta, L. A., Pold, G., Liu, X. A., Frey, S. D., Melillo, J. M., and DeAngelis, K. M. (2020). Microbial diversity drives carbon use efficiency in a model soil. *Nat. Commun.* 11, 3684. doi: 10.1038/s41467-020-17502-z

Durán, P., Thiergart, T., Garrido-Oter, R., Agler, M., Kemen, E., Schulze-Lefert, P., et al. (2018). Microbial interkingdom interactions in roots promote *Arabidopsis* survival. *Cell* 175, 973–983.e14. doi: 10.1016/j.cell.2018.10.020

Edwards, J., Johnson, C., Santos-Medellín, C., Lurie, E., Podishetty, N. K., Bhatnagar, S., et al. (2015). Structure, variation, and assembly of the root-associated microbiomes of rice. *Proc. Natl. Acad. Sci. U.S.A.* 112, E911–E920. doi: 10.1073/pnas.1414592112

Edwards, J. A., Santos-Medellín, C. M., Liechty, Z. S., Nguyen, B., Lurie, E., Eason, S., et al. (2018). Compositional shifts in root-associated bacterial and archaeal microbiota track the plant life cycle in field-grown rice. *PLoS. Biol.* 16, e2003862. doi: 10.1371/journal.pbio.2003862

Eilers, K. G., Lauber, C. L., Knight, R., and Noah, F. (2010). Shifts in bacterial community structure associated with inputs of low molecular weight carbon compounds to soil. *Soil. Biol. Biochem.* 42, 896–903. doi: 10.1016/j.soilbio.2010.02.003

Fan, Y., Chen, J. Q., Shirkey, G., John, R., Wu, S. R., Park, H., et al. (2016). Applications of structural equation modeling (SEM) in ecological studies: an updated review. *Ecol. Process.* 5, 19. doi: 10.1186/s13717-016-0063-3

Fan, M. C., Li, J. J., Luan, X. B., Yang, L., Chen, W. Q., Ma, X., et al. (2023). Biogeographical patterns of rhizosphere microbial communities in *Robinia pseudoacacia* forests along a north-south transect in the Loess Plateau. *Geoderma* 435, 116516. doi: 10.1016/j.geoderma.2023.116516

Felipe, M. R. B., Felipe, J. C. F., Mario, A. L. J., Simone, C. B. B., and Giselle, G. M. F. (2021). Spatial and seasonal responses of diazotrophs and ammonium-oxidizing bacteria to legume-based silvopastoral systems. *Appl. Soil. Ecol.* 158, 103797. doi: 10.1016/j.apsoil.2020.103797

Fitzpatrick, C. R., Copeland, J., Wang, P. W., Guttman, D. S., Kotanen, P. M., and Johnson, M. T. J. (2018). Assembly and ecological function of the root microbiome across angiosperm plant species. *Proc. Natl. Acad. Sci. U.S.A.* 115, E1157–E1165. doi: 10.1073/pnas.1717617115

Fraterrigo, J. M., and Rusak, J. A. (2008). Disturbance-driven changes in the variability of ecological patterns and processes. *Ecol. Lett.* 11, 756–770. doi: 10.1111/j.1461-0248.2008.01191.x

Gao, Y. J., Tariq, A., Zeng, F. J., Sardans, J., Graciano, C., Li, X. Y., et al. (2024). Soil microbial functional profiles of P-cycling reveal drought-induced constraints on P-transformation in a hyper-arid desert ecosystem. *Sci. Total. Environ.* 925, 171767. doi: 10.1016/j.scitotenv.2024.171767

Gao, Y. J., Zeng, F. J., Islam, W., Zhang, Z. H., Du, Y., Zhang, Y. L., et al. (2023). Coexistence desert plants respond to soil phosphorus availability by altering the allocation patterns of foliar phosphorus fractions and acquiring different forms of soil phosphorus. *J. Plant Growth. Regul.* 42, 3770–3784. doi: 10.1007/s00344-022-10836-6

Glassman, S. I., Wang, I. J., and Bruns, T. D. (2017). Environmental filtering by pH and soil nutrients drives community assembly in fungi at fine spatial scales. *Mol. Ecol.* 26, 6960–6973. doi: 10.1111/mec.14414

Glynou, K., Nam, B., Thines, M., and Maciá-Vicente, J. G. (2018). Facultative root-colonizing fungi dominate endophytic assemblages in roots of nonmycorrhizal Microthlaspi species. *New. Phytol.* 217, 1190–1202. doi: 10.1111/nph.14873

Grady, K. L., Sorensen, J. W., Stopnisek, N., Guittar, J., and Shade, A. (2019). Assembly and seasonality of core phyllosphere microbiota on perennial biofuel crops. *Nat. Commun.* 10, 4135. doi: 10.1038/s41467-019-11974-4

Green, L. E., Porras-Alfaro, A., and Sinsabaugh, R. L. (2008). Translocation of nitrogen and carbon integrates biotic crust and grass production in desert grassland. *J. Ecol.* 96, 1076–1085. doi: 10.1111/j.1365-2745.2008.01388.x

Hahsler, M., Hornik, K., and Buchta, C. (2008). Getting things in order: An introduction to the R package seriation. *J. Stat. Software* 25, 1–34. doi: 10.18637/jss.v025.i03

Haichar, F. Z., Marol, C., Berge, O., Rangel-Castro, J. I., Prosser, J. I., Balesdent, J., et al. (2008). Plant host habitat and root exudates shape soil bacterial community structure. *ISME. J.* 2, 1221–1230. doi: 10.1038/ismej.2008.80

Hannula, S. E., Kielak, A. M., Steinauer, K., Huberty, M., Jongen, R., De Long, J. R., et al. (2019). Time after Time: Temporal variation in the effects of grass and forb species on soil bacterial and fungal communities. *mBio* 10, e02635–e02619. doi: 10.1128/mBio.02635-19

Hawkins, B. A., Field, R., Cornell, H. V., Currie, D. J., Guégan, J-F., Kaufman, D. M., et al. (2003). Energy, water, and broad-scale geographic patterns of species richness. *Ecology* 84, 3105–3117. doi: 10.1890/03-8006

He, L. Y., Lai, C. T., Mayes, M. A., Murayama, S., and Xu, X. F. (2021). Microbial seasonality promotes soil respiratory carbon emission in natural ecosystems: A modeling study. *Global. Change. Biol.* 27, 3035–3051. doi: 10.1111/gcb.15627

He, R. J., Zeng, J., Zhao, D. Y., Huang, R., Yu, Z. B., and Wu, Q. L. (2020). Contrasting patterns in diversity and community assembly of phragmites australis root-associated bacterial communities from different seasons. *Appl. Environ. Microb.* 86, e00379–e00320. doi: 10.1128/AEM.00379-20

Hernandez, D. J., David, A. S., Menges, E. S., Searcy, C. A., and Afkhami, M. E. (2021). Environmental stress destabilizes microbial networks. *ISME. J.* 15, 1722–1734. doi: 10.1038/s41396-020-00882-x

Hinsinger, P., Bengough, A. G., Vetterlein, D., and Young, I. M. (2009). Rhizosphere: biophysics, biogeochemistry and ecological relevance. *Plant Soil.* 321, 117–152. doi: 10.1007/s11104-008-9885-9

Hooper, D. U., and Vitousek, P. M. (1998). Effects of plant composition and diversity on nutrient cycling. *Ecol. Monogr.* 68, 121–149. doi: 10.2307/2657146

Howe, A., Stopnisek, N., Dooley, S. K., Yang, F., Grady, K. L., and Shade, A. (2023). Seasonal activities of the phyllosphere microbiome of perennial crops. *Nat. Commun.* 14, 1039. doi: 10.1038/s41467-023-36515-y

Ibáñez, J., Martínez, J., and Schnabel, S. (2007). Desertification due to overgrazing in a dynamic commercial livestock-grass-soil system. *Ecol. Model.* 205, 277–288. doi: 10.1016/j.ecolmodel.2007.02.024

Ibekwe, A. M., Ors, S., Ferreira, J. F. S., Liu, X., Suarez, D. L., Ma, J., et al. (2020). Functional relationships between aboveground and belowground spinach (*Spinacia oleracea* L., cv. *Racoon*) microbiomes impacted by salinity and drought. *Sci. Total. Environ.* 717, 137207. doi: 10.1016/j.scitotenv.2020.137207

Islam, W., Ullah, A., and Zeng, F. J. (2023). Response of total belowground soil biota in *Alhagi sparsifolia* monoculture at different soil vertical profiles in desert ecosystem. *Sci. Total. Environ.* 901, 166027. doi: 10.1016/j.scitotenv.2023.166027

Islam, W., Zeng, F. J., Alotaibi, M. O., and Khan, K. A. (2024a). Unlocking the potential of soil microbes for sustainable desertification management. *Earth-Sci. Rev.* 252, 104738. doi: 10.1016/j.earscirev.2024.104738

Islam, W., Zeng, F. J., Alwutayd, K. M., and Khan, K. A. (2024b). Beneath the Surface: Investigating soil microbial and metazoa communities at various depths in a natural desert ecosystem inhabited by *Karelinia caspia*. *Ecol. Indic.* 159, 111745. doi: 10.1016/j.ecolind.2024.111745

Islam, W., Zeng, F. J., Dar, A. A., and Yousaf, M. S. (2024c). Dynamics of soil biota and nutrients at varied depths in a *Tamarix ramosissima*-dominated natural desert ecosystem: Implications for nutrient cycling and desertification management. *J. Environ. Manage.* 354, 120217. doi: 10.1016/j.jenvman.2024.120217

Jansson, J. K., and Hofmockel, K. S. (2020). Soil microbiomes and climate change. *Nat. Rev. Microbiol.* 18, 35–46. doi: 10.1038/s41579-019-0265-7

Jennifer, A. R., Sam, F., Andrea, P. A., Jose, H., Chris, R., Dylan, R. K., et al. (2022). Biogeography of root-associated fungi in foundation grasses of North American plains. *J. Biogeogr.* 49, 22–37. doi: 10.1111/jbi.14260

Körner, C. (2015). Paradigm shift in plant growth control. *Curr. Opin. Plant Biol.* 25, 107–114. doi: 10.1016/j.pbi.2015.05.003

Lai, L. Y., Wu, C. F., Zhang, H. Q., Zhu, Z. K., Yang, J., Kuzyakov, Y., et al. (2025). Microbial diversity loss and plant genotype modulates rhizosphere microbial β-diversity to constrain soil functioning. *Soil Ecol. Lett.* 7, 250308. doi: 10.1007/s42832-025-0308-0

Lange, M., Eisenhauer, N., Sierra, C. A., Bessler, H., Engels, C., Griffiths, R. I., et al. (2015). Plant diversity increases soil microbial activity and soil carbon storage. *Nat. Commun.* 6, 6707. doi: 10.1038/ncomms7707

Lauber, C. L., Ramirez, K. S., Aanderud, Z., Lennon, J., and Fierer, N. (2013). Temporal variability in soil microbial communities across land-use types. *ISME. J.* 7, 1641–1650. doi: 10.1038/ismej.2013.50

Ledo, A., Smith, P., Zerihun, A., Whitaker, J., Vicente-Vicente, J. L., Qin, Z. C., et al. (2020). Changes in soil organic carbon under perennial crops. *Global. Change. Biol.* 26, 4158–4168. doi: 10.1111/gcb.15120

Lu, X. Y., Yan, Y., Sun, J., Zhang, X. K., Chen, Y. C., Wang, X. D., et al. (2015). Carbon, nitrogen, and phosphorus storage in alpine grassland ecosystems of Tibet: Effects of grazing exclusion. *Ecol. Evol.* 5, 4492–4504. doi: 10.1002/ece3.1732

Maestre, F. T., Delgado-Baquerizo, M., Jeffries, T. C., Eldridge, D. J., Ochoa, V., Gozalo, B., et al. (2015). Increasing aridity reduces soil microbial diversity and abundance in global drylands. *Proc. Natl. Acad. Sci. U.S.A.* 112, 15684–15689. doi: 10.1073/pnas.1516684112

Magoc, T., and Steven, S. L. (2011). FLASH: fast length adjustment of short reads to improve genome assemblies. *Bioinformatics* 27, 2957–2963. doi: 10.1093/bioinformatics/btr507

Makhalanyane, T. P., Angel, V., David, V., Eoin, G., Marc, W., Van, G., et al. (2015). Ecology and biogeochemistry of *Cyanobacteria* in soils, permafrost, aquatic, and cryptic polar habitats. *Biodivers. Conserv.* 24, 819–840. doi: 10.1007/s10531-015-0902-z

Manzoni, S., Taylor, P., Richter, A., Porporato, A., and Ågren, G. I. (2012). Environmental and stoichiometric controls on microbial carbon-use efficiency in soils. *New. Phytol.* 196, 79–91. doi: 10.1111/j.1469-8137.2012.04225.x

Markus, L., Mina, A. R., Georg, D., Dan Frederik, L., Alice, M. O., Simon, A. S., et al. (2024). Stability and carbon uptake of the soil microbial community is determined by differences between rhizosphere and bulk soil. *Soil. Biol. Biochem.* 189, 109280. doi: 10.1016/j.soilbio.2023.109280

Maurice, K., Amélia, B., Robin-Soriano, A., Bryan, V., Hassan, B., Marc-André, S., et al. (2024b). Simulated precipitation in a desert ecosystem reveals specific response of rhizosphere to water and a symbiont response in freshly emitted roots. *Appl. Soil. Ecol.* 199, 105412. doi: 10.1016/j.apsoil.2024.105412

Maurice, K., Laurent-Webb, L., Bourceret, A., Boivin, S., Boukcim, H., Selosse, M. A., et al. (2024a). Networking the desert plant microbiome, bacterial and fungal symbionts structure and assortativity in co-occurrence networks. *Environ. Microbiome.* 19, 65. doi: 10.1186/s40793-024-00610-4

Mendiburu, F. (2020). Agricolae: Statistical procedures for agricultural research. R Package Version 1.3-3. Available online at: https://cran.r-project.org/package=agricolae.

Monson, R. K., Lipson, D. L., Burns, S. P., Turnipseed, A. A., Delany, A. C., Williams, M. W., et al. (2006). Winter forest soil respiration controlled by climate and microbial community composition. *Nature* 439, 711–714. doi: 10.1038/nature04555

Neff, J. C., Reynolds, R. L., Belnap, J., and Lamothe, P. J. (2005). Multi-decadal impacts of grazing on soil physical and biogeochemical properties in southeast Utah. *Ecol. Appl.* 15, 87–95. doi: 10.1890/04-0268

Ning, D., Yuan, M., Wu, L., Zhang, Y., Guo, X., Zhou, X., et al. (2020). A quantitative framework reveals ecological drivers of grassland microbial community assembly in response to warming. *Nat. Commun.* 11, 4717. doi: 10.1038/s41467-020-18560-z

Oksanen, J., Blanchet, F. G., Friendly, M., O'Hara, B., Stevens, M. H. H., Oksanen, M. J., et al. (2017). *Vegan: community ecology package. Ordination methods, diversity analysis and other functions for community and vegetation ecologists. Version 2.4-2.*

Oldroyd, G. E. D., and Leyser, O. (2020). A plant's diet, surviving in a variable nutrient environment. *Science* 368, eaba0196. doi: 10.1126/science.aba0196

Olsen, R. S., and Sommer, L. E. (1982). "Phosphorus," in *Methods of Soil Analysis (Part 2).* American Society of Agronomy, Inc., Soil Science Society of America, Inc. Agronomy Monographs Eds. A. L. Page, R. H. Miller and D. R. Keeney, 15–72.

Philippot, L., Raaijmakers, J. M., Lemanceau, P., and van der Putten, W. H. (2013). Going back to the roots: the microbial ecology of the rhizosphere. *Nat. Rev. Microbiol.* 11, 789–799. doi: 10.1038/nrmicro3109

Porras-Alfaro, A., Herrera, J., Sinsabaugh, R. L., Odenbach, K. J., Lowrey, T., and Natvig, D. O. (2008). Novel root fungal consortium associated with a dominant desert grass. *Appl. Environ. Microb.* 74, 2805–2813. doi: 10.1128/AEM.02769-07

Quast, C., Pruesse, E., Yilmaz, P., Gerken, J., Schweer, T., Yarza, P., et al. (2013). The SILVA ribosomal RNA gene database project: improved data processing and webbased tools. *Nucleic. Acids Res.* 41 (D1), D590–D596. doi: 10.1093/nar/gks1219

Rasche, F., Knapp, D., Kaiser, C., Koranda, M., Kitzler, B., Zechmeister-Boltenstern, S., et al. (2011). Seasonality and resource availability control bacterial and archaeal communities in soils of a temperate beech forest. *ISME. J.* 5, 389–402. doi: 10.1038/ismej.2010.138

R Core Team (2021). R: A language and environment for statistical computing; publisher foundation for statistical computing (Vienna, Austria). Available online at: https://www.R-project.org.

Regan, M. K., Nunan, N., Boeddinghaus, S. R., Vanessa, B., Doreen, B., Steffen, B., et al. (2014). Seasonal controls on grassland microbial biogeography: Are they governed by plants, abiotic properties, or both? *Soil. Biol. Biochem.* 71, 21–30. doi: 10.1016/j.soilbio.2013.12.024

Reinhold-Hurek, B., Bünger, W., Burbano, C. S., Sabale, M., and Hurek, T. (2015). Roots shaping their microbiome: Global hotspots for microbial activity. *Annu. Rev. Phytopathol.* 53, 403–424. doi: 10.1146/annurev-phyto-082712-102342

Rognes, T., Flouri, T., Nichols, B., Quince, C., and Mahé, F. (2016). VSEARCH: a versatile open source tool for metagenomics. *PeerJ* 4, e2584. doi: 10.7717/peerj.2584

Sharhabil, M. Y., Aliyu, A. M., Mustapha, A., and Abdurrashid, H. (2023). Recent advances in the chemistry of nitrogen, phosphorus, and potassium as fertilizers in soil: A review. *Pedosphere* 33, 385–406. doi: 10.1016/j.pedsph.2022.07.012

Siles, J. A., Cajthaml, T., Minerbi, S., and Margesin, R. (2016). Effect of altitude and season on microbial activity, abundance and community structure in *Alpine* forest soils. *FEMS. Microbiol. Ecol.* 92, fiw008. doi: 10.1093/femsec/fiw008

Stegen, J. C., Lin, X., Fredrickson, J. K., and Konopka, A. E. (2015). Estimating and mapping ecological processes influencing microbial community assembly. *Front. Microbiol.* 6. doi: 10.3389/fmicb.2015.00370

Stegen, J. C., Lin, X., Konopka, A. E., and Fredrickson, J. K. (2012). Stochastic and deterministic assembly processes in subsurface microbial communities. *ISME. J.* 6, 1653–1664. doi: 10.1038/ismej.2012.22

Tan, B., Wu, F. Z., Yang, W. Q., and He, X. H. (2014). Snow removal alters soil microbial biomass and enzyme activity in a Tibetan alpine forest. *Appl. Soil. Ecol.* 76, 34–41. doi: 10.1016/j.apsoil.2013.11.015

Tariq, A., Ullah, A., Sardans, J., Zeng, F. J., Graciano, C., Li, X. Y., et al. (2022). *Alhagi sparsifolia*: An ideal phreatophyte for combating desertification and land degradation. *Sci. Total. Environ.* 844, 157228. doi: 10.1016/j.scitotenv.2022.157228

Trivedi, P., Batista, B. D., Bazany, K. E., and Singh, B. K. (2022). Plant-microbiome interactions under a changing world: responses, consequences and perspectives. *New. Phytol.* 234, 1951–1959. doi: 10.1111/nph.18016

Wang, D., Bai, Y., and Qu, J. (2022). The Phragmites root-inhabiting microbiome: A critical review on its composition and environmental application. *Engineering-PRC* 9, 42–50. doi: 10.1016/j.eng.2021.05.016

Wang, H. H., Chu, H. L., Dou, Q., Xie, Q. Z., Tang, M., Sung, C. K., et al. (2018). Phosphorus and nitrogen drive the seasonal dynamics of bacterial communities in *Pinus* forest rhizospheric soil of the qinling mountains. *Front. Microbiol.* 9. doi: 10.3389/fmicb.2018.01930

Wang, Q., Garrity, G. M., Tiedje, J. M., and Cole, J. R. (2007). Naive Bayesian classifier for rapid assignment of rRNA sequences into the new bacterial taxonomy. *Appl. Environ. Microb.* 73, 5261–5267. doi: 10.1128/AEM.00062-07

Wang, J. M., Wang, Y., He, N. P., Ye, Z. Q., Chen, C., Zang, R. G., et al. (2020). Plant functional traits regulate soil bacterial diversity across temperate deserts. *Sci. Total. Environ.* 715, 136976. doi: 10.1016/j.scitotenv.2020.136976

Warra, H. H., Ahmed, M. A., and Nicolau, M. D. (2015). Impact of land cover changes and topography on soil quality in the Kasso catchment, Bale Mountains of southeastern Ethiopia. *Singapore. J. Trop. Geogr.* 36, 357–375. doi: 10.1111/sjtg.12124

Wei, T., and Simko, V. (2013). Corrplot: visualization of a correlation matrix. *Mmwr-Morbid. Mortal. W.* 52, 145–151. doi: 10.1177/002215540405200201

White, E. R., and Hastings, A. (2020). Seasonality in ecology: progress and prospects in theory. *Ecol. Complex.* 44, 100867. doi: 10.1016/j.ecocom.2020.100867

Wu, A. L., Jiao, X. Y., Wang, J. S., Dong, E. W., Guo, J., Wang, L. G., et al. (2021). Sorghum rhizosphere effects reduced soil bacterial diversity by recruiting specific bacterial species under low nitrogen stress. *Sci. Total. Environ.* 770, 144742. doi: 10.1016/j.scitotenv.2020.144742

Wu, Z. Y., Lin, W. X., Li, J. J., Liu, J. F., Li, B. L., Wu, L. K., et al. (2016). Effects of seasonal variations on soil microbial community composition of two typical zonal vegetation types in the Wuyi mountains. *J. Mt. Sci-Engl.* 13, 1056–1065. doi: 10.1007/s11629-015-3599-2

Xiang, Q., Qiao, M., Zhu, D., Giles, M., Neilson, R., Yang, X. R., et al. (2021). Seasonal change is a major driver of soil resistomes at a watershed scale. *ISME. Commun.* 1, 17. doi: 10.1038/s43705-021-00018-y

Xie, L., and Yin, C. (2022). Seasonal variations of soil fungal diversity and communities in subalpine coniferous and broadleaved forests. *Sci. Total. Environ.* 846, 157409. doi: 10.1016/j.scitotenv.2022.157409

Xiong, C., Zhu, Y. G., Wang, J. T., Singh, B., Han, L. L., Shen, J. P., et al. (2021). Host selection shapes crop microbiome assembly and network complexity. *New. Phytol.* 229, 1091–1104. doi: 10.1111/nph.16890

Xu, T. L., Shen, Y. W., Ding, Z. J., and Zhu, B. (2023). Seasonal dynamics of microbial communities in rhizosphere and bulk soils of two temperate forests. *Rhizosphere* 25, 100673. doi: 10.1016/j.rhisph.2023.100673

Yu, Y. Y., Ru, J. Y., Lei, B. H., Han, S. J., Wan, S. Q., and Zheng, J. Q. (2024). Distinct response patterns of soil micro-eukaryotic communities to early-season and late-season precipitation in a semiarid grassland. *Soil. Biol. Biochem.* 194, 109427. doi: 10.1016/j.soilbio.2024.109427

Zhang, Z. H., Chai, X. T., Gao, Y. J., Zhang, B., Lu, Y., Du, Y., et al. (2022b). *Alhagi sparsifolia* harbors a different root-associated mycobiome during different development stages. *Microorganisms* 10, 2376. doi: 10.3390/microorganisms10122376

Zhang, Y. L., Du, Y., Zhang, Z. H., Islam, W., and Zeng, F. J. (2024b). Unveiling the diversity, composition, and dynamics of phyllosphere microbial communities in *Alhagi sparsifolia* across desert basins and seasons in Xinjiang, China. *Front. Microbiol.* 15. doi: 10.3389/fmicb.2024.1361756

Zhang, J. W., Ge, Z. H., Ma, Z. H., Huang, D. Y., and Zhang, J. B. (2022a). Seasonal changes driving shifts of aquatic rhizosphere microbial community structure and the functional properties. *J. Environ. Manage.* 322, 116124. doi: 10.1016/j.jenvman.2022.116124

Zhang, G. L., Jia, J., Zhao, Q. Q., Wang, W., Wang, D. W., and Bai, J. H. (2023). Seasonality and assembly of soil microbial communities in coastal salt marshes invaded by a perennial grass. *J. Environ. Manage.* 331, 117247. doi: 10.1016/j.jenvman.2023.117247

Zhang, Z. H., Tariq, A., Zeng, F. J., Graciano, C., and Zhang, B. (2020). Nitrogen application mitigates drought-induced metabolic changes in *Alhagi* sp*arsifolia* seedlings by regulating nutrient and biomass allocation patterns. *Plant Physiol. Bioch.* 155, 828–841. doi: 10.1016/j.plaphy.2020.08.036

Zhang, J. Y., Zhang, N., Liu, Y. X., Zhang, X. N., Hu, B., Qin, Y., et al. (2018). Root microbiota shift in rice correlates with resident time in the field and developmental stage. *Sci. China. Life. Sci.* 61, 613–621. doi: 10.1007/s11427-018-9284-4

Zhang, J., Zhang, Y. M., and Zhang, Q. (2024a). Host plant traits play a crucial role in shaping the composition of epiphytic microbiota in the arid desert, Northwest China. *J. Arid. Land.* 16, 699–724. doi: 10.1007/s40333-024-0014-2

Zhao, K., Zhang, L., Wang, F., Li, K. K., Zhang, Y. L., and Zhang, B. C. (2024). Dynamics in eukaryotic algal communities regulate bacterial and fungal communities as biocrusts develop in a temperate desert in Central Asia. *Funct. Ecol.* 38, 531–545. doi: 10.1111/1365-2435.14496

Zhong, Y. Q. W., Sorensen, P. O., Zhu, G. Y., Jia, X. Y., Liu, J., Shangguan, Z. P., et al. (2022). Differential microbial assembly processes and co-occurrence networks in the soil-root continuum along an environmental gradient. *iMeta* 1, e18. doi: 10.1002/imt2.18

Zhou, X., Teemu, T., Lucie, M., Chen, L., Pérez-Pérez, J., and Berninger, F. (2024). Global analysis of soil bacterial genera and diversity in response to pH. *Soil. Biol. Biochem.* 198, 109552. doi: 10.1016/j.soilbio.2024.109552

frontiers | Frontiers in Plant Science

TYPE Original Research
PUBLISHED 04 July 2025
DOI 10.3389/fpls.2025.1579142

OPEN ACCESS

EDITED BY
Xiao-Dong Yang,
Ningbo University, China

REVIEWED BY
Yuping Hou,
Ludong University, China
César Marín,
Santo Tomás University, Chile
Shixing Zhou,
Sichuan Agricultural University, China
Xiaoying Jin,
Northeast Forestry University, China

*CORRESPONDENCE
Wei Liu
weiliu@lzb.ac.cn
Meng Zhu
zhumeng@lzb.ac.cn

RECEIVED 18 February 2025
ACCEPTED 11 June 2025
PUBLISHED 04 July 2025

CITATION
Xue Y, Liu W, Feng Q, Zhu M, Zhang J, Wang L, Chen Z and Li X (2025) Effects of vegetation restoration on soil fungi community structure and assembly process in a semiarid alpine mining region. *Front. Plant Sci.* 16:1579142. doi: 10.3389/fpls.2025.1579142

Effects of vegetation restoration on soil fungi community structure and assembly process in a semiarid alpine mining region

Yuanyuan Xue[1,2], Wei Liu[1]*, Qi Feng[1], Meng Zhu[1]*, Jutao Zhang[1], Lingge Wang[1,2], Zexia Chen[1,2] and Xuejiao Li[1,2]

[1]Key Laboratory of Ecological Safety and Sustainable Development in Arid Lands, Northwest Institute of Eco-Environment and Resources, Chinese Academy of Sciences, Lanzhou, China, [2]College of Resources and Environment, University of Chinese Academy of Sciences, Beijing, China

Introduction: Understanding responses of soil fungal community characteristics to vegetation restoration is essential for optimizing artificial restoration strategies in alpine mining ecosystems. Despite its ecological significance, current comprehension regarding the structure composition and assembly mechanisms of soil fungal communities following vegetation restoration in these fragile ecosystems remains insufficient.

Methods: We used the high-throughput sequencing and null model analysis to determine the variations and environmental drivers of soil fungal community structures and assembly processes across different restoration chronosequences (natural plant sites, unrestored sites, 2-year restoration sites, and 6-year restoration sites) in a semiarid alpine coal mining region.

Results: Artificial vegetation restoration significantly enhanced the α diversity of soil fungal communities while reducing β diversity. However, with prolonged restoration duration, we observed a significant decrease in α diversity accompanied by a corresponding increase in β diversity. Moreover, artificial restoration induced substantial modifications in soil fungal community composition. Taxonomic analysis demonstrated a distinct shift in dominant specialist species from Ascomycota in unrestored, natural plant, and 2-year restoration sites to Glomeromycota in 6-year restoration sites. Dispersal limitation and homogeneity selection were the predominant mechanism governing soil fungal community assembly, with its relative contributions varying significantly across restoration stages. In natural plant communities and unrestored sites, the structure of soil fungal community was primarily governed by dispersal limitation. The 2-year restoration sites exhibited a marked transition, with homogeneous selection emerging as the dominant assembly process, primarily influenced by soil sand content, total phosphorus (TP), total potassium (TK), and belowground biomass (BGB). This transition was accompanied by a significant reduction in the contribution of dispersal limitation.

Discussion: As restoration progressed, the importance of homogeneous selection gradually decreased, while dispersal limitation regained prominence,

with community structure being predominantly regulated by soil clay content, soil moisture content (SMC), and TP. Our results underscore the critical role of soil texture and phosphorus availability in shaping soil fungal community dynamics throughout the revegetation process.

KEYWORDS

vegetation restoration, soil fungal community, β diversity, community assembly mechanisms, alpine mining regions

1 Introduction

Coal mining, while contributing to economic development, causes a series of ecological disruptions, such as soil moisture loss, nutrient depletion, plant mortality, and shifts in soil microbial community structure and composition (de Quadros et al., 2016; Chen et al., 2020; Yuan et al., 2021). Numerous studies have found that vegetation restoration can effectively enhance soil nutrient content, improve soil quality, prevent soil erosion, and increase biodiversity, making it one of the most effective measures for mitigating ecological disruptions resulting from mining activities (Dao et al., 2023). A study conducted in the Moa mining area found that soil aggregate stability increased by 66% after planting *Casuarina equisetifolia* (Izquierdo et al., 2005). Dao et al. (2023) observed that during the vegetation recovery process over 5 to 14 years, the composition of soil microbial communities approached that of undisturbed soils. Additionally, Roy et al. (2020) demonstrated that appropriate vegetation interventions on coal mine wastelands, combined with fine-tuned nitrogen and phosphorus fertilizer doses, enabled the optimal growth of sandbuckthorn, thereby promoting and accelerating the ecological restoration of degraded coal mining ecosystems. Thus, the implementation of artificial measures can effectively promote ecological restoration and the recovery of ecosystem functions in mining areas (Chen et al., 2020).

The Muli coal mining area in the Qilian Mountains has abundant coal reserves, and it is not only the source region of the Datong River, but also an important regional water source and ecological safety barrier, occupying a crucial ecological position (Yang et al., 2018; Li et al., 2021). However, the ecosystem of the Muli coal mining area is highly vulnerable due to the cold climate, high altitude, and thin air. Meanwhile, coal mining activities have exacerbated ecosystem degradation, especially in permafrost environments, which will induce a series of problems (Ahirwal and Maiti, 2017). For example, open-pit mining directly removes the surface cover layer, damaging the insulating protective structure of the permafrost layer, accelerating its thawing, and disrupting the thermal balance of the permafrost. This leads to geological hazards such as frost heave and thaw subsidence, which in turn causes habitat degradation for plants and animals. Additionally, the large amount of organic carbon stored in the permafrost is released as CO_2 through microbial decomposition upon thawing, further accelerating global warming (Ji et al., 2022). Thus, the natural restoration process is slow and difficult, and artificial interventions have become essential in the ecological restoration process of mining areas (Luo et al., 2020). Restoration duration is supposed to significantly affect vegetation and soil properties. The research conducted on the Tibetan Plateau by Yuan et al. (2021) indicated that extending the restoration period can significantly promote the accumulation of organic matter and improve soil structure. Additionally, Ma et al. (2019) found that typical vegetation restoration in mining areas positively affected soil quality improvement, while artificial maintenance should be strengthened to prevent soil quality degradation in future ecological management. Furthermore, researchers have observed that with increasing restoration time, the dominance of fungi significantly rises, such as Ascomycota and Zygomycota (Qiang et al., 2020).

As a vital member of the soil ecosystem, soil fungi are essential for nutrient cycling and soil structure development through aggregate formation, while also establishing symbiotic associations with plants to enhance their growth and development (Courty et al., 2010). Researches have demonstrated that Glomeromycota fungi enhances carbon sequestration and promote soil aggregation by producing glomalin-related soil proteins (Agnihotri et al., 2022; Wang et al., 2022). Ascomycota can produce various antimicrobial agents that protect plants from pathogen attack (Jibola-Shittu et al., 2024). And arbuscular mycorrhizal fungi not only supply essential mineral elements to host plants but also enhance resistance to pests, diseases, and abiotic stresses, thereby promoting plant health (Zhang X, et al., 2022). In addition, soil fungi was also used to indicate soil environment changes affected by environmental disturbances. For instance, the relative abundance of Glomeromycota is sensitive to salinity (Krishnamoorthy et al., 2014), while the relative abundance of Mortierellomycota can predict plant growth traits (Zhang et al., 2023). Mycorrhizal fungi have been identified as important predictors of global soil carbon storage (Averill et al., 2014). Diversity is one of the key characteristics for understanding and managing ecosystem functions, as well as evaluating the ecosystem's resilience to disturbances. Generally, higher diversity enhances community stability and increases its ability to resist external disturbances (Liu et al., 2020). Therefore, an increasing number of studies emphasize the necessity of investigating the complete characteristics of fungal communities, including their diversity, structure, assembly, and driving factors.

Presently, most research has primarily focused on the effects of soil properties and plant communities on fungal communities following artificial restoration. In fact, the relative contributions of stochastic and

deterministic processes vary depending on ecological and environmental conditions, while the impact of these processes following artificial restoration were less understood (Myers et al., 2013; Tripathi et al., 2018). After revegetation, the heterogeneity of fungal habitats increased, resulting more complicated assembly processes in fungal communities. Understanding the assembly processes of soil fungal communities under different restoration durations could provide scientific guidance for improving restoration outcomes in alpine mining areas. Especially in open-pit mining, the removal of surface soil leads to ecosystem degradation, resulting in reduced moisture retention capacity and soil organic matter, and the loss of biodiversity (Chen et al., 2020). Furthermore, plant growth and animal reproduction are inhibited by low temperatures and low oxygen levels in alpine mining areas, which significantly decrease plant diversity and soil nutrients (Ganesh et al., 2020). Therefore, we hypothesize that the soil fungal community diversity in unrestored sites of alpine mining areas is relatively low, with community assembly primarily driven by dispersal limitation. Following artificial restoration, increases in vegetation diversity and soil nutrient content promote the diversity of soil fungal community, with community assembly being mainly governed by deterministic processes.

Therefore, the main goals of this study were (1) to explore changes in the composition and diversity of soil fungal communities, and (2) to determine soil fungal community assembly process and dominant driving factors across different restoration chronosequences in alpine mining coalfields.

2 Materials and methods

2.1 Study area

The study area is situated in the Muli coalfields (99°05′E–99°27′E, 38°05′N–38°27′N) of the middle Qilian Mountains, northwestern China (Figure 1). It lies in the northeastern part of the Qinghai-Tibet Plateau with an average elevation of 4100 m.a.s.l. The climate is typical semiarid alpine climate, with mean annual temperature, precipitation, and evaporation reaching to -4°C, 477 mm, and 1050 mm, respectively.

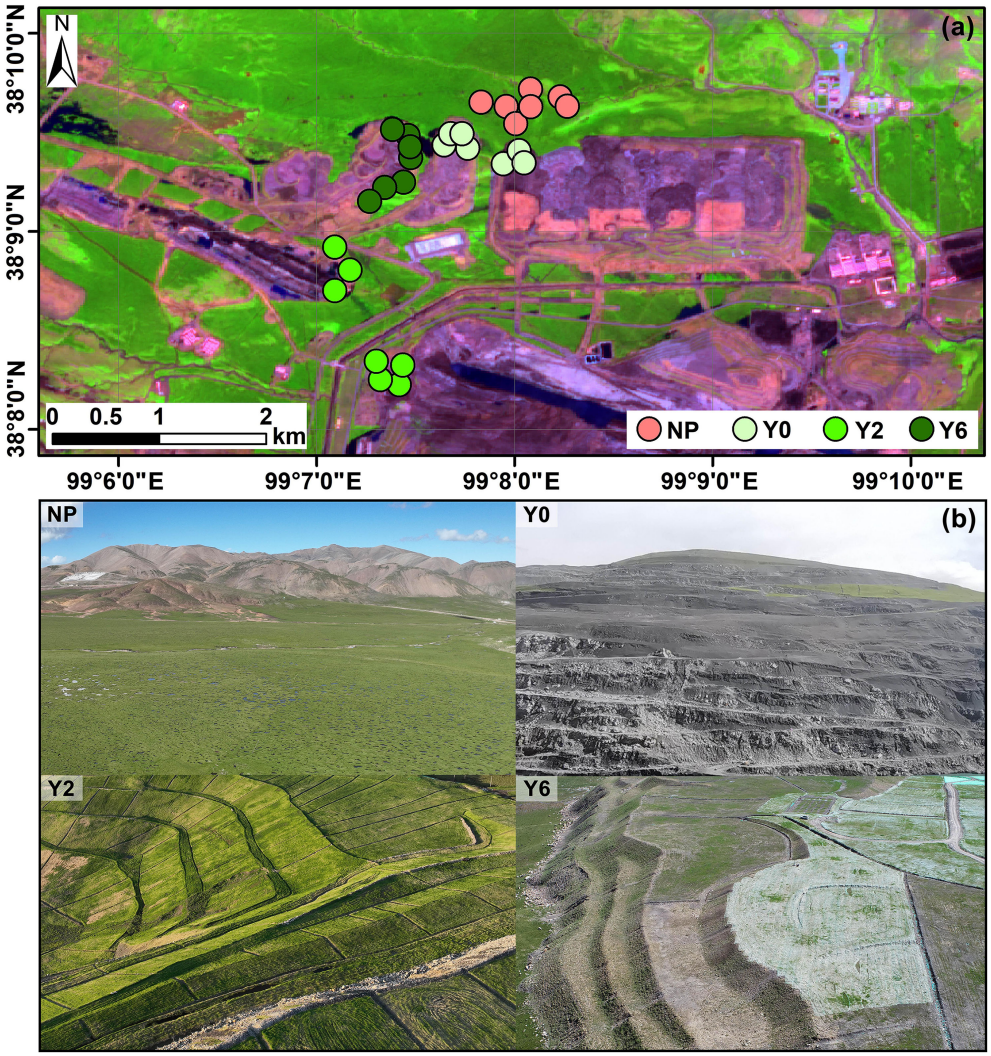

FIGURE 1
Location of sampling points in the Muli coalfield **(a)**, and the landscape of natural plant sites (NP), unrestored sites (Y0), 2-year restoration sites (Y2), and 6-year restoration sites (Y6) in study area **(b)**.

The annual sunshine hours is 2942 h. The region is characterized by glacial landforms at the edge of the plateau, where permafrost (5 to 50 meters) and seasonal frost (1 to 3 meters) are extensively distributed (Bai, 2022). The predominant vegetation types include alpine meadows and alpine wetlands, with the dominant species being *Carex moorcroftii* and *Koeleria tibetica*, and the vegetation coverage is approximately 80%. The main soil type is classified as haplic leptosols according to the World Reference Base for Soil Resources, which is roughly referred to as alpine meadow soils according to the Chinese Soil Genetic Classification.

In the 1960s, small-scale mining activities started gradually, with large-scale extraction beginning in the early 21st century predominantly through open-pit mining with extensive excavation. To mitigating ecological disruptions resulting from mining activities, the government implemented comprehensive ecological remediation initiatives in the mining area between 2014 and 2018. However, persistent illegal coal extraction by certain enterprises led to renewed media exposure of unauthorized mining activities in 2020, generating substantial societal repercussions. In prompt response, governments launched extensive ecological restoration initiatives to rehabilitate the affected areas.

2.2 Plant and soil sample collection and analysis

Soil sampling was conducted in the Muli coalfield in August 2023. We selected soil sampling sites according to the restoration year, i.e., the landscape of natural plant sites (NP), unrestored sites (Y0), 2-year restoration sites (Y2), and 6-year restoration sites (Y6), with a total of 28 soil samples (7 replicates) from 0–20 cm were obtained. We measured Aboveground biomass (AGB), belowground biomass (BGB), litter biomass (Litter), bulk density (BD), soil moisture content (SMC), soil electrical conductivity (EC), pH, soil organic carbon (SOC), total nitrogen (TN), total carbon (TC), total potassium (TK), and phosphorus (TP). The fungal ITS-1 region was amplified with the primer pair ITS1 (5'-CTTGGTCATTTAGAGGAAGTAA-3') and ITS2 (5'-GCTGCGTTCTTCATCGA TGC-3') (Blaalid et al., 2013) to obtain the information of fungal community. More detailed descriptions of sampling protocols and procedures for laboratory analyses can be found in Xue et al. (2025). The raw sequencing reads were deposited in the NCBI database under the accession number PRJNA1208394.

2.3 Statistical analysis

The ANOVA and LSD tests were performed to analyze differences among groups using the 'agricolae' package (Mendiburu, 2017). Plant α diversity indices (iSimpson, Shannon, Simpson and Pielou's indices), fungal community α (Chao1, AEC, Simpson, and Shannon indices) and β diversity indices were also computed (Schloss et al., 2009; Kembel et al., 2010). Additionally, to explore microbial spatial variation (β diversity), we used the Bray-Curtis metric to assess taxonomic variation. The PCoA and ANOSIM were also used to conduct community structure analyses. To characterize specialist OTUs, we computed the specificity and occupancy of each OTU across the four study sites. Specificity reflects the average abundance of an OTU within a given habitat, whereas occupancy indicates its frequency of occurrence across samples (Dufrêne and Legendre, 1997; Gweon et al., 2021). OTUs exhibiting specificity and occupancy values ≥ 0.7 were classified as specialists, indicating their habitat specificity and widespread presence (Gweon et al., 2021). Taxonomic trees were applied to illustrate the distribution and composition of specialist species across the sites by the 'metacoder' package (Foster et al., 2017). To determine the vegetative and edaphic effects on fungal community diversity and structure, we performed a Mantel test (permutations 999) using the 'vegan' package (Sunagawa et al., 2015). Fungal community composition was assessed using Bray-Curtis distances, while environmental dissimilarities were calculated based on Euclidean distances. Additionally, the phylogenetic-bin-based null model analysis (iCAMP) was employed to analyze fungal community assembly processes (Ning et al., 2020). This framework integrates the β-net relatedness index and the Raup-Crick index to evaluate phylogenetic and taxonomic beta diversity, respectively (Stegen et al., 2013; Ning et al., 2020). The relative contributions of five assembly processes, i.e., the heterogeneous selection, homogeneous selection, dispersal limitation, homogenizing dispersal, and drift were quantified, and their variations across the four sites were compared using the Wilcoxon test (Freire-Zapata et al., 2024). More detailed descriptions of the statistical analyses can be found in Xue et al. (2025). All data were processed in R software (version 4.0.2).

3 Results

3.1 Soil fungal community diversity across different restoration stages.

Following 2 years of artificial restoration, the Shannon and Simpson indices exhibited a significant increase (Table 1), whereas β diversity significantly decreased (Figure 2B). As the duration of

TABLE 1 Fungal community α diversity indices among four sites.

Index	Y0	Y2	Y6	NP	*p* value
Chao1	506.07 ± 80.06 a	459.79 ± 72.01 a	340.76 ± 95.44 b	328.50 ± 67.03 b	<0.001 ***
ACE	513.77 ± 89.30 a	524.08 ± 87.36 a	359.85 ± 100.76 b	354.27 ± 45.48 b	<0.001 ***
Shannon	3.33 ± 0.58 b	4.21 ± 0.29 a	3.79 ± 0.35 ab	3.36 ± 0.51 b	0.004 **
Simpson	0.11 ± 0.10 a	0.04 ± 0.02 b	0.06 ± 0.03 ab	0.09 ± 0.05 ab	0.011 *

***, **, and * indicate $p < 0.001$, $p < 0.01$, and $p < 0.05$, respectively.

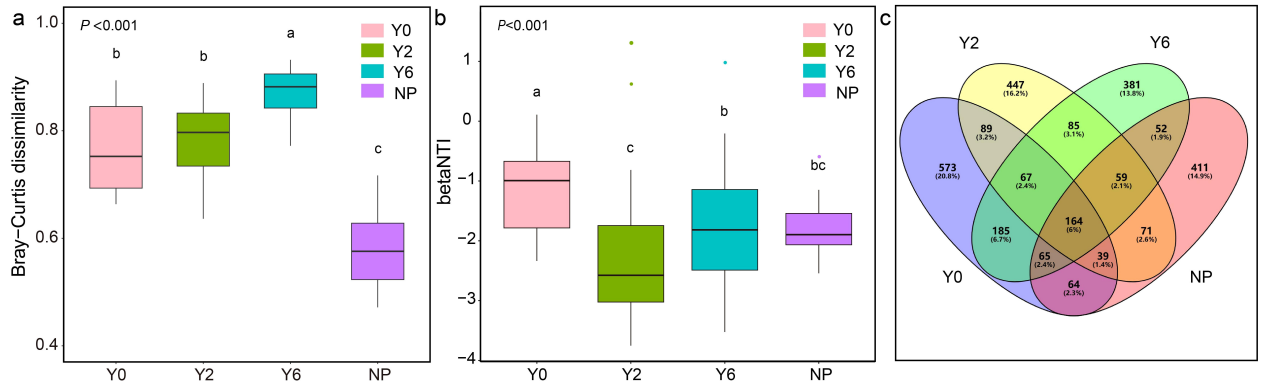

FIGURE 2
Comparisons of fungal community Bray-Curtis dissimilarity **(a)**, betaNTI **(b)**, and OTUs **(c)** among different sampling sites.

restoration progressed, both the richness (Chao1 and ACE indices) and diversity (Shannon and Simpson indices) of the soil fungal communities showed a significant decline, while β diversity experienced a notable increase. Furthermore, no significant differences were detected in neither α diversity nor β diversity of the soil fungal communities between natural plant sites and the 6-year restoration sites. Multivariate statistical analysis, based on Bray-Curtis dissimilarity matrices, revealed significant differences in taxonomic compositions across the four study sites (Figure 2A). Specifically, only 167 OTUs were shared among all four sites, accounting for 6% of the total OTUs, with the unrestored sites, 2-year restored sites, 6-year restored sites, and natural plant sites containing 573, 447, 381, and 411 unique OTUs, respectively (Figure 2C).

3.2 Soil fungal community structure and assembly mechanism across different restoration stages

Based on PCoA, we found that artificial restoration significantly altered the composition of soil fungal communities, which was further supported by ANOSIM results (Figure 3). Ascomycota was the predominant phylum in all sites, exhibiting a significant decrease in relative abundance following artificial restoration (Figure 4A). As the years progressed, its relative abundance continued to decrease significantly. In contrast, Basidiomycota was the second dominant phylum in the unrestored, 2-year restoration, and natural plant sites, with a notable increase in relative abundance in the restoration sites. Glomeromycota was the third dominant phylum in the unrestored and 2-year restoration sites and the second dominant phylum in the 6-year restoration sites, showing a significant increase in relative abundance after 6 years of restoration.

Our study revealed that the dominant fungal genera varied significantly across different sites (Figure 4B). In the unrestored sites, *Liangia* and *Flavocillium* were the dominant genera. After 2 years of artificial restoration, the dominant genera shifted to *Enterocarpus* and *Pseudogymnoascus*. As the restoration period progressed, *Diversispora*, *Coniochaeta*, and *Claroideoglomus* became the dominant genera. In natural plant sites, *Boudiera* and *Microscypha* were the dominant genera. Overall, following artificial restoration, the relative abundance of *Liangia* and *Flavocillium* decreased significantly, with the highest abundance found in natural plant sites. In contrast, the abundance of *Enterocarpus* and *Pseudogymnoascus* increased significantly in the 2-year restoration sites but decreased as the restoration period continued. Their relative abundance was lowest in natural plant sites, suggesting a positive response to long-term artificial restoration. After 6 years of restoration, the abundance of *Diversispora*, *Coniochaeta*, and *Claroideoglomus* increased significantly.

The occupancy and specificity analysis showed that numbers of specialist species in unrestored, 2-year restoration sites, 6-year restoration sites, and natural plant sites were 42, 92, 15, and 54, respectively (Figure 5). Specialist species in the unrestored, 2-year artificial restoration, and natural plant sites were mostly Ascomycota, while Glomeromycota was the predominant group of specialist species in the 6-year artificial restoration sites (Figure 6).

In Figure 7, we found that dispersal limitation and homogeneity selection predominantly governed the soil fungal community in alpine mining areas, but their relative importance varied as the duration of artificial restoration increased. Specifically, dispersal limitation had the highest relative importance in the unrestored and natural plant sites, followed by homogeneity selection. In the wake of artificial restoration, it was discerned that the primary driver shaping fungal communities was homogeneity selection, with dispersal limitation exerting a secondary influence. After artificial restoration, homogeneity selection was identified as making the greatest contribution to structuring fungal communities, followed by dispersal limitation. As the restoration period progressed, the relative importance of homogeneity selection decreased, while that of dispersal limitation increased, thus both homogeneity selection and dispersal limitation jointly dominated the structure of the soil fungal community in the 6-year restoration sites.

We further investigated the influence of environmental factors (Supplementary Table S1) on soil fungal communities in alpine mining region. The results showed that in unrestored sites, soil fungal community structure and diversity were not significantly influenced by soil and vegetation properties (Figure 8A). However,

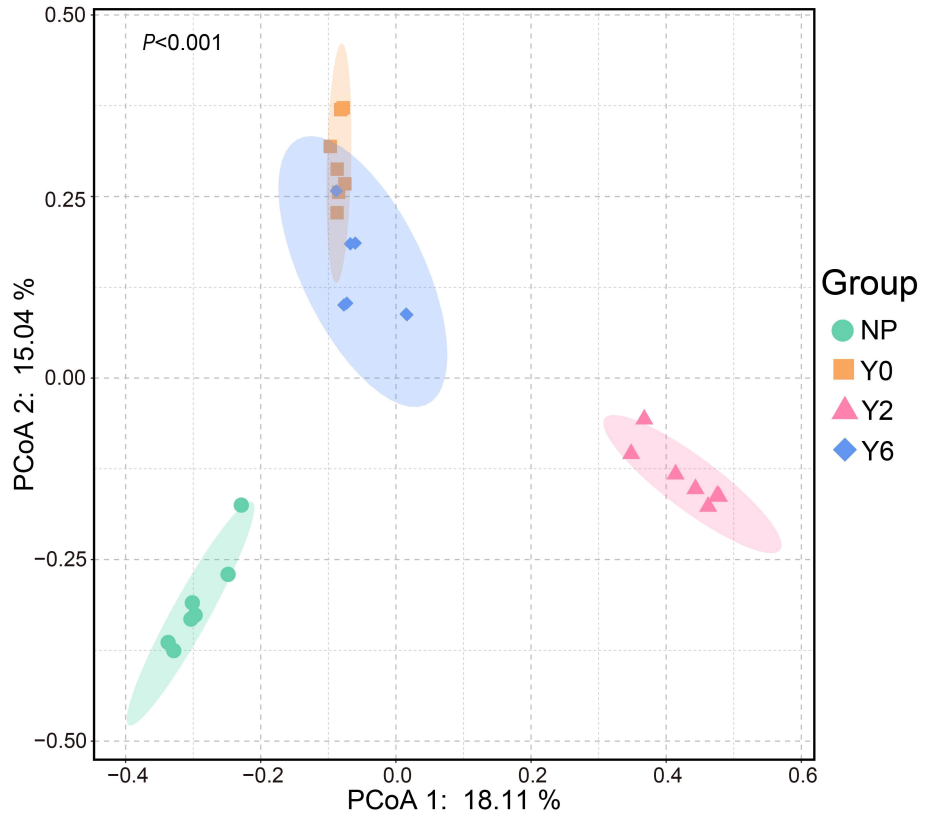

FIGURE 3
Fungal community structures under different sampling sites based on the PCoA analysis.

in 2-year artificial restoration sites, soil fungal community structure was mainly correlated with soil sand, TP, TK, and BGB (Figure 8B). Meanwhile, the diversity of fungal community was significantly influenced by plant Pielou's evenness. As the restoration period progressed, the structure of fungal community was significantly affected by soil clay, SMC, and TP (Figure 8C). While in the natural plant sites, soil pH was the primary factor influencing soil fungal community structure (Figure 8D).

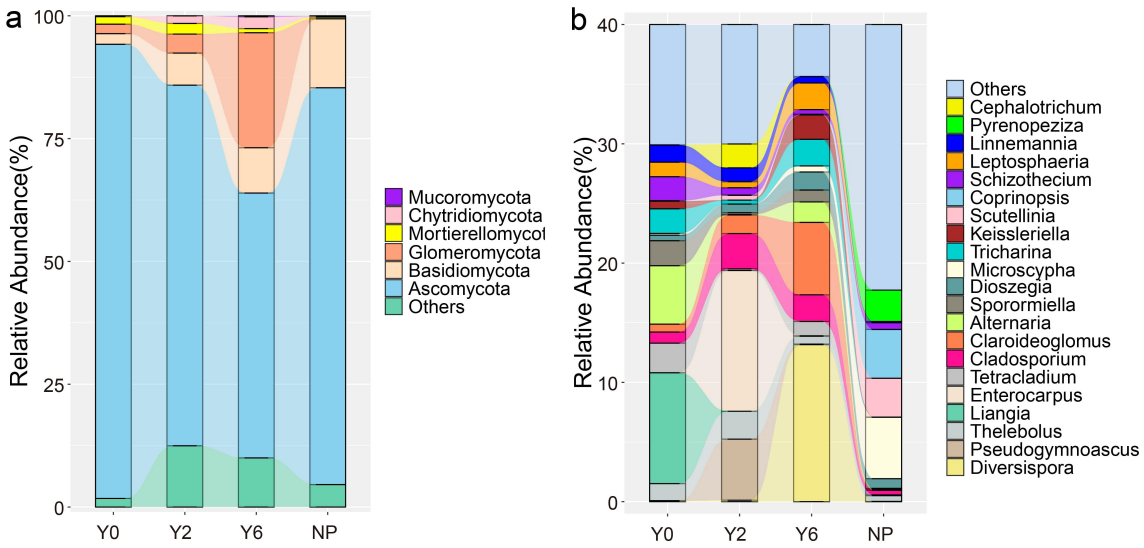

FIGURE 4
The relative abundance of soil fungi at phylum **(a)** and genus **(b)** level from four sites.

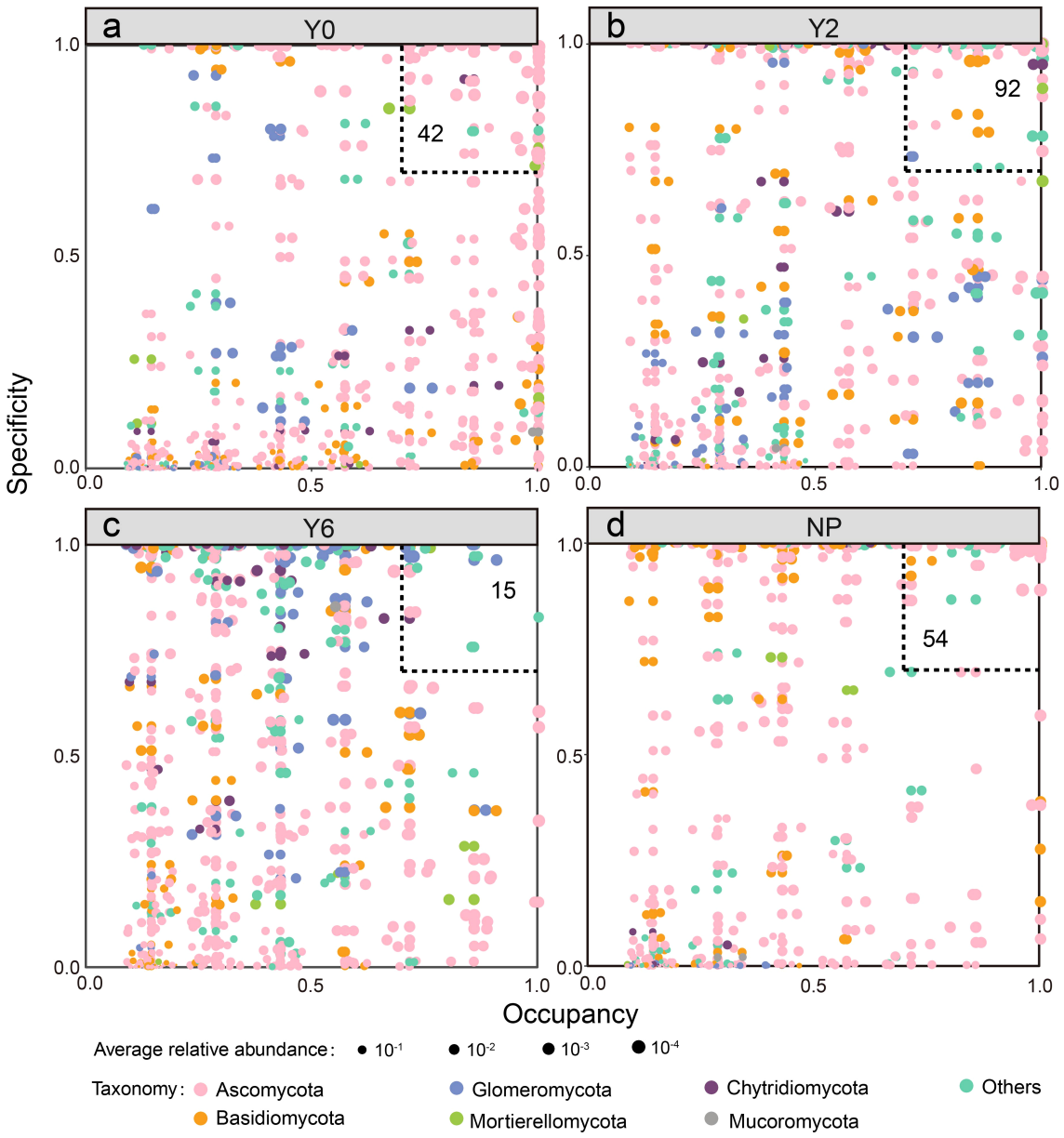

FIGURE 5
The specificity occupancy plot of soil fungal communities in Y0 unrestored sites **(a)**, Y2 2-year artificial restoration sites **(b)**, Y6 6-year artificial restoration sites **(c)**, and NP natural plant sites **(d)**.

4 Discussion

4.1 Soil fungal community diversity across different restoration stages

We employed α and β diversity to assess fungal community diversity. Our results revealed a significant increase in the diversity indices pertaining to soil fungal communities. This may be attributed to the increased plant community richness following 2 years artificial restoration, which promotes the release of various root exudates with binding properties, thereby providing more ecological niches for fungal communities and increasing the α diversity of the fungal community (Butler et al., 2003; Dey et al., 2012; Xu et al., 2022). The restoration process may have also been affected by the addition of sheep dung, which contributed to a swift and significant enhancement of soil nutrient levels, resulting in a more balanced species composition by replacing the dominant species with other species and reducing the number of dominant species in the community (Yang et al., 2024). However, after 2 years of restoration, soil heterogeneity decreased, and the more homogeneous environment selectively filtered species in a similar way, leading to a reduction in β diversity (Nemergut et al., 2013). The fungal community α diversity in 6-year restoration sites was lower than that in 2-year restoration sites. This is probably associated with the depletion of soil nutrients as the intensity of post-restoration management and maintenance has gradually

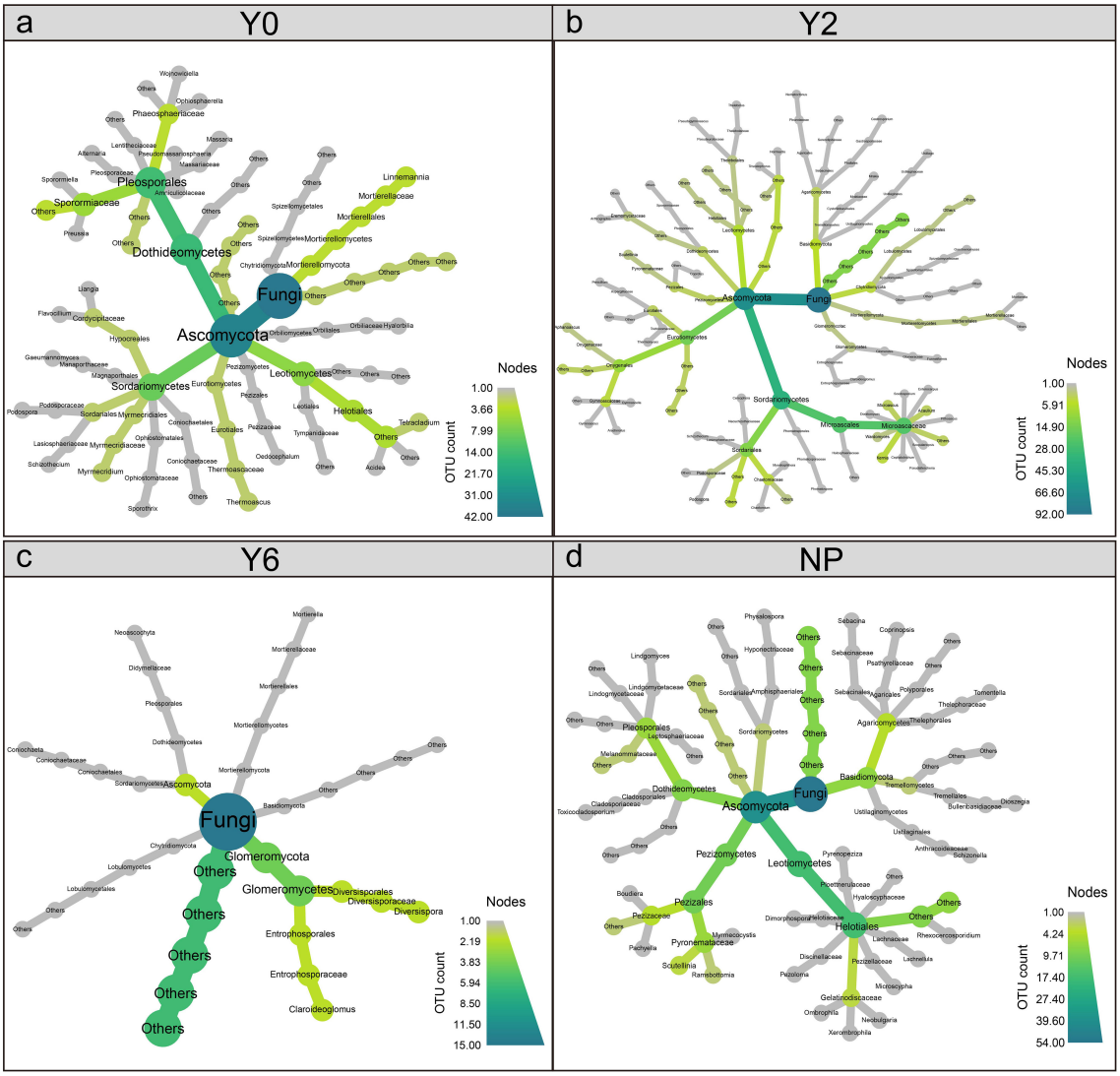

FIGURE 6
The taxonomic trees plotted of soil fungal communities in Y0 unrestored sites **(a)**, Y2 2-year artificial restoration sites **(b)**, Y6 6-year artificial restoration sites **(c)**, and NP natural plant sites **(d)**.

diminished during the later stages of vegetation restoration. While the β diversity of the fungal community may depend on dispersal processes in the 6-year restoration sites (Nemergut et al., 2013; Ernakovich et al., 2022), where the proportion of homogeneous selection significantly decreased and the proportion of dispersal limitation significantly increased, dispersal limitation can increase β diversity by causing spatial aggregation of species (Zhang et al., 2008). Our study observed that fungal community richness was greatest in unrestored soils, potentially due to the extremely low soil nutrient levels, which hinder plant growth. In a barren environment, plants tend to adopt a conservative approach by generating leaf litter abundant in phenolic compounds. Since soil bacteria are less proficient at decomposing such litter, fungi become more dominant in the microbial community, leading to a rise in fungal diversity (Wright et al., 2004), and our findings provide new insights into the mechanisms by which bacteria and fungi are influenced by plants in nutrient-poor soils, offering valuable perspectives for future research. Furthermore, the poor nutrient availability in the unrestored soils restricted the spread of soil fungi, leading to higher β diversity in these soils compared to other sites.

4.2 Soil fungal community structure and assembly mechanism across different restoration stages

Through modifications to the vegetation community composition and soil conditions, artificial restoration has markedly altered the composition and structure of the soil fungal community (Yuan et al., 2021). Ascomycota, being the most abundant and widely distributed fungal group in soil (Al-Sadi et al., 2017; Egidi et al., 2019), possesses dark-colored hyphae and large, multicellular black spores that enable it to endure extreme environmental conditions (Sterflinger, 2006; Bates et al., 2010). Hence, it is unsurprising that

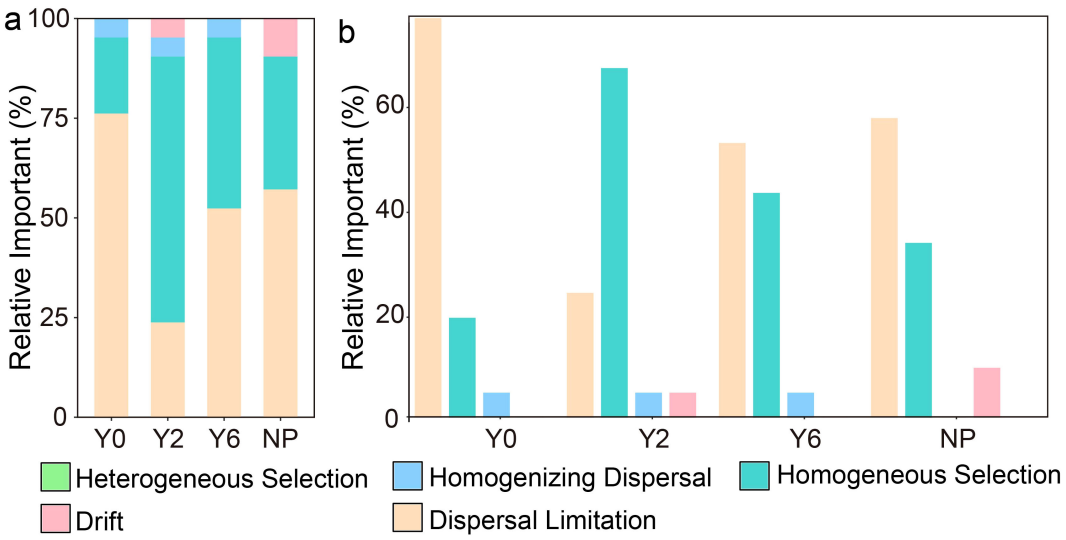

FIGURE 7
Stacked **(a)** and bar **(b)** chart of the relative contribution of each ecological process driving fungal community assembly within four sites based on null model analysis.

Ascomycota dominates across all the study sites. Following 2 years of artificial restoration, the relative abundance of Ascomycota showed a significant decrease, which may be attributed to the elevated total phosphorus levels resulting from the restoration process (Yang et al., 2024). Furthermore, as the restoration period extended, the significant increase in soil pH contributed to the decline in its relative abundance (Zhang Z, et al., 2022).

Following 2 years of restoration, the relative abundance of the *Pseudogymnoascus* within the Ascomycota significantly increased. These species has the capacity to withstand cold stress by allocating nutrients towards the mending and restoration of cellular damage, concurrently reducing the synthesis of proteins necessary for cellular expansion (Bakar et al., 2024). Thus, it is typically found in cold environments such as the Arctic, alpine, and Antarctic regions (Blehert et al., 2009; Vanderwolf et al., 2013; Wilson et al., 2017; Chaturvedi et al., 2018). Previous study indicated that the relative abundance of *Pseudogymnoascus* showed strong positive correlation with soil carbon, nitrogen and phosphorus. The substantial increase in soil nutrient content following 2 years of restoration contributed to a marked rise in its relative abundance. However, after 6 years of restoration, as soil nutrient content significant declined, the relative abundance of *Pseudogymnoascus* correspondingly notably decreased. Additionally, *Pseudogymnoascus* was positively correlated with soil bulk density, thus, the lower soil bulk density will limit the growth of *Pseudogymnoascus* in the unrestored sites. *Coniochaeta* is also a member of Ascomycota, and it engages with plant life through the release of proteins that initiate symbiotic relationships (Challacombe et al., 2019). Its relative abundance significantly increased in the 6-year restoration sites compared to the other three sites, which may be associated with the variety of plant species present.

Members of the Basidiomycota primarily rely on exogenous materials, such as plant litter or soil organic matter, as their main carbon sources for growth and reproduction. They significantly affect the degradation of plant residues, especially the breakdown of recalcitrant macromolecular organic compounds, through the production of oxidative and hydrolytic extracellular enzymes (Entwistle et al., 2018). In contrast to unrestored areas, the artificial restoration sites exhibited a notable rise in plant residues, which correlated with an elevated relative abundance of Basidiomycota. Additionally, Basidiomycota, functioning as saprotrophic fungi, possess the capability to break down lignin and cellulose, even in anaerobic environments (Guo et al., 2018; Kui et al., 2021), which likely explains their highest relative abundance in the natural plant sites. *Microscypha*, one of the major members of Basidiomycota, has been confirmed to possess plant growth-promoting and biocontrol functions (Gao et al., 2023) and is a core species in the root systems and rhizosphere soils of *Leymus chinensis* in alpine meadow (Guo et al., 2024). Our findings also indicated that its relative abundance is highest in the natural plant sites.

Glomeromycota are predominantly composed of arbuscular mycorrhizal fungi, which can establish mutualistic symbioses with the roots of 72% of higher flowering plants (Meng et al., 2023), playing an essential role in plant nutrient uptake and growth (Choi et al., 2018). In comparison to the unaltered areas, the plant community richness in the artificially restored regions increased significantly, resulting in increasing relative abundance of Glomeromycota. It even became the second most dominant group in the 6-year restoration sites, with *Diversispora* and *Claroideoglomus* emerging as the dominant genera in the same sites. However, our findings also indicated that, while the plant community richness was greatest in the natural plant sites, the relative abundance of Glomeromycota was comparatively low. This could be due to the pronounced host specificity inherent in the symbiotic association between Glomeromycota and plants (Liu et al., 2012; Zhang et al., 2023).

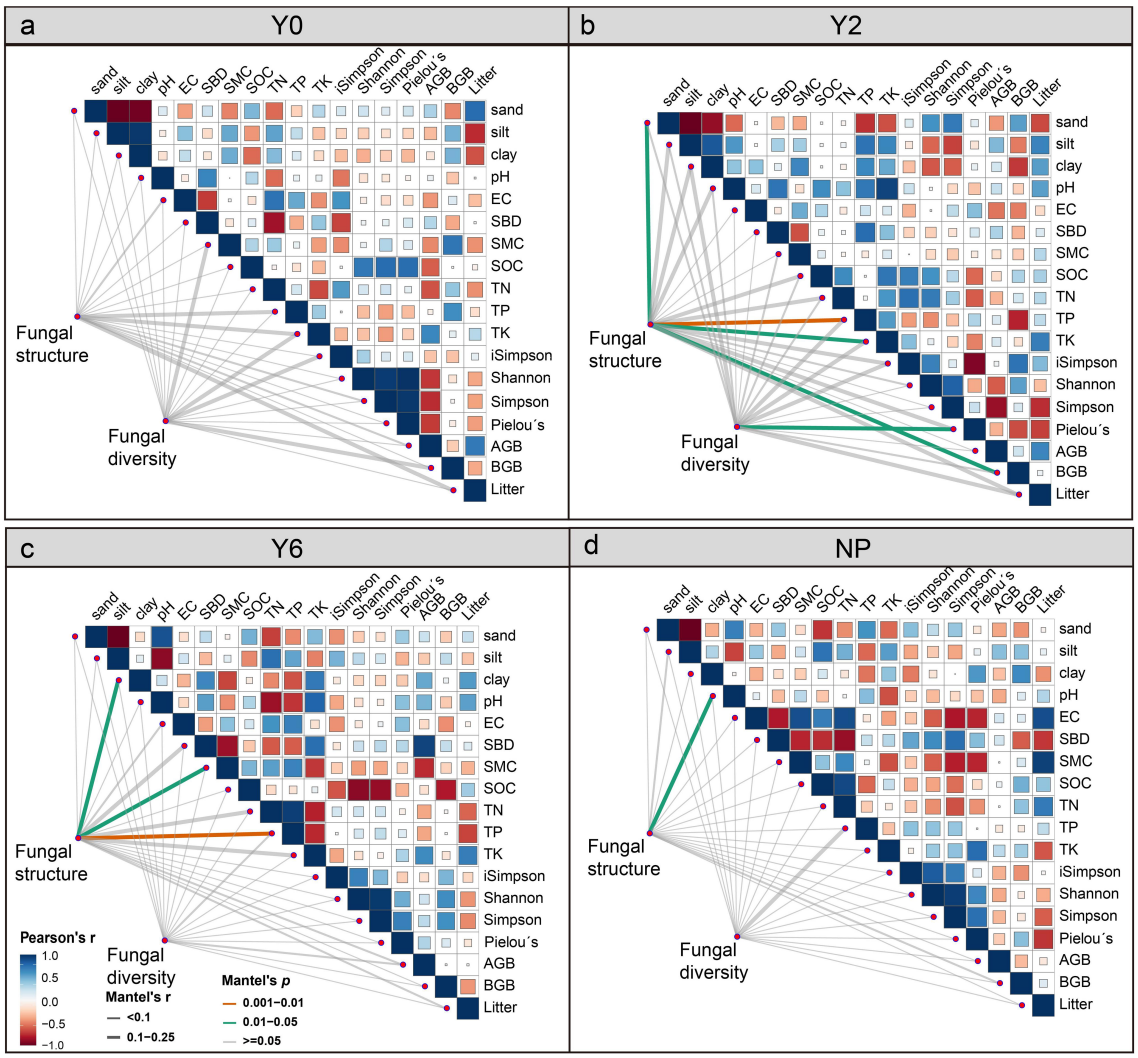

FIGURE 8
Associations of the fungal community structure with environmental factors in Y0 unrestored sites **(a)**, Y2 2-year artificial restoration sites **(b)**, Y6 6-year artificial restoration sites **(c)**, and NP natural plant sites **(d)**.

Artificial restoration impacts not only the composition of dominant species in soil fungal communities but also the processes that govern community assembly. In unrestored sites, the poor soil quality and sparse vegetation restrict fungal growth and reproduction, meaning the community structure is primarily shaped by dispersal limitations, with less influence from environmental factors such as vegetation and soil. In the 2-year restoration sites, significant increases in soil nutrient content, plant diversity, and biomass resulted in soil fungal community structure primarily govern by homogenous selection, with soil and vegetation becoming the primary influencing factors. Mate analysis further revealed that the soil fungal community structure was chiefly determined by soil sand, TP, TK, and BGB. In 6-year restoration sites, decreased soil nutrient content and greater heterogeneity resulted in both homogenous selection and dispersal limitations jointly influencing fungal community structure. Here, the structure was mainly driven by soil clay, SMC, and TP. In natural plant sites, higher BD and SMC impaired soil aeration, thus, the fungal community is primarily influenced by dispersal limitation.

4.3 Limitations and future directions

The current analysis only focuses on the diversity and assembly mechanisms of fungal communities, without integrating the functional aspects of these communities to reveal the dynamic changes in key functional genes. Future research should combine functional gene analysis to clarify the direct relationship between fungal functional activity and ecosystem functioning. This study only collected samples from a single location in the Muli mining area, and future studies should expand the sampling to multiple regions to explore how the relative contributions of environmental filtering and dispersal limitation change across spatial scales. Additionally, this study only collected samples from sites with 2 and 6 years of artificial restoration, which makes it difficult to accurately investigate the

successional characteristics of soil fungal community structure following artificial restoration. Future studies should include longer temporal sequences to more precisely quantify the impact of human interventions on fungal communities.

5 Conclusion

The implementation of artificial restoration measures has substantially augmented the diversity indices of soil fungal communities, while simultaneously causing a notable decline in β diversity in alpine mining areas. As the restoration period extended, the α diversity of soil fungal communities significantly decreased, while β diversity significantly increased. Concurrently, artificial restoration induced significant structural modifications in the soil fungal community composition, with distinctive fungal species accounting for over 82% of the total community in restored sites. Additionally, we found that artificial restoration had a positive effect on Basidiomycota. Dispersal limitation and homogeneity selection were the dominant process driving soil fungal community assembly in alpine mining areas. In the natural plant and unrestored sites, the structure of soil fungal communities was mainly influenced by dispersal limitation, followed by homogeneous selection. After artificial restoration, the structure of soil fungal community primarily was governed by homogeneous selection, following the dispersal limitation. As restoration time progressed, the importance of homogeneous selection decreased, while the relative importance of dispersal limitation notably increased, and the structure of soil fungal community mainly influenced by soil clay, SMC, and TP.

Data availability statement

The original contributions presented in the study are publicly available. This data can be found here: https://www.ncbi.nlm.nih.gov/bioproject/PRJNA1208394/.

Author contributions

YX: Conceptualization, Methodology, Writing – original draft, Writing – review & editing. WL: Conceptualization, Funding acquisition, Resources, Writing – review & editing. QF: Conceptualization, Writing – review & editing. MZ: Methodology, Resources, Writing – review & editing. JZ: Software, Writing – review & editing. LW: Resources, Writing – review & editing. ZC: Software, Writing – review & editing. XL: Software, Writing – review & editing.

Funding

The author(s) declare that financial support was received for the research and/or publication of this article. This research has been funded by the National Key R&D Program of China (Nos. 2022YFF1303301 and 2022YFF1302603), the National Natural Science Fund of China (Nos. 42101115, 52179026, and 42201133), the Gansu Provincial Science and Technology Planning Project (Nos. 23ZDFA018, 23ZDKA017 and 22JR5RA072), Gansu Province Intellectual Property Plan Program (No. 23ZSCQD001), and Excellent Doctoral Student Program of Gansu Province (No. 24JRRA110).

Conflict of interest

The authors declare that the research was conducted in the absence of any commercial or financial relationships that could be construed as a potential conflict of interest.

Generative AI statement

The author(s) declare that no Generative AI was used in the creation of this manuscript.

Publisher's note

Supplementary material

The Supplementary Material for this article can be found online at: https://www.frontiersin.org/articles/10.3389/fpls.2025.1579142/full#supplementary-material

References

Agnihotri, R., Sharma, M. P., Prakash, A., Ramesh, A., Bhattacharjya, S., Patra, A. K., et al. (2022). Glycoproteins of arbuscular mycorrhiza for soil carbon sequestration: Review of mechanisms and controls. *Sci. Total. Environ.* 806, 150571. doi: 10.1016/j.scitotenv.2021.150571

Ahirwal, J., and Maiti, S. K. (2017). Assessment of carbon sequestration potential of revegetated coal mine overburden dumps: a chronosequence study from dry tropical climate. *J. Environ. Manage.* 201, 369–377. doi: 10.1016/j.jenvman.2017.07.003

Al-Sadi, A. M., Al-Khatri, B., Nasehi, A., AI-Shihi, M., AI-Mahmooli, I. H., and Maharachchikumbura, S. S. N. (2017). High fungal diversity and dominance by ascomycota in dam reservoir soils of arid climates. *Int. J. Agric. Biol.* 19, 682–688. doi: 10.17957/IJAB/15.0328

Averill, C., Turner, B. L., and Finzi, A. C. (2014). Mycorrhiza-mediated competition between plants and decomposers drives soil carbon storage. *Nature* 505, 543–545. doi: 10.1038/nature12901

Bai, Y. (2022). *A study on creep characteristics of permafrost layer and its influence on surface subsidence characteristics of underlying coal seam Mining* (Xi'an City, Shaanxi Province, China: Xi'an University of science and technology).

Bakar, N. A., Lau, B. Y. C., González–Aravena, M., Smykla, J., Krzewicka, B., Karsani, S. A., et al. (2024). Geographical diversity of proteomic responses to cold stress in the fungal genus *Pseudogymnoascus*. *Microb. Ecol.* 87, 11. doi: 10.1007/s00248-023-02311-w

Bates, S. T., Iii, T. H. N., Sweat, K. G., and Garcia-Pichel, F. (2010). Fungal communities of lichen-dominated biological soil crusts: diversity, relative microbial biomass, and their relationship to disturbance and crust cover. *J. Arid. Environ.* 74, 1192–1199. doi: 10.1016/j.jaridenv.2010.05.033

Blaalid, R., Kumar, S., Nilsson, R. H., Abarenkov, K., Kirk, P. M., and Kauserud, H. (2013). ITS1 versus ITS2 as DNA metabarcodes for fungi. *Mol. Ecol. Resour.* 13, 218–224. doi: 10.1111/men.2013.13.issue-2

Blehert, D. S., Hicks, A. C., Behr, M., Meteyer, C. U., Berlowski-Zier, B. M., Buckles, E. L., et al. (2009). Bat white-nose syndrome: An emerging fungal pathogen? *Science* 323, 227. doi: 10.1126/science.1163874

Butler, J. L., Williams, M. A., Bottomley, P. J., and David, D. (2003). Microbial community dynamics associated with rhizosphere carbon flow. *Appl. Environ. Microbiol.* 69, 6793–6800. doi: 10.1128/AEM.69.11.6793-6800.2003

Challacombe, J. F., Hesse, C. N., Bramer, L. M., McCue, L. A., Lipton, M., Purvine, S., et al. (2019). Genomes and secretomes of Ascomycota fungi reveal diverse functions in plant biomass decomposition and pathogenesis. *BMC Genom.* 20, 976. doi: 10.1186/s12864-019-6358-x

Chaturvedi, V., DeFiglio, H., and Chaturvedi, S. (2018). Phenotype profiling of white-nose syndrome pathogen *Pseudogymnoascus destructans* and closely-related *Pseudogymnoascus pannorum* reveals metabolic differences underlying fungal lifestyles. *F1000Research* 7, 665. doi: 10.12688/f1000research

Chen, J., Nan, J., Xu, D. L., Mo, L., Zheng, Y. X., Chao, L. M., et al. (2020). Response differences between soil fungal and bacterial communities under opencast coal mining disturbance conditions. *Catena* 194, 104779. doi: 10.1016/j.catena.2020.104779

Choi, J., Summers, W., and Paszkowski, U. (2018). Mechanisms underlying establishment of arbuscular mycorrhizal symbioses. *Ann. Rev. Phytopathol.* 56, 135–160. doi: 10.1146/annurev-phyto-080516-035521

Courty, P. E., Buée, M., Diedhiou, A. G., Frey-Klett, P., Le Tacon, F., Rineau, F., et al. (2010). The role of ectomycorrhizal communities in forest ecosystem processes: New perspectives and emerging concepts. *Soil Biol. Biochem.* 42, 679–698. doi: 10.1016/j.soilbio.2009.12.006

Dao, R. N., Zhang, Y., Li, X. L., Ma, L. X., Tie, X. L., and Lei, S. Y. (2023). Diversity of soil bacteria in alpine coal slag mountain grassland in different vegetation restoration years. *Ann. Microbiol.* 73, 12. doi: 10.1186/s13213-023-01716-9

de Quadros, P. D., Kateryna, Z., Davis-Richardson, A. G., Drew, J. C., Menezes, F. B., Camargo, F. A. D., et al. (2016). Coal mining practices reduce the microbial biomass, richness and diversity of soil. *Appl. Soil Ecol.* 98, 195–203. doi: 10.1016/j.apsoil.2015.10.016

Dey, R., Pal, K. K., and Tilak, K. V. B. R. (2012). Influence of soil and plant types on diversity of rhizobacteria. *Proc. Natl. Acad. Sci. India. Sect. B-Biol. Sci.* 82, 341–352. doi: 10.1007/s40011-012-0030-4

Dufrene, M., and Legendre, P. (1997). Species assemblages and indicator species: the need for a flexible asymmetrical approach. *Ecol. Monogr.* 67, 345–366. doi: 10.2307/2963459

Egidi, E., Delgado-Baquerizo, M., Plett, J. M., Wang, J., Eldridge, D. J., Bargett, R. D., et al. (2019). A few Ascomycota taxa dominate communities worldwide. *Nat. Commun.* 10, 2369. doi: 10.1038/s41467-019-10373-z

Entwistle, E. M., Zak, D. R., and Argiroff, W. A. (2018). Anthropogenic N deposition increases soil C storage by reducing the relative abundance of lignolytic fungi. *Ecol. Monogr.* 88, 225–244. doi: 10.1002/ecm.2018.88.issue-2

Ernakovich, J. G., Barbato, R. A., Rich, V. I., Schädel, C., Hewitt, R. E., Doherty, S. J., et al. (2022). Microbiome assembly in thawing permafrost and its feedbacks to climate. *Glob. Change Biol.* 28, 5007–5026. doi: 10.1111/gcb.v28.17

Foster, Z., Sharpton, T., and Grünwald, N. (2017). Metacoder: an R package for visualization and manipulation of community taxonomic diversity data. *PloS Comput. Biol.* 13, 1–15. doi: 10.1371/journal.pcbi.1005404

Freire-Zapata, V., Holland-Moritz, H., Cronin, R. D., Aroney, S., Smith, D. A., Wilson, R. M., et al. (2024). Microbiome–metabolite linkages drive greenhouse gas dynamics over a permafrost thaw gradient. *Nat. Microbiol.* 9, 2892–2908. doi: 10.1038/s41564-024-01800-z

Ganesh, K. J., Sarah, E. D., and Hugh, W. P. (2020). Seed survival at low temperatures: a potential selecting factor influencing community level changes in high altitudes under climate change. *Crit. Rev. Plant Sci.* 39, 479–492. doi: 10.1080/07352689.2020.1848277

Gao, F., Li, Z. L., Gao, Y. X., Gao, Y., Li, M. Y., Li, C. F., et al. (2023). The effect of long-term controlled-release urea application on the relative abundances of plant growth-promoting microorganisms. *Eur. J. Agron.* 151, 126971. doi: 10.1016/j.eja.2023.126971

Guo, J. J., Liu, W. B., Zhu, C., Luo, G. W., Kong, Y. L., Ling, N., et al. (2018). Bacterial rather fungal community composition is associated with microbial activities and nutrient-use efficiencies in a paddy soil with short-term organic amendments. *Plant Soil* 424, 335–349. doi: 10.1007/s11104-017-3547-8

Guo, J., Xie, Z., Meng, Q., Xu, H., Peng, Q., Wang, B., et al. (2024). Distribution of rhizosphere fungi of *Kobresia humilis* on the Qinghai-Tibet Plateau. *PeerJ.* 12, e16620. doi: 10.7717/peerj.16620

Gweon, H. S., Bowes, M. J., Moorhouse, H. L., Oliver, A. E., Bailey, M. J., Acreman, M. C., et al. (2021). Contrasting community assembly processes structure lotic bacteria metacommunities along the river continuum. *Environ. Microbiol.* 23, 484–498. doi: 10.1111/1462-2920.15337

Izquierdo, I., Caravaca, F., Alguacil, M. M., Hernández, G., and Roldán, A. (2005). Use of microbiological indicators for evaluating success in soil restoration after revegetation of a mining area under subtropical conditions. *Appl. Soil Ecol.* 30, 3–10. doi: 10.1016/j.apsoil.2005.02.004

Ji, X. M., Liu, M. H., Yang, J. L., and Feng, F. J. (2022). Meta-analysis of the impact of freeze-thaw cycles on soil microbial diversity and C and N dynamics. *Soil Biol. Biochem.* 168, 108608. doi: 10.1016/j.soilbio.2022.108608

Jibola-Shittu, M. Y., Heng, Z., Keyhani, N. O., Dang, Y., Chen, R., Liu, S., et al. (2024). Understanding and exploring the diversity of soil microorganisms in tea (*Camellia sinensis*) gardens: toward sustainable tea production. *Front. Microbiol.* 15, 1379879. doi: 10.3389/fmicb.2024.1379879

Kembel, S. W., Helmus, M. R., Cornwell, W. K., Moorlon, H., Ackerly, D. D., Blomberg, S. P., et al. (2010). Picante: R tools for integrating phylogenies and ecology. *Bioinformatics* 26, 1463–1464. doi: 10.1093/bioinformatics/btq166

Krishnamoorthy, R., Kim, K., Kim, C., and Sa, T. (2014). Changes of arbuscular mycorrhizal traits and community structure with respect to soil salinity in a coastal reclamation land. *Soil Biol. Biochem.* 72, 1–10. doi: 10.1016/j.soilbio.2014.01.017

Kui, L., Xiang, G. S., Wang, Y., Wang, Z. J., Li, G. R., Li, D. W., et al. (2021). Large-scale characterization of the soil microbiome in ancient tea plantations using high-throughput 16s rRNA and internal transcribed spacer amplicon sequencing. *Front. Microbiol.* 12, 745225. doi: 10.3389/fmicb.2021.745225

Li, Y. H., Li, X. L., Tang, J. W., Jia, S. B., Zhang, Q. H., Wang, M. H., et al. (2021). Study on "Seven-step" grass planting technology for ecological rehabilitation of frigid zone Muri mining area in Qinghai. *Coal Geol. Chin.* 33, 1674–1803.

Liu, J., Jia, X. Y., Yan, W. M., Zho, Y. Q. W., and Shangguan, Z. P. (2020). Changes in soil microbial community structure during long-term secondary succession. *Land. Degrad. Dev.* 31, 1151–1166. doi: 10.1002/ldr.v31.9

Liu, Y. J., Shi, G. X., Mao, L., Cheng, G., Jiang, S. J., Ma, X. J., et al. (2012). Direct and indirect influences of 8 yr of nitrogen and phosphorus fertilization on Glomeromycota in an alpine meadow ecosystem. *New Phytol.* 194, 523–535. doi: 10.1111/j.1469-8137.2012.04050.x

Luo, Z. B., Ma, J., Chen, F., Li, X. X., Zhang, Q., and Yang, Y. J. (2020). Adaptive development of soil bacterial communities to ecological processes caused by mining activities in the Loess Plateau, China. *Microorganisms* 8, 477. doi: 10.3390/microorganisms8040477

Ma, N., Li, Q., Guo, Y. T., and Li, P. F. (2019). Influence of different years of restoration of typical vegetation to soil quality of Shendong mining area. *Soil Water Conserv. China* 11, 59–62. doi: 10.14123/j.cnki.swcc.2019.0273

Mendiburu, F. D. (2017). Agricolae: Statistical procedures for agricultural research. *J. Am. Stat. Assoc.* 80, 390. doi: 10.2307/2287932

Meng, Y. M., Davison, J., Clarke, J. T., Zobel, M., Gerz, M., Moora, M., et al. (2023). Environmental modulation of plant mycorrhizal traits in the global flora. *Ecol. Lett.* 26, 1862–1876. doi: 10.1111/ele.v26.11

Myers, J. A., Chase, J. M., Jiménez, I., Jørgensen, P. M., Araujo-Murakami, A., Paniagua-Zambrana, N., et al. (2013). Beta-diversity in temperate and tropical forests reflects dissimilar mechanisms of community assembly. *Ecol. Lett.* 16, 151–157. doi: 10.1111/ele.2012.16.issue-2

Nemergut, D. R., Schmidt, S. K., Fukami, T., O'Neill, S. P., Bilinski, T. M., Stanish, L. F., et al. (2013). Patterns and processes of microbial community assembly. *Microbiol. Mol. Biol. Rev.* 77, 342–356. doi: 10.1128/MMBR.00051-12

Ning, D. L., Yuan, M. T., Wu, L. W., Zhang, Y., Guo, X., Zhou, X. S., et al. (2020). A quantitative framework reveals ecological drivers of grassland microbial community assembly in response to warming. *Nat. Commun.* 11, 4717. doi: 10.1038/s41467-020-18560-z

Qiang, W., Yang, B., Liu, Y., Qi, K. B., Yang, T. H., and Pang, X. Y. (2020). Effects of reclamation age on soil microbial communities and enzymatic activities in the sloping citrus orchards of southwestern China. *Appl. Soil Ecol.* 152, 103566. doi: 10.1016/j.apsoil.2020.103566

Roy, R., Wang, J. X., Mostofa, M. G., Fornara, D., Sikdar, A., Sarker, T., et al. (2020). Fine-tuning of soil water and nutrient fertilizer levels for the ecological restoration of coal-mined spoils using Elaeagnus angustifolia. *J. Environ. Manage.* 270, 110855. doi: 10.1016/j.jenvman.2020.110855

Schloss, P. D., Westcott, S. L., Ryabin, T., Hall, J. R., Hartmann, M., Hollister, E. B., et al. (2009). Introducing mothur: open-source, platform-independent, community-supported software for describing and comparing microbial communities. *Appl. Environ. Microb.* 75, 7537–7541. doi: 10.1128/AEM.01541-09

Stegen, J. C., Lin, X. J., Fredrickson, J. K., Chen, X. Y., Kennedy, D. W., Murray, C. J., et al. (2013). Quantifying community assembly processes and identifying features that impose them. *ISME. J.* 7, 2069–2079. doi: 10.1038/ismej.2013.93

Sterflinger, K. (2006). ""Black yeasts and meristematic fungi: ecology, diversity and identification,"," in *Biodiversity and ecophysiology of yeasts*. Eds. G. Peter and C. Rosa (Springer Berlin Heidelberg., Germany), 501–514.

Sunagawa, S., Coelho, L. P., Chaffron, S., Kultima, J. R., Labadie, K., Salazar, G., et al. (2015). Structure and function of the global ocean microbiome. *Science* 348, 6237. doi: 10.1126/science.1261359

Tripathi, B. M., Stegen, J. C., Kim, M., Dong, K., Adams, J. M., and Lee, Y. K. (2018). Soil pH mediates the balance between stochastic and deterministic assembly of bacteria. *ISME. J.* 12, 1072–1083. doi: 10.1038/s41396-018-0082-4

Vanderwolf, K. J., Malloch, D., McAlpine, D. F., and Forbes, G. J. (2013). A world review of fungi, yeasts, and slime molds in caves. *Int. J. Speleol.* 42, 9. doi: 10.5038/1827-806X.42.1.9

Wang, X., Wu, D., Li, S., Chen, T., Chen, R., Yin, L., et al. (2022). Effects of C: N imbalance on soil microbial physiology in subtropical tree plantations associated with ectomycorrhizal and arbuscular mycorrhizal fungi. *Geoderma* 422, 115932. doi: 10.1016/j.geoderma.2022.115932

Wilson, M. B., Held, B. W., Freiborg, A. H., Blanchette, R. A., and Salomon, C. E. (2017). Resource capture and competitive ability of nonpathogenic *Pseudogymnoascus* spp. and *P. destructans*, the cause of white-nose syndrome in bats. *PloS One* 12, e0178968. doi: 10.1371/journal.pone.0178968

Wright, I. J., Reich, P. B., Westoby, M., Ackerly, D. D., Baruch, Z., Bongers, F., et al. (2004). The worldwide leaf economics spectrum. *Nature* 428, 821–827. doi: 10.1038/nature02403

Xu, Y. X., Li, C., Zhu, W. K., Wang, Z. C., Wu, L. C., and Du, A. P. (2022). Effects of enrichmemt planting with native tree species on bacterial community structure and potential impact on Eucalyptus plantations in southern China. *J. For. Res.* 33, 1349–1363. doi: 10.1007/s11676-021-01433-6

Xue, Y. Y., Liu, W., Feng, Q., Zhu, M., Zhang, J. T., Wang, L. G., et al (2025). The role of vegetation restoration in shaping the structure and stability of soil bacterial community of alpine mining regions. *Plant Soil*. doi: 10.1007/s11104-025-07364-z

Yang, X. M., Feng, Q., Zhu, M., Zhang, J. T., Yang, L. S., and Li, R. (2024). The impact of artificial restoration of alpine grasslands in the Qilian Mountains on vegetation, soil bacteria, and soil fungal community diversity. *Microorganisms* 12, 854. doi: 10.3390/microorganisms12050854

Yang, X. G., Li, X. L., Jin, L. Q., and Sun, H. F. (2018). Changes in soil properties of coal mine spoils in an alpine coal mining area after short-term restoration. *Acta Pratac. Sin.* 27, 30–38. doi: 10.11686/cyxb2017350

Yuan, D. Z., Hu, Z. Q., Yang, K., Guo, J. X., Li, P. Y., Li, G. S., et al. (2021). Assessment of the ecological impacts of coal mining and restoration in alpine areas: a case study of the Muli coalfield on the Qinghai-Tibet Plateau. *IEEE* 9, 162919–162934. doi: 10.1109/ACCESS.2021.3133478

Zhang, T., Barry, R. G., Knowles, K., Heginbottom, J. A., and Brown, J. (2008). Statistics and characteristics of permafrost and ground-ice distribution in the northern hemisphere. *Polar. Geogr.* 31, 47–68. doi: 10.1080/10889370802175895

Zhang, Z., Ge, S. B., Fan, L. C., Guo, S., Hu, Q., Ahammed, G. J., et al. (2022). Diversity in rhizospheric microbial communities in tea varieties at different locations and tapping potential beneficial microorganisms. *Front. Microbiol.* 13, 1027444. doi: 10.3389/fmicb.2022.1027444

Zhang, L., Ge, A. H., Toth, T., Yang, F., Wang, Z. C., and An, F. H. (2023). Enrichment of keystone fungal taxa after flue gas desulphurization gypsum application. *Land. Degrad. Dev.* 34, 2276–2287. doi: 10.1002/ldr.v34.8

Zhang, X., Long, H., Huo, D., Awan, M. I., Shao, J., Mahmood, A., et al. (2022). Insights into the functional role of tea microbes on tea growth, quality and resistance against pests and diseases. *Not. Bot. Horti. Agrobo.* 50, 12915. doi: 10.15835/nbha50312915

Frontiers in
Plant Science

Cultivates the science of plant biology and its applications

The most cited plant science journal, which advances our understanding of plant biology for sustainable food security, functional ecosystems and human health.

Discover the latest Research Topics

See more →

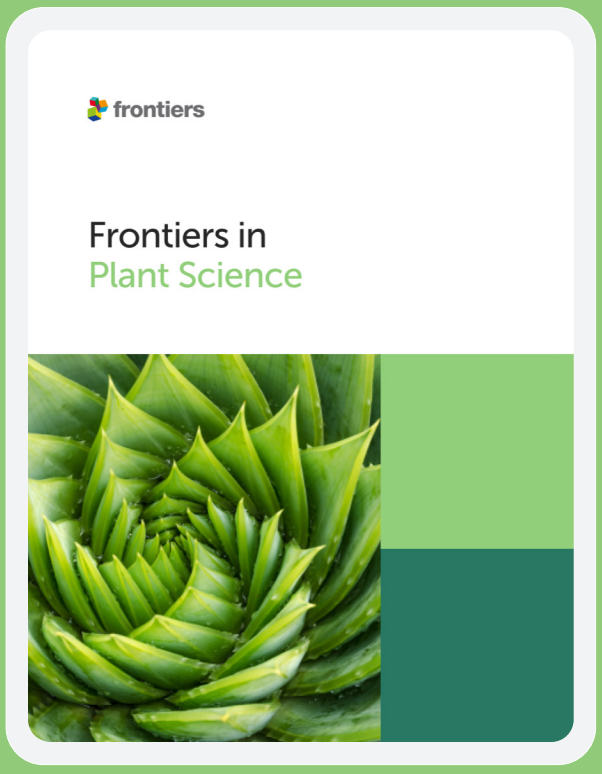

Frontiers

Avenue du Tribunal-Fédéral 34
1005 Lausanne, Switzerland
frontiersin.org

Contact us

+41 (0)21 510 17 00
frontiersin.org/about/contact